ROLE OF NOTCH SIGNALING IN ANGIOGENESIS AND BREAST CANCER

by

KEVIN G. LEONG

B.Sc., The University of British Columbia, 1999

A THESIS SUBMITTED IN PARTIAL FULFILLMENT OF
THE REQUIREMENTS FOR THE DEGREE OF

DOCTOR OF PHILOSOPHY

in

THE FACULTY OF GRADUATE STUDIES

Experimental Medicine

THE UNIVERSITY OF BRITISH COLUMBIA

February 2005

ABSTRACT

The Notch family of transmembrane receptors consists of four members in mammals, Notch1 through Notch4. Upon ligand binding, Notch receptors become activated and participate in intracellular signaling pathways that regulate cell fate decisions. Notch1-3 are expressed on numerous cell types. Because Notch4 is primarily expressed on endothelial cells, we postulated that Notch4 activation would modulate cell fate decisions in an endothelial-specific manner. Angiogenesis, the sprouting of endothelial cells from pre-existing microvessels, requires modulation of the endothelial cell phenotype. We have identified a role for Notch4 activation in the regulation of angiogenesis. Expression of activated Notch4 inhibits endothelial sprouting in vitro and angiogenesis in vivo. Activated Notch4 does not inhibit endothelial cell migration through the extracellular matrix protein fibrinogen, whereas migration through collagen is inhibited. Activated Notch4 increases endothelial cell adhesion to collagen by modulating the affinity state of cell-surface collagen receptors belonging to the β1 integrin family. Specifically, activated Notch4 converts β1 integrin from an inactive, non-ligand-binding state to an active, high-affinity conformation. Our findings suggest that Notch4 activation in endothelial cells inhibits angiogenesis in part by promoting β1 integrin-mediated adhesion to the underlying matrix.

Although Notch signaling regulates normal cellular processes, increasing evidence suggests a role for aberrant Notch signaling in cellular transformation. During tumor progression, epithelial tumor cells often acquire a mesenchymal phenotype through epithelial-to-mesenchymal transition (EMT), a process that promotes invasion and dissemination of cancer cells. In human breast cancer, EMT directly correlates with downregulated expression of the adherens junction protein epithelial (E)-cadherin. Given that Notch pathway elements are

expressed at sites of epithelial-mesenchymal cell-cell interactions during embryogenesis and within primary human breast tumors, we investigated whether Notch signaling would modulate E-cadherin expression in human breast cells. Our studies identify activated Notch signaling as a novel mechanism for the downregulation of E-cadherin expression in normal human breast epithelial cells. In human breast tumor xenografts lacking E-cadherin expression, we show that a soluble inhibitor of Notch signaling attenuates E-cadherin promoter methylation and induces E-cadherin re-expression. This re-induction of E-cadherin in turn inhibits β-catenin nuclear accumulation, resulting in a marked reduction in breast tumor growth and metastasis.

TABLE OF CONTENTS

LIST OF FIGURES

CHAPTER 1

CHAPTER 2

No Figures

CHAPTER 3

CHAPTER 4

CHAPTER 5

LIST OF TABLES

CHAPTER 1

No Tables

CHAPTER 2

CHAPTER 3

No Tables

CHAPTER 4

No Tables

CHAPTER 5

No Tables

LIST OF ABBREVIATIONS

Ab	antibody
ADAM	a disintegrin and metalloprotease
AMF	autocrine motility factor
Ang	angiopoietin
AP	activator protein
APC	adenomatous polyposis coli
ARNT	aryl hydrocarbon receptor nuclear translocator
ATP	adenosine triphosphate
bHLH	basic helix-loop-helix
BrdU	5-bromo-2'-deoxyuridine
C	carboxy-
Ca^{2+}	calcium
CADASIL	cerebral autosomal dominant arteriopathy with subcortical infarcts and leukoencephalopathy
CAM	chorioallantoic membrane
CBF	C protein binding factor
CDH	cadherin
cDNA	complementary deoxyribonucleic acid
CHF	cardiovascular helix-loop-helix factor
CIR	C protein binding factor 1-interacting corepressor
CpG	cytosine-phosphate-guanine
DAPI	4',6-diamidino-2-phenylindole
deltaEF	delta-crystallin/E2-box factor
DGEA	aspartic acid-glycine-glutamic acid-alanine
Dll	Delta-like
DMEM	Dulbecco's modified Eagle's medium
dNTP	2'-deoxynucleoside 5'-triphosphate
DSL	Delta/Serrate/Lag-2
E	embryonic day
E-cadherin	epithelial cadherin
ECM	extracellular matrix
EDTA	ethylenediaminetetraacetic acid
EGF	epidermal growth factor
EMT	epithelial-to-mesenchymal transition
EndoMT	endothelial-to-mesenchymal transition
EpCAM	epithelial cell adhesion molecule
E-selectin	endothelial-selectin
FACS	fluorescence-activated cell sorter
FAK	focal adhesion kinase
FCS	fetal calf serum
FGF	fibroblast growth factor
FGF-R	fibroblast growth factor-receptor
FITC	fluorescein isothiocyanate

GAPDH	glyceraldehyde-3-phosphate dehydrogenase
GBP	glycogen synthase kinase-binding protein
GFOGER	glycine-phenylalanine-hydroxyproline-glycine-glutamic acid-arginine
GFP	green fluorescent protein
GSK3β	glycogen synthase kinase 3β
GTP	guanosine triphosphate
H&E	hematoxylin and eosin
HA	hemagglutinin
HAT	histone acetyltransferase
HAV	histidine-alanine-valine
HDAC	histone deacetylase
HERP	hairy/enhancer-of-split-related repressor protein
HES	hairy/enhancer-of-split
HESR	hairy/enhancer-of-split-related
HEY	hairy/enhancer-of-split-related with YRPW
HEYL	hairy/enhancer-of-split-related with YRPW-like
HGF	hepatocyte growth factor
HIF	hypoxia inducible factor
HMEC	human dermal microvascular endothelial cell
HRT	hairy-related transcription factor
HUVEC	human umbilical vein endothelial cell
IAP	intracisternal A particle
ICAM	intercellular adhesion molecule
IDAPS	isoleucine-aspartic acid-alanine-proline-serine
IRES	internal ribosomal entry site
kDa	kilodalton
LEF	lymphoid enhancer factor
LFA	lymphocyte function-associated
LRP	low density lipoprotein receptor-related protein
L-selectin	lymphocyte-selectin
LTR	long terminal repeat
mAb	monoclonal antibody
Maml	Mastermind-like
MAP	mitogen-activated protein
MASH	mammalian achaete-scute homologue
MATH	mammalian atonal homologue
MDR	multidrug resistance
MHC	major histocompatibility complex
MIG	murine stem cell virus - internal ribosomal entry site - green fluorescent protein
MIY	murine stem cell virus - internal ribosomal entry site - yellow fluorescent protein
MMP	matrix metalloprotease
MMTV	Mouse Mammary Tumor Virus
mRNA	messenger ribonucleic acid

MSCV	murine stem cell virus
MSP	methylation-specific polymerase chain reaction
N	amino-
NFκB	nuclear factor κB
NOD/SCID	non-obese diabetic/severe combined immunodeficient
Notch1IC	Notch1 intracellular domain
Notch4IC	Notch4 intracellular domain
NotchIC	Notch intracellular domain
PBS	phosphate-buffered saline
PCR	polymerase chain reaction
PDZ	PSD-95/Dlg/zonula occludens-1
PECAM	platelet endothelial cell adhesion molecule
PEST	proline-glutamine-serine-threonine
PI3K	phosphatidylinositol 3-kinase
PKC	protein kinase C
PLC	phospholipase C
PlGF	placenta growth factor
P-selectin	platelet-selectin
QIDS	glutamine-isoleucine-aspartic acid-serine
RAM	recombination signal binding protein Jκ-associated module
RBPJκ	recombination signal binding protein Jκ
RGD	arginine-glycine-aspartic acid
RIP	regulated intramembranous proteolysis
RNA	ribonucleic acid
RNAi	ribonucleic acid interference
RNase	ribonuclease
RT-PCR	reverse transcriptase polymerase chain reaction
SDS	sodium dodecyl sulfate
SIP	Smad-interacting protein
SIRT	sirtuin
SKIP	Ski interacting protein
SMRT	silencing mediator of retinoid and thyroid hormone receptor
SNP	single nucleotide polymorphism
SV40	simian virus 40
TACE	tumor necrosis factor α converting enzyme
TAD	transactivation domain
TAE	tris acetic acid
T-ALL	T-cell acute lymphoblastic leukemia
TAN	translocation-associated Notch
TCF	T-cell factor
TCRβ	T-cell receptor β
TE(V/I)GAF	threonine-glutamic acid-(valine/isoleucine)-glycine-alanine-phenylalanine
TFIIA	transcription factor IIA
TFIID	transcription factor IID
TGFβ	transforming growth factor β

Tie	tyrosine kinase with immunoglobulin and epidermal growth factor homology domain
TIMP	tissue inhibitor of metalloprotease
TLE	transducin-like enhancer-of-split
TNFα	tumor necrosis factor α
uPA	urokinase-type plasminogen activator
uPAR	urokinase-type plasminogen activator receptor
VCAM	vascular cell adhesion molecule
VE-cadherin	vascular endothelial cadherin
VEGF	vascular endothelial growth factor
VEGF-R	vascular endothelial growth factor-receptor
VSMC	vascular smooth muscle cell
vWF	von Willebrand factor
WAP	whey acidic protein
WDR	tryptophan-aspartic acid-arginine
Wnt	wingless-type
WRPW	tryptophan-arginine-proline-tryptophan
XNotch	extracellular Notch
YFP	yellow fluorescent protein
YHSW	tyrosine-histidine-serine-tryptophan
YRPW	tyrosine-arginine-proline-tryptophan
ZO	zonula occludens

ACKNOWLEDGEMENTS

Where to begin. First and foremost I would like to thank my parents, David and Peggy Leong, for supporting me both emotionally and financially. They have always believed in my abilities and have been an unwavering source of wisdom and love.

To my older brother Terry Leong and my younger sister Kathryn Leong, I thank you for your honesty and kindness. Sharing with you has made my successes sweeter and my disappointments bearable. I also thank my sister-in-law Amy Leong, for introducing me to my niece Meaghan and my nephew Kyle. I am grateful to my grandparents for their care, and to my many aunts, uncles, and cousins for their words of encouragement.

I would like to acknowledge my colleagues, both past and present, who have influenced my academic career. Thank you to Xiaolong Hu for laying the groundwork on which my research was built, to Ingrid Pollet for providing technical assistance with animal studies, to Fred Wong and Denise McDougal for performing flow cytometry, and to Kyle Niessen for generating cell lines. Thank you to the other members of my laboratory and my department for your support. A special thank you to Maisie Lo. Your encouragement, enthusiasm, and companionship made my thesis writing experience enjoyable. To my graduate committee members, Drs. Peggy Olive, Michel Roberge, and Calvin Roskelley, thank you for your dedication and insight into my research project.

To my research supervisor Dr. Aly Karsan, I am indebted to you for your mentorship. Thank you for providing me with the opportunity to learn and discover.

Last but not least, thank you to the many mice that have given their lives in my pursuit of knowledge. Your sacrifices shall not be in vain. This thesis is dedicated to the memory of my family members who have lost their battles with cancer.

Financial support for my graduate career was provided by a Summer Studentship Award from the Heart and Stroke Foundation of British Columbia and the Yukon, a University Graduate Fellowship Award from the University of British Columbia, a Doctoral Research Award from the Canadian Institutes of Health Research, and a Predoctoral Fellowship Award from the United States Department of Defense.

Chapter 1

INTRODUCTION

1.1 NOTCH

1.1.1 Overview of Notch functions

In 1917, the first documented case of a strain of Drosophila characterized by notches at the ends of their wing blades was reported (Radtke and Raj, 2003). These notches were caused by haploinsufficiency of an unknown gene, which was subsequently cloned in the mid-1980's and identified as the gene coding for the Drosophila transmembrane receptor Notch (Kidd et al., 1986; Wharton et al., 1985). Notch orthologues have since been identified in numerous organisms including mammals (Mumm and Kopan, 2000).

The Notch signaling pathway was originally described as a mechanism for the inhibition of cell differentiation, and has been reported to inhibit neurogenesis (Baker, 2000), myogenesis (Kopan et al., 1994; Nye et al., 1994), granulocytic differentiation (Li et al., 1998b), and T cell development (Robey et al., 1996; Washburn et al., 1997). By maintaining cells in an undifferentiated state, Notch signaling allows cells to respond to inductive cues at appropriate times and thus facilitates the generation of cell diversity (Artavanis-Tsakonas et al., 1995; Weinmaster, 1997). This view of Notch function, however, proved to be oversimplified as Notch signaling can also promote cell differentiation for instance during gliogenesis (Wang and Barres, 2000). Hence activated Notch signaling can either block cell differentiation or direct cells towards an alternate differentiation fate.

In addition to regulating cell fate, Notch signaling has been shown to play a role in cell proliferation (Nicolas et al., 2003; Noseda et al., 2004a; Rangarajan et al., 2001b; Ronchini and

Capobianco, 2001) and apoptosis (Hamada et al., 1999; Han et al., 2000; Jehn et al., 1999; MacKenzie et al., 2004b; Miele and Osborne, 1999; Nair et al., 2003; Rangarajan et al., 2001a; Shelly et al., 1999), as well as three processes directly addressed in this thesis: cell adhesion, blood vessel development, and epithelial-to-mesenchymal transition (EMT).

1.1.2 The Notch receptor and ligand families

1.1.2.1 Notch receptors

Notch is synthesized in the endoplasmic reticulum as a full-length unprocessed protein composed of extracellular, transmembrane, and intracellular domains (Blaumueller et al., 1997). Following transport through the secretory pathway to the trans-golgi network, Notch is cleaved within intracellular vesicles by a furin-like convertase (Logeat et al., 1998) at a site referred to as the S1 cleavage site approximately 70 amino acids N-terminal to the transmembrane domain (Blaumueller et al., 1997; Logeat et al., 1998). Two subunits are thus generated: one consisting of the majority of the extracellular domain and the other consisting of the remainder of the extracellular domain and the complete transmembrane and intracellular domains. These two subunits associate noncovalently via a calcium (Ca^{2+})-coordinated bond (Rand et al., 2000), resulting in the cell-surface expression of a mature heterodimeric Type I transmembrane receptor with an amino (N)-terminal extracellular domain and a carboxy (C)-terminal intracellular domain (Blaumueller et al., 1997) (Figure 1.1).

Notch proteins contain several structural motifs critical to receptor function (Figure 1.1). Epidermal growth factor (EGF)-like repeats are cysteine-rich consensus sequences found in members of the EGF family as well as other growth factor and receptor molecules (Wharton et al., 1985). Within the Notch extracellular domain, numerous EGF-like repeats have been

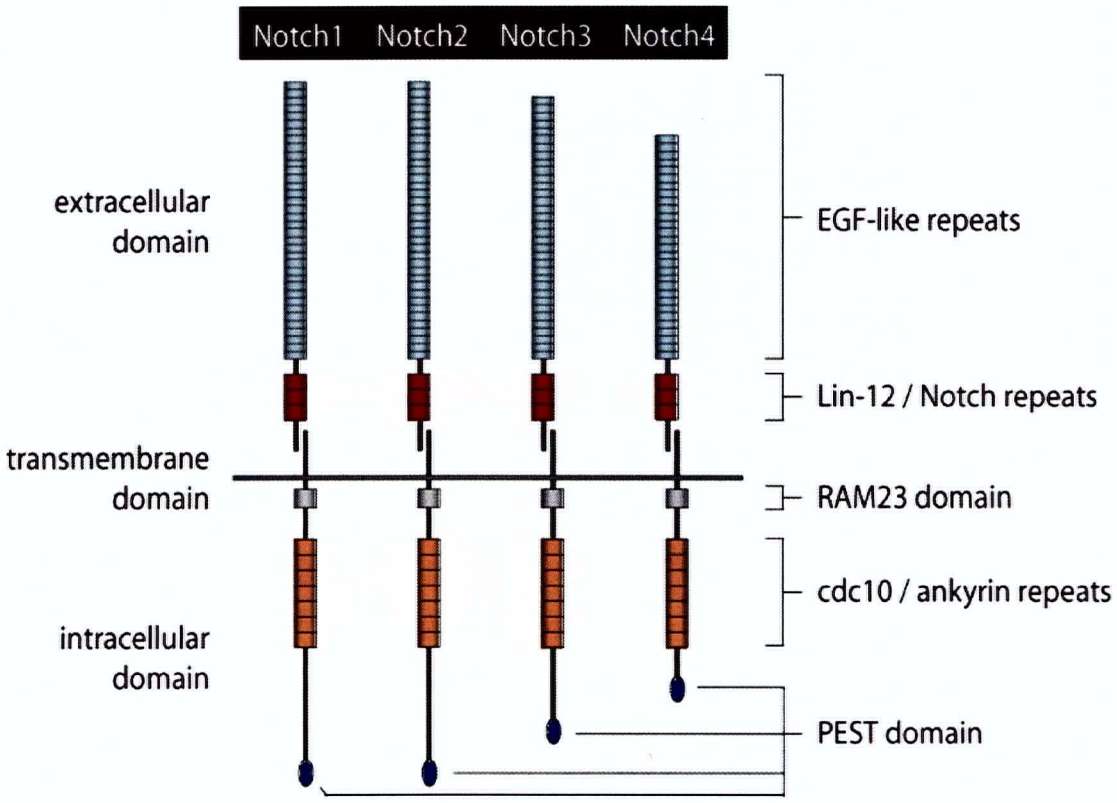

Figure 1.1: The mammalian Notch receptor family. The mammalian Notch receptor family consists of four members: Notch1 through Notch4. Following synthesis in the endoplasmic reticulum, full-length unprocessed Notch proteins are transported to the trans-golgi network where they are cleaved by a furin-like convertase (referred to as S1 cleavage), thus generating two subunits. These two subunits associate non-covalently, giving rise to a mature heterodimeric transmembrane receptor expressed on the cell surface. Notch proteins contain several conserved structural motifs. The extracellular domain contains a variable number of EGF-like repeats involved in ligand binding, and three Lin-12/Notch repeats involved in Notch heterodimerization. The intracellular domain contains a RAM23 domain involved in binding Notch downstream signaling proteins, seven cdc10/ankyrin repeats required for mediating downstream signaling, and a PEST domain involved in Notch protein degradation.

identified and are involved in mediating ligand binding (Rebay et al., 1991). Also located within the Notch extracellular domain are three tandem copies of a Lin-12/Notch repeat essential for the formation of a stable, mature Notch heterodimer (Rand et al., 2000). Within the intracellular domain, Notch proteins contain a recombination signal binding protein Jκ (RBPJκ)-associated module-23 (RAM23) domain involved in binding Notch downstream signaling proteins (Hsieh et al., 1996; Roehl et al., 1996; Tamura et al., 1995). Also involved in mediating downstream signaling are seven tandem copies of a cdc10/ankyrin repeat (Lubman et al., 2004). Flanking the cdc10/ankyrin repeats are three potential nuclear localization signals (Mumm and Kopan, 2000). C-terminal to the cdc10/ankyrin repeats is a putative transactivation domain (TAD) involved in transcriptional activation of downstream Notch target genes (Mumm and Kopan, 2000), followed by a proline-glutamine-serine-threonine (PEST) domain that plays a role in Notch protein degradation (Rogers et al., 1986).

The mammalian family of Notch receptors consists of four members: Notch1-4 (Ellisen et al., 1991; Lardelli et al., 1994; Uyttendaele et al., 1996; Weinmaster et al., 1992) (Figure 1.1). Research presented in this thesis primarily focuses on Notch4 and the potential functional consequences of altered Notch4 signaling. Based upon evolutionary analysis, Notch4 is the most divergent gene in the Notch family (Kortschak et al., 2001). The Notch4 amino acid sequence is 60% similar and 43% identical to the other vertebrate Notch proteins (Uyttendaele et al., 1996). Indeed, Notch4 protein exhibits key structural differences from other Notch family members. Notch4 contains the fewest number of EGF-like repeats in its extracellular domain. Notch4 contains 29 EGF-like repeats, whereas Notch1 and Notch2 both have 36 and Notch3 has 34 (Uyttendaele et al., 1996). The Notch4 intracellular domain is the shortest amongst the mammalian Notch family members (Uyttendaele et al., 1996). Within the intracellular domain,

the PEST domain of Notch4 is significantly shorter than that of the other Notch proteins (Uyttendaele et al., 1996). In addition to structural differences, Notch4 exhibits a relatively restricted expression pattern in normal cells compared to the other Notch proteins. Specifically, Notch4 is primarily expressed on endothelial and endocardial cells (Li et al., 1998a; Shirayoshi et al., 1997; Uyttendaele et al., 1996), although there is recent evidence of Notch4 messenger ribonucleic acid (mRNA) (Vercauteren and Sutherland, 2004) and protein (Dontu et al., 2004) expression in other cell types.

1.1.2.2 Notch ligands

The Notch ligand family consists of five members in mammals: Jagged1/2 and Delta-like (Dll)1/3/4 (Bettenhausen et al., 1995; Dunwoodie et al., 1997; Lindsell et al., 1995; Rao et al., 2000; Shawber et al., 1996) (Figure 1.2). Similar to Notch receptors, Notch ligands are Type I transmembrane proteins (Mumm and Kopan, 2000). Within the extracellular domain, Notch ligands belonging to the Jagged subfamily contain a cysteine-rich region likely involved in the control of Notch receptor binding specificity, as well as a von Willebrand factor (vWF) Type C domain likely involved in ligand oligomerization (Fleming, 1998; Lissemore and Starmer, 1999). Ligands of the Dll subfamily, in contrast, do not contain these motifs (Fleming, 1998). Also located in the extracellular domain of all Notch ligands is a single Delta/Serrate/Lag-2 (DSL) domain which functions as a receptor binding site (Lissemore and Starmer, 1999; Tax et al., 1994), as well as a variable number of EGF-like repeats that may stabilize receptor binding (Lieber et al., 1992). Specifically, Jagged1 and Jagged2 both have 16 EGF-like repeats, Dll1 and Dll4 have eight, and Dll3 has six (Fleming, 1998; Lissemore and Starmer, 1999). The intracellular domain of Notch ligands is required for normal ligand-mediated Notch signaling (Sun and Artavanis-Tsakonas, 1996). Although Notch ligand intracellular domains exhibit

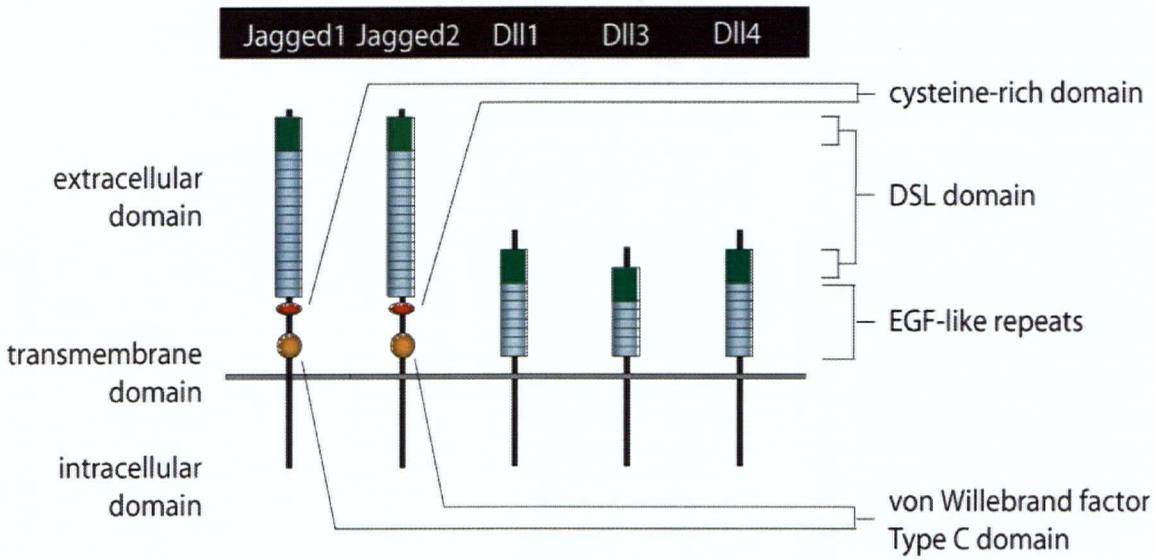

Figure 1.2: The mammalian Notch ligand family. The mammalian Notch ligand family consists of five members: Jagged1/2 and Dll1/3/4. Within the extracellular domain, Jagged family members contain a cysteine-rich region likely involved in the control of Notch receptor binding specificity, as well as a vWF Type C domain likely involved in ligand dimerization. These motifs are not present in Dll family members. Extracellular motifs common to all Notch ligands include a single DSL domain involved in receptor binding, as well as a variable number of EGF-like repeats that may stabilize receptor binding.

relatively few structural motifs (Hock et al., 1998), several reports have highlighted the possibility of nuclear signaling mediated by the ligand intracellular domain (LaVoie and Selkoe, 2003; Sun and Artavanis-Tsakonas, 1996). The Jagged1 intracellular domain contains a PSD-95/Dlg/zonula occludens-1 (ZO-1) (PDZ) domain which mediates intracellular signaling in Jagged1-expressing cells (Ascano et al., 2003). Moreover, this PDZ domain has been shown to be required for Jagged1-induced cellular transformation (Ascano et al., 2003).

1.1.3 Notch receptor activation

1.1.3.1 Ligand-mediated Notch activation

Notch expressed on the cell surface as a heterodimer is the mature, ligand-accessible form of the receptor (Blaumueller et al., 1997). Uncleaved full-length Notch receptors, however, have been reported to be found at the cell surface (Bush et al., 2001; Sakamoto et al., 2002). As well, Notch that has been cleaved within the EGF-like repeat domain and Notch receptors lacking C-terminal sequences have been found at the plasma membrane (Wesley and Mok, 2003; Wesley and Saez, 2000a; Wesley and Saez, 2000b). The functional significance of these alternate Notch receptor forms has not been reported.

In the absence of ligand binding, heterodimeric Notch receptors are inactive (Lindsell et al., 1995; Rebay et al., 1993). The extracellular domain of Notch contains a motif located between the Lin-12/Notch repeats and the transmembrane domain, termed the negative control region, that functions to repress spontaneous Notch signaling (Greenwald, 1994; Kimble et al., 1998; Lieber et al., 1993). Also located within the extracellular domain of Notch receptors are EGF-like repeats 11 and 12, which are both necessary and sufficient to bind Notch ligand (Rebay et al., 1991). Notch ligand binding to Notch receptor on an adjacent cell induces a stress-

based conformational change in the Notch extracellular domain, resulting in the exposure of a proteolytic cleavage site within the Notch extracellular domain referred to as the S2 cleavage site (Mumm et al., 2000; Parks et al., 2000) (Figure 1.3). Following cleavage by the metalloprotease tumor necrosis factor α (TNFα) converting enzyme (TACE) (also known as a disintegrin and metalloprotease 17, ADAM17) (Brou et al., 2000), the newly released Notch extracellular domain is transendocytosed into the ligand-expressing cell (Parks et al., 2000). This process has been identified in both Drosophila and zebrafish and may be mediated by dynamin, a GTPase involved in the generation of clathrin-coated endocytic vesicles that is required for Notch signaling (Le Borgne and Schweisguth, 2003; Seugnet et al., 1997). As a result of transendocytosis, the negative control region of the Notch receptor is removed and thus Notch receptor activation can occur (Mumm and Kopan, 2000).

Following proteolysis at the S2 cleavage site, Notch receptors undergo regulated intramembranous proteolysis (RIP) at a conserved S3 cleavage site located within the transmembrane domain (Saxena et al., 2001). Hence transmembrane-bound Notch is no longer tethered to the cell membrane and the Notch intracellular domain (NotchIC) is released into the cytoplasm, which subsequently translocates into the nucleus to effect Notch signaling (Mumm and Kopan, 2000). S3 cleavage is mediated by a protease that possesses γ-secretase activity (Mumm and Kopan, 2000). Presenilin, a multipass transmembrane protein required for RIP (Wolfe et al., 1999a; Wolfe et al., 1999b), is essential for γ-secretase activity during S3 cleavage of Notch (Mizutani et al., 2001) and has been shown to complex with Notch at the cell membrane (Ray et al., 1999a; Ray et al., 1999b). Because a functional γ-secretase requires a complex of four proteins consisting of presenilin, nicastrin, Pen-2, and Aph-1 (Edbauer et al., 2003), whether presenilin itself is the γ-secretase or not remains to be determined.

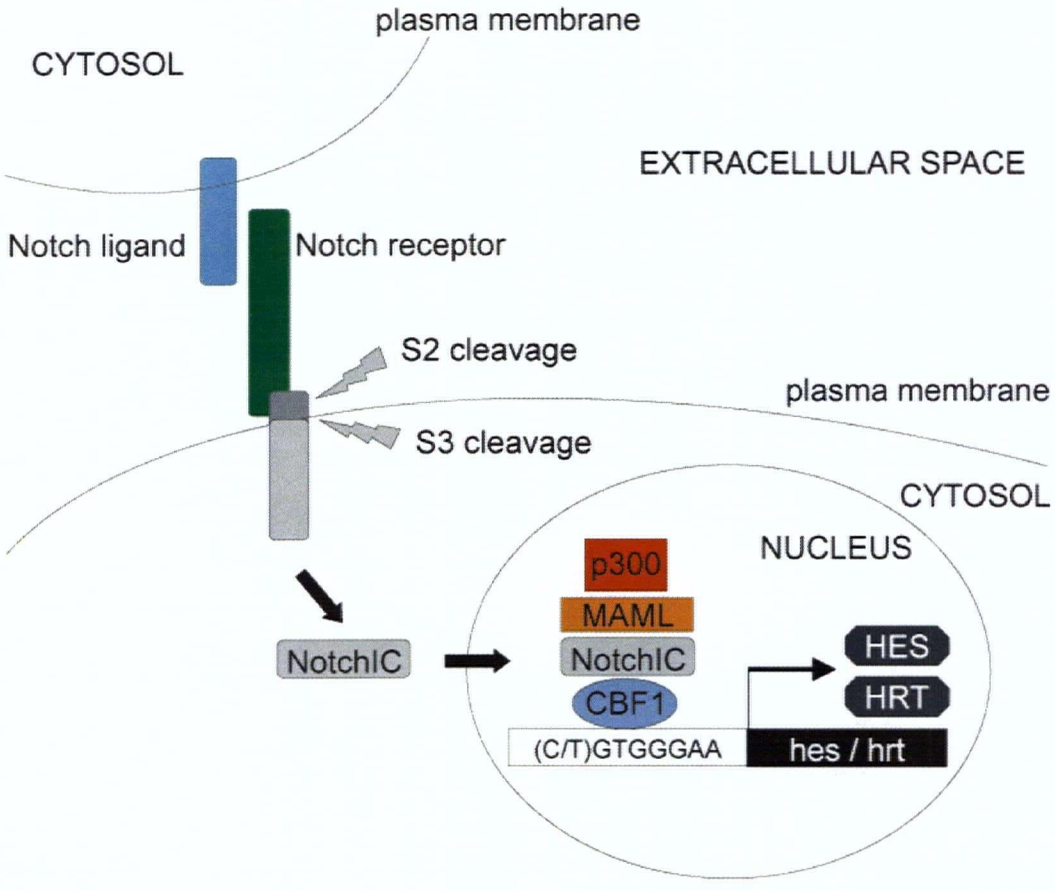

Figure 1.3: Ligand-mediated activation of Notch signaling. Notch expressed on the cell surface as a heterodimer is the mature, ligand-accessible form of the receptor. In the absence of ligand binding, heterodimeric Notch receptors are inactive. When Notch ligand binds to Notch receptor on an adjacent cell, a series of proteolytic cleavages occur (referred to as S2 and S3 cleavages), resulting in release of NotchIC that subsequently translocates into the nucleus. In the absence of nuclear NotchIC, the transcription factor CBF1 binds to the DNA sequence 5'-(C/T)GTGGGAA-3' within Notch target gene promoters and represses transcription. When Notch signaling is activated, nuclear NotchIC binds to CBF1 and, following recruitment of the nuclear protein Maml, results in the formation of a ternary complex that functions as a transcriptional activator. Maml recruits the histone acetyltransferase protein p300, resulting in histone acetylation and conversion of the local chromatin structure to a form amenable to active transcription. Hence transcription of Notch target genes belonging to the HES and HRT families occurs.

1.1.3.2 Constitutive Notch activation

Although Notch proteolytic processing at the S1 cleavage site does not result in Notch activation, processing at both S2 and S3 cleavage sites results in activation of the receptor (Mumm and Kopan, 2000). Translocation of endogenous NotchIC to the nucleus is required for activation of Notch downstream signaling (Mumm and Kopan, 2000). In normal cells, detection of nuclear NotchIC by current biochemical and immunocytochemical techniques has proven extremely difficult as low levels are sufficient to produce a functional response (Rand et al., 2000; Schroeter et al., 1998). To circumvent this limitation, studies involving overexpression of exogenous NotchIC at easily detectable levels have been performed (Capobianco et al., 1997; Iso et al., 2001a). Furthermore, spontaneous processing of the Notch receptor can be achieved by expressing truncated Notch consisting of the intracellular and transmembrane domains without most or all of the extracellular domain (Greenwald, 1994; Mizutani et al., 2001). Such truncated Notch proteins, similar to NotchIC, do not require ligand binding for activation and hence function as constitutively active receptors. Much of our current understanding of Notch signaling has derived from studies utilizing exogenous NotchIC.

1.1.4 Notch signaling

1.1.4.1 CBF1-mediated transcriptional repression

Notch signaling involves the transcriptional activation of downstream target genes by nuclear NotchIC (Mumm and Kopan, 2000) (Figure 1.3). In the absence of nuclear NotchIC, target gene expression is repressed by the transcriptional repressor protein C protein binding factor 1 (CBF1; also known as RBPJκ and KBF2) (Dou et al., 1994; Hsieh and Hayward, 1995). CBF1 is a constitutively expressed transcription factor that binds as a monomer to the

deoxyribonucleic acid (DNA) consensus sequence 5'-(C/T)GTGGGAA-3' within Notch target gene promoters (Brou et al., 1994; Hamaguchi et al., 1992; Ling et al., 1994; Tun et al., 1994). Although the DNA binding domain of CBF1 has been mapped to the central third of the protein (Hsieh and Hayward, 1995; Tang and Kadesch, 2001), CBF1 does not contain a known DNA binding motif (Brou et al., 1994; Tun et al., 1994).

Transcriptional repression by CBF1 is mediated via two distinct mechanisms. The first mechanism involves direct disruption of activated transcription (Olave et al., 1998). Transcription factor IID (TFIID) and transcription factor IIA (TFIIA) are two members of the basal transcription machinery that interact with each other to mediate transcriptional activation (Gill, 2001). CBF1 has been shown to interact with a subunit of TFIID involved in the binding of TFIIA, thus destabilizing their interaction and effectively inhibiting transcription (Olave et al., 1998). The second mechanism of CBF1-mediated transcriptional repression involves the recruitment of corepressor proteins (Hsieh et al., 1999). The corepressor protein KyoT2 has been shown to compete with NotchIC for binding to CBF1 (Taniguchi et al., 1998). CBF1 can also bind to at least two corepressor complexes, whose individual components cooperate to inhibit transcriptional activation (Mumm and Kopan, 2000). Although the exact protein composition of these complexes is not known, several members have been identified. In one such complex, corepressor proteins include CBF1-interacting corepressor (CIR), histone deacetylase (HDAC)-2, and SAP30 (Hsieh et al., 1999; Zhou et al., 2000b). Another more well-defined corepressor complex is composed of silencing mediator of retinoid and thyroid hormone receptor (SMRT), NcoR, HDAC-1, SHARP, and Ski interacting protein (SKIP) (Kao et al., 1998; Oswald et al., 2002; Zhou et al., 2000a; Zhou et al., 2000b). When Notch is not activated, CBF1 directly interacts with SMRT, HDAC-1, SHARP, and SKIP resulting in transcriptional repression (Kao

et al., 1998; Oswald et al., 2002; Zhou et al., 2000a; Zhou et al., 2000b). SKIP may function as an adapter protein during Notch signal activation by mediating the interaction between CBF1 and nuclear NotchIC (Zhou et al., 2000a; Zhou et al., 2000b).

1.1.4.2 Notch-mediated CBF1 transcriptional activation

When Notch signaling is activated, nuclear NotchIC binds to CBF1 and converts CBF1 from a transcriptional repressor to an activator (Mumm and Kopan, 2000; Saxena et al., 2001) (Figure 1.3). Two distinct domains of NotchIC have been shown to interact with CBF1. These include the RAM23 domain of NotchIC which binds to the central third of CBF1, and the cdc10/ankyrin repeat domain of NotchIC which binds to both the N- and C-terminal regions of CBF1 (Hsieh and Hayward, 1995; Tani et al., 2001). NotchIC binding to CBF1 serves two functions: (i) to antagonize the interaction between CBF1 and corepressor proteins and hence alleviate transcriptional repression, and (ii) to recruit coactivator proteins that promote transcriptional activation (Bray and Furriols, 2001).

A model for NotchIC-mediated conversion of CBF1 from a transcriptional repressor to an activator has been proposed (Mumm and Kopan, 2000). In addition to binding CBF1, SKIP can also bind to either SMRT or NotchIC in a mutually exclusive manner (Zhou et al., 2000a; Zhou et al., 2000b). Because SKIP has a higher affinity for NotchIC than SMRT, when NotchIC is present, SKIP-CBF1-SMRT complexes are converted to SKIP-CBF1-NotchIC complexes (Mumm and Kopan, 2000). Furthermore, CBF1 binding to SHARP or NotchIC may be mutually exclusive (Oswald et al., 2002). NotchIC could therefore convert CBF1-SHARP complexes to CBF1-NotchIC complexes (Oswald et al., 2002). Hence nuclear NotchIC displaces corepressor complexes from CBF1.

Although NotchIC contains a transactivation domain, NotchIC itself cannot promote gene transcription (Fryer et al., 2002). Instead, NotchIC must recruit transcriptional coactivators. Histone acetyltransferases (HATs) are enzymes that acetylate histones thereby altering the structure of chromatin to a form amenable to active transcription (Peterson and Laniel, 2004). Several studies have reported a direct interaction between NotchIC and HATs (Kurooka and Honjo, 2000; Oswald et al., 2001). However, others have been unable to detect a direct interaction (Fryer et al., 2002). Mastermind-like (Maml), a nuclear protein that functions as a transcriptional activator, has been shown to be required for Notch signaling (Fryer et al., 2002; Petcherski and Kimble, 2000). Three Maml proteins are expressed in mammals: Maml1/2/3 (Kitagawa et al., 2001; Lin et al., 2002; Wu et al., 2000; Wu et al., 2002). The fact that the three Maml isoforms do not exhibit overlapping expression patterns suggests against functional redundancy (Wu et al., 2002). Maml forms a ternary complex with CBF1-NotchIC via a direct interaction with NotchIC (Wu and Griffin, 2004). Specifically, Maml contains an N-terminal basic domain that binds to the fourth cdc10/ankyrin repeat of NotchIC (Petcherski and Kimble, 2000; Wu and Griffin, 2004). Maml contains two proposed TAD domains: TAD1 within the central region of the protein and TAD2 at the C-terminus (Wu and Griffin, 2004). TAD1 contains a binding site for the HAT protein p300/CBP (Wu and Griffin, 2004). Hence the ternary complex composed of CBF1-NotchIC-Maml functions as a transcriptional activator, resulting in Notch target gene transcription (Mumm and Kopan, 2000).

1.1.4.3 Notch target genes

Numerous genes have been identified as targets of the Notch signaling pathway. Among the primary targets are several genes belonging to the basic helix-loop-helix (bHLH) family of proteins (Iso et al., 2003). These proteins contain two common structural features: a basic

domain and an HLH domain (Murre et al., 1994). The basic domain mediates DNA binding specificity (Murre et al., 1994). The HLH domain serves two functions: (i) it contains hydrophobic residues that facilitate the formation of protein dimers (Murre et al., 1994) and (ii) it positions the basic domains of the dimer to allow for proper DNA binding (Blackwell and Weintraub, 1990; Ma et al., 1994). Hence bHLH proteins bind specific DNA sequences as dimers and modulate gene transcription (Murre et al., 1994). In mammals, members of two families of bHLH proteins contain CBF1 binding sites in their promoters and thus are induced following Notch activation: (i) the hairy/enhancer-of-split (HES) family and (ii) the hairy-related transcription factor (HRT) family (Iso et al., 2003). Both the HES and HRT families function as transcriptional repressors (Iso et al., 2003).

Seven mammalian HES family members have been identified to date (Akazawa et al., 1992; Bae et al., 2000; Bessho et al., 2001; Hirata et al., 2000; Ishibashi et al., 1993; Koyano-Nakagawa et al., 2000; Pissarra et al., 2000; Sasai et al., 1992). However, only four are potential Notch target genes: HES1, HES4, HES5, and HES7 (Iso et al., 2003; MacKenzie et al., 2004a). HES family members repress transcription by three proposed mechanisms. One mechanism involves active repression. Specifically, HES proteins form homodimers and bind to specific DNA consensus sites, with subsequent recruitment of transducin-like enhancer-of-split (TLE) proteins (Kageyama et al., 2000; Paroush et al., 1994). Direct interaction between HES and TLE proteins is mediated by a conserved C-terminal tryptophan-arginine-proline-tryptophan (WRPW) tetrapeptide motif of HES and a C-terminal tryptophan-aspartic acid-arginine (WDR) domain of TLE (Fisher et al., 1996; Grbavec and Stifani, 1996; Jimenez et al., 1997). TLE in turn, via a conserved glycine/proline-rich domain, recruits HDACs (Chen et al., 1999). HES has also been shown to directly bind to the HDAC protein sirtuin-1 (SIRT-1) (Takata and Ishikawa, 2003). As

a result of histone deacetylation by HDACs, the local chromatin structure is altered to a form that opposes gene transcription (Iso et al., 2003). A second mechanism of transcriptional repression by HES involves passive repression. HES can dimerize with bHLH proteins that normally function to activate transcription, thus effectively sequestering them in a non-functional heterodimer complex (Hirata et al., 2000; Sasai et al., 1992). A third mechanism for HES-mediated transcriptional repression involves a repression domain of HES located C-terminal to the bHLH domain, termed the Orange domain (Dawson et al., 1995). Although the mechanism of transcriptional repression mediated by the Orange domain has not been well eludicated, this domain has been shown to be involved in the repression of specific transcriptional activators (Dawson et al., 1995) and may be essential for the repression of several Notch target genes (Castella et al., 2000).

HRT proteins comprise a second family of bHLH proteins induced in response to Notch activation. Also known as hairy/enhancer-of-split-related (HESR), hairy/enhancer-of-split-related with tyrosine-arginine-proline-tryptophan (YRPW) (HEY), HES-related repressor protein (HERP), cardiovascular HLH factor (CHF), and gridlock, the HRT family consists of three members in mammals: (i) HRT1/HESR1/HEY1/HERP2/CHF2; (ii) HRT2/HESR2/HEY2/HERP1/CHF1/gridlock; and (iii) HRT3/HESR3/HEY-like(HEYL)/HERP3 (Iso et al., 2003). Because all three HRT genes exhibit unique and dynamic expression patterns, HRT proteins may not be functionally redundant (Steidl et al., 2000). However, the fact that all three HRT proteins contain nearly identical basic domains raises the possibility that common DNA consensus sequences may be targeted (Nakagawa et al., 1999). Similar to HES proteins, HRT proteins function as transcriptional repressors (Iso et al., 2003). Two mechanisms of HRT-mediated transcriptional repression have been proposed. The first mechanism involves active

repression. HES-mediated active repression utilizes the C-terminal WRPW tetrapeptide motif (Fisher et al., 1996; Grbavec and Stifani, 1996). In contrast, HRT-mediated repression activity does not require a C-terminal tetrapeptide motif, despite the fact that in humans both HRT1 and HRT2 have a C-terminal YRPW motif and HRT3 has a tyrosine-histidine-serine-tryptophan (YHSW) variant motif (Iso et al., 2001b). Hence TLE proteins likely do not participate in HRT-mediated active repression (Iso et al., 2001b). Instead, active repression activity resides primarily in the bHLH domain of HRT proteins (Iso et al., 2001b). HRT proteins have been shown to bind to the mSin3 complex, a corepressor complex composed of at least seven subunits (Iso et al., 2001b). This binding requires the bHLH domain of HRT proteins (Iso et al., 2001b). Among these subunits are mSin3A, a large protein that functions as a scaffold for the formation of the mSin3 complex, as well as the corepressor proteins SMRT, NcoR, HDAC-1, and HDAC-2 (Ayer, 1999; Knoepfler and Eisenman, 1999). Whereas HRT2 can directly interact with mSin3A and NcoR, association with HDACs is indirect (Iso et al., 2001b). HRTs can also repress gene expression via a second mechanism, passive repression. HRT2-mediated repression of vascular endothelial growth factor (VEGF) expression involves this mechanism (Chin et al., 2000). During hypoxia, the transcription factor aryl hydrocarbon receptor nuclear translocator (ARNT; also known as hypoxia inducible factor 1β, HIF1β (Wang et al., 1995)) binds as a heterodimer with HIF1α to the VEGF promoter to induce VEGF expression (Maltepe et al., 1997). HRT2 can directly interact with ARNT, resulting in dissociation of ARNT from DNA and thus inhibition of ARNT/HIF1α-dependent VEGF transcription (Chin et al., 2000).

HES and HRT proteins exhibit sequence similarities (Nakagawa et al., 1999), as well as structural similarities such as the presence of bHLH and Orange domains (Iso et al., 2003). Furthermore, both HES and HRT proteins function to repress gene transcription (Iso et al.,

2003). Despite these common features, several key differences are evident. HES and HRT proteins exhibit different C-terminal tetrapeptide motifs (Iso et al., 2001b). C-terminal to the tetrapeptide motif, HRT proteins contain an additional conserved motif threonine-glutamic acid-(valine/isoleucine)-glycine-alanine-phenylalanine (TE(V/I)GAF) that is not found in HES proteins (Iso et al., 2003). At a corresponding position within the basic domain, HES proteins have a proline residue whereas HRT proteins have a glycine residue (Iso et al., 2003). These respective residues are conserved from Drosophila to humans (Iso et al., 2003). These structural differences, together with the fact that HES and HRT proteins employ different mechanisms for transcriptional repression (Iso et al., 2003), suggest that HES and HRT proteins may regulate both common and different genes (Iso et al., 2001b). Indeed, HES1 binds DNA sequences such as the E box motif CACGTG (Nakagawa et al., 2000), N box motifs (CACNAG) (Takebayashi et al., 1994), class B sites (CANGTG) (Takebayashi et al., 1994), class C sites (CACGNG) (Kim and Siu, 1998), and a class C variant (CACGCA) (Chen et al., 1997a). HRT proteins, on the other hand, preferentially bind to E box motifs. Both HRT1 and HRT2 bind to the E box motif CACGTG (Nakagawa et al., 2000). Interestingly, HRT3 does not bind to the E box motif CACGTG, raising the possibility that HRT3 may function differently from the other HRT proteins (Nakagawa et al., 2000).

In order for DNA binding to occur, bHLH transcriptional repressors must dimerize (Vinson and Garcia, 1992). Cells that express only one of HES or HRT must therefore form homodimers to repress downstream genes (Chin et al., 2000; Kokubo et al., 1999; Leimeister et al., 2000a; Nakagawa et al., 1999; Sasai et al., 1992). In cells that express both HES and HRT proteins, however, heterodimer formation may occur. Studies have shown that HES and HRT proteins can heterodimerize in intact cells in vitro in the absence of DNA, and that repression

mediated by HES-HRT heterodimers is synergistic (Iso et al., 2001b; Leimeister et al., 2000a). Heterodimerization may therefore function as a strategy for the amplification of HES/HRT-mediated transcriptional repression.

Several genes repressed by Notch-induced bHLH proteins have been identified. The gene mammalian achaete-scute homologue-1 (mash1), which encodes for a protein that regulates neuronal differentiation (Casarosa et al., 1999; Cau et al., 1997), contains a class C variant site CACGCA in its promoter (Chen et al., 1997a). HES1 has been shown to directly bind to this site and repress mash1 gene expression (Chen et al., 1997a). Other target genes of HES1 include mammalian atonal homologue-1 (math1) (Akazawa et al., 1995; Ben-Arie et al., 1997; Zine and de Ribaupierre, 2002), neurogenin (Fode et al., 1998; Ma et al., 1998), CD4 (Kim and Siu, 1998), acid α-glucosidase (Yan et al., 2001), p21 (Castella et al., 2000), and hes1 itself (Takebayashi et al., 1994). In vivo target genes of HRT proteins, in contrast, have not been reported (Iso et al., 2003). Interestingly, in cells that express both HES and HRT proteins, the mash1 gene has been suggested to be a target of HES-HRT heterodimers (Iso et al., 2003; Iso et al., 2001b). Furthermore, in vitro experiments suggest that HRT2 may regulate its own expression (Nakagawa et al., 2000).

In addition to bHLH proteins belonging to the HES and HRT families, consensus CBF1 binding sites are found in many genes. The identification of target genes mediated through CBF1 but independent of HES and HRT illustrates the complexity of the Notch signaling pathway. Examples of such genes include p21 (Tun et al., 1994) (although p21 has been suggested to be a target gene of HES1 (Castella et al., 2000)), cyclin D1 (Ronchini and Capobianco, 2001), NFκB2 (Oswald et al., 1998), c-jun (Rangarajan et al., 2001b), major histocompatibility complex (MHC) class I (Israel et al., 1989; Shirakata et al., 1996), CD23 (Ling et al., 1994), β-globin (Lam and

Bresnick, 1998), and erbB2 (Chen et al., 1997b). Adding to the complexity is the identification of Notch signaling pathways independent of CBF1 (Mumm and Kopan, 2000). Moreover, a growing number of modulators of Notch signaling have been described, including Fringe, Deltex, Notchless, and Numb (Haines and Irvine, 2003; Kadesch, 2000).

1.2 THE NOTCH PATHWAY AND DISEASE PATHOGENESIS

1.2.1 Notch ligand-associated diseases

Aberrant expression of Notch ligands can result in disease phenotypes. Jagged1 mutations have been linked to the development of Alagille syndrome, an autosomal dominant disorder characterized by pleiotropic developmental defects that affect numerous organs including the heart, kidney, liver, eye, face, and skeleton (Li et al., 1997; Oda et al., 1997). Clinical features normally manifest within the first two years of age, with a mortality rate of 15-20% (Emerick et al., 1999). Approximately 70% of patients with Alagille syndrome exhibit mutations in Jagged1 (Spinner et al., 2001), with 3-7% of patients exhibiting a complete deletion of the Jagged1 gene (Krantz et al., 1997). Among patients with mutated Jagged1, 83% exhibit nonsense or splice-site mutations that result in the expression of a truncated Jagged1 protein (Ropke et al., 2003). The remaining 17% exhibit missense mutations that cluster around the extracellular domain of Jagged1, in sequences encoding the DSL domain and the first EGF-like repeat (Ropke et al., 2003). Another disease associated with Jagged1 mutations is Familial tetralogy of Fallot, the most common form of complex congenital heart disease (Gridley, 2003). Upregulation of Jagged1 protein expression has been observed in a growing number of human malignancies, including cancers of the cervix (Gray et al., 1999) and prostate (Santagata et al., 2004). Upregulation of Jagged1 mRNA expression has been reported in human pancreatic cancer

(Miyamoto et al., 2003). Jagged2 protein overexpression has also been observed in human malignancies, including pancreatic cancer (Miyamoto et al., 2003) and multiple myeloma (Houde et al., 2004).

Mutations in Dll3 have been identified as a causal factor in the development of spondylocostal dysostosis, a family of related diseases that affects the development of the vertebrae (Bulman et al., 2000). In the autosomal recessive form of this disease, 17 different mutations in Dll3 have been identified (Turnpenny et al., 2003). Structural consequences of these mutations include replacement of an essential amino acid, addition or deletion of cysteine residues within the EGF-like repeats, or truncation of the protein, and hence loss of Dll3 function (Turnpenny et al., 2003). Characteristics of this particular form of the disease include abnormal segmentation of the spine (Kusumi et al., 1998) and rib fusions (Bulman et al., 2000). Dll4 mRNA expression has been detected in the vasculature of human breast and kidney tumors (Mailhos et al., 2001).

1.2.2 Notch receptor-associated diseases

Numerous diseases have been linked to the deregulated expression of Notch receptors. In humans, aberrant Notch1 expression has been identified as a causative factor in the development of T-cell acute lymphoblastic leukemia (T-ALL) (Aster et al., 1994; Ellisen et al., 1991). Analysis of patient samples has revealed a chromosomal translocation, t(7:9)(q34;q34.3), that juxtaposes the C-terminal domain of Notch1 starting from within EGF-like repeat 34 next to the T-cell receptor β (TCRβ) locus (Ellisen et al., 1991). This results in the expression of a truncated constitutively active Notch1, commonly referred to as translocation-associated Notch1 (TAN1) (Ellisen et al., 1991). Subsequent experiments have shown that only those forms of Notch1 capable of activating a CBF1-dependent reporter can induce T-ALL (Aster et al., 2000). In

addition to chromosomal translocation, activating mutations in Notch1 have been identified in more than 50% of human T-ALLs (Weng et al., 2004).

Notch1 has been linked to the development and progression of cervical cancer in humans. In contrast to T-ALL, activation of Notch1 signaling in cervical cancer is primarily ligand-dependent (Rangarajan et al., 2001a). Whereas normal cervical tissues do not express Notch1 protein in differentiated cervical epithelial cells (Zagouras et al., 1995), cervical carcinomas spontaneously overexpress Notch1 (Daniel et al., 1997; Zagouras et al., 1995). Intense cytosolic and nuclear Notch1 staining can be consistently detected by immunohistochemistry (Daniel et al., 1997; Zagouras et al., 1995). Interestingly, in late stage cervical cancers, Notch1 protein expression is reduced (Talora et al., 2002). This downregulation of Notch1 has subsequently been shown to play a role in the maintenance of malignant transformation (Talora et al., 2002). A proposed model is that Notch1 expression in early-stage cervical cancer plays a tumor-promoting function whereas expression in late-stage cervical cancer is tumor-suppressive (Talora et al., 2002). Indeed, a tumor-suppressive function for Notch1 has been demonstrated in mouse skin (Nicolas et al., 2003). In addition to T-ALL and cervical cancer, deregulated Notch1 protein expression has been observed in human malignant melanoma (Nickoloff et al., 2003), as well as human cancers of the colon (Zagouras et al., 1995), lung (Zagouras et al., 1995), and pancreas (Miyamoto et al., 2003). Human breast cancers have been reported to express aberrant Notch1 mRNA (Callahan and Egan, 2004) and protein (Parr et al., 2004; Weijzen et al., 2002).

Similar to Notch1, upregulated Notch2 protein expression has been observed in human cervical cancer (Zagouras et al., 1995). However, in contrast to Notch1, downregulation of Notch2 is not required to maintain the malignancy of late-stage cervical cancers (Talora et al., 2002). Hence advanced cervical cancers display selective loss of Notch1 with retention of

Notch2. Other studies have identified expression of activated Notch2 protein in human malignant melanoma (Nickoloff et al., 2003), as well as Notch2 protein overexpression in human cancers of the colon (Zagouras et al., 1995), pancreas (Miyamoto et al., 2003), and breast (Parr et al., 2004). Overexpression of Notch2 mRNA has been reported in human brain (Fan et al., 2004) and breast (Callahan and Egan, 2004) cancer.

The human disease most closely related to deregulated Notch3 expression is cerebral autosomal dominant arteriopathy with subcortical infarcts and leukoencephalopathy (CADASIL) (Joutel et al., 2000; Joutel et al., 1996). CADASIL is an adult onset disease with a mean clinical presentation at 45 years of age (Chabriat et al., 1995). Typically, mortality occurs approximately 15-20 years post clinical diagnosis (Chabriat et al., 1995). Symptoms include mood disorder, migraine, stroke, and progressive dementia (Chabriat et al., 1995). A common characteristic of this disease is cerebrovascular fragility (Joutel et al., 1996), which results from the loss of vascular smooth muscle cells (VSMC) that surround small cerebral arteries (Jung et al., 1995; Ragno et al., 1995; Tournier-Lasserve et al., 1993). In addition to providing structural support to blood vessels, VSMCs also play a role in the release of VEGF (Ruchoux et al., 2002). Hence VSMC loss results in reduced blood flow to the brain (Bruening et al., 2001). The cause of this disease has been attributed to mutations in Notch3. To date, more than 70 mutations in human Notch3 associated with CADASIL have been described (Hansson et al., 2004). These mutations which can be either missense or splice-site mutations (Joutel et al., 1997), occur exclusively within EGF-like repeats in the Notch3 extracellular domain (Hansson et al., 2004), and always involve either the addition or deletion of a cysteine residue (Joutel et al., 1997). EGF-like repeats normally contain six cysteine residues that participate in the formation of three disulfide bonds per repeat (Joutel et al., 1997). Mutated Notch3, in contrast, contains an odd number of cysteine

residues which inhibits normal disulfide bond formation (Joutel et al., 1997). Potential consequences include conformational changes in Notch3 protein, abnormal receptor proteolytic processing and oligomerization, as well as alterations in ligand binding, post-translational modifications, cell trafficking, and membrane clearance (Joutel et al., 2000; Joutel et al., 1997; Karlstrom et al., 2002). Accumulation of an extracellular Notch3 protein fragment has been detected within the brain vasculature of CADASIL patients (Joutel et al., 2000). Indeed, detection of this fragment within the skin vasculature is commonly used as a diagnosis for CADASIL (Joutel et al., 2001). Additional disease-related alterations in Notch3 include protein overexpression in human malignant melanoma (Nickoloff et al., 2003) and human pancreatic cancer (Miyamoto et al., 2003). Notch3 mRNA expression has been reported in human breast cancer (Callahan and Egan, 2004). Interestingly, Notch3 mRNA was found to be highly expressed in the vasculature of breast tumors, suggesting a role for Notch3 in breast tumor angiogenesis (Callahan and Egan, 2004).

A role for Notch4 in the development of schizophrenia has been suggested (Imai et al., 2001). Recent studies, however, have failed to identify such a relationship (Glatt et al., 2005). Human malignant melanomas (Nickoloff et al., 2003) and pancreatic tumors (Miyamoto et al., 2003) have been shown to overexpress Notch4 protein. A recent report has identified Notch4 mRNA expression in human breast cancer (Callahan and Egan, 2004). A causal role for Notch4 activation in breast cancer development, however, has only been demonstrated in mice.

1.2.2.1 Notch and murine breast cancer

A role for Notch signaling in murine mammary gland tumorigenesis is well recognized. The first study to identify this relationship came from observations of Czech II mice infected with Mouse Mammary Tumor Virus (MMTV) (Gallahan et al., 1987; Jhappan et al., 1992). The

MMTV proviral genome contains enhancer sequences within its long terminal repeats (LTRs), and hence acts as an insertional mutagen by integrating into the genome of infected mammary epithelial cells to cause deregulated expression of adjacent genes (Nusse, 1988). For this reason, genes targeted for MMTV integration are referred to as "int" genes (Nusse, 1988). Czech II mice infected with MMTV develop mammary tumors (Gallahan et al., 1987; Jhappan et al., 1992). Among the mammary tumors that develop, 18% (9 of 45 tumors) exhibit MMTV integration into the gene int3, which coincides with the Notch4 gene locus (Gallahan et al., 1987). Of the tumors displaying MMTV integration into Notch4, 100% (9 of 9 tumors) exhibit integration within the region of Notch4 between the Lin-12/Notch repeats and the transmembrane domain (Gallahan et al., 1987). Hence int3 protein represents a truncated Notch4 protein consisting primarily of a constitutively-active form encoding the transmembrane and intracellular domains (Jhappan et al., 1992). Intracisternal A particles (IAPs) are murine retroviruses which, similar to MMTV, act as insertional mutagens to deregulate gene expression (Christy and Huang, 1988). IAP integration into the Notch4 locus, resulting in the expression of constitutively active Notch4, has been observed in spontaneous mammary tumors in both Czech II (Kordon et al., 1995) and Balb/c mouse strains (Lee et al., 1999). These studies clearly link aberrant Notch4 signaling to murine mammary gland tumorigenesis.

To directly demonstrate that activated Notch4 signaling is oncogenic in the murine mammary gland, transgenic mouse studies have been performed. In wildtype mice, virgin mammary glands consist of a fat pad containing highly organized branching tubules that, during pregnancy, develop secretory lobules responsible for milk production (Daniel and Smith, 1999). Transgenic mice expressing activated Notch4 under the control of the MMTV LTR exhibit impaired mammary gland development and function. In virgin glands of activated Notch4

transgenic mice, the mammary epithelium fails to penetrate the mammary fat pad and therefore does not branch into an organized tree-like structure (Jhappan et al., 1992; Smith et al., 1995). During pregnancy, hormonal changes induce complete development of the ductal system in activated Notch4 transgenic mouse mammary glands; however, secretory lobules do not develop and hence lactation is disrupted (Jhappan et al., 1992). Importantly, these transgenic mice develop mammary carcinomas with 100% penetrance and subsequent metastasis to the lungs (Jhappan et al., 1992; Smith et al., 1995). Transgenic mice expressing activated Notch4 under the control of the whey acidic protein (WAP) promoter have also been studied. Because activity of the WAP promoter is restricted to the secretory mammary epithelium (Burdon et al., 1991), virgin glands of these animals develop normally (Gallahan et al., 1996). The mammary gland at pregnancy, however, exhibits disrupted secretory lobule development and lactation (Gallahan et al., 1996). Similar to MMTV LTR transgenic mice, WAP-Notch4 mice develop mammary carcinomas with 100% penetrance (Gallahan et al., 1996) as well as metastatic lung lesions (Gallahan et al., 1996). A role for Notch1 in murine mammary tumorigenesis has also been reported. c-ErbB2 transgenic mice infected with MMTV develop mammary tumors, some of which exhibit MMTV integration into the Notch1 gene and hence express constitutively activated Notch1 (Dievart et al., 1999). Moreover, expression of either activated Notch1 or activated Notch4 has been shown to induce transformation of mouse mammary epithelial cells in vitro (Dievart et al., 1999; Robbins et al., 1992; Soriano et al., 2000). Hence activated Notch signaling plays a causal role in murine mammary tumorigenesis.

1.2.2.2 Notch and human breast cancer

Several studies have highlighted a potential role for Notch signaling in human breast cancer development. Overexpression of constitutively active Notch4 in normal human breast

epithelial cells induces transformation in vitro (Imatani and Callahan, 2000). Among a panel of human breast cancer cell lines, seven of eight cell lines examined express elevated levels of a Notch4 RNA species corresponding to full-length Notch4 (Imatani and Callahan, 2000). Furthermore, two of these cell lines express an additional Notch4 RNA species encoding a truncated constitutively active Notch4 (Imatani and Callahan, 2000). In a study involving seven breast cancer specimens, Notch1 protein expression was detected in all tumors examined, with normal breast tissue at the margins of tumor sections exhibiting little or no Notch1 protein expression (Weijzen et al., 2002). In a second study involving 25 specimens, mRNAs for all four Notch receptors were expressed at varying frequencies (Callahan and Egan, 2004). A third study involving 97 specimens demonstrated that poorly-differentiated breast tumors were associated with elevated levels of Notch1 protein and reduced patient survival (Parr et al., 2004). Interestingly, well-differentiated breast tumors were associated with elevated levels of Notch2 protein and increased patient survival (Parr et al., 2004). Taken together, these studies suggest an oncogenic role for Notch1 and Notch4 and a tumor-suppressive role for Notch2 in human breast cancer development.

1.3 ANGIOGENESIS

Angiogenesis is a process through which new blood vessels are formed from preexisting vessels (Auerbach and Auerbach, 1994; Hanahan and Folkman, 1996; Risau, 1997). The human circulatory system is generally divided into (i) the macrovasculature, which consists of vessels with a diameter greater than 100 μm and includes arteries and veins, and (ii) the microvasculature, which includes small diameter vessels such as arterioles, capillaries, and venules (Junqueira et al., 1992). Capillaries and postcapillary venules are responsible for the exchange of gases, macromolecules, waste products, and cells between blood and tissue

(Junqueira et al., 1992). Angiogenesis, however, initiates exclusively from postcapillary venules (Carmeliet, 2000). Blood vessels of all calibers are lined by endothelial cells, which undergo extensive functional modulations during angiogenesis (Auerbach and Auerbach, 1994; Hanahan and Folkman, 1996; Risau, 1997).

1.3.1 Mechanism of angiogenesis

Three types of angiogenesis can occur during the growth and remodeling of the vascular network. Intussusception, also known as non-sprouting angiogenesis, involves the splitting of a preexisting vessel into two daughter vessels (Carmeliet, 2000). Initiation of intussusception requires proliferation of endothelial cells within the vessel wall, resulting in widening of the vessel lumen (Risau, 1997). Subsequent formation of transcapillary pillars which divide the lumen in half, followed by invagination of the surrounding periendothelial cells and basement membrane, results in the generation of two functional vessels (Carmeliet, 2000). Another type of angiogenesis is bridging angiogenesis, in which an existing vessel is divided by transendothelial cell bridges into individual vessels (Carmeliet, 2000). The most common form of angiogenesis, however, is sprouting angiogenesis which involves the sprouting of new vessels from preexisting vessels (Carmeliet, 2000).

The mechanism of sprouting angiogenesis has been well elucidated (Figure 1.4). Angiogenesis is controlled by a balance of activators and inhibitors (Hanahan and Folkman, 1996). When the concentration of activators exceeds that of inhibitors, angiogenesis is stimulated. In contrast, when inhibitors dominate over activators, angiogenesis is inhibited. Initiation of the angiogenic response occurs when an excess of angiogenic activators, produced by cells such as inflammatory cells, mast cells, or macrophages, diffuse into nearby tissues (Leek et al., 1994; Sunderkotter et al., 1994). These angiogenic factors bind to specific receptors on the

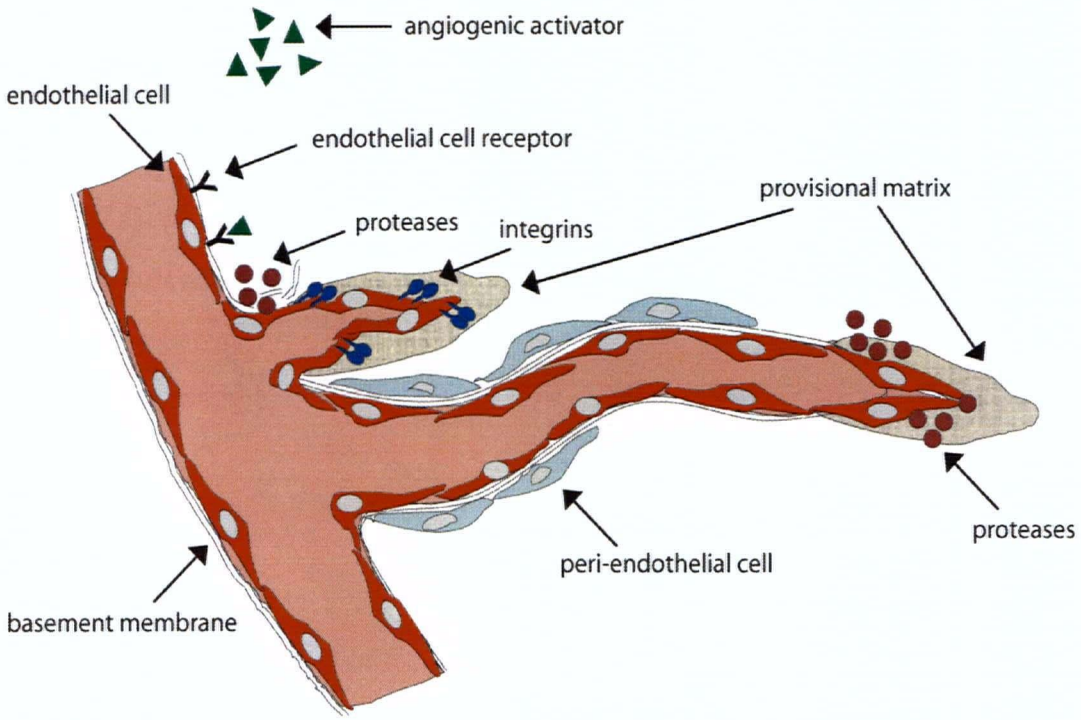

Figure 1.4: Mechanism of angiogenesis. Angiogenesis is controlled by a balance of activators and inhibitors. When the local concentration of activators exceeds that of inhibitors, angiogenesis is stimulated. Angiogenic activators bind to specific receptors on the surface of endothelial cells, resulting in endothelial cell activation. Activated endothelial cells produce proteases that degrade the local basement membrane, as well as nitric oxide that induces vascular permeability. As a result of increased permeability, plasma proteins extravasate from the vessel into the tissue space and form a provisional matrix on which activated endothelial cells migrate. Migration is facilitated by the upregulation of cell-ECM adhesion receptors belonging to the integrin family. Endothelial cells proximal to the migrating tip of the new sprout undergo proliferation, effectively increasing the length of the sprout. As the sprout lengthens, additional proteases are secreted which degrade the tissue at the leading edge of the sprout. Maturation of the new sprout occurs following the recruitment of peri-endothelial cells.

surface of endothelial cells lining preexisting blood vessels, resulting in endothelial cell activation (Brooks, 1996). Activated endothelial cells in turn produce proteinases such as those belonging to the plasminogen activator and matrix metalloprotease (MMP) families, which degrade the local basement membrane thus releasing additional angiogenic factors sequestered within the extracellular matrix (ECM) (Coussens et al., 1999). Activated endothelial cells also produce nitric oxide which induces vasodilation of the existing vessel and an increase in vascular permeability (Carmeliet, 2000). In response to increased permeability, plasma proteins extravasate from the vessel into the tissue space, thus laying down a provisional matrix that will be used by migrating endothelial cells (Carmeliet, 2000). The provisional matrix is primarily composed of fibrin (Dvorak et al., 1995) and fibronectin (Clark et al., 1982). In addition to the production of proteases and nitric oxide, activated endothelial cells undergo a shape change and extend elongated processes such as pseudopodia into the surrounding tissue (Dvorak et al., 1995; Pepper, 1997). Furthermore, these cells upregulate the expression of adhesion molecules such as those belonging to the integrin family, which function to pull the endothelial cell forward toward the angiogenic stimulus (Bazoni et al., 1999; Cockerill et al., 1995). Hence a rudimentary endothelial sprout migrating on the extravascular provisional matrix is formed. Endothelial cells located just proximal to the migrating tip of the sprout begin to proliferate, causing an increase in the length of the sprout (Auerbach and Auerbach, 1994; Hanahan and Folkman, 1996). As the sprout lengthens, additional proteases are produced which degrade tissue in front of the sprout (Stetler-Stevenson, 1999). Endothelial cells trailing the proliferative zone undergo another shape change, stop proliferating, adhere tightly to each other, and begin to form a lumen (Auerbach and Auerbach, 1994; Hanahan and Folkman, 1996). In addition, these endothelial cells deposit a new ECM composed primarily of laminin and collagen type IV (Carey, 1991; Iruela-Arispe et al.,

1991b; Risau and Lemmon, 1988). Both ECM proteins have been shown to promote endothelial cell morphogenesis (Carey, 1991; Iruela-Arispe et al., 1991b; Risau and Lemmon, 1988). Secondary sprouting from the migrating tip results in the formation of a capillary plexus, and the fusion of individual sprouts at their tips closes the loop and circulates blood into the vascularized area (Auerbach and Auerbach, 1994; Hanahan and Folkman, 1996; Risau, 1997). For maturation of new vessels to occur, peri-endothelial cells such as smooth muscle cells or pericytes must be recruited (Carmeliet, 2000). This process serves four functions: (i) to provide structural support to new vessels to prevent rupture or regression; (ii) to assist in the production of ECM proteins; (iii) to maintain endothelial cells in a quiescent state; and (iv) to provide contractile function to modulate vessel caliber (Benjamin et al., 1998; Carmeliet, 2000). Finally, pruning of the vasculature occurs in which vessels lacking peri-endothelial support undergo regression (Benjamin et al., 1998).

1.3.2 Angiogenic activators

Many growth factors and cytokines are known to stimulate angiogenesis. Two angiogenic activators used in this thesis are fibroblast growth factor-2 (FGF-2) and VEGF (Dvorak et al., 1995; Rak and Kerbel, 1997). Whereas FGF-2 exhibits pleiotropic effects and can stimulate numerous cells including endothelial cells and smooth muscle cells, VEGF is primarily an endothelial mitogen (Gospodarowicz et al., 1989; Klagsbrun and Moses, 1999; Leung et al., 1989).

The FGF family consists of 23 members (Wiedlocha and Sorensen, 2004). FGF-2, also known as basic fibroblast growth factor, was the first angiogenic activator to be identified (Shing et al., 1984). FGF-2 is normally sequestered within the ECM through binding to heparan sulfate proteoglycans (Vlodavsky et al., 1991). Following digestion by heparinases, FGF-2 can be

released from the ECM and induce downstream signaling (Vlodavsky et al., 1991). Four FGF-receptor (FGF-R) family members have been identified: FGF-R1/2/3/4 (Jaye et al., 1992; Johnson and Williams, 1993). In addition, alternative splicing can result in the generation of FGF receptor variants (Jaye et al., 1992; Johnson and Williams, 1993). Disruption of either the FGF-R1 or the FGF-R2 gene in mice results in embryonic lethality (Deng et al., 1994; Xu et al., 1998). In contrast, FGF-R3-null mice survive but exhibit skeletal abnormalities (Colvin et al., 1996). Gene disruptions for FGF-R4 have not been described (Cross and Claesson-Welsh, 2001). All four FGF receptors are receptor tyrosine kinases (Jaye et al., 1992; Johnson and Williams, 1993). Induction of angiogenesis by FGF-2 is mediated through FGF-R1 downstream signaling (Plotnikov et al., 1999). Indeed, FGF-R1 has been shown to be essential for the proper development and maintenance of the embryonic vasculature in mice (Lee et al., 2000). FGF-2-null mice, however, exhibit normal embryonic vascular development (Dono et al., 1998). FGF-2 forms a dimer which binds and recruits two FGF-R1 receptor molecules, resulting in FGF-R1 dimerization and autophosphorylation (Klint and Claesson-Welsh, 1999; Plotnikov et al., 1999). Signaling pathways activated by FGF-R1 include the Ras, phosphatidylinositol 3-kinase (PI3K), phospholipase C (PLC), and Src family tyrosine kinase pathways (Cross and Claesson-Welsh, 2001). These pathways in turn induce endothelial cell proliferation, migration, and protease production (Christofori, 1996; Montesano et al., 1986). Moreover, FGF-2 also stimulates angiogenesis by inducing the recruitment of mesenchymal or inflammatory cells (Carmeliet, 2000).

The VEGF cytokine family consists of seven members: VEGF-A, VEGF-B, VEGF-C, VEGF-D, VEGF-E, placenta growth factor-1 (PlGF1), and PlGF2 (Larrivee and Karsan, 2000; Migdal et al., 1998). VEGF-A, the first member to be discovered, was originally identified as

vascular permeability factor due to its ability to induce vascular leakage (Senger et al., 1983). VEGF-A also plays an essential role during vasculogenesis, the process of in situ differentiation of angioblasts into endothelial cells that assemble to form a primitive vessel network (Beck and D'Amore, 1997; Ray et al., 1999b; Risau and Flamme, 1995). Mice heterozygous for VEGF-A die at embryonic day (E)11 and exhibit growth retardation and abnormal blood vessel development (Carmeliet et al., 1996; Ferrara et al., 1996). Homozygous VEGF-A mutants exhibit more severe vascular abnormalities compared to heterozygous mutants (Carmeliet et al., 1996). Alternative splicing of the human VEGF-A gene can give rise to five isoforms: VEGF-A_{121}, VEGF-A_{145}, VEGF-A_{165}, VEGF-A_{189}, and VEGF-A_{206} (Neufeld et al., 1996). Whereas the former three isoforms are freely diffusible proteins, the latter two isoforms are primarily sequestered in the ECM (Neufeld et al., 1996). The VEGF-A isoform used to stimulate angiogenesis in this thesis is VEGF-A_{165}, the most predominant (Cross and Claesson-Welsh, 2001) and biologically active (Neufeld et al., 1999; Neufeld et al., 1996) isoform of VEGF-A.

VEGF ligands form disulfide-linked dimers that bind to members of the VEGF-receptor (VEGF-R) family (Cross and Claesson-Welsh, 2001). Five VEGF-R family members have been identified: (i) VEGF-R1/flt-1; (ii) VEGF-R2/flk-1/KDR; (iii) VEGF-R3/flt-4; (iv) neuropilin-1; and (v) neuropilin-2 (Larrivee and Karsan, 2000). VEGF-A can bind to VEGF-R1, VEGF-R2, neuropilin-1, and neuropilin-2 (Larrivee and Karsan, 2000). VEGF receptors 1/2/3 all share a similar overall structure, which includes an N-terminal extracellular domain containing seven immunoglobulin (Ig)-like domains, a transmembrane domain, and a C-terminal intracellular domain with a two-part tyrosine kinase domain (Petrova et al., 1999). While the second Ig-like domain mediates ligand binding, both the first and third Ig-like domains are required for high-affinity binding (Barleon et al., 1997; Cunningham et al., 1997; Davis-Smyth et al., 1996; Fuh et

al., 1998). Following ligand binding, the fourth Ig-like domain mediates dimerization of VEGF receptors, resulting in receptor autophosphorylation and hence activation of downstream signaling pathways (Barleon et al., 1997).

Mice deficient for VEGF-R2 die around E10, and are characterized by the absence of endothelial cells (Shalaby et al., 1995). Hence no organized blood vessels can be detected at any stage of embryonic development. VEGF-R1-deficient mice also die at E10, and also exhibit vascular defects (Shalaby et al., 1995). However, unlike VEGF-R2 mutant mice, vascular defects in VEGF-R1 mutant mice arise not from a lack of vessels but from the formation of abnormally large and fused vessels (Shalaby et al., 1995). Indeed, VEGF-R1 mutant mice possess an overabundance of endothelial cells (Shalaby et al., 1995). This increased endothelial cell density has been postulated to prevent endothelial cell assembly into normal functional vessels. The fact that endothelial cells are absent in VEGF-R2- but not VEGF-R1-null mice suggests that VEGF-R2 plays a more important role than VEGF-R1 during mouse embryonic development. Indeed, almost all biologically-relevant VEGF signaling has been shown to be mediated by VEGF-R2 (Zachary and Gliki, 2001). VEGF-R2 activation can stimulate endothelial cell migration, proliferation, and survival (Zachary and Gliki, 2001). Signaling mediated by VEGF-R1, in contrast, has not been well elucidated (Zachary and Gliki, 2001). Instead, VEGF-R1 is thought to sequester VEGF and thus function as a negative regulator of VEGF-R2 (Zachary and Gliki, 2001).

1.3.3 Angiogenic inhibitors

Angiogenic inhibitors can be divided into two classes: (i) endogenous angiogenesis inhibitors and (ii) synthetic angiogenesis inhibitors. Among endogenous angiogenesis inhibitors, two of the best-studied are the tumor-derived inhibitors angiostatin and endostatin. Angiostatin is

a 38 kilodalton (kDa) fragment of the serine protease precursor plasminogen first isolated from the urine of mice bearing Lewis lung carcinoma tumors (O'Reilly et al., 1994). Intact plasminogen itself, in contrast to angiostatin, has no anti-angiogenic activity (Zetter, 1998). Angiostatin is not produced by tumor cells directly (Gately et al., 1996). Instead, tumor cells produce and secrete proteases into the circulation which cleave plasminogen to generate angiostatin (Gately et al., 1996). Hence in addition to inhibiting angiogenesis locally, angiostatin can function as a circulating angiogenesis inhibitor that suppresses angiogenesis at distant sites (O'Reilly et al., 1994). The mechanism of action of angiostatin involves interference with adenosine triphosphate (ATP) production (Moser et al., 1999). ATP is normally synthesized by the ATP synthase F1 complex expressed in mitochondria (Alberts et al., 2002). Endothelial cells have been shown to express the ATP synthase F1 complex on the cell surface, which functions to produce ATP that subsequently diffuses into the cell to facilitate numerous intracellular processes (Moser et al., 1999). Angiostatin can bind and inhibit the function of the ATP synthase F1 complex, thus inhibiting endothelial cell proliferation and migration (Moser et al., 1999). Angiostatin can also increase tumor sensitivity to radiation (Gorski et al., 2003).

Endostatin is a 20 kDa fragment of the ECM protein collagen XVIII, a collagen frequently found near blood vessels (O'Reilly et al., 1997). Intact collagen XVIII does not exhibit anti-angiogenic activity (Zetter, 1998). Initially purified from conditioned media of cultured hemangioendothelioma cells (O'Reilly et al., 1997), endostatin has been shown to inhibit endothelial cell function by attenuating growth factor signaling. Specifically, endostatin may downregulate the expression of angiogenic growth factor ligands or receptors, thus inhibiting endothelial cell proliferation (Tee and DiStefano, 2004). Moreover, endostatin can bind with

high-affinity to heparan sulfate proteoglycans on the surface of endothelial cells, thus acting as a competitive inhibitor of growth factor binding (Tee and DiStefano, 2004).

In addition to angiostatin and endostatin, numerous other endogenous angiogenesis inhibitors have been identified. The ECM protein thrombospondin-1 has been shown to block endothelial cell proliferation, migration, and morphogenesis (Bagavandoss and Wilks, 1990; Iruela-Arispe et al., 1991a; Vogel et al., 1993). Tissue inhibitor of metalloproteases (TIMPs), which function to suppress ECM degradation by MMPs, can directly block endothelial cell proliferation and migration (Anand-Apte et al., 1997; Martin et al., 1996; Murphy et al., 1993). Several cytokines possess anti-angiogenic activity, including interleukin-12 (Hiscox and Jiang, 1997), leukemia inhibitory factor (Pepper et al., 1995), platelet factor 4 (Bikfalvi, 2004), and interferon-α/β (Lindner, 2002).

A second class of anti-angiogenic factors consists of synthetic angiogenesis inhibitors. These inhibitors have been designed to block specific steps during the angiogenic cascade. VEGF signaling is a potent inducer of angiogenesis and hence is targeted by numerous synthetic angiogenesis inhibitors. Examples include VEGF antibodies (Abs) that bind to VEGF and prevent its association with VEGF receptors (Adamis et al., 1996; Kim et al., 1993; Presta et al., 1997), VEGF receptor Abs that prevent VEGF binding (Witte et al., 1998), soluble VEGF receptors that sequester VEGF and prevent endogenous receptor activation (Aiello et al., 1995; Goldman et al., 1998; Kendall et al., 1996), and VEGF receptor tyrosine kinase inhibitors that block receptor transphosphorylation (Fong et al., 1999). Synthetic MMP inhibitors that interact with the zinc-binding site of MMPs to block their function prevent MMP-mediated degradation of the ECM during endothelial sprouting (Sledge et al., 1995; Wojtowicz-Praga et al., 1998). Integrin antagonists such as Abs and inhibitor peptides block interaction of endothelial integrins

with ECM proteins (Brooks et al., 1994a; Brooks et al., 1994b; Gutheil et al., 2000). Because integrin ligation to ECM proteins induces cellular survival signals (Giancotti and Ruoslahti, 1999), integrin antagonists prevent these signals and thus induce endothelial cell apoptosis (Brooks et al., 1994b).

Recent studies have demonstrated that some conventional chemotherapeutic drugs, when administered at low doses and on a more frequent schedule, can exhibit anti-angiogenic properties. Such drugs would therefore function not as anti-tumor agents but instead as anti-endothelial agents (Browder et al., 2000; Klement et al., 2000). Examples of drugs that have demonstrated this property include adriamycin (Steiner, 1992), cyclophosphamide (Browder et al., 2000), paclitaxel (Belotti et al., 1996), and vinblastine (Vacca et al., 1999).

1.3.4 Pathological angiogenesis

Angiogenesis plays an important role in numerous physiological processes. These include embryonic development, wound healing, and development and repair of the female reproductive system (Cross and Claesson-Welsh, 2001; Klagsbrun and Moses, 1999). Because angiogenesis is controlled by a balance of angiogenic activators and inhibitors (Hanahan and Folkman, 1996), deregulated angiogenesis can result in the development of pathological disorders (Folkman, 1995; Isner, 1998). Diseases such as diabetic retinopathy, rheumatoid arthritis, and ischemia, as well as chronic inflammation, are all characterized by pathological angiogenesis. Of importance to this thesis is pathological angiogenesis in the context of tumor angiogenesis and metastasis.

1.3.4.1 Tumor angiogenesis

Tumors with a diameter of 1-2 mm or smaller are avascular (Folkman, 1972). Without a blood supply, these tumors cannot grow larger due to rate-limiting diffusion of nutrients and

waste products and hence remain dormant (Folkman, 1971). Despite rapid tumor cell proliferation, a net change in tumor size does not occur due to a concomitant increase in tumor cell apoptosis (Hanahan and Folkman, 1996). In order to initiate blood vessel-dependent growth, avascular tumors engulf adjacent preexisting host organ blood vessels (Holash et al., 1999). Engulfed vessels allow avascular tumors to grow beyond a diameter of 1-2 mm (Denekamp, 1993). For continued tumor expansion to occur, however, tumor cells produce angiogenic activators that stimulate angiogenesis (Zetter, 1998). Host stromal cells recruited to the tumor such as macrophages, mast cells, and lymphocytes, also produce angiogenic activators that facilitate tumor growth (Freeman et al., 1995; Meininger and Zetter, 1992; Miguez et al., 1986). Typically more than one type of angiogenic activator is produced by a single tumor (Kerbel, 2000; Relf et al., 1997). Because the overall activity of newly-produced angiogenic activators exceeds that of locally-produced inhibitors, angiogenesis is activated and tumor growth occurs (Zetter, 1998). Angiogenesis-induced tumor growth does not occur as a result of increased tumor cell proliferation; instead, angiogenesis reduces the rate of tumor cell apoptosis, thus effecting a net expansion of the tumor mass (Holmgren et al., 1995).

Tumor blood vessels are structurally and functionally different from normal blood vessels. Tumor blood vessels can be enlarged and contain abnormal tortuosities, blind ends, corkscrew structures, and atypical branching (Kerbel, 2000; Weidner et al., 1991). Functionally, tumor vessels are highly permeable due to the lack of proper basement membrane deposition and peri-endothelial cell recruitment (Dvorak et al., 1995). The mechanism by which recruitment of peri-endothelial cells is inhibited involves angiopoietin-2 (Ang-2), a secreted glycoprotein that binds to the tyrosine kinase with Ig and EGF homology domains-2 (Tie-2) receptor (Davis et al., 1996). Tie-2 is expressed on the surface of endothelial cells (Partanen and Dumont, 1999), and

normally signals to induce vessel maturation by recruiting peri-endothelial cells to newly-formed vessels (Dumont et al., 1995). Tumors have been shown to produce Ang-2, which binds to Tie-2 and antagonizes Tie-2 signaling, thus preventing tumor blood vessel maturation (Davis et al., 1996; Davis and Yancopoulos, 1999). Tumor blood vessels lack innervation and therefore exhibit abnormal responses to vasoactive stimuli (Mitchell et al., 1994). Blood flow within the tumor vasculature is chaotic (Vaupel et al., 1989). As a result of high tumor interstitial pressure, blood viscosity is increased within the tumor vasculature thus reducing the rate of blood flow (Vaupel et al., 1989). Intermittent flow can also occur, with prolonged periods of stasis or reverse flow (Jain, 1990; Vaupel et al., 1989). Arterio-venous shunting of blood has been reported in tumors (Vaupel et al., 1989). Tumor blood vessels of a mosaic composition have been described in which tumor vessels are lined by both endothelial and tumor cells (Maniotis et al., 1999). This feature of the tumor vasculature, termed vasculogenic mimicry, remains highly controversial (Folberg and Maniotis, 2004). In addition to providing a blood supply to the tumor, the tumor vasculature functions as a route for the spread, or metastasis, of cancer.

1.3.4.2 Tumor metastasis

In general, cancers which do not metastasize do not kill (Miller and Sledge, 1999). Ninety percent of human cancer deaths are caused by metastases (Sporn, 1996). In order for metastases to be established, cancer cells must survive a series of steps (Poste and Fidler, 1980). Each step, however, is rate-limiting since deficiency at any step results in failure of the metastatic process (Poste and Fidler, 1980). Initiation of metastasis involves tumor cell dissemination at the primary tumor site. Tumor cells have been shown to modulate their cell-cell and cell-substrate interactions by modulating the expression and/or adhesive activity of cell adhesion proteins (Webb and Vande Woude, 2000). In addition, both tumor and infiltrating

stromal cells produce chemotactic and chemokinetic factors which enhance tumor cell migration and invasion (Levine et al., 1995; Negus and Balkwill, 1996). Some tumor cells secrete autocrine motility factor (AMF), which binds and activates the AMF receptor expressed on the same tumor cell thus promoting migration and invasion (Nabi et al., 1992). Stromal cells can produce hepatocyte growth factor (HGF), which binds to the Met receptor expressed on tumor cells to induce downstream signaling (Webb and Vaunde Woulde, 2000). HGF stimulation has been shown to induce tumor cell expression of both urokinase-type plasminogen activator (uPA) and its receptor uPAR (Jeffers et al., 1996). VEGF and FGF-2 can also induce uPA expression (Pepper et al., 1990; Pepper et al., 1991). The binding of uPA to uPAR induces the conversion of an inactive plasminogen zymogen into active plasmin, a broad specificity protease that degrades numerous ECM proteins including fibrin, fibronectin, gelatin, laminin, and vitronectin (Mignatti and Rifkin, 1996). Moreover, HGF can induce the expression of several MMPs (Hamasuna et al., 1999). Hence plasmin and MMPs degrade ECM proteins, effectively fragmenting the basement membrane surrounding tumor capillaries. Tumor cells adjacent to such capillaries enter the circulation via intravasation (Zetter, 1998). Both single tumor cells and tumor emboli have been observed to enter the circulation (Nime et al., 1977). When in circulation, tumor cell survival time is dependent upon the tumor cell's ability to avoid apoptosis and immune detection (Webb and Vande Woude, 2000). Tumor cells avoid apoptosis by inducing the expression of survival proteins, or by altering the expression of cell adhesion molecules belonging to the integrin family (Webb and Vande Woude, 2000). Mechanisms used by tumor cells to escape immune surveillance include masking of surface antigens normally recognized by lymphocytes (Marincola et al., 2000), as well as expression of Fas ligand which activates the Fas receptor on the surface of lymphocytes, resulting in lymphocyte apoptosis (O'Connell et al., 1996). Although

many tumor cells in circulation die, a significant proportion survive and attach to the endothelium of organ capillary beds at secondary sites (Zetter, 1998). Whereas initial tumor cell-endothelial cell interactions are weak and are mediated by adhesion proteins of the selectin family (Tedder et al., 1995), strong interactions are mediated by integrins (Saiki et al., 1989). Tumor cell binding to the endothelium induces retraction of endothelial cells, thus exposing the sub-endothelial basement membrane (Nicolson, 1982). Tumor cells readily adhere to the sub-endothelial basement membrane (Abecassis et al., 1987) and therefore extravasate through the vessel wall (Zetter, 1998). Tumor cell extravasation is also facilitated by VEGF-induced disruption of the endothelial barrier in host organ blood vessels (Weis et al., 2004). Subsequent tumor cell proliferation at secondary sites results in the establishment of metastases.

1.3.5 Notch and blood vessel development

Since the start of this thesis project, numerous studies have linked Notch expression and downstream signaling with vascular development and angiogenesis. Mouse gene disruption studies have highlighted the importance of various Notch pathway elements in the development of the vasculature. Jagged1-null mice are lethal at E10.5 and exhibit massive hemorrhaging associated with malformation of the vasculature (Xue et al., 1999). These mice also have defects in angiogenesis (Xue et al., 1999). Similarly, Dll1-null mice die at E10.5 from hemorrhaging (Hrabe de Angelis et al., 1997). Mice homozygous for a hypomorphic Notch2 mutation exhibit disrupted vessel remodeling in multiple vascular beds (McCright et al., 2001). Presenilin-1-null mice are viable until birth, and suffer from severe brain hemorrhage (Shen et al., 1997; Wong et al., 1997). Presenilin-2-null mice are also viable but display only mild hemorrhage compared to presenilin-1-null mice (Herreman et al., 1999). Presenilin-1/presenilin-2 double homozygous deficient mice, however, die at E9.5 and exhibit a severe phenotype associated with delayed

vascularization and a complete lack of blood circulation (Herreman et al., 1999). This phenotype is similar, if not identical, to that observed in Notch1-null mice (Herreman et al., 1999). Notch1 gene disruption is lethal around E10 (Huppert et al., 2000) due to hemorrhaging, with extensive defects in angiogenic vascular remodeling observed in the embryo, yolk sac, and placenta (Krebs et al., 2000). Notch4 gene disruption, in contrast, results in viable mice with no apparent defects (Krebs et al., 2000). The lack of a mutant phenotype in these mice suggests that Notch4 is dispensable for normal embryonic development (Krebs et al., 2000). Interestingly, approximately 50% of Notch1/Notch4 double homozygous deficient mice exhibit more severe vascular defects than Notch1 single null mice (Krebs et al., 2000). Hence a role for Notch4 in embryonic vascular development cannot be excluded. Interestingly, expression of activated Notch4 in the mouse embryonic vasculature, under the control of the VEGF-R2 promoter, results in vascular patterning defects (Uyttendaele et al., 2001). Therefore both increases and decreases in Notch4 signaling result in a common vascular phenotype, disrupted blood vessel development.

The expression of various Notch ligand and receptor family members has been reported in endothelial cells. Of importance to this thesis is that Notch4 is primarily expressed on the endothelium (Uyttendaele et al., 1996). Endothelial-restricted Notch4 mRNA expression is first evident in mice during embryogenesis (Shirayoshi et al., 1997; Uyttendaele et al., 1996) and persists into adulthood (Favre et al., 2003; Johnson et al., 2001; Taichman et al., 2002). Examination of human tissues has revealed selective Notch4 mRNA expression in endothelial cells (Nijjar et al., 2001). By in situ hybridization, Notch target genes of the HRT family have been shown to be highly expressed in blood vessels (Fischer and Gessler, 2003; Leimeister et al., 1999; Leimeister et al., 2000b; Nakagawa et al., 1999). In the murine embryonic vasculature, HRT1 mRNA exhibits an endothelial-restricted expression pattern (Fischer and Gessler, 2003).

HRT2 and HRT3 mRNAs, however, are predominantly expressed in the smooth muscle cell layer surrounding the endothelium, and to a lesser extent the endothelium itself (Fischer and Gessler, 2003). Interestingly, mRNA expression of HES family members is absent or barely detectable in the mouse embryonic vasculature (Kageyama et al., 2000; Sasai et al., 1992). Hence HRT genes, and not HES genes, may be the primary mediators of Notch signaling during vascular development.

Recent studies have identified a role for Notch signaling in the determination of arterial versus venous fate of newly-formed blood vessels. In mouse embryos, mRNA expression of Dll1/3 and Notch2 cannot be detected in vessels (Villa et al., 2001). Jagged1/2, Dll4, and Notch1/3/4 mRNAs, in contrast, are all specifically expressed in arteries and not veins (Villa et al., 2001). Interestingly, only Dll4 and Notch4 mRNAs have been shown to be expressed in capillaries (Villa et al., 2001). Arterial Jagged1 mRNA expression can be detected in both endothelial and smooth muscle cell types (Villa et al., 2001). Notch3, on the other hand, is not expressed in endothelial cells (Joutel et al., 2000). Instead, Notch3 protein has been shown to be expressed in vascular smooth muscle cells (Joutel et al., 2000). In the mouse umbilical cord, Dll4 mRNA expression can be detected in the umbilical artery but not in the adjacent umbilical vein (Shutter et al., 2000). During development of the mouse retina, Dll4 mRNA is expressed in an arterial-restricted pattern (Claxton and Fruttiger, 2004). Indeed, Dll4 is the first Notch ligand to be expressed in arteries (Krebs et al., 2000), and has since been shown to be required in a dosage-sensitive manner for normal arterial development in the mouse (Duarte et al., 2004; Gale et al., 2004). In zebrafish, mRNA expression of the Notch ligand DeltaC can be detected in endothelial cells prior to their acquisition of an arterial fate (Smithers et al., 2000). Endothelial cells that express gridlock (a zebrafish homologue of HRT2) mRNA incorporate exclusively into

arteries and not veins (Zhong et al., 2000). Accordingly, gridlock gene disruption adversely affects the formation of arteries, resulting in expansion of venous regions (Zhong et al., 2000). Hence Notch signaling may promote artery formation through repression of the venous fate. In a rat model of endothelial denudation, regenerating endothelial and smooth muscle cells in injured carotid arteries and aortae exhibit induced mRNA expression of Jagged1/2 and Notch1/2/3/4 (Lindner et al., 2001). Notch signaling may therefore play a role in the arterial vascular response to injury. It should be noted, however, that venous expression of Notch pathway elements has been reported in humans. For example, human umbilical vein endothelial cells (HUVECs) express Notch1/4 and Dll4 mRNAs (Liu et al., 2003) and Dll1 protein (Han et al., 2000), and our laboratory has detected expression of Notch1/2/3/4 and Jagged1 mRNA in HUVEC (Noseda et al., 2004a).

Evidence of cross-talk between Notch and angiogenic growth factor signaling pathways has emerged. Human endothelial cells isolated from different vascular beds, when transduced with either FGF-2 or VEGF, exhibit mRNA induction of various Notch receptors and ligands (Liu et al., 2003). Interestingly, synergistic induction of Notch receptor and ligand mRNA expression in endothelial cells can be achieved by co-transduction of FGF-2 and VEGF (Liu et al., 2003). Stimulation of human arterial endothelial cells with soluble recombinant VEGF but not FGF-2 induces Notch1 and Dll4 mRNA expression (Liu et al., 2003). Our laboratory has shown that Notch4IC can downregulate VEGF-R2 mRNA expression (MacKenzie et al., 2004a). HRT1 overexpression can also downregulate VEGF-R2 mRNA expression, thus attenuating the responsiveness of endothelial cells to VEGF (Henderson et al., 2001). Because the VEGF-R2 gene promoter contains E box binding motifs, activated Notch may act via HRT1 to repress VEGF-R2 expression (Henderson et al., 2001; MacKenzie et al., 2004a). VEGF signaling can

also be attenuated by HRT2-mediated passive repression of VEGF expression. Specifically, HRT2 has been shown to interfere with ARNT transcription factor binding to the VEGF promoter (Chin et al., 2000).

Notch signaling plays a role in endothelial sprouting in vitro and angiogenesis in vivo. HUVEC cultured in three-dimensional fibrin gels as endothelial tubes have been shown to upregulate Dll4, Notch1/4, and HRT1 mRNA expression (Nakatsu et al., 2003). Upregulation of HRT1 in endothelial tubes is postulated to play a role in the establishment of a mature endothelial cell network (Henderson et al., 2001). Low or absent HRT1 expression may be permissive to endothelial proliferation and migration whereas overexpression of HRT1 may block these processes, thus inhibiting the formation of new endothelial tubes (Henderson et al., 2001). Expression of activated Notch1 or overexpression of HES1 has been shown to stabilize endothelial tube formation in Matrigel and induce endothelial cell cycle arrest in two-dimensional cultures in vitro (Liu et al., 2003). Results from our laboratory demonstrate that Jagged1-mediated Notch activation induces cell cycle arrest in primary endothelial cells (Noseda et al., 2004a). These studies suggest that activated Notch signaling inhibits endothelial sprouting in vitro. Accordingly, several studies have shown that inhibited Notch signaling promotes endothelial sprouting in vitro and angiogenesis in vivo. In a collagen gel assay, antisense oligonucleotides directed against Jagged1 enhance FGF-2-induced endothelial tube formation (Zimrin, 1996). Interestingly, HUVEC cultured on fibrin-coated plates and stimulated with FGF-2 have been shown to upregulate expression of a Jagged1 mRNA corresponding to a soluble, non-transmembrane form of Jagged1 (Zimrin, 1996). Overexpression of a complementary DNA (cDNA) encoding this transcript has since been reported to antagonize Notch signaling (Small et al., 2001). In a chick chorioallantoic membrane (CAM) assay, soluble Jagged1 induces

angiogenesis in the chick CAM and hence functions as an angiogenic activator (Wong et al., 2000). Interestingly, expression of activated Notch4 in the rat brain endothelial cell line RBE4 has been shown to promote the formation of microvessel-like structures (Uyttendaele et al., 2000). Hence the effect of Notch signaling on angiogenesis may be dependent upon endothelial cell type. It should be noted, however, that RBE4 cells express the adenovirus E1A oncoprotein, which has been reported to mimic the effects of NotchIC by converting CBF1 from a transcriptional repressor to an activator (Ansieau et al., 2001).

1.4 CELL ADHESION

1.4.1 Overview of cell adhesion molecules

Cells use multiple molecular mechanisms to adhere to other cells as well as to the ECM. Proteins involved in cell-cell and cell-ECM adhesion can be divided into four families: Ig superfamily, selectins, integrins, and cadherins. The Ig superfamily consists of over 100 members that share a characteristic structural motif, the presence of one or more Ig-like domains commonly found in Abs (Alberts et al., 2002). These proteins mediate Ca^{2+}-independent cell-cell adhesion (Alberts et al., 2002). Examples of Ig superfamily members include intercellular adhesion molecule-1 (ICAM-1), vascular cell adhesion molecule-1 (VCAM-1), lymphocyte function-associated protein-1 (LFA-1), and platelet endothelial cell adhesion molecule-1 (PECAM-1) (Alberts et al., 2002). Selectins are a family of cell-surface carbohydrate-binding proteins that mediate Ca^{2+}-dependent transient adhesion between blood cells and the endothelium (Tedder et al., 1995). These interactions allow blood cells to extravasate from the bloodstream into tissues (Bevilacqua, 1993). Three members have been identified: lymphocyte (L)-selectin, platelet (P)-selectin, and endothelial (E)-selectin (Alberts et al., 2002). Similar to

selectins, cell-surface molecules belonging to the integrin and cadherin families mediate Ca^{2+}-dependent cell adhesion (Alberts et al., 2002). Studies presented in this thesis examine the role of integrins and cadherins in angiogenesis and breast cancer, respectively, and therefore these two adhesion protein families are described in detail below.

1.4.2 Integrins

1.4.2.1 Overview of integrin functions

Integrins constitute a large family of cell adhesion proteins expressed on virtually all cell types (Alberts et al., 2002). In addition to mediating cell-cell adhesion, integrins can mediate cell-ECM adhesion by functioning as transmembrane linkers, or integrators, that connect the cytoskeleton to the ECM (Alberts et al., 2002). Integrin ligation by ECM proteins results in the activation of intracellular signaling pathways that regulate numerous cellular processes including proliferation, migration, survival, and differentiation (LaFlamme and Auer, 1996). The phenotype of a cell is directly influenced by the repertoire of integrins expressed on the cell surface (Plow et al., 2000).

1.4.2.2 Integrin receptors

Integrins are heterodimeric receptors, each composed of an α and a β transmembrane glycoprotein subunit, that associate noncovalently to give rise to an asymmetric structure consisting of a single extracellular globular head and two flexible tails (Carrell et al., 1985; Hynes, 1992) (Figure 1.5). Thus far, 18 different α subunits and eight different β subunits have been identified, which associate to give rise to at least 24 distinct α/β heterodimers (Hynes, 2002) (Figure 1.6). Moreover, alternative splicing of integrin subunits has been documented thus contributing to integrin signaling versatility (Hynes, 1992; Sheppard, 2000). Both subunits are

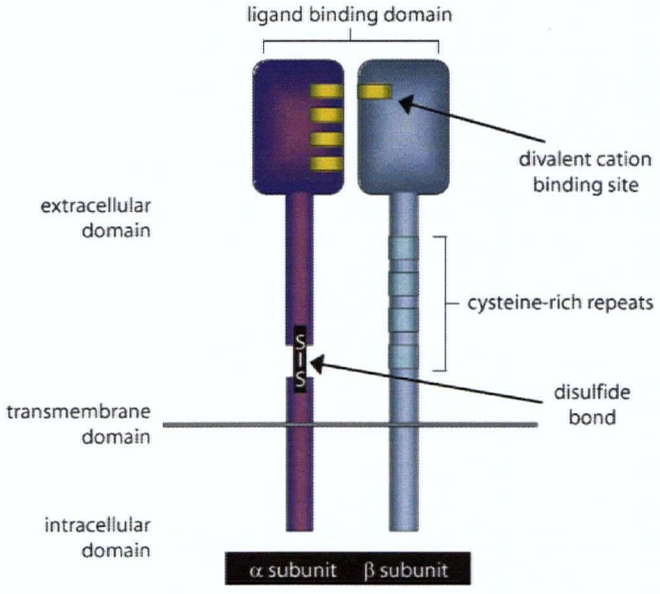

Figure 1.5: Structure of an integrin α/β heterodimer. Each integrin receptor is composed of two transmembrane subunits, called α and β, that are held together by noncovalent bonds. Both α and β subunits consist of a large extracellular domain, transmembrane domain, and a short intracellular domain (with the exception of β4, which has a large intracellular domain). Alpha subunits contain four divalent cation binding sites. In some cases, the α subunit is initially synthesized as a single polypeptide chain, which is then cleaved to form a large extracellular domain and a smaller transmembrane/intracellular domain held together by a disulfide bond. Beta subunits contain a single divalent cation binding site, as well as four cysteine-rich repeats involved in intrasubunit disulfide bonding. Proximal to the divalent cation binding sites of both α and β subunits is a ligand binding domain.

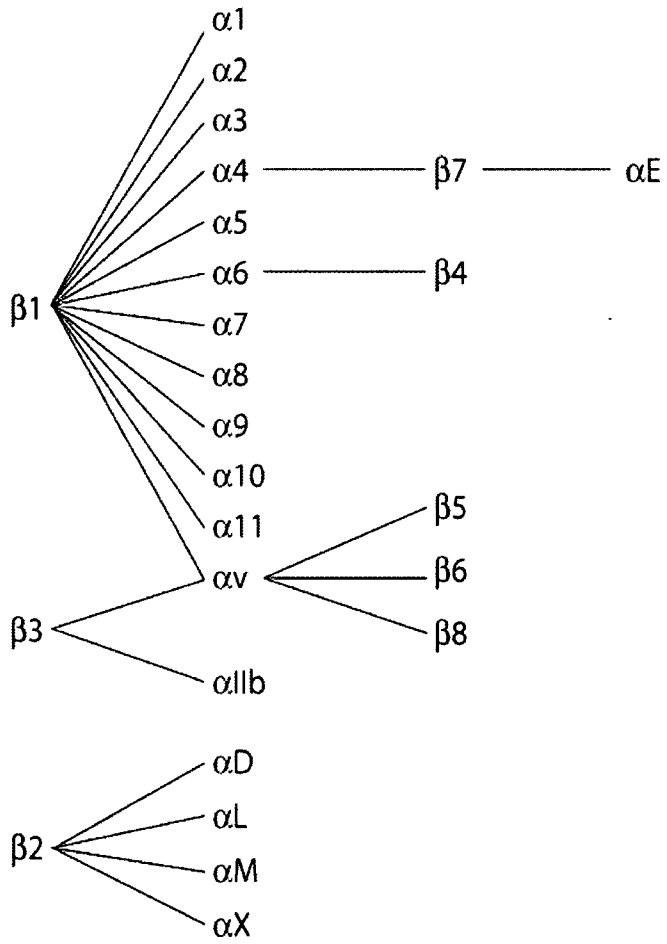

Figure 1.6: Integrin α/β heterodimer combinations. Integrin heterodimers are formed from one α and one β subunit. Thus far, 18 different α subunits and eight different β subunits have been identified, which associate to give rise to at least 24 distinct α/β heterodimers.

required for integrin expression on the cell surface (O'Toole et al., 1989). Alpha subunits range in size from 140-210 kDa and consist of a large extracellular domain followed by a single-pass transmembrane domain and a short intracellular domain (Hynes, 1992) (Figure 1.5). Within the extracellular domain, seven homologous repeating segments fold into a divalent cation binding motif containing four cation binding sites essential for proper integrin function (Tozer et al., 1996). In some cases, the α subunit is initially synthesized as a single polypeptide chain, which is then cleaved to form a large extracellular domain and a smaller transmembrane/intracellular domain held together by a disulfide bond (Alberts et al., 2002). Furin has been identified as an enzyme involved in the endoproteolysis of α subunits (Lehmann et al., 1996). Integrin β subunits typically range in size from 90-130 kDa and have an overall structure similar to that of α subunits (Hynes, 1992). One exception, however, is the β4 subunit which possesses an intracellular domain larger than that of the other β subunits (Sonnenberg et al., 1991). The extracellular domain of all β subunits contains a single divalent cation binding motif and four cysteine-rich repeats involved in intrasubunit disulfide bonding (Calvete et al., 1989). Extracellular divalent cations are essential for the proper formation of integrin heterodimers (Tozer et al., 1996). Heterodimer formation does not involve the intracellular domains of α or β subunits but instead requires the extracellular domains of both subunits (Dana et al., 1991).

1.4.2.3 Integrin ligands

Integrins bind to a diverse set of proteins such as ECM proteins, other cell surface proteins, plasma proteins, and bacterial and viral proteins (Bouvard et al., 2001). Most integrins can recognize several ECM proteins, and individual ECM proteins can bind to several integrins (Hynes, 1987; Ruoslahti and Pierschbacher, 1987). The α and β subunits of an integrin heterodimer both contain several ligand binding sites located just proximal to the divalent cation

binding motif (Sanchez-Mateos et al., 1996). These ligand binding sites are believed to act in a sequential manner. Specifically, one or several binding sites may mediate initial ligand binding which triggers a conformation change that exposes additional binding sites, thus resulting in stable integrin-ligand interactions (Hogg et al., 1994; Stuiver and O'Toole, 1995).

Ligand binding is regulated by the presence of extracellular divalent cations (Tozer et al., 1996). The type of divalent cation, however, directly influences the strength and specificity of the interaction between integrin and ligand (Alberts et al., 2002). Specificity is also mediated by amino acid recognition sequences presented on ligands. For example, the sequence arginine-glycine-aspartic acid (RGD) can be found in the ECM proteins collagen, fibrinogen, fibronectin, and vitronectin, as well as vWF and thrombospondin (Plow et al., 2000). This RGD sequence is recognized by numerous integrins such as $\alpha 3\beta 1$, $\alpha 5\beta 1$, and $\alpha v\beta 3$ (Plow et al., 2000). Integrin binding to ligands containing RGD sequences can be inhibited by treatment with RGD peptides (Andronati et al., 2004). The mere presence of an RGD sequence on a ligand, however, does not ensure recognition by corresponding integrin binding partners. Rather, the context in which an RGD sequence is presented determines whether productive integrin-ligand interactions will occur (Haas and Plow, 1994). These can include the three-dimensional presentation of the RGD sequence, residues flanking the RGD sequence, as well as features specific to the integrin such as the ligand binding motif (Haas and Plow, 1994). Additional examples of recognition sequences are glycine-phenylalanine-hydroxyproline-glycine-glutamic acid-arginine (GFOGER) expressed on collagen and recognized by $\alpha 1\beta 1$ and $\alpha 2\beta 1$, aspartic acid-glycine-glutamic acid-alanine (DGEA) expressed on collagen and recognized by $\alpha 2\beta 1$, isoleucine-aspartic acid-alanine-proline-serine (IDAPS) expressed on fibronectin and recognized by $\alpha 4\beta 1$, and glutamine-isoleucine-

aspartic acid-serine (QIDS) expressed on VCAM-1 and recognized by α4β1 (Hynes, 1992; Plow et al., 2000).

1.4.2.4 Integrin signaling

In response to ECM binding, integrins transmit signals into the cell that activate various intracellular signaling pathways. This type of signal transduction, termed "outside-in signaling", enables the ECM to directly influence cellular phenotype and behavior (Giancotti and Ruoslahti, 1999). Signaling is initiated through integrin ligation. Because ligands and divalent cations share a common binding pocket on the integrin globular head, ligand binding displaces divalent cations thus inducing conformational changes in integrin structure (D'Souza et al., 1994). These conformational changes traverse the plasma membrane and modulate the conformation of the integrin intracellular domains (D'Souza et al., 1994), resulting in integrin clustering within the plane of the plasma membrane (Giancotti and Ruoslahti, 1999). Integrin α subunits have been shown to bind to caveolin-1, a membrane adapter protein that mediates clustering of various transmembrane proteins within the plasma membrane during lipid raft formation (Wary et al., 1996; Wei et al., 1999). Caveolin-1 may aid in integrin clustering since inhibition of caveolin-1 expression blocks integrin signaling (Wary et al., 1996; Wei et al., 1999).

Integrin cytoplasmic tails are devoid of enzymatic activity and hence integrins must associate with adapter proteins for downstream signaling to occur (Giancotti and Ruoslahti, 1999). Integrin α3 and α6 subunits have been shown to bind to CD151, a member of the tetraspanin family consisting of proteins with four transmembrane domains (Kazarov et al., 2002). CD151 may act as a transmembrane linker between the integrin α subunit and intracellular signaling molecules involved in regulating cellular morphology (Kazarov et al., 2002). Recently, the intracellular domain of the integrin αIIb subunit has been shown to bind to

and regulate the signaling activity of protein phosphatase-1 (Vijayan et al., 2004). Following integrin clustering, integrin β-subunit cytoplasmic tails associate with the cytoskeletal proteins talin, α-actinin, vinculin, and paxillin (Lo and Chen, 1994). These proteins in turn induce the assembly of actin filaments, which reorganize into large stress fibres that cause more integrin clustering (Giancotti and Ruoslahti, 1999). The cytoskeletal proteins also recruit enzymes such as Src, protein kinase C (PKC), and focal adhesion kinase (FAK) (Lo and Chen, 1994). Specialized adhesion sites called focal adhesions, composed of integrins, cytoskeletal proteins, and kinases, are thus formed at sites of contact between the ECM and integrins (Lo and Chen, 1994). Intracellular signals originating from focal adhesions have been shown to promote numerous cell processes including proliferation, migration, survival, and differentiation (LaFlamme and Auer, 1996). In addition to "outside-in signaling", integrins can modulate their adhesive activity via "inside-out signaling", i.e. integrins are capable of bidirectional signaling (Giancotti and Ruoslahti, 1999).

1.4.2.5 Regulation of integrin-mediated adhesion

Integrin-mediated adhesion is regulated by two processes, integrin affinity and integrin avidity (Sanchez-Mateos et al., 1996). Changes in integrin affinity and avidity are not mutually exclusive (Shattil et al., 1998; Stewart and Hogg, 1996). Rather, cells can use both processes to modulate ligand binding (Shattil et al., 1998; Stewart and Hogg, 1996).

1.4.2.5.1 *Integrin affinity*

Integrin affinity modulation refers to a change in the attraction of a single integrin for its ligand (Hughes and Pfaff, 1998). This change is rapid and reversible and involves a conformational change in the extracellular ligand binding site of the integrin (Hughes and Pfaff,

1998; Sanchez-Mateos et al., 1996). Integrins normally exist in a low-affinity, non-ligand binding state (Faull et al., 1994; Lollo et al., 1993). Following integrin activation, a transition from low to high-affinity occurs resulting in enhanced cell adhesion (Sanchez-Mateos et al., 1996). The integrin family can be divided into subfamilies based upon a common β subunit (Sanchez-Mateos et al., 1996). Increases in integrin affinity have been demonstrated in β1/2/3/7 subfamilies (Altieri et al., 1988; Crowe et al., 1994; Faull et al., 1993; Shattil et al., 1998). Numerous factors, acting from either inside or outside the cell, can induce activation of integrins.

Modulation of integrin affinity from within the cell occurs via inside-out signaling. Although the exact mechanism of integrin affinity regulation by intracellular signaling pathways remains unknown, a model has been proposed. The α and β subunits of an integrin heterodimer each contain a conserved cytoplasmic membrane-proximal motif, which together form a hinge that locks the integrin in a low-affinity state (Hughes et al., 1996). Sequences C-terminal to the hinge motif also play a role in regulating integrin affinity (O'Toole et al., 1995; Williams et al., 1994). In response to intracellular signals from the mitogen-activated protein (MAP) kinase and PI3K pathways, intracellular proteins bind to the integrin cytoplasmic domains causing a change in the spatial relationship between the α and β subunit tails (Loftus and Liddington, 1997; Williams et al., 1994). This spatial rearrangement disrupts the membrane-proximal hinge (Loftus and Liddington, 1997; Williams et al., 1994), triggering a long-range conformational change that traverses the transmembrane domain to the extracellular region of the integrin thus exposing the ligand binding site (Du et al., 1993). Hence the integrin is activated and in a high-affinity state.

Extracellular factors that regulate integrin affinity include divalent cations and monoclonal Abs (mAbs). Three cations are involved in integrin affinity modulation: Ca^{2+}, Mg^{2+}, and Mn^{2+} (Sanchez-Mateos et al., 1996). The effect of Ca^{2+} on integrin affinity can be inhibitory

or stimulatory, depending on the specific integrin-ligand interaction (Longhurst and Jennings, 1998). In contrast, Mg^{2+} and Mn^{2+} both activate integrins, with Mn^{2+} being the more potent activator of the two cations (Sanchez-Mateos et al., 1996). A mechanism for cation-induced β1 integrin activation has been proposed (Sanchez-Mateos et al., 1996). In the absence of extracellular divalent cations, β1 integrins are in an inactive state that prevents ligand binding. Upon addition of Ca^{2+}, β1 integrins undergo a transition from an inactive to a minimally-active state, but still cannot bind ligands. Upon further addition of Mg^{2+}, β1 integrins are converted from a minimally-active to a partially-active state. It is in this state that β1 integrins can initiate low-affinity ligand binding. For maximum ligand binding to occur, the addition of Mn^{2+} and the removal of Ca^{2+} must follow. These changes result in the conversion of β1 integrins from a partially-active state to a fully-active, high-affinity conformation. Similar to divalent cations, a group of mAbs called activating mAbs can induce integrin activation. Activating mAbs for β1, β2, and β3 integrin families have been described (Arroyo et al., 1993; Frelinger et al., 1991; Ortlepp et al., 1995). Several β1 integrin activating mAbs bind to a conserved regulatory region located between two ligand binding motifs expressed on inactive β1 integrins (Takada and Puzon, 1993). Because this regulatory region contains a structural motif that permits a sharp reversal of polypeptide chain orientation, activating mAb binding is proposed to induce a conformational change in the ligand binding motif that increases integrin affinity (Takada and Puzon, 1993).

1.4.2.5.2 *Integrin avidity*

Integrin avidity modulation refers to a change in the surface density of integrins that affects ligand binding (Hughes and Pfaff, 1998). Because changes in integrin distribution generally occur after ligand binding, integrin avidity is often described as a post-receptor

occupancy event (Sanchez-Mateos et al., 1996). Following ligand binding, integrin interaction with the cytoskeleton results in anchorage of the integrin at a given site, thus altering the integrin diffusion rate within the plasma membrane (Lub et al., 1995; Stewart and Hogg, 1996). Localization of additional integrins to these sites results in focal adhesion formation and integrin clustering (Lo and Chen, 1994). Hence integrin avidity is enhanced without a change in integrin affinity (Sanchez-Mateos et al., 1996). A mechanism of integrin clustering independent of ligand binding has been described. This mechanism involves inside-out signaling pathways that when activated, induce a redistribution of cytoskeletal proteins that interact with integrin cytoplasmic domains to effect integrin clustering (Sanchez-Mateos et al., 1996). Phorbol esters, for example, can activate PKC, which in turn induces actin cytoskeletal reorganization that increases β1 and β2 integrin avidity, not affinity (Danilov and Juliano, 1989; Haverstick et al., 1992).

1.4.2.6 Endothelial integrins

Integrins play an important role in vascular development and angiogenesis (Brooks, 1996). Endothelial cells express αvβ3, αvβ5, α6β4, and β1 integrins (α1-6) (Bischoff, 1997; Hiran et al., 2003). Among these, αvβ3, αvβ5, and β1 integrins have been shown to be required for angiogenesis (Bloch et al., 1997; Brooks, 1996; Eliceiri and Cheresh, 1999). Quiescent endothelial cells express low levels of αvβ3 (Eliceiri and Cheresh, 1998). In contrast, endothelial cells of sprouting blood vessels in vivo express upregulated αvβ3 (Brooks et al., 1994a; Brooks et al., 1994b). Both FGF-2 and VEGF can induce αvβ3 expression in endothelial cells (Brooks et al., 1994b). One function of αvβ3 during angiogenesis may be to promote endothelial cell survival. Function-blocking αvβ3 Abs induce apoptosis of endothelial cells within sprouting vessels in vivo (Brooks et al., 1994b). Furthermore, binding of αvβ3 to ligand increases expression of the anti-apoptotic protein Bcl-2, resulting in enhanced cell survival (Stromblad et

al., 1996). A second function of αvβ3 during angiogenesis may be to promote endothelial cell migration. Specifically, αvβ3 has been shown to bind (Brooks et al., 1996) and localize MMP-2 to the endothelial cell surface (Varner et al., 1995). The role of αvβ5 during angiogenesis is less well known compared to that of αvβ3. Nonetheless, VEGF-induced angiogenesis, and to a lesser extent FGF-2-induced angiogenesis, may require αvβ5 integrins (Friedlander et al., 1995).

Ligation of β1 integrins to four different ECM proteins may modulate the angiogenic response. Specifically, β1 integrins bind to (i) collagen type I, which may regulate endothelial cell adhesion and migration; (ii) fibronectin, which may induce endothelial expression of MMPs; (iii) collagen type IV, which may promote endothelial cell morphogenesis during lumen formation; and (iv) laminin, which may promote endothelial cell differentiation (Brooks, 1996).

1.4.3 Cadherins

1.4.3.1 Overview of the cadherin family

Cadherins constitute a family of transmembrane proteins that primarily function to mediate cell-cell adhesion (Takeichi, 1991). All cadherin family members contain at least one cadherin repeat, a conserved sequence of approximately 110 amino acids that independently folds into an extracellular structural domain (Takeichi, 1990). Each cadherin repeat requires extracellular Ca^{2+} for proper folding, thus conferring rigidity upon the cadherin extracellular domain (Koch et al., 1999) and protection from protease digestion (Grunwald et al., 1981). Cadherin family members can be divided into five subfamilies: (i) classical cadherins, which indirectly link the actin filaments of adjacent cells together in structures called adherens junctions; (ii) desmosomal cadherins, which indirectly link the intermediate filaments of adjacent cells together in structures called desmosomes; (iii) protocadherins, which mediate the formation

of synapses between neurons; (iv) Flamingo cadherins, which are seven-pass transmembrane proteins whose function in mammals remains largely unknown; and (v) cadherin-related proteins, which are unique cadherins that do not fall into the above defined subfamilies (Wheelock and Johnson, 2003). Classical cadherins can be further divided into type I and type II cadherins, based on the presence of an extracellular histidine-alanine-valine (HAV) tripeptide in type I cadherins and the lack thereof in type II cadherins (Wheelock and Johnson, 2003).

1.4.3.2 E-cadherin structure and function

Epithelial (E)-cadherin is a type I classical cadherin that primary functions to mediate cell-cell adhesion between epithelial cells (Wheelock and Johnson, 2003). E-cadherin expression is not restricted to epithelial cells; expression in non-epithelial cells such as erythroid precursors and stromal cells has been reported (Corn et al., 2000). The functional significance of this expression, however, is unknown (Corn et al., 2000). E-cadherin possesses a large N-terminal extracellular domain, a single-pass transmembrane domain, and a C-terminal intracellular domain (Wheelock and Johnson, 2003) (Figure 1.7). The extracellular domain contains five tandem cadherin repeats, each bridged by a Ca^{2+} cation that plays a role in proper protein folding.

The binding specificity of E-cadherin has been mapped to the first cadherin repeat (Overduin et al., 1995). This cadherin repeat contains the HAV tripeptide, which has been shown to be required for cadherin-mediated cell-cell adhesion (Overduin et al., 1995). Cadherin molecules can interact with each other both in cis and in trans (He et al., 2003). Two types of trans-interactions have been described. Homophilic interactions involve the binding of a cadherin molecule on one cell with an identical cadherin molecule on an adjacent cell (Jiang, 1996). Heterophilic interactions involve the binding of a cadherin molecule on one cell with a different

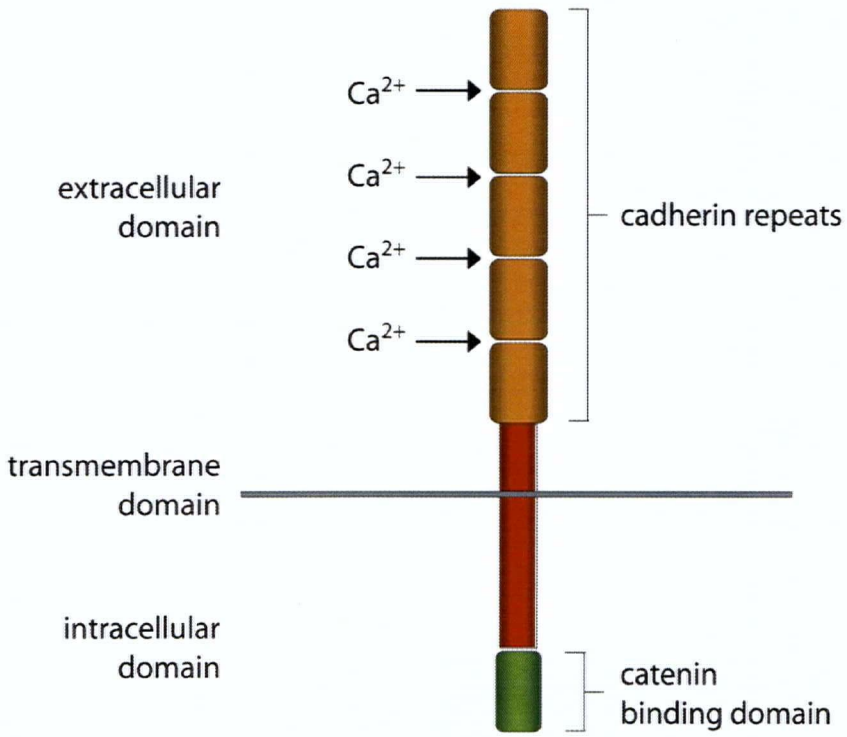

Figure 1.7: Structure of E-cadherin. E-cadherin is composed of an N-terminal extracellular domain, a single-pass transmembrane domain, and a C-terminal intracellular domain. The extracellular domain contains five tandem copies of a cadherin repeat, each bridged by a Ca^{2+} cation that plays a role in proper protein folding. The intracellular domain contains a catenin binding domain.

cadherin molecule on an adjacent cell (Jiang, 1996). In the epithelium, strong cell-cell adhesion is mediated by E-cadherin homophilic interactions (Jiang and Mansel, 2000).

For effective epithelial cell-cell adhesion to occur, the cytoplasmic domain of E-cadherin must be linked to the actin cytoskeleton (Alberts et al., 2002). E-cadherin cannot directly interact with the actin cytoskeleton; rather, this interaction is mediated by a group of cytoplasmic proteins called catenins (Ozawa et al., 1989) (Figure 1.8). Three catenins have been shown to bind the cytoplasmic domain of E-cadherin: β-catenin, γ-catenin, and p120-catenin (Ozawa et al., 1989; Reynolds et al., 1994). β- and γ-catenin bind to the catenin-binding domain present in the E-cadherin cytoplasmic domain in a mutually exclusive manner, and hence can substitute for each other during adherens junction formation (Nieset et al., 1997; Wheelock et al., 2001). In contrast, p120-catenin does not appear to play a structural role in adherens junctions (Thoreson et al., 2000). A fourth catenin, called α-catenin, does not directly interact with E-cadherin but instead binds to β- or γ-catenin (Wheelock and Johnson, 2003). α-catenin in turn interacts with actin filaments either directly or indirectly (via the binding of actin-binding proteins such as α-actinin or vinculin), thus linking the E-cadherin-catenin complex to the cytoskeleton (Wheelock and Johnson, 2003). In addition to playing a structural role in cell-cell adhesion, catenins participate in downstream signaling pathways that modulate cellular responses. Hence E-cadherin has been linked to the regulation of numerous cellular processes including cell proliferation (Gottardi et al., 2001; Kantak and Kramer, 1998; Sasaki et al., 2000; St Croix et al., 1998; Stockinger et al., 2001) and cell survival (Day et al., 1999; Kantak and Kramer, 1998; St Croix et al., 1996; St Croix and Kerbel, 1997).

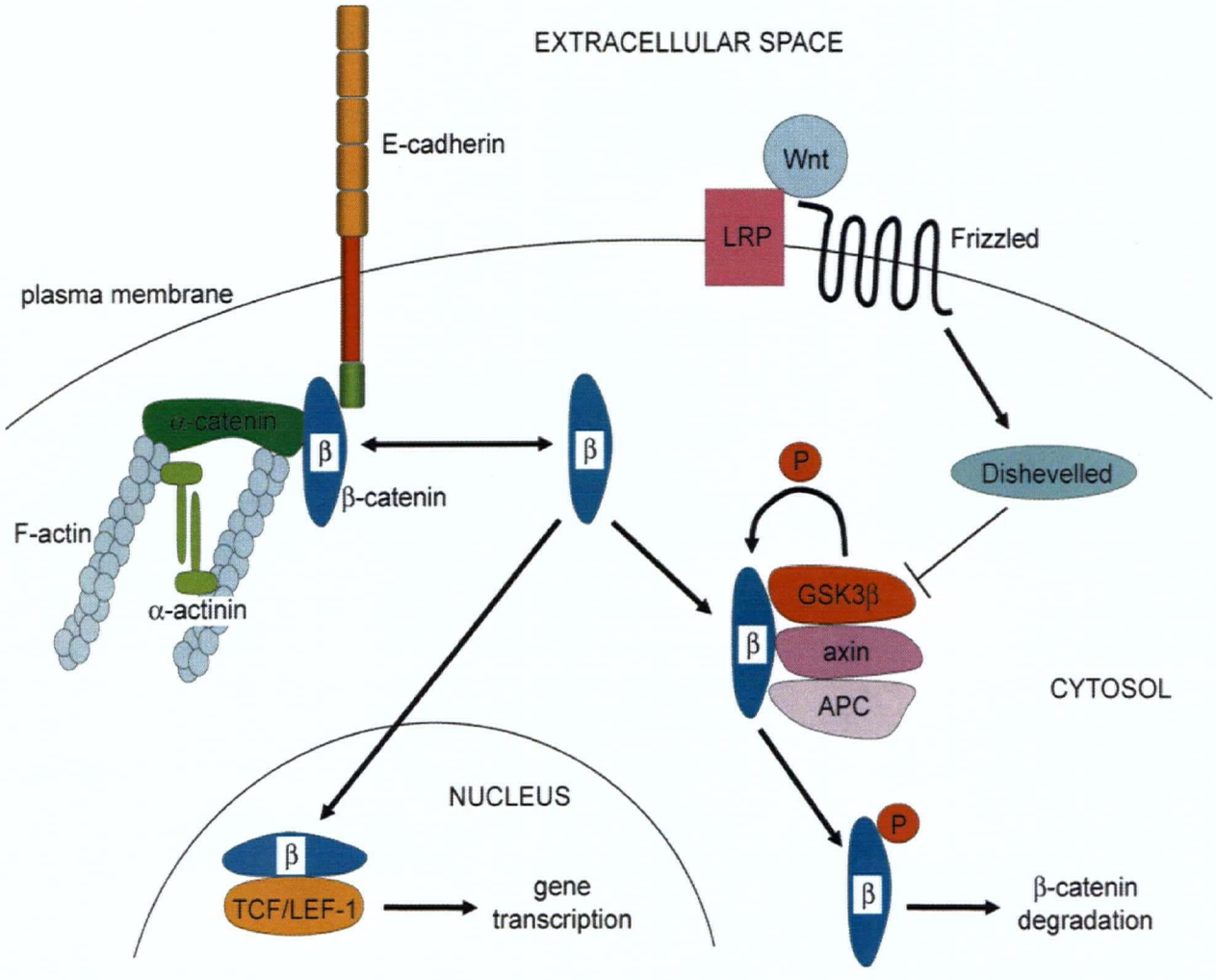

Figure 1.8: The β-catenin signaling pathway. β-catenin is localized to two cellular pools, at the cell surface and in the cytosol. At the cell surface, β-catenin binds to E-cadherin. E-cadherin-bound β-catenin in turn binds to α-catenin, which interacts with actin filaments either directly or indirectly (via the binding of actin-binding proteins such as α-actinin). Hence adherens junctions are formed, which effectively link the E-cadherin cytoplasmic domain to the actin cytoskeleton. β-catenin that is not bound to E-cadherin is found in the cytosol. In the cytosol, the stability of β-catenin is regulated by the Wnt signaling pathway. In the absence of Wnt signaling, β-catenin associates with a macromolecular complex composed of GSK3β, axin, and APC. This macromolecular complex promotes the phosphorylation (P) of β-catenin, resulting in β-catenin ubiquitination and subsequent degradation by the proteasome. In contrast, when Wnt ligand is present, Wnt binds to the receptor molecules Frizzled and LRP to form a ternary complex. This ternary complex activates Dishevelled, which in turn inactivates GSK3β. Hence GSK3β is unable to phosphorylate β-catenin, resulting in β-catenin stabilization and accumulation in the cytosol. Cytosolic β-catenin eventually translocates into the nucleus and binds to the transcription factor TCF/LEF-1, resulting in gene transcription.

1.4.3.3 E-cadherin downstream signaling

Signaling pathways mediated by β-catenin have been extensively studied. β-catenin is localized to two cellular pools: (i) at the cell surface, in adherens junctions that mediate cell-cell adhesion; and (ii) in the cytosol (Nusse, 1997; Papkoff et al., 1996) (Figure 1.8). An equilibrium exists between cell surface and cytosolic pools of β-catenin (Eger et al., 2000; Sanson et al., 1996; Zhu and Watt, 1999). In the cytosol, the stability of β-catenin is regulated by the wingless-type (Wnt) signaling pathway (Nelson and Nusse, 2004). The mammalian Wnt protein family consists of 19 secreted ligands that control cell proliferation, migration, and morphology (Nelson and Nusse, 2004). In the absence of Wnt signaling, β-catenin associates with a macromolecular complex composed of glycogen synthase kinase 3β (GSK3β) and adenomatous polyposis coli (APC), held together by the scaffold protein axin (Ikeda et al., 1998; Kishida et al., 1998; Nelson and Nusse, 2004). GSK3β is a serine/threonine kinase that, when phosphorylated and in an active state, directly binds to and induces phosphorylation of β-catenin (Aberle et al., 1997; Orford et al., 1997). This results in β-catenin ubiquitination and subsequent degradation by the proteasome (Aberle et al., 1997; Orford et al., 1997). GSK3β can also bind and phosphorylate the tumor suppressor protein APC (Rubinfeld et al., 1996). Phosphorylated APC in turn exhibits increased binding to β-catenin, resulting in augmented GSK3β-mediated phosphorylation and degradation of β-catenin (Rubinfeld et al., 1996). Hence β-catenin not associated with cadherins at the cell membrane is rapidly phosphorylated and targeted for degradation (Nelson and Nusse, 2004).

In the presence of Wnt signaling, β-catenin phosphorylation and degradation is inhibited (Nelson and Nusse, 2004). This involves the binding of a secreted Wnt ligand to two receptor molecules, Frizzled and low density lipoprotein (LDL) receptor-related protein (LRP), resulting in a Wnt-Frizzled-LRP ternary complex (Nelson and Nusse, 2004). Through an unknown

mechanism, this ternary complex activates the downstream signaling protein Dishevelled, which in turn directly dephosphorylates and inactivates GSK3β (Nelson and Nusse, 2004). Dishevelled can also recruit GSK-binding protein (GBP), which effectively inactivates GSK3β (Hatsell et al., 2003). Hence GSK3β is unable to phosphorylate β-catenin, resulting in β-catenin stabilization and accumulation in the cytosol (Jiang and Mansel, 2000).

β-catenin accumulation in the cytosol eventually leads to its nuclear translocation (Jiang and Mansel, 2000). Within the nucleus, β-catenin binds to the transcription factor T-cell factor/lymphoid enhancer factor-1 (TCF/LEF-1) (Cadigan and Nusse, 1997). Nuclear β-catenin can also bind to the transcriptional coactivator Pontin52, which may promote the interaction between β-catenin and TCF/LEF-1 (Bauer et al., 1998). The β-catenin-TCF/LEF-1 complex, via transactivation domains provided by β-catenin and a sequence-specific DNA binding domain provided by TCF/LEF-1, initiates transcription of downstream target genes (Hsu et al., 1998; van de Wetering et al., 1997). These include the cell proliferation genes c-myc (He et al., 1998) and cyclin-D1 (Lin et al., 2000), invasion-related genes uPAR (Mann et al., 1999) and MMP-7 (Roose et al., 1999), multidrug resistance gene-1 (MDR-1) (Yamada et al., 2000), E-cadherin transcriptional repressor protein Slug (Conacci-Sorrell et al., 2003), adhesion-related proteins ZO-1 (Mann et al., 1999) and conductin (Jho et al., 2002), components of the transcription factor complex activator protein-1 (AP-1) (Mann et al., 1999), and the transcription factor TCF/LEF-1 (resulting in a positive feedback loop) (Hovanes et al., 2001).

1.5 EPITHELIAL-TO-MESENCHYMAL TRANSITION (EMT)

1.5.1 Physiological EMT

During embryonic development, a fertilized egg divides repeatedly to give rise to numerous epithelial cells which cohere to form epithelial organs (Alberts et al., 2002). In addition to epithelial cells, however, a second cell type with a distinct shape and organization can be recognized (Thiery, 2002). These cells, called mesenchymal cells, exhibit reduced adherence and are found loosely embedded in the ECM which facilitates migration in the extracellular environment (Thiery, 2002). Developmental studies have determined that epithelial cells can undergo a morphological conversion into mesenchymal cells, via a process called EMT (Hay, 1995). Following EMT, mesenchymal cells depart their site of origin and migrate to new microenvironments, where they differentiate into diverse cell types that participate in organ development (Savagner, 2001). Hence EMT is a conserved and fundamental process that governs cellular morphogenesis in multicellular organisms (Thiery, 2002). EMT plays an essential role during embryogenesis, including development of the heart, peripheral nervous system, musculoskeletal system, and most craniofacial structures (Thiery, 2002). In the adult, a partial EMT is required during wound healing, in which keratinocytes exhibit a transient migratory phenotype that facilitates re-epithelialization at the injured site (Paladini et al., 1996). Numerous cytokines have been shown to induce EMT, including EGF, HGF, FGF, and transforming growth factor β (TGFβ) (Savagner, 2001).

1.5.2 Pathological EMT

By virtue of its ability to increase cellular invasiveness, EMT functions as a mechanism for the dissemination of cancer cells during tumor metastasis. Because E-cadherin expression

plays a role in the maintenance of the differentiated epithelial phenotype (Thiery, 2002), E-cadherin functions as a tumor suppressor protein (Berx et al., 1998). During EMT, epithelial cells undergo a dedifferentiation program associated with loss of E-cadherin expression (Thiery, 2002). Indeed, a direct correlation exists between loss of E-cadherin expression and loss of the epithelial phenotype (Behrens et al., 1989). Well-differentiated and less-invasive tumors generally express high E-cadherin levels (Gupta et al., 1997; Oka et al., 1993). Partial/complete loss of E-cadherin expression, in contrast, correlates with loss of differentiation, increased invasiveness and metastasis, increased tumor grade, and poor prognosis (Cadigan and Nusse, 1997; Daniel and Reynolds, 1997; Miller et al., 1999; Polakis et al., 1999).

1.5.2.1 Mechanisms of E-cadherin silencing

Silencing of E-cadherin expression can occur via genetic, epigenetic, and post-translational mechanisms. One genetic mechanism involves mutation of the E-cadherin gene, cadherin (CDH)-1 (Berx et al., 1998). The types of mutations reported include missense mutations, splice site mutations, and truncation mutations (Berx et al., 1998). Thus far, 74 distinct mutation sites in CDH-1 have been identified in various cancer cell lines and tumors (Berx et al., 1998; Berx et al., 1995a). CDH-1 mutation frequently occurs in combination with a second genetic mechanism of E-cadherin silencing, gene deletion, resulting in complete loss of E-cadherin expression (Berx et al., 1998). A third genetic mechanism for E-cadherin silencing involves single nucleotide polymorphism (SNP) (Li et al., 2000). The CDH-1 promoter contains a SNP site located 160 bases upstream of the transcription start site (Li et al., 2000). At this SNP site, the wildtype CDH-1 allele contains a cytosine whereas the polymorphic allele contains an adenine (Li et al., 2000). Although one study has reported a 70% reduction in E-cadherin

transcription in vitro due to the polymorphism (Li et al., 2000), another study has failed to find a relationship between the polymorphism and reduced E-cadherin expression (Cheng et al., 2001).

Two epigenetic mechanisms of E-cadherin silencing directly addressed in this thesis include transcriptional repressor protein expression (Hennig et al., 1996) and promoter hypermethylation (Herman and Baylin, 2003). Transcriptional repressors that inhibit E-cadherin expression include Snail, Slug, Smad-interacting protein 1 (SIP1; also known as ZEB2), delta-crystallin/E2-box factor 1 (delta-EF1; also known as ZEB1), E2A, and Twist (Hajra and Fearon, 2002; Yang et al., 2004). These proteins mediate active repression of E-cadherin expression by binding to E box motifs (CAGGTG) within the CDH-1 promoter. Nuclear β-catenin-TCF/LEF-1 complexes have also been reported to bind and repress the CDH-1 promoter (Jamora et al., 2003). DNA methylation inhibits gene transcription by inducing chromatin condensation, which prevents transcription factor access to gene promoters (Herman and Baylin, 2003). Methylation can occur on cytosine residues at CpG dinucleotides (cytosine and guanine nucleotides linked together by a phosphate bond), which are distributed throughout the genome but exhibit frequent clustering in small stretches of DNA called CpG islands (Herman and Baylin, 2003). The CDH-1 gene contains a CpG island within its promoter which, when hypermethylated, results in reduced E-cadherin transcription (Berx et al., 1995b). Of importance to this thesis is that both transcriptional repressor protein expression and promoter hypermethylation induce reversible downregulation of E-cadherin expression (Conacci-Sorrell et al., 2002), and thus represent targets for reversal of EMT.

E-cadherin silencing can also be mediated by post-translational mechanisms such as E-cadherin shedding (Katayama et al., 1994) and endocytosis (Fujita et al., 2002), which both effectively remove E-cadherin from the cell surface during normal protein turnover.

1.5.2.2 E-cadherin downregulation in breast cancer

One of the best markers of EMT associated with breast cancer progression is the loss of E-cadherin expression (Vincent-Salomon and Thiery, 2003). Two major histological subtypes of breast cancer are ductal and lobular carcinomas (Vincent-Salomon and Thiery, 2003). Although studies suggest a common molecular origin for ductal and lobular tumors, they are morphologically distinct (Roylance et al., 1999). Whereas ductal tumor cells grow in clusters as sheets or cords, lobular tumor cells remain isolated or form narrow cords (Vincent-Salomon and Thiery, 2003). This difference in morphology can be explained by differences in total E-cadherin expression. In ductal tumors, approximately 50% express E-cadherin protein at normal levels with the remaining 50% expressing reduced levels (Gamallo et al., 1993; Moll et al., 1993). In contrast, 85% of lobular tumors exhibit a complete loss of E-cadherin protein expression (De Leeuw et al., 1997). The remaining 15% of lobular tumors that maintain E-cadherin expression nonetheless exhibit abnormal localization of the protein (De Leeuw et al., 1997). Hence E-cadherin downregulation can occur in both ductal and lobular breast cancer, although complete loss of E-cadherin is more common in lobular tumors.

Mechanisms to explain the downregulation of E-cadherin expression in ductal and lobular breast cancers have been identified. Many genetic factors play a role in E-cadherin silencing in breast cancer. Polymorphism in the CDH-1 promoter does not affect E-cadherin expression in ductal or lobular breast tumors, and hence does not confer an increased risk of developing either tumor type (Cheng et al., 2001; Lei et al., 2002). Gene deletion at the CDH-1 locus occurs frequently in both ductal and lobular breast cancer (Berx et al., 1996; Cleton-Jansen et al., 2001). However, an association between gene deletion and decreased E-cadherin expression is evident in lobular (Berx et al., 1996; Cleton-Jansen et al., 2001) but not ductal (De

Leeuw et al., 1997) breast tumors. CDH-1 gene mutations are more common in lobular than ductal breast cancer. In lobular breast tumors, the frequency of CDH-1 gene mutation ranges from 10-56% (Lei et al., 2002). In contrast, ductal breast tumors exhibit CDH-1 mutation frequencies from 0-5% (Kashiwaba et al., 1995; Lei et al., 2002). Genetic factors may work in conjunction with epigenetic factors to modulate E-cadherin expression in breast cancer. Upregulated expression of the E-cadherin transcriptional repressor protein Snail is sufficient to repress E-cadherin transcription (Hajra et al., 2002) and induce EMT in vitro (Cano et al., 2000), and has been reported in high-grade human breast tumors (Blanco et al., 2002). Normal breast epithelia do not display CDH-1 promoter methylation (Graff et al., 1995). In contrast, 50% of ductal tumors (Graff et al., 2000; Nass et al., 2000) and between 41-77% of lobular tumors (Droufakou et al., 2001; Sarrio et al., 2003) exhibit CDH-1 promoter methylation. Overall, these studies demonstrate that both genetic and epigenetic factors contribute to E-cadherin downregulation in breast cancer.

1.5.3 Notch and EMT

Notch target genes are expressed at sites of epithelial-mesenchymal cell-cell interactions during embryogenesis (Mitsiadis et al., 1995; Nakagawa et al., 1999). In an immortalized human keratinocyte cell line, TGFβ stimulation has been shown to induce EMT with an associated downregulation of E-cadherin protein expression (Zavadil et al., 2004). Treatment with antisense HRT1 or functional inactivation of Jagged1, however, inhibits TGFβ-induced downregulation of E-cadherin expression (Zavadil et al., 2004). Although the latter study suggests that Notch signaling may be required for TGFβ-induced EMT in keratinocytes, a direct role for activated Notch signaling in the induction of EMT has not been reported. Recent studies have identified a role for Notch signaling in a specialized type of EMT, endothelial-to-mesenchymal transition

(EndoMT). During murine cardiac development, cardiac endothelial cells (endocardial cells) must undergo a transient EndoMT (Eisenberg and Markwald, 1995). This gives rise to mesenchymal cells that participate in the formation of the endocardial cushion, a specialized embryonic tissue from which the heart valves and septa develop (Eisenberg and Markwald, 1995). In wildtype mice, EndoMT occurs at E9.5 and coincides with Notch1 mRNA expression in both endocardial and mesenchymal cushion cells (Timmerman et al., 2004). In Notch1-null mice, however, endocardial cells remain tightly associated and mesenchymal cells within the cardiac cushion are noticeably absent (Timmerman et al., 2004). A similar phenotype is observed in CBF1-null mice (Timmerman et al., 2004). Hence activated Notch signaling may be required for EndoMT during cardiac development.

During EndoMT, endothelial cells can acquire a migratory phenotype by downregulating the expression of the cell-cell adhesion protein vascular endothelial (VE)-cadherin (Frid et al., 2002). Both VE-cadherin and E-cadherin belong to the classical cadherin subfamily (Wheelock and Johnson, 2003). In porcine aortic endothelial cells, overexpression of activated Notch1 downregulates VE-cadherin expression and induces morphological transformation (Timmerman et al., 2004). Notch signaling may indirectly downregulate VE-cadherin expression via induction of the transcriptional repressor protein Snail. By in vitro luciferase assays, activated Notch1 induces Snail promoter activity, and Snail expression inhibits VE-cadherin promoter activity (Tan et al., 2001; Timmerman et al., 2004). An inverse correlation between Notch and VE-cadherin expression has also been described during murine cardiac development in vivo. In wildtype mouse embryos between E8.5-9.0, VE-cadherin mRNA expression is evident throughout the endocardium (Timmerman et al., 2004). At E9.5, which corresponds to the time of initiation of EndoMT, regions of the endocardium displaying increased Notch1 mRNA

expression also display increased Snail mRNA expression, with a corresponding decrease in VE-cadherin mRNA expression (Timmerman et al., 2004). In contrast, Notch1- or CBF1-null mice at E9.5 exhibit reduced endocardial expression of Snail mRNA and maintained expression of VE-cadherin mRNA (Timmerman et al., 2004). These results suggest that Notch signaling may be required for the downregulation of endocardial cell-cell adhesion during EndoMT.

Research from our laboratory has demonstrated that Notch activation can induce EndoMT in human endothelial cells (Noseda et al., 2004b). Activated Notch4 induces phenotypic changes consistent with EndoMT such as the downregulation of VE-cadherin and the upregulation of various mesenchymal markers (Noseda et al., 2004b). Moreover, cells expressing activated Notch4 exhibit increased migration towards platelet-derived growth factor, a known chemotactic factor for mesenchymal cells (Noseda et al., 2004b). Expression of activated Notch1 or Jagged1 also induces EndoMT (Noseda et al., 2004b). Combined with the fact that Jagged1, Notch1, and Notch4 mRNAs are all expressed in the embryonic murine heart at sites of EndoMT during cardiac development (Noseda et al., 2004b), these results raise the possibility that Jagged1-Notch interactions may induce EndoMT in vivo.

1.6 AIMS OF THE STUDY

It is well known that members of the Notch family of transmembrane receptors play an important role in the regulation of cell fate decisions and differentiation (Artavanis-Tsakonas et al., 1999). At the start of this thesis, several gene disruption studies from mice suggested a role for Notch and its ligands in the regulation of embryonic vascular development (Hrabe de Angelis et al., 1997; Huppert et al., 2000; Xue et al., 1999). Because Notch4 is primarily expressed on the endothelium (Li et al., 1998a; Uyttendaele et al., 1996), we investigated whether enforced expression of activated Notch4 in endothelial cells could inhibit endothelial sprouting in vitro

and angiogenesis in vivo. During the course of our experiments, two separate studies reported that both increases and decreases in Notch signaling result in a common vascular phenotype, disrupted embryonic blood vessel development (Krebs et al., 2000; Uyttendaele et al., 2001). Our studies demonstrate that increased Notch signaling disrupts endothelial sprouting in vitro and angiogenesis in vivo, and more importantly, provide a mechanism with which to explain the common effects of activated and inhibited Notch signaling on angiogenesis.

Recent studies from our laboratory and others have shown that activation of Notch signaling promotes EndoMT, a specialized type of EMT (Noseda et al., 2004b; Timmerman et al., 2004). Although Notch pathway elements are expressed at embryonic sites of epithelial-mesenchymal cell-cell interactions (Mitsiadis et al., 1995; Nakagawa et al., 1999), a direct role for activated Notch signaling in the induction of EMT has not been reported. Given that E-cadherin downregulation directly correlates with EMT in human breast cancer (Thiery, 2002), and that primary human breast cancers express elevated levels of Notch receptors (Callahan and Egan, 2004; Imatani and Callahan, 2000; Parr et al., 2004; Pece et al., 2004; Weijzen et al., 2002), we investigated whether activated Notch signaling would inhibit E-cadherin expression in human breast epithelial cells. We also sought to determine whether inhibition of Notch signaling would re-induce E-cadherin expression in human breast cancer cells previously lacking E-cadherin expression. Together, these experiments would better our understanding of the role of Notch signaling in EMT and breast cancer development.

Overall, two major hypotheses were tested in this thesis: (1) Expression of activated Notch4 in endothelial cells inhibits angiogenesis in part by promoting β1 integrin-mediated adhesion; (2) Inhibition of Notch signaling attenuates breast tumor growth by reversing the mesenchymal phenotype.

Chapter 2

MATERIALS AND METHODS

2.1 TISSUE CULTURE

2.1.1 Cell culture

The human dermal microvascular endothelial cell line HMEC-1 (referred to hereafter as HMEC), transformed with simian virus 40 (SV40) large T antigen (Ades et al., 1992), was provided by the Centers for Disease Control and Prevention (Atlanta, GA). HMEC cell lines were cultured in MCDB 131 medium (Sigma, St. Louis, MO) supplemented with 10% heat-inactivated fetal calf serum (FCS; HyClone, Logan, UT), 10 μg/ml EGF (Sigma), and 100 units/ml each of penicillin and streptomycin (Gibco, Gaithersburg, MD). The avian retroviral packaging cell line Q2bn (gift of K. McNagny, University of British Columbia, Vancouver, BC, Canada) was cultured in Dulbecco's modified Eagle's medium (DMEM; Sigma) supplemented with 10% non-heat-inactivated FCS, 2.5% non-heat-inactivated chicken serum (Sigma), 60 μg/ml conalbumin (Sigma), 50 μM β-mercaptoethanol (Sigma), 2 mM glutamine (Gibco), and 100 units/ml each of penicillin and streptomycin.

The human breast epithelial cell line MCF-10A (gift of P. Sorensen, University of British Columbia) was cultured in a 1:1 mixture of DMEM/F12 (Sigma) supplemented with 5% horse serum (Sigma), 2 mM glutamine, 20 ng/ml EGF, 100 ng/ml cholera toxin (Cedarlane, Hornby, ON, Canada), 10 μg/ml insulin (Sigma), 500 ng/ml hydrocortisone (Sigma), and 100 units/ml each of penicillin and streptomycin. Primary human breast epithelial cells were cultured in Epicult™-B medium (StemCell Technologies, Vancouver, BC, Canada) supplemented with 5% FCS. The human breast carcinoma cell lines MDA-MB-231 (gift of C.D. Roskelley, University

of British Columbia) and T47D (gift of J.T. Emerman, University of British Columbia) and the mouse Lewis lung carcinoma cell line (purchased from American Type Culture Collection, Manassas, VA) were cultured in DMEM supplemented with 10% heat-inactivated calf serum (HyClone), 2 mM glutamine, and 100 units/ml each of penicillin and streptomycin. All cells were maintained at 37°C in an atmosphere of 5% CO_2. Cells were passaged every 3 days by rinsing in phosphate-buffered saline (PBS) and incubating in 0.25% trypsin/1 mM ethylenediaminetetraacetic acid (EDTA; Sigma) for approximately 3 min, followed by replating into tissue culture dishes in new medium.

2.1.2 Primary human breast epithelial cell isolation

Primary human breast epithelial cells were obtained in collaboration with Dr. C. Eaves of the Terry Fox Laboratories (British Columbia Cancer Research Centre, Vancouver, BC, Canada). Discarded tissues from normal premenopausal women undergoing reduction mammoplasty surgeries were enzymatically digested and epithelial cell-enriched fractions were frozen until use, at which time single-cell suspensions were prepared (Stingl et al., 2001). Cells were co-cultured with 1.2 x 10^6 X-irradiated NIH3T3 mouse fibroblasts for 1 day in Epicult™-B medium supplemented with 5% FCS. Following preparation of a single-cell suspension, epithelial cell adhesion molecule (EpCAM)-positive breast epithelial cells were magnetically separated using the human EpCAM selection cocktail EasySep™ (StemCell Technologies), and cultured at a density of 2 x 10^5 cells/plate in 35 mm plates. These 35 mm plates were pre-coated with 2-3 ml Vitrogen™ (67 μg/ml in PBS; Cohesion Technologies, Palo Alto, CA) for 1 hour at 37°C, and washed with PBS prior to use.

2.1.3 Gene transfer

HMEC overexpressing the Notch4 intracellular domain (HMEC-Notch4IC) and HMEC-LNCX cells were constructed by retroviral transduction of a C-terminal hemagglutinin (HA)-tagged human Notch4 cDNA (amino acids 1476-2003) or the empty pLNCX vector control, respectively (Li et al., 1998a). For retroviral transduction, constructs were transiently transfected into the retroviral packaging cell line AmphoPhoenix using Fugene™ 6 Transfection Reagent (Roche Diagnostic Corporation, Indianapolis, IN). Retroviral supernatants were used to transduce HMEC, and stable HMEC lines were obtained by selection in 300 μg/ml G418 (Gibco). Polyclonal HMEC lines were used to avoid artifacts due to retroviral integration site. Chicken retroviral expression vectors were constructed by inserting C-terminal HA-tagged human Notch4IC cDNA into the avian retroviral vector CK (gift of N. Boudreau, University of California, San Francisco, CA and M. Bissell, University of California, Berkeley, CA). Both CK-Notch4IC and the empty vector were transiently transfected into Q2bn cells using Fugene™ 6 Transfection Reagent to generate producer lines.

Retroviral vectors containing an internal ribosomal entry site (IRES) and either yellow fluorescent protein (YFP) or green fluorescent protein (GFP) were used to facilitate sorting of transduced cells. The MIYNotch1IC construct was generated by inserting into the retroviral vector murine stem cell virus (MSCV)-IRES-YFP (MIY, gift of R.K. Humphries, Terry Fox Laboratories) the cDNA encoding human Notch1 intracellular domain (Notch1IC; amino acids 1758 to 2556; gift of S. Artavanis-Tsakonas, Harvard Medical School, Cambridge, MA). The MIYNotch4ICHA construct was generated by inserting into the retroviral vector MIY the cDNA encoding human Notch4IC (amino acids 1476 to 2003) tagged with a C-terminal HA epitope. The MIGXNotch4HA construct was generated by inserting into the retroviral vector MSCV-

IRES-GFP (MIG) the cDNA encoding the entire extracellular domain of human Notch4 (XNotch4; amino acids 1 to 1443) tagged with a C-terminal HA epitope. The MIYE-cadherin construct was generated by inserting into the retroviral vector MIY the cDNA encoding full-length human E-cadherin (gift of B.M. Gumbiner, University of Virginia, Charlottesville, VA). Cells were transduced with empty vector control or vector containing cDNA inserts, and transduced cells were sorted based on YFP or GFP expression using a fluorescence-activated cell sorter (FACS® 440; Becton Dickinson, San Jose, CA).

2.2 PROTEIN ANALYSIS

2.2.1 Immunoblotting

Cultured cells were lysed in 50 mM Tris (Sigma), 150 mM NaCl (Sigma), 2% Triton® X-100 (Fisher Scientific, Suwannee, GA), 10 μg/ml soybean trypsin inhibitor (Sigma), and 200 μM phenylmethylsulfonyl fluoride (Sigma). Tumor tissues were homogenized on ice in 50 mM Hepes (Sigma) buffer, pH 7.6, containing 2% Triton X-100, 5 mM EDTA, and fresh protease inhibitor cocktail (Sigma). Protein concentration was determined using the D_C^{TM} protein assay (Bio-Rad Laboratories, Hercules, CA). Total protein lysates (50 μg) were analyzed by sodium dodecyl sulfate (SDS)- polyacrylamide gel electrophoresis, transferred to nitrocellulose membranes (Bio-Rad Laboratories), and developed by enhanced chemiluminescence (PerkinElmer Life Science, Boston, MA). Membranes were probed with mouse mAbs to HA (Sigma, 1:2000 dilution), E-cadherin (BD Transduction Laboratories, Mississauga, ON, Canada, 1:2500 dilution), total β-catenin (BD Transduction Laboratories, 1:1000 dilution), active β-catenin (Upstate, Lake Placid, NY, 1:500 dilution), and α-tubulin (Sigma, 1:10,000 dilution). Protein expression was quantitated by densitometry. For E-cadherin and total β-catenin

expression, data are presented as the mean ± standard error from (i) 16 MIG tumors and 13 MIGXNotch4HA tumors, and (ii) 12 MIY tumors and 12 MIYE-cadherin tumors. For active β-catenin expression, data are presented as the mean ± standard error from 14 MIG tumors and 11 MIGXNotch4HA tumors.

Concentrated supernatant from cultured cells was obtained by filtering 3 day conditioned medium through a 100,000 kDa molecular weight cut-off Ultrafiltration Membrane (Millipore, Billerica, MA).

2.2.2 Immunofluorescence microscopy

HMEC lines (5 x 10^4) were cultured on coverslips for 48 hours, fixed and permeabilized in cold methanol for 5 min. Non-specific binding was blocked by incubating with PBS containing 5% goat serum (Sigma) and 0.1% Tween® 20 (Fisher Scientific) for 30 min. Following incubation with primary antibody (Ab) (rabbit anti-HA polyclonal Ab, Covance, Princeton, NJ, 1:100 dilution) for 60 min and secondary Ab (Texas Red™-conjugated goat anti-rabbit IgG, Molecular Probes, Eugene, OR, 1:200 dilution) for 30 min, coverslips were mounted on glass slides using an anti-fading solution (FluoroGuard™ Antifade Reagent, Bio-Rad Laboratories) containing 100 ng/ml Hoechst 33258 (Sigma) to stain the nuclei.

MCF-10A cell lines (1 x 10^5) were cultured in chamber culture slides for 7 days. Primary breast epithelial cells (1 x10^5) were cultured in chamber culture slides pre-coated with Vitrogen™ (67 μg/ml in PBS) for 11 days. Cells were washed twice with PBS, fixed in 4% paraformaldehyde (Sigma) in PBS for 10 min, and blocked in PBS containing 10% goat serum for 10 min. Following incubation with mouse mAb to extracellular E-cadherin (10 μg/ml, Chemicon, Temecula, CA) at room temperature for 60 min, chambers were washed twice with PBS and incubated with goat anti-mouse AlexaFluor® 594 (Molecular Probes, 1:100 dilution) at

room temperature in the dark for 30 min. Chambers were washed twice with PBS, nuclei counterstained with 4',6-diamidino-2-phenylindole (DAPI; Sigma) for 5 min, and slides mounted with 50% glycerol.

Tumor cryosections (7 μm thick) were immunostained for E-cadherin, β-catenin, and CD31. For E-cadherin immunofluorescence microscopy, tissues were hydrated in PBS, fixed in 100% ice-cold methanol for 2 min, rinsed in PBS, permeabilized in methanol/acetone (1:1 v/v) for 2 min, rinsed in PBS, blocked in PBS containing 5% goat serum for 45 min, and stained with mouse mAb to E-cadherin (1:500 dilution). For β-catenin immunofluorescence microscopy, tissues were hydrated in PBS, fixed in 4% paraformaldehyde in PBS for 15 min, rinsed in PBS, permeabilized in 0.1% Triton® X-100 for 10 min, rinsed in PBS, blocked in PBS containing 5% goat serum for 45 min, and stained with mouse mAb to β-catenin (1:100 dilution). For CD31 immunofluorescence microscopy, tissues were hydrated in PBS, fixed in 4% paraformaldehyde in PBS for 15 min, rinsed in PBS, blocked in PBS containing 5% goat serum for 45 min, and stained with rat mAb to mouse CD31 (BD Pharmingen, Mississauga, ON, Canada, 1:100 dilution) for 30 min. Following two washes with PBS, tumor sections were incubated with the fluorochrome-conjugated secondary Abs goat anti-mouse AlexaFluor® 594 (1:100 dilution) or goat anti-rat AlexaFluor® 594 (Molecular Probes, 1:100 dilution), nuclei counterstained with DAPI, and slides mounted with Vectashield® (Vector Laboratories, Burlingame, CA). Immunofluorescence was detected with an Axioplan™ II imaging microscope (Carl Zeiss Canada, Toronto, ON, Canada), and images were captured with a 1350EX digital camera (QImaging, Burnaby, BC, Canada).

For quantitation of the percentage CD31 stained area, at least six random fields at 200x magnification were analyzed per tumor using Northern Eclipse™ software (Empix Imaging,

Mississauga, ON, Canada). Vascular density was quantitated by expressing the CD31 stained area as a percentage of the total tumor area. For quantitation of the number of vessels per mm^2, entire tumor sections were analyzed using Northern Eclipse™ software. For MDA-MB-231 tumors, data are expressed as the average percentage CD31 stained area ± standard error from 14 control tumors and 12 XNotch4 tumors, and the average number of vessels per mm^2 ± standard error from 13 control tumors and 16 XNotch4 tumors. For Lewis lung carcinoma tumors, data are expressed as the average percentage CD31 stained area ± standard error from seven control tumors and six XNotch4 tumors, and the average number of vessels per mm^2 ± standard error from 14 control tumors and 16 XNotch4 tumors.

For quantitation of percentage nuclear β-catenin staining, at least six random fields at 200x magnification were analyzed per tumor using Northern Eclipse™ software. Data are presented as the average percentage nuclear β-catenin staining (total number of nuclear β-catenin-positive cells / total number of cells) ± standard error from four control tumors and four XNotch4 tumors.

2.2.3 Immunohistochemistry

CAMs treated with transfected Q2bn cell lines were harvested from E12 embryos, and processed for histological analysis. For hematoxylin and eosin (H&E) staining, CAMs were fixed in formalin overnight at room temperature, dehydrated, and embedded in paraffin. 6 μm sections were cut and stained with H&E. For immunohistological analysis, CAMs were frozen in Tissue-Tek® optimal cutting temperature compound (Somagen Diagnostics, Edmonton, AB, Canada), and 10 μm sections cut and fixed in acetone for 10 min. Sections were hydrated and incubated in 1.5% hydrogen peroxide solution for 5 min to quench endogenous peroxide activity. Non-specific binding was blocked by incubating in goat serum (1:20 dilution) for 20 min. For

vWF staining, sections were incubated with primary Ab (DAKO, Mississauga, ON, Canada, 1:200 dilution), a biotinylated secondary Ab, followed by an avidin conjugate. For HA staining, sections were incubated with primary Ab (mouse anti-HA mAb, 1:500 dilution), secondary Ab (biotinylated goat anti-mouse IgG, DAKO, 1:200 dilution), followed by horseradish peroxidase-conjugated streptavidin (DAKO). Sections were developed with a diaminobenzidine-hydrogen peroxide reaction (Sigma), counterstained with hematoxylin, dehydrated, cleared, and mounted.

Tumor cryosections (7 μm thick) were stained with H&E or rabbit polyclonal Ab to HA (BAbCo, Richmond, CA). A biotinylated goat anti-rabbit IgG (Vector Laboratories, 1:100 dilution) followed by horseradish peroxidase-conjugated streptavidin (Vector Laboratories) were used, nuclei counterstained with hematoxylin, and slides mounted with Permount® (Fisher Scientific).

Immunohistochemistry was examined using an Axioplan™ II imaging microscope and images captured using either a Coolpix™ 990 (Nikon, Tokyo, Japan) or a 1350EX digital camera.

2.2.4 Flow cytometry

Cells were detached by incubation in PBS based enzyme-free cell dissociation buffer (Invitrogen, Carlsbad, CA) for 20 min at 37°C. To reduce nonspecific binding, cells were incubated in 10% heat-inactivated iron-supplemented calf serum (Sigma) in PBS for 30 min at 37°C. The following primary Abs were added to the cells and allowed to incubate at 37°C for 30 min: LM609 (Chemicon, 10 μg/ml), B44 (gift of J. A. Wilkins, University of Manitoba, Winnipeg, MB, Canada, 10 μg/ml), K20 (AMAC Inc., Westbrook, ME, 10 μg/ml), E-cadherin (10 μg/ml). Mouse IgG2a Ab (Sigma, 10 μg/ml) was used as a control. Cells were washed twice in cold PBS, and secondary Ab (goat anti-mouse IgG- fluorescein isothiocyanate (FITC), Sigma,

1:64 dilution; goat anti-mouse AlexaFluor® 594, 1:100 dilution) was added and allowed to incubate an additional 60 min in the dark on ice. After washing cells twice in cold PBS, cells were fixed in 4% paraformaldehyde. Samples were run on an EPICS® ELITE-ESP flow cytometer (Beckman Coulter, Fullerton, CA), and data were analyzed with WinList™ version 2.0 (Verity Software House Inc., Topsham, ME) or FCS Express™ V2 (De Novo Software, Thornhill, ON, Canada). Histograms presented for HMEC lines are from one experiment and are representative of at least three independent experiments. Histograms for MCF-10A cells are from one experiment and are representative of two independent experiments.

For the flow cytometric analysis of cell cycle distribution, HMEC lines were serum starved in 2% FCS in MCDB for 48 hours, and incubated for an additional 24 hours in medium alone (2% FCS in MCDB) or medium supplemented with FGF-2 (R&D Systems, Minneapolis, MN, 15 ng/ml) or $VEGF_{165}$ (R&D Systems, 15 ng/ml). For the last 2 hours of incubation, cells were incubated with 10 μM 5-bromo-2'-deoxyuridine (BrdU; Sigma) at 37°C. Cells were harvested by trypsinization and fixed in 70% ethanol at 4°C for 30 min. After washing in PBS, cells were incubated in 2 M HCl for 30 min to denature DNA, followed by neutralization in serum-free medium. Cells were blocked and permeabilized in 0.5% Triton® X-100 plus 4% calf serum, then incubated with anti-BrdU-FITC conjugated Ab (BD Pharmingen) for 1 hour. Washed cells were stained with 1 μg/ml DAPI in PBS containing 0.5% Triton® X-100. Samples were run on an EPICS® ELITE-ESP flow cytometer, and data were analyzed with WinList™ version 2.0 software. Data are presented as the mean ± standard error of three independent experiments.

2.3 ANGIOGENESIS ASSAYS

2.3.1 Endothelial sprouting assay

Endothelial sprouting was assessed by a modification of the method of Nehls and Drenckhahn (Nehls and Drenckhahn, 1995). Briefly, microcarrier beads coated with gelatin (Cytodex™ 3, Sigma) or positively-charged, cross-linked dextran (Cytodex™ 2, Sigma) were seeded with HMEC lines. When the cells reached confluence on the beads, equal numbers of HMEC-coated beads were embedded in fibrin gels in 96-well plates. For preparation of fibrin gels, bovine fibrinogen (Sigma) was dissolved in PBS at a concentration of 2.5 mg/ml. Aprotinin (Sigma) was added at a concentration of 0.05 mg/ml and the solution filtered through a 0.22 μm filter. Fibrinogen solution was supplemented with FGF-2 (15 ng/ml) or VEGF (15 ng/ml). As a control, fibrinogen solution without angiogenic factor was used. Following transfer of the fibrinogen solution to 96-well plates, HMEC-coated beads were added at an approximate density of 50 beads/well, and clotting was induced by the addition of thrombin (Sigma, 1.2 units/ml). After clotting was complete, gels were equilibrated with 2% FCS in MCDB at 37°C. Following 60 min of incubation, the overlying medium was changed for all wells. MCDB plus 2% FCS alone or containing FGF-2 (15 ng/ml) or VEGF (15 ng/ml) was added to the wells. After 3 days of incubation with daily medium changes, the number of capillary-like tubes formed was quantitated by counting the number of tube-like structures per microcarrier bead (sprouts/bead). Only sprouts greater than 150 μm in length and composed of at least 3 endothelial cells were counted. Data are presented as the mean ± standard deviation of a single experiment done in triplicate and are representative of at least three independent experiments.

For coating of Cytodex™ 2 beads with collagen, beads were resuspended in 1 mg/ml collagen type I (Sigma), allowed to dry overnight on petri dishes, and resuspended in PBS. For

coating of Cytodex™ 2 beads with Abs (IgG2a, 1:1000 dilution; 8A2, gift of J. Harlan, University of Washington, Seattle, WA, 1:1000 dilution; LM534, Chemicon, 1:1000 dilution), beads were incubated with Ab at 37°C for 2 hours, washed twice with PBS, and resuspended in PBS. After incubating the Ab-coated beads with cells for 3 days, the beads were placed in fibrin gels supplemented with the appropriate Ab at 1:1000 dilution.

2.3.2 Chick chorioallantoic membrane (CAM) assay

Fertilized White Leghorn chicken eggs (*Gallus gallus domesticus*) were incubated at 37°C under conditions of constant humidity. All chick eggs were handled according to institutional animal care procedures. On E6, the developing CAM was separated from the shell by opening a small circular window at the broad end of the egg above the air sac. The embryo was checked for normal development, the window sealed with Parafilm®, and the egg returned to the incubator for 2 more days. On E8, transfected Q2bn cell lines were trypsinized and washed in PBS, and 3 x 10^6 cells resuspended in 15 μl of DMEM supplemented with 30 ng/ml VEGF were placed onto nylon meshes (pore size 250 μm, Sefar America, Depew, NY) on the CAM. The cells distribute throughout the mesh and secrete control virus or virus containing Notch4IC. Meshes treated with vehicle alone (15 μl DMEM) were used as negative controls, whereas meshes treated with VEGF (30 ng/ml in 15 μl DMEM) were used as positive controls. Eggs were resealed and returned to the incubator. On E12, images of the CAMs were captured digitally using an Olympus™ SZX9 stereomicroscope (Olympus America, Melville, NY) equipped with a Spot™ RT digital imaging system (Diagnostic Instruments, Sterling Heights, MI). Neovascularization was quantitated for each CAM by counting the number of vessels that entered the mesh area, and dividing by the perimeter of the mesh (vessels/mm). Northern Eclipse™ software was used for manual vessel counting and mesh perimeter measurements. Data

are presented as the mean ± standard error of three independent experiments each done in replicates of 4 to 6 eggs. Following photography, CAMs were harvested and processed for further studies.

For CAMs treated with anti-integrin Abs, fertilized White Leghorn chicken eggs were prepared as described above. Mouse anti-avian β1 integrin Abs TASC (9D11; function-activating β1 integrin Ab, gift of L. F. Reichardt, University of California, San Francisco, CA), V2E9 (non-function-modifying β1 integrin Ab, Developmental Studies Hybridoma Bank, University of Iowa, Iowa City, IA), and W1B10 (function-blocking β1 integrin Ab, Sigma) were prepared at 10 μg/ml in PBS supplemented with 30 ng/ml VEGF. On E8, 20 μl of each Ab preparation was loaded onto 2-mm^3 gelatin sponges (Gelfoam®, Pharmacia Upjohn, Kalamazoo, MI), which were then placed on the surface of the developing CAM. Sponges containing vehicle alone (20 μl of PBS) were used as negative controls, whereas sponges containing 20 μl of 30 ng/ml VEGF in PBS were used as positive controls. CAMs were also treated with a function-blocking mouse anti-human αvβ3 Ab LM609 (which cross-reacts with avian αvβ3 integrin) prepared at 10 μg/ml in PBS containing 30 ng/ml VEGF. LM609 has previously been shown to attenuate VEGF-induced angiogenesis in the CAM (Friedlander et al., 1995), and thus serves as a positive control for angiogenesis inhibition. Eggs were resealed and returned to the incubator. On E10, digital images of the CAMs were captured and analyzed for neovascularization as described above. Data are presented as the mean ± standard error of two independent experiments each done in replicates of 3 to 5 eggs.

2.3.3 Proliferation assay

Proliferation of endothelial cells in response to FGF-2 and VEGF was determined by neutral red uptake. Confluent plates of HMEC lines were serum starved in 2% FCS in MCDB

for 48 hours, and cells plated in 96-well plates at a density of 5 x 10^3 cells/well. After 4 hours incubation to allow cells to bind, overlying medium was removed and the cells treated with 2% FCS in MCDB supplemented with FGF-2 (15 ng/ml) or VEGF (15 ng/ml). As a control, cells were treated with 2% FCS in MCDB alone. Cells were incubated for 0, 24, 48, and 72 hours with daily medium changes. After each time point, wells were emptied and incubated with 100 µl neutral red dye (0.0025% neutral red (Sigma) in MCDB supplemented with 2% FCS). Empty wells were also incubated with neutral red dye for background absorbance correction. After 4 hours of incubation, wells were aspirated and neutral red dye solubilized with 100 µl/well 1% acetic acid in 50% ethanol. Absorbance was determined at 570 nm. Data are presented as the mean ± standard deviation of a single experiment done in triplicate and are representative of at least three independent experiments.

2.3.4 Migration assay

The ability of endothelial cells to migrate towards FGF-2 or VEGF was measured using a Transwell™ filter assay (Corning Costar, Rochester, NY). Polycarbonate filters (8.0 µM pores) of the upper chamber were coated with 50 µl fibrinogen (2.5 mg/ml) or collagen type I (1 mg/ml) in PBS, and allowed to dry overnight. Confluent plates of HMEC cell lines were trypsinized, washed twice with 10 µg/ml soybean trypsin inhibitor, and resuspended in serum-free MCDB medium. 3.5 x 10^4 HMEC cells were placed in the upper chamber, and MCDB medium supplemented with FGF-2 (15 ng/ml) or VEGF (15 ng/ml) was placed in the lower chamber. As a control, MCDB medium without added chemotactic factor was placed in the lower chamber. Following 16 hours of incubation at 37°C, filters were washed in PBS, fixed in 4% paraformaldehyde, and stained with 0.5% crystal violet (Sigma). After removing adherent cells from the upperside of the filter using a cotton swab, all cells that had migrated and adhered to the

underside of the filter were counted using an inverted microscope. Data are presented as the mean ± standard deviation of a single experiment done in triplicate and are representative of at least three independent experiments.

2.3.5 Adhesion assay

High binding 96-well plates (Corning Costar) were coated with 100 μl/well of the following ECM proteins at 20 μg/ml: fibrinogen, fibronectin (Sigma), collagen type I, collagen type IV (Sigma), and vitronectin (Sigma). Control wells were coated with poly-L-lysine (Sigma) at 20 μg/ml. After incubation for 1 hour at 37°C, all wells were aspirated and blocked with 4% BSA in PBS for 30 min at room temperature, followed by washing with PBS. Single cell suspensions were prepared by washing confluent cells once with PBS based enzyme-free cell dissociation buffer, and incubating the cells in the same buffer for 20 min at 37°C. Following resuspension in a mixture of PBS:DMEM (4:1 v/v), 100 μl of the cell suspension at 6 x 10^5 cells/ml was added to each well and incubated at 37°C for 20 min. Plates were then gently washed with PBS, fixed in 4% paraformaldehyde, and stained with 0.5% crystal violet. Following solubilization of dye in 1% SDS in PBS, absorbance was quantitated in an enzyme-linked immunosorbent assay plate reader at 570 nm, with background absorbance subtracted at 630 nm. Data are presented as the mean ± standard deviation of a single experiment done in triplicate and are representative of at least three independent experiments.

For adhesion modulation studies, HMEC lines were incubated with Abs on ice for 20 min. Mouse IgG2a was used at 1:500 dilution, mouse monoclonal function-blocking anti-human β1 integrin Ab P4C10 was used at 1:100, 1:250, and 1:500 dilutions (Gibco) or 2.5 μg/ml (Sigma), mouse monoclonal function-blocking anti-human αvβ3 integrin Ab LM609 was used at 10 μg/ml, and mouse monoclonal function-activating anti-human β1 integrin Ab 8A2 was used at

1 μg/ml. For cells treated with both LM609 and P4C10, 10 μg/ml and 1:100 dilution were used, respectively. For adhesion studies using P4C10, cells were seeded into wells coated with collagen type I and/or collagen type IV. For adhesion studies using 8A2, cells were seeded into wells coated with collagen type I.

2.3.6 Ligand binding assay

The binding of soluble collagen type I to HMEC-LNCX and HMEC-Notch4IC cell lines was examined. HMEC lines were detached by incubation in PBS based enzyme-free cell dissociation buffer for 20 min at 37°C. 5 x 10^5 cells were incubated with FITC-conjugated collagen type I (16.9 molecules of FITC per molecule of collagen, Molecular Probes) in a volume of 100 μl at the following concentrations (μg/ml): 0, 0.1, 1, 10, 100, 500, 1000. After 10 min binding at 37°C, cells were washed 3 times in 1 ml PBS, and fixed in 4% paraformaldehyde. Samples were run on an EPICS® ELITE-ESP flow cytometer, and data were analyzed with WinList™ version 2.0 software. In order to determine the number of molecules of FITC-collagen type I bound per endothelial cell, a fluorescence standard curve was constructed using Quantum™ 24 premixed microbeads (Bangs Laboratories Inc., Fishers, IN). Taking the molecular weight of FITC and collagen type I to be 390 Da and 300 kDa, respectively, and given an FITC:collagen ratio of 16.9, a curve of bound collagen (molecules) versus concentration of FITC-collagen type I conjugate (nM) was generated. Data are presented as the mean ± standard deviation of two independent experiments.

2.4 RIBONUCLEIC ACID (RNA) ANALYSIS

2.4.1 RNA isolation

Total RNA isolation from cultured cells in vitro or tumor tissue in vivo was performed using TRIzol® Reagent (Invitrogen) or an RNeasy® kit (Qiagen, Mississauga, ON, Canada) according to manufacturer's recommendations.

2.4.2 Reverse transcriptase-polymerase chain reaction (RT-PCR)

First strand cDNA was synthesized using 50 μl reactions containing 2.5 μg total RNA and 200 units of Superscript™ II reverse transcriptase (Invitrogen). Following ribonuclease (RNase) H treatment (2 units/reaction; Invitrogen), PCR was performed. Control reactions omitting reverse transcriptase were performed in each experiment. Primer sequences and annealing temperatures are described in Tables 2.1 and 2.2. Entire PCR samples were assessed in 1.5% tris acetic acid (TAE)-agarose gels containing ethidium bromide and quantitated by densitometry. Data are presented as the mean ± standard error from three independent experiments.

For semi-quantitative RT-PCR, individual reactions along with glyceraldehyde-3-phosphate dehydrogenase (GAPDH) control reactions were terminated after the designated number of PCR cycles. Control human cDNA was generated from pooled total RNA isolated from the following human cells: HMEC; vascular smooth muscle cells; cervical cancer cells, SiHa; colon cancer cells, WiDr; kidney epithelial cells, 293T. Control mouse cDNA was generated from pooled total RNA isolated from the following mouse cells: Lewis lung carcinoma cells; endothelial cells, SVEC4-10; fibroblasts, NIH3T3. Data are presented as the mean ± standard error from five control tumors and five XNotch4 tumors.

Table 2.1: PCR Primer Sequences

Gene	Primer Identifier[a]	Species Specificity		Primer Sequences (5' to 3')		Reference
		Human	Mouse			
Jagged1	A	X		Forward:	CTATGATGAGGGGGATGCT	(Noseda et al., 2004a)
	B		X	Forward:	AATGGAGACTCCTTCACCTGT	(Noseda et al., 2004b)
	C	X	X	Reverse:	CGTCCATTCAGGCACTGG	(Noseda et al., 2004b)
Jagged2	A	X		Forward:	TGGGATGCCTGGCACA	This thesis
	B		X	Forward:	CAGGGCACGCGGTGT	This thesis
	C	X	X	Reverse:	CCGGCAGATGCAGGA	This thesis
Delta-like1	A	X		Forward:	GAGGGAGGCCTCGTGGA	This thesis
	B		X	Forward:	TGGTTCTCTCAGAGTTAGCAGAG	This thesis
	C	X	X	Reverse:	AGACCCGAAGTGCCTTTGTA	This thesis
Delta-like3	A	X	X	Forward:	CGGATGCACTCAACAACCT	This thesis
	B	X		Reverse:	GAAGATGGCAGGTAGCTCAA	This thesis
	C		X	Reverse:	ATAGATGTCTCTGGGGAGATGA	This thesis
Delta-like4	A	X	X	Forward:	GCATTGTTTACATTGCATCCTG	This thesis
	B	X		Reverse:	GCAAACCCCAGCAAGAGAC	This thesis
	C		X	Reverse:	GTAGCTCCTGCTTAATGCCAAA	This thesis
Notch1	A	X		Forward:	CACTGTGGGCGGGTCC	(Shou et al., 2001)
	B	X		Reverse:	GTTGTATTGGTTCGGCACCAT	(Shou et al., 2001)
	C		X	Forward:	GGCCACCTCTTCACTGCTTC	(Noseda et al., 2004b)
	D	X	X	Reverse:	CCGGAACTTCTTGGTCTCCA	(Noseda et al., 2004b)
Notch2	A	X		Forward:	AATCCCTGACTCCAGAACG	This thesis
	B		X	Forward:	AACTGGAGAGTCCAAGAAACG	(Noseda et al., 2004b)
	C	X	X	Reverse:	TGGTAGACCAAGTCTGTGATGAT	(Noseda et al., 2004b)
Notch3	A	X		Forward:	TGAGACGCTCGTCAGTTCTT	(Noseda et al., 2004a)
	B		X	Forward:	CACCTTGGCCCCCTAAG	(Noseda et al., 2004b)
	C	X	X	Reverse:	TGGAATGCAGTGAAGTGAGG	(Noseda et al., 2004b)
Notch4	A	X		Forward:	TAGGGCTCCCCAGCTCTC	(Noseda et al., 2004a)
	B		X	Forward:	CAAGCTCCCGTAGTCCTACTTC	(Noseda et al., 2004b)
	C	X	X	Reverse:	GGCAGGTGCCCCCATT	(Noseda et al., 2004b)
HES1	A	X		Forward:	AGGCGGACATTCTGGAAATG	(Muller et al., 2002)
	B	X		Reverse:	CGGTACTTCCCCAGCACACTT	(Muller et al., 2002)
	C		X	Forward:	GGAGAGGCTGCCAAGGTTTT	(Zheng et al., 2000)
	D		X	Reverse:	GCAAATTGGCCGTCAGGA	(Zheng et al., 2000)
	E	X	X	Forward:	CAGCCAGTGTCAACACGACAC	(Zine et al., 2001)
	F	X	X	Reverse:	TCGTTCATGCACTCGCTGAA	This thesis
E-cadherin	A	X		Forward:	CAGCACGTACACAGCCCTAA	(Fujita et al., 2003)
	B	X		Reverse:	ACCTGAGGCTTTGGATTCCT	(Fujita et al., 2003)
	C	X		Forward:	TTAGGTTAGAGGGTTATCGCGT	(Herman et al., 1996)
	D	X		Reverse:	TAACTAAAAATTCACCTACCGAC	(Herman et al., 1996)
	E	X		Forward:	TAATTTTAGGTTAGAGGGTTATTGT	(Herman et al., 1996)
	F	X		Reverse:	CACAACCAATCAACAACACA	(Herman et al., 1996)
	G	X		Forward:	GTTTAGTTTTGGGGAGGGGTT	(Graff et al., 2000)
	H	X		Reverse:	ACTACTACTCCAAAAACCCATAACTAA	(Graff et al., 2000)
Slug	A	X		Forward:	AGATGCATATTCGGACCCAC	(Fujita et al., 2003)
	B	X		Reverse:	CCTCATGTTTGTGCAGGAGA	(Fujita et al., 2003)
Snail	A	X		Forward:	AATCGGAAGCCTAACTACAGCGAG	(Okubo et al., 2001)
	B	X		Reverse:	CCTTGGCCTCAGAGAGCTGG	(Okubo et al., 2001)
SIP1	A	X		Forward:	ACACCCCTGGCACAACAA	This thesis
	B	X		Reverse:	GTGTCACTGCGCTGAAGGTA	This thesis

GAPDH	A	X		Forward:	GGACCTGACCTGCCGTCTAGAA	(Decary et al., 2002)
	B	X		Reverse:	GGTGTCGCTGTTGAAGTCAGAG	(Decary et al., 2002)
	C		X	Forward:	AATGTGTCCGTCGTGGATCT	(Liu et al., 1999)
	D		X	Reverse:	CCCTGTTGCTGTAGCCGTAT	(Liu et al., 1999)
	E	X	X	Forward:	CCCATCACCATCTTCCAG	(MacKenzie et al., 2004b)
	F	X	X	Reverse:	ATGACCTTGCCCACAGCC	(MacKenzie et al., 2004b)

[a]Primer Identifier is a letter assigned to each individual primer. Various combinations of two primers (see Table 2.2 - Primer Set) are used to amplify the target gene of interest.

Table 2.2: PCR Primer Sets and Conditions

Gene	Primer Set[a]	Annealing Temperature (°C)	Product Size (base pairs)
human Jagged1	A/C	53	507
mouse Jagged1	B/C	53	383
human Jagged2	A/C	53	550
mouse Jagged2	B/C	58	550
human Delta-like1	A/C	55	448
mouse Delta-like1	B/C	55	409
human Delta-like3	A/B	55	338
mouse Delta-like3	A/C	55	329
human Delta-like4	A/B	60	456
mouse Delta-like4	A/C	55	473
human Notch1	A/B	55	85
mouse Notch1	C/D	60	529
human Notch2	A/C	53	589
mouse Notch2	B/C	53	583
human Notch3	A/C	53	667
mouse Notch3	B/C	60	449
human Notch4	A/C	60	486
mouse Notch4	B/C	53	486
human HES1	A/B	55	103
mouse HES1	C/D	53	62
human and mouse HES1	E/F	53	307
human E-cadherin	A/B	53	159
human E-cadherin-M	C/D	57	116
human E-cadherin-U	E/F	53	97
human E-cadherin-promoter sequencing	G/H	50	270
human Slug	A/B	53	258
human Snail	A/B	50	400
human SIP1	A/B	53	234
human GAPDH	A/B	53	142
mouse GAPDH	C/D	53	256
human and mouse GAPDH	E/F	53	446

[a]Primer Set is a Primer Identifier pair (see Table 2.1 for individual Primer Identifiers) used to amplify the target gene of interest.

2.5 METHYLATION ASSAYS

2.5.1 Methylation-specific PCR (MSP)

Genomic DNA was isolated from cultured cells or tumor tissue using a DNeasy® Tissue Kit (Qiagen) according to manufacturer's recommendations. One microgram of genomic DNA was bisulfite modified using a CpGenome™ DNA Modification Kit (Chemicon) and eluted in 25 μl Tris-EDTA buffer, according to manufacturer's recommendations. MSP was performed using bisulfite-modified DNA (~120 ng), 5' and 3' primers (each at 400 nM), 2'-deoxynucleoside 5'-triphosphates (dNTPs; Invitrogen) (each at 0.2 mM), 1X PCR buffer, and 0.625 units of HotStarTaq® DNA Polymerase (Qiagen), according to manufacturer's recommendations. Primer sequences and annealing temperatures are described in Tables 2.1 and 2.2. Entire MSP reactions were assessed in 2% TAE-agarose gels containing ethidium bromide. Bands corresponding to methylated and unmethylated PCR products were quantitated by densitometry. Data are expressed as a ratio of methylated over unmethylated PCR products (M/U ratio), and represent the mean ratio ± standard error from five control tumors and five XNotch4 tumors.

2.5.2 Genomic bisulfite sequencing

Bisulfite-modified genomic DNA isolated from tumor tissue was amplified by PCR using primers spanning the E-cadherin proximal promoter. Primer sequences and annealing temperatures are described in Tables 2.1 and 2.2. PCR products were purified, cloned into the pDrive cloning vector (Qiagen), and individual clones sequenced. Five control tumors (a total of 35 MIG clones) and three XNotch4 tumors (a total of 22 XNotch4 clones) were analyzed, and data expressed as the percentage methylation per CpG site (total number of methylated clones / total number of clones).

2.5.3 Global genomic deoxyribonucleic acid (DNA) methylation analysis

Genomic DNA (500 ng) was digested with the restriction enzymes HpaII (New England Biolabs, Pickering, ON, Canada), MspI (New England Biolabs), or McrBC (New England Biolabs). HpaII is unable to digest CpG-methylated DNA, whereas its isoschizomer MspI is not sensitive to CpG methylation and thus is a positive control for DNA digestion. McrBC digests CpG-methylated DNA only in the presence of guanosine triphosphate (GTP). For McrBC digestion, reactions were performed with GTP (McrBC-plus-GTP) or without GTP (McrBC-minus-GTP). Entire reaction mixtures were assessed in 2% TAE-agarose gels containing ethidium bromide. HpaII, MspI, and McrBC-plus-GTP digested DNA products between 2 and 7 kilobases were quantitated by densitometry. For McrBC-minus-GTP reactions, undigested DNA products corresponding to the uppermost DNA band were quantitated by densitometry. Data are expressed as a ratio of HpaII over MspI digested DNA products (HpaII / MspI densitometric ratio), or McrBC-plus-GTP over McrBC-minus-GTP DNA products (+GTP / -GTP densitometric ratio), and represent the mean ratio ± standard error from five control tumors and five XNotch4 tumors.

2.6 TUMORIGENICITY ASSAYS

Female non-obese diabetic/severe combined immunodeficient (NOD/SCID) mice were obtained from the Animal Resource Centre of the British Columbia Cancer Research Centre. For MDA-MB-231 tumor generation, 5 x 10^6 cells were injected subcutaneously into the dorsa of mice. Once tumors were palpable, tumor volume (0.523 x length x width x height) was measured weekly using calipers. For each time point, MDA-MB-231 tumor data are presented as the mean tumor volume ± standard error from (i) 12 MIG tumors and 11 MIGXNotch4HA tumors, and (ii)

12 MIY tumors and 12 MIYE-cadherin tumors. Tumor growth curves for one experiment are presented and are representative of three independent experiments. For Lewis lung carcinoma tumor generation, 2 x 10^6 cells were injected subcutaneously into the dorsa of mice. Once tumors were palpable, tumor volume was measured every two days using calipers. For each time point, Lewis lung carcinoma tumor data are presented as the mean tumor volume ± standard error from six control tumors and seven XNotch4 tumors. Tumor growth curves for one experiment are presented and are representative of three independent experiments.

Following sacrifice of mice, gross images of tumors attached to the dorsal skin flap were captured with an Olympus™ SZX9 stereomicroscope equipped with a Spot™ RT digital camera. Mice bearing MDA-MB-231 tumors (MIG and MIGXNotch4HA, or MIY and MIYE-cadherin) were sacrificed at the same time and the total number and total weight (mg) of metastases determined. Data are presented as the average number of metastases per mouse ± standard error, and the average weight of each metastatic nodule (mg) ± standard error. Metastasis data were determined by analyzing (i) 25 MIG tumors and 27 MIGXNotch4HA tumors, and (ii) 12 MIY tumors and 12 MIYE-cadherin tumors. Animal experiments were approved by the University of British Columbia Institutional Animal Care and Ethics Committee, and all animals were handled according to institutional animal care procedures.

2.7 STATISTICAL ANALYSIS

To determine statistical significance, a one-way analysis of variance with a Tukey test for multiple comparisons was used in all experiments. To assess a correlation between E-cadherin and β-catenin expression, Pearson correlation coefficients were calculated using the statistics program Statistical Package for Social Scientists version 11.0 (SPSS Inc., Chicago, IL). Statistical significance was taken at a P value of ≤ 0.05.

Chapter 3

ACTIVATED NOTCH4 INHIBITS ANGIOGENESIS: ROLE OF β1-INTEGRIN ACTIVATION

3.1 ABSTRACT

Angiogenesis involves modulation of the endothelial cell phenotype. Because activation of Notch in various cell systems has been shown to regulate cell fate decisions, and Notch4 is primarily expressed on endothelial cells, we postulated that Notch4 may be involved in regulating angiogenesis. To answer this question, we expressed the truncated, constitutively-active Notch4IC in endothelial cells. Our studies indicate that activated Notch4 inhibits endothelial sprouting in vitro and angiogenesis in the chick CAM in vivo. Activated Notch4 does not inhibit endothelial cell proliferation, nor does it inhibit endothelial cell migration through fibrinogen towards FGF-2 and VEGF. Migration through collagen, however, was inhibited. We demonstrate that the decreased sprouting of Notch4IC cells from collagen-coated beads is due in part to enhanced β1 integrin-mediated adhesion to collagen. Although endothelial cells expressing Notch4IC do not show increased surface expression of β1 integrins, we show that the β1 integrins are in a high-affinity, active conformation. We also show that activation of β1 integrins with function-activating β1 integrin mAbs, independent of Notch4 expression, is sufficient to inhibit endothelial sprouting in vitro and angiogenesis in vivo. Thus, our results suggest that Notch4 activation in endothelial cells in vivo may inhibit angiogenesis in part by promoting β1 integrin-mediated adhesion to the underlying matrix.

3.2 RESULTS

3.2.1 Constitutively-active Notch4 inhibits endothelial sprouting in vitro

We generated HMEC lines expressing constitutively-active human Notch4IC. A previously described endothelial sprouting assay which mimics the formation of capillary-like tubes in fibrin gels in vitro was used to evaluate the role of Notch4 in angiogenesis (Koblizek et al., 1998; Nehls and Drenckhahn, 1995). Microvascular endothelial cells are seeded as a confluent monolayer onto gelatin-coated beads, which are subsequently embedded in a fibrin gel. Following stimulation by angiogenic factors, endothelial cells migrate off the beads and into the fibrin matrix to form sprouts. Using this in vitro assay, we found that activated Notch4 inhibited spontaneous endothelial sprout formation on gelatin-coated beads, as well as sprouting in response to FGF-2 and VEGF (Figure 3.1A,B). Moreover, the sprouts that formed from Notch4IC cell lines were noted to be shorter than those derived from cells transduced with the empty vector. Notch4IC protein was expressed in HMEC-Notch4IC cells (Figure 3.1C). We typically achieved transduction efficiencies between 50-80%. As expected with polyclonal cell lines, HMEC-Notch4IC cells displayed heterogeneity in staining for Notch4IC protein by immunofluorescence microscopy (Figure 3.1D). The majority of the Notch4IC protein localized to the nucleus of HMEC-Notch4IC cells, which is typical of constitutively-active Notch proteins (Furriols and Bray, 2000). Because HMEC are a transformed endothelial cell line, we repeated the endothelial sprouting assay using primary HUVEC transduced with the Notch4IC construct or the empty vector. Similar to HMEC, activation of Notch4 in HUVEC inhibited endothelial sprouting (data not shown).

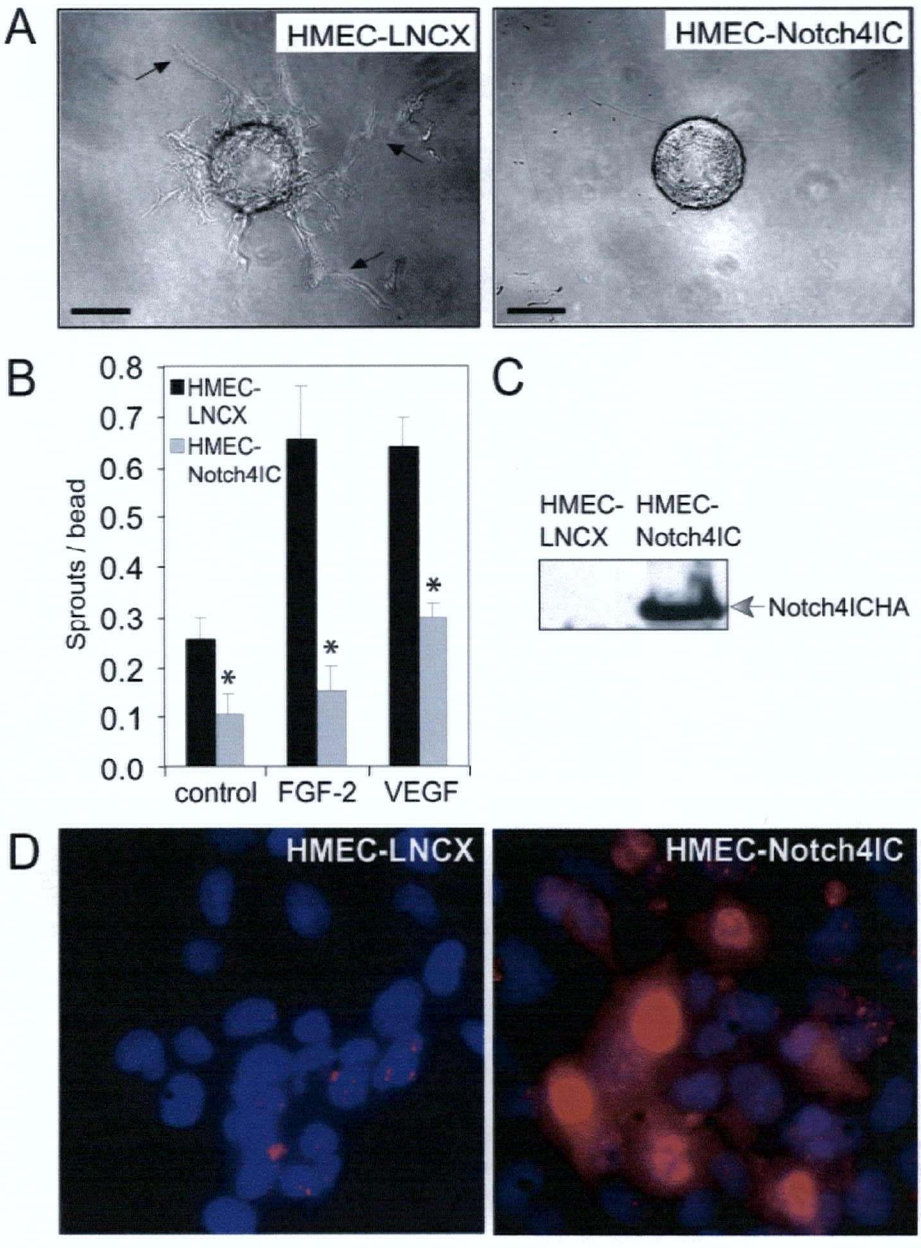

Figure 3.1: Activated Notch4 inhibits endothelial sprouting from gelatin-coated microcarrier beads in vitro. (A) Sprouting of HMEC-LNCX or HMEC-Notch4IC cells from gelatin-coated microcarrier beads embedded in fibrin gels supplemented with either FGF-2 (15 ng/ml) or VEGF (15 ng/ml). Bars represent 100 μm. Arrows indicate endothelial sprouts of sufficient length to be counted. **(B)** Endothelial sprout formation quantitated after 3 days incubation by counting the number of tube-like structures per microcarrier bead (sprouts/bead). Data shown are the mean ± standard deviation of a single experiment done in triplicate and are representative of at least three independent experiments. *Control: $P \leq 0.05$. *FGF-2: $P < 0.01$. *VEGF: $P < 0.001$. **(C)** Immunoblot for expression of HA-tagged Notch4IC in HMEC lines. **(D)** Immunofluorescence of HMEC-LNCX and HMEC-Notch4IC cells stained with Hoechst 33258, as well as anti-HA primary Ab and Texas Red-conjugated secondary Ab to detect HA-tagged Notch4IC protein. Original magnification 40X.

3.2.2 Constitutively-active Notch4 inhibits angiogenesis in vivo

To determine whether activation of Notch4 would inhibit angiogenesis in vivo, we used the CAM assay. The CAM functions as a respiratory structure for gas/nutrient exchange and undergoes intense vascularization (Brooks et al., 1999), thus providing an excellent microenvironment for assessing angiogenesis. Exogenous factors can be placed on the surface of the developing CAM in the presence or absence of a known angiogenic factor to assess anti-angiogenic or pro-angiogenic activity, respectively. As previously described (Boudreau et al., 1997; Jiang et al., 2000), we generated avian retroviral packaging cell lines (Q2bn) transfected with the empty CK vector or CK-Notch4IC. On E8, these CK producer lines, in the presence of VEGF, were placed onto meshes on the chick CAM surface and incubated for an additional 4 days. The cells distribute throughout the mesh and secrete control virus or virus containing Notch4IC which infect the surrounding proliferating cells, the majority of which are endothelial. CAMs transduced with the empty vector demonstrated normal angiogenesis in response to VEGF, whereas angiogenesis was markedly inhibited by the expression of Notch4IC (Figure 3.2A,B). Expression of Notch4IC protein was detected in transfected Q2bn cells (Figure 3.2C).

Histological analysis was performed on sections of harvested CAMs. For H&E stained sections, areas of the CAMs proximal to the Q2bn-containing mesh were analyzed. H&E staining of CK vector-transduced CAMs revealed the presence of numerous blood vessels in the subchorionic mesenchyme (Figure 3.3A). In contrast, CAMs transduced with CK-Notch4IC exhibited a marked reduction in blood vessels close to the mesh (Figure 3.3B). Immunohistochemistry was also performed on CAM sections, and areas proximal to the mesh examined. Staining for the endothelial-specific marker vWF (Sehested and Hou-Jensen, 1981) confirmed the presence of blood vessels in CK vector-transduced CAMs (Figure 3.3C).

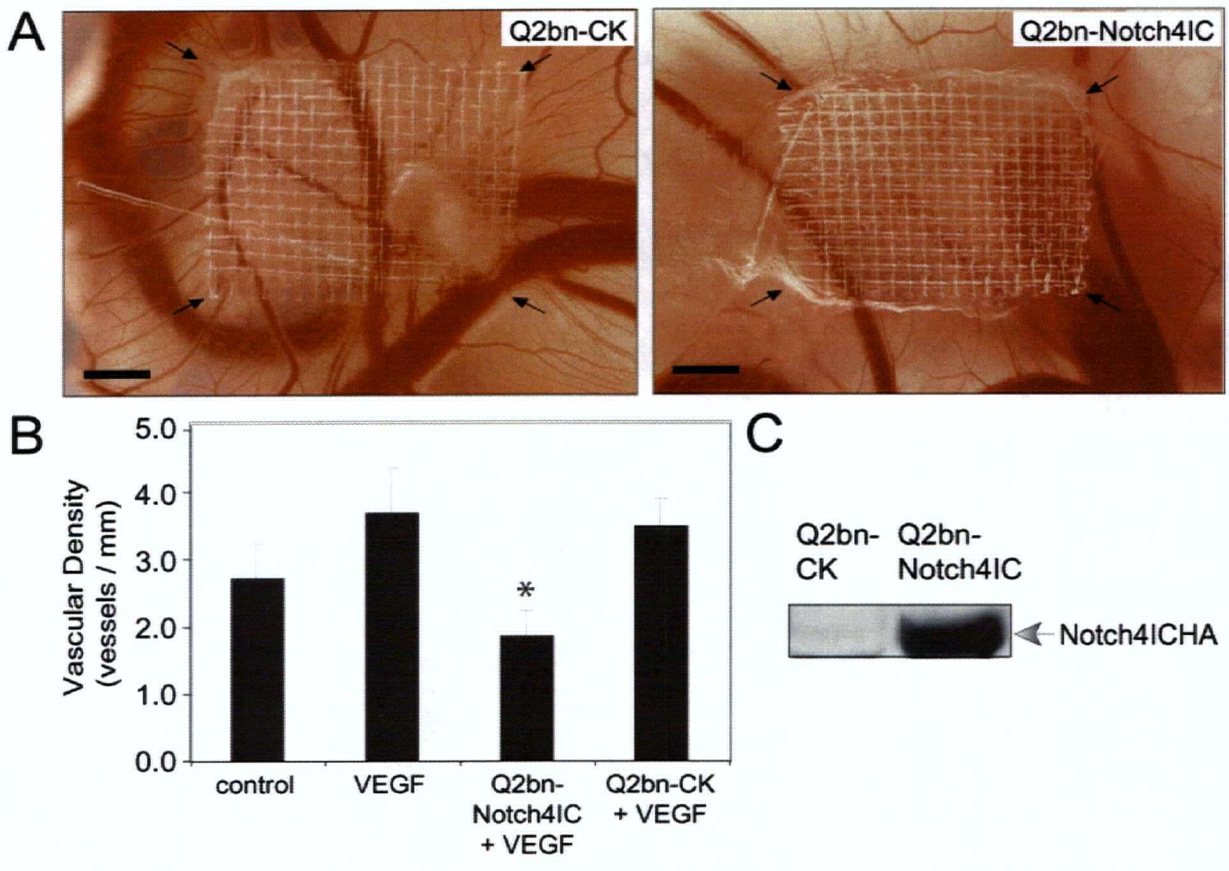

Figure 3.2: Activated Notch4 inhibits angiogenesis in the chick CAM in vivo. The avian retroviral packaging cell line Q2bn was transfected with the empty vector CK (Q2bn-CK) or CK-Notch4IC (Q2bn-Notch4IC). On day 9, transfected Q2bn cell lines were placed onto nylon meshes on the CAM surface in the presence of VEGF (30 ng/ml). The grafted cells distribute throughout the mesh and secrete control virus or virus containing Notch4IC. Control CAMs were treated with medium alone or medium supplemented with VEGF. Images of the CAMs were captured on day 12. **(A)** CAMs treated with Q2bn-CK or Q2bn-Notch4IC cell lines in the presence of VEGF. Arrows indicate the edges of the nylon mesh. Bars represent 1 mm. **(B)** Vascular density quantitated after 4 days incubation by counting the number of vessels that entered the mesh area and dividing by the perimeter of the mesh (vessels/mm). Data shown are the mean ± standard error of three experiments each done in replicates of 4-6 eggs. *CK versus Notch4IC: $P < 0.00001$. **(C)** Immunoblot for expression of HA-tagged Notch4IC in Q2bn cell lines.

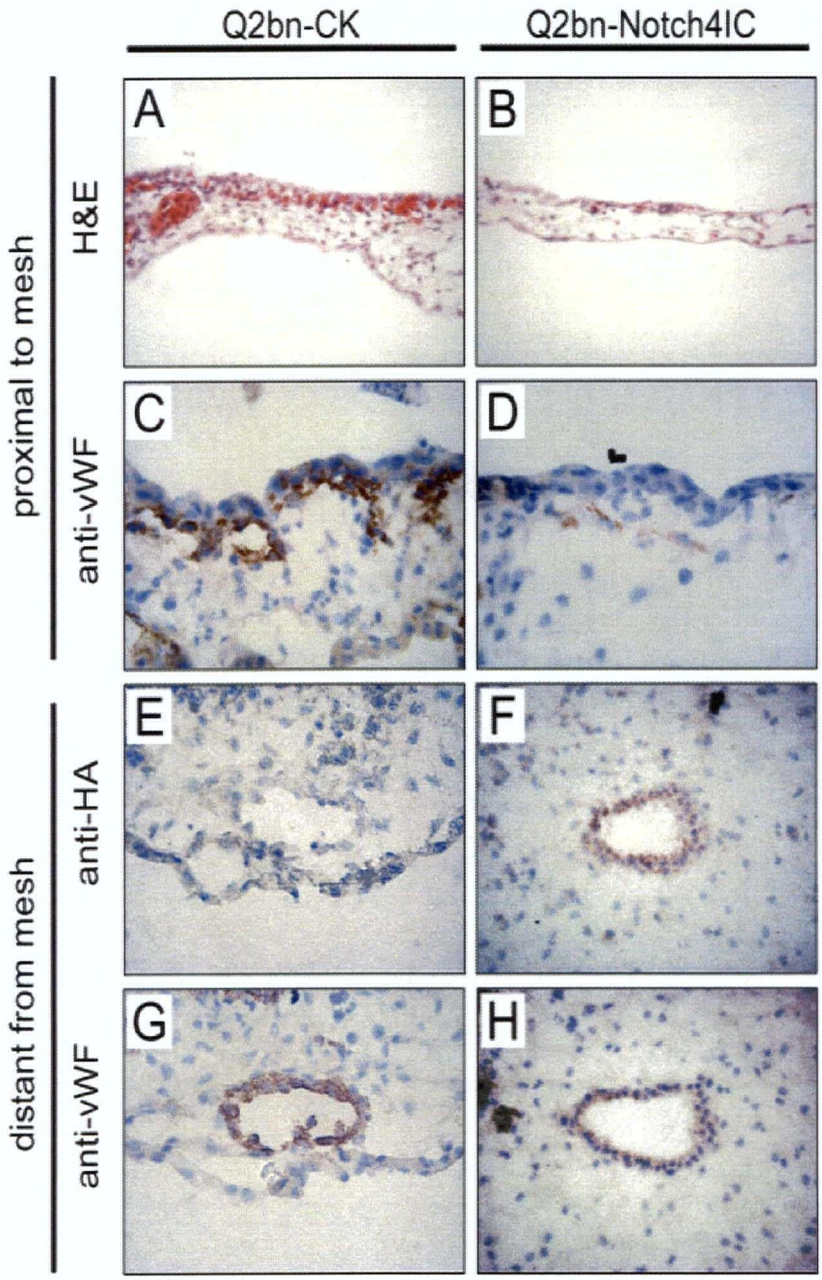

Figure 3.3: Immunohistochemical analysis of Notch4IC expression in the CAM. Q2bn packaging cells transfected with the vector control (Q2bn-CK) or Notch4IC (Q2bn-Notch4IC) were placed onto nylon meshes on the CAM surface. Treated CAMs were harvested on day 12 and sections prepared. **(A-D)** CAM sections proximal to mesh. H&E staining of Q2bn-CK treated CAM (A) or Q2bn-Notch4IC treated CAM (B). Anti-vWF staining of Q2bn-CK treated CAM (C) or Q2bn-Notch4IC treated CAM (D). **(E-H)** CAM sections distant from mesh. Anti-HA staining of Q2bn-CK treated CAM (E) or Q2bn-Notch4IC treated CAM (F). Anti-vWF staining of Q2bn-CK treated CAM (G) or Q2bn-Notch4IC treated CAM (H). Original magnifications: 40X (A,B,C,D,F,H) and 63X (E,G).

Notch4IC-transduced CAMs, in contrast, showed minimal staining for vWF (Figure 3.3D), confirming inhibition of blood vessel formation.

To assess expression of the HA-tagged Notch4IC protein in endothelial cells, serial sections were stained with Abs against HA and vWF. Because Notch4IC-transduced CAMs were nearly devoid of small vessels proximal to the mesh, colocalization of staining was examined in vessels distant from the mesh. As expected for CK vector-transduced CAMs, vessels distant from the mesh did not stain for HA (Figure 3.3E) but did for vWF (Figure 3.3G). Analysis of Notch4IC-transduced CAMs demonstrated that vessels distant from the mesh exhibited co-staining for HA (Figure 3.3F) and vWF (Figure 3.3H). Our findings suggest that expression of Notch4IC in vessels that feed the area of the mesh inhibits VEGF-induced endothelial sprouting and angiogenesis. In order to elucidate a possible mechanism(s) by which activated Notch4 inhibits endothelial sprouting in vitro and angiogenesis in vivo, we investigated the effects of Notch4IC expression on endothelial cell functions related to the angiogenic process using various in vitro assays.

3.2.3 Notch4 inhibition of endothelial sprouting in vitro cannot be explained by reduced endothelial cell proliferation

Endothelial cell proliferation enables newly formed sprouts to increase in length and extend into the surrounding matrix. To determine whether reduced proliferation was a possible reason for the decreased sprouting of Notch4IC endothelial cells, we performed neutral red proliferation assays. When plated on normal tissue culture substrata, Notch4IC cells and control cells exhibited similar proliferation rates over 72 hours (the incubation time for the endothelial sprouting assay) (Figure 3.4A). In fact, proliferation rates were the same when cells were grown in serum-containing medium, or medium supplemented with FGF-2 or VEGF. Proliferation on

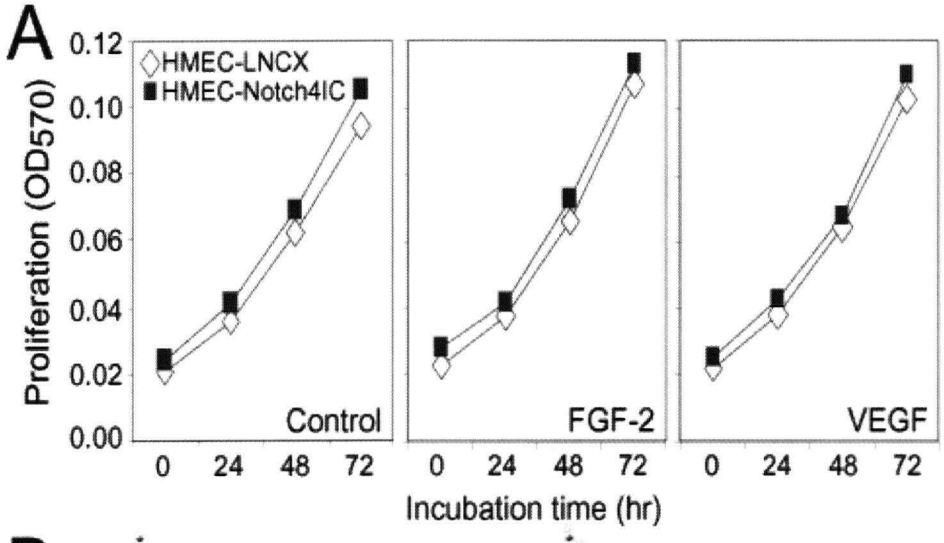

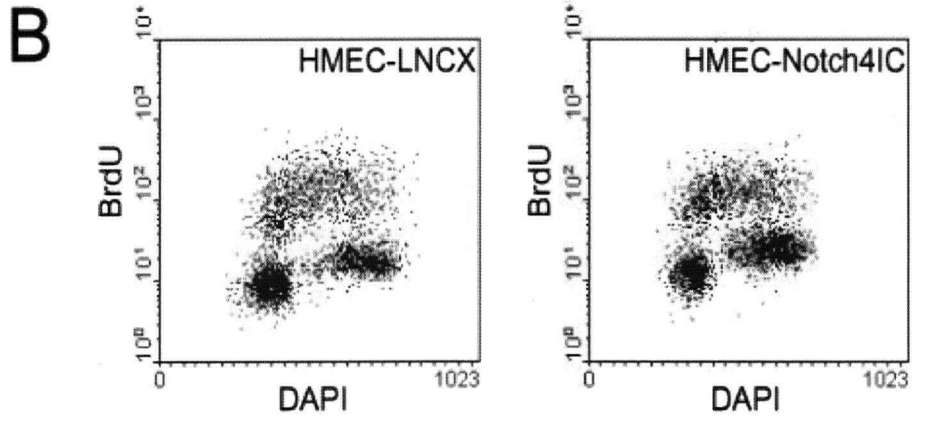

C

	HMEC-LNCX			HMEC-Notch4IC		
	G_0/G_1	S	G_2/M	G_0/G_1	S	G_2/M
Control	44 ± 1%	29 ± 4%	25 ± 3%	36 ± 4%	30 ± 4%	30 ± 7%
FGF-2	37 ± 4%	34 ± 2%	24 ± 1%	35 ± 3%	30 ± 5%	33 ± 3%
VEGF	41 ± 1%	33 ± 2%	26 ± 5%	38 ± 6%	32 ± 3%	27 ± 6%

Figure 3.4: Activated Notch4 does not inhibit HMEC proliferation. (A) Neutral red assay for proliferation. HMEC-LNCX and HMEC-Notch4IC cell proliferation was assayed over 72 hours in medium alone, or medium supplemented with FGF-2 (15 ng/ml) or VEGF (15 ng/ml). Data shown are the mean absorbances from a single experiment done in triplicate and are representative of at least three independent experiments. **(B)** Cell cycle distribution for HMEC-LNCX and HMEC-Notch4IC cells stimulated with VEGF. Cells were stained with DAPI for total DNA content and pulse-labeled with BrdU to detect DNA synthesis, and analyzed by flow cytometry. **(C)** Cell cycle distributions for HMEC-LNCX and HMEC-Notch4IC cells cultured in medium alone or medium supplemented with FGF-2 (15 ng/ml) or VEGF (15 ng/ml). Data shown are the mean ± standard error of three independent experiments.

fibrinogen- and collagen-coated surfaces was also investigated, and was found to be equivalent for Notch4IC cells and control cells (data not shown).

To confirm that Notch4IC does not affect HMEC cell cycle kinetics, we performed flow cytometry on HMEC lines pulse-labeled with BrdU and co-stained with DAPI. Both control and Notch4IC cells exhibited similar cell cycle distributions and BrdU incorporation in the absence or presence of growth factor (see Figure 3.4B for representative samples of VEGF-stimulated HMEC-LNCX and HMEC-Notch4IC, and Figure 3.4C for distribution percentages). Overall, the proliferation studies performed demonstrate that control and Notch4IC cells proliferate at similar rates. Hence the inhibition of HMEC-Notch4IC cell sprouting in vitro cannot be explained by a decrease in Notch4IC cell proliferation.

3.2.4 Notch4 inhibits endothelial cell migration through collagen but not fibrinogen

In order for capillaries to sprout, endothelial cells need to migrate toward a stimulus. To examine whether defective migration could explain the Notch4-induced inhibition of sprouting, we performed chemotaxis assays using Transwell filters coated with either fibrinogen or collagen. When filters were coated with fibrinogen, both control cells and Notch4IC-expressing cells exhibited similar degrees of chemotaxis towards FGF-2 and VEGF (Figure 3.5). Migration through collagen-coated filters towards FGF-2 or VEGF, however, was reduced for Notch4IC cells compared to control cells (Figure 3.5). These data suggest that activated Notch4 does not affect the intrinsic motility of HMEC cells, but influences endothelial cell migration in a matrix-dependent manner.

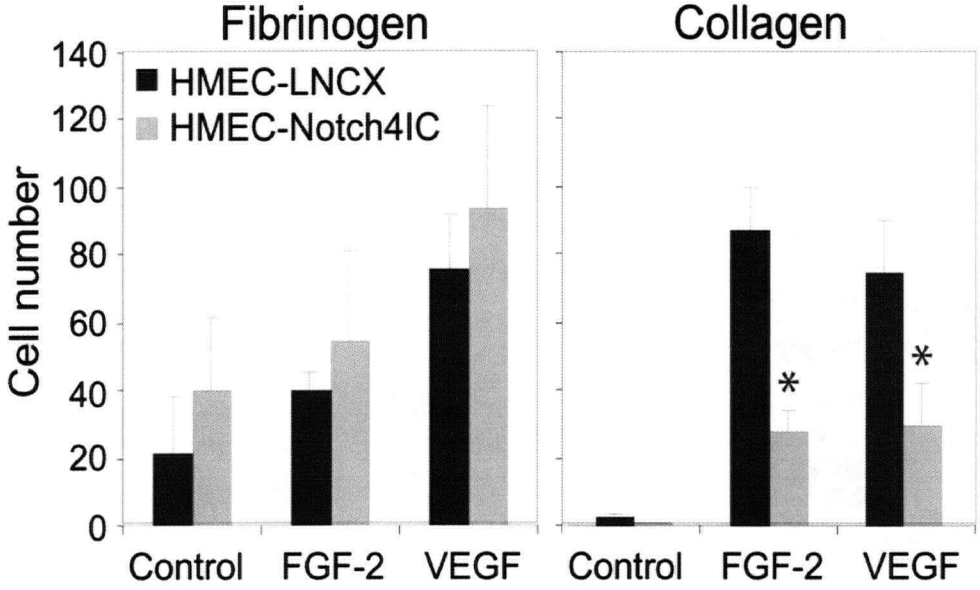

Figure 3.5: Activated Notch4 inhibits endothelial cell migration through collagen but not fibrinogen. Migration of HMEC-LNCX and HMEC-Notch4IC cells towards control medium, or medium supplemented with FGF-2 (15 ng/ml) or VEGF (15 ng/ml) was assayed using Transwell filters coated with fibrinogen or collagen type I. Following 16 hours of incubation, cells that had migrated and adhered to the underside of the filter were stained and counted. Data shown are the mean ± standard deviation of a single experiment done in triplicate and are representative of at least three independent experiments. *FGF-2: $P < 0.01$. *VEGF: $P \leq 0.05$.

3.2.5 Notch4 promotes adhesion to ECM proteins through β1 integrins

Modulation of both cell surface integrin levels and integrin affinity are crucial events throughout the course of capillary tube formation (Bloch et al., 1997; Grant et al., 1989) and cell migration (Lauffenburger and Horwitz, 1996). Therefore, to explain the matrix-specific inhibition of HMEC-Notch4IC migration, we investigated whether Notch4 activation affects endothelial cell adhesion to ECM proteins. Notch4IC-expressing cells exhibited increased adherence to various ECM proteins (Figure 3.6A). In contrast, when adhesion was mediated by charge interactions alone (on poly-L-lysine-coated wells), Notch4IC cells and control cells both adhered to the same degree (Figure 3.6A). Regulation of αvβ3 and β1 integrins is required for angiogenesis (Bloch et al., 1997; Eliceiri and Cheresh, 1999). Because activation of Notch4 promoted adhesion to fibronectin, collagen type I, and collagen type IV, all of which are β1 integrin substrates (Figure 3.6A), we postulated that the pattern of increased adhesion was due to effects of Notch4 activation on β1 integrin expression or function. Using the function-blocking β1 integrin Ab P4C10 (Carter et al., 1990), we confirmed that the majority of the increased HMEC-Notch4IC cell adhesion to collagen type I (Figure 3.6B,C) or collagen type IV (Figure 3.6C) was mediated by β1 integrins. A function-blocking Ab directed against αvβ3 integrin (LM609) (Cheresh, 1987), however, did not affect HMEC-Notch4IC cell adhesion to collagen type I (Figure 3.6B). LM609 concentrations of up to 20 μg/ml were tested, with no effect on collagen type I adhesion (data not shown). Interestingly, when LM609 and P4C10 were used in combination, the inhibition of HMEC-Notch4IC cell adhesion to collagen type I was less effective than P4C10 used alone (Figure 3.6B). Although the reason(s) for the attenuated blocking is not clear, this may be due in part to steric hindrance.

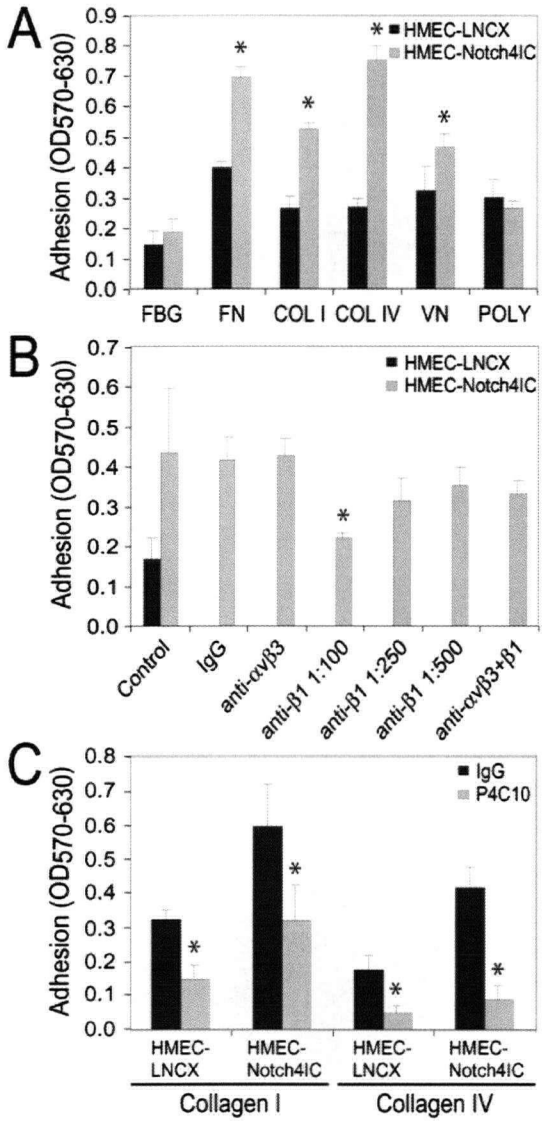

Figure 3.6: Activated Notch4 promotes endothelial cell adhesion to various ECM proteins through β1 integrins. (A) Adhesion of HMEC-LNCX and HMEC-Notch4IC cells to ECM proteins. Plates were coated with the following proteins: FBG, fibrinogen; FN, fibronectin; COL I, collagen type I; COL IV, collagen type IV; VN, vitronectin; POLY, poly-L-lysine. Adherent cells were fixed, stained, and solubilized, and absorbance read at 570 nm with background absorbance subtracted at 630 nm. *FN: $P < 0.001$. *COL I: $P < 0.001$. *COL IV: $P < 0.001$. *VN: $P \leq 0.05$. **(B)** Adhesion of HMEC-LNCX and HMEC-Notch4IC cells in the presence of function-blocking Abs against αvβ3 and β1 integrins. Adhesion assays were performed on plates coated with collagen type I. HMEC-LNCX and HMEC-Notch4IC cells were pre-incubated with IgG2a (1:100 dilution), anti-αvβ3 Ab (LM609, 10 μg/ml), and anti-β1 Ab (P4C10, 1:100, 1:250, and 1:500 dilutions). For cells treated with both αvβ3 and β1 Abs, 10 μg/ml and 1:100 dilution were used, respectively. * Anti-β1 1:100 dilution versus IgG: $P < 0.01$. **(C)** Adhesion of HMEC-LNCX and HMEC-Notch4IC cells in the presence of a function-blocking β1 integrin Ab. Adhesion assays were performed on plates coated with collagen type I or collagen type IV. Cells were pre-incubated with IgG2a (1:500 dilution) or anti-β1 Ab (P4C10, 2.5 μg/ml). Adhesion data shown are the mean ± standard deviation of a single experiment done in triplicate and are representative of at least three independent experiments. *Collagen I LNCX: $P < 0.001$. *Collagen I Notch4IC: $P \leq 0.05$. *Collagen IV LNCX: $P < 0.01$. *Collagen IV Notch4IC: $P < 0.001$.

We next tested whether Notch4IC affected the expression levels of αvβ3 and β1 integrins at the cell surface. Using flow cytometry, we demonstrated that neither αvβ3 nor β1 integrin levels were upregulated on the surface of HMEC-Notch4IC cells compared to controls (Figure 3.7A). In fact, in most experiments, there was decreased β1 integrin, but not αvβ3, on the surface of HMEC-Notch4IC cells. Non-ligand-binding (inactive or low-affinity) integrins can be converted to a ligand-binding (active or high-affinity) state via inside-out signaling (Hynes, 1987). Our findings of increased β1 integrin-mediated adhesion without increased β1 integrin expression suggest that Notch4IC may participate in an inside-out signaling process that promotes β1 integrin affinity. To test this hypothesis, we performed ligand binding assays using FITC-conjugated collagen type I. Binding of soluble collagen type I to HMEC-Notch4IC cells was greater than that for HMEC control cells (Figure 3.7B). Because HMEC-Notch4IC cells exhibit increased binding to soluble collagen type I (Figure 3.7B) without a corresponding increase in total β1 integrin expression (Figure 3.7A), our findings suggest that HMEC-Notch4IC cells display a greater number of β1 integrins in a high-affinity, active conformation, compared to control cells.

To confirm the increased proportion of active β1 integrin on the surface of HMEC-Notch4IC cells, Notch4IC cells and control cells were stained with Abs that specifically recognize active β1 integrin (B44) (Ni et al., 1998; Wilkins et al., 1996) or total β1 integrin (K20) (Takada and Puzon, 1993), and mean fluorescence ratios (active β1 / total β1) were determined by flow cytometry. Notch4IC cells, compared to control cells, displayed a greater proportion of β1 integrin receptors in a high-affinity state (Figure 3.8A). Based on our findings, we reasoned that if β1 integrins expressed on HMEC-Notch4IC cells were already in a high-affinity state, we would not be able to further increase β1 integrin-mediated adhesion to collagen. Using a

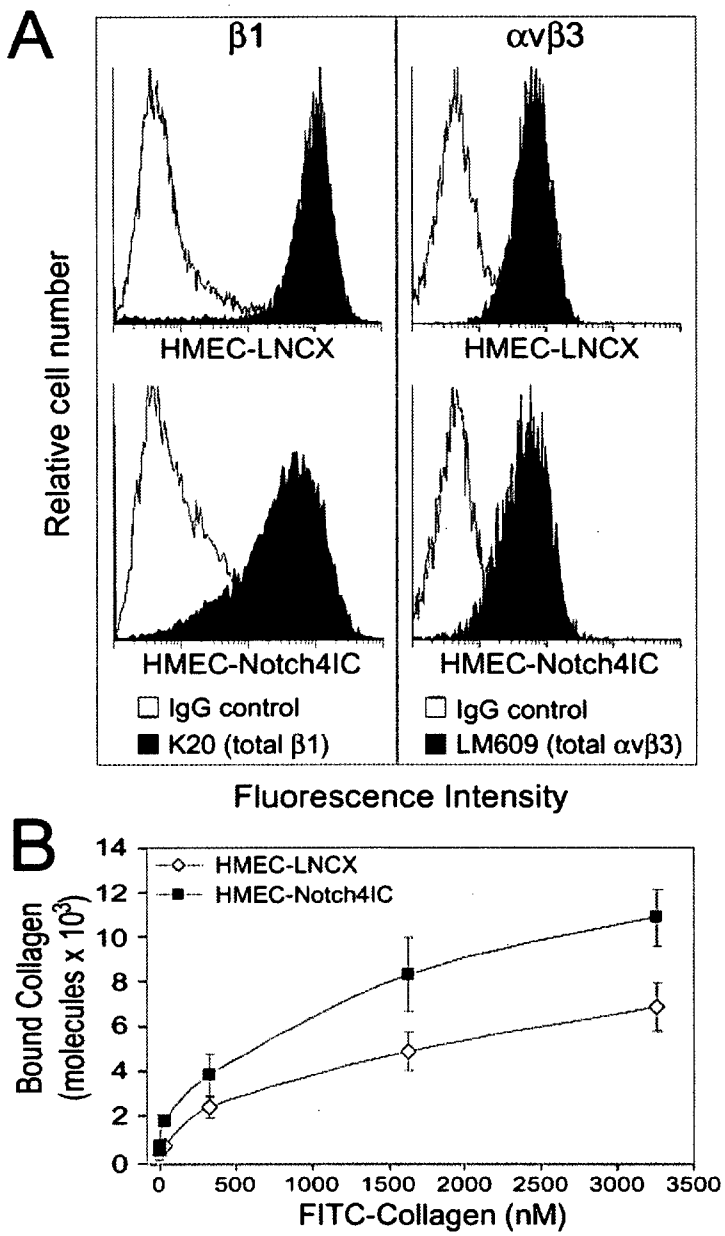

Figure 3.7: Activated Notch4 does not increase endothelial cell-surface expression of β1 integrins but enhances binding of soluble collagen. (A) Expression of αvβ3 and β1 integrins on the surface of HMEC-LNCX and HMEC-Notch4IC cells. Cells were incubated with Abs (IgG-control, K20-total β1, LM609-total αvβ3) and analyzed by flow cytometry. Histograms shown are representative of at least three independent experiments. **(B)** Binding curve of soluble collagen to HMEC-LNCX and HMEC-Notch4IC cells. FITC-conjugated collagen type I was incubated with cells at the indicated concentrations, and the samples analyzed by flow cytometry. Binding data shown are the mean ± standard deviation of two independent experiments.

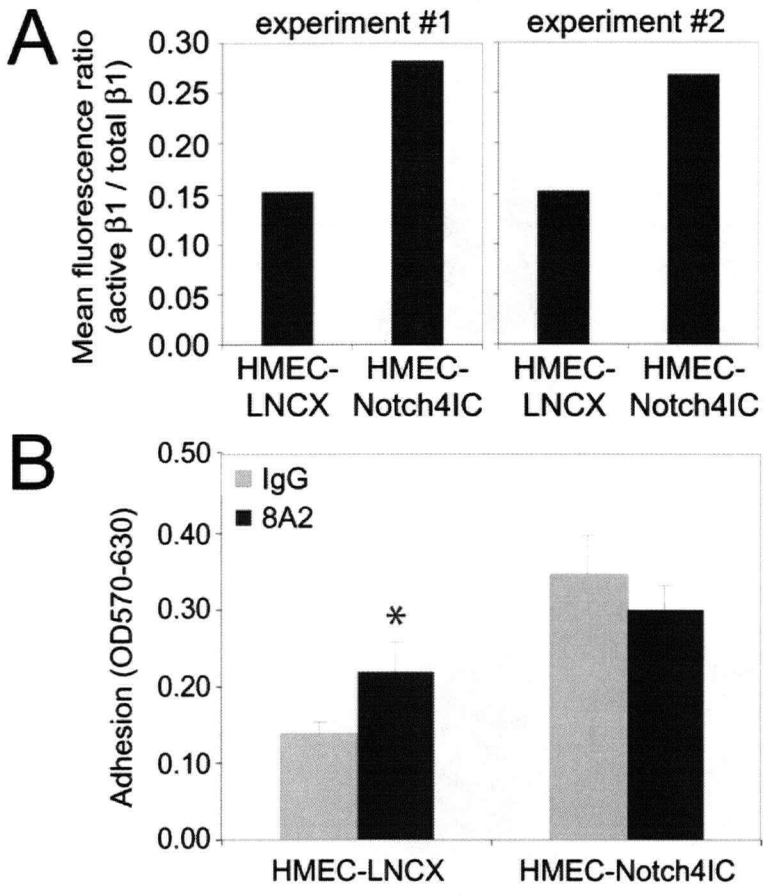

Figure 3.8: Activated Notch4-expressing cells display β1 integrins in a high-affinity conformation. (A) Mean fluorescence ratios of active β1 to total β1 on the surface of HMEC-LNCX and HMEC-Notch4IC cells. Cells were incubated with Abs (B44-active β1, K20-total β1) and assessed by flow cytometry. Data shown are from two independent experiments. **(B)** HMEC-Notch4IC cell adhesion to collagen cannot be increased by function-activating β1 integrin Abs. HMEC-LNCX and HMEC-Notch4IC cells pre-incubated with the function-activating β1 integrin Ab 8A2 were added to collagen type I-coated wells. Adherent cells were fixed, stained, and solubilized, and absorbance read at 570 nm with background absorbance subtracted at 630 nm. Data shown are the mean ± standard deviation of a single experiment done in triplicate and are representative of at least three independent experiments. *$P \leq 0.05$.

function-activating β1 integrin Ab (8A2) (Kovach et al., 1992), we found that whereas HMEC-LNCX cell adhesion to collagen type I could be increased, 8A2 was unable to increase HMEC-Notch4IC cell adhesion to collagen type I (Figure 3.8B). Taken together, our findings demonstrate that Notch4IC cells already display β1 integrins in a fully-active conformation.

3.2.6 Increased β1 integrin-mediated adhesion plays a role in the Notch4 inhibition of endothelial sprouting

Our data suggest that the inhibited sprouting of Notch4IC cells in vitro may be explained in part by an increased affinity to gelatin (denatured collagen)-coated beads, and that this high-affinity adhesive state (which presumably cannot be "turned off" due to the constitutive activation of Notch4) prevents the Notch4IC cells from migrating off the beads and into the fibrin gel. This would suggest that if Notch4IC cells were seeded onto beads by charge interaction rather than β1 integrin-mediated adhesion, the ability to form sprouts would be restored. To test this hypothesis, HMEC-Notch4IC cells were seeded onto dextran-coated microcarrier beads, and the beads were embedded into fibrin gels. In this assay, we noted that HMEC-Notch4IC cells formed sprouts to a similar extent as HMEC-LNCX cells (Figure 3.9). Hence in the absence of a β1 integrin substrate with which to interact, Notch4IC cells are capable of forming sprouts. As a control, dextran-coated beads were further coated with collagen type I, and then seeded with HMEC-Notch4IC cells. Similar to results shown in Figure 3.1B, sprouting of HMEC-Notch4IC cells from these collagen-recoated beads was inhibited (Figure 3.9).

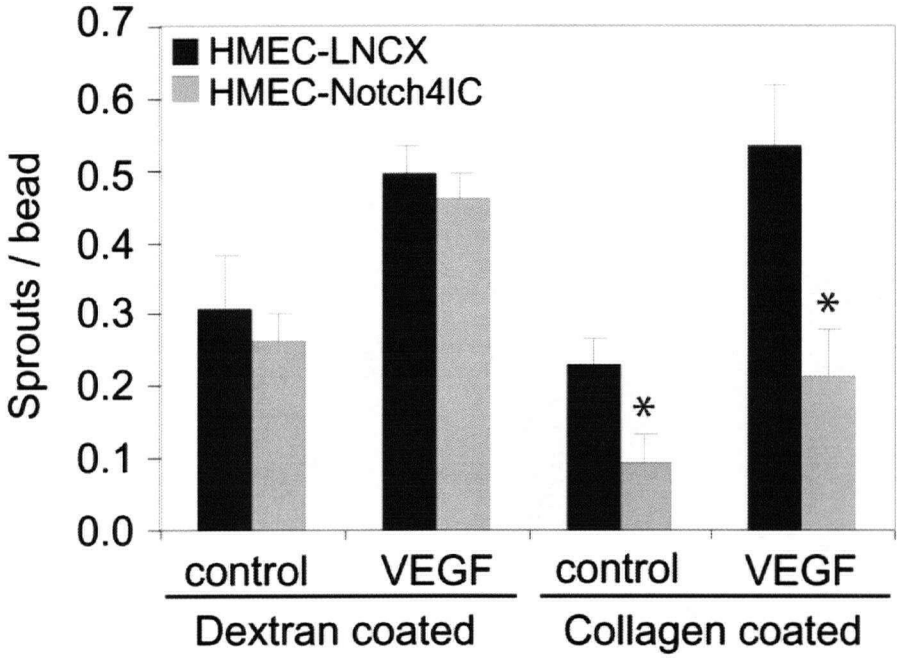

Figure 3.9: Activated Notch4 does not inhibit endothelial sprouting from dextran-coated microcarrier beads in vitro. Dextran-coated microcarrier beads were seeded with HMEC-LNCX or HMEC-Notch4IC cells. Equal numbers of beads were embedded in fibrin gels containing control medium or medium supplemented with VEGF (15 ng/ml). Endothelial sprout formation was quantitated after 3 days incubation. As a control, dextran-coated beads were coated with collagen type I, which were then seeded with HMEC cell lines. Data shown are the mean ± standard deviation of a single experiment done in triplicate and are representative of at least three independent experiments. *Control: $P < 0.01$. *VEGF: $P < 0.01$.

3.2.7 Activation of β1 integrins is sufficient to inhibit endothelial sprouting in vitro and angiogenesis in vivo

Our findings described thus far demonstrate that expression of activated Notch4 in endothelial cells inhibits angiogenesis both in vitro and in vivo, in part by promoting β1 integrin activation. To determine whether activation of β1 integrins alone (independent of constitutively-active Notch4 expression) was sufficient to inhibit angiogenesis, we performed in vitro and in vivo experiments using Abs that specifically activate β1 integrins.

Using the in vitro sprouting model with untransduced parental HMEC cells, we investigated the effect of the function-activating β1 integrin Ab 8A2 on VEGF-induced sprouting. Dextran-coated beads were preincubated with either 8A2 or LM534, a non-function-modifying β1 Ab (Takada and Puzon, 1993). These beads were subsequently seeded with parental HMEC, and incubated for three days to allow parental HMEC to produce and secrete their own matrix proteins (many of which are β1 integrin substrates) onto the bead surface (Kramer et al., 1985). Whereas VEGF was able to induce sprouting of parental HMEC from beads coated with LM534, sprouting from 8A2-coated beads was reduced (Figure 3.10A). Hence β1 integrin activation was sufficient to inhibit VEGF-induced endothelial sprouting in vitro. Using the in vivo chick CAM assay, VEGF-induced angiogenesis was examined in the presence of various anti-avian β1 integrin Abs (Figure 3.10B,C). CAMs were treated with TASC (a function-activating β1 integrin Ab) (Cruz et al., 1997; Neugebauer and Reichardt, 1991), V2E9 (a non-function-modifying β1 integrin Ab) (Hayashi et al., 1990), or W1B10 (a function-blocking β1 integrin Ab) (Cruz et al., 1997). Whereas VEGF was able to induce angiogenesis in CAMs treated with V2E9 and W1B10, CAMs treated with TASC exhibited decreased angiogenesis (Figure 3.10B,C). In fact, angiogenesis in TASC-treated CAMs was reduced to a level similar to that of CAMs treated with LM609 (Figure 3.10B,C), a function-blocking αvβ3

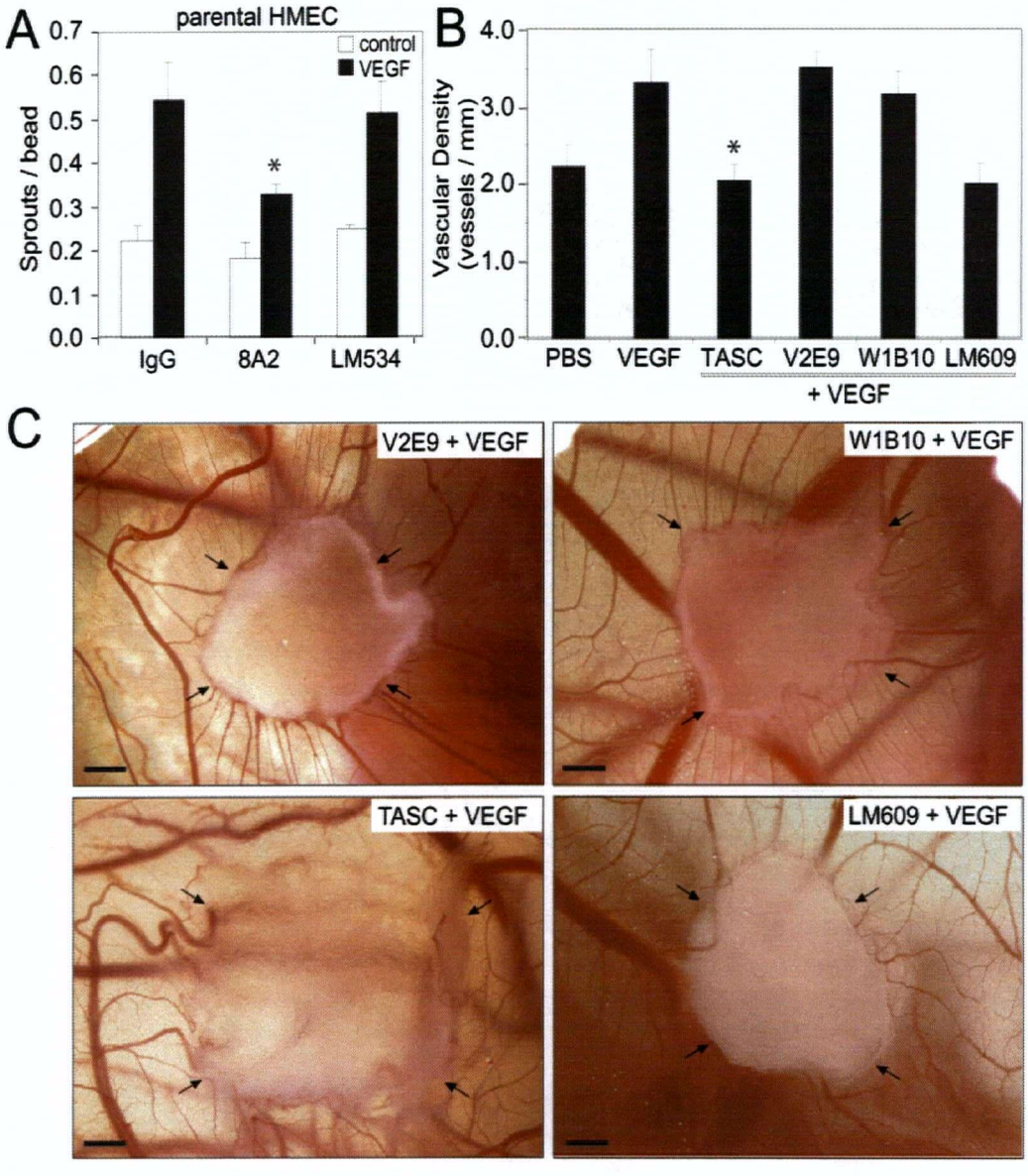

Figure 3.10: Activation of β1 integrins alone, independent of Notch4 activation, is sufficient to inhibit endothelial sprouting in vitro and angiogenesis in vivo. (A) In vitro sprouting of parental HMEC from microcarrier beads coated with anti-β1 integrin Abs. Dextran-coated microcarrier beads were pre-incubated with IgG control Ab, a function-activating β1 integrin Ab (8A2), or a non-function-modifying β1 integrin Ab (LM534). Data shown are the mean ± standard deviation of a single experiment done in triplicate and are representative of at least three independent experiments. *8A2 versus IgG: $P \leq 0.05$. *8A2 versus LM534: $P \leq 0.05$. **(B)** Angiogenesis in the chick CAM in the presence of anti-β1 integrin Abs. The following Abs were used: TASC (function-activating β1 integrin Ab), V2E9 (non-function-modifying β1 integrin Ab), W1B10 (function-blocking β1 integrin Ab), LM609 (function-blocking αvβ3 integrin Ab). Abs (10 μg/ml) plus VEGF (30 ng/ml) were loaded onto gelatin sponges, and the sponges placed on the CAMs of day 8 embryos. As controls, sponges containing PBS or VEGF (30 ng/ml) were placed on CAMs. Angiogenesis was quantitated on day 10. Data shown are the mean ± standard error of two experiments each done in replicates of 3-5 eggs. *TASC versus VEGF: $P \leq 0.05$. *TASC versus V2E9: $P < 0.0001$. **(C)** CAMs treated with V2E9, W1B10, TASC, and LM609 Abs, all in the presence of VEGF. CAMs shown are representative of two independent experiments. Arrows indicate the corners of the sponges. Bars represent 1 mm.

integrin Ab previously shown to attenuate VEGF-induced angiogenesis in the CAM (Friedlander et al., 1995). Taken together, our findings demonstrate that activation of β1 integrins, and hence increased adhesion through β1 integrins, is sufficient to inhibit VEGF-induced endothelial sprouting in vitro and angiogenesis in vivo.

3.3 DISCUSSION

Quiescent endothelial cells are normally anchored by their abluminal surface to a collagen-rich matrix (Carey, 1991; Iruela-Arispe et al., 1991b; Risau and Lemmon, 1988). At the initiation of angiogenesis, the mature collagen-containing matrix is degraded and replaced by a provisional matrix composed of fibrin (Dvorak et al., 1995) and fibronectin (Clark et al., 1982) upon which endothelial cells migrate and proliferate. The endothelial sprouting assay used in our studies mimics angiogenesis in vivo. Specifically, microvascular endothelial cells are seeded as a monolayer onto gelatin-coated beads, and are then induced by angiogenic factors to migrate into a fibrin matrix to form sprouts. We report that endothelial cells expressing Notch4IC exhibit inhibited sprouting in vitro (Figures 3.1 and 3.9), and that this inhibition can be explained in part by an increase in Notch4IC cell adhesion to collagen (Figures 3.6, 3.7, and 3.8). By enhancing cell adherence to collagen-coated beads, activated Notch4 prevents migration of the cells into the fibrin matrix. This is in accordance with our migration studies, in which Notch4IC cell migration through collagen, but not fibrinogen, is inhibited (Figure 3.5). Proliferation rates, on the other hand, are similar in HMEC-Notch4IC and control cells (Figure 3.4). Our in vivo studies demonstrate that Notch4IC expression in the chick CAM inhibits VEGF-induced angiogenesis (Figures 3.2 and 3.3). Based on our in vitro findings, the inhibition of angiogenesis in vivo may be due in part to enhanced endothelial cell adhesion to matrix proteins, thereby inhibiting vascular remodeling in the CAM. Since the completion of this thesis, results from our laboratory

have determined that Notch4IC-induced inhibition of endothelial sprouting requires the cdc10/ankyrin repeats of Notch4, and involves both CBF1-dependent and -independent pathways (MacKenzie et al., 2004a). Hence enhanced Notch4IC cell adhesion to collagen likely involves signaling mediated by the cdc10/ankyrin repeats.

Cell migration requires the coordinated activation and deactivation of integrins (Lauffenburger and Horwitz, 1996). As a cell migrates across a matrix, integrins at the leading edge of the cell adhere to the substrate (Huttenlocher et al., 1996). At the same time, integrins at the trailing edge of the cell detach from the substrate to allow the cell to progress forward (Palecek et al., 1998). Thus during the sprouting process of angiogenesis, integrin affinity states are constantly being modulated. Although $\alpha v\beta 3$ integrin has been shown to play a critical role in angiogenesis, several studies also delineate the essential contribution of $\beta 1$ integrins to endothelial morphogenesis (Bloch et al., 1997; Eliceiri and Cheresh, 1999). Our data show that activated Notch4 increases endothelial cell adhesion (Figure 3.6), and that enhanced $\beta 1$ integrin affinity plays a role in this increased adhesion (Figures 3.7 and 3.8). Hence the ability of Notch4 to inhibit endothelial sprouting in vitro and angiogenesis in vivo may be related in part to its ability to increase the ligand-binding affinity of $\beta 1$ integrins. Other potential mechanisms, however, may act in concert with $\beta 1$ integrin activation to mediate the observed Notch4 effect.

There is much evidence demonstrating that suppression of integrin activation is a physiological mechanism with which to control integrin-dependent cell adhesion and migration (Hughes and Pfaff, 1998). In addition, regulation of integrin activation has been reported to precede differentiation in several cell types. Regulation of $\beta 1$ integrin activity has been reported in neurogenic and myogenic differentiation, two processes that are also modulated by Notch (Boettiger et al., 1995; Neugebauer and Reichardt, 1991). In a baboon model, it has previously

been shown in uninjured saphenous arteries that endothelial cells and vascular smooth muscle cells express an epitope characteristic of β1 integrins in a high-affinity state (Koyama et al., 1996). However, six weeks following balloon injury, regenerating endothelial cells did not express this ligand-induced epitope, although there was no decrease in the expression of total β1 integrin (Koyama et al., 1996). In the same study, activation of β1 integrins with the function-activating β1 integrin Ab 8A2 inhibited the migration of endothelial cells in vitro (Koyama et al., 1996). Together, these findings suggest that activated β1 integrin is required to maintain endothelial cells in a quiescent state, but in order to repair arteries and possibly to allow neovascularization, dyshesion by downregulating β1 integrin affinity is required. In fact, activation of β1 integrins on human endothelial cells has been shown to inhibit capillary tube formation in collagen gels in vitro (Gamble et al., 1999). We report that activation of β1 integrins on endothelial cells, independent of Notch4 activation, inhibits endothelial sprouting in vitro (Figure 3.10A).

We demonstrate that β1 integrin activation can inhibit angiogenesis in the chick CAM in vivo (Figure 3.10B,C). In a previous study using function-blocking Abs directed against specific α integrin subunits, a combination of α1-blocking and α2-blocking Abs was shown to inhibit VEGF-induced angiogenesis in a mouse Matrigel plug assay (Senger et al., 1997). These findings suggest that blocking α1β1 and α2β1 integrin function can inhibit VEGF-induced angiogenesis (Senger et al., 1997). Although these results may seem contradictory to our data demonstrating that blocking β1 integrin function does not inhibit VEGF-induced angiogenesis in the chick CAM (Figure 3.10B,C), it is important to note that the effect of function-blocking/activating Abs directed against the β1 integrin subunit in the Matrigel plug assay was not reported. Because numerous α-β1 integrin heterodimers are implicated in angiogenesis

(Bauer et al., 1992; Davis et al., 1993), blocking the function of only the α1 and α2 subunits may result in a different phenotype from that seen when the function of all β1 integrins is blocked. Alternatively, the different results may reflect intrinsic differences in the experimental models used. Indeed, the function-blocking β1 integrin Ab CSAT has been reported to disrupt vascular development and lumen formation when micro-injected into quail embryos (Drake et al., 1992), whereas the same CSAT Ab does not affect FGF-2- or TNFα-induced angiogenesis in the chick CAM (Brooks et al., 1994a).

Our work demonstrates that constitutive Notch4 activation inhibits vascular remodeling. Importantly, our studies provide a possible mechanism with which to explain the common vascular defects observed in mutant mice with either increased (Uyttendaele et al., 2001) or decreased (Krebs et al., 2000) Notch signaling. Because Notch plays a role in cell fate decisions, Notch signaling must be precisely regulated and hence requires cessation of receptor signaling at certain times (Artavanis-Tsakonas et al., 1999; Milner and Bigas, 1999; Weinmaster, 2000). Similarly, because cell adhesion influences cell functions such as migration and cell phenotype, modulation of cell adhesion must be strictly regulated (Bloch et al., 1997; Gamble et al., 1993; Lauffenburger and Horwitz, 1996; Palecek et al., 1997; Ruoslahti and Engvall, 1997). Therefore, it is possible that knocking out Notch4 and Notch1 results in a loss of cell-ECM adhesion and hence inhibited vascular remodeling, whereas constitutive Notch4 activation results in excessive cell-ECM adhesion, thereby effectively fixing the cells in place. Taken together, our studies as well as the studies of Krebs et al. (Krebs et al., 2000) and Uyttendaele et al. (Uyttendaele et al., 2001) reveal that altered Notch4 signaling results in disrupted blood vessel development.

Because Notch4 expression is restricted to the endothelium (Uyttendaele et al., 1996), and because Notch4 is the only Notch receptor expressed in capillary endothelium (Villa et al.,

2001), our findings implicate selective activation of Notch4 as a possible method with which to inhibit angiogenesis in pathological contexts. However, because our studies involve a constitutively-active, overexpressed form of Notch4 in endothelial cells, the physiological relevance of the data must be interpreted with caution. Further studies using ligands specific for Notch4 will be important to determine whether ligand-induced activation of Notch4 also inhibits angiogenesis.

Chapter 4

NOTCH SIGNAL INHIBITION ATTENUATES BREAST TUMOR GROWTH BY REVERSING THE MESENCHYMAL PHENOTYPE

4.1 ABSTRACT

During tumor progression, tumor cells of epithelial origin often acquire a mesenchymal phenotype through EMT, a process that promotes invasion and dissemination of cancer cells (Vincent-Salomon and Thiery, 2003). Recent studies from our laboratory and others have shown that activation of Notch signaling promotes a specialized type of EMT, EndoMT (Noseda et al., 2004b; Timmerman et al., 2004). Given that Notch pathway elements are expressed at sites of epithelial-mesenchymal cell-cell interactions during embryogenesis (Mitsiadis et al., 1995; Nakagawa et al., 1999) and within primary human breast tumors (Callahan and Egan, 2004; Imatani and Callahan, 2000; Parr et al., 2004; Pece et al., 2004; Weijzen et al., 2002), and that loss of E-cadherin directly correlates with EMT in human breast cancer (Behrens et al., 1989), we determined whether Notch signaling would modulate E-cadherin expression and hence breast tumorigenesis. We have identified activated Notch signaling as a novel mechanism for the downregulation of E-cadherin expression in human breast epithelial cells. We demonstrate that inhibition of Notch signaling attenuates E-cadherin promoter methylation and induces E-cadherin re-expression in human breast tumor cells previously lacking E-cadherin expression, resulting in restricted β-catenin nuclear accumulation and a marked reduction in tumor growth and metastasis.

4.2 RESULTS

4.2.1 Activated Notch signaling inhibits E-cadherin expression in human breast epithelial cells

We transduced the E-cadherin-positive human breast epithelial cell line MCF-10A with a retroviral vector (MIY) containing YFP linked to Notch1IC or Notch4IC through an internal ribosomal entry site. Expression of Notch1IC or Notch4IC induced cytologic changes consistent with EMT, such as cell scattering and the acquisition of a spindle-shaped morphology (Figure 4.1A). Notch1IC or Notch4IC expression also reduced E-cadherin expression (Figure 4.1B,C). Because MCF-10A are an immortalized human breast epithelial cell line (Tait et al., 1990), we determined whether Notch1IC or Notch4IC expression would inhibit E-cadherin expression in primary breast epithelial cells. Similar to MCF-10A, primary human breast epithelial cells transduced with activated Notch1 or Notch4 downregulated E-cadherin expression (Figure 4.2).

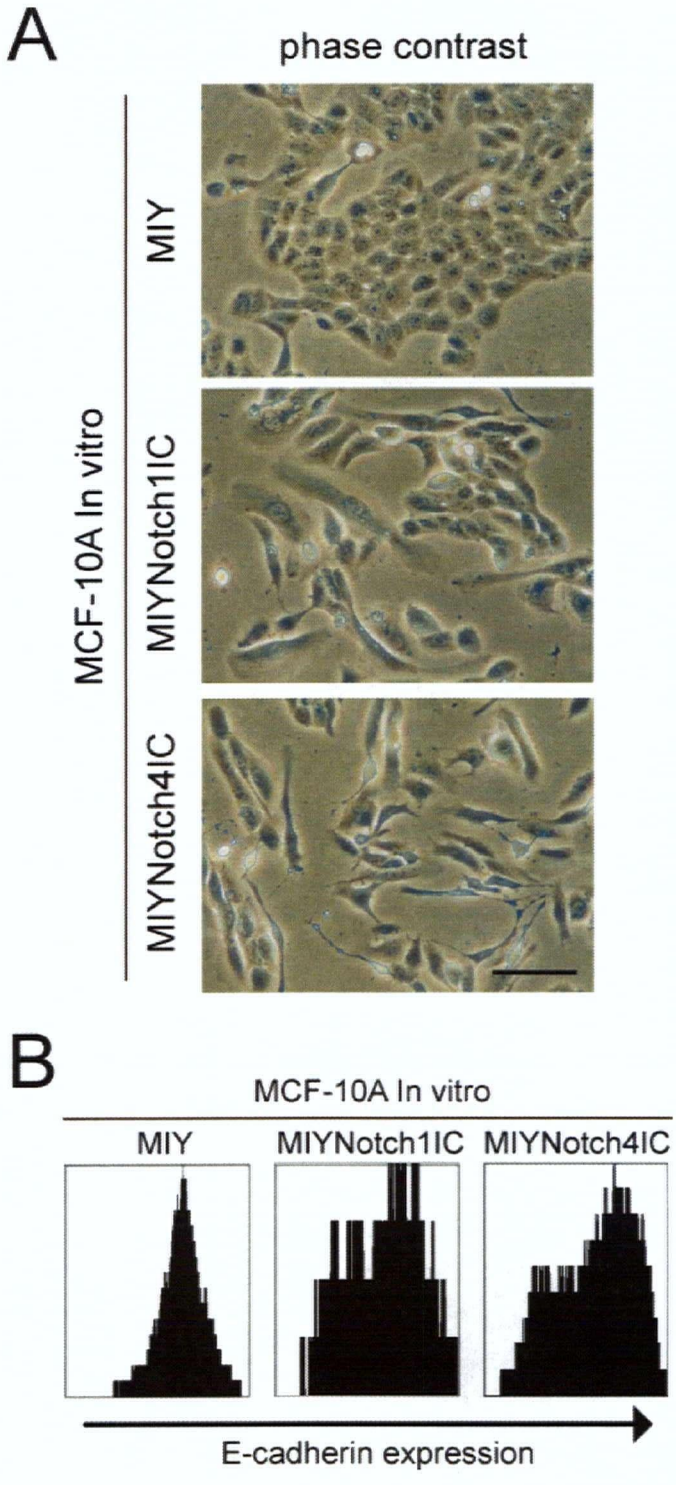

Figure 4.1 (Part 1): Activated Notch signaling inhibits E-cadherin expression in MCF-10A human breast epithelial cells. (A) Phase contrast images of MCF-10A cells transduced with MIY, MIYNotch1IC, or MIYNotch4IC. Bar, 100 μm. **(B)** Flow cytometry histograms for surface E-cadherin expression in MCF-10A cell lines. Data shown are from one experiment and are representative of two independent experiments. **(C)** (see next page).

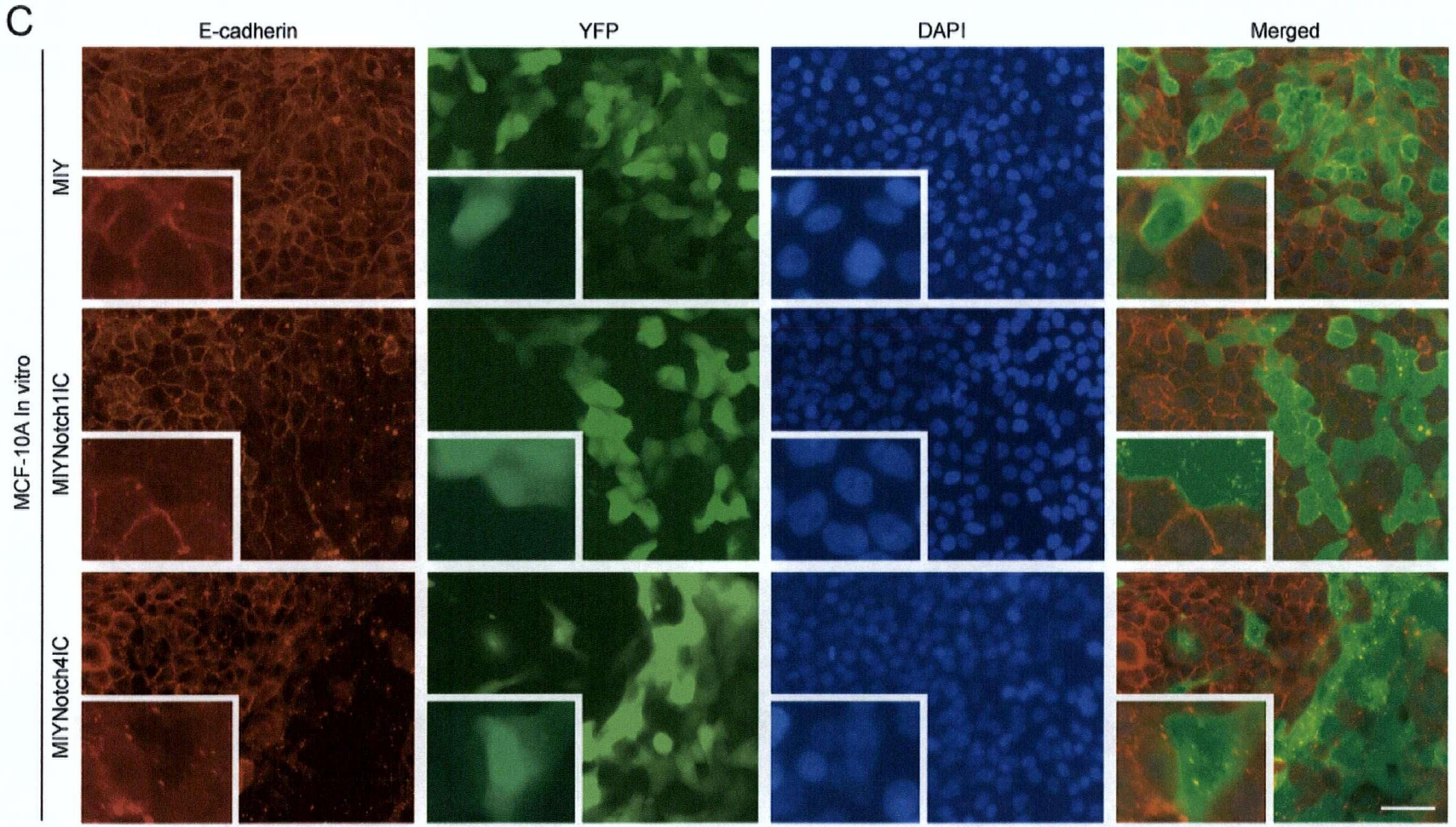

Figure 4.1 (Part 2): Activated Notch signaling inhibits E-cadherin expression in MCF-10A human breast epithelial cells. (C) Immunofluorescence for E-cadherin (red), YFP (yellow), and DAPI (blue) in MCF-10A cell lines. Bar, 50 μm. Insets represent close-up magnifications of 6-8 cells.

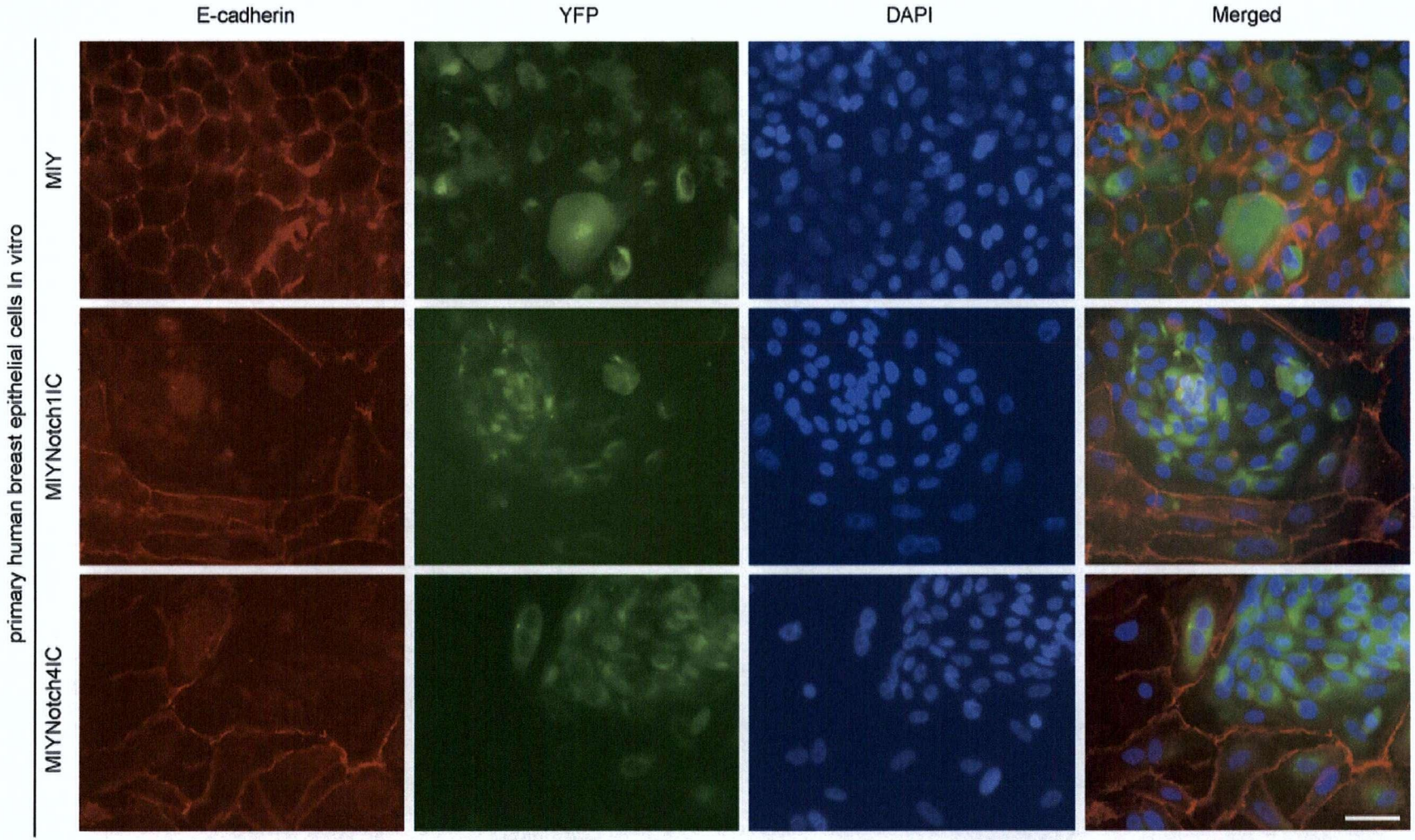

Figure 4.2: Activated Notch signaling inhibits E-cadherin expression in primary human breast epithelial cells. Immunofluorescence for E-cadherin (red), YFP (yellow), and DAPI (blue) in primary human breast epithelial cells transduced with MIY, MIYNotch1IC, or MIYNotch4IC. Bar, 100 μm.

4.2.2 Notch signal inhibition reduces human breast tumor growth in vivo

Having demonstrated that activated Notch signaling is associated with a decrease in E-cadherin expression in human breast epithelial cells, we sought to determine whether inhibition of Notch signaling would induce re-expression of E-cadherin and inhibit tumor growth in MDA-MB-231 human breast tumors. MDA-MB-231 cells are E-cadherin-negative despite possessing one wildtype E-cadherin gene, and thus exhibit reversible E-cadherin silencing (van de Wetering et al., 2001). We also performed experiments with mouse Lewis lung carcinoma cells, which express barely detectable levels of E-cadherin protein (Foty and Steinberg, 1997). Both cell types expressed multiple Notch receptors and ligands (Figure 4.3A); however, MDA-MB-231 cells exhibited approximately a 5-fold greater expression of the key Notch target gene HES1 (Figure 4.3B).

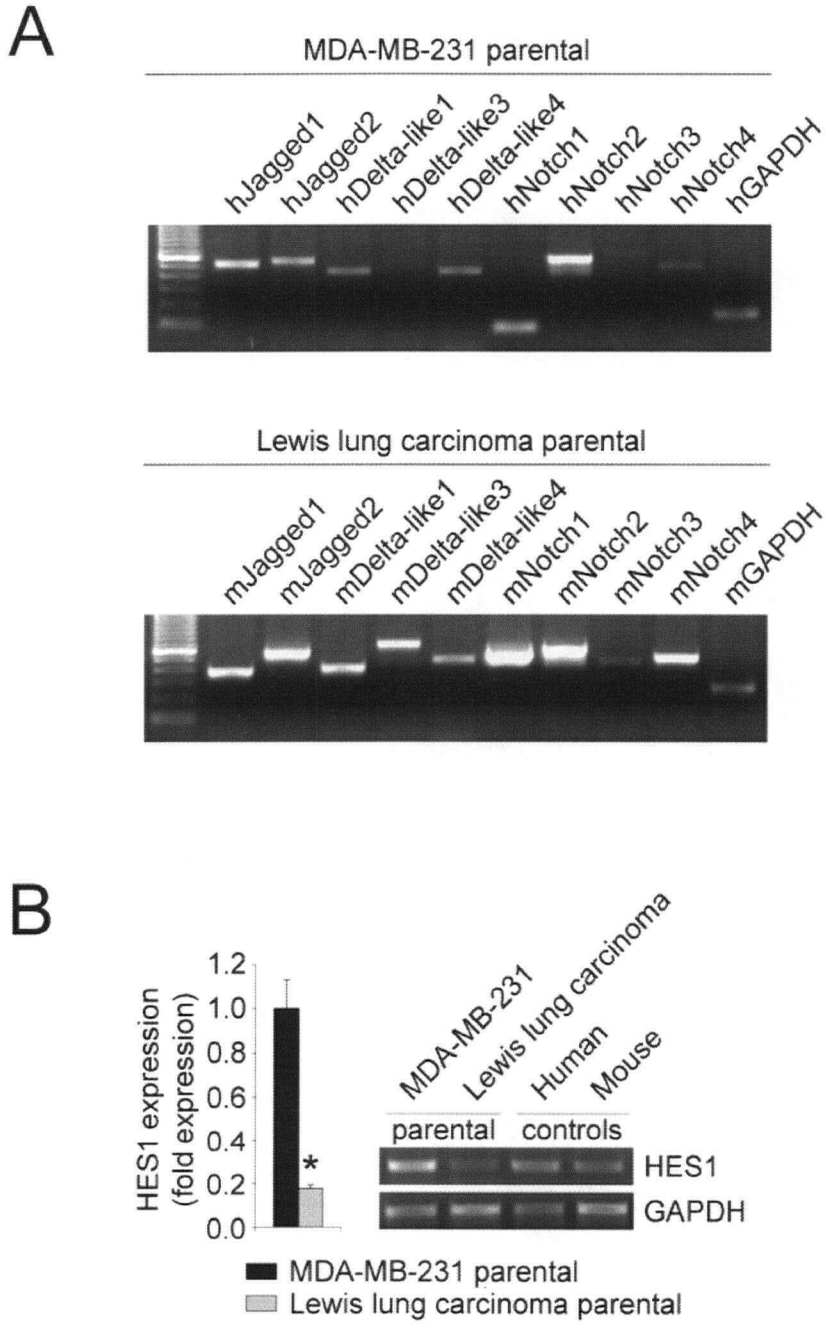

Figure 4.3: MDA-MB-231 and Lewis lung carcinoma parental tumor cells both express Notch ligands and receptors, with MDA-MB-231 cells expressing greater levels of HES1. **(A)** RT-PCR for expression of human Notch ligands and receptors in MDA-MB-231 parental cells and mouse Notch ligands and receptors in Lewis lung carcinoma parental cells. Human-specific primer sets do not recognize mouse targets, and mouse-specific primer sets do not recognize human targets. **(B)** RT-PCR for expression of the Notch target gene HES1 in MDA-MB-231 and Lewis lung carcinoma parental cells. Primers were designed to recognize both human and mouse HES1. Data shown represent mean ± standard error from three independent experiments. *P < 0.01.

The most commonly used inhibitors of Notch signaling are the γ-secretase inhibitors, which block proteolytic processing of transmembrane Notch (Das et al., 2004). However, these inhibitors are not specific for Notch signaling as they also block signaling by other receptors such as ErbB4 (Lee et al., 2002). To specifically inhibit Notch signaling, we generated a retroviral construct expressing the soluble extracellular domain of human Notch4 (XNotch4). We transduced XNotch4 cDNA into MDA-MB-231 or Lewis lung carcinoma cells and confirmed secretion of the soluble protein (Figure 4.4). When implanted subcutaneously into immunodeficient mice, XNotch4 inhibited MDA-MB-231 but not Lewis lung carcinoma tumor growth (Figure 4.5A). We confirmed in vivo expression of XNotch4 protein in both tumor types (Figure 4.5B). In addition to reduced growth of the primary tumor, inhibition of Notch signaling reduced both the number and average weight of metastatic nodules in axillary and subiliac lymph node regions in XNotch4 mice (Figure 4.6). Neither control nor XNotch4 mice exhibited metastases in internal organs (data not shown). By semi-quantitative RT-PCR using two primer sets, one specific for human HES1 and the other for mouse HES1, we confirmed in MDA-MB-231 xenografts that XNotch4 inhibited Notch signaling specifically in the human tumor cells and not in the murine stromal cell compartment (Figure 4.7A,B). Also, HES1 mRNA levels were not altered between Lewis lung carcinoma tumors expressing vector or XNotch4 (Figure 4.7C). These findings may explain the lack of tumor growth inhibition in Lewis lung carcinoma tumors expressing XNotch4 (Figure 4.5A).

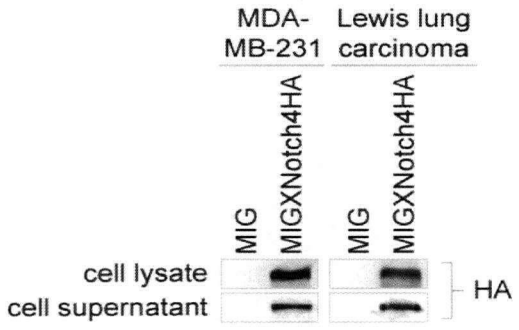

Figure 4.4: XNotch4 protein is secreted. Immunoblot for expression of HA-tagged XNotch4 in MDA-MB-231 and Lewis lung carcinoma cell lines transduced with MIG or MIGXNotch4HA. Concentrated supernatant from cultured cells was obtained by filtering 3 day conditioned medium through a 100,000 kDa molecular weight cut-off Ultrafiltration Membrane.

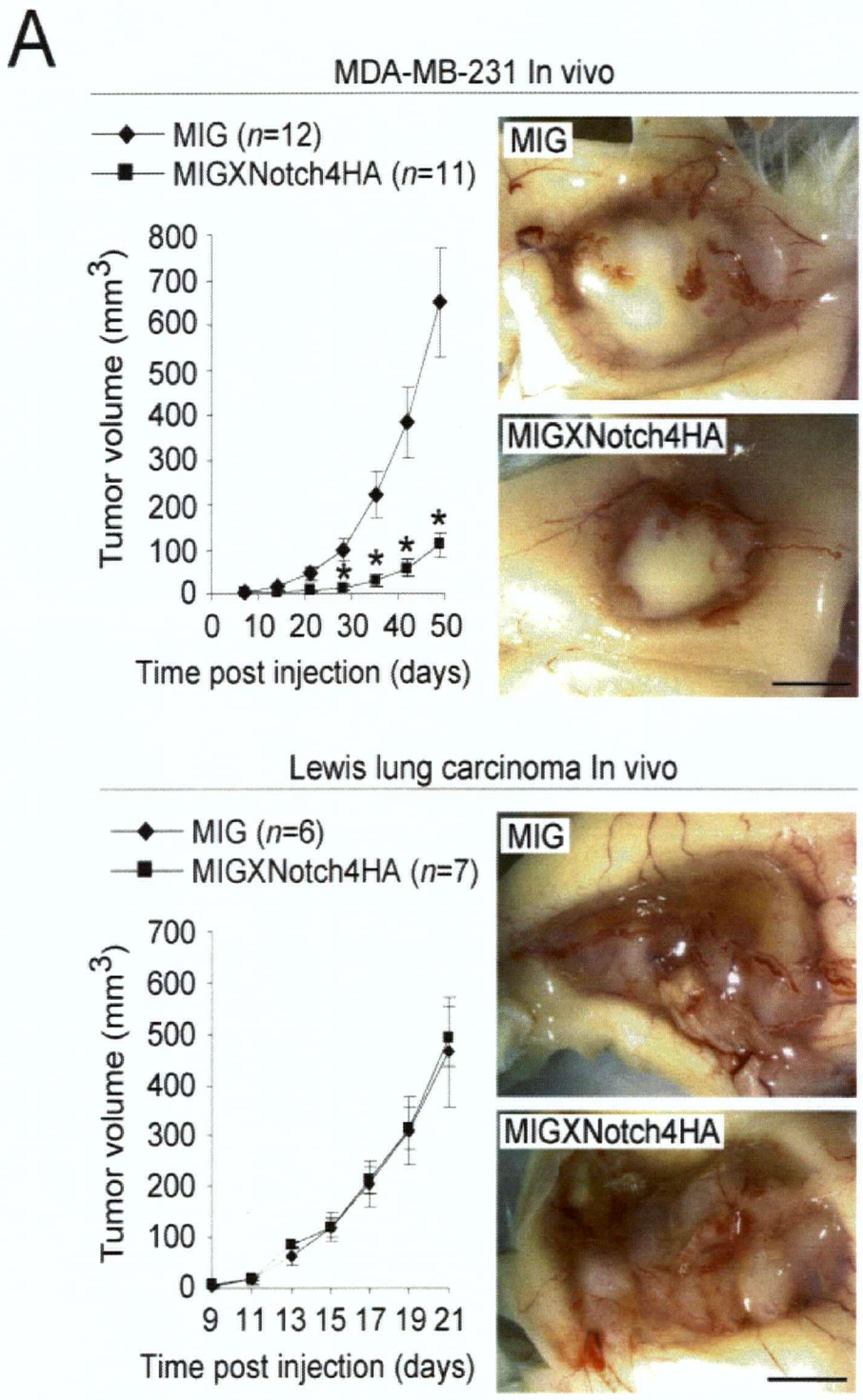

Figure 4.5 (Part 1): Notch signal inhibition reduces human breast tumor growth in vivo. (A) Tumor growth curves for MDA-MB-231 and Lewis lung carcinoma cell lines grown as xenografts in the dorsa of mice. MDA-MB-231 and Lewis lung carcinoma tumor volumes were measured weekly and every two days, respectively. Representative macroscopic images of tumors at the time of sacrifice are shown. Bar, 5 mm. *P < 0.01. **(B)** (see next page).

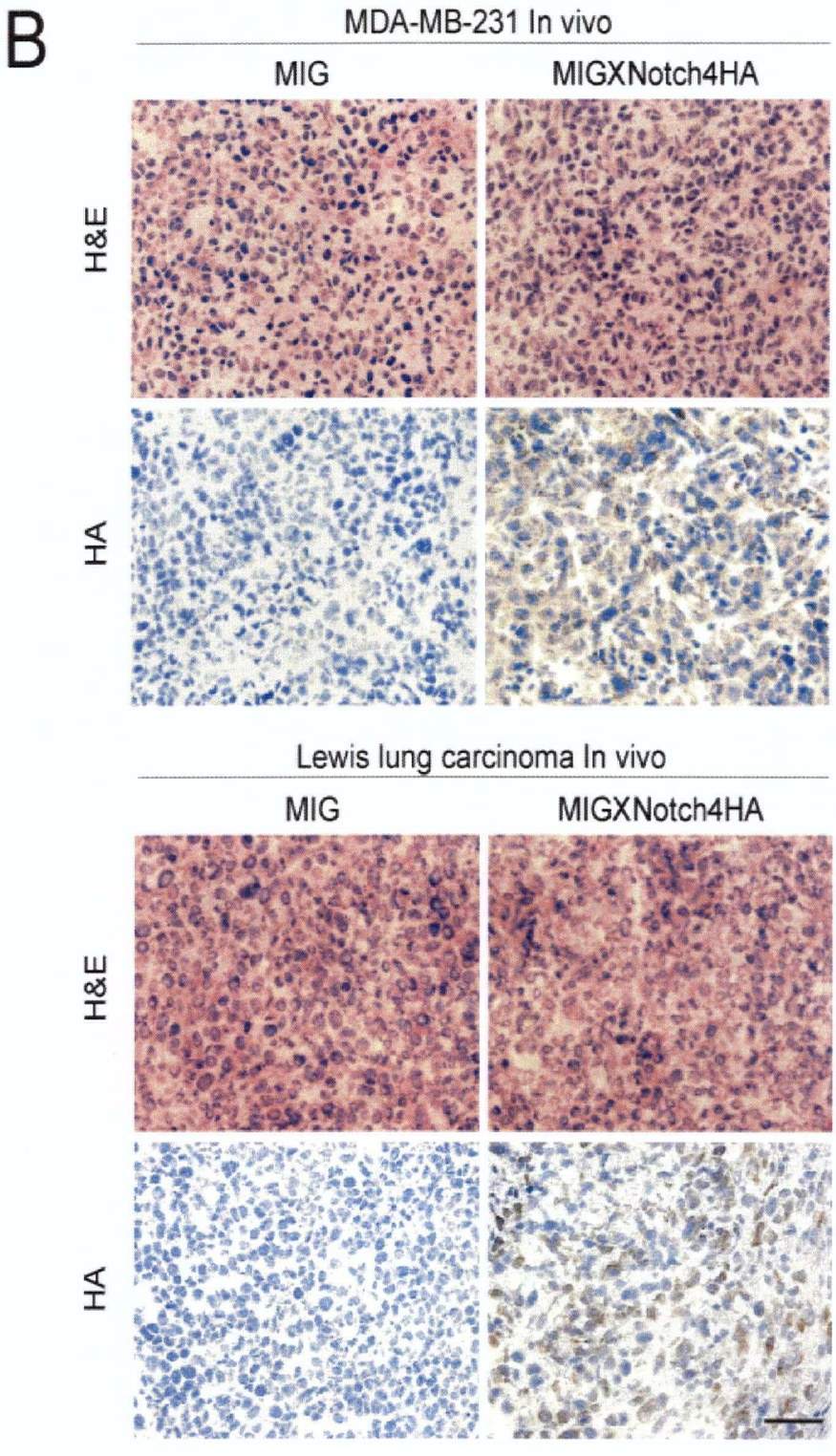

Figure 4.5 (Part 2): Notch signal inhibition reduces human breast tumor growth in vivo. (B) Immunostaining for XNotch4HA expression in MDA-MB-231 and Lewis lung carcinoma tumors. H&E staining is also shown. Bar, 50 μm.

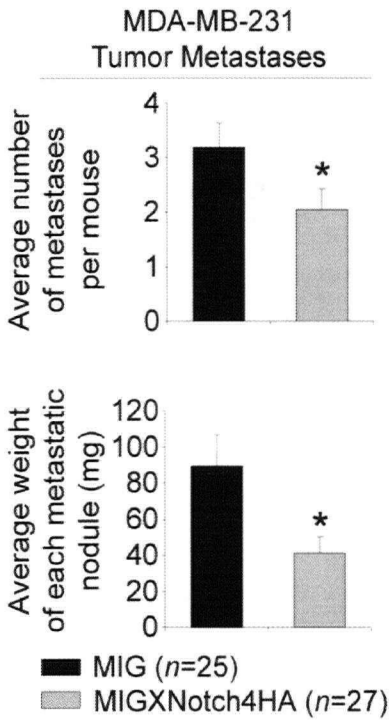

Figure 4.6: Notch signal inhibition reduces metastasis of human breast tumors in vivo. Quantitation of metastases in MDA-MB-231 tumor-bearing mice. Control and XNotch4 mice were sacrificed at the same time, mice were examined for metastases, and the total number and total weight of metastases determined. Data shown represent the average number of metastases per mouse ± standard error, and the average weight of each metastatic nodule ± standard error. *P ≤ 0.05. Metastasis data were determined by analyzing 25 MIG tumors and 27 MIGXNotch4HA tumors.

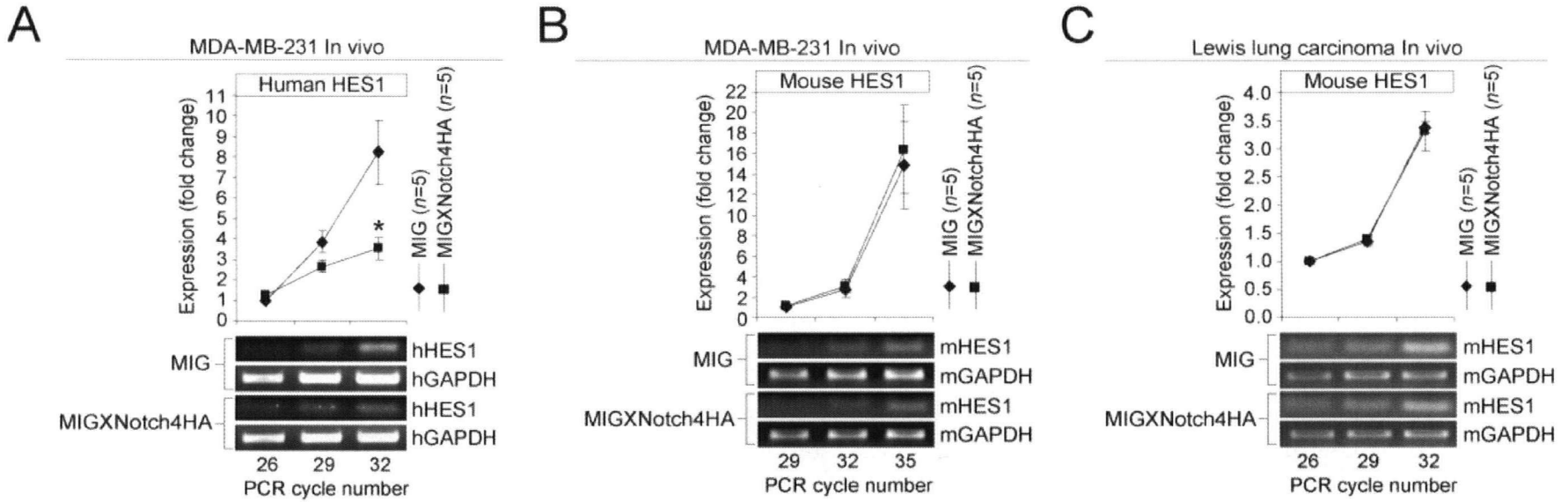

Figure 4.7: Soluble XNotch4 inhibits Notch signaling specifically in the tumor cell compartment of MDA-MB-231 tumors in vivo. Total RNA was harvested from MDA-MB-231 and Lewis lung carcinoma tumors, and reverse-transcribed into cDNA. For semi-quantitative RT-PCR, individual reactions along with GAPDH control reactions were terminated after the designated number of PCR cycles. **(A)** Semi-quantitative RT-PCR for expression of the Notch target gene HES1 specifically in the tumor cell compartment of MDA-MB-231 tumors. Data shown represent mean ± standard error. *P < 0.0001. **(B)** Semi-quantitative RT-PCR for HES1 expression in the host cell compartment of MDA-MB-231 tumors. Data shown represent mean ± standard error. **(C)** Semi-quantitative RT-PCR for HES1 expression in Lewis lung carcinoma tumors. Data shown represent mean ± standard error.

Although data from this thesis and other studies (Krebs et al., 2000; Uyttendaele et al., 2001) demonstrate that aberrant Notch signaling results in disrupted in vivo embryonic blood vessel development, we did not observe differences in vascular density in implanted tumors in response to XNotch4 (Figure 4.8A,B). This suggests that inhibition of angiogenesis is not the mechanism by which XNotch4 inhibits MDA-MB-231 tumor growth. However, because angiogenesis inhibitors can induce tumor regression without altering vascular density (Hlatky et al., 2002), vascular density alone may not provide a good evaluation of anti-angiogenic activity. Hence an anti-angiogenic role for XNotch4 cannot be completely ruled out.

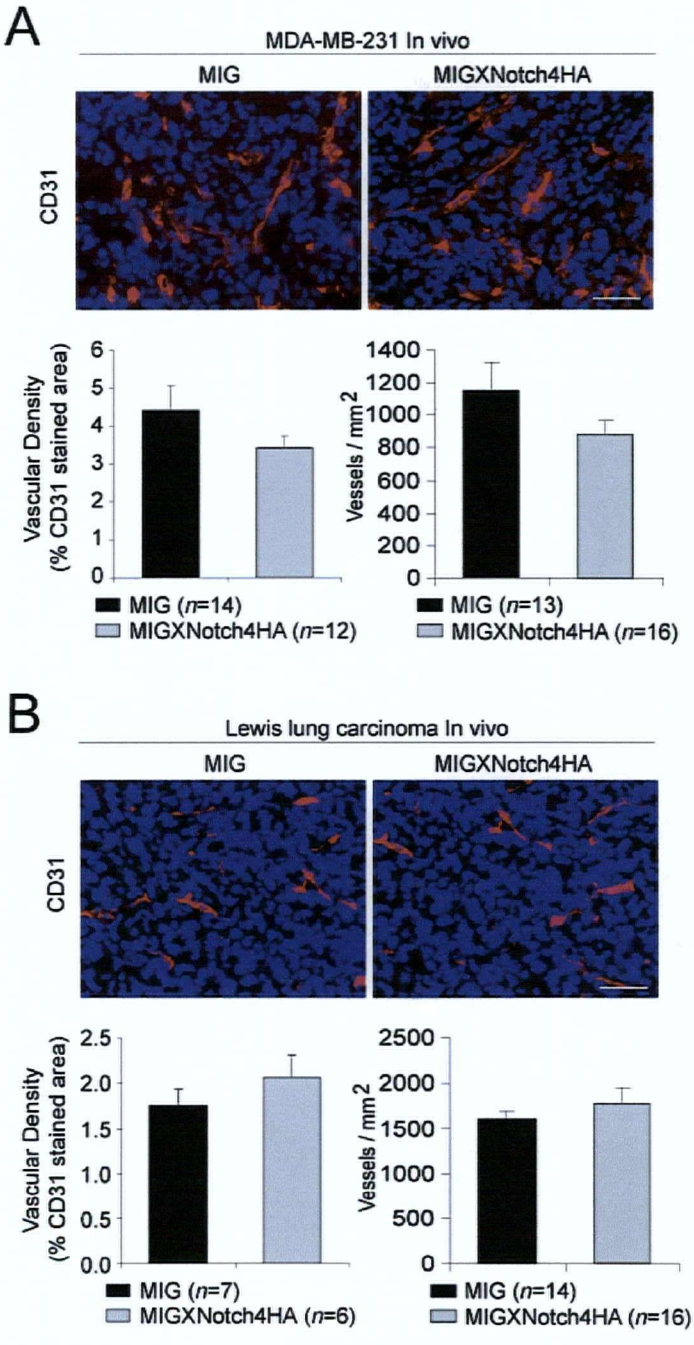

Figure 4.8: Soluble XNotch4 does not affect vascular density in vivo. (A) Vascular density in MDA-MB-231 tumors in vivo. Immunostaining for the endothelial marker CD31 (red) and DAPI (blue). Bar, 50 μm. Vascular density was quantitated by expressing the CD31 stained area as a percentage of the total tumor area, and by number of vessels per mm^2. Data shown represent mean ± standard error. **(B)** Vascular density in Lewis lung carcinoma tumors in vivo. Immunostaining for CD31 (red) and DAPI (blue). Bar, 50 μm. Vascular density was quantitated by expressing the CD31 stained area as a percentage of the total tumor area, and by number of vessels per mm^2. Data shown represent mean ± standard error.

4.2.3 Notch signal inhibition induces E-cadherin expression in human breast tumors in vivo

We examined MDA-MB-231 tumor xenografts to determine whether Notch inhibition induced re-expression of E-cadherin. XNotch4 but not control tumors expressed E-cadherin protein (Figure 4.9A). Because the Ab used recognizes both human and mouse E-cadherin, RT-PCR was performed with human E-cadherin-specific primers. Human E-cadherin transcripts were detected only in tumors in which Notch was inhibited (Figure 4.9B), suggesting transcriptional reversal of E-cadherin repression specifically in the human tumor xenografted cells. By immunofluorescence microscopy, E-cadherin staining was detected at the plasma membrane in response to Notch inhibition (Figure 4.9C), indicating a functional re-expression of E-cadherin.

β-catenin contributes to breast tumorigenesis by translocating into the nucleus to modulate the expression of genes involved in cell proliferation, invasion, and EMT (Conacci-Sorrell et al., 2003; Crawford et al., 1999; He et al., 1998; Lin et al., 2000). When bound to E-cadherin, however, signaling-competent nuclear β-catenin levels diminish resulting in suppression of cell proliferation and invasion (Wong and Gumbiner, 2003). Because β-catenin binding to cadherins stabilizes catenin expression (Wheelock et al., 2001), we determined whether E-cadherin re-expression in XNotch4 tumors modulated β-catenin expression. Whereas control tumors expressed low levels of β-catenin protein, levels were increased in XNotch4 tumors, which correlated positively with E-cadherin expression (Figure 4.9A). Importantly, however, β-catenin was present at the plasma membrane when Notch was inhibited, but exhibited cytoplasmic/nuclear localization in control tumors (Figure 4.9C). Indeed, we detected a significantly lower proportion of nuclear β-catenin-positive tumor cells in XNotch4 tumors compared to that of control tumors (Figure 4.9D), which was confirmed by immunoblot analysis

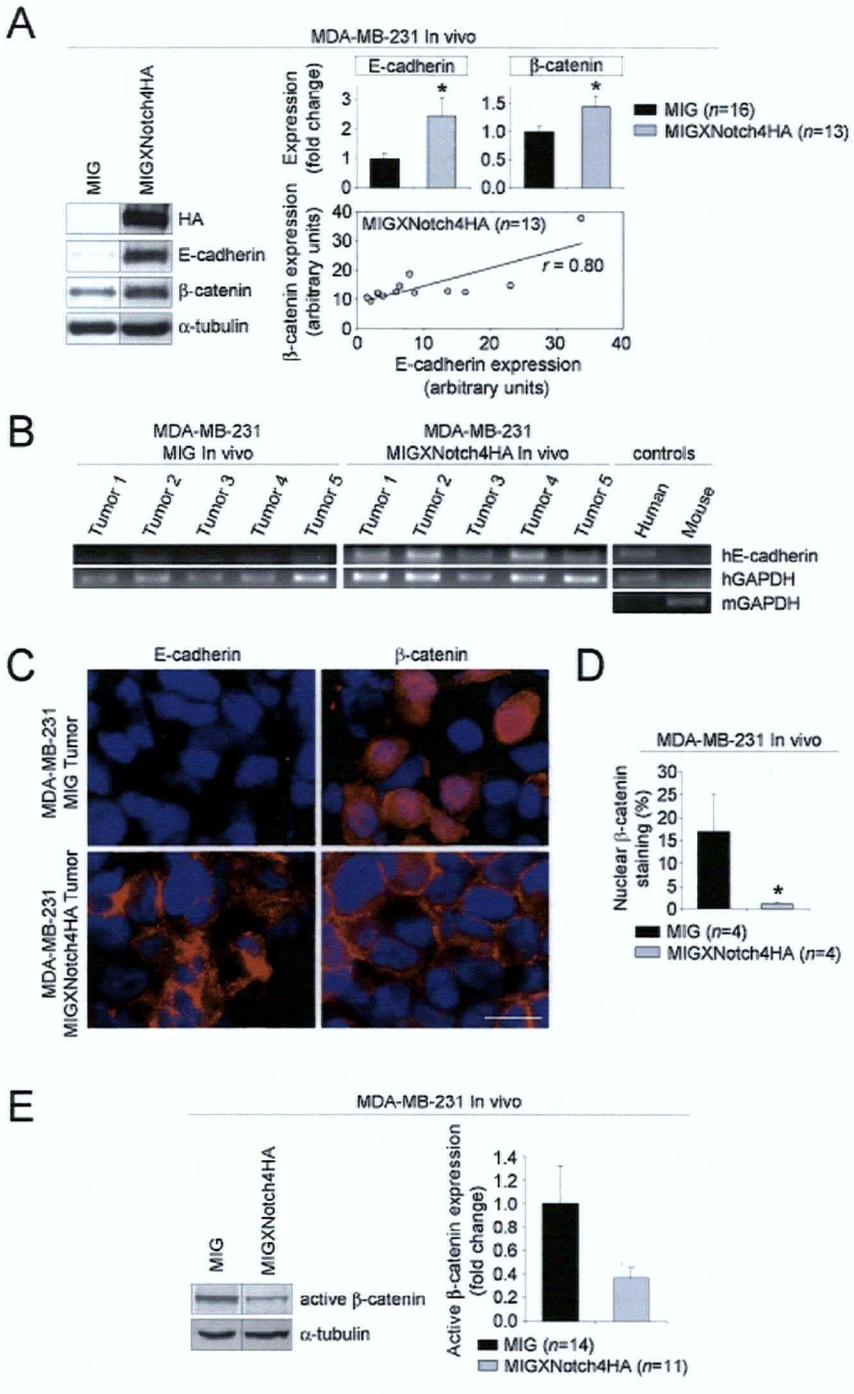

Figure 4.9: Notch signal inhibition induces E-cadherin expression in xenografted human breast tumor cells in vivo. (A) Immunoblot for expression of XNotch4HA, E-cadherin, β-catenin, and tubulin in MDA-MB-231 tumors. Total protein lysates were prepared from tumor tissue. Data shown represent mean ± standard error. *P ≤ 0.05. Positive correlation, P < 0.01. **(B)** RT-PCR for expression of human E-cadherin in MDA-MB-231 tumors. Total RNA was isolated from MDA-MB-231 tumors, and reverse-transcribed into cDNA. Primers recognize human but not mouse E-cadherin. **(C)** Immunofluorescence for E-cadherin (left panels; red), β-catenin (right panels; red), and DAPI (blue) in MDA-MB-231 tumors. Bar, 15 μm. **(D)** Quantitation of nuclear β-catenin staining in MDA-MB-231 tumors. Data shown represent mean ± standard error. *P ≤ 0.05. **(E)** Immunoblot for expression of active β-catenin and tubulin in MDA-MB-231 tumors in vivo. Data shown represent mean ± standard error.

of tumor lysates with an Ab specific for active β-catenin (Figure 4.9E). These results suggest that inhibition of Notch signaling reverses the mesenchymal phenotype by re-inducing expression of E-cadherin, which in turn inhibits β-catenin nuclear translocation to elicit an inhibition of tumor growth.

4.2.4 Expression of E-cadherin alone is sufficient to inhibit human breast tumor growth in vivo

To determine whether re-expression of E-cadherin alone (independent of Notch signal inhibition) was sufficient to inhibit MDA-MB-231 tumor growth, we transduced MDA-MB-231 cells with human E-cadherin cDNA and grew xenografts in mice. E-cadherin overexpression had a similar effect on MDA-MB-231 tumors as that of XNotch4-induced E-cadherin expression. Overexpression of E-cadherin inhibited tumor growth (Figure 4.10A). E-cadherin expression also inhibited MDA-MB-231 metastasis formation (Figure 4.10B). We confirmed E-cadherin expression and β-catenin induction in E-cadherin-overexpressing tumors (Figure 4.10C), and observed a positive correlation between E-cadherin and β-catenin expression (Figure 4.10C). By immunofluorescence microscopy, we detected plasma membrane staining for both E-cadherin and β-catenin (Figure 4.10D). Taken together with our XNotch4 tumor data, our results show that XNotch4-induced re-expression of E-cadherin plays a causal role in the inhibition of MDA-MB-231 tumor growth and metastasis.

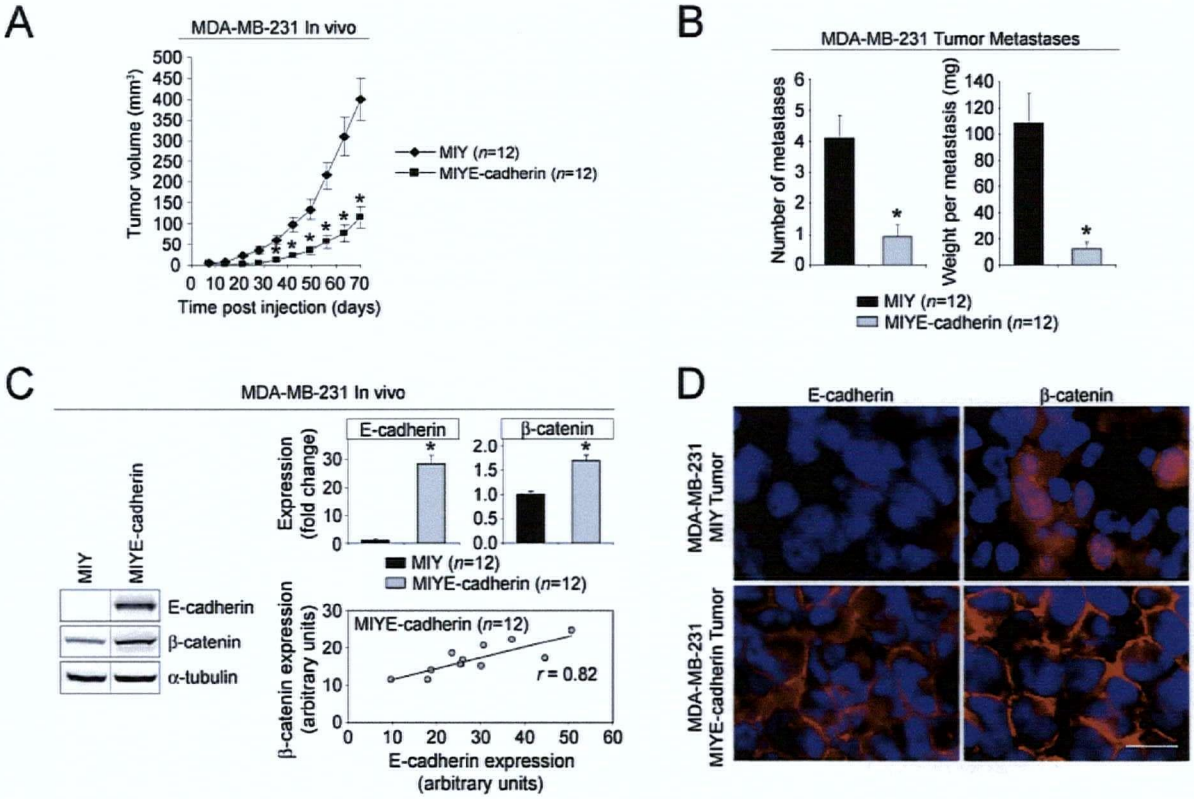

Figure 4.10: Expression of E-cadherin alone, independent of Notch signal inhibition, is sufficient to inhibit human breast tumor growth in vivo. (A) Tumor growth curves for MDA-MB-231 cells transduced with MIY or MIYE-cadherin grown as xenografts in mice. Tumor volumes were measured weekly. *P < 0.001. **(B)** Immunoblot for expression of E-cadherin, β-catenin, and tubulin in MDA-MB-231 tumors. Total protein lysates were prepared from tumor tissue. Data shown represent mean ± standard error. *E-cadherin: P < 0.0000001; *β-catenin: P < 0.0001. Positive correlation, P < 0.001. **(C)** Immunofluorescence for E-cadherin (left panels; red), β-catenin (right panels; red) and DAPI (blue) in MDA-MB-231 tumors. Bar, 15 μm. **(D)** Quantitation of metastases in MDA-MB-231 tumor-bearing mice. After sacrifice, mice were examined for lymph node metastases and the total number and total weight of metastases determined. Data shown represent mean ± standard error. *P < 0.001.

4.2.5 Induction of E-cadherin expression is mediated by attenuated E-cadherin promoter methylation

Our findings demonstrate that inhibited Notch signaling attenuates MDA-MB-231 tumor growth by inducing E-cadherin re-expression. To elucidate a possible mechanism(s) by which inhibited Notch signaling re-induces E-cadherin expression, we investigated the effects of Notch signal inhibition on known mechanisms of E-cadherin silencing. E-cadherin expression can be repressed by several mechanisms including gene mutation, gene deletion, shedding, endocytosis, transcriptional repression, and promoter hypermethylation (Berx et al., 1998; Fujita et al., 2002; Hennig et al., 1996; Herman and Baylin, 2003; Katayama et al., 1994). The latter two mechanisms have been reported to play a role in E-cadherin silencing in MDA-MB-231 cells (Graff et al., 1995; Hajra et al., 2002). The E-cadherin proximal promoter, containing binding sites for E-cadherin transcriptional repressors and sites of promoter methylation, is shown in Figure 4.11.

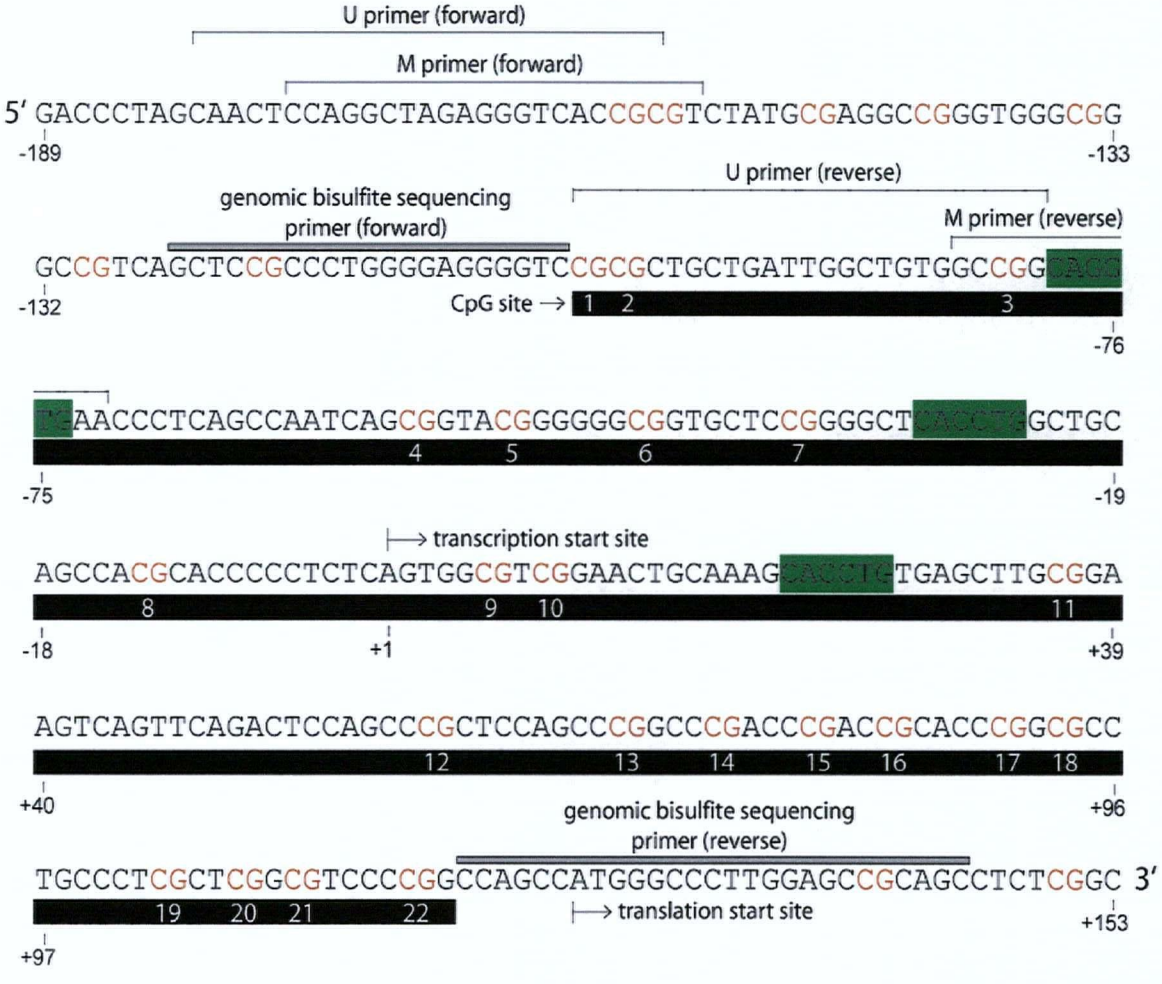

Figure 4.11: The human E-cadherin proximal promoter. The human E-cadherin gene from positions -189 to +153 relative to the transcription start site is shown. Three E-boxes ( ) recognized by E-cadherin transcriptional repressor proteins are indicated. For MSP, primer recognition sequences for methylated (M) and unmethylated (U) primer sets are shown. For genomic bisulfite sequencing, primer recognition sequences are shown, as are the 22 CpG sites (**CG**) analyzed within the E-cadherin promoter from positions -104 to +118 ( ) relative to the transcription start site. The translation start site is also indicated.

E-cadherin transcriptional repressor proteins function by binding to the E-cadherin promoter and blocking gene transcription (Hennig et al., 1996). We assessed the expression of three E-cadherin transcriptional repressor proteins, Slug/Snail/SIP1, in control and XNotch4 tumors by semi-quantitative RT-PCR. Expression of these three transcriptional repressor proteins did not differ between control and XNotch4 tumors (Figure 4.12). Thus E-cadherin re-expression in XNotch4 tumors cannot be explained by inhibited expression of Slug, Snail, or SIP1.

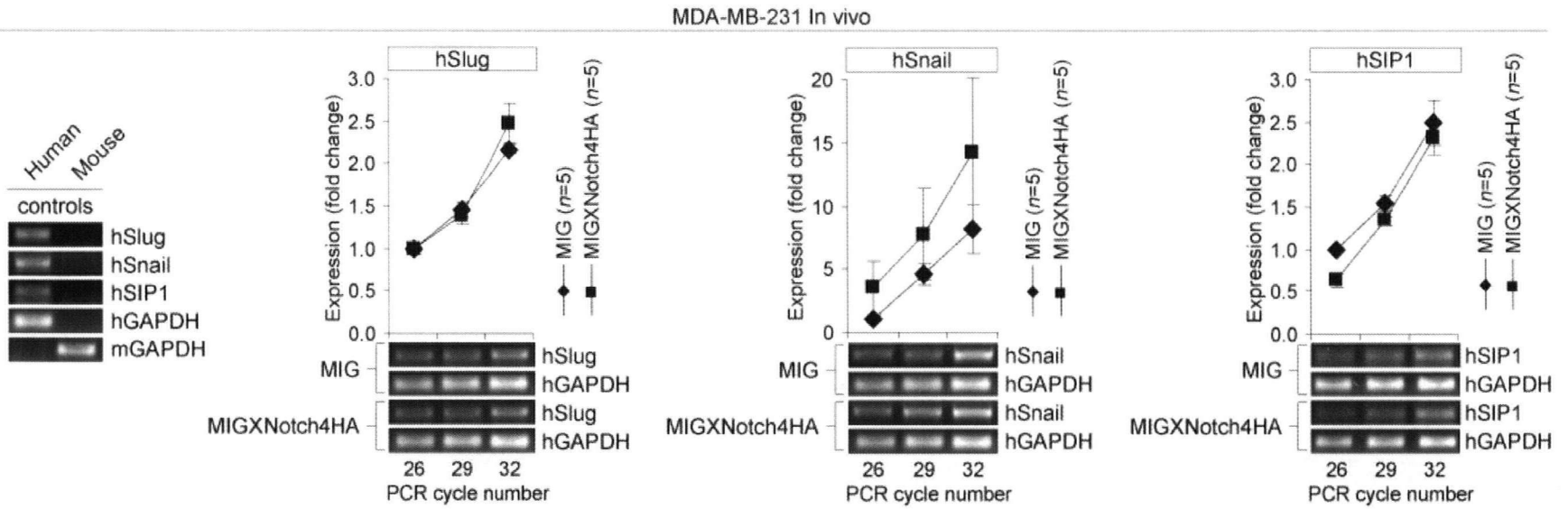

Figure 4.12: Notch signal inhibition does not affect the expression of E-cadherin transcriptional repressor proteins. Semi-quantitative RT-PCR for expression of human Slug, Snail, and SIP1 in MDA-MB-231 tumors. Total RNA was harvested from MDA-MB-231 tumors and reverse-transcribed into cDNA. For semi-quantitative RT-PCR, individual reactions along with GAPDH control reactions were terminated after the designated number of PCR cycles. Primers recognize human but not mouse target genes. Data shown represent mean ± standard error.

The E-cadherin promoter contains numerous CpG sites which, when methylated on the corresponding cytosine residue, can result in E-cadherin silencing (Berx et al., 1995b). In a previous study of MDA-MB-231 cells in vitro, nearly every CpG site analyzed within the E-cadherin proximal promoter was found to be methylated (Graff et al., 2000). We assessed the status of E-cadherin promoter methylation within MDA-MB-231 tumor xenografts using two methods: MSP (Herman et al., 1996) and genomic bisulfite sequencing (Graff et al., 1997). Both methods require bisulfite modification of genomic DNA, which converts unmethylated cytosines to uracils while methylated cytosines remain unchanged. MSP utilizes primers designed against DNA sequences containing one or more CpG sites (Figure 4.11); thus amplification of a PCR product is dependent on the methylation status of the target gene. Genomic bisulfite sequencing utilizes primers designed against DNA sequences that are relatively free of CpG sites, but which amplify a region of DNA containing a high density of CpG sites (Graff et al., 1997) (Figure 4.11). Hence the methylation status of the target gene can be inferred from the DNA sequence. Importantly, CpG methylation in this region of DNA has been shown to be tightly associated with loss of E-cadherin expression (Graff et al., 1997). By both MSP and genomic bisulfite sequencing, E-cadherin promoter methylation in XNotch4 tumors was found to be reduced compared to control tumors (Figure 4.13A,B). In a previous genomic bisulfite sequencing study examining the same E-cadherin promoter region as that analyzed in this thesis, reduced E-cadherin promoter methylation at 9 of 21 CpG sites was associated with E-cadherin re-expression in MDA-MB-231 cells (Graff et al., 1997). We detected reduced E-cadherin promoter methylation at 16 of 22 CpG sites examined (Figure 4.13B). These results suggest that XNotch4 re-induces E-cadherin expression by attenuating E-cadherin promoter methylation.

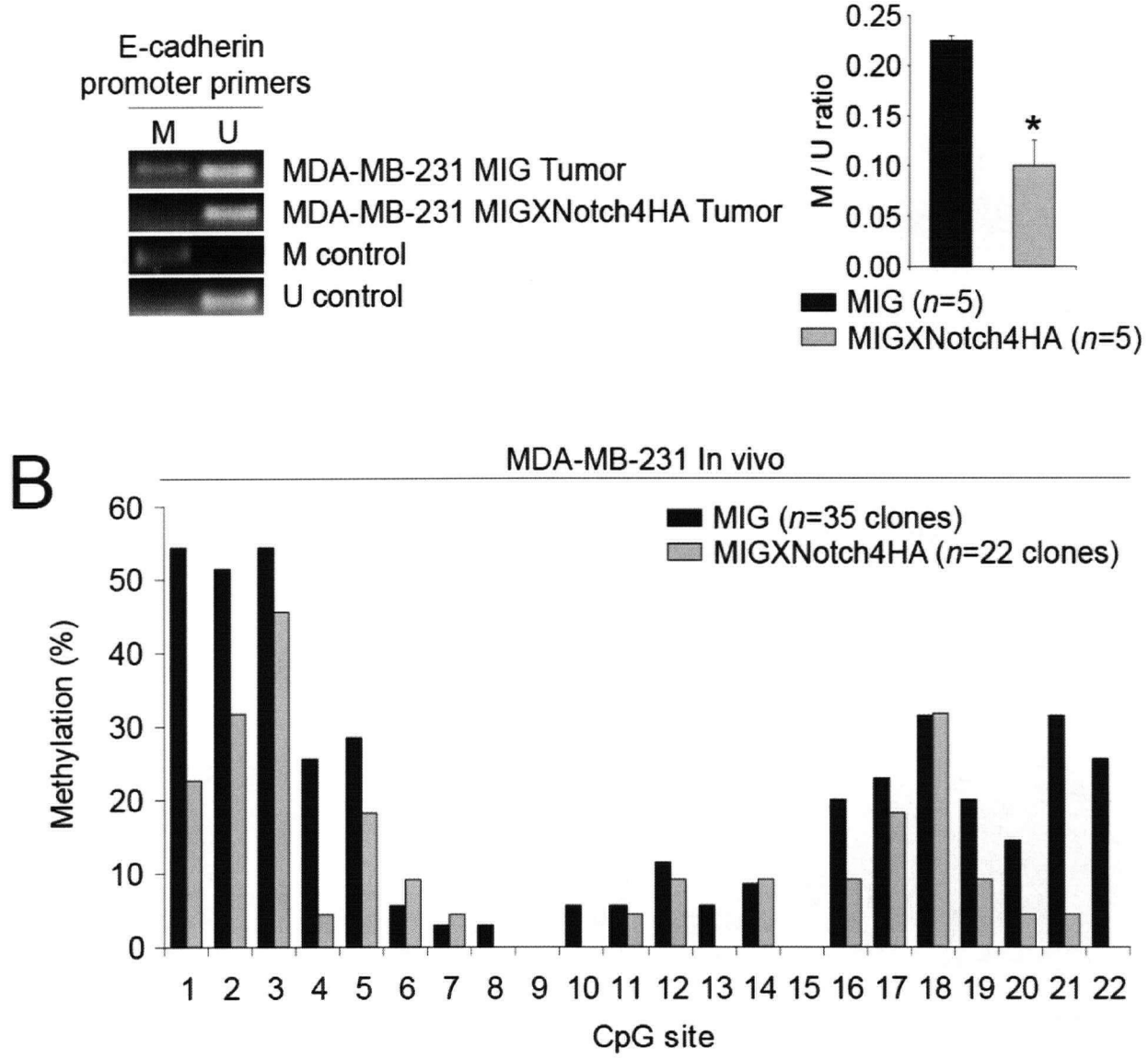

Figure 4.13 (Part 1): Notch signal inhibition attenuates E-cadherin promoter methylation, but does not induce a generalized demethylation of the genome. (A) MSP to assess the methylation status of the E-cadherin promoter in MDA-MB-231 tumors. Genomic DNA was isolated from MDA-MB-231 tumors, bisulfite-treated, and PCR performed using primers specific for methylated (M) or unmethylated (U) E-cadherin promoter. Amplified M and U products were quantitated by densitometry and expressed as an M/U ratio. Data shown represent mean ± standard error. *P < 0.001. **(B)** Genomic bisulfite sequencing to assess methylation status of the E-cadherin promoter in MDA-MB-231 tumors. Bisulfite-treated genomic DNA from MDA-MB-231 tumors was amplified by PCR, PCR products cloned into the pDrive cloning vector, resultant constructs transformed into bacteria, and individual clones sequenced. A total of 22 CpG sites within the E-cadherin proximal promoter (-114 to +109) were analyzed. Data shown represent the percentage methylation observed at each CpG site. Paired t-test across all 22 CpG sites: P ≤ 0.05. **(C)** and **(D)** (see next page).

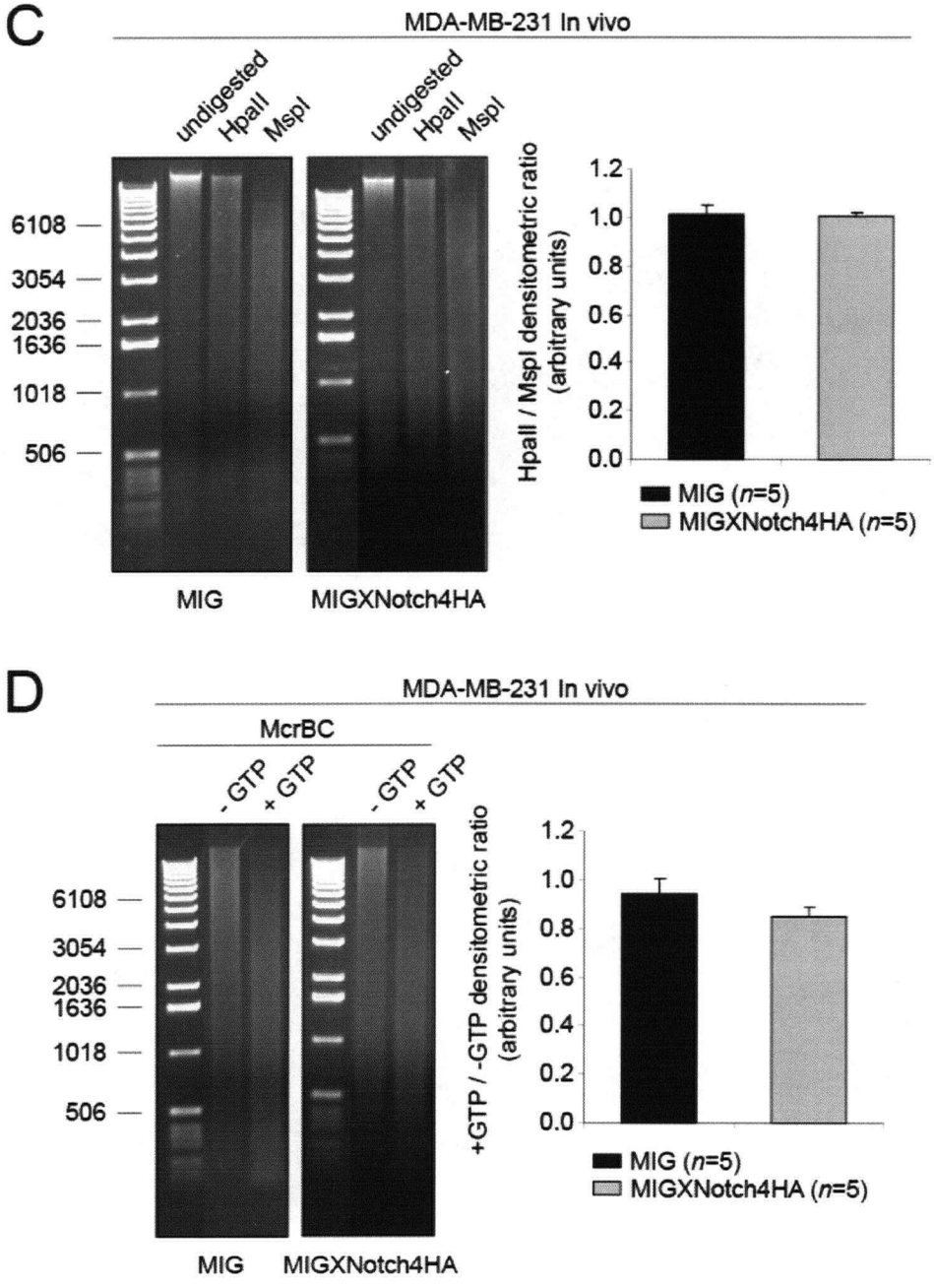

Figure 4.13 (Part 2): Notch signal inhibition attenuates E-cadherin promoter methylation, but does not induce a generalized demethylation of the genome. (C) HpaII or MspI digestion of unmodified genomic DNA isolated from MDA-MB-231 tumors. HpaII is unable to digest CpG-methylated DNA, whereas its isoschizomer MspI is not sensitive to CpG methylation. The relative degree of methylation of total genomic DNA was estimated by dividing densitometric scans of HpaII digests between 2 and 7 kb by that of MspI digests between 2 and 7 kb. A molecular weight ladder (in base pairs) is shown. **(D)** McrBC digestion of unmodified genomic DNA isolated from MDA-MB-231 tumors. McrBC digests CpG-methylated DNA in the presence of GTP. The relative degree of methylation of total genomic DNA was estimated by dividing densitometric scans between 2 and 7 kb of digests with GTP by densitometric scans of the uppermost undigested DNA band in reactions without GTP. A molecular weight ladder (in base pairs) is shown.

We next sought to determine whether XNotch4 induced global demethylation of the genome. We used DNA restriction enzymes that differentially cleave unmodified DNA based on the methylation status of their DNA recognition sequences. Specifically, we used the restriction enzymes (i) HpaII, which is unable to digest CpG-methylated DNA, and (ii) MspI, an isoschizomer of HpaII that digests DNA regardless of methylation status and thus serves as a positive control for DNA digestion (Fernandez-Peralta et al., 1994). We also used the restriction enzyme McrBC, which digests CpG-methylated DNA only in the presence of GTP (Sutherland et al., 1992). Genomic DNA from MDA-MB-231 control and XNotch4 tumors was digested, along with a control reaction for undigested DNA. DNA products were quantitated by densitometry, and the relative level of global genomic DNA methylation was expressed as a ratio of HpaII over MspI digested DNA products (HpaII over MspI densitometric ratio), or a ratio of McrBC-plus-GTP over McrBC-minus-GTP DNA products (+GTP over -GTP densitometric ratio). We detected similar levels of genomic DNA digestion from both control and XNotch4 tumors (Figure 4.13C,D). Importantly, because we did not detect a generalized demethylation of the genome, Notch signal inhibition may selectively induce demethylation of the E-cadherin promoter and potentially other Notch-specific promoters. Because in vitro treatment of MDA-MB-231 cells with methylation inhibitors alone can induce E-cadherin re-expression (Graff et al., 1995; Hurtubise and Momparler, 2004; Sarrio et al., 2004), our results suggest that inhibition of Notch signaling re-induces E-cadherin expression by attenuating E-cadherin promoter methylation.

4.3 DISCUSSION

Data presented in this thesis are the first to identify activated Notch signaling as a mechanism for EMT in tumorigenesis, and demonstrate proof-of-principle for targeting Notch

signaling for reversion of EMT and the invasive mesenchymal phenotype. We show that activated Notch signaling inhibits E-cadherin expression in MCF-10A and primary human breast epithelial cells (Figures 4.1 and 4.2). Using XNotch4 as a soluble inhibitor of Notch signaling, we demonstrate that inhibition of Notch activation in human MDA-MB-231 breast tumors can reduce tumor growth and metastasis in vivo (Figure 4.5). XNotch4 inhibits E-cadherin promoter methylation (Figure 4.13), resulting in re-expression of E-cadherin and subsequent attenuation of β-catenin nuclear localization (Figure 4.9).

Inhibitors of Notch signaling can be selective or nonselective. Selective inhibitors specifically target individual Notch receptors, and include mAbs (Dontu et al., 2004; Yasutomo et al., 2000), antisense (Garces et al., 1997; Rangarajan et al., 2001b; Weijzen et al., 2002; Yasutomo et al., 2000), and RNA interference (RNAi) (Presente et al., 2004; Presente et al., 2002). To simultaneously target all Notch receptors, however, a nonselective inhibitor must be used. These include γ-secretase inhibitors (Das et al., 2004), soluble Notch ligands (Chitnis et al., 1995; Hukriede et al., 1997; Small et al., 2001; Sun and Artavanis-Tsakonas, 1996), and soluble Notch receptors (Garces et al., 1997; Nickoloff et al., 2002; Rangarajan et al., 2001b; Shimizu et al., 1999; Small et al., 2001). Because γ-secretase inhibitors block signaling pathways in addition to Notch (Lee et al., 2002), and because soluble Notch ligands may actually promote Notch signaling (Dontu et al., 2004; Fitzgerald and Greenwald, 1995; Han et al., 2000; Li et al., 1998a; Nickoloff et al., 2002), we have used soluble Notch4 receptor as a nonselective inhibitor of Notch signaling.

In normal breast epithelia, E-cadherin promoter methylation does not occur and thus cells maintain an epithelial phenotype (Graff et al., 1995). However, methylation of the E-cadherin promoter has been detected in various breast cancer cell lines, as well as in breast cancers of both

ductal and lobular histological subtypes (Droufakou et al., 2001; Graff et al., 2000; Nass et al., 2000; Sarrio et al., 2003). Importantly, in E-cadherin-negative breast tumors that exhibit a mesenchymal phenotype, such as lobular breast cancer, E-cadherin promoter methylation has been reported to be the most frequent mechanism of E-cadherin silencing (Droufakou et al., 2001). The fact that gene silencing by promoter methylation is a reversible epigenetic change has led to the development of inhibitors of methylation for the clinical management of cancer. Two commonly used methylation inhibitors, 5-azacytidine and deoxy-5-azacytidine, induce demethylation by covalently binding enzymes involved in DNA methylation (Momparler, 1985; Vesely, 1985). However, because these drugs must incorporate into DNA to exert their function (Ferguson et al., 1997; Jackson-Grusby et al., 1997), the likelihood of toxic side effects have limited their use. In the clinic, methylation inhibitors have shown promise for the treatment of hematological malignancies but not solid tumors (Aparicio and Weber, 2002). Our findings have identified inhibitors of Notch signaling as potential new therapeutics for the reversal of E-cadherin promoter methylation and hence the mesenchymal phenotype.

Notch ligands interact with Notch receptors via EGF-like repeats 11 and 12 (Rebay et al., 1991). In our studies, the entire extracellular domain of human Notch4 was used as an inhibitor of ligand-activated Notch signaling. Several reports have demonstrated inhibition of Notch signaling using a recombinant extracellular Notch fragment consisting of only EGF-like repeats 11 and 12 (Garces et al., 1997; Nickoloff et al., 2002; Rangarajan et al., 2001b). These results raise the possibility of using smaller recombinant Notch fragments as novel therapeutic agents in the treatment of breast cancer. However, because Notch signaling is involved in numerous cell processes, therapeutic use of inhibitors of Notch signaling will undoubtedly have side effects. Furthermore, because Notch1 has been suggested to function as a tumor suppressor in skin

(Nicolas et al., 2003), lung (Sriuranpong et al., 2001), and prostate (Shou et al., 2001) cells, potential side effects of blocked Notch signaling in these cells must be considered. Nonetheless, inhibitors of Notch signaling have the potential to be viable and effective anti-cancer agents in the treatment of human breast cancer, and possibly other cancers where Notch is activated.

Chapter 5

SUMMARY, PERSPECTIVES, AND FUTURE DIRECTIONS

Data presented in Chapter 3 of this thesis highlight a role for Notch signaling in angiogenesis. We demonstrate that activated Notch4 inhibits endothelial sprouting in vitro and angiogenesis in vivo, and that this inhibition is due at least in part to an increase in β1 integrin-mediated adhesion. In order for angiogenesis to occur, endothelial cells must migrate along a provisional matrix and form primitive endothelial sprouts (Carmeliet, 2000). This migration is regulated by coordinated changes in the adhesive activity of integrins, which function to direct the endothelial cells toward an angiogenic stimulus (Bazoni et al., 1999; Cockerill et al., 1995). Our data show that activated Notch4, via induction of an inside-out signaling pathway, converts β1 integrins from an inactive, low-affinity binding state to an active, high-affinity binding state. Hence endothelial cell adhesion to β1 integrin ligands is enhanced, effectively locking the endothelial cells in place and thus inhibiting endothelial cell migration and angiogenesis.

Activated Notch4 does not increase the surface expression level of β1 integrins, but instead increases the affinity state of individual β1 integrin receptors. Modulation of β1 integrin avidity, however, remains a possibility. Indeed, regulation of cell-ECM binding typically involves changes in both integrin affinity and avidity (Shattil et al., 1998; Stewart and Hogg, 1996). Integrin avidity is commonly referred to as a post-receptor occupancy event because changes in integrin distribution generally occur after ligand binding (Sanchez-Mateos et al., 1996). Changes in integrin avidity can also occur independent of ligand binding (Sanchez-Mateos et al., 1996). Determining whether activated Notch signaling modulates β1 integrin avidity via an inside-out signaling pathway would greatly enhance our understanding of integrin avidity modulation.

Because angiogenesis plays an important role during tumor growth and metastasis (Zetter, 1998), our results identify Notch signal activation as a potential method with which to inhibit tumor angiogenesis. One model to test this hypothesis would involve expressing activated Notch4 specifically in the mouse endothelial cell compartment of a human tumor xenograft. A major drawback of this tumor angiogenesis model, however, is that Notch4IC must be expressed within tumor endothelial cells for a potential anti-angiogenic effect to occur. Because data presented in this thesis as well as other studies (Krebs et al., 2000; Uyttendaele et al., 2001) demonstrate that both increases and decreases in Notch signaling result in disrupted embryonic blood vessel development, soluble inhibitors of Notch signaling (which do not require intracellular expression to effect function) may present an alternative method with which to inhibit tumor angiogenesis.

In Chapter 4 of this thesis, a role for Notch signaling in EMT is described. Using the human breast epithelial cell line MCF-10A, we show that expression of activated Notch induces cytologic changes consistent with EMT such as cell scattering and the acquisition of a spindle-shaped phenotype. We also demonstrate that activated Notch downregulates E-cadherin expression, a hallmark cellular change commonly associated with EMT (Vincent-Salomon and Thiery, 2003). Activated Notch also downregulates E-cadherin expression in primary human breast epithelial cells. These data suggest an oncogenic role for activated Notch during breast cancer development; however, the tumorigenic potential of these NotchIC-expressing cells has not been tested.

Induction of angiogenesis and EMT both contribute to tumor progression by supplying the tumor with a vascular supply during growth (Zetter, 1998), and by downregulating cell-cell adhesion during invasion (Thiery, 2002), respectively. Having demonstrated a role for Notch

signaling in angiogenesis and EMT, we sought to determine whether inhibited Notch signaling would inhibit angiogenesis and/or EMT in a human tumor xenograft model in mice. In Chapter 4, in vivo experiments utilizing XNotch4 as a soluble inhibitor of Notch signaling are described. We used the highly tumorigenic MDA-MB-231 human breast cancer cell line which, despite possessing one wildtype E-cadherin gene (van de Wetering et al., 2001), displays a mesenchymal phenotype and lacks E-cadherin protein expression (Sarrio et al., 2004). We transduced MDA-MB-231 cells with XNotch4, confirmed secretion of XNotch4, and grew tumors in immunodeficient mice. Hence tumor cells and infiltrating mouse endothelial cells were continuously exposed to XNotch4 protein. In this tumor model, XNotch4 inhibits MDA-MB-231 tumor growth in vivo.

XNotch4 does not affect vascular density in MDA-MB-231 tumors. However, because changes in vascular density may not accurately reflect anti-angiogenic activity (Hlatky et al., 2002), additional angiogenesis experiments such as the chick CAM and Matrigel plug assays may provide a better assessment of the anti-angiogenic potential of XNotch4. We demonstrate that XNotch4 induces E-cadherin re-expression associated with attenuated E-cadherin promoter methylation. Furthermore, we show that E-cadherin re-expression inhibits β-catenin nuclear localization, which may explain the XNotch4-mediated inhibition of MDA-MB-231 tumor growth. Hence inhibition of Notch signaling attenuates MDA-MB-231 tumor growth by reversing the mesenchymal phenotype.

Our results suggest inhibition of Notch signaling as a new mechanism for the reversal of E-cadherin promoter methylation. However, we have not demonstrated a causal role for activated Notch signaling in E-cadherin promoter methylation. Moreover, we must identify the Notch target gene(s) involved in the downregulation and potential methylation of the E-cadherin protein

and gene, respectively. Our data demonstrate that XNotch4 inhibits HES1 expression in vivo. Inhibition of HES1-mediated Notch signaling may therefore play a role in the attenuation of E-cadherin promoter methylation, resulting in E-cadherin re-expression in XNotch4 tumors. XNotch4-mediated downregulation of other Notch target genes, however, remains a possibility. Identifying the Notch target genes that play a role in E-cadherin promoter methylation would allow us to design therapeutics that specifically inhibit these target genes. Such therapeutics could potentially be used to treat E-cadherin-negative cancers in which E-cadherin promoter methylation has been identified as a causal factor for E-cadherin silencing.

We have shown that XNotch4 can induce E-cadherin re-expression in MDA-MB-231 cells in vivo. Demonstrating this effect in other cancer cells in which Notch is activated, and that possess a wildtype E-cadherin gene but lack E-cadherin protein expression, would argue against a cell-type-specific effect of XNotch4. We have shown that transduction of MDA-MB-231 cells with E-cadherin cDNA is sufficient to inhibit tumor growth in vivo. To prove that E-cadherin re-induction by XNotch4 is a causal factor in the inhibition of MDA-MB-231 tumor growth, E-cadherin knockdown in XNotch4 cells to determine whether tumor growth is restored would be required. This could be achieved by co-transducing MDA-MB-231 cells with XNotch4 and an E-cadherin RNAi construct, followed by tumor growth in mice. By preventing E-cadherin upregulation, β-catenin re-localization to the plasma membrane should be prevented, thus maintaining tumor growth in vivo.

To achieve continuous exposure of tumor cells to XNotch4 protein, our in vivo experiments utilized transduction of XNotch4 cDNA into tumor cells, which results in tumor cell-mediated production of XNotch4. To demonstrate clinical applicability of our results,

purified recombinant XNotch4 protein could be produced and injected directly into the tumor or via the tail vein, and effects on tumor growth assessed.

In conclusion, the studies presented in this thesis identify a role for Notch signaling in angiogenesis and breast cancer development. Importantly, our findings provide proof-of-principle for Notch signal activation as a mechanism for the inhibition of angiogenesis, and for Notch signal inhibition as a mechanism for the inhibition of human breast tumor growth.

REFERENCES

Abecassis, J., Millon-Collard, R., Klein-Soyer, C., Nicora, F., Fricker, J. P., Beretz, A., Eber, M., Muller, D., and Cazenave, J. P. (1987). Adhesion of human breast cancer cell line MCF-7 to human vascular endothelial cells in culture. Enhancement by activated platelets. Int J Cancer *40*, 525-531.

Aberle, H., Bauer, A., Stappert, J., Kispert, A., and Kemler, R. (1997). beta-catenin is a target for the ubiquitin-proteasome pathway. Embo J *16*, 3797-3804.

Adamis, A. P., Shima, D. T., Tolentino, M. J., Gragoudas, E. S., Ferrara, N., Folkman, J., D'Amore, P. A., and Miller, J. W. (1996). Inhibition of vascular endothelial growth factor prevents retinal ischemia-associated iris neovascularization in a nonhuman primate. Arch Ophthalmol *114*, 66-71.

Ades, E. W., Candal, F. J., Swerlick, R. A., George, V. G., Summers, S., Bosse, D. C., and Lawley, T. J. (1992). HMEC-1: establishment of an immortalized human microvascular endothelial cell line. J Invest Dermatol *99*, 683-690.

Aiello, L. P., Pierce, E. A., Foley, E. D., Takagi, H., Chen, H., Riddle, L., Ferrara, N., King, G. L., and Smith, L. E. (1995). Suppression of retinal neovascularization in vivo by inhibition of vascular endothelial growth factor (VEGF) using soluble VEGF-receptor chimeric proteins. Proc Natl Acad Sci U S A *92*, 10457-10461.

Akazawa, C., Ishibashi, M., Shimizu, C., Nakanishi, S., and Kageyama, R. (1995). A mammalian helix-loop-helix factor structurally related to the product of Drosophila proneural gene atonal is a positive transcriptional regulator expressed in the developing nervous system. J Biol Chem *270*, 8730-8738.

Akazawa, C., Sasai, Y., Nakanishi, S., and Kageyama, R. (1992). Molecular characterization of a rat negative regulator with a basic helix-loop-helix structure predominantly expressed in the developing nervous system. J Biol Chem *267*, 21879-21885.

Alberts, B., Johnson, A., Lewis, J., Raff, M., Roberts, K., and Walter, P. (2002). Molecular Biology of the Cell, 4th edn (New York & London, Garland Publishing Inc.).

Altieri, D. C., Bader, R., Mannucci, P. M., and Edgington, T. S. (1988). Oligospecificity of the cellular adhesion receptor Mac-1 encompasses an inducible recognition specificity for fibrinogen. J Cell Biol *107*, 1893-1900.

Anand-Apte, B., Pepper, M. S., Voest, E., Montesano, R., Olsen, B., Murphy, G., Apte, S. S., and Zetter, B. (1997). Inhibition of angiogenesis by tissue inhibitor of metalloproteinase-3. Invest Ophthalmol Vis Sci *38*, 817-823.

Andronati, S. A., Karaseva, T. L., and Krysko, A. A. (2004). Peptidomimetics - antagonists of the fibrinogen receptors: molecular design, structures, properties and therapeutic applications. Curr Med Chem *11*, 1183-1211.

Ansieau, S., Strobl, L. J., and Leutz, A. (2001). Activation of the Notch-regulated transcription factor CBF1/RBP-Jkappa through the 13SE1A oncoprotein. Genes Dev *15*, 380-385.

Aparicio, A., and Weber, J. S. (2002). Review of the clinical experience with 5-azacytidine and 5-aza-2'-deoxycytidine in solid tumors. Curr Opin Investig Drugs *3*, 627-633.

Arroyo, A. G., Garcia-Pardo, A., and Sanchez-Madrid, F. (1993). A high affinity conformational state on VLA integrin heterodimers induced by an anti-beta 1 chain monoclonal antibody. J Biol Chem *268*, 9863-9868.

Artavanis-Tsakonas, S., Matsuno, K., and Fortini, M. E. (1995). Notch signaling. Science *268*, 225-232.

Artavanis-Tsakonas, S., Rand, M. D., and Lake, R. J. (1999). Notch signaling: cell fate control and signal integration in development. Science *284*, 770-776.

Ascano, J. M., Beverly, L. J., and Capobianco, A. J. (2003). The C-terminal PDZ-ligand of JAGGED1 is essential for cellular transformation. J Biol Chem *278*, 8771-8779.

Aster, J., Pear, W., Hasserjian, R., Erba, H., Davi, F., Luo, B., Scott, M., Baltimore, D., and Sklar, J. (1994). Functional analysis of the TAN-1 gene, a human homolog of Drosophila notch. Cold Spring Harb Symp Quant Biol *59*, 125-136.

Aster, J. C., Xu, L., Karnell, F. G., Patriub, V., Pui, J. C., and Pear, W. S. (2000). Essential roles for ankyrin repeat and transactivation domains in induction of T-cell leukemia by notch1. Mol Cell Biol *20*, 7505-7515.

Auerbach, W., and Auerbach, R. (1994). Angiogenesis inhibition. Pharmac Ther *63*, 265-311.

Ayer, D. E. (1999). Histone deacetylases: transcriptional repression with SINers and NuRDs. Trends Cell Biol *9*, 193-198.

Bae, S., Bessho, Y., Hojo, M., and Kageyama, R. (2000). The bHLH gene Hes6, an inhibitor of Hes1, promotes neuronal differentiation. Development *127*, 2933-2943.

Bagavandoss, P., and Wilks, J. W. (1990). Specific inhibition of endothelial cell proliferation by thrombospondin. Biochem Biophys Res Commun *170*, 867-872.

Baker, N. E. (2000). Notch signaling in the nervous system. Pieces still missing from the puzzle. Bioessays *22*, 264-273.

Barleon, B., Totzke, F., Herzog, C., Blanke, S., Kremmer, E., Siemeister, G., Marme, D., and Martiny-Baron, G. (1997). Mapping of the sites for ligand binding and receptor dimerization at the extracellular domain of the vascular endothelial growth factor receptor FLT-1. J Biol Chem *272*, 10382-10388.

Bauer, A., Huber, O., and Kemler, R. (1998). Pontin52, an interaction partner of beta-catenin, binds to the TATA box binding protein. Proc Natl Acad Sci U S A *95*, 14787-14792.

Bauer, J., Margolis, M., Schreiner, C., Edgell, C. J., Azizkhan, J., Lazarowski, E., and Juliano, R. L. (1992). In vitro model of angiogenesis using a human endothelium-derived permanent cell line: contributions of induced gene expression, G-proteins, and integrins. J Cell Physiol *153*, 437-449.

Bazoni, G., Dejana, E., and Lampugnani, M. G. (1999). Endothelial adhesion molecules in the development of the vascular tree: the garden of forking paths. Curr Opin Cell Biol *11*, 573-581.

Beck, L., Jr., and D'Amore, P. A. (1997). Vascular development: cellular and molecular regulation. Faseb J *11*, 365-373.

Behrens, J., Mareel, M. M., Van Roy, F. M., and Birchmeier, W. (1989). Dissecting tumor cell invasion: epithelial cells acquire invasive properties after the loss of uvomorulin-mediated cell-cell adhesion. J Cell Biol *108*, 2435-2447.

Belotti, D., Vergani, V., Drudis, T., Borsotti, P., Pitelli, M. R., Viale, G., Giavazzi, R., and Taraboletti, G. (1996). The microtubule-affecting drug paclitaxel has antiangiogenic activity. Clin Cancer Res *2*, 1843-1849.

Ben-Arie, N., Bellen, H. J., Armstrong, D. L., McCall, A. E., Gordadze, P. R., Guo, Q., Matzuk, M. M., and Zoghbi, H. Y. (1997). Math1 is essential for genesis of cerebellar granule neurons. Nature *390*, 169-172.

Benjamin, L. E., Hemo, I., and Keshet, E. (1998). A plasticity window for blood vessel remodelling is defined by pericyte coverage of the preformed endothelial network and is regulated by PDGF-B and VEGF. Development *125*, 1591-1598.

Berx, G., Becker, K. F., Hofler, H., and van Roy, F. (1998). Mutations of the human E-cadherin (CDH1) gene. Hum Mutat *12*, 226-237.

Berx, G., Cleton-Jansen, A. M., Nollet, F., de Leeuw, W. J., van de Vijver, M., Cornelisse, C., and van Roy, F. (1995a). E-cadherin is a tumour/invasion suppressor gene mutated in human lobular breast cancers. Embo J *14*, 6107-6115.

Berx, G., Cleton-Jansen, A. M., Strumane, K., de Leeuw, W. J., Nollet, F., van Roy, F., and Cornelisse, C. (1996). E-cadherin is inactivated in a majority of invasive human lobular breast cancers by truncation mutations throughout its extracellular domain. Oncogene *13*, 1919-1925.

Berx, G., Staes, K., van Hengel, J., Molemans, F., Bussemakers, M. J., van Bokhoven, A., and van Roy, F. (1995b). Cloning and characterization of the human invasion suppressor gene E-cadherin (CDH1). Genomics *26*, 281-289.

Bessho, Y., Miyoshi, G., Sakata, R., and Kageyama, R. (2001). Hes7: a bHLH-type repressor gene regulated by Notch and expressed in the presomitic mesoderm. Genes Cells *6*, 175-185.

Bettenhausen, B., Hrabe de Angelis, M., Simon, D., Guenet, J. L., and Gossler, A. (1995). Transient and restricted expression during mouse embryogenesis of Dll1, a murine gene closely related to Drosophila Delta. Development *121*, 2407-2418.

Bevilacqua, M. P. (1993). Endothelial-leukocyte adhesion molecules. Annu Rev Immunol *11*, 767-804.

Bikfalvi, A. (2004). Platelet factor 4: an inhibitor of angiogenesis. Semin Thromb Hemost *30*, 379-385.

Bischoff, J. (1997). Cell adhesion and angiogenesis. J Clin Invest *99*, 373-376.

Blackwell, T. K., and Weintraub, H. (1990). Differences and similarities in DNA-binding preferences of MyoD and E2A protein complexes revealed by binding site selection. Science *250*, 1104-1110.

Blanco, M. J., Moreno-Bueno, G., Sarrio, D., Locascio, A., Cano, A., Palacios, J., and Nieto, M. A. (2002). Correlation of Snail expression with histological grade and lymph node status in breast carcinomas. Oncogene *21*, 3241-3246.

Blaumueller, C. M., Qi, H., Zagouras, P., and Artavanis-Tsakonas, S. (1997). Intracellular cleavage of Notch leads to a heterodimeric receptor on the plasma membrane. Cell *90*, 281-291.

Bloch, W., Forsberg, E., Lentini, S., Brakebusch, C., Martin, K., Krell, H. W., Weidle, U. H., Addicks, K., and Fassler, R. (1997). β1 integrin is essential for teratoma growth and angiogenesis. J Cell Biol *139*, 265-278.

Boettiger, D., Enomoto-Iwamoto, M., Yoon, H. Y., Hofer, U., Menko, A. S., and Chiquet-Ehrismann, R. (1995). Regulation of integrin alpha 5 beta 1 affinity during myogenic differentiation. Dev Biol *169*, 261-272.

Boudreau, N., Andrews, C., Srebrow, A., Ravanpay, A., and Cheresh, D. A. (1997). Induction of the angiogenic phenotype by Hox D3. J Cell Biol *139*, 257-264.

Bouvard, D., Brakebusch, C., Gustafsson, E., Aszodi, A., Bengtsson, T., Berna, A., and Fassler, R. (2001). Functional consequences of integrin gene mutations in mice. Circ Res *89*, 211-223.

Bray, S., and Furriols, M. (2001). Notch pathway: making sense of suppressor of hairless. Curr Biol *11*, R217-221.

Brooks, P. C. (1996). Role of integrins in angiogenesis. Eur J Cancer *32A*, 2423-2429.

Brooks, P. C., Clark, R. A., and Cheresh, D. A. (1994a). Requirement of vascular integrin alpha v beta 3 for angiogenesis. Science *264*, 569-571.

Brooks, P. C., Montgomery, A. M., and Cheresh, D. A. (1999). Use of the 10-day-old chick embryo model for studying angiogenesis. Methods Mol Biol *129*, 257-269.

Brooks, P. C., Montgomery, A. M., Rosenfeld, M., Reisfeld, R. A., Hu, T., Klier, G., and Cheresh, D. A. (1994b). Integrin alpha v beta 3 antagonists promote tumor regression by inducing apoptosis of angiogenic blood vessels. Cell *79*, 1157-1164.

Brooks, P. C., Stromblad, S., Sanders, L. C., von Schalscha, T. L., Aimes, R. T., Stetler-Stevenson, W. G., Quigley, J. P., and Cheresh, D. A. (1996). Localization of matrix metalloproteinase MMP-2 to the surface of invasive cells by interaction with integrin alpha v beta 3. Cell *85*, 683-693.

Brou, C., Logeat, F., Gupta, N., Bessia, C., LeBail, O., Doedens, J. R., Cumano, A., Roux, P., Black, R. A., and Israel, A. (2000). A novel proteolytic cleavage involved in Notch signaling: the role of the disintegrin-metalloprotease TACE. Mol Cell *5*, 207-216.

Brou, C., Logeat, F., Lecourtois, M., Vandekerckhove, J., Kourilsky, P., Schweisguth, F., and Israel, A. (1994). Inhibition of the DNA-binding activity of Drosophila suppressor of hairless and of its human homolog, KBF2/RBP-J kappa, by direct protein-protein interaction with Drosophila hairless. Genes Dev *8*, 2491-2503.

Browder, T., Butterfield, C. E., Kraling, B. M., Shi, B., Marshall, B., O'Reilly, M. S., and Folkman, J. (2000). Antiangiogenic scheduling of chemotherapy improves efficacy against experimental drug-resistant cancer. Cancer Res *60*, 1878-1886.

Bruening, R., Dichgans, M., Berchtenbreiter, C., Yousry, T., Seelos, K. C., Wu, R. H., Mayer, M., Brix, G., and Reiser, M. (2001). Cerebral autosomal dominant arteriopathy with subcortical infarcts and leukoencephalopathy: decrease in regional cerebral blood volume in hyperintense subcortical lesions inversely correlates with disability and cognitive performance. AJNR Am J Neuroradiol *22*, 1268-1274.

Bulman, M. P., Kusumi, K., Frayling, T. M., McKeown, C., Garrett, C., Lander, E. S., Krumlauf, R., Hattersley, A. T., Ellard, S., and Turnpenny, P. D. (2000). Mutations in the human delta homologue, DLL3, cause axial skeletal defects in spondylocostal dysostosis. Nat Genet *24*, 438-441.

Burdon, T., Sankaran, L., Wall, R. J., Spencer, M., and Hennighausen, L. (1991). Expression of a whey acidic protein transgene during mammary development. Evidence for different mechanisms of regulation during pregnancy and lactation. J Biol Chem *266*, 6909-6914.

Bush, G., diSibio, G., Miyamoto, A., Denault, J. B., Leduc, R., and Weinmaster, G. (2001). Ligand-induced signaling in the absence of furin processing of Notch1. Dev Biol *229*, 494-502.

Cadigan, K. M., and Nusse, R. (1997). Wnt signaling: a common theme in animal development. Genes Dev *11*, 3286-3305.

Callahan, R., and Egan, S. E. (2004). Notch signaling in mammary development and oncogenesis. J Mammary Gland Biol Neoplasia *9*, 145-163.

Calvete, J. J., Henschen, A., and Gonzalez-Rodriguez, J. (1989). Complete localization of the intrachain disulphide bonds and the N-glycosylation points in the alpha-subunit of human platelet glycoprotein IIb. Biochem J *261*, 561-568.

Cano, A., Perez-Moreno, M. A., Rodrigo, I., Locascio, A., Blanco, M. J., del Barrio, M. G., Portillo, F., and Nieto, M. A. (2000). The transcription factor snail controls epithelial-mesenchymal transitions by repressing E-cadherin expression. Nat Cell Biol *2*, 76-83.

Capobianco, A. J., Zagouras, P., Blaumueller, C. M., Artavanis-Tsakonas, S., and Bishop, J. M. (1997). Neoplastic transformation by truncated alleles of human NOTCH1/TAN1 and NOTCH2. Mol Cell Biol *17*, 6265-6273.

Carey, D. J. (1991). Control of growth and differentiation of vascular cells by extracellular matrix proteins. Annu Rev Physiol *53*, 161-177.

Carmeliet, P. (2000). Mechanisms of angiogenesis and arteriogenesis. Nat Med *6*, 389-395.

Carmeliet, P., Ferreira, V., Breier, G., Pollefeyt, S., Kieckens, L., Gertsenstein, M., Fahrig, M., Vandenhoeck, A., Harpal, K., Eberhardt, C., *et al.* (1996). Abnormal blood vessel development and lethality in embryos lacking a single VEGF allele. Nature *380*, 435-439.

Carrell, N. A., Fitzgerald, L. A., Steiner, B., Erickson, H. P., and Phillips, D. R. (1985). Structure of human platelet membrane glycoproteins IIb and IIIa as determined by electron microscopy. J Biol Chem *260*, 1743-1749.

Carter, W. G., Wayner, E. A., Bouchard, T. S., and Kaur, P. (1990). The role of integrins alpha 2 beta 1 and alpha 3 beta 1 in cell-cell and cell-substrate adhesion of human epidermal cells. J Cell Biol *110*, 1387-1404.

Casarosa, S., Fode, C., and Guillemot, F. (1999). Mash1 regulates neurogenesis in the ventral telencephalon. Development *126*, 525-534.

Castella, P., Sawai, S., Nakao, K., Wagner, J. A., and Caudy, M. (2000). HES-1 repression of differentiation and proliferation in PC12 cells: role for the helix 3-helix 4 domain in transcription repression. Mol Cell Biol *20*, 6170-6183.

Cau, E., Gradwohl, G., Fode, C., and Guillemot, F. (1997). Mash1 activates a cascade of bHLH regulators in olfactory neuron progenitors. Development *124*, 1611-1621.

Chabriat, H., Vahedi, K., Iba-Zizen, M. T., Joutel, A., Nibbio, A., Nagy, T. G., Krebs, M. O., Julien, J., Dubois, B., Ducrocq, X., and et al. (1995). Clinical spectrum of CADASIL: a study of 7 families. Cerebral autosomal dominant arteriopathy with subcortical infarcts and leukoencephalopathy. Lancet *346*, 934-939.

Chen, G., Fernandez, J., Mische, S., and Courey, A. J. (1999). A functional interaction between the histone deacetylase Rpd3 and the corepressor groucho in Drosophila development. Genes Dev *13*, 2218-2230.

Chen, H., Thiagalingam, A., Chopra, H., Borges, M. W., Feder, J. N., Nelkin, B. D., Baylin, S. B., and Ball, D. W. (1997a). Conservation of the Drosophila lateral inhibition pathway in human lung cancer: a hairy-related protein (HES-1) directly represses achaete-scute homolog-1 expression. Proc Natl Acad Sci U S A *94*, 5355-5360.

Chen, Y., Fischer, W. H., and Gill, G. N. (1997b). Regulation of the ERBB-2 promoter by RBPJkappa and NOTCH. J Biol Chem *272*, 14110-14114.

Cheng, C. W., Wu, P. E., Yu, J. C., Huang, C. S., Yue, C. T., Wu, C. W., and Shen, C. Y. (2001). Mechanisms of inactivation of E-cadherin in breast carcinoma: modification of the two-hit hypothesis of tumor suppressor gene. Oncogene *20*, 3814-3823.

Cheresh, D. A. (1987). Human endothelial cells synthesize and express an Arg-Gly-Asp-directed adhesion receptor involved in attachment to fibrinogen and von Willebrand factor. Proc Natl Acad Sci U S A *84*, 6471-6475.

Chin, M. T., Maemura, K., Fukumoto, S., Jain, M. K., Layne, M. D., Watanabe, M., Hsieh, C. M., and Lee, M. E. (2000). Cardiovascular basic helix loop helix factor 1, a novel transcriptional repressor expressed preferentially in the developing and adult cardiovascular system. J Biol Chem *275*, 6381-6387.

Chitnis, A., Henrique, D., Lewis, J., Ish-Horowicz, D., and Kintner, C. (1995). Primary neurogenesis in Xenopus embryos regulated by a homologue of the Drosophila neurogenic gene Delta. Nature *375*, 761-766.

Christofori, G. (1996). The role of fibroblast growth factors in tumour progression and angiogenesis (Oxford, Oxford University Press).

Christy, R. J., and Huang, R. C. (1988). Functional analysis of the long terminal repeats of intracisternal A-particle genes: sequences within the U3 region determine both the efficiency and direction of promoter activity. Mol Cell Biol *8*, 1093-1102.

Clark, R. A., DellaPelle, P., Manseau, E., Lanigan, J. M., Dvorak, H. F., and Colvin, R. B. (1982). Blood vessel fibronectin increases in conjunction with endothelial cell proliferation and capillary ingrowth during wound healing. J Invest Dermatol *79*, 269-276.

Claxton, S., and Fruttiger, M. (2004). Periodic Delta-like 4 expression in developing retinal arteries. Gene Expr Patterns *5*, 123-127.

Cleton-Jansen, A. M., Callen, D. F., Seshadri, R., Goldup, S., McCallum, B., Crawford, J., Powell, J. A., Settasatian, C., van Beerendonk, H., Moerland, E. W., *et al.* (2001). Loss of heterozygosity mapping at chromosome arm 16q in 712 breast tumors reveals factors that influence delineation of candidate regions. Cancer Res *61*, 1171-1177.

Cockerill, G. W., Gamble, J. R., and Vadas, M. A. (1995). Angiogenesis: models and modulators. Int Rev Cytol *159*, 113-160.

Colvin, J. S., Bohne, B. A., Harding, G. W., McEwen, D. G., and Ornitz, D. M. (1996). Skeletal overgrowth and deafness in mice lacking fibroblast growth factor receptor 3. Nat Genet *12*, 390-397.

Conacci-Sorrell, M., Simcha, I., Ben-Yedidia, T., Blechman, J., Savagner, P., and Ben-Ze'ev, A. (2003). Autoregulation of E-cadherin expression by cadherin-cadherin interactions: the roles of beta-catenin signaling, Slug, and MAPK. J Cell Biol *163*, 847-857.

Conacci-Sorrell, M., Zhurinsky, J., and Ben-Ze'ev, A. (2002). The cadherin-catenin adhesion system in signaling and cancer. J Clin Invest *109*, 987-991.

Corn, P. G., Smith, B. D., Ruckdeschel, E. S., Douglas, D., Baylin, S. B., and Herman, J. G. (2000). E-cadherin expression is silenced by 5' CpG island methylation in acute leukemia. Clin Cancer Res *6*, 4243-4248.

Coussens, L. M., Raymond, W. W., Bergers, G., Laig-Webster, M., Behrendtsen, O., Werb, Z., Caughey, G. H., and Hanahan, D. (1999). Inflammatory mast cells up-regulate angiogenesis during squamous epithelial carcinogenesis. Genes Dev *13*, 1382-1397.

Crawford, H. C., Fingleton, B. M., Rudolph-Owen, L. A., Goss, K. J., Rubinfeld, B., Polakis, P., and Matrisian, L. M. (1999). The metalloproteinase matrilysin is a target of beta-catenin transactivation in intestinal tumors. Oncogene *18*, 2883-2891.

Cross, M. J., and Claesson-Welsh, L. (2001). FGF and VEGF function in angiogenesis: signalling pathways, biological responses and therapeutic inhibition. Trends Pharmacol Sci *22*, 201-207.

Crowe, D. T., Chiu, H., Fong, S., and Weissman, I. L. (1994). Regulation of the avidity of integrin alpha 4 beta 7 by the beta 7 cytoplasmic domain. J Biol Chem *269*, 14411-14418.

Cruz, M. T., Dalgard, C. L., and Ignatius, M. J. (1997). Functional partitioning of beta1 integrins revealed by activating and inhibitory mAbs. J Cell Sci *110*, 2647-2659.

Cunningham, S. A., Stephan, C. C., Arrate, M. P., Ayer, K. G., and Brock, T. A. (1997). Identification of the extracellular domains of Flt-1 that mediate ligand interactions. Biochem Biophys Res Commun *231*, 596-599.

Dana, N., Fathallah, D. M., and Arnaout, M. A. (1991). Expression of a soluble and functional form of the human beta 2 integrin CD11b/CD18. Proc Natl Acad Sci U S A *88*, 3106-3110.

Daniel, B., Rangarajan, A., Mukherjee, G., Vallikad, E., and Krishna, S. (1997). The link between integration and expression of human papillomavirus type 16 genomes and cellular changes in the evolution of cervical intraepithelial neoplastic lesions. J Gen Virol *78*, 1095-1101.

Daniel, C. W., and Smith, G. H. (1999). The mammary gland: a model for development. J Mammary Gland Biol Neoplasia *4*, 3-8.

Daniel, J. M., and Reynolds, A. B. (1997). Tyrosine phosphorylation and cadherin/catenin function. Bioessays *19*, 883-891.

Danilov, Y. N., and Juliano, R. L. (1989). Phorbol ester modulation of integrin-mediated cell adhesion: a postreceptor event. J Cell Biol *108*, 1925-1933.

Das, I., Craig, C., Funahashi, Y., Jung, K. M., Kim, T. W., Byers, R., Weng, A. P., Kutok, J. L., Aster, J. C., and Kitajewski, J. (2004). Notch oncoproteins depend on gamma-secretase/presenilin activity for processing and function. J Biol Chem *279*, 30771-30780.

Davis, C. M., Danehower, S. C., Laurenza, A., and Molony, J. L. (1993). Identification of a role of the vitronectin receptor and protein kinase C in the induction of endothelial cell vascular formation. J Cell Biochem *51*, 206-218.

Davis, S., Aldrich, T. H., Jones, P. F., Acheson, A., Compton, D. L., Jain, V., Ryan, T. E., Bruno, J., Radziejewski, C., Maisonpierre, P. C., and Yancopoulos, G. D. (1996). Isolation of angiopoietin-1, a ligand for the TIE2 receptor, by secretion-trap expression cloning. Cell *87*, 1161-1169.

Davis, S., and Yancopoulos, G. D. (1999). The angiopoietins: Yin and Yang in angiogenesis. Curr Top Microbiol Immunol *237*, 173-185.

Davis-Smyth, T., Chen, H., Park, J., Presta, L. G., and Ferrara, N. (1996). The second immunoglobulin-like domain of the VEGF tyrosine kinase receptor Flt-1 determines ligand binding and may initiate a signal transduction cascade. Embo J *15*, 4919-4927.

Dawson, S. R., Turner, D. L., Weintraub, H., and Parkhurst, S. M. (1995). Specificity for the hairy/enhancer of split basic helix-loop-helix (bHLH) proteins maps outside the bHLH domain and suggests two separable modes of transcriptional repression. Mol Cell Biol *15*, 6923-6931.

Day, M. L., Zhao, X., Vallorosi, C. J., Putzi, M., Powell, C. T., Lin, C., and Day, K. C. (1999). E-cadherin mediates aggregation-dependent survival of prostate and mammary epithelial cells through the retinoblastoma cell cycle control pathway. J Biol Chem *274*, 9656-9664.

De Leeuw, W. J., Berx, G., Vos, C. B., Peterse, J. L., Van de Vijver, M. J., Litvinov, S., Van Roy, F., Cornelisse, C. J., and Cleton-Jansen, A. M. (1997). Simultaneous loss of E-cadherin and catenins in invasive lobular breast cancer and lobular carcinoma in situ. J Pathol *183*, 404-411.

Decary, S., Decesse, J. T., Ogryzko, V., Reed, J. C., Naguibneva, I., Harel-Bellan, A., and Cremisi, C. E. (2002). The retinoblastoma protein binds the promoter of the survival gene bcl-2 and regulates its transcription in epithelial cells through transcription factor AP-2. Mol Cell Biol *22*, 7877-7888.

Denekamp, J. (1993). Review article: angiogenesis, neovascular proliferation and vascular pathophysiology as targets for cancer therapy. Br J Radiol *66*, 181-196.

Deng, C. X., Wynshaw-Boris, A., Shen, M. M., Daugherty, C., Ornitz, D. M., and Leder, P. (1994). Murine FGFR-1 is required for early postimplantation growth and axial organization. Genes Dev *8*, 3045-3057.

Dievart, A., Beaulieu, N., and Jolicoeur, P. (1999). Involvement of Notch1 in the development of mouse mammary tumors. Oncogene *18*, 5973-5981.

Dono, R., Texido, G., Dussel, R., Ehmke, H., and Zeller, R. (1998). Impaired cerebral cortex development and blood pressure regulation in FGF-2-deficient mice. Embo J *17*, 4213-4225.

Dontu, G., Jackson, K. W., McNicholas, E., Kawamura, M. J., Abdallah, W. M., and Wicha, M. S. (2004). Role of Notch signaling in cell-fate determination of human mammary stem/progenitor cells. Breast Cancer Res *6*, R605-615.

Dou, S., Zeng, X., Cortes, P., Erdjument-Bromage, H., Tempst, P., Honjo, T., and Vales, L. D. (1994). The recombination signal sequence-binding protein RBP-2N functions as a transcriptional repressor. Mol Cell Biol *14*, 3310-3319.

Drake, C. J., Davis, L. A., and Little, C. D. (1992). Antibodies to beta 1-integrins cause alterations of aortic vasculogenesis, in vivo. Dev Dyn *193*, 83-91.

Droufakou, S., Deshmane, V., Roylance, R., Hanby, A., Tomlinson, I., and Hart, I. R. (2001). Multiple ways of silencing E-cadherin gene expression in lobular carcinoma of the breast. Int J Cancer *92*, 404-408.

D'Souza, S. E., Haas, T. A., Piotrowicz, R. S., Byers-Ward, V., McGrath, D. E., Soule, H. R., Cierniewski, C., Plow, E. F., and Smith, J. W. (1994). Ligand and cation binding are dual functions of a discrete segment of the integrin beta 3 subunit: cation displacement is involved in ligand binding. Cell *79*, 659-667.

Du, X., Gu, M., Weisel, J. W., Nagaswami, C., Bennett, J. S., Bowditch, R., and Ginsberg, M. H. (1993). Long range propagation of conformational changes in integrin alpha IIb beta 3. J Biol Chem *268*, 23087-23092.

Duarte, A., Hirashima, M., Benedito, R., Trindade, A., Diniz, P., Bekman, E., Costa, L., Henrique, D., and Rossant, J. (2004). Dosage-sensitive requirement for mouse Dll4 in artery development. Genes Dev *18*, 2474-2478.

Dumont, D. J., Fong, G. H., Puri, M. C., Gradwohl, G., Alitalo, K., and Breitman, M. L. (1995). Vascularization of the mouse embryo: a study of flk-1, tek, tie, and vascular endothelial growth factor expression during development. Dev Dyn *203*, 80-92.

Dunwoodie, S. L., Henrique, D., Harrison, S. M., and Beddington, R. S. (1997). Mouse Dll3: a novel divergent Delta gene which may complement the function of other Delta homologues during early pattern formation in the mouse embryo. Development *124*, 3065-3076.

Dvorak, H. F., Brown, L. F., Detmar, M., and Dvorak, A. M. (1995). Vascular permeability factor/vascular endothelial growth factor, microvascular hyperpermeability, and angiogenesis. Am J Pathol *146*, 1029-1039.

Edbauer, D., Winkler, E., Regula, J. T., Pesold, B., Steiner, H., and Haass, C. (2003). Reconstitution of gamma-secretase activity. Nat Cell Biol *5*, 486-488.

Eger, A., Stockinger, A., Schaffhauser, B., Beug, H., and Foisner, R. (2000). Epithelial mesenchymal transition by c-Fos estrogen receptor activation involves nuclear translocation of

beta-catenin and upregulation of beta-catenin/lymphoid enhancer binding factor-1 transcriptional activity. J Cell Biol *148*, 173-188.

Eisenberg, L. M., and Markwald, R. R. (1995). Molecular regulation of atrioventricular valvuloseptal morphogenesis. Circ Res *77*, 1-6.

Eliceiri, B. P., and Cheresh, D. A. (1998). The role of alphav integrins during angiogenesis. Mol Med *4*, 741-750.

Eliceiri, B. P., and Cheresh, D. A. (1999). The role of alphav integrins during angiogenesis: insights into potential mechanisms of action and clinical development. J Clin Invest *103*, 1227-1230.

Ellisen, L. W., Bird, J., West, D. C., Soreng, A. L., Reynolds, T. C., Smith, S. D., and Sklar, J. (1991). TAN-1, the human homolog of the Drosophila notch gene, is broken by chromosomal translocations in T lymphoblastic neoplasms. Cell *66*, 649-661.

Emerick, K. M., Rand, E. B., Goldmuntz, E., Krantz, I. D., Spinner, N. B., and Piccoli, D. A. (1999). Features of Alagille syndrome in 92 patients: frequency and relation to prognosis. Hepatology *29*, 822-829.

Fan, X., Mikolaenko, I., Elhassan, I., Ni, X., Wang, Y., Ball, D., Brat, D. J., Perry, A., and Eberhart, C. G. (2004). Notch1 and notch2 have opposite effects on embryonal brain tumor growth. Cancer Res *64*, 7787-7793.

Faull, R. J., Kovach, N. L., Harlan, J. M., and Ginsberg, M. H. (1993). Affinity modulation of integrin alpha 5 beta 1: regulation of the functional response by soluble fibronectin. J Cell Biol *121*, 155-162.

Faull, R. J., Kovach, N. L., Harlan, J. M., and Ginsberg, M. H. (1994). Stimulation of integrin-mediated adhesion of T lymphocytes and monocytes: two mechanisms with divergent biological consequences. J Exp Med *179*, 1307-1316.

Favre, C. J., Mancuso, M., Maas, K., McLean, J. W., Baluk, P., and McDonald, D. M. (2003). Expression of genes involved in vascular development and angiogenesis in endothelial cells of adult lung. Am J Physiol Heart Circ Physiol *285*, H1917-1938.

Ferguson, A. T., Vertino, P. M., Spitzner, J. R., Baylin, S. B., Muller, M. T., and Davidson, N. E. (1997). Role of estrogen receptor gene demethylation and DNA methyltransferase.DNA adduct formation in 5-aza-2'deoxycytidine-induced cytotoxicity in human breast cancer cells. J Biol Chem *272*, 32260-32266.

Fernandez-Peralta, A. M., Navarro, P., Tagarro, I., and Gonzalez-Aguilera, J. J. (1994). Digestion of human chromosomes by means of the isoschizomers MspI and HpaII. Genome *37*, 770-774.

Ferrara, N., Carver-Moore, K., Chen, H., Dowd, M., Lu, L., O'Shea, K. S., Powell-Braxton, L., Hillan, K. J., and Moore, M. W. (1996). Heterozygous embryonic lethality induced by targeted inactivation of the VEGF gene. Nature *380*, 439-442.

Fischer, A., and Gessler, M. (2003). Hey genes in cardiovascular development. Trends Cardiovasc Med *13*, 221-226.

Fisher, A. L., Ohsako, S., and Caudy, M. (1996). The WRPW motif of the hairy-related basic helix-loop-helix repressor proteins acts as a 4-amino-acid transcription repression and protein-protein interaction domain. Mol Cell Biol *16*, 2670-2677.

Fitzgerald, K., and Greenwald, I. (1995). Interchangeability of Caenorhabditis elegans DSL proteins and intrinsic signalling activity of their extracellular domains in vivo. Development *121*, 4275-4282.

Fleming, R. J. (1998). Structural conservation of Notch receptors and ligands. Semin Cell Dev Biol *9*, 599-607.

Fode, C., Gradwohl, G., Morin, X., Dierich, A., LeMeur, M., Goridis, C., and Guillemot, F. (1998). The bHLH protein NEUROGENIN 2 is a determination factor for epibranchial placode-derived sensory neurons. Neuron *20*, 483-494.

Folberg, R., and Maniotis, A. J. (2004). Vasculogenic mimicry. Apmis *112*, 508-525.

Folkman, J. (1971). Tumor angiogenesis: therapeutic implications. N Engl J Med *285*, 1182-1186.

Folkman, J. (1972). Anti-angiogenesis: new concept for therapy of solid tumors. Ann Surg *175*, 409-416.

Folkman, J. (1995). Angiogenesis in cancer, vascular, rheumatoid and other disease. Nat Med *1*, 27-31.

Fong, T. A., Shawver, L. K., Sun, L., Tang, C., App, H., Powell, T. J., Kim, Y. H., Schreck, R., Wang, X., Risau, W., *et al.* (1999). SU5416 is a potent and selective inhibitor of the vascular endothelial growth factor receptor (Flk-1/KDR) that inhibits tyrosine kinase catalysis, tumor vascularization, and growth of multiple tumor types. Cancer Res *59*, 99-106.

Foty, R. A., and Steinberg, M. S. (1997). Measurement of tumor cell cohesion and suppression of invasion by E- or P-cadherin. Cancer Res *57*, 5033-5036.

Freeman, M. R., Schneck, F. X., Gagnon, M. L., Corless, C., Soker, S., Niknejad, K., Peoples, G. E., and Klagsbrun, M. (1995). Peripheral blood T lymphocytes and lymphocytes infiltrating human cancers express vascular endothelial growth factor: a potential role for T cells in angiogenesis. Cancer Res *55*, 4140-4145.

Frelinger, A. L., 3rd, Du, X. P., Plow, E. F., and Ginsberg, M. H. (1991). Monoclonal antibodies to ligand-occupied conformers of integrin alpha IIb beta 3 (glycoprotein IIb-IIIa) alter receptor affinity, specificity, and function. J Biol Chem *266*, 17106-17111.

Frid, M. G., Kale, V. A., and Stenmark, K. R. (2002). Mature vascular endothelium can give rise to smooth muscle cells via endothelial-mesenchymal transdifferentiation: in vitro analysis. Circ Res *90*, 1189-1196.

Friedlander, M., Brooks, P. C., Shaffer, R. W., Kincaid, C. M., Varner, J. A., and Cheresh, D. A. (1995). Definition of two angiogenic pathways by distinct alpha v integrins. Science *270*, 1500-1502.

Fryer, C. J., Lamar, E., Turbachova, I., Kintner, C., and Jones, K. A. (2002). Mastermind mediates chromatin-specific transcription and turnover of the Notch enhancer complex. Genes Dev *16*, 1397-1411.

Fuh, G., Li, B., Crowley, C., Cunningham, B., and Wells, J. A. (1998). Requirements for binding and signaling of the kinase domain receptor for vascular endothelial growth factor. J Biol Chem *273*, 11197-11204.

Fujita, N., Jaye, D. L., Kajita, M., Geigerman, C., Moreno, C. S., and Wade, P. A. (2003). MTA3, a Mi-2/NuRD complex subunit, regulates an invasive growth pathway in breast cancer. Cell *113*, 207-219.

Fujita, Y., Krause, G., Scheffner, M., Zechner, D., Leddy, H. E., Behrens, J., Sommer, T., and Birchmeier, W. (2002). Hakai, a c-Cbl-like protein, ubiquitinates and induces endocytosis of the E-cadherin complex. Nat Cell Biol *4*, 222-231.

Furriols, M., and Bray, S. (2000). Dissecting the mechanisms of suppressor of hairless function. Dev Biol *227*, 520-532.

Gale, N. W., Dominguez, M. G., Noguera, I., Pan, L., Hughes, V., Valenzuela, D. M., Murphy, A. J., Adams, N. C., Lin, H. C., Holash, J., *et al.* (2004). Haploinsufficiency of delta-like 4 ligand results in embryonic lethality due to major defects in arterial and vascular development. Proc Natl Acad Sci U S A *101*, 15949-15954.

Gallahan, D., Jhappan, C., Robinson, G., Hennighausen, L., Sharp, R., Kordon, E., Callahan, R., Merlino, G., and Smith, G. H. (1996). Expression of a truncated Int3 gene in developing secretory mammary epithelium specifically retards lobular differentiation resulting in tumorigenesis. Cancer Res *56*, 1775-1785.

Gallahan, D., Kozak, C., and Callahan, R. (1987). A new common integration region (int-3) for mouse mammary tumor virus on mouse chromosome 17. J Virol *61*, 218-220.

Gamallo, C., Palacios, J., Suarez, A., Pizarro, A., Navarro, P., Quintanilla, M., and Cano, A. (1993). Correlation of E-cadherin expression with differentiation grade and histological type in breast carcinoma. Am J Pathol *142*, 987-993.

Gamble, J., Meyer, G., Noack, L., Furze, J., Matthias, L., Kovach, N., Harlan, J., and Vadas, M. (1999). beta(1) integrin activation inhibits in vitro tube formation: Effects on cell migration, vacuole coalescence and lumen formation. Endothelium *7*, 23-34.

Gamble, J. R., Matthias, L. J., Meyer, G., Kaur, P., Russ, G., Faull, R., Berndt, M. C., and Vadas, M. A. (1993). Regulation of in vitro capillary tube formation by anti-integrin antibodies. J Cell Biol *121*, 931-943.

Garces, C., Ruiz-Hidalgo, M. J., de Mora, J. F., Park, C., Miele, L., Goldstein, J., Bonvini, E., Porras, A., and Laborda, J. (1997). Notch-1 controls the expression of fatty acid-activated transcription factors and is required for adipogenesis. J Biol Chem *272*, 29729-29734.

Gately, S., Twardowski, P., Stack, M. S., Patrick, M., Boggio, L., Cundiff, D. L., Schnaper, H. W., Madison, L., Volpert, O., Bouck, N., *et al.* (1996). Human prostate carcinoma cells express enzymatic activity that converts human plasminogen to the angiogenesis inhibitor, angiostatin. Cancer Res *56*, 4887-4890.

Giancotti, F. G., and Ruoslahti, E. (1999). Integrin signaling. Science *285*, 1028-1032.

Gill, G. (2001). Regulation of the initiation of eukaryotic transcription. Essays Biochem *37*, 33-43.

Glatt, S. J., Wang, R. S., Yeh, Y. C., Tsuang, M. T., and Faraone, S. V. (2005). Five NOTCH4 polymorphisms show weak evidence for association with schizophrenia: evidence from meta-analyses. Schizophr Res *73*, 281-290.

Goldman, C. K., Kendall, R. L., Cabrera, G., Soroceanu, L., Heike, Y., Gillespie, G. Y., Siegal, G. P., Mao, X., Bett, A. J., Huckle, W. R., *et al.* (1998). Paracrine expression of a native soluble vascular endothelial growth factor receptor inhibits tumor growth, metastasis, and mortality rate. Proc Natl Acad Sci U S A *95*, 8795-8800.

Gorski, D. H., Mauceri, H. J., Salloum, R. M., Halpern, A., Seetharam, S., and Weichselbaum, R. R. (2003). Prolonged treatment with angiostatin reduces metastatic burden during radiation therapy. Cancer Res *63*, 308-311.

Gospodarowicz, D., Abraham, J. A., and Schilling, J. (1989). Isolation and characterization of a vascular endothelial cell mitogen produced by pituitary-derived folliculo stellate cells. Proc Natl Acad Sci U S A *86*, 7311-7315.

Gottardi, C. J., Wong, E., and Gumbiner, B. M. (2001). E-cadherin suppresses cellular transformation by inhibiting beta-catenin signaling in an adhesion-independent manner. J Cell Biol *153*, 1049-1060.

Graff, J. R., Gabrielson, E., Fujii, H., Baylin, S. B., and Herman, J. G. (2000). Methylation patterns of the E-cadherin 5' CpG island are unstable and reflect the dynamic, heterogeneous loss of E-cadherin expression during metastatic progression. J Biol Chem *275*, 2727-2732.

Graff, J. R., Herman, J. G., Lapidus, R. G., Chopra, H., Xu, R., Jarrard, D. F., Isaacs, W. B., Pitha, P. M., Davidson, N. E., and Baylin, S. B. (1995). E-cadherin expression is silenced by DNA hypermethylation in human breast and prostate carcinomas. Cancer Res *55*, 5195-5199.

Graff, J. R., Herman, J. G., Myohanen, S., Baylin, S. B., and Vertino, P. M. (1997). Mapping patterns of CpG island methylation in normal and neoplastic cells implicates both upstream and downstream regions in de novo methylation. J Biol Chem *272*, 22322-22329.

Grant, D. S., Tashiro, K. I., Segui-Real, B., Yamada, Y., Martin, G. R., and Kleinman, H. K. (1989). Two different laminin domains mediate the differentiation of human endothelial cells into capillary-like structures *in vitro*. Cell *58*, 933-943.

Gray, G. E., Mann, R. S., Mitsiadis, E., Henrique, D., Carcangiu, M. L., Banks, A., Leiman, J., Ward, D., Ish-Horowitz, D., and Artavanis-Tsakonas, S. (1999). Human ligands of the Notch receptor. Am J Pathol *154*, 785-794.

Grbavec, D., and Stifani, S. (1996). Molecular interaction between TLE1 and the carboxyl-terminal domain of HES-1 containing the WRPW motif. Biochem Biophys Res Commun *223*, 701-705.

Greenwald, I. (1994). Structure/function studies of lin-12/Notch proteins. Curr Biol *4*, 556-562.

Gridley, T. (2003). Notch signaling and inherited disease syndromes. Hum Mol Genet *12*, R9-13.

Grunwald, G. B., Bromberg, R. E., Crowley, N. J., and Lilien, J. (1981). Enzymatic dissection of embryonic cell adhesive mechanisms. II. Developmental regulation of an endogenous adhesive system in the chick neural retina. Dev Biol *86*, 327-338.

Gupta, S. K., Douglas-Jones, A. G., Jasani, B., Morgan, J. M., Pignatelli, M., and Mansel, R. E. (1997). E-cadherin (E-cad) expression in duct carcinoma in situ (DCIS) of the breast. Virchows Arch *430*, 23-28.

Gutheil, J. C., Campbell, T. N., Pierce, P. R., Watkins, J. D., Huse, W. D., Bodkin, D. J., and Cheresh, D. A. (2000). Targeted antiangiogenic therapy for cancer using Vitaxin: a humanized monoclonal antibody to the integrin alphavbeta3. Clin Cancer Res *6*, 3056-3061.

Haas, T. A., and Plow, E. F. (1994). Integrin-ligand interactions: a year in review. Curr Opin Cell Biol *6*, 656-662.

Haines, N., and Irvine, K. D. (2003). Glycosylation regulates Notch signalling. Nat Rev Mol Cell Biol *4*, 786-797.

Hajra, K. M., Chen, D. Y., and Fearon, E. R. (2002). The SLUG zinc-finger protein represses E-cadherin in breast cancer. Cancer Res *62*, 1613-1618.

Hajra, K. M., and Fearon, E. R. (2002). Cadherin and catenin alterations in human cancer. Genes Chromosomes Cancer *34*, 255-268.

Hamada, Y., Kadokawa, Y., Okabe, M., Ikawa, M., Coleman, J. R., and Tsujimoto, Y. (1999). Mutation in ankyrin repeats of the mouse Notch2 gene induces early embryonic lethality. Development *126*, 3415-3424.

Hamaguchi, Y., Yamamoto, Y., Iwanari, H., Maruyama, S., Furukawa, T., Matsunami, N., and Honjo, T. (1992). Biochemical and immunological characterization of the DNA binding protein (RBP-J kappa) to mouse J kappa recombination signal sequence. J Biochem (Tokyo) *112*, 314-320.

Hamasuna, R., Kataoka, H., Moriyama, T., Itoh, H., Seiki, M., and Koono, M. (1999). Regulation of matrix metalloproteinase-2 (MMP-2) by hepatocyte growth factor/scatter factor (HGF/SF) in human glioma cells: HGF/SF enhances MMP-2 expression and activation accompanying up-regulation of membrane type-1 MMP. Int J Cancer *82*, 274-281.

Han, W., Ye, Q., and Moore, M. A. (2000). A soluble form of human Delta-like-1 inhibits differentiation of hematopoietic progenitor cells. Blood *95*, 1616-1625.

Hanahan, D., and Folkman, J. (1996). Patterns and emerging mechanisms of the angiogenic switch during tumorigenesis. Cell *86*, 353-364.

Hansson, E. M., Lendahl, U., and Chapman, G. (2004). Notch signaling in development and disease. Semin Cancer Biol *14*, 320-328.

Hatsell, S., Rowlands, T., Hiremath, M., and Cowin, P. (2003). Beta-catenin and Tcfs in mammary development and cancer. J Mammary Gland Biol Neoplasia *8*, 145-158.

Haverstick, D. M., Sakai, H., and Gray, L. S. (1992). Lymphocyte adhesion can be regulated by cytoskeleton-associated, PMA-induced capping of surface receptors. Am J Physiol *262*, C916-926.

Hay, E. D. (1995). An overview of epithelio-mesenchymal transformation. Acta Anat (Basel) *154*, 8-20.

Hayashi, Y., Haimovich, B., Reszka, A., Boettiger, D., and Horwitz, A. (1990). Expression and function of chicken integrin beta 1 subunit and its cytoplasmic domain mutants in mouse NIH 3T3 cells. J Cell Biol *110*, 175-184.

He, T. C., Sparks, A. B., Rago, C., Hermeking, H., Zawel, L., da Costa, L. T., Morin, P. J., Vogelstein, B., and Kinzler, K. W. (1998). Identification of c-MYC as a target of the APC pathway. Science *281*, 1509-1512.

He, W., Cowin, P., and Stokes, D. L. (2003). Untangling desmosomal knots with electron tomography. Science *302*, 109-113.

Henderson, A. M., Wang, S. J., Taylor, A. C., Aitkenhead, M., and Hughes, C. C. (2001). The basic helix-loop-helix transcription factor HESR1 regulates endothelial cell tube formation. J Biol Chem *276*, 6169-6176.

Hennig, G., Lowrick, O., Birchmeier, W., and Behrens, J. (1996). Mechanisms identified in the transcriptional control of epithelial gene expression. J Biol Chem *271*, 595-602.

Herman, J. G., and Baylin, S. B. (2003). Gene silencing in cancer in association with promoter hypermethylation. N Engl J Med *349*, 2042-2054.

Herman, J. G., Graff, J. R., Myohanen, S., Nelkin, B. D., and Baylin, S. B. (1996). Methylation-specific PCR: a novel PCR assay for methylation status of CpG islands. Proc Natl Acad Sci U S A *93*, 9821-9826.

Herreman, A., Hartmann, D., Annaert, W., Saftig, P., Craessaerts, K., Serneels, L., Umans, L., Schrijvers, V., Checler, F., Vanderstichele, H., *et al.* (1999). Presenilin 2 deficiency causes a mild pulmonary phenotype and no changes in amyloid precursor protein processing but enhances the embryonic lethal phenotype of presenilin 1 deficiency. Proc Natl Acad Sci U S A *96*, 11872-11877.

Hiran, T. S., Mazurkiewicz, J. E., Kreienberg, P., Rice, F. L., and LaFlamme, S. E. (2003). Endothelial expression of the alpha6beta4 integrin is negatively regulated during angiogenesis. J Cell Sci *116*, 3771-3781.

Hirata, H., Ohtsuka, T., Bessho, Y., and Kageyama, R. (2000). Generation of structurally and functionally distinct factors from the basic helix-loop-helix gene Hes3 by alternative first exons. J Biol Chem *275*, 19083-19089.

Hiscox, S., and Jiang, W. G. (1997). Interleukin-12, an emerging anti-tumour cytokine. In Vivo *11*, 125-132.

Hlatky, L., Hahnfeldt, P., and Folkman, J. (2002). Clinical application of antiangiogenic therapy: microvessel density, what it does and doesn't tell us. J Natl Cancer Inst *94*, 883-893.

Hock, B., Bohme, B., Karn, T., Yamamoto, T., Kaibuchi, K., Holtrich, U., Holland, S., Pawson, T., Rubsamen-Waigmann, H., and Strebhardt, K. (1998). PDZ-domain-mediated interaction of the Eph-related receptor tyrosine kinase EphB3 and the ras-binding protein AF6 depends on the kinase activity of the receptor. Proc Natl Acad Sci U S A *95*, 9779-9784.

Hogg, N., Clive Landis, R., Bates, P. A., Stanley, P., and Randi, A. M. (1994). The sticking point: How integrins bind to their ligands. Trends Cell Biol *4*, 379-382.

Holash, J., Maisonpierre, P. C., Compton, D., Boland, P., Alexander, C. R., Zagzag, D., Yancopoulos, G. D., and Wiegand, S. J. (1999). Vessel cooption, regression, and growth in tumors mediated by angiopoietins and VEGF. Science *284*, 1994-1998.

Holmgren, L., O'Reilly, M. S., and Folkman, J. (1995). Dormancy of micrometastases: balanced proliferation and apoptosis in the presence of angiogenesis suppression. Nat Med *1*, 149-153.

Houde, C., Li, Y., Song, L., Barton, K., Zhang, Q., Godwin, J., Nand, S., Toor, A., Alkan, S., Smadja, N. V., *et al.* (2004). Overexpression of the NOTCH ligand JAG2 in malignant plasma cells from multiple myeloma patients and cell lines. Blood *104*, 3697-3704.

Hovanes, K., Li, T. W., Munguia, J. E., Truong, T., Milovanovic, T., Lawrence Marsh, J., Holcombe, R. F., and Waterman, M. L. (2001). Beta-catenin-sensitive isoforms of lymphoid enhancer factor-1 are selectively expressed in colon cancer. Nat Genet *28*, 53-57.

Hrabe de Angelis, M., McIntyre, J., 2nd, and Gossler, A. (1997). Maintenance of somite borders in mice requires the Delta homologue DII1. Nature *386*, 717-721.

Hsieh, J. J., and Hayward, S. D. (1995). Masking of the CBF1/RBPJ kappa transcriptional repression domain by Epstein-Barr virus EBNA2. Science *268*, 560-563.

Hsieh, J. J., Henkel, T., Salmon, P., Robey, E., Peterson, M. G., and Hayward, S. D. (1996). Truncated mammalian Notch1 activates CBF1/RBPJk-repressed genes by a mechanism resembling that of Epstein-Barr virus EBNA2. Mol Cell Biol *16*, 952-959.

Hsieh, J. J., Zhou, S., Chen, L., Young, D. B., and Hayward, S. D. (1999). CIR, a corepressor linking the DNA binding factor CBF1 to the histone deacetylase complex. Proc Natl Acad Sci U S A *96*, 23-28.

Hsu, S. C., Galceran, J., and Grosschedl, R. (1998). Modulation of transcriptional regulation by LEF-1 in response to Wnt-1 signaling and association with beta-catenin. Mol Cell Biol *18*, 4807-4818.

Hughes, P. E., Diaz-Gonzalez, F., Leong, L., Wu, C., McDonald, J. A., Shattil, S. J., and Ginsberg, M. H. (1996). Breaking the integrin hinge. A defined structural constraint regulates integrin signaling. J Biol Chem *271*, 6571-6574.

Hughes, P. E., and Pfaff, M. (1998). Integrin affinity modulation. Trends Cell Biol *8*, 359-364.

Hukriede, N. A., Gu, Y., and Fleming, R. J. (1997). A dominant-negative form of Serrate acts as a general antagonist of Notch activation. Development *124*, 3427-3437.

Huppert, S. S., Le, A., Schroeter, E. H., Mumm, J. S., Saxena, M. T., Milner, L. A., and Kopan, R. (2000). Embryonic lethality in mice homozygous for a processing-deficient allele of Notch1. Nature *405*, 966-970.

Hurtubise, A., and Momparler, R. L. (2004). Evaluation of antineoplastic action of 5-aza-2'-deoxycytidine (Dacogen) and docetaxel (Taxotere) on human breast, lung and prostate carcinoma cell lines. Anticancer Drugs *15*, 161-167.

Huttenlocher, A., Ginsberg, M. H., and Horwitz, A. F. (1996). Modulation of cell migration by integrin-mediated cytoskeletal linkages and ligand-binding affinity. J Cell Biol *134*, 1551-1562.

Hynes, R. O. (1987). Integrins: a family of cell surface receptors. Cell *48*, 549-554.

Hynes, R. O. (1992). Integrins: versatility, modulation, and signaling in cell adhesion. Cell *69*, 11-25.

Hynes, R. O. (2002). Integrins: bidirectional, allosteric signaling machines. Cell *110*, 673-687.

Ikeda, S., Kishida, S., Yamamoto, H., Murai, H., Koyama, S., and Kikuchi, A. (1998). Axin, a negative regulator of the Wnt signaling pathway, forms a complex with GSK-3beta and beta-catenin and promotes GSK-3beta-dependent phosphorylation of beta-catenin. Embo J *17*, 1371-1384.

Imai, K., Harada, S., Kawanishi, Y., Tachikawa, H., Okubo, T., and Suzuki, T. (2001). The (CTG)n polymorphism in the NOTCH4 gene is not associated with schizophrenia in Japanese individuals. BMC Psychiatry *1*, 1.

Imatani, A., and Callahan, R. (2000). Identification of a novel NOTCH-4/INT-3 RNA species encoding an activated gene product in certain human tumor cell lines. Oncogene *19*, 223-231.

Iruela-Arispe, M. L., Bornstein, P., and Sage, H. (1991a). Thrombospondin exerts an antiangiogenic effect on cord formation by endothelial cells in vitro. Proc Natl Acad Sci U S A *88*, 5026-5030.

Iruela-Arispe, M. L., Hasselaar, P., and Sage, H. (1991b). Differential expression of extracellular proteins is correlated with angiogenesis in vitro. Lab Invest *64*, 174-186.

Ishibashi, M., Sasai, Y., Nakanishi, S., and Kageyama, R. (1993). Molecular characterization of HES-2, a mammalian helix-loop-helix factor structurally related to Drosophila hairy and Enhancer of split. Eur J Biochem *215*, 645-652.

Isner, J. M. (1998). Angiogenesis (Philadelphia, Lippencott-Raven).

Iso, T., Kedes, L., and Hamamori, Y. (2003). HES and HERP families: multiple effectors of the Notch signaling pathway. J Cell Physiol *194*, 237-255.

Iso, T., Sartorelli, V., Chung, G., Shichinohe, T., Kedes, L., and Hamamori, Y. (2001a). HERP, a new primary target of Notch regulated by ligand binding. Mol Cell Biol *21*, 6071-6079.

Iso, T., Sartorelli, V., Poizat, C., Iezzi, S., Wu, H. Y., Chung, G., Kedes, L., and Hamamori, Y. (2001b). HERP, a novel heterodimer partner of HES/E(spl) in Notch signaling. Mol Cell Biol *21*, 6080-6089.

Israel, A., Yano, O., Logeat, F., Kieran, M., and Kourilsky, P. (1989). Two purified factors bind to the same sequence in the enhancer of mouse MHC class I genes: one of them is a positive regulator induced upon differentiation of teratocarcinoma cells. Nucleic Acids Res *17*, 5245-5257.

Jackson-Grusby, L., Laird, P. W., Magge, S. N., Moeller, B. J., and Jaenisch, R. (1997). Mutagenicity of 5-aza-2'-deoxycytidine is mediated by the mammalian DNA methyltransferase. Proc Natl Acad Sci U S A *94*, 4681-4685.

Jain, R. K. (1990). Vascular and interstitial barriers to delivery of therapeutic agents in tumors. Cancer Metastasis Rev *9*, 253-266.

Jamora, C., DasGupta, R., Kocieniewski, P., and Fuchs, E. (2003). Links between signal transduction, transcription and adhesion in epithelial bud development. Nature *422*, 317-322.

Jaye, M., Schlessinger, J., and Dionne, C. A. (1992). Fibroblast growth factor receptor tyrosine kinases: molecular analysis and signal transduction. Biochim Biophys Acta *1135*, 185-199.

Jeffers, M., Rong, S., and Vande Woude, G. F. (1996). Enhanced tumorigenicity and invasion-metastasis by hepatocyte growth factor/scatter factor-met signalling in human cells concomitant with induction of the urokinase proteolysis network. Mol Cell Biol *16*, 1115-1125.

Jehn, B. M., Bielke, W., Pear, W. S., and Osborne, B. A. (1999). Cutting edge: protective effects of notch-1 on TCR-induced apoptosis. J Immunol *162*, 635-638.

Jhappan, C., Gallahan, D., Stahle, C., Chu, E., Smith, G. H., Merlino, G., and Callahan, R. (1992). Expression of an activated Notch-related int-3 transgene interferes with cell differentiation and induces neoplastic transformation in mammary and salivary glands. Genes Dev *6*, 345-355.

Jho, E. H., Zhang, T., Domon, C., Joo, C. K., Freund, J. N., and Costantini, F. (2002). Wnt/beta-catenin/Tcf signaling induces the transcription of Axin2, a negative regulator of the signaling pathway. Mol Cell Biol *22*, 1172-1183.

Jiang, B. H., Zheng, J. Z., Aoki, M., and Vogt, P. K. (2000). Phosphatidylinositol 3-kinase signaling mediates angiogenesis and expression of vascular endothelial growth factor in endothelial cells. Proc Natl Acad Sci U S A *97*, 1749-1753.

Jiang, W. G. (1996). E-cadherin and its associated protein catenins, cancer invasion and metastasis. Br J Surg *83*, 437-446.

Jiang, W. G., and Mansel, R. E. (2000). E-cadherin complex and its abnormalities in human breast cancer. Surg Oncol *9*, 151-171.

Jimenez, G., Paroush, Z., and Ish-Horowicz, D. (1997). Groucho acts as a corepressor for a subset of negative regulators, including Hairy and Engrailed. Genes Dev *11*, 3072-3082.

Johnson, D. E., and Williams, L. T. (1993). Structural and functional diversity in the FGF receptor multigene family. Adv Cancer Res *60*, 1-41.

Johnson, J., Espinoza, T., McGaughey, R. W., Rawls, A., and Wilson-Rawls, J. (2001). Notch pathway genes are expressed in mammalian ovarian follicles. Mech Dev *109*, 355-361.

Joutel, A., Andreux, F., Gaulis, S., Domenga, V., Cecillon, M., Battail, N., Piga, N., Chapon, F., Godfrain, C., and Tournier-Lasserve, E. (2000). The ectodomain of the Notch3 receptor accumulates within the cerebrovasculature of CADASIL patients. J Clin Invest *105*, 597-605.

Joutel, A., Corpechot, C., Ducros, A., Vahedi, K., Chabriat, H., Mouton, P., Alamowitch, S., Domenga, V., Cecillion, M., Marechal, E., *et al.* (1996). Notch3 mutations in CADASIL, a hereditary adult-onset condition causing stroke and dementia. Nature *383*, 707-710.

Joutel, A., Favrole, P., Labauge, P., Chabriat, H., Lescoat, C., Andreux, F., Domenga, V., Cecillon, M., Vahedi, K., Ducros, A., *et al.* (2001). Skin biopsy immunostaining with a Notch3 monoclonal antibody for CADASIL diagnosis. Lancet *358*, 2049-2051.

Joutel, A., Vahedi, K., Corpechot, C., Troesch, A., Chabriat, H., Vayssiere, C., Cruaud, C., Maciazek, J., Weissenbach, J., Bousser, M. G., *et al.* (1997). Strong clustering and stereotyped nature of Notch3 mutations in CADASIL patients. Lancet *350*, 1511-1515.

Jung, H. H., Bassetti, C., Tournier-Lasserve, E., Vahedi, K., Arnaboldi, M., Arifi, V. B., and Burgunder, J. M. (1995). Cerebral autosomal dominant arteriopathy with subcortical infarcts and leukoencephalopathy: a clinicopathological and genetic study of a Swiss family. J Neurol Neurosurg Psychiatry *59*, 138-143.

Junqueira, L. C., Carnero, J., and Kelley, R. O. (1992). Basic Histology, 7th ed. edn (Norwalk, Appleton & Lange).

Kadesch, T. (2000). Notch signaling: a dance of proteins changing partners. Exp Cell Res *260*, 1-8.

Kageyama, R., Ohtsuka, T., and Tomita, K. (2000). The bHLH gene Hes1 regulates differentiation of multiple cell types. Mol Cells *10*, 1-7.

Kantak, S. S., and Kramer, R. H. (1998). E-cadherin regulates anchorage-independent growth and survival in oral squamous cell carcinoma cells. J Biol Chem *273*, 16953-16961.

Kao, H. Y., Ordentlich, P., Koyano-Nakagawa, N., Tang, Z., Downes, M., Kintner, C. R., Evans, R. M., and Kadesch, T. (1998). A histone deacetylase corepressor complex regulates the Notch signal transduction pathway. Genes Dev *12*, 2269-2277.

Karlstrom, H., Beatus, P., Dannaeus, K., Chapman, G., Lendahl, U., and Lundkvist, J. (2002). A CADASIL-mutated Notch 3 receptor exhibits impaired intracellular trafficking and maturation but normal ligand-induced signaling. Proc Natl Acad Sci U S A *99*, 17119-17124.

Kashiwaba, M., Tamura, G., Suzuki, Y., Maesawa, C., Ogasawara, S., Sakata, K., and Satodate, R. (1995). Epithelial-cadherin gene is not mutated in ductal carcinomas of the breast. Jpn J Cancer Res *86*, 1054-1059.

Katayama, M., Hirai, S., Kamihagi, K., Nakagawa, K., Yasumoto, M., and Kato, I. (1994). Soluble E-cadherin fragments increased in circulation of cancer patients. Br J Cancer *69*, 580-585.

Kazarov, A. R., Yang, X., Stipp, C. S., Sehgal, B., and Hemler, M. E. (2002). An extracellular site on tetraspanin CD151 determines alpha 3 and alpha 6 integrin-dependent cellular morphology. J Cell Biol *158*, 1299-1309.

Kendall, R. L., Wang, G., and Thomas, K. A. (1996). Identification of a natural soluble form of the vascular endothelial growth factor receptor, FLT-1, and its heterodimerization with KDR. Biochem Biophys Res Commun *226*, 324-328.

Kerbel, R. S. (2000). Tumor angiogenesis: past, present and the near future. Carcinogenesis *21*, 505-515.

Kidd, S., Kelley, M. R., and Young, M. W. (1986). Sequence of the notch locus of Drosophila melanogaster: relationship of the encoded protein to mammalian clotting and growth factors. Mol Cell Biol *6*, 3094-3108.

Kim, H. K., and Siu, G. (1998). The notch pathway intermediate HES-1 silences CD4 gene expression. Mol Cell Biol *18*, 7166-7175.

Kim, K. J., Li, B., Winer, J., Armanini, M., Gillett, N., Phillips, H. S., and Ferrara, N. (1993). Inhibition of vascular endothelial growth factor-induced angiogenesis suppresses tumour growth in vivo. Nature *362*, 841-844.

Kimble, J., Henderson, S., and Crittenden, S. (1998). Notch/LIN-12 signaling: transduction by regulated protein slicing. Trends Biochem Sci *23*, 353-357.

Kishida, S., Yamamoto, H., Ikeda, S., Kishida, M., Sakamoto, I., Koyama, S., and Kikuchi, A. (1998). Axin, a negative regulator of the wnt signaling pathway, directly interacts with adenomatous polyposis coli and regulates the stabilization of beta-catenin. J Biol Chem *273*, 10823-10826.

Kitagawa, M., Oyama, T., Kawashima, T., Yedvobnick, B., Kumar, A., Matsuno, K., and Harigaya, K. (2001). A human protein with sequence similarity to Drosophila mastermind coordinates the nuclear form of notch and a CSL protein to build a transcriptional activator complex on target promoters. Mol Cell Biol *21*, 4337-4346.

Klagsbrun, M., and Moses, M. A. (1999). Molecular angiogenesis. Chem Biol *6*, R217-224.

Klement, G., Baruchel, S., Rak, J., Man, S., Clark, K., Hicklin, D. J., Bohlen, P., and Kerbel, R. S. (2000). Continuous low-dose therapy with vinblastine and VEGF receptor-2 antibody induces sustained tumor regression without overt toxicity. J Clin Invest *105*, R15-24.

Klint, P., and Claesson-Welsh, L. (1999). Signal transduction by fibroblast growth factor receptors. Front Biosci *4*, D165-177.

Knoepfler, P. S., and Eisenman, R. N. (1999). Sin meets NuRD and other tails of repression. Cell *99*, 447-450.

Koblizek, T. I., Weiss, C., Yancopoulos, G. D., Deutsch, U., and Risau, W. (1998). Angiopoietin-1 induces sprouting angiogenesis *in vitro*. Curr Biol *8*, 529-532.

Koch, A. W., Bozic, D., Pertz, O., and Engel, J. (1999). Homophilic adhesion by cadherins. Curr Opin Struct Biol *9*, 275-281.

Kokubo, H., Lun, Y., and Johnson, R. L. (1999). Identification and expression of a novel family of bHLH cDNAs related to Drosophila hairy and enhancer of split. Biochem Biophys Res Commun *260*, 459-465.

Kopan, R., Nye, J. S., and Weintraub, H. (1994). The intracellular domain of mouse Notch: A constitutively activated repressor of myogenesis directed at the basic helix-loop-helix region of *MyoD*. Development *120*, 2385-2396.

Kordon, E. C., Smith, G. H., Callahan, R., and Gallahan, D. (1995). A novel non-mouse mammary tumor virus activation of the Int-3 gene in a spontaneous mouse mammary tumor. J Virol *69*, 8066-8069.

Kortschak, R. D., Tamme, R., and Lardelli, M. (2001). Evolutionary analysis of vertebrate Notch genes. Dev Genes Evol *211*, 350-354.

Kovach, N. L., Carlos, T. M., Yee, E., and Harlan, J. M. (1992). A monoclonal antibody to beta 1 integrin (CD29) stimulates VLA-dependent adherence of leukocytes to human umbilical vein endothelial cells and matrix components. J Cell Biol *116*, 499-509.

Koyama, N., Seki, J., Vergel, S., Mattsson, E. J., Yednock, T., Kovach, N. L., Harlan, J. M., and Clowes, A. W. (1996). Regulation and function of an activation-dependent epitope of the beta 1 integrins in vascular cells after balloon injury in baboon arteries and in vitro. Am J Pathol *148*, 749-761.

Koyano-Nakagawa, N., Kim, J., Anderson, D., and Kintner, C. (2000). Hes6 acts in a positive feedback loop with the neurogenins to promote neuronal differentiation. Development *127*, 4203-4216.

Kramer, R. H., Fuh, G. M., and Karasek, M. A. (1985). Type IV collagen synthesis by cultured human microvascular endothelial cells and its deposition into the subendothelial basement membrane. Biochemistry *24*, 7423-7430.

Krantz, I. D., Rand, E. B., Genin, A., Hunt, P., Jones, M., Louis, A. A., Graham, J. M., Jr., Bhatt, S., Piccoli, D. A., and Spinner, N. B. (1997). Deletions of 20p12 in Alagille syndrome: frequency and molecular characterization. Am J Med Genet *70*, 80-86.

Krebs, L. T., Xue, Y., Norton, C. R., Shutter, J. R., Maguire, M., Sundberg, J. P., Gallahan, D., Closson, V., Kitajewski, J., Callahan, R., *et al.* (2000). Notch signaling is essential for vascular morphogenesis in mice. Genes Dev *14*, 1343-1352.

Kurooka, H., and Honjo, T. (2000). Functional interaction between the mouse notch1 intracellular region and histone acetyltransferases PCAF and GCN5. J Biol Chem *275*, 17211-17220.

Kusumi, K., Sun, E. S., Kerrebrock, A. W., Bronson, R. T., Chi, D. C., Bulotsky, M. S., Spencer, J. B., Birren, B. W., Frankel, W. N., and Lander, E. S. (1998). The mouse pudgy mutation disrupts Delta homologue Dll3 and initiation of early somite boundaries. Nat Genet *19*, 274-278.

LaFlamme, S. E., and Auer, K. L. (1996). Integrin signaling. Semin Cancer Biol *7*, 111-118.

Lam, L. T., and Bresnick, E. H. (1998). Identity of the beta-globin locus control region binding protein HS2NF5 as the mammalian homolog of the notch-regulated transcription factor suppressor of hairless. J Biol Chem *273*, 24223-24231.

Lardelli, M., Dahlstrand, J., and Lendahl, U. (1994). The novel Notch homologue mouse Notch 3 lacks specific epidermal growth factor-repeats and is expressed in proliferating neuroepithelium. Mech Dev *46*, 123-136.

Larrivee, B., and Karsan, A. (2000). Signaling pathways induced by vascular endothelial growth factor (review). Int J Mol Med *5*, 447-456.

Lauffenburger, D. A., and Horwitz, A. F. (1996). Cell migration: a physically integrated molecular process. Cell *84*, 359-369.

LaVoie, M. J., and Selkoe, D. J. (2003). The Notch ligands, Jagged and Delta, are sequentially processed by alpha-secretase and presenilin/gamma-secretase and release signaling fragments. J Biol Chem *278*, 34427-34437.

Le Borgne, R., and Schweisguth, F. (2003). Notch signaling: endocytosis makes delta signal better. Curr Biol *13*, R273-275.

Lee, H. J., Jung, K. M., Huang, Y. Z., Bennett, L. B., Lee, J. S., Mei, L., and Kim, T. W. (2002). Presenilin-dependent gamma-secretase-like intramembrane cleavage of ErbB4. J Biol Chem *277*, 6318-6323.

Lee, J. S., Haruna, T., Ishimoto, A., Honjo, T., and Yanagawa, S. (1999). Intracisternal type A particle-mediated activation of the Notch4/int3 gene in a mouse mammary tumor: generation of truncated Notch4/int3 mRNAs by retroviral splicing events. J Virol *73*, 5166-5171.

Lee, S. H., Schloss, D. J., and Swain, J. L. (2000). Maintenance of vascular integrity in the embryo requires signaling through the fibroblast growth factor receptor. J Biol Chem *275*, 33679-33687.

Leek, R. D., Harris, A. L., and Lewis, C. E. (1994). Cytokine networks in solid human tumors: regulation of angiogenesis. J Leukoc Biol *56*, 423-435.

Lehmann, M., Rigot, V., Seidah, N. G., Marvaldi, J., and Lissitzky, J. C. (1996). Lack of integrin alpha-chain endoproteolytic cleavage in furin-deficient human colon adenocarcinoma cells LoVo. Biochem J *317*, 803-809.

Lei, H., Sjoberg-Margolin, S., Salahshor, S., Werelius, B., Jandakova, E., Hemminki, K., Lindblom, A., and Vorechovsky, I. (2002). CDH1 mutations are present in both ductal and lobular breast cancer, but promoter allelic variants show no detectable breast cancer risk. Int J Cancer *98*, 199-204.

Leimeister, C., Dale, K., Fischer, A., Klamt, B., Hrabe de Angelis, M., Radtke, F., McGrew, M. J., Pourquie, O., and Gessler, M. (2000a). Oscillating expression of c-Hey2 in the presomitic

mesoderm suggests that the segmentation clock may use combinatorial signaling through multiple interacting bHLH factors. Dev Biol *227*, 91-103.

Leimeister, C., Externbrink, A., Klamt, B., and Gessler, M. (1999). Hey genes: a novel subfamily of hairy- and Enhancer of split related genes specifically expressed during mouse embryogenesis. Mech Dev *85*, 173-177.

Leimeister, C., Schumacher, N., Steidl, C., and Gessler, M. (2000b). Analysis of HeyL expression in wild-type and Notch pathway mutant mouse embryos. Mech Dev *98*, 175-178.

Leung, D. W., Cachianes, G., Kuang, W. J., Goeddel, D. V., and Ferrara, N. (1989). Vascular endothelial growth factor is a secreted angiogenic mitogen. Science *246*, 1306-1309.

Levine, M. D., Liotta, L. A., and Stracke, M. L. (1995). Stimulation and regulation of tumor cell motility in invasion and metastasis. Exs *74*, 157-179.

Li, L., Huang, G. M., Banta, A. B., Deng, Y., Smith, T., Dong, P., Friedman, C., Chen, L., Trask, B. J., Spies, T., *et al.* (1998a). Cloning, characterization, and the complete 56.8-kilobase DNA sequence of the human Notch4 gene. Genomics *51*, 45-58.

Li, L., Krantz, I. D., Deng, Y., Genin, A., Banta, A. B., Collins, C. C., Qi, M., Trask, B. J., Kuo, W. L., Cochran, J., *et al.* (1997). Alagille syndrome is caused by mutations in human Jagged1, which encodes a ligand for Notch1. Nat Genet *16*, 243-251.

Li, L., Milner, L. A., Deng, Y., Iwata, M., Banta, A., Graf, L., Marcovina, S., Friedman, C., Trask, B. J., Hood, L., and Torok-Storb, B. (1998b). The human homolog of rat Jagged1 expressed by marrow stroma inhibits differentiation of 32D cells through interaction with Notch1. Immunity *8*, 43-55.

Li, L. C., Chui, R. M., Sasaki, M., Nakajima, K., Perinchery, G., Au, H. C., Nojima, D., Carroll, P., and Dahiya, R. (2000). A single nucleotide polymorphism in the E-cadherin gene promoter alters transcriptional activities. Cancer Res *60*, 873-876.

Lieber, T., Kidd, S., Alcamo, E., Corbin, V., and Young, M. W. (1993). Antineurogenic phenotypes induced by truncated Notch proteins indicate a role in signal transduction and may point to a novel function for Notch in nuclei. Genes Dev *7*, 1949-1965.

Lieber, T., Wesley, C. S., Alcamo, E., Hassel, B., Krane, J. F., Campos-Ortega, J. A., and Young, M. W. (1992). Single amino acid substitutions in EGF-like elements of Notch and Delta modify Drosophila development and affect cell adhesion in vitro. Neuron *9*, 847-859.

Lin, S. E., Oyama, T., Nagase, T., Harigaya, K., and Kitagawa, M. (2002). Identification of new human mastermind proteins defines a family that consists of positive regulators for notch signaling. J Biol Chem *277*, 50612-50620.

Lin, S. Y., Xia, W., Wang, J. C., Kwong, K. Y., Spohn, B., Wen, Y., Pestell, R. G., and Hung, M. C. (2000). Beta-catenin, a novel prognostic marker for breast cancer: its roles in cyclin D1 expression and cancer progression. Proc Natl Acad Sci U S A *97*, 4262-4266.

Lindner, D. J. (2002). Interferons as antiangiogenic agents. Curr Oncol Rep *4*, 510-514.

Lindner, V., Booth, C., Prudovsky, I., Small, D., Maciag, T., and Liaw, L. (2001). Members of the Jagged/Notch gene families are expressed in injured arteries and regulate cell phenotype via alterations in cell matrix and cell-cell interaction. Am J Pathol *159*, 875-883.

Lindsell, C. E., Shawber, C. J., Boulter, J., and Weinmaster, G. (1995). Jagged: a mammalian ligand that activates Notch1. Cell *80*, 909-917.

Ling, P. D., Hsieh, J. J., Ruf, I. K., Rawlins, D. R., and Hayward, S. D. (1994). EBNA-2 upregulation of Epstein-Barr virus latency promoters and the cellular CD23 promoter utilizes a common targeting intermediate, CBF1. J Virol *68*, 5375-5383.

Lissemore, J. L., and Starmer, W. T. (1999). Phylogenetic analysis of vertebrate and invertebrate Delta/Serrate/LAG-2 (DSL) proteins. Mol Phylogenet Evol *11*, 308-319.

Liu, L., Zeng, M., and Stamler, J. S. (1999). Hemoglobin induction in mouse macrophages. Proc Natl Acad Sci U S A *96*, 6643-6647.

Liu, Z. J., Shirakawa, T., Li, Y., Soma, A., Oka, M., Dotto, G. P., Fairman, R. M., Velazquez, O. C., and Herlyn, M. (2003). Regulation of Notch1 and Dll4 by vascular endothelial growth factor in arterial endothelial cells: implications for modulating arteriogenesis and angiogenesis. Mol Cell Biol *23*, 14-25.

Lo, S. H., and Chen, L. B. (1994). Focal adhesion as a signal transduction organelle. Cancer Metastasis Rev *13*, 9-24.

Loftus, J. C., and Liddington, R. C. (1997). Cell adhesion in vascular biology. New insights into integrin-ligand interaction. J Clin Invest *99*, 2302-2306.

Logeat, F., Bessia, C., Brou, C., LeBail, O., Jarriault, S., Seidah, N. G., and Israel, A. (1998). The Notch1 receptor is cleaved constitutively by a furin-like convertase. Proc Natl Acad Sci U S A *95*, 8108-8112.

Lollo, B. A., Chan, K. W., Hanson, E. M., Moy, V. T., and Brian, A. A. (1993). Direct evidence for two affinity states for lymphocyte function-associated antigen 1 on activated T cells. J Biol Chem *268*, 21693-21700.

Longhurst, C. M., and Jennings, L. K. (1998). Integrin-mediated signal transduction. Cell Mol Life Sci *54*, 514-526.

Lub, M., van Kooyk, Y., and Figdor, C. G. (1995). Ins and outs of LFA-1. Immunol Today *16*, 479-483.

Lubman, O. Y., Korolev, S. V., and Kopan, R. (2004). Anchoring notch genetics and biochemistry; structural analysis of the ankyrin domain sheds light on existing data. Mol Cell *13*, 619-626.

Ma, P. C., Rould, M. A., Weintraub, H., and Pabo, C. O. (1994). Crystal structure of MyoD bHLH domain-DNA complex: perspectives on DNA recognition and implications for transcriptional activation. Cell *77*, 451-459.

Ma, Q., Chen, Z., del Barco Barrantes, I., de la Pompa, J. L., and Anderson, D. J. (1998). neurogenin1 is essential for the determination of neuronal precursors for proximal cranial sensory ganglia. Neuron *20*, 469-482.

MacKenzie, F., Duriez, P., Larrivee, B., Chang, L., Pollet, I., Wong, F., Yip, C., and Karsan, A. (2004a). Notch4-induced inhibition of endothelial sprouting requires the ankyrin repeats and involves signaling through RBP-Jkappa. Blood *104*, 1760-1768.

MacKenzie, F., Duriez, P., Wong, F., Noseda, M., and Karsan, A. (2004b). Notch4 inhibits endothelial apoptosis via RBP-Jkappa-dependent and -independent pathways. J Biol Chem *279*, 11657-11663.

Mailhos, C., Modlich, U., Lewis, J., Harris, A., Bicknell, R., and Ish-Horowicz, D. (2001). Delta4, an endothelial specific notch ligand expressed at sites of physiological and tumor angiogenesis. Differentiation *69*, 135-144.

Maltepe, E., Schmidt, J. V., Baunoch, D., Bradfield, C. A., and Simon, M. C. (1997). Abnormal angiogenesis and responses to glucose and oxygen deprivation in mice lacking the protein ARNT. Nature *386*, 403-407.

Maniotis, A. J., Folberg, R., Hess, A., Seftor, E. A., Gardner, L. M., Pe'er, J., Trent, J. M., Meltzer, P. S., and Hendrix, M. J. (1999). Vascular channel formation by human melanoma cells in vivo and in vitro: vasculogenic mimicry. Am J Pathol *155*, 739-752.

Mann, B., Gelos, M., Siedow, A., Hanski, M. L., Gratchev, A., Ilyas, M., Bodmer, W. F., Moyer, M. P., Riecken, E. O., Buhr, H. J., and Hanski, C. (1999). Target genes of beta-catenin-T cell-factor/lymphoid-enhancer-factor signaling in human colorectal carcinomas. Proc Natl Acad Sci U S A *96*, 1603-1608.

Marincola, F. M., Jaffee, E. M., Hicklin, D. J., and Ferrone, S. (2000). Escape of human solid tumors from T-cell recognition: molecular mechanisms and functional significance. Adv Immunol *74*, 181-273.

Martin, D. C., Ruther, U., Sanchez-Sweatman, O. H., Orr, F. W., and Khokha, R. (1996). Inhibition of SV40 T antigen-induced hepatocellular carcinoma in TIMP-1 transgenic mice. Oncogene *13*, 569-576.

McCright, B., Gao, X., Shen, L., Lozier, J., Lan, Y., Maguire, M., Herzlinger, D., Weinmaster, G., Jiang, R., and Gridley, T. (2001). Defects in development of the kidney, heart and eye vasculature in mice homozygous for a hypomorphic Notch2 mutation. Development *128*, 491-502.

Meininger, C. J., and Zetter, B. R. (1992). Mast cells and angiogenesis. Semin Cancer Biol *3*, 73-79.

Miele, L., and Osborne, B. (1999). Arbiter of differentiation and death: Notch signaling meets apoptosis. J Cell Physiol *181*, 393-409.

Migdal, M., Huppertz, B., Tessler, S., Comforti, A., Shibuya, M., Reich, R., Baumann, H., and Neufeld, G. (1998). Neuropilin-1 is a placenta growth factor-2 receptor. J Biol Chem *273*, 22272-22278.

Mignatti, P., and Rifkin, D. B. (1996). Plasminogen activators and matrix metalloproteinases in angiogenesis. Enzyme Protein *49*, 117-137.

Miguez, M., Davel, L., and de Lustig, E. S. (1986). Lymphocyte-induced angiogenesis: correlation with the metastatic incidence of two murine mammary adenocarcinomas. Invasion Metastasis *6*, 313-320.

Miller, J. R., Hocking, A. M., Brown, J. D., and Moon, R. T. (1999). Mechanism and function of signal transduction by the Wnt/beta-catenin and Wnt/Ca2+ pathways. Oncogene *18*, 7860-7872.

Miller, K. D., and Sledge, G. W., Jr. (1999). Toward checkmate: biology and breast cancer therapy for the new millennium. Invest New Drugs *17*, 417-427.

Milner, L. A., and Bigas, A. (1999). Notch as a mediator of cell fate determination in hematopoiesis: evidence and speculation. Blood *93*, 2431-2448.

Mitchell, B. S., Schumacher, U., and Kaiserling, E. (1994). Are tumours innervated? Immunohistological investigations using antibodies against the neuronal marker protein gene product 9.5 (PGP 9.5) in benign, malignant and experimental tumours. Tumour Biol *15*, 269-274.

Mitsiadis, T. A., Lardelli, M., Lendahl, U., and Thesleff, I. (1995). Expression of Notch 1, 2 and 3 is regulated by epithelial-mesenchymal interactions and retinoic acid in the developing mouse tooth and associated with determination of ameloblast cell fate. J Cell Biol *130*, 407-418.

Miyamoto, Y., Maitra, A., Ghosh, B., Zechner, U., Argani, P., Iacobuzio-Donahue, C. A., Sriuranpong, V., Iso, T., Meszoely, I. M., Wolfe, M. S., *et al.* (2003). Notch mediates TGF alpha-induced changes in epithelial differentiation during pancreatic tumorigenesis. Cancer Cell *3*, 565-576.

Mizutani, T., Taniguchi, Y., Aoki, T., Hashimoto, N., and Honjo, T. (2001). Conservation of the biochemical mechanisms of signal transduction among mammalian Notch family members. Proc Natl Acad Sci U S A *98*, 9026-9031.

Moll, R., Mitze, M., Frixen, U. H., and Birchmeier, W. (1993). Differential loss of E-cadherin expression in infiltrating ductal and lobular breast carcinomas. Am J Pathol *143*, 1731-1742.

Momparler, R. L. (1985). Molecular, cellular and animal pharmacology of 5-aza-2'-deoxycytidine. Pharmacol Ther *30*, 287-299.

Montesano, R., Vassalli, J. D., Baird, A., Guillemin, R., and Orci, L. (1986). Basic fibroblast growth factor induces angiogenesis in vitro. Proc Natl Acad Sci U S A *83*, 7297-7301.

Moser, T. L., Stack, M. S., Asplin, I., Enghild, J. J., Hojrup, P., Everitt, L., Hubchak, S., Schnaper, H. W., and Pizzo, S. V. (1999). Angiostatin binds ATP synthase on the surface of human endothelial cells. Proc Natl Acad Sci U S A *96*, 2811-2816.

Muller, P., Kietz, S., Gustafsson, J. A., and Strom, A. (2002). The anti-estrogenic effect of all-trans-retinoic acid on the breast cancer cell line MCF-7 is dependent on HES-1 expression. J Biol Chem *277*, 28376-28379.

Mumm, J. S., and Kopan, R. (2000). Notch signaling: from the outside in. Dev Biol *228*, 151-165.

Mumm, J. S., Schroeter, E. H., Saxena, M. T., Griesemer, A., Tian, X., Pan, D. J., Ray, W. J., and Kopan, R. (2000). A ligand-induced extracellular cleavage regulates gamma-secretase-like proteolytic activation of Notch1. Mol Cell *5*, 197-206.

Murphy, A. N., Unsworth, E. J., and Stetler-Stevenson, W. G. (1993). Tissue inhibitor of metalloproteinases-2 inhibits bFGF-induced human microvascular endothelial cell proliferation. J Cell Physiol *157*, 351-358.

Murre, C., Bain, G., van Dijk, M. A., Engel, I., Furnari, B. A., Massari, M. E., Matthews, J. R., Quong, M. W., Rivera, R. R., and Stuiver, M. H. (1994). Structure and function of helix-loop-helix proteins. Biochim Biophys Acta *1218*, 129-135.

Nabi, I. R., Watanabe, H., and Raz, A. (1992). Autocrine motility factor and its receptor: role in cell locomotion and metastasis. Cancer Metastasis Rev *11*, 5-20.

Nair, P., Somasundaram, K., and Krishna, S. (2003). Activated Notch1 inhibits p53-induced apoptosis and sustains transformation by human papillomavirus type 16 E6 and E7 oncogenes through a PI3K-PKB/Akt-dependent pathway. J Virol *77*, 7106-7112.

Nakagawa, O., McFadden, D. G., Nakagawa, M., Yanagisawa, H., Hu, T., Srivastava, D., and Olson, E. N. (2000). Members of the HRT family of basic helix-loop-helix proteins act as transcriptional repressors downstream of Notch signaling. Proc Natl Acad Sci U S A *97*, 13655-13660.

Nakagawa, O., Nakagawa, M., Richardson, J. A., Olson, E. N., and Srivastava, D. (1999). HRT1, HRT2, and HRT3: a new subclass of bHLH transcription factors marking specific cardiac, somitic, and pharyngeal arch segments. Dev Biol *216*, 72-84.

Nakatsu, M. N., Sainson, R. C., Aoto, J. N., Taylor, K. L., Aitkenhead, M., Perez-del-Pulgar, S., Carpenter, P. M., and Hughes, C. C. (2003). Angiogenic sprouting and capillary lumen formation modeled by human umbilical vein endothelial cells (HUVEC) in fibrin gels: the role of fibroblasts and Angiopoietin-1. Microvasc Res *66*, 102-112.

Nass, S. J., Herman, J. G., Gabrielson, E., Iversen, P. W., Parl, F. F., Davidson, N. E., and Graff, J. R. (2000). Aberrant methylation of the estrogen receptor and E-cadherin 5' CpG islands increases with malignant progression in human breast cancer. Cancer Res *60*, 4346-4348.

Negus, R. P., and Balkwill, F. R. (1996). Cytokines in tumour growth, migration and metastasis. World J Urol *14*, 157-165.

Nehls, V., and Drenckhahn, D. (1995). A novel, microcarrier-based *in vitro* assay for rapid and reliable quantification of three-dimensional cell migration and angiogenesis. Microvasc Res *50*, 311-322.

Nelson, W. J., and Nusse, R. (2004). Convergence of Wnt, beta-catenin, and cadherin pathways. Science *303*, 1483-1487.

Neufeld, G., Cohen, T., Gengrinovitch, S., and Poltorak, Z. (1999). Vascular endothelial growth factor (VEGF) and its receptors. Faseb J *13*, 9-22.

Neufeld, G., Cohen, T., Gitay-Goren, H., Poltorak, Z., Tessler, S., Sharon, R., Gengrinovitch, S., and Levi, B. Z. (1996). Similarities and differences between the vascular endothelial growth factor (VEGF) splice variants. Cancer Metastasis Rev *15*, 153-158.

Neugebauer, K. M., and Reichardt, L. F. (1991). Cell-surface regulation of beta 1-integrin activity on developing retinal neurons. Nature *350*, 68-71.

Ni, H., Li, A., Simonsen, N., and Wilkins, J. A. (1998). Integrin activation by dithiothreitol or Mn2+ induces a ligand-occupied conformation and exposure of a novel NH2-terminal regulatory site on the beta1 integrin chain. J Biol Chem *273*, 7981-7987.

Nickoloff, B. J., Osborne, B. A., and Miele, L. (2003). Notch signaling as a therapeutic target in cancer: a new approach to the development of cell fate modifying agents. Oncogene *22*, 6598-6608.

Nickoloff, B. J., Qin, J. Z., Chaturvedi, V., Denning, M. F., Bonish, B., and Miele, L. (2002). Jagged-1 mediated activation of notch signaling induces complete maturation of human keratinocytes through NF-kappaB and PPARgamma. Cell Death Differ *9*, 842-855.

Nicolas, M., Wolfer, A., Raj, K., Kummer, J. A., Mill, P., van Noort, M., Hui, C. C., Clevers, H., Dotto, G. P., and Radtke, F. (2003). Notch1 functions as a tumor suppressor in mouse skin. Nat Genet *33*, 416-421.

Nicolson, G. L. (1982). Metastatic tumor cell attachment and invasion assay utilizing vascular endothelial cell monolayers. J Histochem Cytochem *30*, 214-220.

Nieset, J. E., Redfield, A. R., Jin, F., Knudsen, K. A., Johnson, K. R., and Wheelock, M. J. (1997). Characterization of the interactions of alpha-catenin with alpha-actinin and beta-catenin/plakoglobin. J Cell Sci *110*, 1013-1022.

Nijjar, S. S., Crosby, H. A., Wallace, L., Hubscher, S. G., and Strain, A. J. (2001). Notch receptor expression in adult human liver: a possible role in bile duct formation and hepatic neovascularization. Hepatology *34*, 1184-1192.

Nime, F. A., Rosen, P. P., Thaler, H. T., Ashikari, R., and Urban, J. A. (1977). Prognostic significance of tumor emboli in intramammary lymphatics in patients with mammary carcinoma. Am J Surg Pathol *1*, 25-30.

Noseda, M., Chang, L., McLean, G., Grim, J. E., Clurman, B. E., Smith, L. L., and Karsan, A. (2004a). Notch activation induces endothelial cell cycle arrest and participates in contact inhibition: role of p21Cip1 repression. Mol Cell Biol *24*, 8813-8822.

Noseda, M., McLean, G., Niessen, K., Chang, L., Pollet, I., Montpetit, R., Shahidi, R., Dorovini-Zis, K., Li, L., Beckstead, B., *et al.* (2004b). Notch activation results in phenotypic and functional changes consistent with endothelial-to-mesenchymal transformation. Circ Res *94*, 910-917.

Nusse, R. (1988). The int genes in mammary tumorigenesis and in normal development. Trends Genet *4*, 291-295.

Nusse, R. (1997). A versatile transcriptional effector of Wingless signaling. Cell *89*, 321-323.

Nye, J. S., Kopan, R., and Axel, R. (1994). An activated Notch suppresses neurogenesis and myogenesis but not gliogenesis in mammalian cells. Development *120*, 2421-2430.

O'Connell, J., O'Sullivan, G. C., Collins, J. K., and Shanahan, F. (1996). The Fas counterattack: Fas-mediated T cell killing by colon cancer cells expressing Fas ligand. J Exp Med *184*, 1075-1082.

Oda, T., Elkahloun, A. G., Pike, B. L., Okajima, K., Krantz, I. D., Genin, A., Piccoli, D. A., Meltzer, P. S., Spinner, N. B., Collins, F. S., and Chandrasekharappa, S. C. (1997). Mutations in the human Jagged1 gene are responsible for Alagille syndrome. Nat Genet *16*, 235-242.

Oka, H., Shiozaki, H., Kobayashi, K., Inoue, M., Tahara, H., Kobayashi, T., Takatsuka, Y., Matsuyoshi, N., Hirano, S., Takeichi, M., and et al. (1993). Expression of E-cadherin cell adhesion molecules in human breast cancer tissues and its relationship to metastasis. Cancer Res *53*, 1696-1701.

Okubo, T., Truong, T. K., Yu, B., Itoh, T., Zhao, J., Grube, B., Zhou, D., and Chen, S. (2001). Down-regulation of promoter 1.3 activity of the human aromatase gene in breast tissue by zinc-finger protein, snail (SnaH). Cancer Res *61*, 1338-1346.

Olave, I., Reinberg, D., and Vales, L. D. (1998). The mammalian transcriptional repressor RBP (CBF1) targets TFIID and TFIIA to prevent activated transcription. Genes Dev *12*, 1621-1637.

O'Reilly, M. S., Boehm, T., Shing, Y., Fukai, N., Vasios, G., Lane, W. S., Flynn, E., Birkhead, J. R., Olsen, B. R., and Folkman, J. (1997). Endostatin: an endogenous inhibitor of angiogenesis and tumor growth. Cell *88*, 277-285.

O'Reilly, M. S., Holmgren, L., Shing, Y., Chen, C., Rosenthal, R. A., Moses, M., Lane, W. S., Cao, Y., Sage, E. H., and Folkman, J. (1994). Angiostatin: a novel angiogenesis inhibitor that mediates the suppression of metastases by a Lewis lung carcinoma. Cell *79*, 315-328.

Orford, K., Crockett, C., Jensen, J. P., Weissman, A. M., and Byers, S. W. (1997). Serine phosphorylation-regulated ubiquitination and degradation of beta-catenin. J Biol Chem *272*, 24735-24738.

Ortlepp, S., Stephens, P. E., Hogg, N., Figdor, C. G., and Robinson, M. K. (1995). Antibodies that activate beta 2 integrins can generate different ligand binding states. Eur J Immunol *25*, 637-643.

Oswald, F., Kostezka, U., Astrahantseff, K., Bourteele, S., Dillinger, K., Zechner, U., Ludwig, L., Wilda, M., Hameister, H., Knochel, W., *et al.* (2002). SHARP is a novel component of the Notch/RBP-Jkappa signalling pathway. Embo J *21*, 5417-5426.

Oswald, F., Liptay, S., Adler, G., and Schmid, R. M. (1998). NF-kappaB2 is a putative target gene of activated Notch-1 via RBP-Jkappa. Mol Cell Biol *18*, 2077-2088.

Oswald, F., Tauber, B., Dobner, T., Bourteele, S., Kostezka, U., Adler, G., Liptay, S., and Schmid, R. M. (2001). p300 acts as a transcriptional coactivator for mammalian Notch-1. Mol Cell Biol *21*, 7761-7774.

O'Toole, T. E., Loftus, J. C., Plow, E. F., Glass, A. A., Harper, J. R., and Ginsberg, M. H. (1989). Efficient surface expression of platelet GPIIb-IIIa requires both subunits. Blood *74*, 14-18.

O'Toole, T. E., Ylanne, J., and Culley, B. M. (1995). Regulation of integrin affinity states through an NPXY motif in the beta subunit cytoplasmic domain. J Biol Chem *270*, 8553-8558.

Overduin, M., Harvey, T. S., Bagby, S., Tong, K. I., Yau, P., Takeichi, M., and Ikura, M. (1995). Solution structure of the epithelial cadherin domain responsible for selective cell adhesion. Science *267*, 386-389.

Ozawa, M., Baribault, H., and Kemler, R. (1989). The cytoplasmic domain of the cell adhesion molecule uvomorulin associates with three independent proteins structurally related in different species. Embo J *8*, 1711-1717.

Paladini, R. D., Takahashi, K., Bravo, N. S., and Coulombe, P. A. (1996). Onset of re-epithelialization after skin injury correlates with a reorganization of keratin filaments in wound edge keratinocytes: defining a potential role for keratin 16. J Cell Biol *132*, 381-397.

Palecek, S. P., Huttenlocher, A., Horwitz, A. F., and Lauffenburger, D. A. (1998). Physical and biochemical regulation of integrin release during rear detachment of migrating cells. J Cell Sci *111*, 929-940.

Palecek, S. P., Loftus, J. C., Ginsberg, M. H., Lauffenburger, D. A., and Horwitz, A. F. (1997). Integrin-ligand binding properties govern cell migration speed through cell-substratum adhesiveness. Nature *385*, 537-540.

Papkoff, J., Rubinfeld, B., Schryver, B., and Polakis, P. (1996). Wnt-1 regulates free pools of catenins and stabilizes APC-catenin complexes. Mol Cell Biol *16*, 2128-2134.

Parks, A. L., Klueg, K. M., Stout, J. R., and Muskavitch, M. A. (2000). Ligand endocytosis drives receptor dissociation and activation in the Notch pathway. Development *127*, 1373-1385.

Paroush, Z., Finley, R. L., Jr., Kidd, T., Wainwright, S. M., Ingham, P. W., Brent, R., and Ish-Horowicz, D. (1994). Groucho is required for Drosophila neurogenesis, segmentation, and sex determination and interacts directly with hairy-related bHLH proteins. Cell *79*, 805-815.

Parr, C., Watkins, G., and Jiang, W. G. (2004). The possible correlation of Notch-1 and Notch-2 with clinical outcome and tumour clinicopathological parameters in human breast cancer. Int J Mol Med *14*, 779-786.

Partanen, J., and Dumont, D. J. (1999). Functions of Tie1 and Tie2 receptor tyrosine kinases in vascular development. Curr Top Microbiol Immunol *237*, 159-172.

Pece, S., Serresi, M., Santolini, E., Capra, M., Hulleman, E., Galimberti, V., Zurrida, S., Maisonneuve, P., Viale, G., and Di Fiore, P. P. (2004). Loss of negative regulation by Numb over Notch is relevant to human breast carcinogenesis. J Cell Biol *167*, 215-221.

Pepper, M. S. (1997). Manipulating angiogenesis: From basic science to the bedside. Arterioscler Thromb Vasc Biol *17*, 605-619.

Pepper, M. S., Belin, D., Montesano, R., Orci, L., and Vassalli, J. D. (1990). Transforming growth factor-beta 1 modulates basic fibroblast growth factor-induced proteolytic and angiogenic properties of endothelial cells in vitro. J Cell Biol *111*, 743-755.

Pepper, M. S., Ferrara, N., Orci, L., and Montesano, R. (1991). Vascular endothelial growth factor (VEGF) induces plasminogen activators and plasminogen activator inhibitor-1 in microvascular endothelial cells. Biochem Biophys Res Commun *181*, 902-906.

Pepper, M. S., Ferrara, N., Orci, L., and Montesano, R. (1995). Leukemia inhibitory factor (LIF) inhibits angiogenesis in vitro. J Cell Sci *108*, 73-83.

Petcherski, A. G., and Kimble, J. (2000). LAG-3 is a putative transcriptional activator in the C. elegans Notch pathway. Nature *405*, 364-368.

Peterson, C. L., and Laniel, M. A. (2004). Histones and histone modifications. Curr Biol *14*, R546-551.

Petrova, T. V., Makinen, T., and Alitalo, K. (1999). Signaling via vascular endothelial growth factor receptors. Exp Cell Res *253*, 117-130.

Pissarra, L., Henrique, D., and Duarte, A. (2000). Expression of hes6, a new member of the Hairy/Enhancer-of-split family, in mouse development. Mech Dev *95*, 275-278.

Plotnikov, A. N., Schlessinger, J., Hubbard, S. R., and Mohammadi, M. (1999). Structural basis for FGF receptor dimerization and activation. Cell *98*, 641-650.

Plow, E. F., Haas, T. A., Zhang, L., Loftus, J., and Smith, J. W. (2000). Ligand binding to integrins. J Biol Chem *275*, 21785-21788.

Polakis, P., Hart, M., and Rubinfeld, B. (1999). Defects in the regulation of beta-catenin in colorectal cancer. Adv Exp Med Biol *470*, 23-32.

Poste, G., and Fidler, I. J. (1980). The pathogenesis of cancer metastasis. Nature *283*, 139-146.

Presente, A., Boyles, R. S., Serway, C. N., de Belle, J. S., and Andres, A. J. (2004). Notch is required for long-term memory in Drosophila. Proc Natl Acad Sci U S A *101*, 1764-1768.

Presente, A., Shaw, S., Nye, J. S., and Andres, A. J. (2002). Transgene-mediated RNA interference defines a novel role for notch in chemosensory startle behavior. Genesis *34*, 165-169.

Presta, L. G., Chen, H., O'Connor, S. J., Chisholm, V., Meng, Y. G., Krummen, L., Winkler, M., and Ferrara, N. (1997). Humanization of an anti-vascular endothelial growth factor monoclonal antibody for the therapy of solid tumors and other disorders. Cancer Res *57*, 4593-4599.

Radtke, F., and Raj, K. (2003). The role of Notch in tumorigenesis: oncogene or tumour suppressor? Nat Rev Cancer *3*, 756-767.

Ragno, M., Tournier-Lasserve, E., Fiori, M. G., Manca, A., Patrosso, M. C., Ferlini, A., Sirocchi, G., Trojano, L., Chabriat, H., and Salvi, F. (1995). An Italian kindred with cerebral autosomal dominant arteriopathy with subcortical infarcts and leukoencephalopathy (CADASIL). Ann Neurol *38*, 231-236.

Rak, J., and Kerbel, R. S. (1997). bFGF and tumor angiogenesis--back in the limelight? Nature Med *3*, 1083-1084.

Rand, M. D., Grimm, L. M., Artavanis-Tsakonas, S., Patriub, V., Blacklow, S. C., Sklar, J., and Aster, J. C. (2000). Calcium depletion dissociates and activates heterodimeric notch receptors. Mol Cell Biol *20*, 1825-1835.

Rangarajan, A., Syal, R., Selvarajah, S., Chakrabarti, O., Sarin, A., and Krishna, S. (2001a). Activated Notch1 signaling cooperates with papillomavirus oncogenes in transformation and generates resistance to apoptosis on matrix withdrawal through PKB/Akt. Virology *286*, 23-30.

Rangarajan, A., Talora, C., Okuyama, R., Nicolas, M., Mammucari, C., Oh, H., Aster, J. C., Krishna, S., Metzger, D., Chambon, P., *et al.* (2001b). Notch signaling is a direct determinant of keratinocyte growth arrest and entry into differentiation. Embo J *20*, 3427-3436.

Rao, P. K., Dorsch, M., Chickering, T., Zheng, G., Jiang, C., Goodearl, A., Kadesch, T., and McCarthy, S. (2000). Isolation and characterization of the notch ligand delta4. Exp Cell Res *260*, 379-386.

Ray, W. J., Yao, M., Mumm, J., Schroeter, E. H., Saftig, P., Wolfe, M., Selkoe, D. J., Kopan, R., and Goate, A. M. (1999a). Cell surface presenilin-1 participates in the gamma-secretase-like proteolysis of Notch. J Biol Chem *274*, 36801-36807.

Ray, W. J., Yao, M., Nowotny, P., Mumm, J., Zhang, W., Wu, J. Y., Kopan, R., and Goate, A. M. (1999b). Evidence for a physical interaction between presenilin and Notch. Proc Natl Acad Sci U S A *96*, 3263-3268.

Rebay, I., Fehon, R. G., and Artavanis-Tsakonas, S. (1993). Specific truncations of Drosophila Notch define dominant activated and dominant negative forms of the receptor. Cell *74*, 319-329.

Rebay, I., Fleming, R. J., Fehon, R. G., Cherbas, L., Cherbas, P., and Artavanis-Tsakonas, S. (1991). Specific EGF repeats of Notch mediate interactions with Delta and Serrate: implications for Notch as a multifunctional receptor. Cell *67*, 687-699.

Relf, M., LeJeune, S., Scott, P. A., Fox, S., Smith, K., Leek, R., Moghaddam, A., Whitehouse, R., Bicknell, R., and Harris, A. L. (1997). Expression of the angiogenic factors vascular endothelial cell growth factor, acidic and basic fibroblast growth factor, tumor growth factor beta-1, platelet-derived endothelial cell growth factor, placenta growth factor, and pleiotrophin in human primary breast cancer and its relation to angiogenesis. Cancer Res *57*, 963-969.

Reynolds, A. B., Daniel, J., McCrea, P. D., Wheelock, M. J., Wu, J., and Zhang, Z. (1994). Identification of a new catenin: the tyrosine kinase substrate p120cas associates with E-cadherin complexes. Mol Cell Biol *14*, 8333-8342.

Risau, W. (1997). Mechanisms of angiogenesis. Nature *386*, 671-674.

Risau, W., and Flamme, I. (1995). Vasculogenesis. Annu Rev Cell Dev Biol *11*, 73-91.

Risau, W., and Lemmon, V. (1988). Changes in the vascular extracellular matrix during embryonic vasculogenesis and angiogenesis. Dev Biol *125*, 441-450.

Robbins, J., Blondel, B. J., Gallahan, D., and Callahan, R. (1992). Mouse mammary tumor gene int-3: a member of the notch gene family transforms mammary epithelial cells. J Virol *66*, 2594-2599.

Robey, E., Chang, D., Itano, A., Cado, D., Alexander, H., Lans, D., Weinmaster, G., and Salmon, P. (1996). An activated form of Notch influences the choice between CD4 and CD8 T cell lineages. Cell *87*, 483-492.

Roehl, H., Bosenberg, M., Blelloch, R., and Kimble, J. (1996). Roles of the RAM and ANK domains in signaling by the C. elegans GLP-1 receptor. Embo J *15*, 7002-7012.

Rogers, S., Wells, R., and Rechsteiner, M. (1986). Amino acid sequences common to rapidly degraded proteins: the PEST hypothesis. Science *234*, 364-368.

Ronchini, C., and Capobianco, A. J. (2001). Induction of cyclin D1 transcription and CDK2 activity by Notch(ic): implication for cell cycle disruption in transformation by Notch(ic). Mol Cell Biol *21*, 5925-5934.

Roose, J., Huls, G., van Beest, M., Moerer, P., van der Horn, K., Goldschmeding, R., Logtenberg, T., and Clevers, H. (1999). Synergy between tumor suppressor APC and the beta-catenin-Tcf4 target Tcf1. Science *285*, 1923-1926.

Ropke, A., Kujat, A., Graber, M., Giannakudis, J., and Hansmann, I. (2003). Identification of 36 novel Jagged1 (JAG1) mutations in patients with Alagille syndrome. Hum Mutat *21*, 100.

Roylance, R., Gorman, P., Harris, W., Liebmann, R., Barnes, D., Hanby, A., and Sheer, D. (1999). Comparative genomic hybridization of breast tumors stratified by histological grade reveals new insights into the biological progression of breast cancer. Cancer Res *59*, 1433-1436.

Rubinfeld, B., Albert, I., Porfiri, E., Fiol, C., Munemitsu, S., and Polakis, P. (1996). Binding of GSK3beta to the APC-beta-catenin complex and regulation of complex assembly. Science *272*, 1023-1026.

Ruchoux, M. M., Brulin, P., Brillault, J., Dehouck, M. P., Cecchelli, R., and Bataillard, M. (2002). Lessons from CADASIL. Ann N Y Acad Sci *977*, 224-231.

Ruoslahti, E., and Engvall, E. (1997). Integrins and vascular extracellular matrix assembly. J Clin Invest *99*, 1149-1152.

Ruoslahti, E., and Pierschbacher, M. D. (1987). New perspectives in cell adhesion: RGD and integrins. Science *238*, 491-497.

Saiki, I., Murata, J., Iida, J., Sakurai, T., Nishi, N., Matsuno, K., and Azuma, I. (1989). Antimetastatic effects of synthetic polypeptides containing repeated structures of the cell adhesive Arg-Gly-Asp (RGD) and Tyr-Ile-Gly-Ser-Arg (YIGSR) sequences. Br J Cancer *60*, 722-728.

Sakamoto, K., Ohara, O., Takagi, M., Takeda, S., and Katsube, K. (2002). Intracellular cell-autonomous association of Notch and its ligands: a novel mechanism of Notch signal modification. Dev Biol *241*, 313-326.

Sanchez-Mateos, P., Cabanas, C., and Sanchez-Madrid, F. (1996). Regulation of integrin function. Semin Cancer Biol *7*, 99-109.

Sanson, B., White, P., and Vincent, J. P. (1996). Uncoupling cadherin-based adhesion from wingless signalling in Drosophila. Nature *383*, 627-630.

Santagata, S., Demichelis, F., Riva, A., Varambally, S., Hofer, M. D., Kutok, J. L., Kim, R., Tang, J., Montie, J. E., Chinnaiyan, A. M., *et al.* (2004). JAGGED1 expression is associated with prostate cancer metastasis and recurrence. Cancer Res *64*, 6854-6857.

Sarrio, D., Moreno-Bueno, G., Hardisson, D., Sanchez-Estevez, C., Guo, M., Herman, J. G., Gamallo, C., Esteller, M., and Palacios, J. (2003). Epigenetic and genetic alterations of APC and CDH1 genes in lobular breast cancer: relationships with abnormal E-cadherin and catenin expression and microsatellite instability. Int J Cancer *106*, 208-215.

Sarrio, D., Perez-Mies, B., Hardisson, D., Moreno-Bueno, G., Suarez, A., Cano, A., Martin-Perez, J., Gamallo, C., and Palacios, J. (2004). Cytoplasmic localization of p120ctn and E-cadherin loss characterize lobular breast carcinoma from preinvasive to metastatic lesions. Oncogene *23*, 3272-3283.

Sasai, Y., Kageyama, R., Tagawa, Y., Shigemoto, R., and Nakanishi, S. (1992). Two mammalian helix-loop-helix factors structurally related to Drosophila hairy and Enhancer of split. Genes Dev *6*, 2620-2634.

Sasaki, C. Y., Lin, H., Morin, P. J., and Longo, D. L. (2000). Truncation of the extracellular region abrogrates cell contact but retains the growth-suppressive activity of E-cadherin. Cancer Res *60*, 7057-7065.

Savagner, P. (2001). Leaving the neighborhood: molecular mechanisms involved during epithelial-mesenchymal transition. Bioessays *23*, 912-923.

Saxena, M. T., Schroeter, E. H., Mumm, J. S., and Kopan, R. (2001). Murine notch homologs (N1-4) undergo presenilin-dependent proteolysis. J Biol Chem *276*, 40268-40273.

Schroeter, E. H., Kisslinger, J. A., and Kopan, R. (1998). Notch-1 signalling requires ligand-induced proteolytic release of intracellular domain. Nature *393*, 382-386.

Sehested, M., and Hou-Jensen, K. (1981). Factor VIII related antigen as an endothelial cell marker in benign and malignant diseases. Virchows Arch A Pathol Anat Histol *391*, 217-225.

Senger, D. R., Claffey, K. P., Benes, J. E., Perruzzi, C. A., Sergiou, A. P., and Detmar, M. (1997). Angiogenesis promoted by vascular endothelial growth factor: regulation through alpha1beta1 and alpha2beta1 integrins. Proc Natl Acad Sci U S A *94*, 13612-13617.

Senger, D. R., Galli, S. J., Dvorak, A. M., Perruzzi, C. A., Harvey, V. S., and Dvorak, H. F. (1983). Tumor cells secrete a vascular permeability factor that promotes accumulation of ascites fluid. Science *219*, 983-985.

Seugnet, L., Simpson, P., and Haenlin, M. (1997). Requirement for dynamin during Notch signaling in Drosophila neurogenesis. Dev Biol *192*, 585-598.

Shalaby, F., Rossant, J., Yamaguchi, T. P., Gertsenstein, M., Wu, X. F., Breitman, M. L., and Schuh, A. C. (1995). Failure of blood-island formation and vasculogenesis in Flk-1-deficient mice. Nature *376*, 62-66.

Shattil, S. J., Kashiwagi, H., and Pampori, N. (1998). Integrin signaling: the platelet paradigm. Blood *91*, 2645-2657.

Shawber, C., Boulter, J., Lindsell, C. E., and Weinmaster, G. (1996). Jagged2: a serrate-like gene expressed during rat embryogenesis. Dev Biol *180*, 370-376.

Shelly, L. L., Fuchs, C., and Miele, L. (1999). Notch-1 inhibits apoptosis in murine erythroleukemia cells and is necessary for differentiation induced by hybrid polar compounds. J Cell Biochem *73*, 164-175.

Shen, J., Bronson, R. T., Chen, D. F., Xia, W., Selkoe, D. J., and Tonegawa, S. (1997). Skeletal and CNS defects in Presenilin-1-deficient mice. Cell *89*, 629-639.

Sheppard, D. (2000). In vivo functions of integrins: lessons from null mutations in mice. Matrix Biol *19*, 203-209.

Shimizu, K., Chiba, S., Kumano, K., Hosoya, N., Takahashi, T., Kanda, Y., Hamada, Y., Yazaki, Y., and Hirai, H. (1999). Mouse jagged1 physically interacts with notch2 and other notch receptors. Assessment by quantitative methods. J Biol Chem *274*, 32961-32969.

Shing, Y., Folkman, J., Sullivan, R., Butterfield, C., Murray, J., and Klagsbrun, M. (1984). Heparin affinity: purification of a tumor-derived capillary endothelial cell growth factor. Science *223*, 1296-1299.

Shirakata, Y., Shuman, J. D., and Coligan, J. E. (1996). Purification of a novel MHC class I element binding activity from thymus nuclear extracts reveals that thymic RBP-Jkappa/CBF1 binds to NF-kappaB-like elements. J Immunol *156*, 4672-4679.

Shirayoshi, Y., Yuasa, Y., Suzuki, T., Sugaya, K., Kawase, E., Ikemura, T., and Nakatsuji, N. (1997). Proto-oncogene of int-3, a mouse Notch homologue, is expressed in endothelial cells during early embryogenesis. Genes Cells *2*, 213-224.

Shou, J., Ross, S., Koeppen, H., de Sauvage, F. J., and Gao, W. Q. (2001). Dynamics of notch expression during murine prostate development and tumorigenesis. Cancer Res *61*, 7291-7297.

Shutter, J. R., Scully, S., Fan, W., Richards, W. G., Kitajewski, J., Deblandre, G. A., Kintner, C. R., and Stark, K. L. (2000). Dll4, a novel Notch ligand expressed in arterial endothelium. Genes Dev *14*, 1313-1318.

Sledge, G. W., Jr., Qulali, M., Goulet, R., Bone, E. A., and Fife, R. (1995). Effect of matrix metalloproteinase inhibitor batimastat on breast cancer regrowth and metastasis in athymic mice. J Natl Cancer Inst *87*, 1546-1550.

Small, D., Kovalenko, D., Kacer, D., Liaw, L., Landriscina, M., Di Serio, C., Prudovsky, I., and Maciag, T. (2001). Soluble Jagged 1 represses the function of its transmembrane form to induce the formation of the Src-dependent chord-like phenotype. J Biol Chem *276*, 32022-32030.

Smith, G. H., Gallahan, D., Diella, F., Jhappan, C., Merlino, G., and Callahan, R. (1995). Constitutive expression of a truncated INT3 gene in mouse mammary epithelium impairs differentiation and functional development. Cell Growth Differ *6*, 563-577.

Smithers, L., Haddon, C., Jiang, Y. J., and Lewis, J. (2000). Sequence and embryonic expression of deltaC in the zebrafish. Mech Dev *90*, 119-123.

Sonnenberg, A., Calafat, J., Janssen, H., Daams, H., van der Raaij-Helmer, L. M., Falcioni, R., Kennel, S. J., Aplin, J. D., Baker, J., Loizidou, M., and et al. (1991). Integrin alpha 6/beta 4 complex is located in hemidesmosomes, suggesting a major role in epidermal cell-basement membrane adhesion. J Cell Biol *113*, 907-917.

Soriano, J. V., Uyttendaele, H., Kitajewski, J., and Montesano, R. (2000). Expression of an activated Notch4(int-3) oncoprotein disrupts morphogenesis and induces an invasive phenotype in mammary epithelial cells in vitro. Int J Cancer *86*, 652-659.

Spinner, N. B., Colliton, R. P., Crosnier, C., Krantz, I. D., Hadchouel, M., and Meunier-Rotival, M. (2001). Jagged1 mutations in alagille syndrome. Hum Mutat *17*, 18-33.

Sporn, M. B. (1996). The war on cancer. Lancet *347*, 1377-1381.

Sriuranpong, V., Borges, M. W., Ravi, R. K., Arnold, D. R., Nelkin, B. D., Baylin, S. B., and Ball, D. W. (2001). Notch signaling induces cell cycle arrest in small cell lung cancer cells. Cancer Res *61*, 3200-3205.

St Croix, B., Florenes, V. A., Rak, J. W., Flanagan, M., Bhattacharya, N., Slingerland, J. M., and Kerbel, R. S. (1996). Impact of the cyclin-dependent kinase inhibitor p27Kip1 on resistance of tumor cells to anticancer agents. Nat Med *2*, 1204-1210.

St Croix, B., and Kerbel, R. S. (1997). Cell adhesion and drug resistance in cancer. Curr Opin Oncol *9*, 549-556.

St Croix, B., Sheehan, C., Rak, J. W., Florenes, V. A., Slingerland, J. M., and Kerbel, R. S. (1998). E-Cadherin-dependent growth suppression is mediated by the cyclin-dependent kinase inhibitor p27(KIP1). J Cell Biol *142*, 557-571.

Steidl, C., Leimeister, C., Klamt, B., Maier, M., Nanda, I., Dixon, M., Clarke, R., Schmid, M., and Gessler, M. (2000). Characterization of the human and mouse HEY1, HEY2, and HEYL genes: cloning, mapping, and mutation screening of a new bHLH gene family. Genomics *66*, 195-203.

Steiner, R. (1992). Angiostatic activity of anticancer agents in the chick embryo chorioallantoic membrane (CHE-CAM) assay. Exs *61*, 449-454.

Stetler-Stevenson, W. G. (1999). Matrix metalloproteinases in angiogenesis: a moving target for therapeutic intervention. J Clin Invest *103*, 1237-1241.

Stewart, M., and Hogg, N. (1996). Regulation of leukocyte integrin function: affinity vs. avidity. J Cell Biochem *61*, 554-561.

Stingl, J., Eaves, C. J., Zandieh, I., and Emerman, J. T. (2001). Characterization of bipotent mammary epithelial progenitor cells in normal adult human breast tissue. Breast Cancer Res Treat *67*, 93-109.

Stockinger, A., Eger, A., Wolf, J., Beug, H., and Foisner, R. (2001). E-cadherin regulates cell growth by modulating proliferation-dependent beta-catenin transcriptional activity. J Cell Biol *154*, 1185-1196.

Stromblad, S., Becker, J. C., Yebra, M., Brooks, P. C., and Cheresh, D. A. (1996). Suppression of p53 activity and p21WAF1/CIP1 expression by vascular cell integrin alphaVbeta3 during angiogenesis. J Clin Invest *98*, 426-433.

Stuiver, I., and O'Toole, T. E. (1995). Regulation of integrin function and cellular adhesion. Stem Cells *13*, 250-262.

Sun, X., and Artavanis-Tsakonas, S. (1996). The intracellular deletions of Delta and Serrate define dominant negative forms of the Drosophila Notch ligands. Development *122*, 2465-2474.

Sunderkotter, C., Steinbrink, K., Goebeler, M., Bhardwaj, R., and Sorg, C. (1994). Macrophages and angiogenesis. J Leukoc Biol *55*, 410-422.

Sutherland, E., Coe, L., and Raleigh, E. A. (1992). McrBC: a multisubunit GTP-dependent restriction endonuclease. J Mol Biol *225*, 327-348.

Taichman, D. B., Loomes, K. M., Schachtner, S. K., Guttentag, S., Vu, C., Williams, P., Oakey, R. J., and Baldwin, H. S. (2002). Notch1 and Jagged1 expression by the developing pulmonary vasculature. Dev Dyn *225*, 166-175.

Tait, L., Soule, H. D., and Russo, J. (1990). Ultrastructural and immunocytochemical characterization of an immortalized human breast epithelial cell line, MCF-10. Cancer Res *50*, 6087-6094.

Takada, Y., and Puzon, W. (1993). Identification of a regulatory region of integrin beta 1 subunit using activating and inhibiting antibodies. J Biol Chem *268*, 17597-17601.

Takata, T., and Ishikawa, F. (2003). Human Sir2-related protein SIRT1 associates with the bHLH repressors HES1 and HEY2 and is involved in HES1- and HEY2-mediated transcriptional repression. Biochem Biophys Res Commun *301*, 250-257.

Takebayashi, K., Sasai, Y., Sakai, Y., Watanabe, T., Nakanishi, S., and Kageyama, R. (1994). Structure, chromosomal locus, and promoter analysis of the gene encoding the mouse helix-loop-helix factor HES-1. Negative autoregulation through the multiple N box elements. J Biol Chem *269*, 5150-5156.

Takeichi, M. (1990). Cadherins: a molecular family important in selective cell-cell adhesion. Annu Rev Biochem *59*, 237-252.

Takeichi, M. (1991). Cadherin cell adhesion receptors as a morphogenetic regulator. Science *251*, 1451-1455.

Talora, C., Sgroi, D. C., Crum, C. P., and Dotto, G. P. (2002). Specific down-modulation of Notch1 signaling in cervical cancer cells is required for sustained HPV-E6/E7 expression and late steps of malignant transformation. Genes Dev *16*, 2252-2263.

Tamura, K., Taniguchi, Y., Minoguchi, S., Sakai, T., Tun, T., Furukawa, T., and Honjo, T. (1995). Physical interaction between a novel domain of the receptor Notch and the transcription factor RBP-J kappa/Su(H). Curr Biol *5*, 1416-1423.

Tan, C., Costello, P., Sanghera, J., Dominguez, D., Baulida, J., de Herreros, A. G., and Dedhar, S. (2001). Inhibition of integrin linked kinase (ILK) suppresses beta-catenin-Lef/Tcf-dependent transcription and expression of the E-cadherin repressor, snail, in APC-/- human colon carcinoma cells. Oncogene *20*, 133-140.

Tang, Z., and Kadesch, T. (2001). Identification of a novel activation domain in the Notch-responsive transcription factor CSL. Nucleic Acids Res *29*, 2284-2291.

Tani, S., Kurooka, H., Aoki, T., Hashimoto, N., and Honjo, T. (2001). The N- and C-terminal regions of RBP-J interact with the ankyrin repeats of Notch1 RAMIC to activate transcription. Nucleic Acids Res *29*, 1373-1380.

Taniguchi, Y., Furukawa, T., Tun, T., Han, H., and Honjo, T. (1998). LIM protein KyoT2 negatively regulates transcription by association with the RBP-J DNA-binding protein. Mol Cell Biol *18*, 644-654.

Tax, F. E., Yeargers, J. J., and Thomas, J. H. (1994). Sequence of C. elegans lag-2 reveals a cell-signalling domain shared with Delta and Serrate of Drosophila. Nature *368*, 150-154.

Tedder, T. F., Steeber, D. A., Chen, A., and Engel, P. (1995). The selectins: vascular adhesion molecules. Faseb J *9*, 866-873.

Tee, D., and DiStefano, J., 3rd (2004). Simulation of tumor-induced angiogenesis and its response to anti-angiogenic drug treatment: mode of drug delivery and clearance rate dependencies. J Cancer Res Clin Oncol *130*, 15-24.

Thiery, J. P. (2002). Epithelial-mesenchymal transitions in tumour progression. Nat Rev Cancer *2*, 442-454.

Thoreson, M. A., Anastasiadis, P. Z., Daniel, J. M., Ireton, R. C., Wheelock, M. J., Johnson, K. R., Hummingbird, D. K., and Reynolds, A. B. (2000). Selective uncoupling of p120(ctn) from E-cadherin disrupts strong adhesion. J Cell Biol *148*, 189-202.

Timmerman, L. A., Grego-Bessa, J., Raya, A., Bertran, E., Perez-Pomares, J. M., Diez, J., Aranda, S., Palomo, S., McCormick, F., Izpisua-Belmonte, J. C., and de la Pompa, J. L. (2004). Notch promotes epithelial-mesenchymal transition during cardiac development and oncogenic transformation. Genes Dev *18*, 99-115.

Tournier-Lasserve, E., Joutel, A., Melki, J., Weissenbach, J., Lathrop, G. M., Chabriat, H., Mas, J. L., Cabanis, E. A., Baudrimont, M., Maciazek, J., and et al. (1993). Cerebral autosomal dominant arteriopathy with subcortical infarcts and leukoencephalopathy maps to chromosome 19q12. Nat Genet *3*, 256-259.

Tozer, E. C., Hughes, P. E., and Loftus, J. C. (1996). Ligand binding and affinity modulation of integrins. Biochem Cell Biol *74*, 785-798.

Tun, T., Hamaguchi, Y., Matsunami, N., Furukawa, T., Honjo, T., and Kawaichi, M. (1994). Recognition sequence of a highly conserved DNA binding protein RBP-J kappa. Nucleic Acids Res *22*, 965-971.

Turnpenny, P. D., Whittock, N., Duncan, J., Dunwoodie, S., Kusumi, K., and Ellard, S. (2003). Novel mutations in DLL3, a somitogenesis gene encoding a ligand for the Notch signalling pathway, cause a consistent pattern of abnormal vertebral segmentation in spondylocostal dysostosis. J Med Genet *40*, 333-339.

Uyttendaele, H., Closson, V., Wu, G., Roux, F., Weinmaster, G., and Kitajewski, J. (2000). Notch4 and Jagged-1 induce microvessel differentiation of rat brain endothelial cells. Microvasc Res *60*, 91-103.

Uyttendaele, H., Ho, J., Rossant, J., and Kitajewski, J. (2001). Vascular patterning defects associated with expression of activated Notch4 in embryonic endothelium. Proc Natl Acad Sci U S A *98*, 5643-5648.

Uyttendaele, H., Marazzi, G., Wu, G., Yan, Q., Sassoon, D., and Kitajewski, J. (1996). Notch4/int-3, a mammary proto-oncogene, is an endothelial cell-specific mammalian Notch gene. Development *122*, 2251-2259.

Vacca, A., Iurlaro, M., Ribatti, D., Minischetti, M., Nico, B., Ria, R., Pellegrino, A., and Dammacco, F. (1999). Antiangiogenesis is produced by nontoxic doses of vinblastine. Blood *94*, 4143-4155.

van de Wetering, M., Barker, N., Harkes, I. C., van der Heyden, M., Dijk, N. J., Hollestelle, A., Klijn, J. G., Clevers, H., and Schutte, M. (2001). Mutant E-cadherin breast cancer cells do not display constitutive Wnt signaling. Cancer Res *61*, 278-284.

van de Wetering, M., Cavallo, R., Dooijes, D., van Beest, M., van Es, J., Loureiro, J., Ypma, A., Hursh, D., Jones, T., Bejsovec, A., *et al.* (1997). Armadillo coactivates transcription driven by the product of the Drosophila segment polarity gene dTCF. Cell *88*, 789-799.

Varner, J. A., Brooks, P. C., and Cheresh, D. A. (1995). REVIEW: the integrin alpha V beta 3: angiogenesis and apoptosis. Cell Adhes Commun *3*, 367-374.

Vaupel, P., Kallinowski, F., and Okunieff, P. (1989). Blood flow, oxygen and nutrient supply, and metabolic microenvironment of human tumors: a review. Cancer Res *49*, 6449-6465.

Vercauteren, S. M., and Sutherland, H. J. (2004). Constitutively active Notch4 promotes early human hematopoietic progenitor cell maintenance while inhibiting differentiation and causes lymphoid abnormalities in vivo. Blood *104*, 2315-2322.

Vesely, J. (1985). Mode of action and effects of 5-azacytidine and of its derivatives in eukaryotic cells. Pharmacol Ther *28*, 227-235.

Vijayan, K. V., Liu, Y., Li, T. T., and Bray, P. F. (2004). Protein phosphatase 1 associates with the integrin alphaIIb subunit and regulates signaling. J Biol Chem *279*, 33039-33042.

Villa, N., Walker, L., Lindsell, C. E., Gasson, J., Iruela-Arispe, M. L., and Weinmaster, G. (2001). Vascular expression of Notch pathway receptors and ligands is restricted to arterial vessels. Mech Dev *108*, 161-164.

Vincent-Salomon, A., and Thiery, J. P. (2003). Host microenvironment in breast cancer development: epithelial-mesenchymal transition in breast cancer development. Breast Cancer Res *5*, 101-106.

Vinson, C. R., and Garcia, K. C. (1992). Molecular model for DNA recognition by the family of basic-helix-loop-helix-zipper proteins. New Biol *4*, 396-403.

Vlodavsky, I., Bar-Shavit, R., Ishai-Michaeli, R., Bashkin, P., and Fuks, Z. (1991). Extracellular sequestration and release of fibroblast growth factor: a regulatory mechanism? Trends Biochem Sci *16*, 268-271.

Vogel, T., Guo, N. H., Krutzsch, H. C., Blake, D. A., Hartman, J., Mendelovitz, S., Panet, A., and Roberts, D. D. (1993). Modulation of endothelial cell proliferation, adhesion, and motility by recombinant heparin-binding domain and synthetic peptides from the type I repeats of thrombospondin. J Cell Biochem *53*, 74-84.

Wang, G. L., Jiang, B. H., Rue, E. A., and Semenza, G. L. (1995). Hypoxia-inducible factor 1 is a basic-helix-loop-helix-PAS heterodimer regulated by cellular O2 tension. Proc Natl Acad Sci U S A *92*, 5510-5514.

Wang, S., and Barres, B. A. (2000). Up a notch: instructing gliogenesis. Neuron *27*, 197-200.

Wary, K. K., Mainiero, F., Isakoff, S. J., Marcantonio, E. E., and Giancotti, F. G. (1996). The adaptor protein Shc couples a class of integrins to the control of cell cycle progression. Cell *87*, 733-743.

Washburn, T., Schweighoffer, E., Gridley, T., Chang, D., Fowlkes, B. J., Cado, D., and Robey, E. (1997). Notch activity influences the alphabeta versus gammadelta T cell lineage decision. Cell *88*, 833-843.

Webb, C., and Vaunde Woulde, G. (2000). Met Gene, John Wiley & Sons).

Webb, C. P., and Vande Woude, G. F. (2000). Genes that regulate metastasis and angiogenesis. J Neurooncol *50*, 71-87.

Wei, Y., Yang, X., Liu, Q., Wilkins, J. A., and Chapman, H. A. (1999). A role for caveolin and the urokinase receptor in integrin-mediated adhesion and signaling. J Cell Biol *144*, 1285-1294.

Weidner, N., Semple, J. P., Welch, W. R., and Folkman, J. (1991). Tumor angiogenesis and metastasis--correlation in invasive breast carcinoma. N Engl J Med *324*, 1-8.

Weijzen, S., Rizzo, P., Braid, M., Vaishnav, R., Jonkheer, S. M., Zlobin, A., Osborne, B. A., Gottipati, S., Aster, J. C., Hahn, W. C., *et al.* (2002). Activation of Notch-1 signaling maintains the neoplastic phenotype in human Ras-transformed cells. Nat Med *8*, 979-986.

Weinmaster, G. (1997). The ins and outs of notch signaling. Mol Cell Neurosci *9*, 91-102.

Weinmaster, G. (2000). Notch signal transduction: a real rip and more. Curr Opin Genet Dev *10*, 363-369.

Weinmaster, G., Roberts, V. J., and Lemke, G. (1992). Notch2: a second mammalian Notch gene. Development *116*, 931-941.

Weis, S., Cui, J., Barnes, L., and Cheresh, D. (2004). Endothelial barrier disruption by VEGF-mediated Src activity potentiates tumor cell extravasation and metastasis. J Cell Biol *167*, 223-229.

Weng, A. P., Ferrando, A. A., Lee, W., Morris, J. P. t., Silverman, L. B., Sanchez-Irizarry, C., Blacklow, S. C., Look, A. T., and Aster, J. C. (2004). Activating mutations of NOTCH1 in human T cell acute lymphoblastic leukemia. Science *306*, 269-271.

Wesley, C. S., and Mok, L. P. (2003). Regulation of Notch signaling by a novel mechanism involving suppressor of hairless stability and carboxyl terminus-truncated notch. Mol Cell Biol *23*, 5581-5593.

Wesley, C. S., and Saez, L. (2000a). Analysis of notch lacking the carboxyl terminus identified in Drosophila embryos. J Cell Biol *149*, 683-696.

Wesley, C. S., and Saez, L. (2000b). Notch responds differently to Delta and Wingless in cultured Drosophila cells. J Biol Chem *275*, 9099-9101.

Wharton, K. A., Johansen, K. M., Xu, T., and Artavanis-Tsakonas, S. (1985). Nucleotide sequence from the neurogenic locus notch implies a gene product that shares homology with proteins containing EGF-like repeats. Cell *43*, 567-581.

Wheelock, M. J., and Johnson, K. R. (2003). Cadherins as modulators of cellular phenotype. Annu Rev Cell Dev Biol *19*, 207-235.

Wheelock, M. J., Soler, A. P., and Knudsen, K. A. (2001). Cadherin junctions in mammary tumors. J Mammary Gland Biol Neoplasia *6*, 275-285.

Wiedlocha, A., and Sorensen, V. (2004). Signaling, internalization, and intracellular activity of fibroblast growth factor. Curr Top Microbiol Immunol *286*, 45-79.

Wilkins, J. A., Li, A., Ni, H., Stupack, D. G., and Shen, C. (1996). Control of beta1 integrin function. Localization of stimulatory epitopes. J Biol Chem *271*, 3046-3051.

Williams, M. J., Hughes, P. E., O'Toole, T. E., and Ginsberg, M. H. (1994). The inner world of cell adhesion: integrin cytoplasmic domains. Trends Cell Biol *4*, 109-112.

Witte, L., Hicklin, D. J., Zhu, Z., Pytowski, B., Kotanides, H., Rockwell, P., and Bohlen, P. (1998). Monoclonal antibodies targeting the VEGF receptor-2 (Flk1/KDR) as an anti-angiogenic therapeutic strategy. Cancer Metastasis Rev *17*, 155-161.

Wojtowicz-Praga, S., Torri, J., Johnson, M., Steen, V., Marshall, J., Ness, E., Dickson, R., Sale, M., Rasmussen, H. S., Chiodo, T. A., and Hawkins, M. J. (1998). Phase I trial of Marimastat, a novel matrix metalloproteinase inhibitor, administered orally to patients with advanced lung cancer. J Clin Oncol *16*, 2150-2156.

Wolfe, M. S., De Los Angeles, J., Miller, D. D., Xia, W., and Selkoe, D. J. (1999a). Are presenilins intramembrane-cleaving proteases? Implications for the molecular mechanism of Alzheimer's disease. Biochemistry *38*, 11223-11230.

Wolfe, M. S., Xia, W., Ostaszewski, B. L., Diehl, T. S., Kimberly, W. T., and Selkoe, D. J. (1999b). Two transmembrane aspartates in presenilin-1 required for presenilin endoproteolysis and gamma-secretase activity. Nature *398*, 513-517.

Wong, A. S., and Gumbiner, B. M. (2003). Adhesion-independent mechanism for suppression of tumor cell invasion by E-cadherin. J Cell Biol *161*, 1191-1203.

Wong, M. K., Prudovsky, I., Vary, C., Booth, C., Liaw, L., Mousa, S., Small, D., and Maciag, T. (2000). A non-transmembrane form of Jagged-1 regulates the formation of matrix-dependent chord-like structures. Biochem Biophys Res Commun *268*, 853-859.

Wong, P. C., Zheng, H., Chen, H., Becher, M. W., Sirinathsinghji, D. J., Trumbauer, M. E., Chen, H. Y., Price, D. L., Van der Ploeg, L. H., and Sisodia, S. S. (1997). Presenilin 1 is required for Notch1 and Dll1 expression in the paraxial mesoderm. Nature *387*, 288-292.

Wu, L., Aster, J. C., Blacklow, S. C., Lake, R., Artavanis-Tsakonas, S., and Griffin, J. D. (2000). MAML1, a human homologue of Drosophila mastermind, is a transcriptional co-activator for NOTCH receptors. Nat Genet *26*, 484-489.

Wu, L., and Griffin, J. D. (2004). Modulation of Notch signaling by mastermind-like (MAML) transcriptional co-activators and their involvement in tumorigenesis. Semin Cancer Biol *14*, 348-356.

Wu, L., Sun, T., Kobayashi, K., Gao, P., and Griffin, J. D. (2002). Identification of a family of mastermind-like transcriptional coactivators for mammalian notch receptors. Mol Cell Biol *22*, 7688-7700.

Xu, X., Weinstein, M., Li, C., Naski, M., Cohen, R. I., Ornitz, D. M., Leder, P., and Deng, C. (1998). Fibroblast growth factor receptor 2 (FGFR2)-mediated reciprocal regulation loop between FGF8 and FGF10 is essential for limb induction. Development *125*, 753-765.

Xue, Y., Gao, X., Lindsell, C. E., Norton, C. R., Chang, B., Hicks, C., Gendron-Maguire, M., Rand, E. B., Weinmaster, G., and Gridley, T. (1999). Embryonic lethality and vascular defects in mice lacking the Notch ligand Jagged1. Hum Mol Genet *8*, 723-730.

Yamada, T., Takaoka, A. S., Naishiro, Y., Hayashi, R., Maruyama, K., Maesawa, C., Ochiai, A., and Hirohashi, S. (2000). Transactivation of the multidrug resistance 1 gene by T-cell factor 4/beta-catenin complex in early colorectal carcinogenesis. Cancer Res *60*, 4761-4766.

Yan, B., Heus, J., Lu, N., Nichols, R. C., Raben, N., and Plotz, P. H. (2001). Transcriptional regulation of the human acid alpha-glucosidase gene. Identification of a repressor element and its transcription factors Hes-1 and YY1. J Biol Chem *276*, 1789-1793.

Yang, J., Mani, S. A., Donaher, J. L., Ramaswamy, S., Itzykson, R. A., Come, C., Savagner, P., Gitelman, I., Richardson, A., and Weinberg, R. A. (2004). Twist, a master regulator of morphogenesis, plays an essential role in tumor metastasis. Cell *117*, 927-939.

Yasutomo, K., Doyle, C., Miele, L., Fuchs, C., and Germain, R. N. (2000). The duration of antigen receptor signalling determines CD4+ versus CD8+ T-cell lineage fate. Nature *404*, 506-510.

Zachary, I., and Gliki, G. (2001). Signaling transduction mechanisms mediating biological actions of the vascular endothelial growth factor family. Cardiovasc Res *49*, 568-581.

Zagouras, P., Stifani, S., Blaumueller, C. M., Carcangiu, M. L., and Artavanis-Tsakonas, S. (1995). Alterations in Notch signaling in neoplastic lesions of the human cervix. Proc Natl Acad Sci U S A *92*, 6414-6418.

Zavadil, J., Cermak, L., Soto-Nieves, N., and Bottinger, E. P. (2004). Integration of TGF-beta/Smad and Jagged1/Notch signalling in epithelial-to-mesenchymal transition. Embo J *23*, 1155-1165.

Zetter, B. R. (1998). Angiogenesis and tumor metastasis. Annu Rev Med *49*, 407-424.

Zheng, J. L., Shou, J., Guillemot, F., Kageyama, R., and Gao, W. Q. (2000). Hes1 is a negative regulator of inner ear hair cell differentiation. Development *127*, 4551-4560.

Zhong, T. P., Rosenberg, M., Mohideen, M. A., Weinstein, B., and Fishman, M. C. (2000). gridlock, an HLH gene required for assembly of the aorta in zebrafish. Science *287*, 1820-1824.

Zhou, S., Fujimuro, M., Hsieh, J. J., Chen, L., and Hayward, S. D. (2000a). A role for SKIP in EBNA2 activation of CBF1-repressed promoters. J Virol *74*, 1939-1947.

Zhou, S., Fujimuro, M., Hsieh, J. J., Chen, L., Miyamoto, A., Weinmaster, G., and Hayward, S. D. (2000b). SKIP, a CBF1-associated protein, interacts with the ankyrin repeat domain of NotchIC To facilitate NotchIC function. Mol Cell Biol *20*, 2400-2410.

Zhu, A. J., and Watt, F. M. (1999). beta-catenin signalling modulates proliferative potential of human epidermal keratinocytes independently of intercellular adhesion. Development *126*, 2285-2298.

Zimrin, A. B., Pepper, M.S., McMahon, G.A., Nguyen, F., Montesano, R., Maciag, T. (1996). An antisense oligonucleotide to the notch ligand jagged enhances fibroblast growth factor-induced angiogenesis in vitro. J Biol Chem *271*, 32499-32502.

Zine, A., Aubert, A., Qiu, J., Therianos, S., Guillemot, F., Kageyama, R., and de Ribaupierre, F. (2001). Hes1 and Hes5 activities are required for the normal development of the hair cells in the mammalian inner ear. J Neurosci *21*, 4712-4720.

Zine, A., and de Ribaupierre, F. (2002). Notch/Notch ligands and Math1 expression patterns in the organ of Corti of wild-type and Hes1 and Hes5 mutant mice. Hear Res *170*, 22-31.

APPENDIX

The following is a list of publications I have achieved during my Graduate School career, listed in order of publication date. For each publication, I have summarized the major findings and have indicated my contribution to the published data. Actual publications are included at the end of this thesis.

1) Leong, K. G., and Karsan, A. (2000). Signaling pathways mediated by tumor necrosis factor alpha. Histol Histopathol *15*, 1303-1325.

   - This review is a summary of the molecular mechanisms of tumor necrosis factor alpha signal transduction.
   - I wrote this review for a graduate course in signal transduction pathways.

2) Roskelley, C. D., Williams, D. E., McHardy, L. M., Leong, K. G., Troussard, A., Karsan, A., Andersen, R. J., Dedhar, S., and Roberge, M. (2001). Inhibition of tumor cell invasion and angiogenesis by motuporamines. Cancer Res *61*, 6788-6794.

   - This peer-reviewed article identifies motuporamine C as a novel inhibitor of tumor cell invasion and angiogenesis.
   - I generated the following data:
     Figure 7. Motuporamine C inhibits endothelial sprouting in vitro.
     Figure 8. Motuporamine C inhibits angiogenesis in vivo.
     Figure 9. Motuporamine C does not inhibit HUVEC proliferation or survival.

3) Leong, K. G., Hu, X., Li, L., Noseda, M., Larrivee, B., Hull, C., Hood, L., Wong, F., and Karsan, A. (2002). Activated Notch4 inhibits angiogenesis: role of beta 1-integrin activation. Mol Cell Biol *22*, 2830-2841.

   - Data in this peer-reviewed article are presented in my thesis.

4) Litwin, C., Leong, K. G., Zapf, R., Sutherland, H., Naiman, S. C., and Karsan, A. (2002). Role of the microenvironment in promoting angiogenesis in acute myeloid leukemia. Am J Hematol *70*, 22-30.

   - This peer-reviewed article highlights a role for bone marrow environmental factors in the induction of angiogenesis in acute myeloid leukemia.
   - C. Litwin and I contributed equally to the published work.
   - I generated the following data:
     Figure 5. Endothelial sprouting in vitro in response to conditioned media from bone marrow aspirates.
     Figure 6. Angiogenesis on the chick chorioallantoic membrane in response to conditioned media from bone marrow aspirates.

5) Pollet, I., Opina, C. J., Zimmerman, C., Leong, K. G., Wong, F., and Karsan, A. (2003). Bacterial lipopolysaccharide directly induces angiogenesis through TRAF6-mediated activation of NF-kappaB and c-Jun N-terminal kinase. Blood *102*, 1740-1742.

- This peer-reviewed article demonstrates a direct endothelial-stimulatory role for lipopolysaccharide (LPS) in the initiation of angiogenesis through tumor necrosis factor receptor associated factor 6 (TRAF6)-dependent signaling pathways.
- I generated the following data:
  Figure 2. Inhibition of TRAF6 signaling on the chick CAM inhibits LPS- but not FGF-2-induced angiogenesis.

This page intentionally blank

Histol Histopathol (2000) 15: 1303-1325

http://www.ehu.es/histol-histopathol

Histology and Histopathology
Cellular and Molecular Biology

Invited Review

Signaling pathways mediated by tumor necrosis factor α

K.G. Leong[1] and A. Karsan[1,2]

Departments of [1]Experimental Medicine and [2]Pathology and Laboratory Medicine, University of British Columbia, Vancouver, British Columbia, Canada

Summary. Tumor necrosis factor α (TNFα) has been shown to trigger many signaling pathways. Following oligomerization by TNFα, the receptors TNF-RI and TNF-RII associate with adapter molecules via specific protein-protein interactions. The subsequent recruitment of downstream molecules to the receptor complex enables propagation of the TNFα signal. Two cellular responses to TNFα have been well documented, the induction of cell death and the activation of gene transcription for cell survival. TNFα-induced apoptosis involves the activation of caspase cascades, which culminate in the cleavage of specific cellular substrates to effect cell death. TNFα has also been implicated in various caspase-independent cell death processes. Two transcription factors activated by TNFα are nuclear factor κB (NFκB) and activating protein 1 (AP-1). Pathways that promote the activation of these transcription factors involve signaling molecules such as kinases, phospholipases, and sphingomyelinases. In addition to increased survival (anti-apoptotic) gene expression, NFκB and AP-1 also induce the expression of genes involved in inflammation, cell growth, and signal regulation. The past decade has witnessed the identification of numerous signaling intermediates implicated in TNFα cellular responses. This article reviews the molecular mechanisms of TNFα signal transduction. In particular, pathways involved in cell death and transcription factor activation are discussed.

Key words: Tumor necrosis factor, Signal transduction, Apoptosis, NFκB, AP-1

Abbreviations

AIF: apoptosis inducing factor; AP-1: activating protein 1; ASK1: apoptosis signal-regulating kinase 1; ASMase: acidic sphingomyelinase; CARD: caspase activating recruitment domain; CARDIAK: CARD containing ICE-associated kinase; c-IAP: cellular inhibitor of apoptosis; CLAP: CARD-like apoptotic protein; CRD: cysteine-rich domain; DED: death effector domain; ERK: extracellular signal regulated kinase; FADD: Fas associated death domain; FAN: factor associated with NSMase; GCK(R): germinal center kinase (related); ICE: interleukin-1ß converting enzyme; IRAK: interleukin-1 receptor-associated kinase; JNK: c-Jun N-terminal kinase; MAPK: mitogen activated protein kinase; NIK: NFκB-inducing kinase; NFκB: nuclear factor κB; NSD: NSMase domain; NSMase: neutral sphingomyelinase; RAIDD: RIP-associated ICH-1 homologous death domain; RIP: receptor interacting protein; SODD: silencer of death domains; TACE: TNFα converting enzyme; TANK: TRAF-associated NFκB activator; TNFα: tumor necrosis factor alpha; TNF-R: TNF receptor; TRADD: TNF receptor associated death domain; TRAF: TNF receptor associated factor

Offprint requests to: Aly Karsan, Department of Pathology and Laboratory Medicine, UBC McDonald Research Laboratories, St. Paul's Hospital, Room B292, 1081 Burrard St., Vancouver, BC. Canada V6Z 1Y6. e-mail: akarsan@mrl.ubc.ca

Introduction

The effects of tumor necrosis factor α (TNFα) have been implicated in numerous physiological and pathological conditions. Until recently, knowledge concerning the global effects of TNFα far outweighed that of its cellular effects. Over the last few years, key players involved in mediating the cellular effects of TNFα have been identified. We now know that TNFα activates cell death pathways as well as transcription factors that signal survival pathways. This review will focus on the TNFα signaling pathways that enable cell death and transcription factor activation to occur.

The role of tumor necrosis factor α in health and disease

In 1893, a New York surgeon by the name of W.B. Coley was the first to document the effects of TNFα (Orlinick and Chao, 1998), although TNFα itself had not yet been identified. In 1975, an endotoxin-induced factor isolated from macrophages was discovered (Carswell et

al., 1975). This factor was named tumor necrosis factor alpha (TNFα), because of its ability to kill tumor cells *in vitro* and to cause hemorrhagic necrosis of solid tumors *in vivo*. Concurrent with the discovery of TNFα, another macrophage-derived factor known as cachectin was identified (Beutler et al., 1985b). Cachectin is responsible for the development of cachexia, a wasting syndrome commonly associated with chronic disease states (Beutler and Cerami, 1987; Tracey and Cerami, 1993). Such diseases may include chronic parasitic infection, acquired immunodeficiency syndrome (AIDS), malaria, tuberculosis, and cancer. Cachexia is characterized by the prevention of fat storage and the suppression of muscle- and fat-specific gene expression leading to weight loss (Tracey and Cerami, 1993). Sequence comparison between TNFα and cachectin revealed the two factors to be identical (Beutler et al., 1985a). Since then, TNFα has been purified and crystallized, and its tertiary and quaternary structures characterized.

TNFα is a pleiotropic cytokine involved in a wide variety of physiological conditions. Endogenous TNFα is an important mediator of natural immunity, and has been shown to be essential for the development of a successful response to microbial infection (Echtenacher et al., 1990). Its production at sites of bacterial or viral invasion serves to recruit and activate defense mechanisms. TNFα has also been implicated in inflammatory conditions, by inducing the synthesis of proinflammatory mediators. Other diverse responses influenced by TNFα include cell proliferation and differentiation (Heller and Kronke, 1994), cell death (Kerr et al., 1972; Famularo et al., 1994; Ware et al., 1996), neuroprotection (Cheng et al., 1994), and neurotransmission (Tancredi et al., 1992).

The strength and duration of TNFα expression greatly influences the effect of this cytokine. When produced inappropriately, pathological conditions may ensue. The development of septic shock (Kramer et al., 1995) and autoimmune diseases such as rheumatoid arthritis (Elliott et al., 1994; Feldmann et al., 1995; Taupin et al., 1997) have been correlated with high systemic levels of TNFα. In addition, sustained activation of TNFα is associated with multiple organ failure (Landow and Andersen, 1994), multiple sclerosis (Selmaj et al., 1991; Raine, 1995), cardiac dysfunction (Meldrum, 1998), atherosclerosis (Rus et al., 1991), ischemia-reperfusion injury (Meldrum and Donnahoo, 1999), insulin resistance (Hotamisligil et al., 1995; Peraldi and Spiegelman, 1998), and inflammatory bowel diseases (Brynskov et al., 1994). Unraveling the molecular mechanisms of TNFα action may contribute to the development of novel and effective therapies for treatment of TNFα-related diseases.

The TNF ligand family

TNFα is the prototypical member of a large family of ligands designated the TNF ligand family. The original family consisted of two members: the macrophage-derived TNFα and the T lymphocyte-derived LT-α (lymphotoxin-α/TNFß). Additional members have since been added to the family. These include FasL/CD95L, CD40L, CD27L, CD30L, LT-ß, OX40L, 4-1BBL, Apo2L/TRAIL, Apo3L/TWEAK, RANKL/TRANCE/ODF/OPGL, and GITRL (Smith and Ross, 1993; Armitage, 1994; Gruss and Dower, 1995; Nocentini et al., 1997; Gurney et al., 1999; Takahashi et al., 1999). With the exception of LT-α, all of the other family members are type II membrane proteins. Characteristics include a C-terminal extracellular domain, a single transmembrane domain, followed by a short N-terminal cytoplasmic domain. All members share 20-25% homology in a 150 amino acid stretch in the extracellular domain, required for binding to their cognate receptors (reviewed in Baker and Reddy, 1996; Orlinick and Chao, 1998).

The human genome contains a single copy of the TNFα gene, located within the major histocompatibility complex (MHC) locus on chromosome six (Nedwin et al., 1985a; Browning et al., 1993). In addition to macrophages/monocytes, TNFα is also produced by lymphocytes, mast cells, fibroblasts, and hepatocytes (Vassalli, 1992; Vandenabeele et al., 1995; Wallach, 1997; Zhang et al., 1997; Yan et al., 1999). Secretion from macrophages usually occurs in response to an inflammatory stimulus such as lipopolysaccharide (LPS) (Pauli, 1994). Activation of antigen receptors on T lymphocytes can induce TNFα production, whereas aggregation of high-affinity IgE receptors on mast cells is sufficient to trigger cytokine secretion (Zhang et al., 1997). The fact that activated mast cells secrete TNFα implicates TNFα as a major player in immediate inflammatory responses (Thomas et al., 1996). Production of TNFα can occur within 2 to 3 hours post induction, with maximum synthesis achieved after 48 hours (Nedwin et al., 1985b). The rate of production has been shown to increase by a factor of several thousand in macrophages activated by LPS (Bazzoni and Beutler, 1996). Enhanced TNFα synthesis functions as a distress signal both in an autocrine and paracrine fashion, triggering protective mechanisms designed to cope with infection.

TNFα is initially produced as a 26 kDa membrane-bound proform (proTNFα) (Perez et al., 1990). The extracellular domain of proTNFα contains a membrane-proximal metalloprotease cleavage site (Blobel, 1997). Specifically, a metalloprotease of the disintegrin family named TACE (TNFα converting enzyme, also known as ADAM-17) is responsible for cleaving proTNFα to the 17 kDa soluble TNFα form (Black et al., 1997; Moss et al., 1997). Both forms of TNFα are active and capable of binding to their cellular receptors, although distinct roles have been demonstrated for the individual forms of TNFα (Perez et al., 1990).

The TNF receptor superfamily

Members of the TNF ligand family interact with their cognate receptors, all of which belong to a group of

receptors collectively known as the TNF receptor superfamily. The criteria for classifying cell surface receptors are based on structural and mechanistic features. With respect to the TNF receptor family, all members are type I membrane proteins with their C-terminal domains located in the interior of the cell. Furthermore, all members contain highly conserved cysteine-rich domains (CRDs) in their extracellular region (Beutler and van Huffel, 1994). Although the number of CRDs within different receptors varies from two to six, each CRD contains six cysteine residues interspersed within a 40 amino acid stretch (Smith et al., 1994; Ashkenazi and Dixit, 1998). The TNF receptor superfamily consists of TNF-RI (TNF-R55, p55-TNFR, CD120a), TNF-RII (TNF-R75, p75-TNFR, CD120b), TNF-RIII (TNF-RP), Fas (Apo1), OX-40, 4-1BB, CD27, CD30, CD40, poxvirus gene products PV-T2 and PV-A53R, p75 NGFR, TRAMP (Apo3, DR3, LARD, Ws1), CAR1, TRAIL-RI (DR4), TRAIL-R2 (Apo2, DR5, KILLER, TRICK2), DR6, and RANK (Itoh and Nagata, 1993; Smith and Ross, 1993; Armitage, 1994; Gruss and Dower, 1995; Brojatsch et al., 1996; Kitson et al., 1996; Pan et al., 1997a,b; Ashkenazi and Dixit, 1998). In addition, TRAIL has at least three decoy receptors, DcR1 (TRAIL-R3, TRID), DcR2 (TRAIL-R4), and DcR3 (Ashkenazi and Dixit, 1999).

TNFα interacts with two receptors, TNF-RI and TNF-RII (Loetscher et al., 1990; Nophar et al., 1990; Schall et al., 1990; Smith et al., 1990). Both receptors can be found on the surface of most cells (Vandenabeele et al., 1995), although they are expressed in different amounts. On a per cell basis, the number of TNF-RII receptors far surpasses that of TNF-RI (Fiers et al., 1995). The fact that TNF-RI expression is constitutive and non-inducible and that TNF-RII expression is inducible may account for the varying expression levels (Newton and Decicco, 1999). Another difference between these receptors involves their localization within the cell. During steady-state conditions, the majority of TNF-RI molecules are found in the perinuclear Golgi complex (Jones et al., 1999). In contrast, most TNF-RII molecules are expressed on the cell surface. TNF-RI and TNF-RII molecules localized to the cell membrane exist as glycoproteins. Their extracellular domains contain four CRDs, all of which are essential for efficient ligand binding (Marsters et al., 1992). Both receptors contain a single transmembrane domain, but there is no homology evident in their cytoplasmic domains (Tartaglia and Goeddel, 1992). In addition, neither TNF-RI nor TNF-RII contains intrinsic tyrosine or serine/threonine kinase domains. Differences between their cytoplasmic domains account for the different signaling pathways initiated by the two receptors.

Ligand-receptor interactions

Membrane-bound and soluble forms of TNFα are both capable of forming homotrimers, due to the presence of a ß-sheet sandwich structural motif within each monomer (Browning et al., 1993). Only trimeric TNFα can interact with TNF-RI and TNF-RII receptors. The interfaces between the TNFα subunits comprising the trimer are required for receptor binding (Banner et al., 1993). With respect to both receptors, structural studies have demonstrated a role for the CRDs present in the extracellular domain for ligand binding (Beutler and van Huffel, 1994). Trimerization of either TNF-RI or TNF-RII by trimeric TNFα triggers a cellular response.

TNF-RI and TNF-RII have similar affinities for soluble TNFα (Grell et al., 1995). Dissociation rates, however, vary between the two receptors. TNFα bound to TNF-RII has a fast off rate relative to TNFα bound to TNF-RI (Tartaglia et al., 1993b). Because concentrations of TNFα in normal physiological conditions are low (Adolf et al., 1994), TNFα should favor the activation of TNF-RI. This may explain why TNF-RI is involved in a majority of the actions mediated by TNFα. Membrane-bound TNFα, on the other hand, exhibits a greater affinity for TNF-RII (Grell, 1995; Grell et al., 1995). Therefore, TNF-RII may be important during local inflammatory reactions that involve intercellular contacts.

Binding of TNFα to either TNF-RI or TNF-RII has been shown to induce shedding of the receptor extracellular domain. A cleavage site has been localized to a small region flanked by the CRD and transmembrane domains (Brakebusch et al., 1994). Shedding represents a mechanism for regulating the surface expression of both receptors. A second regulatory mechanism is also established upon receptor cleavage. Because the soluble forms of the receptors retain their ability to bind TNFα (Gatanaga et al., 1990), the shed extracellular domains function as inhibitors of TNFα and downregulate the bioavailability of the cytokine (Van Zee et al., 1992; van der Poll et al., 1995; Aderka, 1996). Binding of TNFα to either receptor can also lead to internalization of the TNFα-receptor complex, followed by subsequent degradation of the ligand (Tsujimoto et al., 1985; Boldin et al., 1995a; Bradley et al., 1995). Hence the ability of TNFα to bind to receptor and initiate intracellular signaling mechanisms is strictly regulated.

Signal transduction by TNFα

Numerous signaling pathways have been characterized for TNFα in multiple subcellular compartments, which include the plasma membrane, cytosol, endosomes, mitochondria, and nucleus. Among the many diverse cellular effects of TNFα, two effects have garnered the most attention: (1) the initiation of cell death, and (2) the activation of transcription factors leading to the expression of genes, some of which promote cell survival.

Cell death pathways activated by TNFα

The demise of a cell can occur by two mechanisms: necrosis and/or apoptosis. TNFα can elicit both

mechanisms of cell death. The specific death pathway activated by TNFα in a cell is dependent on such variables as cell type, TNFα dosage, and the local microenvironment. Necrosis occurs when a cell is subjected to overwhelming external injury, either from physical stress or toxic agents (Kerr et al., 1972; Majno and Joris, 1995). Necrotic cell death involves activation of the complement system or stimulation of granule release from cytotoxic T lymphocytes. In both situations, the integrity of the target cell lipid bilayer is challenged. An osmotic imbalance is created that leads to cell swelling, followed by a sudden collapse of the cell (Grooten et al., 1993). Cellular contents are then released into the cell surroundings. Apoptosis is a form of programmed cell death where the cell actively participates in its own destruction. Apoptotic death plays an important role in the regulation of development and growth (Tomei and Cope, 1994), as well as the elimination of unwanted cells (Hebert et al., 1996; Jacobson et al., 1997). Characteristics of apoptosis include chromatin condensation, DNA degradation into oligonucleosomal fragments, and membrane blebbing (Duvall and Wyllie, 1986). An important difference between apoptosis and necrosis is the confinement of cellular contents within membrane-bound particles during apoptosis. These particles can then be phagocytosed without the risk of intracellular enzyme leakage (Majno and Joris, 1995; Hart et al., 1996).

In most cell types, induction of apoptosis by TNFα cannot occur without inhibiting the expression of new genes (Itoh and Nagata, 1993). This can be achieved through the addition of RNA synthesis inhibitors such as actinomycin D, or protein synthesis inhibitors such as cycloheximide. The inhibition of new gene expression is essential because TNFα has been shown to induce the expression of anti-apoptotic proteins (Karsan, 1998; Malek et al., 1998). In general, activation of the TNFα survival pathway inhibits activation of the death pathway (Natoli et al., 1998). In transformed cells or virally-infected cells, however, TNFα alone is capable of inducing cell death (Beyaert and Fiers, 1994). The increased sensitivity of these cells to TNFα may be due to the lack of a transient protective factor that renders normal cells resistant to TNFα-induced cytotoxicity.

The role of TNF-RI in apoptosis

Apoptotic signaling is primarily mediated by TNF-

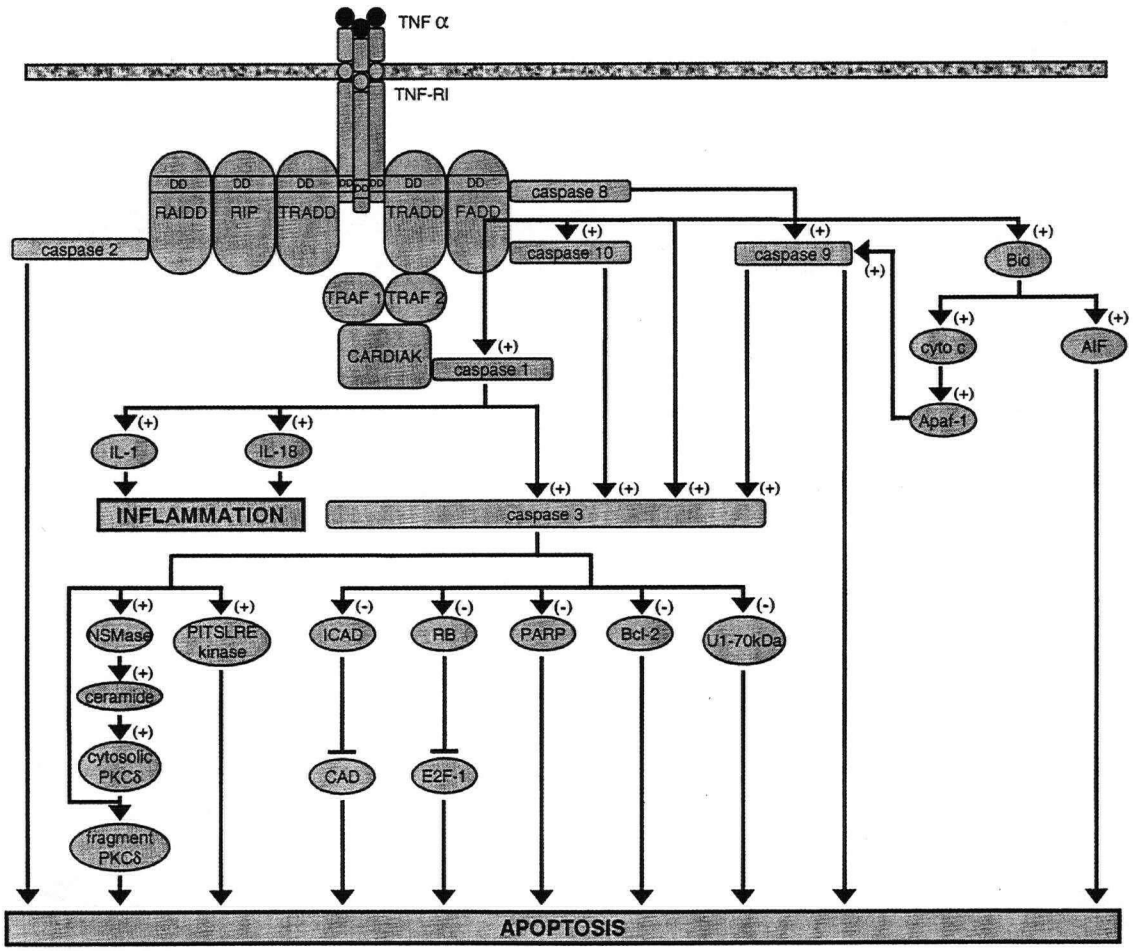

Fig. 1. Caspase activation pathways. These signal transduction pathways are specific for TNF-RI. Trimerization of TNF-RI by TNFα initiates the signaling cascade. The net effect of caspase activation is apoptotic cell death. Refer to the text for abbreviations of signaling components.

RI (Tartaglia et al., 1993c). Because TNF-RI is devoid of catalytic activity, it utilizes cellular proteins as adapter molecules for propagating the death signal. The cytoplasmic domain of TNF-RI contains a region termed the death domain, which has been shown to be essential for TNFα-induced cytotoxicity (Tartaglia et al., 1993a). The death domain folds into a series of antiparallel amphipathic α-helices with exposed charged residues, which functions as a dimerization motif (Huang et al., 1996). Associations between various death domain-containing proteins are facilitated by this motif, thus enabling propagation of the death signal within the cell. Subsequent activation of protease cascades leads to the apoptotic demise of the cell. The proteases involved belong to a family of aspartyl-directed cysteine proteases termed caspases.

The caspase activation pathways. In the basal state without bound TNFα, a protein named SODD (silencer of death domains) is associated with the death domain of TNF-RI and prevents signal transduction (Jiang et al., 1999). Upon binding trimeric TNFα, however, SODD rapidly dissociates and enables aggregation of the TNF-RI death domains to occur. A death domain-containing protein named TRADD (TNF receptor associated death domain), which exhibits high affinity for the aggregated TNF-RI death domains, is recruited to the receptor complex (Hsu et al., 1995, 1996b) (Fig. 1). TNF-RI - TRADD complexes are relatively stable. Similar to TNF-RI, TRADD is devoid of enzymatic activity and thus functions as an adapter protein. The death domain of TRADD directly interacts with the death domain of FADD (Fas associated death domain, also known as MORT1) (Boldin et al., 1995b; Chinnaiyan et al., 1995). Although TRADD-FADD complexes are stable, TNF-RI-TRADD-FADD multimeric complexes require additional proteins for stability (Hsu et al., 1996b). The C-terminal death domain of FADD does not play a role in the further propagation of the death signal; instead, an N-terminal domain termed the DED (death effector domain) is required (Boldin et al., 1995b; Chinnaiyan et al., 1995). The interaction between TRADD and FADD exposes the DED of FADD (Muzio et al., 1996).

A domain analogous to the DED, called the CARD domain (caspase activating recruitment domain), is found in the prodomain of various upstream caspases (Hofmann et al., 1997). Procaspase 8 (FLICE/MACH/Mch5) contains two DED (CARD) domains at its N-terminus (Boldin et al., 1996; Muzio et al., 1996). FADD and procaspase 8 bind through their DED (CARD) domains. Recruitment of procaspase 8 to the receptor signaling complex results in oligomerization of procaspase 8, thereby enabling activation of its mild autoproteolytic activity (Yeh et al., 1998; Zhang et al., 1998). The induced proximity of two or more procaspase 8 molecules results in the excision of the procaspase 8 prodomain (Muzio et al., 1998), followed by further cleavage to fragments of approximately 20 kDa and 10 kDa. These fragments form a dimer, and two dimers combine to form a tetramer, thus yielding an active caspase.

Active caspase 8 is capable of activating procaspase 9 (Pan et al., 1998). Processing of procaspase 9 to its active form, however, may not be a direct action of caspase 8. Instead, a signaling pathway involving the mitochondria is involved. Caspase 8 cleaves the cytosolic protein Bid, releasing a C-terminal fragment (Li et al., 1998; Luo et al., 1998). Translocation of this Bid fragment to the mitochondria causes loss of mitochondrial transmembrane potential and release of cytochrome c (Li et al., 1998). Normally, pH and electrical gradients exist across the inner mitochondrial membrane (Kroemer et al., 1997). When the inner mitochondrial membrane becomes permeable to water and solutes, however, a reduction in mitochondrial transmembrane potential occurs, which triggers the release of AIF (apoptosis inducing factor), cytochrome c, and procaspases 2, 3, and 9 (Liu et al., 1996a; Susin et al., 1996, 1999; Cai et al., 1998). AIF translocates to the nucleus to effect the degradation of DNA into large fragments (Lorenzo et al., 1999). Because Apaf-1 has a CARD domain, it is able to interact with procaspase 9 (Mch6/APAF3) in the presence of cytochrome c and dATP (Zou et al., 1997; Pan et al., 1998). The induced proximity of two or more procaspase 9 molecules causes autoactivation of procaspase 9 and subsequent cleavage to its active form (Srinivasula et al., 1998). Active caspase 9 cleaves and activates procaspase 3 (YAMA/CPP32/apopain) (Budihardjo et al., 1999). Recently, a CARD domain-containing protein named CLAP (CARD-like apoptotic protein) has been shown to function downstream of caspase 8 (Srinivasula et al., 1999). CLAP was able to activate the Apaf-1-caspase 9 pathway. Furthermore, the CARD and C-terminal domains of CLAP demonstrate low levels of proapoptotic activity. The CARD domain also exerts a dominant negative effect on TNFα-induced anti-apoptotic activity. Hence CLAP may enhance the induction of apoptosis by TNFα. In addition to the activation of procaspase 9, caspase 8 also cleaves and activates procaspase 3 (Tewari et al., 1995b), which is directly involved with the manifestation of the apoptotic phenotype (Yuan, 1997; Hirata et al., 1998; Stennicke et al., 1998). Caspase 8 may also cleave and activate procaspase 1 (ICE, interleukin-1 ß converting enzyme) (Beutler, 1999), which is required for processing proIL-1b and proIL-18 into their active forms (Schonbeck et al., 1997; Saha et al., 1999). Therefore, caspases are involved in both death and inflammatory signaling by TNFα.

In addition to interacting with procaspase 8 during downstream death signal propagation, FADD can also interact with procaspase 10 (Vincenz and Dixit, 1997). Binding is mediated by DED (CARD) domains located at the N-terminus of both proteins (Fernandes-Alnemri et al., 1996; Vincenz and Dixit, 1997). Activation of procaspase 10 occurs in a manner similar to that of procaspase 8, where receptor oligomerization leads to

the aggregation of procaspase 10 molecules, and hence autocatalytic cleavage into active caspase 10 (Fernandes-Alnemri et al., 1996; Vincenz and Dixit, 1997; Yuan, 1997; Ashkenazi and Dixit, 1998). Receptor oligomerization can also function to bring procaspase 8 and procaspase 10 into close proximity, thus facilitating the activation of these caspases by each other (Vincenz and Dixit, 1997). Active caspase 10 can activate the executioner procaspase 3 (Stennicke et al., 1998). To date, three isoforms of caspase 10 have been identified, caspase 10a (Mch4), caspase 10b (FLICE2), and the recently identified caspase 10c (Ng et al., 1999). TNFα specifically stimulates the expression of caspase 10c mRNA through an unidentified pathway. Caspase 10c is insoluble and forms filamentous structures known as DEFs (death effector filaments) (Siegel et al., 1998; Ng et al., 1999). DEFs are postulated to be involved in intracellular caspase recruitment and activation, thus effectively enhancing the apoptotic response of TNFα.

The adapter protein TRADD also recruits the death domain-containing protein RIP (receptor interacting protein) to the TNF-RI receptor signaling complex, mediated by the death domains of the two proteins (Hsu et al., 1996a). The domain structure of RIP consists of a C-terminal death domain and an N-terminal kinase domain (Stanger et al., 1995), separated by a unique intermediate domain (Hsu et al., 1996a). RIP is an active serine/threonine protein kinase (Hsu et al., 1996a). Propagation of the death signal, however, does not require kinase activity. Instead, RIP utilizes its death domain and functions as an adapter protein to recruit RAIDD (RIP-associated ICH-1 homologous death domain, also known as CRADD) to the receptor complex (Ahmad et al., 1997; Duan and Dixit, 1997). Because RAIDD possesses a DED (CARD) domain, it is able to interact with procaspase 2 (ICH-1). Subsequent activation of caspase 2 may assist in the apoptotic demise of the cell, although the direct substrates of caspase 2 have yet to be identified. A RIP-like kinase called RIP3 has been shown to interact with RIP and to activate various caspases (Yu et al., 1999). Similar to RIP, the kinase domain of RIP3 is not involved in the induction of apoptosis. RIP, in addition to playing a role in apoptosis, is also involved in TNFα-induced anti-apoptotic responses through the activation of transcription factors (Hsu et al., 1996a; Kelliher et al., 1998). Caspase 8 can cleave RIP to the cleavage product RIPc, thus effectively blocking the induction of the anti-apoptotic response (Lin et al., 1999). Furthermore, RIPc can strengthen the interaction between TRADD and FADD, thereby enhancing the cytotoxic effects of TNFα.

Finally, TRADD can recruit TRAF (TNF receptor associated factor) proteins to TNF-RI (Hsu et al., 1996b). Although TRAFs primarily participate in the activation of anti-apoptotic signals induced by TNFα, they are also involved in death signaling. Six different TRAFs (TRAF1-6) have been identified (reviewed in Arch et al., 1998). Among these, only TRAF1 and TRAF2 have been shown to be involved in apoptosis thus far (Hsu et al., 1996b). All TRAF proteins exhibit homology in a conserved C-terminal 150 amino acid region called the TRAF domain (Rothe et al., 1994). The TRAF domain itself is divided into N-terminal and C-terminal portions, TRAF-N and TRAF-C, respectively. Dimerization of TRAF proteins is mediated by the TRAF domains. Despite the ability of TRAF1 and TRAF2 to homodimerize *in vitro*, only TRAF1-TRAF2 heterodimers have been detected *in vivo*. Interaction between TRADD and TRAF1-TRAF2 heterodimers occurs via the N-terminal TRAF-binding domain of TRADD and the TRAF-C domain of TRAF2 (Hsu et al., 1996b). Downstream signaling involves association of the TRAF1-TRAF2 heterodimer with the serine/threonine kinase CARDIAK (CARD containing ICE-associated kinase, also known as RIP2/RICK) (Thome et al., 1998). Via a C-terminal DED (CARD) domain, CARDIAK can interact with a homologous domain in procaspase 1. This interaction results in the activation of procaspase 1, independent of the kinase activity of CARDIAK (McCarthy et al., 1998; Thome et al., 1998). TNFα treatment is capable of inducing apoptosis by activating procaspase 1 in the nucleus (Mao et al., 1998). This novel TNFα action has led to the identification of a nuclear localization signal within the prodomain of procaspase 1. TNFα is able to induce nuclear translocation of procaspase 1, perhaps by facilitating the removal of repressor proteins that mask the nuclear localization signal. Subsequent activation of procaspase 1 within the nucleus may lead to cleavage of nuclear death substrates (Cohen, 1997; Nicholson and Thornberry, 1997).

Execution of the apoptotic death sentence. The main executioner caspase in TNFα-induced apoptosis is caspase 3. It can cleave numerous cytoplasmic and nuclear substrates within the cell, thus manifesting the apoptotic phenotype. One such substrate is the anti-apoptotic protein Bcl-2 (Cheng et al., 1997). Cleavage of Bcl-2 into N-terminal and C-terminal products acts as a positive feedback mechanism to enhance cell death. The C-terminal Bcl-2 cleavage product acts as a proapoptotic protein. However, preventing Bcl-2 cleavage does not alter the kinetics of TNFα-induced death (Johnson and Boise, 1999). PITSLRE kinase, another substrate of caspase 3, is cleaved into its active form upon TNFα treatment (Lahti et al., 1995). The active kinase facilitates the execution of apoptosis. I-CAD is an inhibitor protein that binds to CAD (caspase-activated DNase) and sequestors CAD in the cytosol (Enari et al., 1998). Upon cleavage of I-CAD by caspase 3, CAD is able to migrate to the nucleus where it digests DNA into internucleosomal fragments, yielding the characteristic DNA laddering pattern of apoptosis (Sakahira et al., 1998). The 70 kDa component of the U1 small nuclear ribonucleoprotein (U1-70 kDa) is also cleaved by caspase 3 (Tewari et al., 1995a), which compromises the RNA splicing process. TNFα can induce RB

(retinoblastoma) protein degradation via activation of caspase 3 (Tan et al., 1997). RB is normally found in the cytosol complexed to E2F-1, a factor that can induce apoptosis when overexpressed (Shan and Lee, 1994). When cleaved by caspase 3, RB can no longer suppress the action of E2F-1, thus amplifying the death response to TNFα.

Caspase 3 is known to cleave PARP (Poly(ADP-ribose) polymerase) during TNFα-induced apoptosis (Nicholson et al., 1995; Tewari et al., 1995b). PARP is a repair enzyme that is activated in the presence of DNA damage (reviewed in D'Amours et al., 1999). During DNA repair, PARP consumes vast amounts of NAD^+, which leads to depletion of cellular ATP levels. It has been postulated that because apoptosis is a highly ATP-dependent process, insufficient ATP would shift the cell death pathway towards necrosis. Consequences would include damage to neighboring cells and the generation of inflammatory responses. To avoid such a fate, caspase 3 cleaves PARP into its inactive form and hence prevents apoptotic cells from entering necrosis.

Caspase 3 can activate neutral sphingomyelinase (NSMase), a membrane-bound enzyme involved in the generation of ceramide (Yuan, 1997). The upregulated production of ceramide induces a translocation of membrane-associated PKCδ to the cytosol (Emoto et al., 1995). Cytosolic PKCδ is susceptible to caspase 3 cleavage, thus forming a PKCδ fragment. Translocation of PKCδ to the cytosol is required for TNFα-induced apoptosis (Sawai et al., 1997).

Regulation of TNFα-induced apoptosis. A protein structurally similar to caspase 8, called c-FLIP (Casper/MRIT/FLAME/CASH), is involved in regulating the activation of caspase 8 (Goltsev et al., 1997; Han et al., 1997; Inohara et al., 1997; Irmler et al., 1997; Rasper et al., 1998). Although c-FLIP shares extensive homology with caspase 8, including the presence of a DED domain, c-FLIP is not a functional caspase because it lacks several key residues necessary for catalysis (Shu et al., 1997). c-FLIP has been reported to be anti-apoptotic as well as proapoptotic (Goltsev et al., 1997). Interactions of c-FLIP with both TRAF-2 and FADD have been demonstrated. Simultaneous binding of procaspase 8 and procaspase 3 to c-FLIP can also take place. Following recruitment to the TNF-RI receptor complex, the DED domain of c-FLIP may act in a FADD-like fashion to bind procaspase 8, thus preventing oligomerization and activation of caspase 8 by FADD (Hu et al., 1997; Shu et al., 1997; Thome et al., 1997). Another potential function of c-FLIP may be to localize procaspase 3 to the vicinity of procaspase 8, thus facilitating activation of procaspase 3 by procaspase 8 (Shu et al., 1997). Additional studies need to be performed to better determine the function of c-FLIP in apoptosis.

Several proteins belonging to the c-IAP (cellular inhibitor of apoptosis) family have been implicated in TNFα-induced apoptosis inhibition (reviewed in Clem and Duckett, 1997). c-IAP1 has been found to associate directly with the TNF-RI receptor signaling complex (Shu et al., 1996). In addition, both c-IAP1 and c-IAP2 can bind to TRAF1 and TRAF2 (Shu et al., 1996; Uren et al., 1996), as well as to CARDIAK (Inohara et al., 1998; McCarthy et al., 1998; Thome et al., 1998). The mechanism with which c-IAPs perturb the TNFα apoptotic signal may be at the level of caspase activation. Specifically, c-IAPs have been shown to directly inhibit some TNFα-activated caspases (Deveraux and Reed, 1999).

Mitochondria and cell death induction by TNFα. As mentioned previously, the propagation of the TNFα-induced apoptotic signal can involve the disruption of mitochondrial integrity, with the subsequent release of procaspases, AIF, and cytochrome c (Liu et al., 1996a; Susin et al., 1996). TNFα can also affect the mitochondria via a pathway independent of caspase 8 activation. Following treatment of susceptible cells with TNFα, the distribution of mitochondria within the target cell is modified (De Vos et al., 1998). Specifically, the mitochondria translocate from an initial dispersed pattern to a perinuclear cluster. The region of the cytoplasmic domain of TNF-RI immediately adjacent to the membrane is required for mitochondrial translocation. In an untreated cell, motor proteins called kinesins facilitate the intracellular movement of cargo along microtubules towards the cell periphery (Vale, 1987). TNF-RI with liganded TNFα sends a signal via its membrane-proximal region to inhibit kinesin function, perhaps by activating caspases (De Vos et al., 1998). Unable to direct mitochondrial movement away from the nucleus, perinuclear clustering of mitochondria occurs. The net effect of kinesin inactivity is an enhancement of cell death.

TNFα acting through TNF-RI can also induce necrotic cell death in various cell types (Vercammen et al., 1998). This process is independent of caspase activation. Instead, the mechanism may involve the delivery of exogenous TNFα directly to the mitochondria via a TNF-binding protein in the inner mitochondrial membrane (Ledgerwood et al., 1998). TNFα also induces the formation of reactive oxygen intermediates by the mitochondria, which may cause necrosis of the target cell (Schulze-Osthoff et al., 1992, 1993; Goossens et al., 1995; Vercammen et al., 1998).

The role of TNF-RII in apoptosis

TNFα binding to TNF-RI is the major ligand-receptor interaction involved in apoptotic signal transduction (Hohmann et al., 1990; Thoma et al., 1990; Tartaglia et al., 1993a). TNF-RII, unlike TNF-RI, does not possess a death domain and hence is unable to recruit death adapter proteins such as TRADD. Under some circumstances, however, TNF-RII may also be involved in inducing cell death (Heller et al., 1992; Bigda et al., 1994; Medvedev et al., 1994). For example, TNF-RII is

a major player in the apoptotic demise of mature $CD8^+$ T lymphocytes (Zheng et al., 1995). Two roles for TNF-RII in apoptotic signaling have been postulated. First, TNF-RII may increase the local TNFα concentration so as to enhance death signaling from TNF-RI. The dissociation rate of TNFα from TNF-RII is significantly greater than that for TNF-RI (Tartaglia et al., 1993b). Hence TNF-RII can perform a ligand passing function and bind many molecules of TNFα, which are then rapidly passed on to TNF-RI (Tartaglia et al., 1993b; Declercq et al., 1998; Haridas et al., 1998). Second, TNF-RII may induce degradation of TRAF2 or inhibit TRAF2 function, thereby preventing the activation of anti-apoptotic processes by TNFα (Duckett and Thompson, 1997; Weiss et al., 1998). Although TRAF2 is involved in TNF-RI death signaling, its major function is in the transduction of anti-apoptotic signals.

Transcription factor activation pathways of TNFα signaling

The activation of transcription factors is a major cellular effect induced by TNFα. These transcription factors regulate the expression of genes whose products are responsible for many of the physiological and pathological effects of TNFα. The principal transcription factors activated are NFκB (nuclear factor κB) and AP-1 (activating protein 1).

NFκB activation is associated with TNFα-induced cellular protection (Beg and Baltimore, 1996; Liu et al., 1996b; Van Antwerp et al., 1996; Wang et al., 1996). NFκB, a member of the Rel family of transcription factors, functions as a homo- or heterodimer formed from five possible subunits: p50/105 (NFκB1), p52/100 (NFκB2), p65 (RelA), RelB, and c-Rel (reviewed in Baeuerle and Henkel, 1994; Siebenlist et al., 1994). The p50 and p52 subunits are synthesized as inactive precursors, p105 and p100, respectively, that are subsequently processed into their active forms. All of the subunits share homology in a N-terminal 300 amino acid region, which is important for dimer formation, nuclear translocation, and DNA binding. The most common form of NFκB consists of a p50 and p65 heterodimer (Baeuerle and Henkel, 1994; Thanos and Maniatis, 1995). Heterodimeric NFκB is sequestered in the cytosol in an inactive state via noncovalent interactions with the IκB family of inhibitor proteins (Baeuerle and Baltimore, 1988, 1989; Beg et al., 1992; Baldwin, 1996). IκB effectively masks the nuclear localization signal on NFκB. When IκB is degraded, NFκB translocates to the nucleus and participates in the regulation of numerous genes, many of which are involved in anti-apoptotic and inflammatory responses (Baeuerle and Henkel, 1994).

AP-1 is a member of the basic region leucine zipper family of transcription factors (Karin et al., 1997). Similar to NFκB, AP-1 is also a homo- or heterodimer. Subunits for AP-1 include c-Jun, c-Fos, and members of the ATF (activating transcription factor) family. Activation of AP-1 is regulated by three of the five known mammalian MAPK (mitogen activated protein kinase) protein families, which are activated upon TNFα treatment (reviewed in Karin, 1995; Woodgett et al., 1996; Paul et al., 1997; Kyriakis, 1999). Specifically, JNK (c-Jun N-terminal kinase, also known as SAPK1), p38 (SAPK2), and ERK (extracellular signal regulated kinase) function to upregulate and phosphorylate the subunits of AP-1. Phosphorylated subunits are transcriptionally active, and can translocate to the nucleus and initiate gene expression (Karin, 1995). Various proinflammatory genes have been shown to be targeted by AP-1 (Reimold et al., 1996). Although some reports suggest that AP-1 is involved in TNFα-induced cellular protection mechanisms (Roulston et al., 1998),

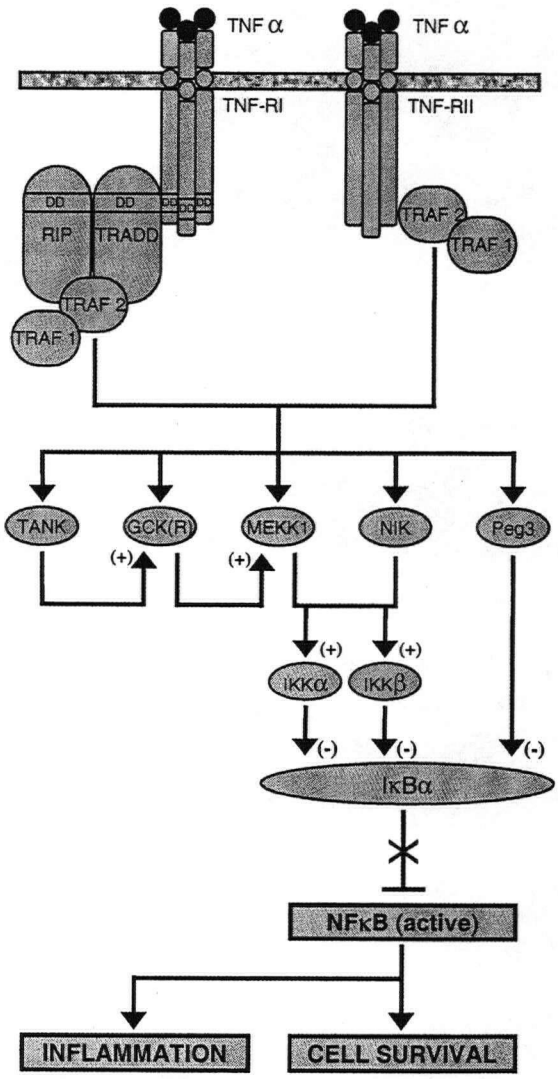

Fig. 2. NFkB activation pathways common to both TNF-RI and TNF-RII. Binding of TNFα to either receptor initiates the signaling cascade. Activation of NFkB results in expression of genes for cell survival and inflammation. Refer to the text for abbreviations of signaling components.

others have implicated AP-1 in the induction of apoptosis (Singh et al., 1995). Activation of the JNK pathway is often associated with stress-induced apoptosis (Hoeflich et al., 1999), although other studies do not show a distinct role for JNK in apoptotic cell death (Liu et al., 1996b). Further research may help to clarify these discrepancies.

The NFκB activation pathways

Pathways common to both TNF-RI and TNF-RII. Both TNF-RI and TNF-RII are capable of activating NFκB independently (Laegreid et al., 1994; Rothe et al., 1994, 1995; Hsu et al., 1995). TNFα binding to either receptor can lead to the degradation of IκB (Fig. 2). As noted previously, RIP plays a role in TNFα-induced apoptosis via interactions with the TNF-RI receptor complex. RIP is also critical for TNFα-induced NFκB activation (Hsu et al., 1996a). The intermediate domain of RIP, which enables RIP to act as a scaffold for TRAF1-TRAF2 heterodimers, is essential for this function (Hsu et al., 1996a). With respect to TNF-RII, this receptor can directly associate with TRAF1-TRAF2 heterodimers, mediated by interactions between TRAF2 and the C-terminal domain of TNF-RII (Rothe et al., 1994). Hence TRAF2 is recruited to both the TNF-RI and TNF-RII receptor complexes.

TRAF2 has been shown to interact with NIK (NFκB-inducing kinase) through the WK1 motif within the TRAF domain (Malinin et al., 1997; Song et al., 1997; Lin et al., 1998). NIK shares sequence homology with members of the MAPKKK family (Eder, 1997; Robinson and Cobb, 1997), but is unable to directly phosphorylate IκBα (Fischer et al., 1999). Instead, the activation of NFκB is regulated by a high molecular weight complex called the signalsome (also known as the IKK (IκB kinase) complex) (Woronicz et al., 1997). Components of the signalsome include NIK, IKKα (IKK1/CHUK), and IKKß (IKK2) (DiDonato et al., 1997; Malinin et al., 1997; Mercurio et al., 1997; Regnier et al., 1997; Woronicz et al., 1997; Zandi et al., 1997). Two adapter proteins are also present in the signalsome, IKKγ (NEMO/IKK associated protein 1) (Rothwarf et al., 1998) and IKAP (IKK complex associated protein) (Cohen et al., 1998), which may serve to stabilize the complex. NIK preferentially binds and phosphorylates IKKα, although interactions with IKKß do occur (Woronicz et al., 1997; Ling et al., 1998; Nakano et al., 1998; Fischer et al., 1999). When phosphorylated, IKKα and IKKß are activated and can phosphorylate IκBα on two serine residues (Ser32 and Ser36) (Chen et al., 1995; Traenckner et al., 1995; DiDonato et al., 1997). An IκBα-Ub (ubiquitin) ligase has a high affinity for phosphorylated IκBα, and can catalyze the ubiquitination of IκBα (Suzuki et al., 1999). Proteasome complexes then recognize the ubiquitinated protein and target it for degradation (Zandi et al., 1997). Because IκBα is no longer able to sequester NFκB in the cytosol, NFκB translocates to the nucleus and activates transcription.

Three additional proteins are recruited via TRAF2 to the receptor complex: TANK (TRAF-associated NFκB activator) (Cheng and Baltimore, 1996), GCK(R) (germinal center kinase (related)) (Yuasa et al., 1998; Chin et al., 1999), and MEKK1 (Baud et al., 1999). All three proteins participate in a relay mechanism towards NFκB activation. TANK activates GCK(R) (Chin et al., 1999), which in turn activates MEKK1 (Shi and Kehrl, 1997), which subsequently activates both IKKα and IKKß (Lee et al., 1998). Although MEKK1 can activate both IKKα and IKKß, activation of IKKα by MEKK1 far exceeds that of IKKß (Lee et al., 1997; Nakano et al., 1998). The fact that MEKK1 has been shown to be a component of the signalsome complex (Mercurio et al., 1997) has added credence to the proposal that MEKK1 is the principal kinase involved in NFκB activation (Lee et al., 1998). A fourth protein that interacts with TRAF2 is Peg3 (Pw1) (Relaix et al., 1998). This protein causes the dissociation of IκBα from NFκB, thus activating the transcription factor.

Pathways specific for TNF-RI. Several NFκB activation pathways mediated by TNF-RI alone have been characterized. One pathway involves IRAK (interleukin-1 receptor-associated kinase), which is a death domain-containing protein (Feinstein et al., 1995; Trofimova et al., 1996). IRAK is capable of direct interaction with TNF-RI via its death domain, and hence can initiate signaling independent of TRADD binding (Vig et al., 1999). Complex formation between IRAK and NIK has been demonstrated. Binding to NIK results in activation of IKKα and IKKß, and thus the activation of NFκB.

Activation of NFκB by the protein p62 specifically involves the TNF-RI receptor complex (Sanz et al., 1999). RIP, a component of the TNF-RI-TRADD-RIP trimeric complex, binds via its intermediate domain to p62. This intermediate domain also mediates interactions between RIP and TRAF2 (Hsu et al., 1996a). Association studies have revealed that the interactions of TRAF2 and p62 with RIP are not antagonistic (Sanz et al., 1999). p62 contains a dimerization domain upstream of its RIP-binding site, which is able to bind to members of the aPKC (atypical protein kinase C) family of proteins, namely PKCζ and PKCλ/i (Puls et al., 1997; Sanchez et al., 1998). Both aPKC proteins are recruited to the receptor complex, where they can activate IKKß and induce NFκB activation (Lallena et al., 1999).

A signal transduction pathway involving PI3K (phosphoinositide 3-kinase) is able to activate NFκB. PI3K is a heterodimer composed of a p110 catalytic subunit and a p85 regulatory subunit (reviewed in Carpenter and Cantley, 1996). Formation of active PI3K can only occur if both subunits have been phosphorylated. TNFα binding to TNF-RI eventually leads to the activation of an as yet unknown tyrosine kinase activity, which is capable of phosphorylating the p85 subunit (Guo and Donner, 1996). The mechanism for p110 subunit activation has been characterized, and

involves the Grb2 protein. Grb2 is a cytoplasmic protein with two SH3 domains, one located at each terminus. An intracellular region of TNF-RI, designated the PLAP motif, binds to the C-terminal SH3 domain of Grb2. With its N-terminal SH3 domain, Grb2 interacts with SOS (Lowenstein et al., 1992; Hildt and Oess, 1999). SOS is a guanine nucleotide exchange factor that binds inactive Ras-GDP and converts it to the active Ras-GTP. Ras-GTP is then able to phosphorylate the p110 subunit. Association of the phosphorylated p85 and p110 subunits forms an active PI3K molecule. The substrate for PI3K is generated via another signaling pathway initiated by TNF-RI. The protein PIP5K (phosphatidylinositol 4-phosphate 5-kinase) has been shown to interact with the juxtamembrane region of TNF-RI (Castellino et al., 1997). PIP5K catalyzes the conversion of PtdIns4P (phosphatidylinositol 4-phosphate) to PIP_2 (phosphatidylinositol 4,5-bisphosphate). PI3K phosphorylates PIP_2 to form PIP_3 (phosphatidylinositol 3,4,5-trisphosphate). Both PIP_2 and PIP_3 have a high affinity towards proteins containing PH (pleckstrin homology) domains (Lassing and Lindberg, 1988; Hemmings, 1997; Klippel et al., 1997; Stokoe et al., 1997; Downward, 1998). Hence two PH domain-containing proteins, Akt and a specific serine/threonine kinase that activates Akt, are recruited to the receptor complex. Active Akt is able to activate IKKα and thereby induce NFκB activation (Ozes et al., 1999). Furthermore, Akt has been shown to phosphorylate and inactivate BAD, a pro-apoptotic molecule of the Bcl-2 family (Yang et al., 1995; White, 1996).

The JNK kinase activation pathways

Pathways common to both TNF-RI and TNF-RII. TRAF2 is a major conduit of JNK activation. Because both the TNF-RI and TNF-RII receptor complexes are able to recruit TRAF2, both receptors have been implicated in JNK activation (Rothe et al., 1995; Natoli et al., 1997). Both receptors are also able to recruit TRAF2 for NFκB activation (Laegreid et al., 1994; Rothe et al., 1994, 1995; Hsu et al., 1995). Hence it is not surprising that some signal transduction mechanisms are shared between the two activation pathways. One such mechanism is the activation of MEKK1, described earlier. Briefly, TRAF2 interacts with three proteins, TANK, GCK(R), and MEKK1. TANK activates GCK(R), which in turn activates MEKK1. It is at this point in the cascade where the two activation pathways bifurcate. MEKK1 has been shown to be a potent activator of the JNK pathway (Minden et al., 1994). MEKK1 activates MKK4 (JNKK/SEK1/SKK1/SAPKK1/Mek4), which in turn activates JNK (Liu et al., 1996b; Natoli et al., 1997).

Interaction between TRAF2 and ASK1 (apoptosis signal-regulating kinase 1) triggers another pathway for JNK activation (Nishitoh et al., 1998). ASK1, a member of the MAPKKK family, contains a C-terminal kinase domain. When ASK1 is in its latent state, the regions flanking the kinase domain interact with each other, thus effectively masking the kinase domain (Ichijo et al., 1997; Chang et al., 1998; Nishitoh et al., 1998). Upon binding to TRAF2, however, this inhibitory interaction is displaced. Active ASK1 directly activates two members of the MAPKK family, MKK4 (Ichijo et al., 1997) and MKK7 (Moriguchi et al., 1997). These kinases in turn activate JNK (Liu et al., 1996b; Moriguchi et al., 1997; Natoli et al., 1997). CARDIAK, another TRAF2-interacting protein, is also capable of activating the JNK pathway (Thome et al., 1998). The kinase domain of CARDIAK is not required for JNK activation. Instead, the CARD domain of CARDIAK is responsible. An additional function of CARDIAK is the activation of NFκB (Thome et al., 1998), although the mechanism for this activation has not been elucidated. Finally, JNK can also be activated by TRAF-2 interactions with caspase 8, caspase 10, or c-FLIP. This pathway requires the DED of the latter three proteins, but is independent of their protease activities (Chaudhary et al., 1999).

Active JNK can phosphorylate and activate various transcription factors, including c-Jun, ATF2, Elk-1, and CREB (Liu et al., 1996b; Natoli et al., 1997; Reinhard et al., 1997). CREB proteins may enhance the transcriptional activity of NFκB (Zhong et al., 1997). Elk-1 induces the expression of c-Fos (Karin, 1995). c-Jun, ATF2, and c-Fos are subunits of the AP-1 transcription factor. Hence the JNK pathway influences gene expression by promoting the formation of the AP-1 complex.

Pathways specific for TNF-RI. A TNF-RI-specific signaling pathway described previously, involving the activation of PI3K and the subsequent production of PIP_3, also assists in the activation of JNK. Upon TNFα treatment, a signaling cascade involving PI3K and the downstream mediator Rac has been shown to result in JNK activation (Kim et al., 1999). A molecule downstream from Rac, namely $cPLA_2$ (cytosolic phospholipase A_2), is also activated (Kim and Kim, 1997). $cPLA_2$ activation can result in increased c-Fos expression as well as JNK activation (Kim et al., 1999), both of which enhance the function of AP-1. More work is needed to identify the various players in this signaling cascade.

The p38 kinase activation pathways

Both TNF-RI and TNF-RII can stimulate pathways leading to p38 kinase activation. Following recruitment of TRAF2 to the receptor complex, ASK1 is known to bind TRAF2 (Nishitoh et al., 1998). ASK1 (a MAPKKK) can directly activate three MAPKKs that have been identified as activators of p38 kinase. These are MKK2, MKK3, and MKK6 (Derijard et al., 1995; Kyriakis and Avruch, 1996; Winston et al., 1997). In addition, evidence suggests that the intermediate domain of RIP may associate with a p38-specific MAPKKK

enzyme, although such an enzyme has not yet been identified (Yuasa et al., 1998). Substrates for p38 kinase include ATF2 and $cPLA_2$. Activation of both substrates assists in AP-1 transcription factor formation. Activation of $cPLA_2$ can also lead to NFκB activation. MAPKAP kinases 2 and 3 are also substrates for p38 kinase (Stokoe et al., 1992; Ludwig et al., 1996). When activated by p38 kinase, both MAPKAP kinases can directly phosphorylate mammalian hsp25/27 (heat shock protein 25/27) (Engel et al., 1995). Immediately following TNFα treatment, phosphorylated hsp25/27 proteins are known to aggregate to form large oligomers (Mehlen et al., 1995, 1997). These oligomers function to protect the cell from reactive oxygen species generated by TNFα (Park et al., 1998; Preville et al., 1998).

The ERK kinase activation pathways

The activation of ERK kinase is specifically mediated by TNF-RI. ERK activation involves a previously described receptor complex consisting of TNF-RI, Grb2, SOS, and Ras-GTP. The target of Ras-GTP in the ERK pathway is c-Raf-1 (Avruch et al., 1994). However, Ras-GTP alone cannot activate c-Raf-1 (Hildt and Oess, 1999). Rather, TNFα upregulates PKCζ kinase (Das et al., 1999), which acts in concert with Ras-GTP to phosphorylate and activate c-Raf-1 (Berra et al., 1995). Activated c-Raf-1 then activates MEK1 (Winston et al., 1995), which in turn activates ERK1/2 (Vietor et al., 1993). ERK1/2 can activate the transcription factor Elk1, thus promoting transcription of c-Fos and the subsequent formation of AP-1 (Karin, 1995).

The neutral sphingomyelinase pathway

The binding of TNFα to TNF-RI can induce the activation of neutral sphingomyelinase (NSMase), a C type phospholipase localized to the plasma membrane. A region adjacent to the death domain of TNF-RI, designated the NSD (NSMase domain), is necessary for NSMase activation (Adam et al., 1996). A WD-repeat protein called FAN (factor associated with NSMase) binds to the NSD domain of TNF-RI (Adam-Klages et al., 1996), and acts as an adapter to recruit NSMase to the receptor complex. NSMase cleaves sphingomyelin located in the plasma membrane, generating ceramide (Dressler et al., 1992; Wiegmann et al., 1994). It was thought that one of the functions of TNFα-induced ceramide was to induce apoptosis, although this view is now controversial (Kolesnick et al., 1994; Adam-Klages et al., 1996; Hannun, 1996). Signaling pathways mediated by ceramide have been linked to the activation of transcription factors (Schutze et al., 1992), as well as the production of proinflammatory metabolites (Heller and Kronke, 1994). TNFα-induced ceramide is known to increase c-Fos expression (Kim et al., 1999), to activate PLA_2 (Lin et al., 1993; Wiegmann et al., 1994), and to activate NFκB (Yang et al., 1993). Direct downstream targets of ceramide include CAPK (ceramide activated protein kinase) (Liu et al., 1994), CAPP (ceramide activated protein phosphatase) (Wolff et al., 1994), and PKCζ (Lozano et al., 1994; Muller et al., 1995).

Activation of CAPK by ceramide induces the binding of CAPK to c-Raf-1 (Yao et al., 1995). CAPK can then phosphorylate c-Raf-1. As mentioned before, activation of c-Raf-1 may require cooperative phosphorylation by more than one kinase. The Grb2-SOS-Ras pathway may provide this additional phosphorylation for activating c-Raf-1 (Hildt and Oess, 1999). Ceramide-activated PKCζ may also participate in c-Raf-1 activation (Berra et al., 1995). Some reports indicate that ceramide may be able to phosphorylate and activate c-Raf-1 directly (Pfeilschifter and Huwiler, 1998). Active c-Raf-1 targets MEK1 for activation (Yao et al., 1995), thus leading to the activation of ERK1/2 (Vietor et al., 1993; Bird et al., 1994). Downstream signaling events following ERK1/2 activation include the activation of both Elk-1 (Karin, 1995) and PLA_2 (Lin et al., 1993). Elk-1-induced c-Fos production leads to AP-1 formation, whereas PLA_2-induced phosphatidylcholine degradation leads to arachidonic acid production. Arachidonic acid can induce the activation of JNK (Rizzo and Carlo-Stella, 1996). In addition, it can act as a substrate to further propagate TNFα signaling.

Arachidonic acid is a substrate for both lipoxygenase and cyclooxygenase. Lipoxygenase oxidizes arachidonic acid to produce leukotrienes and other lipoxygenase metabolites (Samuelsson et al., 1987). Effects of these metabolites include the induction of c-Fos expression (Haliday et al., 1991) and the generation of reactive oxygen intermediates (Samuelsson et al., 1987). In fact, reactive oxygen intermediates can act as cofactors to promote c-Fos production (Yamauchi et al., 1989), as well as promote the activation of NFκB (Schreck et al., 1991). Conversely, the reactive oxygen intermediates produced may also potentiate the cytotoxic effects of TNFα (Chang et al., 1992). When arachidonic acid is targeted by cyclooxygenase, prostaglandins are produced. Prostaglandins, along with leukotrienes, are proinflammatory mediators that can increase blood flow and enhance capillary permeability. These effects can contribute to TNFα-induced inflammatory responses (Heller and Kronke, 1994).

TNFα binding to TNF-RI has been shown to stimulate the production of diacylglycerol (Schutze et al., 1991). The signaling pathway leading to diacylglycerol production involves activation of PC-PLC (phosphatidylcholine dependent phospholipase C) by the death domain of TNF-RI (Schutze et al., 1992; Wiegmann et al., 1994). Activated PC-PLC converts phosphatidylcholine to diacylglycerol, which in turn activates a TNFα-responsive isotype of PKC that triggers the induction of c-Jun and c-Fos (Fain and Berridge, 1978; Michell et al., 1979; Brenner et al., 1989).

Ceramide can be cleaved by ceramidase to generate sphingosine (Kolesnick and Golde, 1994; Hannun, 1996;

Spiegel and Merrill, 1996). Subsequent cleavage of sphingosine by sphingosine kinase yields sphingosine-1-phosphate. In this signaling pathway, activation of sphingosine kinase is mediated by the actions of either sphingomyelinase or ceramidase. Recently, a sphingomyelinase- and ceramidase-independent activation of sphingosine kinase by TNFα has been detected (Xia et al., 1999). The mechanism of this novel signaling pathway, however, is currently unknown. Sphingosine-1-phosphate activates anti-apoptotic and inflammatory pathways (Xia et al., 1999). In addition to activating NFκB and stimulating ERK activity, sphingosine-1-phosphate can also inhibit the function of caspase 3. Hence sphingosine-1-phosphate plays a role in TNFα-induced cell protection mechanisms.

The acidic sphingomyelinase pathway

Similar to NSMase, acidic sphingomyelinase (ASMase) is also a C type phospholipase. Activation of ASMase can only occur through TNF-RI. Furthermore, because ASMase is localized to acidic compartments of the cell such as lysosomes, TNF-RI must be internalized for ASMase activation to occur (Schutze et al., 1999). The ASMase pathway is initiated when TNF-RI, present at the plasma membrane, activates PC-PLC. Propagation of the signal can occur if the diacylglycerol produced from lipid hydrolysis is in close proximity with TNF-RI, so that some diacylglycerol is incorporated into endosomes during TNF-RI internalization. Following endosome formation, lysosomes containing ASMase fuse with the endosome, thereby effectively approximating TNF-RI and ASMase. The interior of the fusion vesicle is now optimal for ASMase activity to occur. Activation of ASMase requires both diacyl-glycerol and the extracellular domain of TNF-RI (which is located within the lumen of the vesicle) (Kolesnick, 1987; Schutze et al., 1992; Wiegmann et al., 1999). Also, TNF-RI must be associated with both TRADD and FADD for ASMase activation to occur (Adam-Klages et al., 1998). TRADD and FADD are believed to enhance the stability of TNF-RI, thus enabling the extracellular domain of TNF-RI to activate ASMase. Activation of ASMase leads to the generation of ceramide (Merrill et al., 1993; Spence, 1993), which can induce NFκB activation (Machleidt et al., 1994; Reddy et al., 1994). Ceramide can also bind and activate the lysosomal protease cathepsin D, thereby contributing to TNFα-induced cell death (Wickel et al., 1998).

Gene expression following TNFα-induced transcription factor activation

Four categories of genes are induced following TNFα treatment. These include anti-apoptotic genes, proinflammatory genes, mitogenic genes, and signal regulatory genes.

Anti-apoptotic gene expression. Concomitant with activation of apoptotic pathways, induction of protective proteins provides cells with resistance to TNFα-induced cytotoxicity. Both NFκB and AP-1 participate in cell survival. In response to TNFα, several anti-apoptotic proteins are induced. These include A1, an anti-apoptotic protein of the Bcl-2 family, the zinc finger protein A20, the reactive oxygen intermediate scavenger enzyme manganese superoxide dismutase, plasminogen activator inhibitor 2, c-IAPs, TRAF2, and IEX-1L (Krikos et al., 1992; Karsan et al., 1996; Uren et al., 1996; Deveraux et al., 1997; Moriguchi et al., 1997; Hu et al., 1998; Wu et al., 1998). Of interest, both A1 and A20 have also been reported to inhibit NFκB activation in addition to inhibiting apoptosis (Jaattela et al., 1996; Stroka et al., 1999).

Proinflammatory gene expression. Inflammation is a major physiological effect induced by TNFα. Both NFκB and AP-1 can participate in the production of proinflammatory mediators. This includes upregulation of cell adhesion molecules such as E-selectin, intracellular adhesion molecules 1 and 2, and vascular cell adhesion molecule 1 (De Luca et al., 1994; Barnes and Karin, 1997; Farina et al., 1997; Subramaniam et al., 1997), as well as production of various chemokines such as monocyte chemoattractant protein 1, interleukin-8, and macrophage inhibitory protein 2a (Barnes and Karin, 1997; Ueda et al., 1997; Roger et al., 1998). Additional proinflammatory-related genes induced by TNFα include interleukin-6, prostaglandin H synthase 2, platelet activating factor, and the matrix metalloproteases, collagenase and stromelysin (Barnes and Karin, 1997).

Mitogenic gene expression. Both NFκB and AP-1 can enhance the expression of growth promoting genes in response to TNFα treatment (Arch et al., 1998). One such gene is granulocyte-macrophage colony stimulating factor (Munker et al., 1986). Granulocyte-macrophage colony stimulating factor is known to enhance monocyte and granulocyte production, as well as to promote the growth of pluripotent and erythroid stem cells (reviewed in de Groot et al., 1998).

Signal regulatory gene expression. TNFα can activate regulatory systems within a cell to limit the magnitude and duration of TNFα-induced inflammatory responses. TNFα-activated NFκB and AP-1 can increase the synthesis of TNFα which may modulate the immune response in a positive or negative fashion (Takashiba et al., 1993). The increased production of TNFα may act to kill effector cells, and thus restrict the immune response (Swantek et al., 1997). On the other hand, cells already exposed to sublethal doses of TNFα are partially resistant to the cytotoxic effects of TNFα, which may potentiate the inflammatory response. NFκB can induce the synthesis of IκBα, which can rapidly restore the inhibitory protein levels to render NFκB activation transient (Baldwin, 1996). The expression of factors involved in a TNFα negative feedback loop, such as

interleukin-10 (Platzer et al., 1995), corticosteroids (Van der Poll et al., 1991), and prostanoids (Dayer et al., 1985), functions to suppress the production of TNFα. NFκB has also been shown to induce the expression of TRAF1 and TRAF2 (Wang et al., 1998; Schwenzer et al., 1999). TRAF expression has been postulated to play a role in feedback regulation of activated receptors.

Conclusions

A plethora of knowledge has accumulated over the past decade with respect to the mechanisms of TNFα signal transduction. Many of the intracellular signaling molecules have been identified. Detailed molecular pathways have been established from the point of signal initiation mediated by ligand-receptor interactions at the plasma membrane, to the point of gene transcription within the nucleus. The mechanisms involved in cell death induction by TNFα have also been characterized. Factors influencing the balance of opposing signaling pathways, however, remain to be identified. With this vast amount of data available at hand, potential clinical applications for TNFα may become more apparent. Understanding the complex nature of TNFα signaling allows the rational development of therapies to modulate TNFα function. It is important, however, to realize that many of the components of the signaling pathways and their interaction partners were identified under nonphysiological conditions, including overexpression studies and targeted null mutations in animals. Furthermore, signaling mechanisms may be cell-type specific, as evidenced by the contradicting results in the literature. Clearly, much remains to be learned about the relationship between the cellular and global effects of TNFα.

Acknowledgements. This work was funded by grants to A.K. from the Heart and Stroke Foundation of British Columbia and the Yukon and the Medical Research Council of Canada. A.K. is a Clinician-Scientist of the Medical Research Council of Canada.

References

Adam D., Wiegmann K., Adam-Klages S., Ruff A. and Kronke M. (1996). A novel cytoplasmic domain of the p55 tumor necrosis factor receptor initiates the neutral sphingomyelinase pathway. J. Biol. Chem. 271, 14617-14622.

Adam-Klages S., Adam D., Wiegmann K., Struve S., Kolanus W., Schneider-Mergener J. and Kronke M. (1996). FAN, a novel WD-repeat protein, couples the p55 TNF-receptor to neutral sphingomyelinase. Cell 86, 937-947.

Adam-Klages S., Schwandner R., Adam D., Kreder D., Bernardo K. and Kronke M. (1998). Distinct adapter proteins mediate acid versus neutral sphingomyelinase activation through the p55 receptor for tumor necrosis factor. J. Leukoc. Biol. 63, 678-682.

Aderka D. (1996). The potential biological and clinical significance of the soluble tumor necrosis factor receptors. Cytokine Growth Factor Rev. 7, 231-240.

Adolf R.A., Grell M. and Scheurich P. (1994). Tumor necrosis factor. In: Epidermal growth factors and cytokines. Luger T.A. and Schwartz T. (eds). Marcel Dekker. New York. pp 63-88.

Ahmad M., Srinivasula S.M., Wang L., Talanian R.V., Litwack G., Fernandes-Alnemri T. and Alnemri E.S. (1997). CRADD, a novel human apoptotic adaptor molecule for caspase-2, and FasL/tumor necrosis factor receptor-interacting protein RIP. Cancer Res. 57, 615-619.

Arch R.H., Gedrich R.W. and Thompson C.B. (1998). Tumor necrosis factor receptor-associated factors (TRAFs) - a family of adapter proteins that regulates life and death. Genes Dev. 12, 2821-2830.

Armitage R.J. (1994). Tumor necrosis factor receptor superfamily members and their ligands. Curr. Opin. Immunol. 6, 407-413.

Ashkenazi A. and Dixit V.M. (1998). Death receptors: signaling and modulation. Science 281, 1305-1308.

Ashkenazi A. and Dixit V.M. (1999). Apoptosis control by death and decoy receptors. Curr. Opin. Cell Biol. 11, 255-260.

Avruch J., Zhang X.F. and Kyriakis J.M. (1994). Raf meets Ras: completing the framework of a signal transduction pathway. Trends Biochem. Sci. 19, 279-283.

Baeuerle P.A. and Baltimore D. (1988). Activation of DNA-binding activity in an apparently cytoplasmic precursor of the NF-kappa B transcription factor. Cell 53, 211-217.

Baeuerle P.A. and Baltimore D. (1989). A 65-kappaD subunit of active NF-kappaB is required for inhibition of NF-kappaB by I kappaB. Genes Dev. 3, 1689-1698.

Baeuerle P.A. and Henkel T. (1994). Function and activation of NF-kappa B in the immune system. Annu. Rev. Immunol. 12, 141-179.

Baker S.J. and Reddy E.P. (1996). Transducers of life and death: TNF receptor superfamily and associated proteins. Oncogene 12, 1-9.

Baldwin A.S. Jr. (1996). The NF-kappa B and I kappa B proteins: new discoveries and insights. Annu. Rev. Immunol. 14, 649-683.

Banner D.W., Janes W., Gentz R., Schoenfeld H.J., Broger C., Loetscher H. and Lesslauer W. (1993). Crystal structure of the soluble human 55 kd TNF receptor-human TNF beta complex: implications for TNF receptor activation. Cell 73, 431-445.

Barnes P.J. and Karin M. (1997). Nuclear factor-kappaB: a pivotal transcription factor in chronic inflammatory diseases. N. Engl. J. Med. 336, 1066-1071.

Baud V., Liu Z.G., Bennett B., Suzuki N., Xia Y. and Karin M. (1999). Signaling by proinflammatory cytokines: oligomerization of TRAF2 and TRAF6 is sufficient for JNK and IKK activation and target gene induction via an amino-terminal effector domain. Genes Dev. 13, 1297-1308.

Bazzoni F. and Beutler B. (1996). Seminars in medicine of the Beth Israel Hospital, Boston: The tumor necrosis factor ligand and receptor families. N. Engl. J. Med. 334, 1717-1725.

Beg A.A. and Baltimore D. (1996). An essential role for NF-kappaB in preventing TNF-alpha-induced cell death. Science 274, 782-784.

Beg A.A., Ruben S.M., Scheinman R.I., Haskill S., Rosen C.A. and Baldwin A.S. Jr. (1992). I kappa B interacts with the nuclear localization sequences of the subunits of NF-kappa B: a mechanism for cytoplasmic retention [published erratum appears in Genes Dev 1992 Dec;6(12B):2664-5]. Genes Dev. 6, 1899-1913.

Berra E., Diaz-Meco M.T., Lozano J., Frutos S., Municio M.M., Sanchez P., Sanz L. and Moscat J. (1995). Evidence for a role of MEK and MAPK during signal transduction by protein kinase C zeta. EMBO J. 14, 6157-6163.

Beutler B.A. (1999). The role of tumor necrosis factor in health and disease. J. Rheumatol. 26 Suppl. 57, 16-21.

Beutler B. and Cerami A. (1987). Cachectin: a monokine implicated as a mediator of cachexia and shock. Lymphokines 14, 203-222.

Beutler B. and van Huffel C. (1994). Unraveling function in the TNF ligand and receptor families. Science 264, 667-668.

Beutler B., Greenwald D., Hulmes J.D., Chang M., Pan Y.C., Mathison J., Ulevitch R. and Cerami A. (1985a). Identity of tumour necrosis factor and the macrophage-secreted factor cachectin. Nature 316, 552-554.

Beutler B., Mahoney J., Le Trang N., Pekala P. and Cerami A. (1985b). Purification of cachectin, a lipoprotein lipase-suppressing hormone secreted by endotoxin-induced RAW 264.7 cells. J. Exp. Med. 161, 984-995.

Beyaert R. and Fiers W. (1994). Molecular mechanisms of tumor necrosis factor-induced cytotoxicity. What we do understand and what we do not. FEBS Lett. 340, 9-16.

Bigda J., Beletsky I., Brakebusch C., Varfolomeev Y., Engelmann H., Bigda J., Holtmann H. and Wallach D. (1994). Dual role of the p75 tumor necrosis factor (TNF) receptor in TNF cytotoxicity. J. Exp. Med. 180, 445-460.

Bird T.A., Kyriakis J.M., Tyshler L., Gayle M., Milne A. and Virca G.D. (1994). Interleukin-1 activates p54 mitogen-activated protein (MAP) kinase/stress-activated protein kinase by a pathway that is independent of p21ras, Raf-1, and MAP kinase kinase. J. Biol. Chem. 269, 31836-31844.

Black R.A., Rauch C.T., Kozlosky C.J., Peschon J.J., Slack J.L., Wolfson M.F., Castner B.J., Stocking K.L., Reddy P., Srinivasan S., Nelson N., Boiani N., Schooley K.A., Gerhart M., Davis R., Fitzner J.N., Johnson R.S., Paxton R.J., March C.J. and Cerretti D.P. (1997). A metalloproteinase disintegrin that releases tumour-necrosis factor- alpha from cells. Nature 385, 729-733.

Blobel C.P. (1997). Metalloprotease-disintegrins: links to cell adhesion and cleavage of TNF alpha and Notch. Cell 90, 589-592.

Boldin M.P., Goncharov T.M., Goltsev Y.V. and Wallach D. (1996). Involvement of MACH, a novel MORT1/FADD-interacting protease, in Fas/APO-1- and TNF receptor-induced cell death. Cell 85, 803-815.

Boldin M.P., Mett I.L., Varfolomeev E.E., Chumakov I., Shemer-Avni Y., Camonis J.H. and Wallach D. (1995a). Self-association of the "death domains" of the p55 tumor necrosis factor (TNF) receptor and Fas/APO1 prompts signaling for TNF and Fas/APO1 effects. J. Biol. Chem. 270, 387-391.

Boldin M.P., Varfolomeev E.E., Pancer Z., Mett I.L., Camonis J.H. and Wallach D. (1995b). A novel protein that interacts with the death domain of Fas/APO1 contains a sequence motif related to the death domain. J. Biol. Chem. 270, 7795-7798.

Bradley J.R., Thiru S. and Pober J.S. (1995). Disparate localization of 55-kd and 75-kd tumor necrosis factor receptors in human endothelial cells. Am. J. Pathol. 146, 27-32.

Brakebusch C., Varfolomeev E.E., Batkin M. and Wallach D. (1994). Structural requirements for inducible shedding of the p55 tumor necrosis factor receptor. J. Biol. Chem. 269, 32488-32496.

Brenner D.A., Angel P., Chojkier M. and Karin M. (1989). Prolonged activation of jun and collagenase genes by tumour necrosis factor-alpha. Nature 337, 661-663.

Brojatsch J., Naughton J., Rolls M.M., Zingler K. and Young J.A. (1996). CAR1, a TNFR-related protein, is a cellular receptor for cytopathic avian leukosis-sarcoma viruses and mediates apoptosis. Cell 87, 845-855.

Browning J.L., Ngam-ek A., Lawton P., DeMarinis J., Tizard R., Chow E.P., Hession C., Foley S.F. and Ware C.F. (1993). Lymphotoxin beta, a novel member of the TNF family that forms a heteromeric complex with lymphotoxin on the cell surface. Cell 72, 847-856.

Brynskov J., Nielsen O.H., Ahnfelt-Ronne I. and Bendtzen K. (1994). Cytokines (immunoinflammatory hormones) and their natural regulation in inflammatory bowel disease (Crohn's disease and ulcerative colitis): a review. Dig. Dis. 12, 290-304.

Budihardjo I., Oliver H., Lutter M., Luo X. and Wang X. (1999). Biochemical pathways of caspase activation during apoptosis. Annu. Rev. Cell Dev. Biol. 15, 269-290.

Cai J., Yang J. and Jones D.P. (1998). Mitochondrial control of apoptosis: the role of cytochrome c. Biochim. Biophys. Acta 1366, 139-149.

Carpenter C.L. and Cantley L.C. (1996). Phosphoinositide kinases. Curr. Opin. Cell Biol. 8, 153-158.

Carswell E.A., Old L.J., Kassel R.L., Green S., Fiore N. and Williamson B. (1975). An endotoxin-induced serum factor that causes necrosis of tumors. Proc. Natl. Acad. Sci. USA 72, 3666-3670.

Castellino A.M., Parker G.J., Boronenkov I.V., Anderson R.A. and Chao M.V. (1997). A novel interaction between the juxtamembrane region of the p55 tumor necrosis factor receptor and phosphatidylinositol-4-phosphate 5-kinase. J. Biol. Chem. 272, 5861-5870.

Chang D.J., Ringold G.M. and Heller R.A. (1992). Cell killing and induction of manganous superoxide dismutase by tumor necrosis factor-alpha is mediated by lipoxygenase metabolites of arachidonic acid. Biochem. Biophys. Res. Commun. 188, 538-546.

Chang H.Y., Nishitoh H., Yang X., Ichijo H. and Baltimore D. (1998). Activation of apoptosis signal-regulating kinase 1 (ASK1) by the adapter protein Daxx. Science 281, 1860-1863.

Chaudhary P.M., Eby M.T., Jasmin A. and Hood L. (1999). Activation of the c-Jun N-terminal kinase/stress-activated protein kinase pathway by overexpression of caspase-8 and its homologs. J. Biol. Chem. 274, 19211-19219.

Chen Z., Hagler J., Palombella V.J., Melandri F., Scherer D., Ballard D. and Maniatis T. (1995). Signal-induced site-specific phosphorylation targets I kappa B alpha to the ubiquitin-proteasome pathway. Genes Dev. 9, 1586-1597.

Cheng B., Christakos S. and Mattson M.P. (1994). Tumor necrosis factors protect neurons against metabolic-excitotoxic insults and promote maintenance of calcium homeostasis. Neuron 12, 139-153.

Cheng E.H., Kirsch D.G., Clem R.J., Ravi R., Kastan M.B., Bedi A., Ueno K. and Hardwick J.M. (1997). Conversion of Bcl-2 to a Bax-like death effector by caspases. Science 278, 1966-1968.

Cheng G. and Baltimore D. (1996). TANK, a co-inducer with TRAF2 of TNF and CD 40L-mediated NF-kappaB activation. Genes Dev. 10, 963-973.

Chin A.I., Shu J., Shan Shi C., Yao Z., Kehrl J.H. and Cheng G. (1999). TANK potentiates tumor necrosis factor receptor-associated factor-mediated c-Jun N-terminal kinase/stress-activated protein kinase activation through the germinal center kinase pathway. Mol. Cell. Biol. 19, 6665-6672.

Chinnaiyan A.M., Tewari M. and Dixit V.M. (1995). FADD, a novel death domain-containing protein, interacts with the death domain of Fas and initiates apoptosis. Cell 81, 505-512.

Clem R.J. and Duckett C.S. (1997). The iap genes: Unique arbitrators of cell death. Trends Cell Biol. 7, 337-339.

Cohen G.M. (1997). Caspases: the executioners of apoptosis. Biochem. J. 326, 1-16.

Cohen L., Henzel W.J. and Baeuerle P.A. (1998). IKAP is a scaffold

protein of the IkappaB kinase complex. Nature 395, 292-296.

D'Amours D., Desnoyers S. and Poirier G.G. (1999). Poly(ADP-ribosyl)ation reactions in the regulation of nuclear functions. Biochem. J. 342, 249-268.

Das S., Bhattacharyya S., Ghosh S. and Majumdar S. (1999). TNF-alpha induced altered signaling mechanism in human neutrophil. Mol. Cell. Biochem. 197, 97-108.

Dayer J.M., Beutler B. and Cerami A. (1985). Cachectin/tumor necrosis factor stimulates collagenase and prostaglandin E2 production by human synovial cells and dermal fibroblasts. J. Exp. Med. 162, 2163-2168.

de Groot R.P., Coffer P.J. and Koenderman L. (1998). Regulation of proliferation, differentiation and survival by the IL- 3/IL-5/GM-CSF receptor family. Cell. Signal. 10, 619-628.

De Luca L.G., Johnson D.R., Whitley M.Z., Collins T. and Pober J.S. (1994). cAmp and tumor necrosis factor competitively regulate transcriptional activation through and nuclear factor binding to the cAMP-responsive element/activating transcription factor element of the endothelial leukocyte adhesion molecule-1 (E-selectin) promoter. J. Biol. Chem. 269, 19193-19196.

De Vos K., Goossens V., Boone E., Vercammen D., Vancompernolle K., Vandenabeele P., Haegeman G., Fiers W. and Grooten J. (1998). The 55-kDa tumor necrosis factor receptor induces clustering of mitochondria through its membrane-proximal region. J. Biol. Chem. 273, 9673-9680.

Declercq W., Denecker G., Fiers W. and Vandenabeele P. (1998). Cooperation of both TNF receptors in inducing apoptosis: involvement of the TNF receptor-associated factor binding domain of the TNF receptor 75. J. Immunol. 161, 390-399.

Derijard B., Raingeaud J., Barrett T., Wu I.H., Han J., Ulevitch R.J. and Davis R.J. (1995). Independent human MAP-kinase signal transduction pathways defined by MEK and MKK isoforms [published erratum appears in Science 1995 Jul 7;269(5220):17]. Science 267, 682-685.

Deveraux Q.L. and Reed J.C. (1999). IAP family proteins-suppressors of apoptosis. Genes Dev. 13, 239-252.

Deveraux Q.L., Takahashi R., Salvesen G.S. and Reed J.C. (1997). X-linked IAP is a direct inhibitor of cell-death proteases. Nature 388, 300-304.

DiDonato J.A., Hayakawa M., Rothwarf D.M., Zandi E. and Karin M. (1997). A cytokine-responsive IkappaB kinase that activates the transcription factor NF-kappaB. Nature 388, 548-554.

Downward J. (1998). Lipid-regulated kinases: some common themes at last. Science 279, 673-674.

Dressler K.A., Mathias S. and Kolesnick R.N. (1992). Tumor necrosis factor-alpha activates the sphingomyelin signal transduction pathway in a cell-free system. Science 255, 1715-1718.

Duan H. and Dixit V.M. (1997). RAIDD is a new 'death' adaptor molecule. Nature 385, 86-89.

Duckett C.S. and Thompson C.B. (1997). CD30-dependent degradation of TRAF2: implications for negative regulation of TRAF signaling and the control of cell survival. Genes Dev. 11, 2810-2821.

Duvall E. and Wyllie A.H. (1986). Death and the cell. Immunol. Today 7, 115-119.

Echtenacher B., Falk W., Mannel D.N. and Krammer P.H. (1990). Requirement of endogenous tumor necrosis factor/cachectin for recovery from experimental peritonitis. J. Immunol. 145, 3762-3766.

Eder J. (1997). Tumour necrosis factor alpha and interleukin 1 signalling: do MAPKK kinases connect it all? Trends Pharmacol. Sci. 18, 319-322.

Elliott M.J., Maini R.N., Feldmann M., Kalden J.R., Antoni C., Smolen J.S., Leeb B., Breedveld F.C., Macfarlane J.D., Bijl H. and Woody J.N. (1994). Randomised double-blind comparison of chimeric monoclonal antibody to tumour necrosis factor alpha (cA2) versus placebo in rheumatoid arthritis. Lancet. 344, 1105-1110.

Emoto Y., Manome Y., Meinhardt G., Kisaki H., Kharbanda S., Robertson M., Ghayur T., Wong W.W., Kamen R., Weichselbaum R. and Kufe D. (1995). Proteolytic activation of protein kinase C delta by an ICE-like protease in apoptotic cells. EMBO J. 14, 6148-6156.

Enari M., Sakahira H., Yokoyama H., Okawa K., Iwamatsu A. and Nagata S. (1998). A caspase-activated DNase that degrades DNA during apoptosis, and its inhibitor ICAD [published erratum appears in Nature 1998 May 28;393(6683):396]. Nature 391, 43-50.

Engel K., Ahlers A., Brach M.A., Herrmann F. and Gaestel M. (1995). MAPKAP kinase 2 is activated by heat shock and TNF-alpha: *in vivo* phosphorylation of small heat shock protein results from stimulation of the MAP kinase cascade. J. Cell. Biochem. 57, 321-330.

Fain J.N. and Berridge M.J. (1978). Relationship between 5-hydroxytryptamine activation of phosphatidylinositol hydrolysis and calcium-ion entry in Calliphora salivary glands. Biochem. Soc. Trans. 6, 1038-1039.

Famularo G., De Simone C., Tzantzoglou S. and Trinchieri V. (1994). Apoptosis, anti-apoptotic compounds and TNF-alpha release. Immunol. Today 15, 495-496.

Farina A.R., Cappabianca L., Mackay A.R., Tiberio A., Tacconelli A., Tessitore A., Frati L., Martinotti S. and Gulino A. (1997). Transcriptional regulation of intercellular adhesion molecule 1 by phorbol ester in human neuroblastoma cell line SK-N-SH involves jun- and fos-containing activator protein 1 site binding complex(es). Cell Growth Differ. 8, 789-800.

Feinstein E., Kimchi A., Wallach D., Boldin M. and Varfolomeev E. (1995). The death domain: a module shared by proteins with diverse cellular functions. Trends Biochem. Sci. 20, 342-344.

Feldmann M., Brennan F.M., Elliott M.J., Williams R.O. and Maini R.N. (1995). TNF alpha is an effective therapeutic target for rheumatoid arthritis. Ann. NY Acad. Sci. 766, 272-278.

Fernandes-Alnemri T., Armstrong R.C., Krebs J., Srinivasula S.M., Wang L., Bullrich F., Fritz L.C., Trapani J.A., Tomaselli K.J., Litwack G. and Alnemri E.S. (1996). *In vitro* activation of CPP32 and Mch3 by Mch4, a novel human apoptotic cysteine protease containing two FADD-like domains. Proc. Natl. Acad. Sci. USA 93, 7464-7469.

Fiers W., Beyaert R., Boone E., Cornelis S., Declercq W., Decoster E., Denecker G., Depuydt B., De Valck D., De Wilde G., Goossens V., Grooten J., Haegeman G., Heyninck K., Penning L., Plaisance S., Vancompernolle K., Van Criekinge W., Vandenabeele P., Vanden Berghe W., Van de Craen M., Vandevoorde V. and Vercammen D. (1995). TNF-induced intracellular signaling leading to gene induction or to cytotoxicity by necrosis or by apoptosis. J. Inflamm. 47, 67-75.

Fischer C., Page S., Weber M., Eisele T., Neumeier D. and Brand K. (1999). Differential effects of lipopolysaccharide and tumor necrosis factor on monocytic IkappaB kinase signalsome activation and IkappaB proteolysis. J. Biol. Chem. 274, 24625-24632.

Gatanaga T., Hwang C.D., Kohr W., Cappuccini F., Lucci J.A.d., Jeffes E.W., Lentz R., Tomich J., Yamamoto R.S. and Granger G.A. (1990). Purification and characterization of an inhibitor (soluble tumor necrosis factor receptor) for tumor necrosis factor and lymphotoxin obtained from the serum ultrafiltrates of human cancer patients. Proc. Natl. Acad. Sci. USA 87, 8781-8784.

Goltsev Y.V., Kovalenko A.V., Arnold E., Varfolomeev E.E., Brodianskii V.M. and Wallach D. (1997). CASH, a novel caspase homologue with death effector domains. J. Biol. Chem. 272, 19641-19644.

Goossens V., Grooten J., De Vos K. and Fiers W. (1995). Direct evidence for tumor necrosis factor-induced mitochondrial reactive oxygen intermediates and their involvement in cytotoxicity. Proc. Natl. Acad. Sci. USA 92, 8115-8119.

Grell M. (1995). Tumor necrosis factor (TNF) receptors in cellular signaling of soluble and membrane-expressed TNF. J. Inflamm. 47, 8-17.

Grell M., Douni E., Wajant H., Lohden M., Clauss M., Maxeiner B., Georgopoulos S., Lesslauer W., Kollias G., Pfizenmaier K. and Scheurich P. (1995). The transmembrane form of tumor necrosis factor is the prime activating ligand of the 80 kDa tumor necrosis factor receptor. Cell 83, 793-802.

Grooten J., Goossens V., Vanhaesebroeck B. and Fiers W. (1993). Cell membrane permeabilization and cellular collapse, followed by loss of dehydrogenase activity: early events in tumour necrosis factor-induced cytotoxicity. Cytokine 5, 546-555.

Gruss H.J. and Dower S.K. (1995). Tumor necrosis factor ligand superfamily: involvement in the pathology of malignant lymphomas. Blood 85, 3378-3404.

Guo D. and Donner D.B. (1996). Tumor necrosis factor promotes phosphorylation and binding of insulin receptor substrate 1 to phosphatidylinositol 3-kinase in 3T3-L1 adipocytes. J. Biol. Chem. 271, 615-618.

Gurney A.L., Marsters S.A., Huang R.M., Pitti R.M., Mark D.T., Baldwin D.T., Gray A.M., Dowd A.D., Brush A.D., Heldens A.D., Schow A.D., Goddard A.D., Wood W.I., Baker K.P., Godowski P.J. and Ashkenazi A. (1999). Identification of a new member of the tumor necrosis factor family and its receptor, a human ortholog of mouse GITR. Curr. Biol. 9, 215-218.

Haliday E.M., Ramesha C.S. and Ringold G. (1991). TNF induces c-fos via a novel pathway requiring conversion of arachidonic acid to a lipoxygenase metabolite. EMBO J. 10, 109-115.

Han D.K., Chaudhary P.M., Wright M.E., Friedman C., Trask B.J., Riedel R.T., Baskin D.G., Schwartz S.M. and Hood L. (1997). MRIT, a novel death-effector domain-containing protein, interacts with caspases and BclXL and initiates cell death. Proc. Natl. Acad. Sci. USA 94, 11333-11338.

Hannun Y.A. (1996). Functions of ceramide in coordinating cellular responses to stress. Science 274, 1855-1859.

Haridas V., Darnay B.G., Natarajan K., Heller R. and Aggarwal B.B. (1998). Overexpression of the p80 TNF receptor leads to TNF-dependent apoptosis, nuclear factor-kappa B activation, and c-Jun kinase activation. J. Immunol. 160, 3152-3162.

Hart S.P., Haslett C. and Dransfield I. (1996). Recognition of apoptotic cells by phagocytes. Experientia 52, 950-956.

Hebert M.J., Takano T., Holthofer H. and Brady H.R. (1996). Sequential morphologic events during apoptosis of human neutrophils. Modulation by lipoxygenase-derived eicosanoids. J. Immunol. 157, 3105-3115.

Heller R.A. and Kronke M. (1994). Tumor necrosis factor receptor-mediated signaling pathways. J. Cell Biol. 126, 5-9.

Heller R.A., Song K., Fan N. and Chang D.J. (1992). The p70 tumor necrosis factor receptor mediates cytotoxicity. Cell 70, 47-56.

Hemmings B.A. (1997). Akt signaling: linking membrane events to life and death decisions. Science 275, 628-630.

Hildt E. and Oess S. (1999). Identification of Grb2 as a novel binding partner of tumor necrosis factor (TNF) receptor I. J. Exp. Med. 189, 1707-1714.

Hirata H., Takahashi A., Kobayashi S., Yonehara S., Sawai H., Okazaki T., Yamamoto K. and Sasada M. (1998). Caspases are activated in a branched protease cascade and control distinct downstream processes in Fas-induced apoptosis. J. Exp. Med. 187, 587-600.

Hoeflich K.P., Yeh W.C., Yao Z., Mak T.W. and Woodgett J.R. (1999). Mediation of TNF receptor-associated factor effector functions by apoptosis signal-regulating kinase-1 (ASK1). Oncogene 18, 5814-5820.

Hofmann K., Bucher P. and Tschopp J. (1997). The CARD domain: a new apoptotic signalling motif. Trends Biochem. Sci. 22, 155-156.

Hohmann H.P., Brockhaus M., Baeuerle P.A., Remy R., Kolbeck R. and van Loon A.P. (1990). Expression of the types A and B tumor necrosis factor (TNF) receptors is independently regulated, and both receptors mediate activation of the transcription factor NF-kappa B. TNF alpha is not needed for induction of a biological effect via TNF receptors. J. Biol. Chem. 265, 22409-22417.

Hotamisligil G.S., Arner P., Caro J.F., Atkinson R.L. and Spiegelman B.M. (1995). Increased adipose tissue expression of tumor necrosis factor-alpha in human obesity and insulin resistance. J. Clin. Invest. 95, 2409-2415.

Hsu H., Xiong J. and Goeddel D.V. (1995). The TNF receptor 1-associated protein TRADD signals cell death and NF-kappa B activation. Cell 81, 495-504.

Hsu H., Huang J., Shu H.B., Baichwal V. and Goeddel D.V. (1996a). TNF-dependent recruitment of the protein kinase RIP to the TNF receptor- 1 signaling complex. Immunity 4, 387-396.

Hsu H., Shu H.B., Pan M.G. and Goeddel D.V. (1996b). TRADD-TRAF2 and TRADD-FADD interactions define two distinct TNF receptor 1 signal transduction pathways. Cell 84, 299-308.

Hu S., Vincenz C., Ni J., Gentz R. and Dixit V.M. (1997). I-FLICE, a novel inhibitor of tumor necrosis factor receptor-1- and CD-95-induced apoptosis. J. Biol. Chem. 272, 17255-17257.

Hu X., Yee E., Harlan J.M., Wong F. and Karsan A. (1998). Lipopolysaccharide induces the antiapoptotic molecules, A1 and A20, in microvascular endothelial cells. Blood 92, 2759-2765.

Huang B., Eberstadt M., Olejniczak E.T., Meadows R.P. and Fesik S.W. (1996). NMR structure and mutagenesis of the Fas (APO-1/CD95) death domain. Nature 384, 638-641.

Ichijo H., Nishida E., Irie K., ten Dijke P., Saitoh M., Moriguchi T., Takagi M., Matsumoto K., Miyazono K. and Gotoh Y. (1997). Induction of apoptosis by ASK1, a mammalian MAPKKK that activates SAPK/JNK and p38 signaling pathways. Science 275, 90-94.

Inohara N., del Peso L., Koseki T., Chen S. and Nunez G. (1998). RICK, a novel protein kinase containing a caspase recruitment domain, interacts with CLARP and regulates CD95-mediated apoptosis [published erratum appears in J. Biol. Chem. 1998 Jul 17;273(29):18675]. J. Biol. Chem. 273, 12296-12300.

Inohara N., Koseki T., Hu Y., Chen S. and Nunez G. (1997). CLARP, a death effector domain-containing protein interacts with caspase-8 and regulates apoptosis. Proc. Natl. Acad. Sci. USA 94, 10717-10722.

Irmler M., Thome M., Hahne M., Schneider P., Hofmann K., Steiner V., Bodmer J.L., Schroter M., Burns K., Mattmann C., Rimoldi D., French L.E. and Tschopp J. (1997). Inhibition of death receptor signals by cellular FLIP. Nature 388, 190-195.

Itoh N. and Nagata S. (1993). A novel protein domain required for apoptosis. Mutational analysis of human Fas antigen. J. Biol. Chem.

268, 10932-10937.

Jaattela M., Mouritzen H., Elling F. and Bastholm L. (1996). A20 zinc finger protein inhibits TNF and IL-1 signaling. J. Immunol. 156, 1166-1173.

Jacobson M.D., Weil M. and Raff M.C. (1997). Programmed cell death in animal development. Cell 88, 347-354.

Jiang Y., Woronicz J.D., Liu W. and Goeddel D.V. (1999). Prevention of constitutive TNF receptor 1 signaling by silencer of death domains [published erratum appears in Science 1999 Mar 19;283(5409):1852]. Science 283, 543-546.

Johnson B.W. and Boise L.H. (1999). Bcl-2 and caspase inhibition cooperate to inhibit tumor necrosis factor-alpha-induced cell death in a Bcl-2 cleavage-independent fashion. J. Biol. Chem. 274, 18552-18558.

Jones S.J., Ledgerwood E.C., Prins J.B., Galbraith J., Johnson D.R., Pober J.S. and Bradley J.R. (1999). TNF recruits TRADD to the plasma membrane but not the trans-Golgi network, the principal subcellular location of TNF-R1. J. Immunol. 162, 1042-1048.

Karin M. (1995). The regulation of AP-1 activity by mitogen-activated protein kinases. J. Biol. Chem. 270, 16483-16486.

Karin M., Liu Z. and Zandi E. (1997). AP-1 function and regulation. Curr. Opin. Cell Biol. 9, 240-246.

Karsan A. (1998). Tumor necrosis factor and endothelial cell death. Trends Cardiovasc. Med. 8, 19-24.

Karsan A., Yee E. and Harlan J.M. (1996). Endothelial cell death induced by tumor necrosis factor-alpha is inhibited by the Bcl-2 family member, A1. J. Biol. Chem. 271, 27201-27204.

Kelliher M.A., Grimm S., Ishida Y., Kuo F., Stanger B.Z. and Leder P. (1998). The death domain kinase RIP mediates the TNF-induced NF-kappaB signal. Immunity 8, 297-303.

Kerr J.F., Wyllie A.H. and Currie A.R. (1972). Apoptosis: a basic biological phenomenon with wide-ranging implications in tissue kinetics. Br. J. Cancer 26, 239-257.

Kim B.C. and Kim J.H. (1997). Nuclear signalling by rac GTPase: essential role of phospholipase A2. Biochem. J. 326, 333-337.

Kim B.C., Lee M.N., Kim J.Y., Lee S.S., Chang J.D., Kim S.S., Lee S.Y. and Kim J.H. (1999). Roles of phosphatidylinositol 3-kinase and Rac in the nuclear signaling by tumor necrosis factor-alpha in rat-2 fibroblasts. J. Biol. Chem. 274, 24372-24377.

Kitson J., Raven T., Jiang Y.P., Goeddel D.V., Giles K.M., Pun K.T., Grinham C.J., Brown R. and Farrow S.N. (1996). A death-domain-containing receptor that mediates apoptosis. Nature 384, 372-375.

Klippel A., Kavanaugh W.M., Pot D. and Williams L.T. (1997). A specific product of phosphatidylinositol 3-kinase directly activates the protein kinase Akt through its pleckstrin homology domain. Mol. Cell. Biol. 17, 338-344.

Kolesnick R.N. (1987). 1,2-Diacylglycerols but not phorbol esters stimulate sphingomyelin hydrolysis in GH3 pituitary cells. J. Biol. Chem. 262, 16759-16762.

Kolesnick R. and Golde D.W. (1994). The sphingomyelin pathway in tumor necrosis factor and interleukin-1 signaling. Cell 77, 325-328.

Kolesnick R.N., Haimovitz-Friedman A. and Fuks Z. (1994). The sphingomyelin signal transduction pathway mediates apoptosis for tumor necrosis factor, Fas, and ionizing radiation. Biochem. Cell Biol. 72, 471-474.

Kramer B., Machleidt T., Wiegmann K. and Kronke M. (1995). Superantigen-induced transcriptional activation of the human TNF gene promoter in T cells. J. Inflamm. 45, 183-192.

Krikos A., Laherty C.D. and Dixit V.M. (1992). Transcriptional activation of the tumor necrosis factor alpha-inducible zinc finger protein, A20, is mediated by kappa B elements. J. Biol. Chem. 267, 17971-17976.

Kroemer G., Zamzami N. and Susin S.A. (1997). Mitochondrial control of apoptosis. Immunol. Today 18, 44-51.

Kyriakis J.M. (1999). Activation of the AP-1 transcription factor by inflammatory cytokines of the TNF family. Gene Expr. 7, 217-231.

Kyriakis J.M. and Avruch J. (1996). Protein kinase cascades activated by stress and inflammatory cytokines. Bioessays 18, 567-577.

Laegreid A., Medvedev A., Nonstad U., Bombara M.P., Ranges G., Sundan A. and Espevik T. (1994). Tumor necrosis factor receptor p75 mediates cell-specific activation of nuclear factor kappa B and induction of human cytomegalovirus enhancer. J. Biol. Chem. 269, 7785-7791.

Lahti J.M., Xiang J., Heath L.S., Campana D. and Kidd V.J. (1995). PITSLRE protein kinase activity is associated with apoptosis. Mol. Cell. Biol. 15, 1-11.

Lallena M.J., Diaz-Meco M.T., Bren G., Paya C.V. and Moscat J. (1999). Activation of IkappaB kinase beta by protein kinase C isoforms. Mol. Cell. Biol. 19, 2180-2188.

Landow L. and Andersen L.W. (1994). Splanchnic ischaemia and its role in multiple organ failure. Acta. Anaesthesiol. Scand. 38, 626-639.

Lassing I. and Lindberg U. (1988). Evidence that the phosphatidylinositol cycle is linked to cell motility. Exp. Cell Res. 174, 1-15.

Ledgerwood E.C., Prins J.B., Bright N.A., Johnson D.R., Wolfreys K., Pober J.S. and Bradley J.R. (1998). Tumor necrosis factor is delivered to mitochondria where a tumor necrosis factor-binding protein is localized. Lab. Invest. 78, 1583-1589.

Lee F.S., Hagler J., Chen Z.J. and Maniatis T. (1997). Activation of the IkappaB alpha kinase complex by MEKK1, a kinase of the JNK pathway. Cell. 88, 213-222.

Lee F.S., Peters R.T., Dang L.C. and Maniatis T. (1998). MEKK1 activates both IkappaB kinase alpha and IkappaB kinase beta. Proc. Natl. Acad. Sci. USA 95, 9319-9324.

Li H., Zhu H., Xu C.J. and Yuan J. (1998). Cleavage of BID by caspase 8 mediates the mitochondrial damage in the Fas pathway of apoptosis. Cell 94, 491-501.

Lin L.L., Wartmann M., Lin A.Y., Knopf J.L., Seth A. and Davis R.J. (1993). cPla2 is phosphorylated and activated by Map kinase. Cell 72, 269-278.

Lin X., Mu Y., Cunningham E.T. Jr., Marcu K.B., Geleziunas R. and Greene W.C. (1998). Molecular determinants of NF-kappaB-inducing kinase action. Mol. Cell. Biol. 18, 5899-5907.

Lin Y., Devin A., Rodriguez Y. and Liu Z.G. (1999). Cleavage of the death domain kinase RIP by caspase-8 prompts TNF-induced apoptosis. Genes Dev. 13, 2514-2526.

Ling L., Cao Z. and Goeddel D.V. (1998). NF-kappaB-inducing kinase activates IKK-alpha by phosphorylation of Ser- 176. Proc. Natl. Acad. Sci. USA 95, 3792-3797.

Liu J., Mathias S., Yang Z. and Kolesnick R.N. (1994). Renaturation and tumor necrosis factor-alpha stimulation of a 97-kDa ceramide-activated protein kinase. J. Biol. Chem. 269, 3047-3052.

Liu X., Kim C.N., Yang J., Jemmerson R. and Wang X. (1996a). Induction of apoptotic program in cell-free extracts: requirement for dATP and cytochrome c. Cell 86, 147-157.

Liu Z.G., Hsu H., Goeddel D.V. and Karin M. (1996b). Dissection of TNF receptor 1 effector functions: JNK activation is not linked to apoptosis while NF-kappaB activation prevents cell death. Cell 87, 565-576.

Loetscher H., Pan Y.C., Lahm H.W., Gentz R., Brockhaus M., Tabuchi

H. and Lesslauer W. (1990). Molecular cloning and expression of the human 55 kd tumor necrosis factor receptor. Cell 61, 351-359.

Lorenzo H.K., Susin S.A., Penninger J. and Kroemer G. (1999). Apoptosis inducing factor (AIF): a phylogenetically old, caspase-independent effector of cell death. Cell Death Differ. 6, 516-524.

Lowenstein E.J., Daly R.J., Batzer A.G., Li W., Margolis B., Lammers R., Ullrich A., Skolnik E.Y., Bar-Sagi D. and Schlessinger J. (1992). The SH2 and SH3 domain-containing protein GRB2 links receptor tyrosine kinases to ras signaling. Cell 70, 431-442.

Lozano J., Berra E., Municio M.M., Diaz-Meco M.T., Dominguez I., Sanz L. and Moscat J. (1994). Protein kinase C zeta isoform is critical for kappa B-dependent promoter activation by sphingomyelinase. J. Biol. Chem. 269, 19200-19202.

Ludwig S., Engel K., Hoffmeyer A., Sithanandam G., Neufeld B., Palm D., Gaestel M. and Rapp U.R. (1996). 3pK, a novel mitogen-activated protein (MAP) kinase-activated protein kinase, is targeted by three MAP kinase pathways. Mol. Cell. Biol. 16, 6687-6697.

Luo X., Budihardjo I., Zou H., Slaughter C. and Wang X. (1998). Bid, a Bcl2 interacting protein, mediates cytochrome c release from mitochondria in response to activation of cell surface death receptors. Cell 94, 481-490.

Machleidt T., Wiegmann K., Henkel T., Schutze S., Baeuerle P. and Kronke M. (1994). Sphingomyelinase activates proteolytic I kappa B-alpha degradation in a cell-free system. J. Biol. Chem. 269, 13760-13765.

Majno G. and Joris I. (1995). Apoptosis, oncosis, and necrosis. An overview of cell death. Am. J. Pathol. 146, 3-15.

Malek N.P., Pluempe J., Kubicka S., Manns M.P. and Trautwein C. (1998). Molecular mechanisms of TNF receptor-mediated signaling. Recent Results Cancer Res. 147, 97-106.

Malinin N.L., Boldin M.P., Kovalenko A.V. and Wallach D. (1997). MAP3K-related kinase involved in NF-kappaB induction by TNF, CD95 and IL-1. Nature 385, 540-544.

Mao P.L., Jiang Y., Wee B.Y. and Porter A.G. (1998). Activation of caspase-1 in the nucleus requires nuclear translocation of pro-caspase-1 mediated by its prodomain. J. Biol. Chem. 273, 23621-23624.

Marsters S.A., Frutkin A.D., Simpson N.J., Fendly B.M. and Ashkenazi A. (1992). Identification of cysteine-rich domains of the type 1 tumor necrosis factor receptor involved in ligand binding. J. Biol. Chem. 267, 5747-5750.

McCarthy J.V., Ni J. and Dixit V.M. (1998). RIP2 is a novel NF-kappaB-activating and cell death-inducing kinase. J. Biol. Chem. 273, 16968-16975.

Medvedev A.E., Sundan A. and Espevik T. (1994). Involvement of the tumor necrosis factor receptor p75 in mediating cytotoxicity and gene regulating activities. Eur. J. Immunol. 24, 2842-2849.

Mehlen P., Hickey E., Weber L.A. and Arrigo A.P. (1997). Large unphosphorylated aggregates as the active form of hsp27 which controls intracellular reactive oxygen species and glutathione levels and generates a protection against TNFalpha in NIH-3T3-ras cells. Biochem. Biophys. Res. Commun. 241, 187-192.

Mehlen P., Mehlen A., Guillet D., Preville X. and Arrigo A.P. (1995). Tumor necrosis factor-alpha induces changes in the phosphorylation, cellular localization, and oligomerization of human hsp27, a stress protein that confers cellular resistance to this cytokine. J. Cell. Biochem. 58, 248-259.

Meldrum D.R. (1998). Tumor necrosis factor in the heart. Am. J. Physiol. 274, R577-595.

Meldrum D.R. and Donnahoo K.K. (1999). Role of TNF in mediating renal insufficiency following cardiac surgery: evidence of a postbypass cardiorenal syndrome. J. Surg. Res. 85, 185-199.

Mercurio F., Zhu H., Murray B.W., Shevchenko A., Bennett B.L., Li J., Young D.B., Barbosa M., Mann M., Manning A. and Rao A. (1997). IKK-1 and IKK-2: cytokine-activated IkappaB kinases essential for NF- kappaB activation. Science 278, 860-866.

Merrill A.H. Jr., Hannun Y.A. and Bell R.M. (1993). Introduction: sphingolipids and their metabolites in cell regulation. Adv. Lipid Res. 25, 1-24.

Michell R.H., Kirk C.J. and Billah M.M. (1979). Hormonal stimulation of phosphatidylinositol breakdown with particular reference to the hepatic effects of vasopressin. Biochem. Soc. Trans. 7, 861-865.

Minden A., Lin A., McMahon M., Lange-Carter C., Derijard B., Davis R.J., Johnson G.L. and Karin M. (1994). Differential activation of ERK and JNK mitogen-activated protein kinases by Raf-1 and MEKK. Science 266, 1719-1723.

Moriguchi T., Toyoshima F., Masuyama N., Hanafusa H., Gotoh Y. and Nishida E. (1997). A novel SAPK/JNK kinase, MKK7, stimulated by TNFalpha and cellular stresses. EMBO J. 16, 7045-7053.

Moss M.L., Jin S.L., Milla M.E., Burkhart W., Carter H.L., Chen W.J., Clay W.C., Didsbury J.R., Hassler D., Hoffman C.R., Kost T.A., Lambert M.H., Leesnitzer M.A., McCauley P., McGeehan G., Mitchell J., Moyer M., Pahel G., Rocque W., Overton L.K., Schoenen F., Seaton T., Su J.L., Warner J., Willard D. and Becherer J.D. (1997). Cloning of a disintegrin metalloproteinase that processes precursor tumour-necrosis factor-alpha [published erratum appears in Nature 1997 Apr 17;386(6626):738]. Nature 385, 733-736.

Muller G., Ayoub M., Storz P., Rennecke J., Fabbro D. and Pfizenmaier K. (1995). PKC zeta is a molecular switch in signal transduction of TNF-alpha, bifunctionally regulated by ceramide and arachidonic acid. EMBO J. 14, 1961-1969.

Munker R., Gasson J., Ogawa M. and Koeffler H.P. (1986). Recombinant human TNF induces production of granulocyte-monocyte colony- stimulating factor. Nature 323, 79-82.

Muzio M., Chinnaiyan A.M., Kischkel F.C., Shevchenko A., Ni J., Scaffidi C., Bretz J.D., Zhang M., Gentz R., Mann M., Krammer P.H., Peter M.E. and Dixit V.M. (1996). FLICE, a novel FADD-homologous ICE/CED-3-like protease, is recruited to the CD95 (Fas/APO-1) death-inducing signaling complex. Cell 85, 817-827.

Muzio M., Stockwell B.R., Stennicke H.R., Salvesen G.S. and Dixit V.M. (1998). An induced proximity model for caspase-8 activation. J. Biol. Chem. 273, 2926-2930.

Nakano H., Shindo M., Sakon S., Nishinaka S., Mihara M., Yagita H. and Okumura K. (1998). Differential regulation of IkappaB kinase alpha and beta by two upstream kinases, NF-kappaB-inducing kinase and mitogen-activated protein kinase/ERK kinase kinase-1. Proc. Natl. Acad. Sci. USA 95, 3537-3542.

Natoli G., Costanzo A., Guido F., Moretti F. and Levrero M. (1998). Apoptotic, non-apoptotic, and anti-apoptotic pathways of tumor necrosis factor signalling. Biochem. Pharmacol. 56, 915-920.

Natoli G., Costanzo A., Ianni A., Templeton D.J., Woodgett J.R., Balsano C. and Levrero M. (1997). Activation of SAPK/JNK by TNF receptor 1 through a noncytotoxic TRAF2- dependent pathway. Science 275, 200-203.

Nedwin G.E., Naylor S.L., Sakaguchi A.Y., Smith D., Jarrett-Nedwin J., Pennica D., Goeddel D.V. and Gray P.W. (1985a). Human lymphotoxin and tumor necrosis factor genes: structure, homology and chromosomal localization. Nucleic Acids Res. 13, 6361-6373.

Nedwin G.E., Svedersky L.P., Bringman T.S., Palladino M.A. Jr. and Goeddel D.V. (1985b). Effect of interleukin 2, interferon-gamma, and mitogens on the production of tumor necrosis factors alpha and beta. J. Immunol. 135, 2492-2497.

Newton R.C. and Decicco C.P. (1999). Therapeutic potential and strategies for inhibiting tumor necrosis factor-alpha. J. Med. Chem. 42, 2295-2314.

Ng P.W., Porter A.G. and Janicke R.U. (1999). Molecular cloning and characterization of two novel pro-apoptotic isoforms of caspase-10. J. Biol. Chem. 274, 10301-10308.

Nicholson D.W. and Thornberry N.A. (1997). Caspases: killer proteases. Trends Biochem. Sci. 22, 299-306.

Nicholson D.W., Ali A., Thornberry N.A., Vaillancourt J.P., Ding C.K., Gallant M., Gareau Y., Griffin P.R., Labelle M., Lazebnik Y.A., Munday N.A., Raju S.M., Smulson M.E., Yamin T.-T., Yu V.L. and Miller D.K. (1995). Identification and inhibition of the ICE/CED-3 protease necessary for mammalian apoptosis. Nature 376, 37-43.

Nishitoh H., Saitoh M., Mochida Y., Takeda K., Nakano H., Rothe M., Miyazono K. and Ichijo H. (1998). ASK1 is essential for JNK/SAPK activation by TRAF2. Mol. Cell. 2, 389-395.

Nocentini G., Giunchi L., Ronchetti S., Krausz L.T., Bartoli A., Moraca R., Migliorati G. and Riccardi C. (1997). A new member of the tumor necrosis factor/nerve growth factor receptor family inhibits T cell receptor-induced apoptosis. Proc. Natl. Acad. Sci. USA 94, 6216-6221.

Nophar Y., Kemper O., Brakebusch C., Englemann H., Zwang R., Aderka D., Holtmann H. and Wallach D. (1990). Soluble forms of tumor necrosis factor receptors (TNF-Rs). The cDNA for the type I TNF-R, cloned using amino acid sequence data of its soluble form, encodes both the cell surface and a soluble form of the receptor. EMBO J. 9, 3269-3278.

Orlinick J.R. and Chao M.V. (1998). TNF-related ligands and their receptors. Cell. Signal. 10, 543-551.

Ozes O.N., Mayo L.D., Gustin J.A., Pfeffer S.R., Pfeffer L.M. and Donner D.B. (1999). NF-kappaB activation by tumour necrosis factor requires the Akt serine- threonine kinase. Nature 401, 82-85.

Pan G. and Dixit V.M. (1998). Caspase-9, Bcl-XL, and Apaf-1 form a ternary complex. J. Biol. Chem. 273, 5841-5845.

Pan G., Chinnaiyan A.M., Gentz R., Ebner R., Ni J. and Dixit V.M. (1997a). The receptor for the cytotoxic ligand TRAIL. Science 276, 111-113.

Pan G., Ni J., Wei Y.F., Yu G., Gentz R. and Dixit V.M. (1997b). An antagonist decoy receptor and a death domain-containing receptor for TRAIL. Science 277, 815-818.

Park Y.M., Han M.Y., Blackburn R.V. and Lee Y.J. (1998). Overexpression of HSP25 reduces the level of TNF alpha-induced oxidative DNA damage biomarker, 8-hydroxy-2'-deoxyguanosine, in L929 cells. J. Cell. Physiol. 174, 27-34.

Paul A., Wilson S., Belham C.M., Robinson C.J., Scott P.H., Gould G.W. and Plevin R. (1997). Stress-activated protein kinases: activation, regulation and function. Cell. Signal. 9, 403-410.

Pauli U. (1994). Control of tumor necrosis factor gene expression. Crit. Rev. Eukaryot Gene Expr. 4, 323-344.

Peraldi P. and Spiegelman B. (1998). TNF-alpha and insulin resistance: summary and future prospects. Mol. Cell. Biochem. 182, 169-175.

Perez C., Albert I., DeFay K., Zachariades N., Gooding L. and Kriegler M. (1990). A nonsecretable cell surface mutant of tumor necrosis factor (TNF) kills by cell-to-cell contact. Cell 63, 251-258.

Pfeilschifter J. and Huwiler A. (1998). Identification of ceramide targets in interleukin-1 and tumor necrosis factor-alpha signaling in mesangial cells. Kidney Int. Suppl. 67, S34-39.

Platzer C., Meisel C., Vogt K., Platzer M. and Volk H.D. (1995). Up-regulation of monocytic IL-10 by tumor necrosis factor-alpha and cAMP elevating drugs. Int. Immunol. 7, 517-523.

Preville X., Schultz H., Knauf U., Gaestel M. and Arrigo A.P. (1998). Analysis of the role of Hsp25 phosphorylation reveals the importance of the oligomerization state of this small heat shock protein in its protective function against TNFalpha- and hydrogen peroxide-induced cell death. J. Cell. Biochem. 69, 436-452.

Puls A., Schmidt S., Grawe F. and Stabel S. (1997). Interaction of protein kinase C zeta with ZIP, a novel protein kinase C-binding protein. Proc. Natl. Acad. Sci. USA 94, 6191-6196.

Raine C.S. (1995). Multiple sclerosis: TNF revisited, with promise. Nat. Med. 1, 211-214.

Rasper D.M., Vaillancourt J.P., Hadano S., Houtzager V.M., Seiden I., Keen S.L., Tawa P., Xanthoudakis S., Nasir J., Martindale D., Koop B.F., Peterson E.P., Thornberry N.A., Huang J., MacPherson D.P., Black S.C., Hornung F., Lenardo M.J., Hayden M.R., Roy S. and Nicholson D.W. (1998). Cell death attenuation by 'Usurpin', a mammalian DED-caspase homologue that precludes caspase-8 recruitment and activation by the CD-95 (Fas, APO-1) receptor complex. Cell Death Differ. 5, 271-288.

Reddy S.A., Chaturvedi M.M., Darnay B.G., Chan H., Higuchi M. and Aggarwal B.B. (1994). Reconstitution of nuclear factor kappa B activation induced by tumor necrosis factor requires membrane-associated components. Comparison with pathway activated by ceramide. J. Biol. Chem. 269, 25369-25372.

Regnier C.H., Song H.Y., Gao X., Goeddel D.V., Cao Z. and Rothe M. (1997). Identification and characterization of an IkappaB kinase. Cell 90, 373-383.

Reimold A.M., Grusby M.J., Kosaras B., Fries J.W., Mori R., Maniwa S., Clauss I.M., Collins T., Sidman R.L., Glimcher M.J. and Glimcher L.H. (1996). Chondrodysplasia and neurological abnormalities in ATF-2-deficient mice. Nature 379, 262-265.

Reinhard C., Shamoon B., Shyamala V. and Williams L.T. (1997). Tumor necrosis factor alpha-induced activation of c-jun N-terminal kinase is mediated by TRAF2. EMBO J. 16, 1080-1092.

Relaix F., Wei X.J., Wu X. and Sassoon D.A. (1998). Peg3/Pw1 is an imprinted gene involved in the TNF-NFkappaB signal transduction pathway. Nat. Genet. 18, 287-291.

Rizzo M.T. and Carlo-Stella C. (1996). Arachidonic acid mediates interleukin-1 and tumor necrosis factor-alpha-induced activation of the c-jun amino-terminal kinases in stromal cells. Blood 88, 3792-3800.

Robinson M.J. and Cobb M.H. (1997). Mitogen-activated protein kinase pathways. Curr. Opin. Cell Biol. 9, 180-186.

Roger T., Out T., Mukaida N., Matsushima K., Jansen H. and Lutter R. (1998). Enhanced AP-1 and NF-kappaB activities and stability of interleukin 8 (IL-8) transcripts are implicated in IL-8 mRNA superinduction in lung epithelial H292 cells. Biochem. J. 330, 429-435.

Rothe M., Sarma V., Dixit V.M. and Goeddel D.V. (1995). TRAF2-mediated activation of NF-kappa B by TNF receptor 2 and CD40. Science 269, 1424-1427.

Rothe M., Wong S.C., Henzel W.J. and Goeddel D.V. (1994). A novel family of putative signal transducers associated with the cytoplasmic domain of the 75 kDa tumor necrosis factor receptor. Cell 78, 681-692.

Rothwarf D.M., Zandi E., Natoli G. and Karin M. (1998). IKK-gamma is an essential regulatory subunit of the IkappaB kinase complex. Nature 395, 297-300.

Roulston A., Reinhard C., Amiri P. and Williams L.T. (1998). Early activation of c-Jun N-terminal kinase and p38 kinase regulate cell survival in response to tumor necrosis factor alpha. J. Biol. Chem. 273, 10232-10239.

Rus H.G., Niculescu F. and Vlaicu R. (1991). Tumor necrosis factor-alpha in human arterial wall with atherosclerosis. Atherosclerosis 89, 247-254.

Saha N., Moldovan F., Tardif G., Pelletier J.P., Cloutier J.M. and Martel-Pelletier J. (1999). Interleukin-1beta-converting enzyme/caspase-1 in human osteoarthritic tissues: localization and role in the maturation of interleukin-1beta and interleukin-18. Arthritis Rheum. 42, 1577-1587.

Sakahira H., Enari M. and Nagata S. (1998). Cleavage of CAD inhibitor in CAD activation and DNA degradation during apoptosis. Nature 391, 96-99.

Samuelsson B., Dahlen S.E., Lindgren J.A., Rouzer C.A. and Serhan C.N. (1987). Leukotrienes and lipoxins: structures, biosynthesis, and biological effects. Science 237, 1171-1176.

Sanchez P., De Carcer G., Sandoval I.V., Moscat J. and Diaz-Meco M.T. (1998). Localization of atypical protein kinase C isoforms into lysosome-targeted endosomes through interaction with p62. Mol. Cell. Biol. 18, 3069-3080.

Sanz L., Sanchez P., Lallena M.J., Diaz-Meco M.T. and Moscat J. (1999). The interaction of p62 with RIP links the atypical PKCs to NF-kappaB activation. EMBO J. 18, 3044-3053.

Sawai H., Okazaki T., Takeda Y., Tashima M., Sawada H., Okuma M., Kishi S., Umehara H. and Domae N. (1997). Ceramide-induced translocation of protein kinase C-delta and -epsilon to the cytosol. Implications in apoptosis. J. Biol. Chem. 272, 2452-2458.

Schall T.J., Lewis M., Koller K.J., Lee A., Rice G.C., Wong G.H., Gatanaga T., Granger G.A., Lentz R., Raab H., Kohr W.J. and Goeddel D.V. (1990). Molecular cloning and expression of a receptor for human tumor necrosis factor. Cell 61, 361-370.

Schonbeck U., Mach F., Bonnefoy J.Y., Loppnow H., Flad H.D. and Libby P. (1997). Ligation of CD40 activates interleukin 1beta-converting enzyme (caspase- 1) activity in vascular smooth muscle and endothelial cells and promotes elaboration of active interleukin 1beta. J. Biol. Chem. 272, 19569-19574.

Schreck R., Rieber P. and Baeuerle P.A. (1991). Reactive oxygen intermediates as apparently widely used messengers in the activation of the NF-kappa B transcription factor and HIV-1. EMBO J. 10, 2247-2258.

Schulze-Osthoff K., Bakker A.C., Vanhaesebroeck B., Beyaert R., Jacob W.A. and Fiers W. (1992). Cytotoxic activity of tumor necrosis factor is mediated by early damage of mitochondrial functions. Evidence for the involvement of mitochondrial radical generation. J. Biol. Chem. 267, 5317-5323.

Schulze-Osthoff K., Beyaert R., Vandevoorde V., Haegeman G. and Fiers W. (1993). Depletion of the mitochondrial electron transport abrogates the cytotoxic and gene-inductive effects of TNF. EMBO J. 12, 3095-3104.

Schutze S., Berkovic D., Tomsing O., Unger C. and Kronke M. (1991). Tumor necrosis factor induces rapid production of 1'2'diacylglycerol by a phosphatidylcholine-specific phospholipase C. J. Exp. Med. 174, 975-988.

Schutze S., Potthoff K., Machleidt T., Berkovic D., Wiegmann K. and Kronke M. (1992). TNF activates NF-kappa B by phosphatidylcholine-specific phospholipase C-induced "acidic" sphingomyelin breakdown. Cell 71, 765-776.

Schutze S., Machleidt T., Adam D., Schwandner R., Wiegmann K., Kruse M.L., Heinrich M., Wickel M. and Kronke M. (1999). Inhibition of receptor internalization by monodansylcadaverine selectively blocks p55 tumor necrosis factor receptor death domain signaling. J. Biol. Chem. 274, 10203-10212.

Schwenzer R., Siemienski K., Liptay S., Schubert G., Peters N., Scheurich P., Schmid R.M. and Wajant H. (1999). The human tumor necrosis factor (TNF) receptor-associated factor 1 gene (TRAF1) is up-regulated by cytokines of the TNF ligand family and modulates TNF-induced activation of NF-kappaB and c-Jun N-terminal kinase. J. Biol. Chem. 274, 19368-19374.

Selmaj K., Raine C.S., Cannella B. and Brosnan C.F. (1991). Identification of lymphotoxin and tumor necrosis factor in multiple sclerosis lesions. J. Clin. Invest. 87, 949-954.

Shan B. and Lee W.H. (1994). Deregulated expression of E2F-1 induces S-phase entry and leads to apoptosis. Mol. Cell. Biol. 14, 8166-8173.

Shi C.S. and Kehrl J.H. (1997). Activation of stress-activated protein kinase/c-Jun N-terminal kinase, but not NF-kappaB, by the tumor necrosis factor (TNF) receptor 1 through a TNF receptor-associated factor 2- and germinal center kinase related-dependent pathway. J. Biol. Chem. 272, 32102-32107.

Shu H.B., Halpin D.R. and Goeddel D.V. (1997). Casper is a FADD- and caspase-related inducer of apoptosis. Immunity 6, 751-763.

Shu H.B., Takeuchi M. and Goeddel D.V. (1996). The tumor necrosis factor receptor 2 signal transducers TRAF2 and c- IAP1 are components of the tumor necrosis factor receptor 1 signaling complex. Proc. Natl. Acad. Sci. USA 93, 13973-13978.

Siebenlist U., Franzoso G. and Brown K. (1994). Structure, regulation and function of NF-kappa B. Annu. Rev. Cell Biol. 10, 405-455.

Siegel R.M., Martin D.A., Zheng L., Ng S.Y., Bertin J., Cohen J. and Lenardo M.J. (1998). Death-effector filaments: novel cytoplasmic structures that recruit caspases and trigger apoptosis. J. Cell Biol. 141, 1243-1253.

Singh N., Sun Y., Nakamura K., Smith M.R. and Colburn N.H. (1995). C-JUN/AP-1 as possible mediators of tumor necrosis factor-alpha-induced apoptotic response in mouse JB6 tumor cells. Oncol. Res. 7, 353-362.

Smith C.A., Davis T., Anderson D., Solam L., Beckmann M.P., Jerzy R., Dower S.K., Cosman D. and Goodwin R.G. (1990). A receptor for tumor necrosis factor defines an unusual family of cellular and viral proteins. Science 248, 1019-1023.

Smith C.A., Farrah T. and Goodwin R.G. (1994). The TNF receptor superfamily of cellular and viral proteins: activation, costimulation, and death. Cell 76, 959-962.

Smith P.J. and Ross D.A. (1993). Tubed radial fascial flap and reconstruction of the flexor apparatus in the forearm [published erratum appears in J. Hand Surg. [Am] 1994 Nov;19(6):1064]. J. Hand Surg. [Am] 18, 959-962.

Song H.Y., Regnier C.H., Kirschning C.J., Goeddel D.V. and Rothe M. (1997). Tumor necrosis factor (TNF)-mediated kinase cascades: bifurcation of nuclear factor-kappaB and c-jun N-terminal kinase (JNK/SAPK) pathways at TNF receptor-associated factor 2. Proc. Natl. Acad. Sci. USA 94, 9792-9796.

Spence M.W. (1993). Sphingomyelinases. Adv. Lipid Res. 26, 3-23.

Spiegel S. and Merrill A.H. Jr. (1996). Sphingolipid metabolism and cell

growth regulation. FASEB J. 10, 1388-1397.

Srinivasula S.M., Ahmad M., Fernandes-Alnemri T. and Alnemri E.S. (1998). Autoactivation of procaspase-9 by Apaf-1-mediated oligomerization. Mol. Cell. 1, 949-957.

Srinivasula S.M., Ahmad M., Lin J.H., Poyet J.L., Fernandes-Alnemri T., Tsichlis P.N. and Alnemri E.S. (1999). CLAP, a novel caspase recruitment domain-containing protein in the tumor necrosis factor receptor pathway, regulates NF-kappaB activation and apoptosis. J. Biol. Chem. 274, 17946-17954.

Stanger B.Z., Leder P., Lee T.H., Kim E. and Seed B. (1995). RIP: a novel protein containing a death domain that interacts with Fas/APO-1 (CD95) in yeast and causes cell death. Cell 81, 513-523.

Stennicke H.R., Jurgensmeier J.M., Shin H., Deveraux Q., Wolf B.B., Yang X., Zhou Q., Ellerby H.M., Ellerby L.M., Bredesen D., Green D.R., Reed J.C., Froelich C.J. and Salvesen G.S. (1998). Procaspase-3 is a major physiologic target of caspase-8. J. Biol. Chem. 273, 27084-27090.

Stokoe D., Engel K., Campbell D.G., Cohen P. and Gaestel M. (1992). Identification of MAPKAP kinase 2 as a major enzyme responsible for the phosphorylation of the small mammalian heat shock proteins. FEBS Lett. 313, 307-313.

Stokoe D., Stephens L.R., Copeland T., Gaffney P.R., Reese C.B., Painter G.F., Holmes A.B., McCormick F. and Hawkins P.T. (1997). Dual role of phosphatidylinositol-3,4,5-trisphosphate in the activation of protein kinase B. Science 277, 567-570.

Stroka D.M., Badrichani A.Z., Bach F.H. and Ferran C. (1999). Overexpression of A1, an NF-kappaB-inducible anti-apoptotic bcl gene, inhibits endothelial cell activation. Blood 93, 3803-3810.

Subramaniam M., Saffaripour S., Van De Water L., Frenette P.S., Mayadas T.N., Hynes R.O. and Wagner D.D. (1997). Role of endothelial selectins in wound repair. Am. J. Pathol. 150, 1701-1709.

Susin S.A., Lorenzo H.K., Zamzami N., Marzo I., Brenner C., Larochette N., Prevost M.C., Alzari P.M. and Kroemer G. (1999). Mitochondrial release of caspase-2 and -9 during the apoptotic process. J. Exp. Med. 189, 381-394.

Susin S.A., Zamzami N., Castedo M., Hirsch T., Marchetti P., Macho A., Daugas E., Geuskens M. and Kroemer G. (1996). Bcl-2 inhibits the mitochondrial release of an apoptogenic protease. J. Exp. Med. 184, 1331-1341.

Suzuki H., Chiba T., Kobayashi M., Takeuchi M., Furuichi K. and Tanaka K. (1999). *In vivo* and *in vitro* recruitment of an IkappaBalpha-ubiquitin ligase to IkappaBalpha phosphorylated by IKK, leading to ubiquitination. Biochem. Biophys. Res. Commun. 256, 121-126.

Swantek J.L., Cobb M.H. and Geppert T.D. (1997). Jun N-terminal kinase/stress-activated protein kinase (JNK/SAPK) is required for lipopolysaccharide stimulation of tumor necrosis factor alpha (TNF-alpha) translation: glucocorticoids inhibit TNF-alpha translation by blocking JNK/SAPK. Mol. Cell. Biol. 17, 6274-6282.

Takahashi N., Udagawa N. and Suda T. (1999). A new member of tumor necrosis factor ligand family, ODF/OPGL/TRANCE/RANKL, regulates osteoclast differentiation and function. Biochem. Biophys. Res. Commun. 256, 449-455.

Takashiba S., Shapira L., Amar S. and Van Dyke T.E. (1993). Cloning and characterization of human TNF alpha promoter region. Gene 131, 307-308.

Tan X., Martin S.J., Green D.R. and Wang J.Y.J. (1997). Degradation of retinoblastoma protein in tumor necrosis factor- and CD95-induced cell death. J. Biol. Chem. 272, 9613-9616.

Tancredi V., Grassi F., Tarroni P., Palmieri G., Santoni A. and Eusebi F. (1992). Tumor necrosis factor alters synaptic transmission in rat hippocampal slices. Neurosci. Lett. 146, 176-178.

Tartaglia L.A. and Goeddel D.V. (1992). Two TNF receptors. Immunol. Today 13, 151-153.

Tartaglia L.A., Ayres T.M., Wong G.H. and Goeddel D.V. (1993a). A novel domain within the 55 kd TNF receptor signals cell death. Cell 74, 845-853.

Tartaglia L.A., Pennica D. and Goeddel D.V. (1993b). Ligand passing: the 75-kDa tumor necrosis factor (TNF) receptor recruits TNF for signaling by the 55-kDa TNF receptor. J. Biol. Chem. 268, 18542-18548.

Tartaglia L.A., Rothe M., Hu Y.F. and Goeddel D.V. (1993c). Tumor necrosis factor's cytotoxic activity is signaled by the p55 TNF receptor. Cell 73, 213-216.

Taupin V., Renno T., Bourbonniere L., Peterson A.C., Rodriguez M. and Owens T. (1997). Increased severity of experimental autoimmune encephalomyelitis, chronic macrophage/microglial reactivity, and demyelination in transgenic mice producing tumor necrosis factor-alpha in the central nervous system. Eur. J. Immunol. 27, 905-913.

Tewari M., Beidler D.R. and Dixit V.M. (1995a). CrmA-inhibitable cleavage of the 70-kDa protein component of the U1 small nuclear ribonucleoprotein during Fas- and tumor necrosis factor-induced apoptosis. J. Biol. Chem. 270, 18738-18741.

Tewari M., Quan L.T., O'Rourke K., Desnoyers S., Zeng Z., Beidler D.R., Poirier G.G., Salvesen G.S. and Dixit V.M. (1995b). Yama/CPP32 beta, a mammalian homolog of CED-3, is a CrmA-inhibitable protease that cleaves the death substrate poly(ADP-ribose) polymerase. Cell 81, 801-809.

Thanos D. and Maniatis T. (1995). NF-kappa B: a lesson in family values. Cell 80, 529-532.

Thoma B., Grell M., Pfizenmaier K. and Scheurich P. (1990). Identification of a 60-kD tumor necrosis factor (TNF) receptor as the major signal transducing component in TNF responses. J. Exp. Med. 172, 1019-1023.

Thomas P.S., Pennington D.W., Schreck R.E., Levine T.M. and Lazarus S.C. (1996). Authentic 17 kDa tumour necrosis factor alpha is synthesized and released by canine mast cells and up-regulated by stem cell factor. Clin. Exp. Allergy 26, 710-718.

Thome M., Hofmann K., Burns K., Martinon F., Bodmer J.L., Mattmann C. and Tschopp J. (1998). Identification of CARDIAK, a RIP-like kinase that associates with caspase-1. Curr. Biol. 8, 885-888.

Thome M., Schneider P., Hofmann K., Fickenscher H., Meinl E., Neipel F., Mattmann C., Burns K., Bodmer J.L., Schroter M., Scaffidi C., Krammer P.H., Peter M.E. and Tschopp J. (1997). Viral FLICE-inhibitory proteins (FLIPs) prevent apoptosis induced by death receptors. Nature 386, 517-521.

Tomei L.D. and Cope F.O. (1994). Apoptosis II: the molecular basis of apoptosis in disease. Cold Spring Harbor Laboratory. Cold Spring Harbor. New York.

Tracey K.J. and Cerami A. (1993). Tumor necrosis factor, other cytokines and disease. Annu. Rev. Cell Biol. 9, 317-343.

Traenckner E.B., Pahl H.L., Henkel T., Schmidt K.N., Wilk S. and Baeuerle P.A. (1995). Phosphorylation of human I kappa B-alpha on serines 32 and 36 controls I kappa B-alpha proteolysis and NF-kappa B activation in response to diverse stimuli. EMBO J. 14, 2876-2883.

Trofimova M., Sprenkle A.B., Green M., Sturgill T.W., Goebl M.G. and

Harrington M.A. (1996). Developmental and tissue-specific expression of mouse pelle-like protein kinase. J. Biol. Chem. 271, 17609-17612.

Tsujimoto M., Yip Y.K. and Vilcek J. (1985). Tumor necrosis factor: specific binding and internalization in sensitive and resistant cells. Proc. Natl. Acad. Sci. USA 82, 7626-7630.

Ueda A., Ishigatsubo Y., Okubo T. and Yoshimura T. (1997). Transcriptional regulation of the human monocyte chemoattractant protein-1 gene. Cooperation of two NF-kappaB sites and NF-kappaB/Rel subunit specificity. J. Biol. Chem. 272, 31092-31099.

Uren A.G., Pakusch M., Hawkins C.J., Puls K.L. and Vaux D.L. (1996). Cloning and expression of apoptosis inhibitory protein homologs that function to inhibit apoptosis and/or bind tumor necrosis factor receptor-associated factors. Proc. Natl. Acad. Sci. USA 93, 4974-4978.

Vale R.D. (1987). Intracellular transport using microtubule-based motors. Annu. Rev. Cell Biol. 3, 347-378.

Van Antwerp D.J., Martin S.J., Kafri T., Green D.R. and Verma I.M. (1996). Suppression of TNF-alpha-induced apoptosis by NF-kappaB. Science 274, 787-789.

Van der Poll T., Romijn J.A., Endert E., Borm J.J., Buller H.R. and Sauerwein H.P. (1991). Tumor necrosis factor mimics the metabolic response to acute infection in healthy humans. Am. J. Physiol. 261, E457-465.

van der Poll T., Calvano S.E., Kumar A., Braxton C.C., Coyle S.M., Barbosa K., Moldawer L.L. and Lowry S.F. (1995). Endotoxin induces downregulation of tumor necrosis factor receptors on circulating monocytes and granulocytes in humans. Blood 86, 2754-2759.

Van Zee K.J., Kohno T., Fischer E., Rock C.S., Moldawer L.L. and Lowry S.F. (1992). Tumor necrosis factor soluble receptors circulate during experimental and clinical inflammation and can protect against excessive tumor necrosis factor alpha *in vitro* and *in vivo*. Proc. Natl. Acad. Sci. USA 89, 4845-4849.

Vandenabeele P., Declerq W., Beyaert R. and Fiers W. (1995). Two tumor necrosis factor receptors: structure and function. Trends Cell Biol. 5, 392-399.

Vassalli P. (1992). The pathophysiology of tumor necrosis factors. Annu. Rev. Immunol. 10, 411-452.

Vercammen D., Beyaert R., Denecker G., Goossens V., Van Loo G., Declercq W., Grooten J., Fiers W. and Vandenabeele P. (1998). Inhibition of caspases increases the sensitivity of L929 cells to necrosis mediated by tumor necrosis factor. J. Exp. Med. 187, 1477-1485.

Vietor I., Schwenger P., Li W., Schlessinger J. and Vilcek J. (1993). Tumor necrosis factor-induced activation and increased tyrosine phosphorylation of mitogen-activated protein (MAP) kinase in human fibroblasts. J. Biol. Chem. 268, 18994-18999.

Vig E., Green M., Liu Y., Donner D.B., Mukaida N., Goebl M.G. and Harrington M.A. (1999). Modulation of tumor necrosis factor and interleukin-1-dependent NF- kappaB activity by mPLK/IRAK. J. Biol. Chem. 274, 13077-13084.

Vincenz C. and Dixit V.M. (1997). Fas-associated death domain protein interleukin-1beta-converting enzyme 2 (FLICE2), an ICE/Ced-3 homologue, is proximally involved in CD95- and p55-mediated death signaling. J. Biol. Chem. 272, 6578-6583.

Wallach D. (1997). Cell death induction by TNF: a matter of self control. Trends Biochem. Sci. 22, 107-109.

Wang C.Y., Mayo M.W. and Baldwin A.S. Jr. (1996). TNF- and cancer therapy-induced apoptosis: potentiation by inhibition of NF-kappaB. Science 274, 784-787.

Wang C.Y., Mayo M.W., Korneluk R.G., Goeddel D.V. and Baldwin A.S. Jr. (1998). NF-kappaB antiapoptosis: induction of TRAF1 and TRAF2 and c-IAP1 and c-IAP2 to suppress caspase-8 activation. Science 281, 1680-1683.

Ware C.F., VanArsdale S. and VanArsdale T.L. (1996). Apoptosis mediated by the TNF-related cytokine and receptor families. J. Cell. Biochem. 60, 47-55.

Weiss T., Grell M., Siemienski K., Muhlenbeck F., Durkop H., Pfizenmaier K., Scheurich P. and Wajant H. (1998). TNFR80-dependent enhancement of TNFR60-induced cell death is mediated by TNFR-associated factor 2 and is specific for TNFR60. J. Immunol. 161, 3136-3142.

White E. (1996). Life, death, and the pursuit of apoptosis. Genes Dev. 10, 1-15.

Wickel M., Heinrich M., Rosenbaum C., Gahr J., Schwandner R., Kreder D., Brunner J., Kronke M. and Schutze S. (1998). Identification of cathepsin D as a novel ceramide-target involved in TNF signaling. J. Interferon Cytokine Res. 18, A-77 (Abstract).

Wiegmann K., Schutze S., Machleidt T., Witte D. and Kronke M. (1994). Functional dichotomy of neutral and acidic sphingomyelinases in tumor necrosis factor signaling. Cell 78, 1005-1015.

Wiegmann K., Schwandner R., Krut O., Yeh W.C., Mak T.W. and Kronke M. (1999). Requirement of FADD for tumor necrosis factor-induced activation of acid sphingomyelinase. J. Biol. Chem. 274, 5267-5270.

Winston B.W., Chan E.D., Johnson G.L. and Riches D.W. (1997). Activation of p38mapk, MKK3, and MKK4 by TNF-alpha in mouse bone marrow-derived macrophages. J. Immunol. 159, 4491-4497.

Winston B.W., Remigio L.K. and Riches D.W. (1995). Preferential involvement of MEK1 in the tumor necrosis factor-alpha-induced activation of p42mapk/erk2 in mouse macrophages. J. Biol. Chem. 270, 27391-27394.

Wolff R.A., Dobrowsky R.T., Bielawska A., Obeid L.M. and Hannun Y.A. (1994). Role of ceramide-activated protein phosphatase in ceramide-mediated signal transduction. J. Biol. Chem. 269, 19605-19609.

Woodgett J.R., Kyriakis J.M., Avruch J., Zon L.I., Zanke B. and Templeton D.J. (1996). Reconstitution of novel signalling cascades responding to cellular stresses. Philos. Trans. R. Soc. Lond. B. Biol. Sci. 351, 135-141; discussion 142.

Woronicz J.D., Gao X., Cao Z., Rothe M. and Goeddel D.V. (1997). IkappaB kinase-beta: NF-kappaB activation and complex formation with IkappaB kinase-alpha and NIK. Science 278, 866-869.

Wu M.X., Ao Z., Prasad K.V., Wu R. and Schlossman S.F. (1998). IEX-1L, an apoptosis inhibitor involved in NF-kappaB-mediated cell survival. Science 281, 998-1001.

Xia P., Wang L., Gamble J.R. and Vadas M.A. (1999). Activation of sphingosine kinase by tumor necrosis factor-alpha inhibits apoptosis in human endothelial cells. J. Biol. Chem. 274, 34499-34505.

Yamauchi N., Kuriyama H., Watanabe N., Neda H., Maeda M. and Niitsu Y. (1989). Intracellular hydroxyl radical production induced by recombinant human tumor necrosis factor and its implication in the killing of tumor cells *in vitro*. Cancer Res. 49, 1671-1675.

Yan Z., Yang D.C. and Jett M. (1999). Cholera toxin induces tumor necrosis factor alpha production in human monocytes. Mol. Cell. Biol. Res. Commun. 2, 124-130.

Yang E., Zha J., Jockel J., Boise L.H., Thompson C.B. and Korsmeyer

S.J. (1995). Bad, a heterodimeric partner for Bcl-XL and Bcl-2, displaces Bax and promotes cell death. Cell 80, 285-291.

Yang Z., Costanzo M., Golde D.W. and Kolesnick R.N. (1993). Tumor necrosis factor activation of the sphingomyelin pathway signals nuclear factor kappa B translocation in intact HL-60 cells. J. Biol. Chem. 268, 20520-20523.

Yao B., Zhang Y., Delikat S., Mathias S., Basu S. and Kolesnick R. (1995). Phosphorylation of Raf by ceramide-activated protein kinase. Nature 378, 307-310.

Yeh W.C., Pompa J.L., McCurrach M.E., Shu H.B., Elia A.J., Shahinian A., Ng M., Wakeham A., Khoo W., Mitchell K., El-Deiry W.S., Lowe S.W., Goeddel D.V. and Mak T.W. (1998). FADD: essential for embryo development and signaling from some, but not all, inducers of apoptosis. Science 279, 1954-1958.

Yu P.W., Huang B.C., Shen M., Quast J., Chan E., Xu X., Nolan G.P., Payan D.G. and Luo Y. (1999). Identification of RIP3, a RIP-like kinase that activates apoptosis and NFkappaB. Curr. Biol. 9, 539-542.

Yuan J. (1997). Transducing signals of life and death. Curr. Opin. Cell Biol. 9, 247-251.

Yuasa T., Ohno S., Kehrl J.H. and Kyriakis J.M. (1998). Tumor necrosis factor signaling to stress-activated protein kinase (SAPK)/Jun NH2-terminal kinase (JNK) and p38. Germinal center kinase couples TRAF2 to mitogen-activated protein kinase/ERK kinase kinase 1 and SAPK while receptor interacting protein associates with a mitogen-activated protein kinase kinase kinase upstream of MKK6 and p38. J. Biol. Chem. 273, 22681-22692.

Zandi E., Rothwarf D.M., Delhase M., Hayakawa M. and Karin M. (1997). The IkappaB kinase complex (IKK) contains two kinase subunits, IKKalpha and IKKbeta, necessary for IkappaB phosphorylation and NF-kappaB activation. Cell 91, 243-252.

Zhang C., Baumgartner R.A., Yamada K. and Beaven M.A. (1997). Mitogen-activated protein (MAP) kinase regulates production of tumor necrosis factor-alpha and release of arachidonic acid in mast cells. Indications of communication between p38 and p42 MAP kinases. J. Biol. Chem. 272, 13397-13402.

Zhang J., Cado D., Chen A., Kabra N.H. and Winoto A. (1998). Fas-mediated apoptosis and activation-induced T-cell proliferation are defective in mice lacking FADD/Mort1. Nature 392, 296-300.

Zheng L., Fisher G., Miller R.E., Peschon J., Lynch D.H. and Lenardo M.J. (1995). Induction of apoptosis in mature T cells by tumour necrosis factor. Nature 377, 348-351.

Zhong H., SuYang H., Erdjument-Bromage H., Tempst P. and Ghosh S. (1997). The transcriptional activity of NF-kappaB is regulated by the IkappaB-associated PKAc subunit through a cyclic AMP-independent mechanism. Cell 89, 413-424.

Zou H., Henzel W.J., Liu X., Lutschg A. and Wang X. (1997). Apaf-1, a human protein homologous to *C. elegans* CED-4, participates in cytochrome c-dependent activation of caspase-3. Cell 90, 405-413.

Accepted June 16, 2000

This page intentionally blank

[CANCER RESEARCH 61, 6788–6794, September 15, 2001]

Inhibition of Tumor Cell Invasion and Angiogenesis by Motuporamines[1]

Calvin D. Roskelley, David E. Williams, Lianne M. McHardy, Kevin G. Leong, Armelle Troussard, Aly Karsan, Raymond J. Andersen, Shoukat Dedhar, and Michel Roberge[2]

Departments of Anatomy [C. D. R., L. M. M.], Chemistry and Oceanography (EOS) [D. E. W., R. J. A.], and Biochemistry and Molecular Biology [L. M. M., M. R.], University of British Columbia, Vancouver, British Columbia V6T 1Z3; Departments of Pathology and Medical Biophysics, British Columbia Cancer Agency, Vancouver, British Columbia V5Z 1L3 [K. G. L., A. K.]; and Jack Bell Research Laboratories, Vancouver, British Columbia V6H 3Z6 [A. T., S. D.], Canada

ABSTRACT

Tissue invasion is an important determinant of angiogenesis and metastasis and constitutes an attractive target for cancer therapy. We have developed an assay to identify agents that inhibit invasion by mechanisms other than inhibition of cell attachment or cytotoxicity. A screen of marine sponge extracts identified motuporamines as micromolar inhibitors of invasion of basement membrane gels by MDA-231 breast carcinoma, PC-3 prostate carcinoma, and U-87 and U-251 glioma cells. Motuporamine C inhibits cell migration in monolayer cultures and impairs actin-mediated membrane ruffling at the leading edge of lamellae. Motuporamine C also reduces β1-integrin activation, raising the possibility that it interferes with "inside-out" signaling to integrins. In addition, motuporamine C inhibits angiogenesis in an *in vitro* sprouting assay with human endothelial cells and an *in vivo* chick chorioallantoic membrane assay. The motuporamines show little or no toxicity or inhibition of cell proliferation, and they are structurally simple and easy to synthesize, making them attractive drug candidates.

INTRODUCTION

The ability of cancer cells to invade adjacent tissues and to stimulate neovascularization is critical to tumor growth and metastasis (1). Tissue invasion allows primary tumors to disseminate and form metastases, the cause of 90% of cancer deaths (2). Tumors also stimulate the formation of new blood vessels without which they cannot grow beyond a size of 1–2 mm and cannot metastasize (3). Consequently, the elucidation of the mechanisms governing metastasis and angiogenesis and the development of therapies aimed at preventing these processes are the focus of intense research.

Invasion, angiogenesis, and metastasis all require cells to modify their adhesion to other cells and to the extracellular matrix, to break down the matrix, and to migrate through the breaches thus created (3, 4). Therefore, agents that inhibit the movement of tumor cells and endothelial cells through the extracellular matrix have the potential to be of considerable therapeutic value.

We have developed a quantitative assay suitable for testing crude natural extracts for inhibitors of this process. In an initial small-scale screen, we found that a family of marine sponge alkaloids, the motuporamines, inhibit the invasion of metastatic MDA-231 breast carcinoma cells. In subsequent testing, we demonstrate that motuporamine C interferes with the migration and leading edge ruffling of human breast cancer cells, prostate carcinoma cells, and glioma cells. In addition, motuporamine C inhibits angiogenesis in both an *in vitro* sprouting assay and an *in vivo* chick chorioallantoic membrane assay. These properties, combined with its low cytotoxicity and ease of synthesis, make motuporamine C an attractive drug candidate.

Received 4/5/01; accepted 7/18/01.

The costs of publication of this article were defrayed in part by the payment of page charges. This article must therefore be hereby marked *advertisement* in accordance with 18 U.S.C. Section 1734 solely to indicate this fact.

[1] Supported by the Canadian Breast Cancer Research Initiative (to C. D. R., M. R.), the Natural Sciences and Engineering Research Council of Canada (to R. J. A.), and the National Cancer Institute of Canada (S. D., A. K.).

[2] To whom requests for reprints should be addressed, at Department of Biochemistry and Molecular Biology, University of British Columbia, 2146 Health Sciences Mall, Vancouver, British Columbia, Canada V6T 1Z3. Phone: (604) 822-2304; Fax: (604) 822-5227; E-mail: michel@otter.biochem.ubc.ca.

MATERIALS AND METHODS

Cell Culture. Human breast carcinoma MDA-231 and MDA-453 cells, prostate carcinoma PC-3 cells, and glioma U-87 and U-251 cells were routinely maintained in monolayer culture in DMEM:Ham's F-12 (1:1) medium containing 5% FBS[3] and 50 units/ml gentamicin. HUVECs were isolated by flushing fresh umbilical cord veins with RPMI followed by collagenase A in RPMI (0.13 mg/ml). The cords were then filled with collagenase A and incubated at room temperature for 30 min. After massaging the cords to dislodge cells, the contents were flushed with RPMI and harvested by centrifugation. The cell pellet was washed with RPMI and suspended in MCDB medium supplemented with 10% FBS, 10% iron-supplemented FBS, 16 units/ml heparin, 20 μg/ml endothelial cell growth supplement (Collaborative Biomedical Products), 2 mM glutamine, and 100 units/ml each of penicillin and streptomycin. For the initial passage, cells were plated onto dishes coated with 0.2% gelatin to promote HUVEC attachment. Subsequent passages were performed using standard tissue culture-treated dishes. All of the cells were maintained at 37°C in 5% CO_2.

Marine Organism Collection and Extract Preparation. Approximately 250 g each of marine sponges were collected by hand, using scuba, from tropical Pacific Ocean reefs off Motupore and Madang in Papua, New Guinea. Samples were deep frozen on site and transported to Vancouver, British Columbia, Canada over dry ice. Voucher samples of each are kept in methanol at −20°C at the University of British Columbia for taxonomic identification. Extracts were prepared by homogenizing 200 g of each sponge sample in methanol. The homogenates were filtered and concentrated *in vacuo* to give a gummy residue. About 1 mg was dissolved in 100 μl of DMSO for use in the invasion inhibition screen.

Three-step Assay for Invasion Inhibitors. Reconstituted basement membrane (Matrigel; Collaborative Biomedical Products) was diluted 1:1 in ice-cold DMEM:Ham's F-12, and 50 μl was distributed into each well of ice-cold 96-well cell culture plates. The plates were transferred to a 37°C incubator overnight to allow the Matrigel to polymerize and adhere to the plastic. On top of the Matrigel was added 100 μl of growth medium warmed to 37°C, with or without 1 μl of sponge extract dissolved in DMSO, followed by 100 μl of medium containing 60,000 highly invasive MDA-231 cells. Addition of 1 μl of DMSO served as a negative control and 125 μM LY294002 served as a positive control. The cells were then incubated for 2.5 h to allow invasion to take place. After incubation, cells had either invaded the Matrigel or failed to invade and settled on the surface of the Matrigel. The cell culture medium was then removed without disturbing the cells using the aspiration function of a Bio-Tek ELx405 96-well plate washer with the aspiration needles positioned about 2 mm above the surface of the Matrigel. The attached cells that failed to invade were recovered by detaching them from the surface of the Matrigel by incubation with 200 μl of 0.125% trypsin in HBSS for 30 min at 37°C. The cells were then suspended by pipetting up and down three times using the 100-μl setting of a hand-held pipettor, and 100 μl were withdrawn and transferred to fresh plates without Matrigel containing 100 μl of medium supplemented with 30% FBS. The cells were then incubated overnight to allow attachment of cells to the plastic surface, and live cells were measured using the MTT assay (5).

Isolation of Motuporamines. A portion of the sponge (86 g) was extracted repeatedly with methanol. The combined methanol extracts were concentrated *in vacuo* and partitioned between water and ethyl acetate to give a water layer active in the assay. *n*-butyl alcohol extracted the bioactive material from the

[3] The abbreviations used are: FBS, fetal bovine serum; HUVEC, human umbilical vein endothelial cell; VEGF, vascular endothelial growth factor; MTT, 3-(4,5-dimethylthiazol-2-yl)-2,5-diphenyltetrazolium bromide; CAM, chorioallantoic membrane.

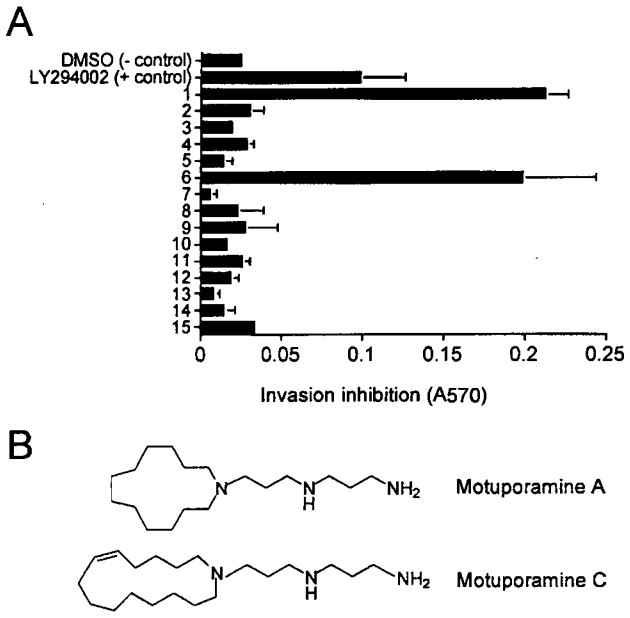

Fig. 1. Inhibition of invasion by two crude sponge extracts and chemical structures of motuporamines A and C. *A*, MDA-231 cells were incubated with Matrigel in the presence of sponge extracts for 2.5 h as described in "Materials and Methods." Cells that failed to invade were recovered by trypsinization and replated. After overnight incubation, live cells were measured using the MTT assay in which the absorbance at 570 nm provides a quantitative measure of the number of cells that failed to invade. Shown are averages and SD of duplicate measurements of the effects of DMSO (negative control), 125 μM LY294002 (positive control), and 15 of the sponge extracts. *B*, structural formulae of motuporamines isolated from extract #1 from *Xestospongia exigua*.

water layer. Concentration of the *n*-butyl alcohol extracts *in vacuo* gave an active residue that was suspended in water adjusted to pH >12 by addition of NaOH. Extraction of the basic aqueous solution with CH_2Cl_2 followed by evaporation of the combined CH_2Cl_2 extracts *in vacuo* gave a residue active in the assay. The bioactive residue was first fractionated via Sephadex LH20 chromatography eluting with methanol followed by a second Sephadex LH20 chromatography eluting with the mixed solvent system ethyl acetate/methanol/water (20:5:2). The active materials were further fractionated by reversed-phase high-performance liquid chromatography [eluent, 2% trifluoroacetic acid in methanol/water (11:9)] to give pure samples of the known compounds motuporamines A and C (6), a sample of monoacetylmotuporamine C (an artifact resulting from reaction of motuporamine C with ethyl acetate during purification), and mixtures of a number of minor related analogues. Diacetylated derivatives of the motuporamines were prepared by dissolving them in pyridine/acetic anhydride (3:1) and stirring at room temperature for 16 h. Removal of the reagents by evaporation *in vacuo* gave diacetylated motuporamines that were purified via reversed-phase high-performance liquid chromatography [eluent, acetonitrile/0.6% trifluoroactic acid in H_2O (2:3)].

Integrin Activation State. Integrin expression on the cell surface was analyzed by flow cytometry. PC3 cells were serum-starved overnight and then incubated for 1 h in medium without serum containing the indicated concentrations of motuporamine C. Cells were washed and harvested by scraping. Cells were suspended in 200 μl of PBS (pH 7.4), 20 mM glucose, and 1% BSA and incubated with 4 μg of anti-activated β1 integrin (MAB2079Z; Chemicon) or total-β1 integrin (Upstate Biotechnology) monoclonal antibody. After a 45-min incubation at room temperature, cells were incubated with 1 μg of FITC-conjugated antimouse secondary antibody (Jackson Laboratories) for 30 min at room temperature. Cells were analyzed on a Coulter EXPO XL4 flow cytometer. Experiments were performed in duplicate and repeated three times.

Endothelial Sprouting Assay. Endothelial sprouting was assessed by a modification of the method used by Nehls and Drenckhahn (7). Briefly, microcarrier beads coated with denatured collagen (Cytodex 3; Sigma Chemical Co.) were seeded with HUVECs and embedded in fibrin gels in 96-well plates. For preparation of fibrin gels, bovine fibrinogen was dissolved in MCDB medium at a concentration of 2.5 mg/ml. Aprotinin was added at a concentration of 0.05 mg/ml, and the solution was passed through a 0.22-μm filter. The fibrinogen solution was supplemented with 15 ng/ml VEGF. As a control, fibrinogen solution without VEGF was used. Motuporamine C was also added at different concentrations, and the fibrinogen solutions were transferred to 96-well plates together with HUVEC-coated beads at a density of 50 beads/well. Clotting was induced by the addition of thrombin (1.2 units/ml). After clotting was complete, gels were equilibrated with MCDB medium containing 5% FBS at 37°C. After 60 min of incubation, the medium was replaced with medium with or without motuporamine C. After 3 days of incubation with daily changes of the medium, the number of capillary-like tubes formed/microcarrier bead (sprouts/bead) was counted by microscopy, monitoring at least 150 beads for each treatment. Only sprouts greater that 150 μm in length and composed of at least three endothelial cells were counted.

Chick CAM Assay for Angiogenesis. Fertilized White Leghorn chicken eggs were incubated at 37°C under conditions of constant humidity. On embryonic day 6, the developing CAM was separated from the shell by opening a small circular window at the broad end of the egg above the air sac. The opening was sealed with Parafilm, and the eggs were incubated for 2 more days. Motuporamine C was prepared in PBS supplemented with 30 ng/ml VEGF. On day 8, 20 μl was loaded onto 2-mm^3 gelatin sponges (Gelfoam; Pharmacia Upjohn) that were placed on the surface of the developing CAM. Sponges containing vehicle alone (20 μl of PBS) were used as negative controls, whereas sponges containing 20 μl of 30 ng/ml VEGF in PBS were used as positive controls. Eggs were resealed and returned to the incubator. On day 10, images of CAM were captured digitally using an Olympus SZX9 stereomicroscope equipped with a Spot RT digital imaging system (Diagnostic Instruments).

Cell Viability and Proliferation Assays. HUVEC viability was determined as follows. Cells were plated in 96-well plates at 1.5×10^5 cells/well. When cells reached 95% confluency, motuporamine C was added at different concentrations and for different times, with daily change of medium and drug, and cell viability was measured by incubating cells with 100 μl of 0.005% neutral red in cell culture medium for 4 h. The medium was removed, and 100 μl of 1% acetic acid in 50% ethanol was added/well to solubilize the dye and absorbance was measured at 550 nm. HUVEC proliferation was determined as follows. Cells were plated in 96-well plates at 5×10^3 cells/well and incubated with different concentrations of motuporamine C, with daily change of medium and drug. Cell proliferation was measured at 0, 24, 48, and 72 h using neutral red as described above. MDA 231 proliferation was determined as follows. Cells were plated in 96-well plates at 1×10^3 cells and treated with different concentrations of motuporamine C for 24 h. Proliferation was measured at different times using the MTT assay (5).

RESULTS

Three-step Screen for Invasion Inhibitors. The "outgrowth" assay and the "Boyden chamber" assay are widely used to study invasion. In the former, cells are suspended in liquid Matrigel followed by

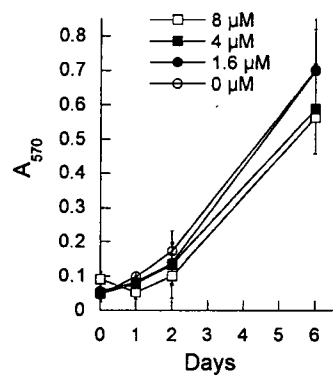

Fig. 2. Effect of motuporamine C on cell proliferation. MDA-231 cells plated in a 96-well plate at a density of 1000 cells/well were exposed to the indicated concentrations of motuporamine C at day 0. Twenty-four h later (day 1), the compound was removed and the cells were allowed to proliferate in the absence of compound. Cell proliferation was measured using the MTT assay at the indicated days. Averages and SD of quadruplicate measurements are shown.

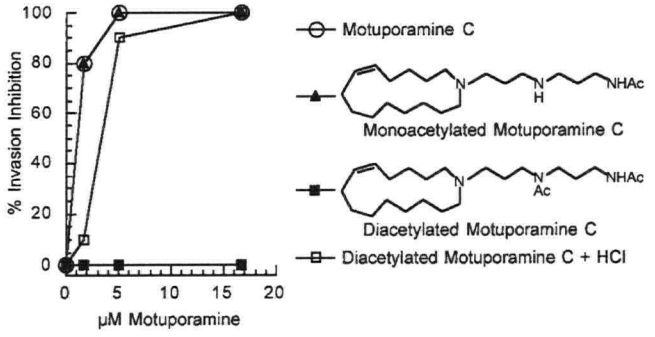

Fig. 3. Importance of the tail amines for invasion inhibition. Motuporamine C and derivatives were prepared and tested at different concentrations in the invasion inhibition assay.

gelling, and invasion is then assayed morphologically as the cells form outgrowths into the gel (8). In the latter, Matrigel is pre-gelled upon a porous filter support. Cells are then placed on the Matrigel, and invasion is quantified by measuring the number of cells that cross to the other side of the Matrigel/filter barrier, usually in response to a chemotactic agent (9). Both assays have proven very useful for studying mechanisms that regulate invasion, but they have drawbacks that make them less suited for screening for invasion inhibitors. The major drawback of outgrowth assays is the difficulty in quantifying changes in cell morphology. The Boyden chamber assays do generate quantitative data, but they are unable to discriminate between agents that affect invasion, adhesion, and cell viability.

Nature is a prime source of drug leads (10). However, an inherent problem with using crude natural extracts in cell-based screens is that 10–20% of the extracts are toxic to cells at the dilutions that generate optimal hit rates because of the high concentrations of salts and other materials they contain. To avoid unacceptably high numbers of false-positive results, a screen needs to distinguish invasion inhibition attributable to a specific inhibitor from that caused by cell death or toxicity. We have combined the principles of the Matrigel outgrowth and the Boyden chamber assays in a three-step screen for invasion inhibitors. The assay is quantitative and screens sequentially for compounds that prevent invasion of Matrigel, do not prevent cell attachment to Matrigel, and are not cytotoxic.

We first tested the suitability of the assay for drug screening using a small selection of crude methanol extracts from marine sponges. Two-hundred and thirty extracts were tested at 50–100 μg/ml. Two-hundred and twenty-eight extracts showed absorbance readings close to or below those of the DMSO carrier negative controls (0.025). Two extracts showed strong inhibition of invasion (Fig. 1*A*) higher than LY294002, a phosphatidylinositol 3-kinase inhibitor known to inhibit invasion (11).

Isolation and Identification of Motuporamines. The active compounds were purified from extract #1 as described in "Materials and Methods," using the assay to guide fractionation. The sponge yielding extract #6 resembled the first sponge and contained the same active compounds. The active compounds were identified as motuporamine A and motuporamine C (Fig. 1*B*), two macrocyclic alkaloids with a spermidine-like "tail" (6). The compounds showed concentration-dependent activity with IC_{50} of 3 μM for motuporamine A and 1 μM for motuporamine C. Only motuporamine C was obtained in sufficient quantities for further study. As expected from the design of the screening assay, motuporamine C did not inhibit the proliferation of MDA-231 cells at a concentration close to the IC_{50} for invasion inhibition (Fig. 2). Higher concentrations of 4 and 8 μM showed only a mild inhibition of cell proliferation.

Importance of the Spermidine-like Tail for Activity. A conspicuous feature of motuporamines is their spermidine-like tail, which carries positive charges at physiological pH. To examine the role of the tail in invasion inhibition, motuporamine C was acetylated at one or both amines of the tail, and the compounds were tested for activity.

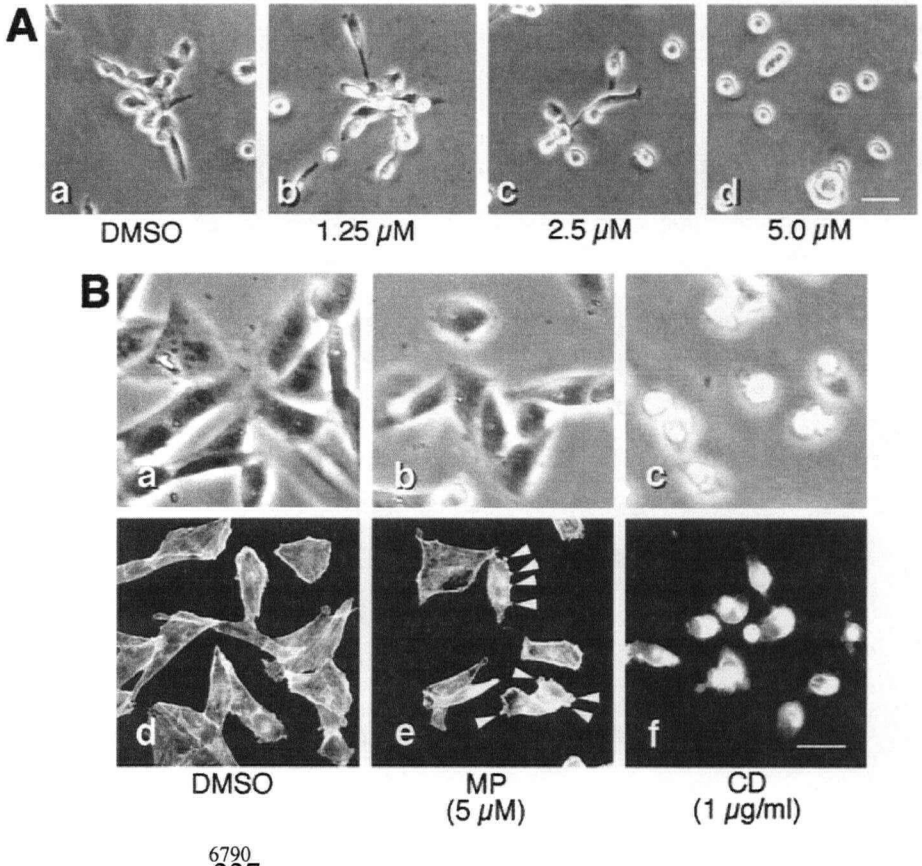

Fig. 4. Motuporamine C inhibits invasion of basement membrane gels and subtly affects cell morphology in monolayer culture. *A*, MDA-231 cells were plated on Matrigel in the presence of the vehicle control (*DMSO*; 0.1%) or the indicated concentrations of motuporamine C for 4 h (*bar*, 20 μm). *B*, MDA-231 cells were pre-spread in monolayer culture after attachment to tissue culture plastic and then treated with the vehicle control (*DMSO*) or 5 μM motuporamine C or 1 μg/ml cytochalasin D (*CD*) for 4 h. Cell morphology was then assessed by phase contrast microscopy of live cultures (*parts a–c*), and actin was visualized by rhodamine-phalloidin staining (*parts d–f*; *arrowheads*, small discontinuous aggregations of actin at cell edges; *bar*, 15 μm).

Table 1 *Comparison of the ability of motuporamine C (5 μM) to inhibit basement membrane invasion, inhibit migration in wounded monolayers, and disrupt leading edge actin-based ruffles in four different tumor lines*

Activity	MDA-231 breast carcinoma	PC-3 prostate carcinoma	U-87 glioma	U-251 glioma
Inhibition of basement membrane invasion	++[a]	+[b]	++	+++
Inhibition of migration	++	+	ND[c]	+++
Disruption of leading edge ruffles	++	++	ND[d]	++

[a] For each category, MDA-231 was designated the standard with a value of ++.
[b] At 4 h after treatment, the inhibitory effect on PC-3 was less than for MDA-231; however, the inhibition was greater for PC-3 at later time points (*i.e.*, 24 h).
[c] ND, not done; this cell line did not form confluent monolayers that could be wounded.
[d] ND, not done; this cell line did not form clearly discernible leading edge ruffles under control conditions.

Acetylation of the terminal amino group had no effect on activity, whereas acetylation of both the terminal and central amines caused a complete loss of activity (Fig. 3). HCl treatment of diacetylated motuporamine C removed both acetates and restored activity (Fig. 3). Therefore, the terminal amino group is dispensable for activity, but the central amine is absolutely required.

Morphological Analysis of Invasion Inhibition by Motuporamine C. MDA-231 cells are highly invasive, both *in vivo* and *in vitro* (12). These cells become spindle-shaped and move into basement membrane gels within 4 h. Incubation of the cells with motuporamine C at the time of plating prevented these morphological responses (Fig. 4*A*). It is noteworthy that the motuporamine C concentration that strongly inhibited basement membrane invasion (5 μM) did not cause the cells to detach from the matrix. Instead, the cells remained rounded, attached, and, for the most part, single (Fig. 4*A*, *part d*). Motuporamine C (5 μM) had similar morphological effects on prostate carcinoma (PC-3) and glioma (U-251 and U-87) cells (Table 1). Therefore, the activity observed in the initial three-step screen using MDA-231 cells correctly identified motuporamine C as a cancer cell invasion inhibitor, and the follow-up morphological experiments with other cell lines indicates widespread *in vitro* efficacy.

The actin cytoskeleton regulates changes in cell shape (13). The

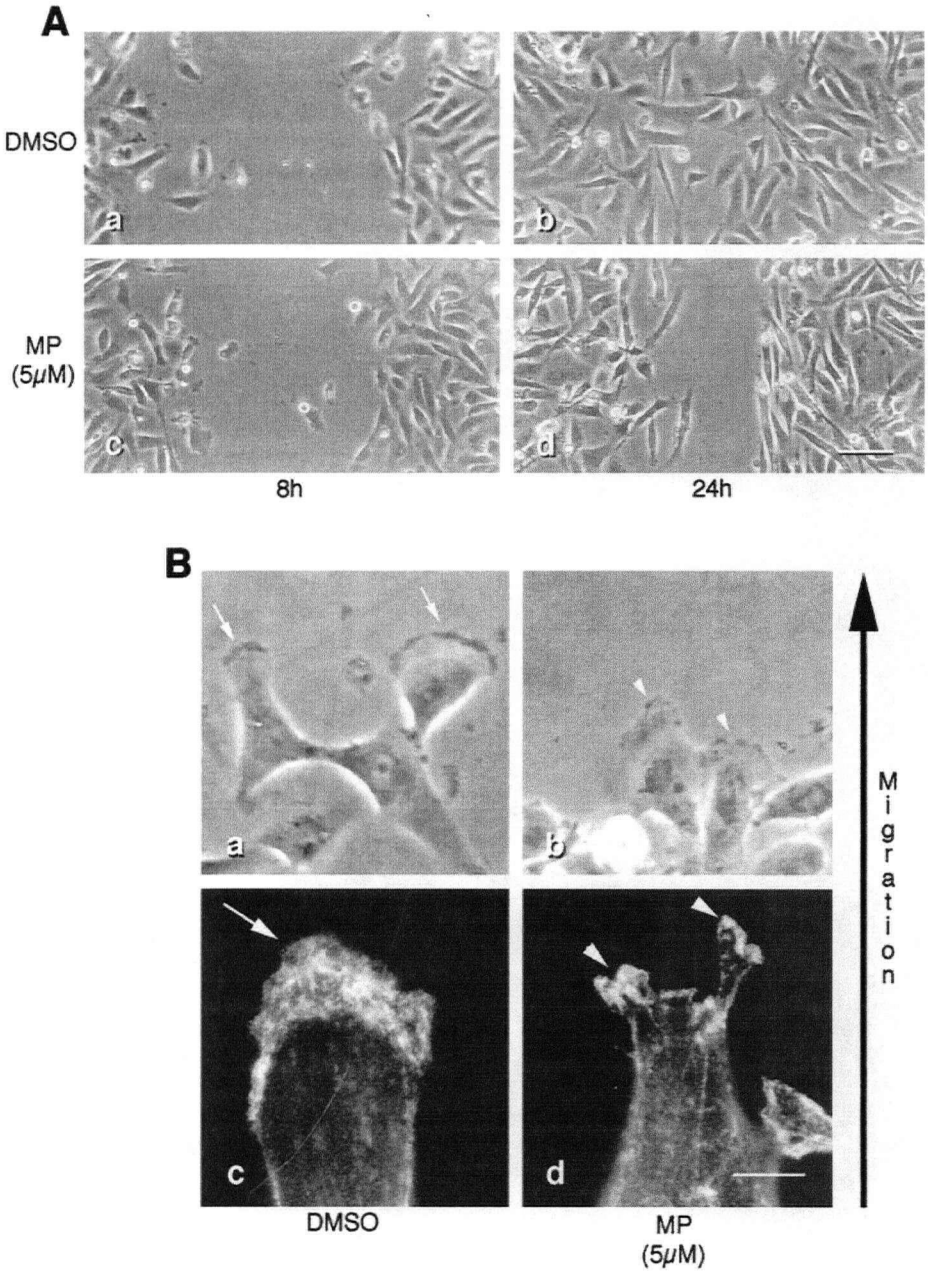

Fig. 5. Motuporamine C inhibits cell migration and perturbs actin ruffling in leading lamellae. *A*, confluent MDA-231 cell monolayers were wounded with a sterile toothpick (*vertical orientation* in the micrographs), and cells were allowed to migrate into the wound over a 24-h period in the presence of the vehicle control (*DMSO*) or 5 μM motuporamine C (*MP*; *bar*, 30 μm). *B*, MDA-231 monolayers were wounded and maintained for 8 h in the presence of DMSO or 5 μM motuporamine C and then photographed live by phase contrast microscopy or stained for filamentous actin with rhodamine-phalloidin. The wound is located in the *top* portion of each photomicrograph. The *black arrow* on the *right* indicates the direction of cell migration (*white arrows*, continuous membrane ruffles in control cultures; *white arrowheads*, discontinuous ruffles in motuporamine treated cultures; *bar*, 20 μm for *parts a* and *b* and 10 μm for *parts c* and *d*).

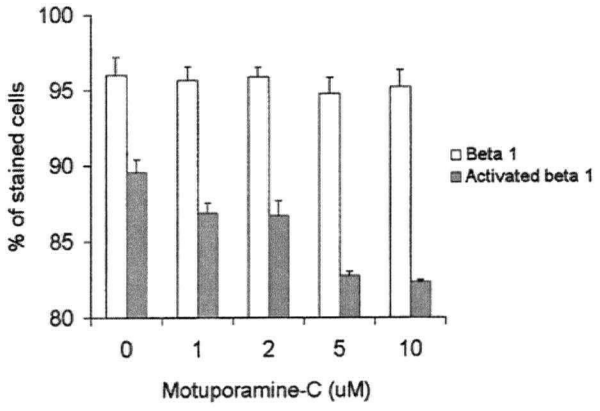

Fig. 6. Motuporamine C decreases β1-integrin activation. PC-3 prostate carcinoma cells in serum-free monolayer culture were treated with the indicated dose of motuporamine C for 1 h. The percentage of cells expressing either total (activated and nonactivated) or only activated β1 integrin on their surface was then determined by flow cytometry.

observation that motuporamine C-treated MDA-231 cells remained rounded but attached on malleable basement membrane gels suggested that it might be acting to disrupt the actin cytoskeleton. To test this, we plated MDA-231 cells on a rigid tissue culture plastic in the presence of serum. When motuporamine C was added at the time of plating, it slowed cell spreading slightly but it did not prevent it (data not shown). When cells were first allowed to attach and spread on the tissue culture plastic substratum, subsequent treatment with motuporamine C did not cause cell rounding, although the cells retracted slightly (Fig. 4*B*). The effects of motuporamine C treatment on the actin cytoskeleton of pre-spread cells was subtle. Cytoplasmic actin stress fibers were still visible, but small discrete "buttons" of actin localization were observed at cell edges (Fig. 4*B*, *arrowheads*). In contrast, treatment of pre-spread cells with the filamentous actin disrupting agent cytochalasin D (1 μg/ml) caused cells to round up and cytoplasmic actin filaments to disassemble (Fig. 4*B*). Therefore, motuporamine C did not cause a global disruption of the actin cytoskeleton in MDA-231 cells.

Motuporamine C Decreases Cell Migration. The subtle effects of motuporamine C on cell shape and the actin cytoskeleton led us to suspect that it might inhibit invasion, at least in part, by decreasing cell migration. Therefore, we examined cell migration across "wounded" monolayers on a tissue culture plastic substratum. A sterile toothpick was drawn across a confluent monolayer of MDA-231 cells leaving a cell-free gap of about 100 μm. In control cultures, the cells migrated into the gap and obliterated it within 24 h (Fig. 5*A*). In contrast, in cultures treated with motuporamine C (5 μM) a significant gap was still present at 24 h. This inhibition of migration was also observed in prostate carcinoma and one of the glioma cell lines tested (Table 1). Although no significant differences in wound closure were observed between control and motuporamine C-treated MDA-231 cell cultures after only 8 h of treatment, we did notice a slight morphological difference at this earlier time point. In control cultures, cells at the edge of the wound had broad leading lamellae that were located in the direction of migration. As expected in migrating cells, the leading edge of control lamellae was continuous and phase-dark, which is indicative of ruffling membranes (Fig. 5*B*, *part a*). This was confirmed by phalloidin staining, which demonstrated filamentous actin condensation in the ruffles (Fig. 5*B*, *part b*). These lamellae were along their leading edges with actin condensations throughout. In contrast, cells treated with motuporamine C had only small and discontinuous ruffles along their leading edges (Fig. 5*B*, *part c*). These small ruffles contained discrete patches of actin condensation (Fig. 5*B*, *part d*), similar to the "button-like" condensations observed in pre-spread nonmigrating cells (see Fig. 4*B*, *part e*). We also observed this fragmentation of leading edge ruffles in prostate carcinoma and glioma cell lines (Table 1).

Motuporamine C Partially Inhibits Integrin Activation. When cells in monolayer culture migrate, actin-containing membrane ruffles at the edge of the leading lamellae are the sites at which adhesive contacts between the cell and substratum are initiated. It is now accepted that during cell migration, such contacts are strengthened and weakened in a cyclical manner. Changes in the strength of adhesion may be modulated by changes in the affinity of integrins for their ligands, a process that can be regulated from the cell interior, the so-called "inside-out" signaling (14). To determine whether motuporamine C affected the affinity of a major class of integrins, we analyzed the reactivity of PC-3 cells to an antibody that recognizes only the "activated" form of β1-containing integrins (15). As shown in Fig. 6, exposure of PC-3 cells to motuporamine C resulted in a small dose-dependent reduction of the binding of the "activated" β1 antibody compared with the total β1 antibody. The results show that motuporamine C exposure causes conformational changes in β1-integrins leading to a decrease of "activated" β1 on the surface of PC-3 cells. This effect of motuporamine C was subtle but highly reproducible, consistent with the effects on cell spreading and migration (see Figs. 4 and 5 above) in the absence of discernable effects on cell adhesion *per se*.

Motuporamine C Inhibits Endothelial Sprouting and Angiogenesis. The formation of new blood vessels requires endothelial cells to invade the extracellular matrix, raising the possibility that motuporamine C also inhibits angiogenesis. This was tested using an *in vitro* endothelial sprouting assay and an *in vivo* CAM assay. In the endothelial sprouting

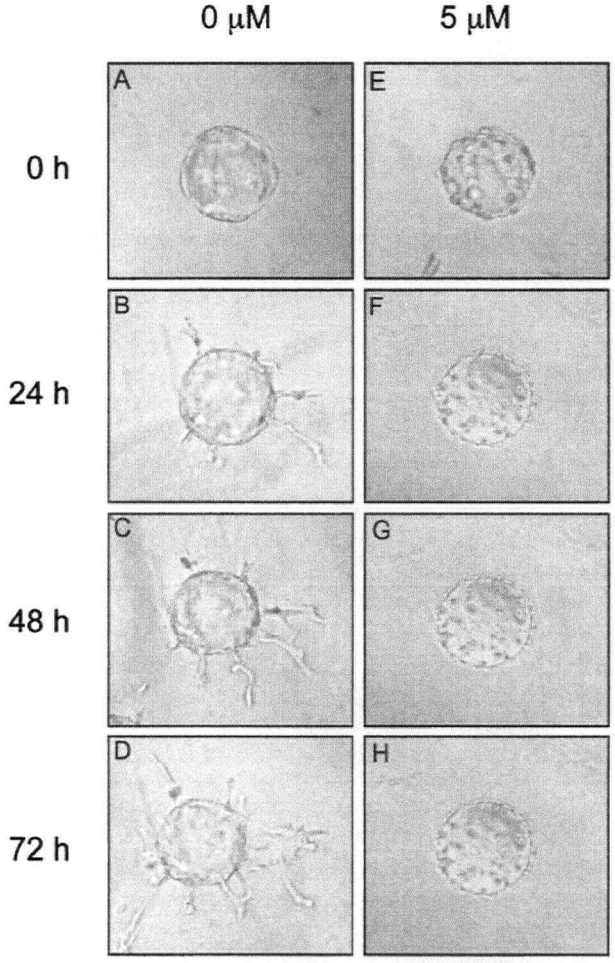

Fig. 7. Motuporamine C inhibits endothelial cell sprouting *in vitro*. HUVEC-coated beads were incubated in the presence of 15 ng/ml VEGF with the indicated concentrations of motuporamine C. Phase contrast micrographs of a typical bead were taken at the indicated times to illustrate the effects of the compound on sprout formation and cell morphology.

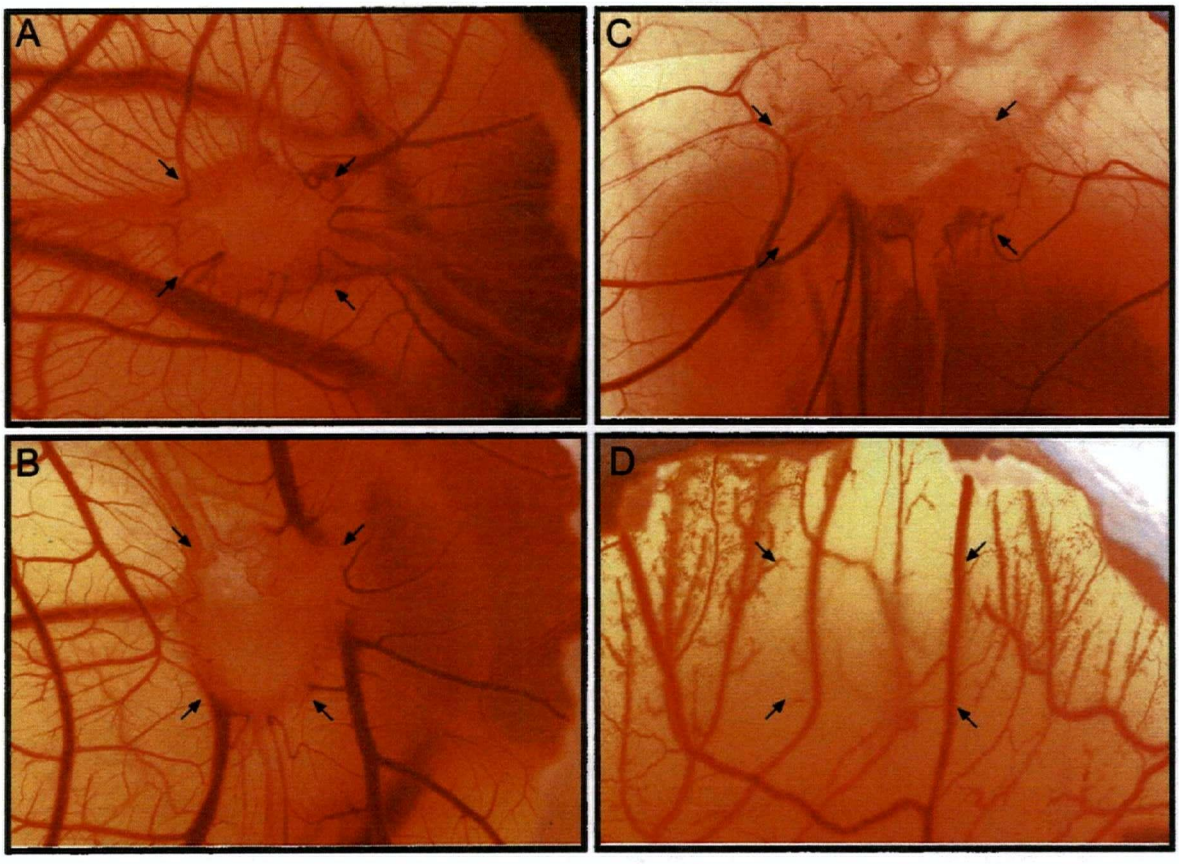

Fig. 8. Motuporamine C inhibits angiogenesis *in vivo*. Photographs of developing CAMs incubated for 2 days with VEGF (*A*) or VEGF and motuporamine C at 2.5 μM (*B*), 5 μM (*C*), or 10 μM (*D*). The *arrows* indicate the corners of the gelatin sponges containing VEGF and the compounds.

assay, HUVECs are seeded onto collagen-coated beads. Exposure to VEGF stimulates the formation of capillary-like tubes, the number and length of which may be measured over time by microscopy (Fig. 7). In two separate experiments, endothelial sprouting quantitated at 72 h was inhibited by 88% and 93% with 5 μM motuporamine C and was inhibited completely with 10 μM motuporamine C (see Fig. 7 for examples). In the CAM assay, angiogenesis in response to VEGF (30 ng/ml) was reduced by treatment with 2.5 μM and 5 μM motuporamine C and was completely inhibited at 10 μM motuporamine C (Fig. 8). Motuporamine C was not toxic in the CAM assay when tested at concentrations of up to 25 μM (data not shown).

Finally, we examined the effects of motuporamine C on the survival and proliferation of HUVECs. Incubation of rapidly proliferating HUVECs with different concentrations of motuporamine C for up to 3 days did not inhibit cell proliferation (Fig. 9*A*). Exposure of confluent, nonproliferating HUVEC monolayers to different motuporamine concentrations for up to 3 days also had no effects on cell survival (Fig. 9*B*). Therefore, as was the case for invasion, motuporamine C does not inhibit angiogenesis through toxic or antiproliferative effects.

DISCUSSION

Invasion and angiogenesis are important determinants of tumor progression and, as such, constitute attractive targets for cancer therapy. Extracts from marine invertebrates, particularly sponges, are a rich source of secondary metabolites with potential as lead compounds for the development of therapeutic drugs (16). To search for inhibitors of invasion and angiogenesis in natural extracts, we sought to establish a quantitative assay that would be simple yet able to eliminate cell death and inhibition of attachment as causes of invasion inhibition. The assay described here achieves this by screening sequentially for compounds that inhibit invasion into Matrigel, do not prevent cell attachment to Matrigel, and do not kill the cells. A small-scale screen showed activity in an extract of the Papua, New Guinea sponge *Xestospongia exigua* (Kirkpatrick), and assay-guided fractionation led to the isolation of motuporamines as potent and efficacious inhibitors of invasion and angiogenesis.

The motuporamines are a family of relatively simple macrocyclic alkaloids containing a spermidine-like substructure (6). Comparison of the activities of the natural compounds and simple chemical modification of the tail of motuporamine C provided initial structure-activity information. The positively charged amine in the middle of

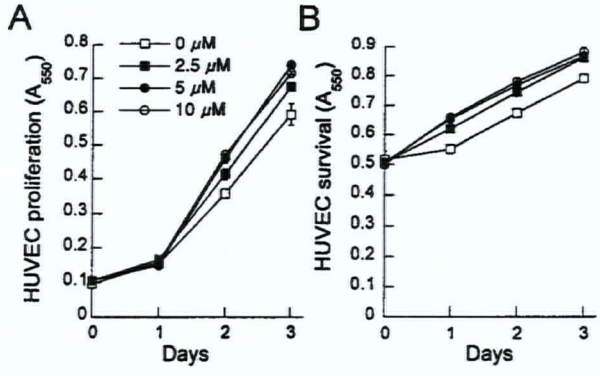

Fig. 9. Motuporamine does not inhibit HUVEC proliferation or survival. Different concentrations of motuporamine C were added at day 0 to rapidly dividing HUVECs (*A*) or near-confluent HUVECs (*B*), and medium and compound were changed daily. Proliferation and survival were measured at the indicated times as described in "Materials and Methods."

the tail is a critical determinant of activity because its acetylation completely abrogated anti-invasion activity. However, acetylation of the terminal amino group had no detectable effect. The size of the macrocyclic ring had an influence on activity because motuporamines with smaller rings were slightly less active. Simple and inexpensive motuporamine synthetic schemes have been published recently (17, 18) that will make possible further structure-activity study and eliminate dependence on natural sources.

The motuporamines show some resemblance to squalamine, an angiogenesis inhibitor (19) currently in Phase II clinical trials for the treatment of advanced non-small cell lung cancer (20). Squalamine was isolated from dogfish shark liver and is a much more complex molecule composed of spermidine attached to C-3 of a steroid core with a sulfated side chain. The observation that both classes of compounds decrease cell migration, inhibit angiogenesis, and are composed of a macrocyclic ring attached to a polyamine raises the possibility that they act in a similar fashion. However, although the mechanism of action of squalamine is still unclear, it appears to inhibit both cell proliferation and migration (19). Motuporamine C inhibits migration with little effect on proliferation, suggesting that the two compounds may have distinct cellular targets.

In this study, we carried out preliminary cell biological studies in an effort to broadly define the mechanism of action of motuporamine C. We found that doses of motuporamine C that inhibit both tumor cell invasion and endothelial cell angiogenesis are not cytotoxic to cancer cell lines and HUVECs. This characteristic, which was built into the original screen, is an important consideration with respect to the possible therapeutic usefulness of the drug. Invasive tumor cells in malleable basement membrane gels and endothelial cells in malleable fibrin gels remained rounded in the presence of motuporamine C. This could have been explained by global disruption of the actin cytoskeleton. However, experiments in monolayer culture do not support this possibility because cells were able to spread and form cytoplasmic actin stress fibers.

The ability of motuporamines to decrease tumor cell movement through basement membrane gels and endothelial cell movement through fibrin gels suggests that the drug acts to inhibit cell-mediated degradation of extracellular matrix and/or inhibit cell motility. It has not yet been determined whether motuporamine C alters matrix degradation. However, we have demonstrated that the compound decreased tumor cell motility and subtly altered the organization of filamentous actin at the cell margin. In particular, we observed an impairment of actin-mediated membrane ruffling in the leading lamellae of cells induced to migrate by wounding. This suggests at least two possible classes of molecular targets. The first class is the Rho-family GTPases, most specifically Rac, the activity of which is required for the formation of leading lamellae and ruffles (21, 22). The second class consists of molecules that regulate actin polymerization within ruffles. These include the Arp2/3 complex and regulators such as WASP (23). Cellular adhesion to the extracellular matrix itself leads to the activation of Rho family GTPases and subcellular actin rearrangements, including those associated with leading edge ruffling (24). Importantly, these events also provide feedback via an as yet poorly defined "inside-out" signaling mechanism to regulate the affinity of cell surface integrin receptors for their extracellular matrix ligands (25). It has been proposed that such changes in integrin affinity help regulate the maturation of transient focal complexes at the leading edge of migrating cells into more mature, stable focal complexes in the cell body (26). Motuporamine C may act to dampen this inside-out signaling because it subtly decreased the affinity state of $\beta 1$ integrins. Despite this modest decrease, we did not observe any disruption of tumor cell attachment to either basement membrane gels or tissue culture plastic. To our knowledge, compounds with analogous structure have not been documented to have effects on adhesion. We are currently addressing this by examining focal adhesion complex formation and signaling on a number of defined extracellular matrices.

Compounds that have the potential for inhibiting tumor cell invasion and angiogenesis are attractive candidates for cancer therapy. In combination with conventional cytotoxic chemotherapy agents, they may prove to be efficacious in controlling cancer progression. We are now carrying out experiments to evaluate the antitumor, antiangiogenesis, and antimetastasis activity of motuporamine C in animals and structure-activity studies to identify additional compounds for *in vivo* testing. Motuporamines showing *in vivo* activity will become attractive novel drug candidates.

ACKNOWLEDGMENTS

We thank Edmund Au and Lindsay Chung for technical assistance and Hilary Anderson for critical reading of the manuscript.

REFERENCES

1. Hanahan, D., and Weinberg, R. A. The hallmarks of cancer. Cell, *100:* 57–70, 2000.
2. Sporn, M. B. The war on cancer. Lancet, *347:* 1377–1381, 1996.
3. Wyke, J. A. Overview-burgeoning promise in metastasis research. Eur. J. Cancer, *36:* 1589–1594, 2000.
4. Carmeliet, P., and Jain, R. K. Angiogenesis in cancer and other diseases. Nature (Lond.), *407:* 249–257, 2000.
5. Mossman, T. Rapid colorimetric assay for cellular growth and survival: application to proliferation and cytotoxicity assays. J. Immunol. Methods, *65:* 55–63, 1983.
6. Williams, D. E., Lassota, P., and Andersen, R. J. Motuporamines A-C, cytotoxic alkaloids isolated from the marine sponge *Xestospongia exigua* (Kirkpatrick). J. Org. Chem., *63:* 4838–4841, 1998.
7. Nehls, V., and Drenckhahn, D. A novel, microcarrier-based *in vitro* assay for rapid and reliable quantification of three-dimensional cell migration and angiogenesis. Microvasc. Res., *50:* 311–322, 1995.
8. Bae, S. N., Arand, G., Azzam, H., Pavasant, P., Torri, J., Frandsen, T. L., and Thompson, E. W. Molecular and cellular analysis of basement membrane invasion by human breast cancer cells in Matrigel-based *in vitro* assays. Breast Cancer Res. Treat., *24:* 241–255, 1993.
9. Price, J. T., and Thompson, E. W. Models for studying cellular invasion of basement membranes. Methods Mol. Biol., *129:* 231–250, 1999.
10. Cragg, G. M., Newman, D. J., and Snader, K. M. Natural products in drug discovery and development. J. Nat. Prod. (Lloydia), *60:* 52–60, 1997.
11. Saeki, Y., Seya, T., Hazeki, K., Ui, M., Hazeki, O., and Akedo, H. Involvement of phosphoinositide 3-kinase in regulation of adhesive activity of highly metastatic hepatoma cells. J. Biochem. (Tokyo), *124:* 1020–1025, 1998.
12. Kohn, E. C., Francis, E. A., Liotta, L. A., and Schiffmann, E. Heterogeneity of the motility responses in malignant tumor cells: a biological basis for the diversity and homing of metastatic cells. Int. J. Cancer, *46:* 287–292, 1990.
13. Friedl, P., and Brocker, E-B. The biology of cell locomotion within three-dimensional extracellular matrix. Cell. Mol. Life Sci., *57:* 41–64, 2000.
14. Dedhar, S. Integrins and signal transduction. Curr. Opin. Hematol., *6:* 37–43, 1999.
15. Luque, A., Gomez, M., Puzon, W., Takada, Y., Sanchez-Madrid, F., and Cabanas, C. Activated conformations of very late activation integrins detected by a group of antibodies (HUTS) specific for a novel regulatory region (355–425) of the common $\beta 1$ chain. J. Biol. Chem., *271:* 11067–11075, 1996.
16. Faulkner, D. J. Chemical riches from the oceans. Chem. Br., *39:* 680–684, 1995.
17. Baldwin, J. E., Vollmer, H. R., and Lee, V. Total synthesis of cytotoxic sponge alkaloids motuporamines. Tetrahedron Lett., *40:* 5401–5404, 1999.
18. Goldring, W. P. D., Hodder, A. S., and Weiler, L. Synthesis of macrocyclic lactams and lactones via ring-closing olefin metathesis. Tetrahedron Lett., *39:* 4955–4958, 1998.
19. Sills, A. K. J., Williams, J. I., Tyler, B. M., Epstein, D. S., Sipos, E. P., Davis, J. D., McLane, M. P., Pitchford, S., Cheshire, K., Gannon, F. H., Kinney, W. A., Chao, T. L., Donowitz, M., Laterra, J., Zasloff, M., and Brem, H. Squalamine inhibits angiogenesis and solid tumor growth *in vivo* and perturbs embryonic vasculature. Cancer Res., *58:* 2784–2792, 1998.
20. Deplanque, G., and Harris, A. L. Anti-angiogenic agents: clinical trial design and therapies in development. Eur. J. Cancer, *36:* 1713–1724, 2000.
21. Kraynov, V. S., Chamberlain, C., Bokoch, G. M., Schwartz, M. A., Slabaugh, S., and Hahn, K. M. Localized rac activation dynamics visualized in living cells. Science (Wash. DC), *290:* 333–337, 2000.
22. Schmitz, A. A., Govek, E. E., Bottner, B., and Van Aelst, L. Rho GTPases: signaling, migration, and invasion. Exp. Cell Res., *261:* 1–12, 2000.
23. Welch, M. D. The world according to Arp: regulation of actin nucleation by the Arp2/3 complex. Trends Cell Biol., *9:* 423–427, 1999.
24. Giancotti, F. G., and Ruoslahti, E. Integrin signaling. Science (Wash. DC), *285:* 1028–1032, 1999.
25. Schwartz, M. A., and Shattil, S. J. Signaling networks linking integrins and rho family GTPases. Trends Biochem Sci., *25:* 388–391, 2000.
26. Maheshwari, G., Brown, G., Lauffenburger, D. A., Wells, A., and Griffith, L. G. Cell adhesion and motility depend on nanoscale RGD clustering. J. Cell Sci., *113:* 1677–1686, 2000.

This page intentionally blank

MOLECULAR AND CELLULAR BIOLOGY, Apr. 2002, p. 2830–2841 Vol. 22, No. 8
0270-7306/02/$04.00+0 DOI: 10.1128/MCB.22.8.2830–2841.2002

Activated Notch4 Inhibits Angiogenesis: Role of β1-Integrin Activation

Kevin G. Leong,[1,2] Xiaolong Hu,[3] Linheng Li,[4] Michela Noseda,[2,3] Bruno Larrivée,[1,2] Christopher Hull,[2,3] Leroy Hood,[5] Fred Wong,[2,3] and Aly Karsan[1,2,3]*

Departments of Experimental Medicine[1] and Pathology and Laboratory Medicine,[3] University of British Columbia and British Columbia Cancer Agency, and Department of Medical Biophysics, British Columbia Cancer Agency,[2] Vancouver, British Columbia V5Z 1L3, Canada; Stem Cell Research Laboratory, Stowers Institute for Medical Research, Kansas City, Missouri 64110[4]; and Institute for Systems Biology, Seattle, Washington 98105[5]

Received 22 May 2001/Returned for modification 7 July 2001/Accepted 9 January 2002

Notch4 is a member of the Notch family of transmembrane receptors that is expressed primarily on endothelial cells. Activation of Notch in various cell systems has been shown to regulate cell fate decisions. The sprouting of endothelial cells from microvessels, or angiogenesis, involves the modulation of the endothelial cell phenotype. Based on the function of other Notch family members and the expression pattern of Notch4, we postulated that Notch4 activation would modulate angiogenesis. Using an in vitro endothelial-sprouting assay, we show that expression of constitutively active Notch4 in human dermal microvascular endothelial cells (HMEC-1) inhibits endothelial sprouting. We also show that activated Notch4 inhibits vascular endothelial growth factor (VEGF)-induced angiogenesis in the chick chorioallantoic membrane in vivo. Activated Notch4 does not inhibit HMEC-1 proliferation or migration through fibrinogen. However, migration through collagen is inhibited. Our data show that Notch4 cells exhibit increased β1-integrin-mediated adhesion to collagen. HMEC-1 expressing activated Notch4 do not have increased surface expression of β1-integrins. Rather, we demonstrate that Notch4-expressing cells display β1-integrin in an active, high-affinity conformation. Furthermore, using function-activating β1-integrin antibodies, we demonstrate that activation of β1-integrins is sufficient to inhibit VEGF-induced endothelial sprouting in vitro and angiogenesis in vivo. Our findings suggest that constitutive Notch4 activation in endothelial cells inhibits angiogenesis in part by promoting β1-integrin-mediated adhesion to the underlying matrix.

Angiogenesis, the formation of new blood vessels from existing vessels, is a complex process requiring modulation of multiple endothelial cell functions (3, 30, 62). The formation of capillary sprouts from the existing microvasculature occurs secondary to an inciting stimulus that results in increased vascular permeability, accumulation of extravascular fibrin, and local proteolytic degradation of the basement membrane (20, 59). The endothelial cells overlying the disrupted region become activated, change shape, and extend elongated processes into the surrounding tissue (20, 59). Directed migration toward the angiogenic stimulus results in the formation of a column of endothelial cells (3, 30, 62). Just proximal to the migrating tip of the column is a region of proliferating cells (3, 30). These proliferating endothelial cells cause an increase in the length of the sprout. Proximal to the proliferative zone, the endothelial cells undergo another shape change, adhere tightly to each other, and begin to form a lumen (3, 30). Secondary sprouting from the migrating tip results in a capillary plexus, and the fusion of individual sprouts at their tips closes the loop and circulates blood into the vascularized area (3, 30, 62). Throughout this process the function and expression of various adhesion proteins, including those of the integrin family, are tightly regulated (5, 15). Several growth factors and cytokines are known to stimulate angiogenesis, the best-studied of which are vascular endothelial growth factor (VEGF), and fibroblast growth factor 2 (FGF-2; basic FGF) (20, 60).

During development, equipotential cells choose between alternative cell fates. Interactions between the Notch transmembrane receptor and its various ligands on adjacent cells can determine cell fate (2, 51). Notch is also involved in signaling between heterotypic cells to modulate differentiation (2, 51). The importance of Notch in mammalian differentiation is highlighted by several mutations responsible for human disease (22, 37, 48). Engagement of Notch by a ligand results in cleavage of the receptor within or close to the plasma membrane, with subsequent translocation of the C-terminal intracellular domain (NotchIC) to the nucleus (64, 71). Because activation of Notch requires ligand-dependent cleavage of the intracellular domain, enforced expression of NotchIC results in a constitutively active form of the receptor (29, 61). Enforced expression of the truncated intracellular domain of Notch proteins inhibits differentiation pathways in several models but is required for differentiation in other systems (6, 27, 41).

Four mammalian Notch homologues have been identified to date (Notch1 to -4) (47, 51, 74). Recently, the full-length form of Notch4 was cloned from mice and humans (47, 74). Notch4 is evolutionarily distant from the other members of the Notch family (47). Distinct structural features of Notch4 include fewer epidermal growth factor-like repeats and an intracellular domain significantly shorter than those of other Notch members (74). Of interest to us is that Notch4 is primarily expressed on the endothelium and the endocardium (47, 68, 74).

Given that Notch4 is primarily expressed on endothelial cells, we postulated that Notch4 may be involved in regulating

* Corresponding author. Mailing address: Department of Medical Biophysics, British Columbia Cancer Research Centre, 601 West 10th Ave., Vancouver, British Columbia, Canada V5Z 1L3. Phone: (604) 877-6248. Fax: (604) 877-6002. E-mail: akarsan@bccancer.bc.ca.

angiogenesis. To answer this question, we expressed the truncated, constitutively active intracellular domain of Notch4 (Notch4IC) in endothelial cells. Our studies indicate that activated Notch4 inhibits the sprouting of human dermal microvascular endothelial cells (HMEC-1) in vitro and angiogenesis in the chick chorioallantoic membrane (CAM) in vivo. Activated Notch4 does not inhibit proliferation of HMEC-1, nor does it inhibit their migration through fibrinogen toward angiogenic factors FGF-2 and VEGF. However, activated Notch4 does inhibit migration through collagen. We demonstrate that the decreased sprouting of Notch4IC cells from collagen-coated beads is due in part to enhanced β1-integrin-mediated adhesion to collagen. Although endothelial cells expressing Notch4IC do not show increased surface expression of β1-integrins, we show that the β1-integrins are in a high-affinity, active conformation. We also show that activation of β1-integrins with function-activating β1-integrin monoclonal antibodies, independent of Notch4 expression, is sufficient to inhibit endothelial sprouting in vitro and angiogenesis in vivo. Thus, our results suggest that Notch4 activation in endothelial cells in vivo may inhibit angiogenesis in part by promoting β1-integrin-mediated adhesion to the underlying matrix.

MATERIALS AND METHODS

Cell culture. The HMEC-1 (referred to hereafter as HMEC) line (1) was provided by the Centers for Disease Control and Prevention (Atlanta, Ga.). HMEC lines were cultured in MCDB medium supplemented with 10% heat-inactivated fetal calf serum (FCS), 10 μg of epidermal growth factor/ml, and 100 U each of penicillin and streptomycin/ml. The avian retroviral packaging cell line Q2bn (gift from K. McNagny, University of British Columbia) was cultured in Dulbecco's modified Eagle's medium (DMEM) supplemented with 10% non-heat-inactivated FCS, 2.5% non-heat-inactivated chicken serum, 60 μg of conalbumin/ml, 50 μM β-mercaptoethanol, 2 mM glutamine, and 100 U each of penicillin and streptomycin/ml. All cells were maintained at 37°C in 5% CO_2.

Gene transfer. HMEC-Notch4IC and HMEC-LNCX were constructed by retroviral transduction of cDNA encoding a C-terminal hemagglutinin (HA)-tagged human Notch4 (amino acids 1476 to 2003) or of the empty pLNCX vector control, respectively (47). The method of transduction has previously been described (39). Stable HMEC lines were obtained by selection in 300 μg of G-418 (Gibco)/ml. Polyclonal HMEC lines were used to avoid artifacts due to the retroviral integration site. Chicken retroviral expression vectors were constructed by inserting C-terminal HA-tagged human Notch4IC cDNA into the avian retroviral vector CK (gift from N. Boudreau, University of California, San Francisco, and M. Bissell, University of California, Berkeley). Both CK-Notch4IC and the empty vector were transiently transfected into Q2bn cells with Fugene 6 transfection reagent (Boehringer Mannheim) to generate producer lines.

Immunoblotting and immunofluorescence. For immunoblotting, total cellular extracts were prepared from HMEC or Q2bn lines by lysing 10^5 cells in a solution containing 50 mM Tris, 150 mM NaCl, 2% Triton X-100, 10 μg of soybean trypsin inhibitor/ml, and 200 μM phenylmethylsulfonyl fluoride and were analyzed by sodium dodecyl sulfate-polyacrylamide gel electrophoresis and immunoblotting as previously described (19).

For immunofluorescence, HMEC lines (5×10^4 cells) were cultured on coverslips for 48 h, fixed, and permeabilized in cold methanol for 5 min. Nonspecific binding was blocked by incubation with phosphate-buffered saline (PBS) containing 5% goat serum and 0.1% Tween 20. Following incubation with a primary antibody (rabbit anti-HA polyclonal antibody; 1:100 dilution) for 1 h and a secondary antibody (Texas red-conjugated goat anti-rabbit immunoglobulin G [IgG]; 1:200 dilution) for 30 min, coverslips were mounted on glass slides with an antifading solution (FluoroGuard antifade reagent; Bio-Rad) containing 100 ng of Hoechst 33258 (Sigma)/ml to stain the nuclei. Immunofluorescence was examined using an Axioplan 2 imaging microscope (Zeiss), and images were captured with a DVC-1310M digital camera (Digital Video Camera Company).

Endothelial-sprouting assay. Endothelial sprouting was assessed by a modification of the method of Nehls and Drenckhahn (53). Briefly, microcarrier beads coated with gelatin (Cytodex 3; Sigma) or positively charged, cross-linked dextran (Cytodex 2; Sigma) were seeded with HMEC lines. When the cells reached confluence on the beads, equal numbers of HMEC-coated beads were embedded in fibrin gels in 96-well plates. For preparation of fibrin gels, bovine fibrinogen was dissolved in PBS at a concentration of 2.5 mg/ml. Aprotinin was added at a concentration of 0.05 mg/ml, and the solution was filtered through a 0.22-μm-pore-size filter. Fibrinogen solution was supplemented with FGF-2 (15 ng/ml) or VEGF (15 ng/ml). As a control, fibrinogen solution without angiogenic factor was used. Following transfer of the fibrinogen solution to 96-well plates, HMEC-coated beads were added at a density of 50 beads/well, and clotting was induced by the addition of thrombin (1.2 U/ml). After clotting was complete, gels were equilibrated with MCDB–2% FCS at 37°C. Following 60 min of incubation, the overlying medium was changed for all wells. MCDB–2% FCS, either alone or containing FGF-2 (15 ng/ml) or VEGF (15 ng/ml), was added to the wells. After 3 days of incubation with daily medium changes, the number of capillary-like tubes formed was quantitated by counting the number of tube-like structures per microcarrier bead (sprouts per bead). Only sprouts greater than 150 μm in length and composed of at least three endothelial cells were counted.

For coating Cytodex 2 beads with collagen, beads were resuspended in 1 mg of collagen type I/ml, allowed to dry overnight on petri dishes, and resuspended in PBS. For coating Cytodex 2 beads with antibodies (IgG2a, 1:1,000 dilution [Sigma]; 8A2, 1:1,000 dilution [gift from J. Harlan, University of Washington]; LM534, 1:1,000 dilution [Chemicon]), beads were incubated with antibodies at 37°C for 2 h, washed twice with PBS, and resuspended in PBS. After the antibody-coated beads were incubated with cells for 3 days, the beads were placed in fibrin gels supplemented with the appropriate antibody at 1:1,000 dilution.

CAM assay. Fertilized White Leghorn chicken (*Gallus gallus domesticus*) eggs were incubated at 37°C under conditions of constant humidity. All chicken eggs were handled according to institutional animal care procedures. On embryonic day 6, the developing CAM was separated from the shell by opening a small circular window at the broad end of the egg above the air sac. The embryos were checked for normal development, the window was sealed with Parafilm, and the eggs were returned to the incubator for two more days. On day 8, transfected Q2bn cell lines were trypsinized and washed in PBS, and 3×10^6 cells resuspended in 15 μl of DMEM supplemented with 30 ng of VEGF/ml were placed onto nylon meshes (pore size, 250 μm; Sefar America) on the CAM. The cells distribute throughout the mesh and secrete control virus or virus containing Notch4IC. Meshes treated with vehicle alone (15 μl of DMEM) were used as negative controls, whereas meshes treated with VEGF (30 ng/ml in 15 μl of DMEM) were used as positive controls. Eggs were resealed and returned to the incubator. On day 12, images of the CAMs were captured digitally with an Olympus SZX9 stereomicroscope (Olympus America) equipped with a Spot RT digital imaging system (Diagnostic Instruments). Neovascularization was quantitated for each CAM by counting the number of vessels that entered the mesh area and dividing by the perimeter of the mesh (vessels per millimeter). Northern Eclipse, version 6.0 (Empix Imaging, Inc.), was used for manual vessel counting and mesh perimeter measurements. Following photography, CAMs were harvested and processed for further studies.

For CAMs treated with anti-integrin antibodies, fertilized White Leghorn chicken eggs were prepared as described above. Mouse anti-avian β1-integrin antibodies TASC (9D11; function-activating β1-integrin antibody; gift of L. F. Reichardt, University of California, San Francisco), V2E9 (non-function-modifying β1-integrin antibody; Developmental Studies Hybridoma Bank, University of Iowa), and W1B10 (function-blocking β1-integrin antibody; Sigma) were prepared at 10 μg/ml in PBS supplemented with 30 ng of VEGF/ml. On day 8, 20 μl of each antibody preparation was loaded onto 2-mm^3 gelatin sponges (Gelfoam; Pharmacia Upjohn), which were then placed on the surface of the developing CAM. Sponges containing vehicle alone (20 μl of PBS) were used as negative controls, whereas sponges containing 20 μl of VEGF at 30 ng/ml in PBS were used as positive controls. CAMs were also treated with function-blocking mouse anti-human αvβ3 antibody LM609 (which cross-reacts with avian αvβ3 integrin; Chemicon) prepared at 10 μg/ml in PBS containing 30 ng of VEGF/ml. LM609 has previously been shown to attenuate VEGF-induced angiogenesis in the CAM (23) and thus serves as a positive control for angiogenesis inhibition. Eggs were resealed and returned to the incubator. On day 10, digital images of the CAMs were captured and analyzed for neovascularization as described above.

Immunohistochemistry. CAMs treated with transfected Q2bn cell lines were harvested from day 12 embryos and processed for histological analysis. For hematoxylin and eosin (H&E) staining, CAMs were fixed in formalin overnight at room temperature, dehydrated, and embedded in paraffin. Sections (6 μm thick) were cut and stained with H&E. For immunohistological analysis, CAMs were frozen in Tissue-Tek optimal cutting temperature compound (Somagen) and 10-μm-thick sections were cut and fixed in acetone for 10 min. Sections were

hydrated and incubated in 1.5% hydrogen peroxide solution for 5 min to quench endogenous peroxide activity. Nonspecific binding was blocked by incubation in normal goat serum (1:20 dilution) for 20 min. For von Willebrand factor (vWF) staining, sections were incubated with a primary antibody (1:200 dilution; DAKO) and a biotinylated secondary antibody, followed by an avidin conjugate. For HA staining, sections were incubated with a primary antibody (mouse anti-HA monoclonal antibody, 1:500 dilution) and a secondary antibody (biotinylated goat anti-mouse IgG, 1:200 dilution), followed by peroxidase-conjugated streptavidin (DAKO). All sections were developed with a diaminobenzidine-hydrogen peroxide reaction (Sigma), counterstained with hematoxylin, dehydrated, cleared, and mounted. CAM sections were examined with an Axioplan 2 imaging microscope (Zeiss), and images were captured with a Coolpix 990 digital camera (Nikon).

Proliferation assay. Proliferation of endothelial cells in response to angiogenic factors FGF-2 and VEGF was determined by two methods: (i) neutral red uptake and (ii) flow-cytometric analysis for total DNA content (DAPI [4′,6′-diamidino-2-phenylindole]) and bromodeoxyuridine (BrdU) incorporation. For the neutral red assay (19, 49), confluent plates of HMEC lines were serum starved in MCDB–2% FCS for 48 h and cells were plated in 96-well plates at a density of 5×10^3 cells/well. After 4 h of incubation to allow cells to bind, overlay medium was removed and the cells were treated with MCDB–2% FCS supplemented with FGF-2 (15 ng/ml) or VEGF (15 ng/ml). As a control, cells were treated with MCDB–2% FCS alone. Cells were incubated for 0, 24, 48, and 72 h with daily medium changes. After each time point, wells were emptied and incubated with 100 μl of neutral red dye (0.0025% neutral red in MCDB–2% FCS). Empty wells were also incubated with neutral red dye for background absorbance correction. After 4 h of incubation, wells were aspirated and neutral red dye was solubilized with 100 μl of 1% acetic acid–50% ethanol per well. Absorbance was determined at 570 nm.

For the flow-cytometric analysis of cell cycle distribution, HMEC lines were serum starved in MCDB–2% FCS for 48 h and incubated for an additional 24 h in medium alone (MCDB–2% FCS) or medium supplemented with FGF-2 (15 ng/ml) or VEGF (15 ng/ml). For the last 2 h of incubation, cells were incubated with 10 μM BrdU (Sigma) at 37°C. Cells were harvested by trypsinization and fixed in 70% ethanol at 4°C for 30 min. After being washed in PBS, cells were incubated in 2 M HCl for 30 min to denature DNA, followed by neutralization in serum-free medium. Cells were blocked and permeabilized in 0.5% Triton X-100–4% calf serum and then incubated with an anti-BrdU fluorescein isothiocyanate (FITC)-conjugated antibody (Pharmingen) for 1 h. Washed cells were stained with 1 μg of DAPI/ml in PBS containing 0.5% Triton X-100. Samples were run on an EPICS ELITE-ESP flow cytometer (Beckman Coulter), and data were analyzed with WinList, version 2.0, software (Verity Software House, Inc.).

Migration assay. The ability of endothelial cells to migrate toward FGF-2 or VEGF was measured by a Transwell filter assay (Corning Costar), as previously described (13). Briefly, polycarbonate filters (8.0-μm pores) of the upper chamber were coated with 50 μl of fibrinogen (2.5 mg/ml) or collagen type I (1 mg/ml) in PBS and allowed to dry overnight. Confluent plates of HMEC lines were trypsinized, washed twice with 10 μg of soybean trypsin inhibitor/ml, and resuspended in serum-free MCDB medium. HMEC (3.5×10^4) were placed in the upper chamber, and MCDB medium supplemented with FGF-2 (15 ng/ml) or VEGF (15 ng/ml) was placed in the lower chamber. As a control, MCDB medium without an added chemotactic factor was placed in the lower chamber. Following 16 h of incubation at 37°C, filters were washed in PBS, fixed in 4% paraformaldehyde, and stained with 0.5% crystal violet. After adherent cells were removed from the upper side of the filter with a cotton swab, cells that had migrated and adhered to the underside of the filter were counted with an inverted microscope.

Adhesion assay. High-binding 96-well plates (Corning Costar) were coated with 100 μl of the following matrix proteins/well at 20 μg/ml: fibrinogen, fibronectin, collagen type I, collagen type IV, and vitronectin. Control wells were coated with poly-L-lysine at 20 μg/ml. After incubation for 1 h at 37°C, all wells were aspirated and blocked with 4% bovine serum albumin in PBS for 30 min at room temperature, followed by washing with PBS. Single-cell suspensions were prepared by washing confluent cells once with PBS-based enzyme-free cell dissociation buffer (Gibco) and incubating the cells in the same buffer for 20 min at 37°C, as described previously (70). Following resuspension in a mixture of PBS-DMEM (4:1 [vol/vol]), 100 μl of the cell suspension at 6×10^5 cells/ml was added to each well and incubated at 37°C for 20 min. Plates were then gently washed with PBS, fixed in 4% paraformaldehyde, and stained with 0.5% crystal violet. Following solubilization of dye in 1% sodium dodecyl sulfate in PBS, absorbance was quantitated in an enzyme-linked immunosorbent assay plate reader at 570 nm, with background absorbance subtracted at 630 nm.

For adhesion modulation studies, HMEC lines were incubated with antibodies on ice for 20 min. Mouse IgG2a (Sigma) was used at 1:500 dilution; mouse monoclonal function-blocking anti-human β1-integrin antibody P4C10 was used at 1:100, 1:250, and 1:500 dilutions (Gibco) or at 2.5 μg/ml (Sigma); mouse monoclonal function-blocking anti-human αvβ3-integrin antibody LM609 (Chemicon) was used at 10 μg/ml; and mouse monoclonal function-activating anti-human β1-integrin antibody 8A2 was used at 1 μg/ml. For cells treated with both LM609 and P4C10, a concentration of 10 μg/ml and a 1:100 dilution, respectively, were used. For adhesion studies using P4C10, cells were seeded into wells coated with collagen type I and/or collagen type IV. For adhesion studies using 8A2, cells were seeded into wells coated with collagen type I.

Flow cytometry for integrin expression levels. HMEC lines were detached by incubation in PBS-based enzyme-free cell dissociation buffer for 20 min at 37°C. To reduce nonspecific binding, cells were incubated in PBS–10% heat-inactivated iron-supplemented calf serum for 30 min at 37°C. Primary antibodies LM609 (10 μg/ml; Chemicon), B44 (10 μg/ml; gift from J. A. Wilkins, University of Manitoba), and K20 (10 μg/ml; AMAC, Inc.) were added to the cells, and the cells and antibodies were allowed to incubate at 37°C for 30 min. A mouse IgG2a antibody (10 μg/ml; Sigma) was used as a control. Cells were washed twice in cold PBS, and a secondary antibody (goat anti-mouse IgG-FITC, 1:64 dilution; Sigma) was added, and the cells and the antibody were allowed to incubate for an additional 60 min in the dark on ice. After cells were washed twice in cold PBS, they were fixed in 4% paraformaldehyde. Samples were run on an EPICS ELITE-ESP flow cytometer (Beckman Coulter), and data were analyzed with WinList, version 2.0 (Verity Software House, Inc.).

Ligand-binding assay. The binding of soluble collagen type I to HMEC-LNCX and HMEC-Notch4IC lines was examined. HMEC lines were detached by incubation in PBS-based enzyme-free cell dissociation buffer for 20 min at 37°C. Cells (5×10^5) were incubated with FITC-conjugated collagen type I (16.9 molecules of FITC per molecule of collagen; Molecular Probes) in a volume of 100 μl at 0, 0.1, 1, 10, 100, 500, and 1,000 μg/ml. After 10 min of binding at 37°C, cells were washed three times in 1 ml of PBS and fixed in 4% paraformaldehyde. Samples were run on an EPICS ELITE-ESP flow cytometer (Beckman Coulter), and data were analyzed with WinList, version 2.0 (Verity Software House, Inc.). To determine the number of molecules of FITC-collagen type I bound per endothelial cell, a standard fluorescence curve was constructed by using Quantum 24 premixed microbeads (Bangs Laboratories, Inc.). Taking the molecular mass of FITC and collagen type I to be 390 Da and 300 kDa, respectively, and given an FITC/collagen ratio of 16.9, a curve of bound collagen (molecules) versus concentration (nanomolar) of FITC-collagen type I conjugate was generated.

RESULTS

Constitutively active Notch4 inhibits endothelial sprouting in vitro. Given the role of Notch in modulating cell fate decisions, we postulated that the endothelium-specific Notch4 would modulate endothelial sprouting. To address this issue, we generated HMEC lines that express a truncated intracellular form of human Notch4, Notch4IC, which is constitutively active. A previously described endothelial-sprouting assay which mimics the formation of capillary-like tubes in fibrin gels in vitro was used to evaluate the role of Notch4 in angiogenesis (40, 53). Using this in vitro assay, we found that activated Notch4 blocked spontaneous endothelial sprout formation on gelatin-coated beads, as well as sprouting in response to FGF-2 and VEGF (Fig. 1A and B). Moreover, the sprouts that formed from Notch4IC-expressing cell lines were noted to be shorter than those derived from cells transduced with the empty vector. Figure 1C shows the expression of Notch4IC protein in HMEC-Notch4IC as determined by immunoblotting. Expression of the Notch4IC construct in HMEC was also analyzed by immunofluorescence. We typically achieve transduction efficiencies between 50 and 80%. As expected with polyclonal cell lines, HMEC-Notch4IC display heterogeneity in staining for the Notch4IC protein (Fig. 1D). The majority of the Notch4IC protein localizes to the nuclei of HMEC-Notch4IC, which is typical of constitutively active Notch proteins (24).

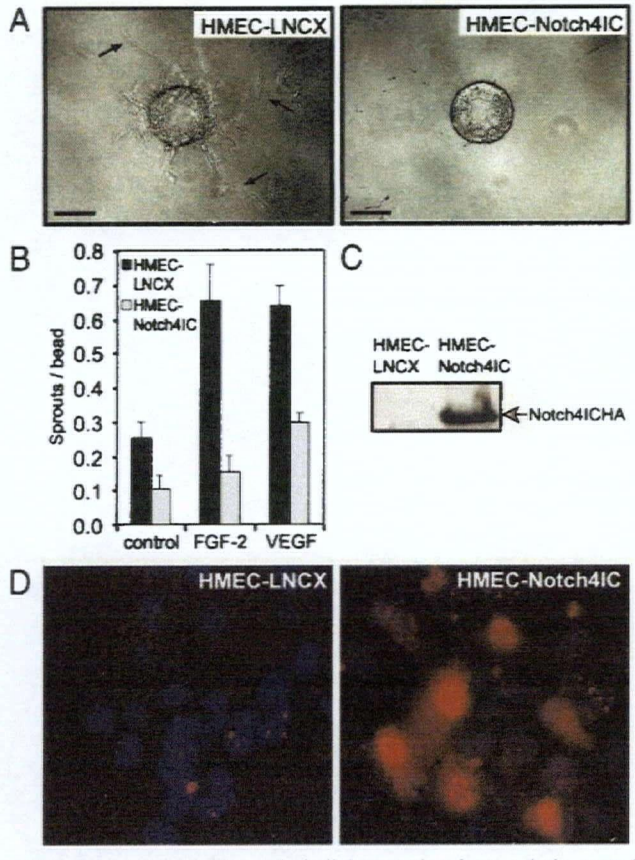

FIG. 1. Notch4 inhibits endothelial sprouting from gelatin-coated microcarrier beads in vitro. (A) Gelatin-coated microcarrier beads were seeded with HMEC-LNCX or HMEC-Notch4IC. When cells reached confluence on the beads, equal numbers of beads were embedded in fibrin gels supplemented with either FGF-2 (15 ng/ml) or VEGF (15 ng/ml). Bars, 100 μm. Arrows, endothelial sprouts of sufficient length to be counted. (B) Endothelial sprout formation quantitated after 3 days of incubation by counting the number of tube-like structures per microcarrier bead (sprouts per bead). Data are the means ± standard deviations from a single experiment done in triplicate and are representative of at least three independent experiments. (C) Expression of HA-tagged Notch4IC in HMEC lines by immunoblotting total cellular extracts with the anti-HA monoclonal antibody. (D) Immunofluorescence of HMEC-LNCX and HMEC-Notch4IC stained with Hoechst 33258, as well as an anti-HA primary antibody and a Texas red-conjugated secondary antibody to detect HA-tagged Notch4IC protein. Original magnification, ×40.

Because HMEC are a transformed endothelial cell line, we repeated the endothelial-sprouting assay using primary human umbilical vein endothelial cells (HUVEC) transduced with the Notch4IC construct or the empty vector. As for HMEC, activation of Notch4 in HUVEC blocked endothelial sprouting (data not shown).

Constitutively active Notch4 inhibits angiogenesis in vivo. To determine whether activation of Notch4 would inhibit angiogenesis in vivo, we used a chick CAM assay. The CAM functions as a respiratory structure for gas-nutrient exchange and undergoes intense vascularization (11), thus providing an excellent microenvironment for assessing angiogenesis. As previously described (9, 36), we generated avian retroviral packaging cell lines (Q2bn) transfected with the empty CK vector or CK-Notch4IC. On embryonic day 8, these CK producer lines, in the presence of VEGF, were placed on meshes on the chick CAM surface and incubated for an additional 4 days. The cells distribute throughout the mesh and secrete control virus or virus containing Notch4IC, which infects the surrounding proliferating cells, the majority of which are endothelial. CAMs transduced with the empty vector demonstrated normal angiogenesis in response to VEGF, whereas angiogenesis was markedly inhibited by the expression of Notch4IC (Fig. 2A and B). Expression of the Notch4IC protein in transfected Q2bn cells is shown in Fig. 2C.

Histological analysis was performed on sections of harvested CAMs. For H&E-stained sections, areas of the CAMs proximal to the Q2bn-containing mesh were analyzed. H&E staining of CK vector-transduced CAMs revealed the presence of numerous blood vessels in the subchorionic mesenchyme (Fig. 3A). In contrast, CAMs transduced with CK-Notch4IC exhibited a marked reduction in blood vessels close to the mesh (Fig. 3B). Immunohistochemistry was also performed on CAM sections and areas proximal to the mesh examined. Staining for the endothelium-specific marker vWF (65) confirmed the presence of blood vessels in CK vector-transduced CAMs (Fig. 3C). Notch4IC-transduced CAMs, on the other hand, showed minimal staining for vWF (Fig. 3D), confirming inhibition of blood vessel formation.

To assess expression of the HA-tagged Notch4IC protein in endothelial cells, serial sections were stained with antibodies against HA and vWF. Because Notch4IC-transduced CAMs were nearly devoid of small vessels proximal to the mesh, colocalization of staining was examined in vessels distant from the mesh. As expected for CK vector-transduced CAMs, vessels distant from the mesh did not stain for HA (Fig. 3E) but did stain for vWF (Fig. 3G). Analysis of Notch4IC-transduced CAMs demonstrated that vessels distant from the mesh exhibited costaining for HA (Fig. 3F) and vWF (Fig. 3H). Our findings suggest that expression of Notch4IC in vessels that feed the area of the mesh inhibits VEGF-induced endothelial sprouting and angiogenesis. To elucidate a possible mechanism(s) by which activated Notch4 inhibits endothelial sprouting in vitro and angiogenesis in vivo, we investigated the effects of Notch4IC expression on endothelial cell functions related to the angiogenic process by using various in vitro assays.

Notch4 inhibition of endothelial sprouting in vitro cannot be explained by reduced endothelial cell proliferation. Endothelial cell proliferation enables newly formed sprouts to increase in length and extend into the surrounding matrix. To determine whether reduced proliferation was a possible reason for the decreased sprouting of Notch4IC-expressing endothelial cells, we performed neutral red proliferation assays. When plated on normal tissue culture substrata, Notch4IC-expressing cells and control cells exhibited similar proliferation rates over 72 h (the incubation time for the endothelial-sprouting assay) (Fig. 4A). In fact, proliferation rates for cells grown in serum-containing medium were the same as those for cells grown in medium supplemented with FGF-2 or VEGF. Proliferation on fibrinogen- and collagen-coated surfaces was also investigated and was found to be equivalent for Notch4IC-expressing cells and control cells (data not shown).

To confirm that Notch4IC does not affect HMEC cell cycle kinetics, we performed flow cytometry on HMEC lines pulse-

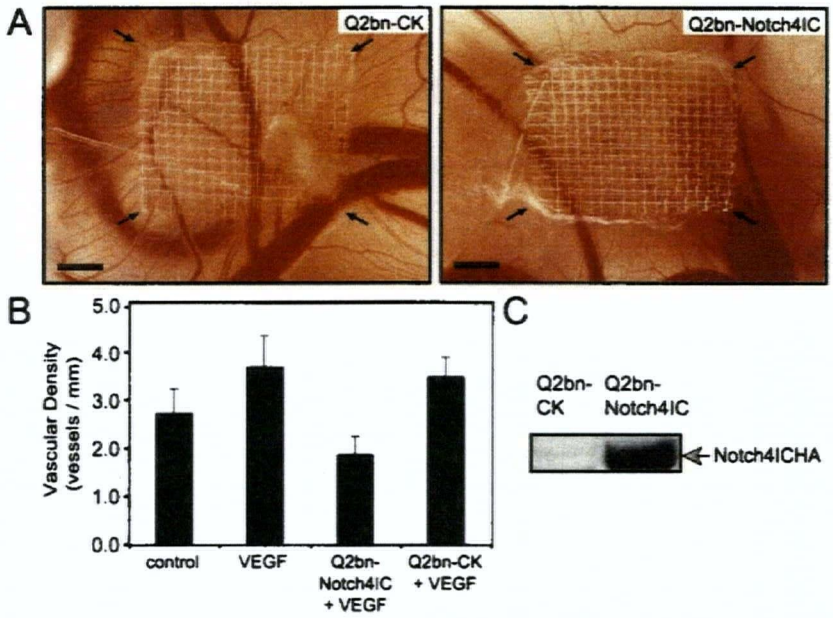

FIG. 2. Notch4 inhibits angiogenesis in the chick CAM in vivo. The avian retroviral packaging cell line Q2bn was transfected with empty vector CK (Q2bn-CK) or CK-Notch4IC (Q2bn-Notch4IC). On day 9, transfected Q2bn cell lines were placed onto nylon meshes on the CAM surface in the presence of VEGF (30 ng/ml). The grafted cells distribute throughout the mesh and secrete control virus or virus containing Notch4IC. Control CAMs were treated with medium alone or medium supplemented with VEGF. Images of the CAMs were captured on day 12. (A) CAMs treated with Q2bn-CK or Q2bn-Notch4IC cell lines in the presence of VEGF. Arrows, edges of the nylon mesh. Bars, 1 mm. (B) Vascular density quantitated after 4 days of incubation by counting the number of vessels that entered the mesh area and dividing by the perimeter of the mesh (vessels per millimeter). Data are the means ± standard errors from three experiments each done in replicates of four to six eggs. (C) Expression of HA-tagged Notch4IC in Q2bn cell lines verified by immunoblotting total cellular extracts with the anti-HA monoclonal antibody.

labeled with BrdU and costained with DAPI. Control and Notch4IC-expressing cells exhibited similar cell cycle distributions and levels of BrdU incorporation in the absence or presence of a growth factor (Fig. 4B shows representative samples of VEGF-stimulated HMEC-LNCX and HMEC-Notch4IC, and Fig. 4C shows distribution percentages). Overall, the proliferation studies performed demonstrate that control and Notch4IC-expressing cells proliferate at similar rates. Hence the inhibited sprouting of HMEC-Notch4IC in the in vitro endothelial-sprouting experiments cannot be explained by a decrease in proliferation of Notch4IC-expressing cells.

Notch4 inhibits endothelial cell migration through collagen but not fibrinogen. For capillaries to sprout, endothelial cells need to migrate toward a stimulus. To examine whether defective migration could explain the Notch4 inhibition of sprouting, we performed chemotaxis assays using Transwell filters coated with either fibrinogen or collagen. When filters were coated with fibrinogen, control cells and Notch4IC-expressing cells exhibited similar degrees of chemotaxis toward FGF-2 and VEGF (Fig. 5). Migration through collagen-coated filters toward FGF-2 or VEGF, however, for Notch4IC-expressing cells was less than that for control cells (Fig. 5). These data suggest that activated Notch4 does not affect the intrinsic motility of HMEC cells but influences endothelial cell migration in a matrix-dependent manner.

Notch4 promotes adhesion to extracellular matrix proteins through β1-integrins. Modulation of cell surface integrin levels as well as integrin affinity is a crucial event throughout the course of capillary tube formation (7, 28) and cell migration (46). Therefore, to explain the matrix-specific inhibition of HMEC-Notch4IC migration, we investigated whether Notch4 activation affects endothelial cell adhesion to extracellular matrix proteins. Figure 6A shows that Notch4IC-expressing cells exhibited increased adherence to various matrix proteins. In contrast, when adhesion was mediated by charge interactions alone, Notch4IC-expressing cells and control cells adhered to poly-L-lysine to the same degree. Regulation of αvβ3- and β1-integrins is required for angiogenesis (7, 21). Because activation of Notch4 promoted adhesion to the β1-integrin substrates tested (Fig. 6A), we postulated that the pattern of increased adhesion was due to effects of Notch4 activation on β1-integrin expression or function. Using function-blocking β1-integrin antibody P4C10 (12), we confirmed that the majority of the increased HMEC-Notch4IC adhesion to collagen type I (Fig. 6B and C) or collagen type IV (Fig. 6C) was mediated by β1-integrins. A function-blocking antibody directed against αvβ3-integrin (LM609) (14), however, did not affect HMEC-Notch4IC adhesion to collagen type I (Fig. 6B). LM609 concentrations of up to 20 μg/ml were tested, with no effect on collagen type I adhesion (data not shown). Interestingly, when LM609 and P4C10 were used in combination, the inhibition of HMEC-Notch4IC adhesion to collagen type I was less effective than when P4C10 was used alone (Fig. 6B). Although the reason(s) for the attenuated blocking is not clear, in part this may be due to steric hindrance.

We next tested whether Notch4IC affected the expression levels of αvβ3- and β1-integrins at the cell surface. Using flow cytometry, we demonstrated that neither αvβ3- nor β1-integrin levels were upregulated on the surface of HMEC-Notch4IC compared to levels for controls (Fig. 7A). In fact, in most

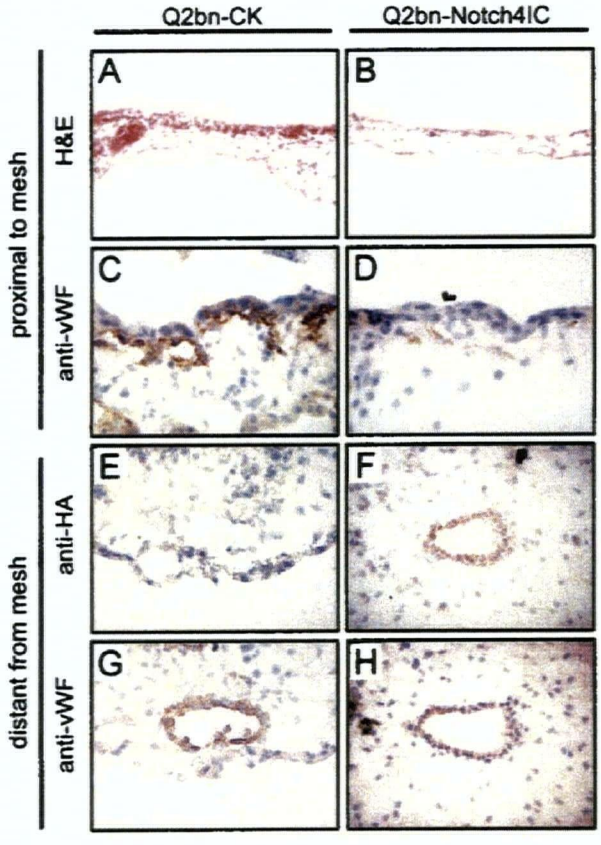

FIG. 3. Immunohistochemical analysis of Notch4IC expression in the CAM. Q2bn packaging cells transfected with the vector control (Q2bn-CK) or Notch4IC (Q2bn-Notch4IC) were placed onto nylon meshes on the CAM surface. Treated CAMs were harvested on day 12, and sections were prepared. (A to D) CAM sections proximal to mesh. Shown is H&E staining of Q2bn-CK-treated (A) and Q2bn-Notch4IC-treated (B) CAMs and anti-vWF staining of Q2bn-CK-treated (C) and Q2bn-Notch4IC-treated (D) CAMs. (E to H) CAM sections distant from mesh. Shown is anti-HA staining of Q2bn-CK-treated (E) and Q2bn-Notch4IC-treated (F) CAMs and anti-vWF staining of Q2bn-CK-treated (G) and Q2bn-Notch4IC-treated (H) CAMs. Original magnifications: ×40 (A to D, F, and H) and ×63 (E and G).

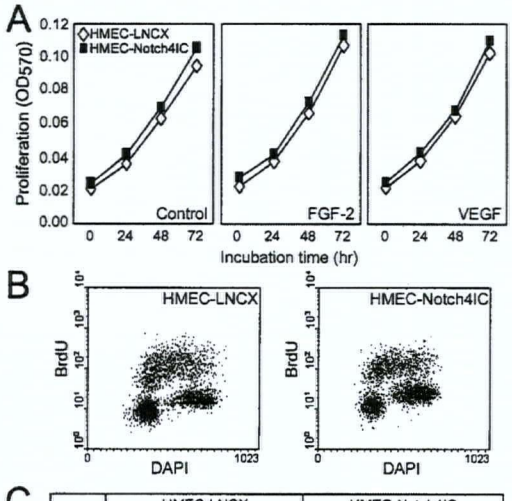

	HMEC-LNCX			HMEC-Notch4IC		
	G_0/G_1	S	G_2/M	G_0/G_1	S	G_2/M
Control	44 ± 1%	29 ± 4%	25 ± 3%	36 ± 4%	30 ± 4%	30 ± 7%
FGF-2	37 ± 4%	34 ± 2%	24 ± 1%	35 ± 3%	30 ± 5%	33 ± 3%
VEGF	41 ± 1%	33 ± 2%	26 ± 5%	38 ± 6%	32 ± 3%	27 ± 6%

FIG. 4. Notch4 does not inhibit HMEC proliferation. (A) Neutral red assay for proliferation. HMEC-LNCX and HMEC-Notch4IC proliferation in medium alone and in medium supplemented with FGF-2 (15 ng/ml) or VEGF (15 ng/ml) was assayed over 72 h. Data are the mean absorbances from a single experiment done in triplicate and are representative of at least three independent experiments. OD_{570}, optical density at 570 nm. (B) Cell cycle distribution for HMEC-LNCX and HMEC-Notch4IC stimulated with VEGF. Cells were stained with DAPI for total DNA content and pulse-labeled with BrdU to detect DNA synthesis and analyzed by flow cytometry. (C) Cell cycle distributions for HMEC-LNCX and HMEC-Notch4IC cultured in medium alone or medium supplemented with FGF-2 (15 ng/ml) or VEGF (15 ng/ml). Data are the means ± standard errors from three independent experiments.

experiments, there was decreased β1-integrin, but not αvβ3-integrin, on the surface of HMEC-Notch4IC. Integrins can exist at the cell surface in at least two conformational states, a ligand-binding (active or high-affinity) conformation and a non-ligand-binding (inactive or low-affinity) conformation (33). Increased affinity of integrins for their ligand(s) can be regulated by intracellular events, a process referred to as inside-out signaling (33). Our findings of increased β1-integrin-mediated adhesion without increased β1-integrin expression suggest that Notch4IC may participate in an inside-out signaling process that promotes β1-integrin affinity. To test this hypothesis, we performed ligand-binding assays using FITC-conjugated collagen type I. The binding of soluble collagen type I to HMEC-Notch4IC was greater than that to control HMEC (Fig. 7B). Because HMEC-Notch4IC exhibit increased binding to soluble collagen type I (Fig. 7B) without a corresponding increase in total β1-integrin expression (Fig. 7A), our findings suggest that HMEC-Notch4IC display a greater number of β1-integrins in a high-affinity, active conformation, than control cells.

To confirm the increased proportion of active β1-integrin on the surface of HMEC-Notch4IC, Notch4IC-expressing cells and control cells were stained with antibodies that specifically recognize active β1-integrin (B44) (55, 78) or total β1-integrin

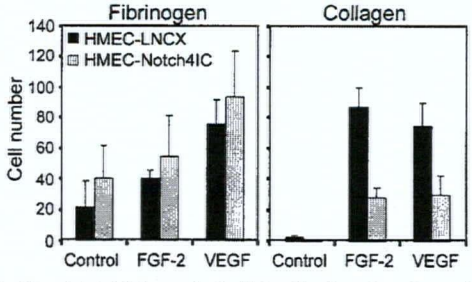

FIG. 5. Notch4 inhibits endothelial cell migration through collagen but not fibrinogen. Migration of HMEC-LNCX and HMEC-Notch4IC toward control medium and medium supplemented with FGF-2 (15 ng/ml) or VEGF (15 ng/ml) was assayed by using Transwell filters coated with fibrinogen or collagen type I. Following 16 h of incubation, cells that had migrated and adhered to the underside of the filter were stained and counted. Data are the means ± standard deviations from a single experiment done in triplicate and are representative of at least three independent experiments.

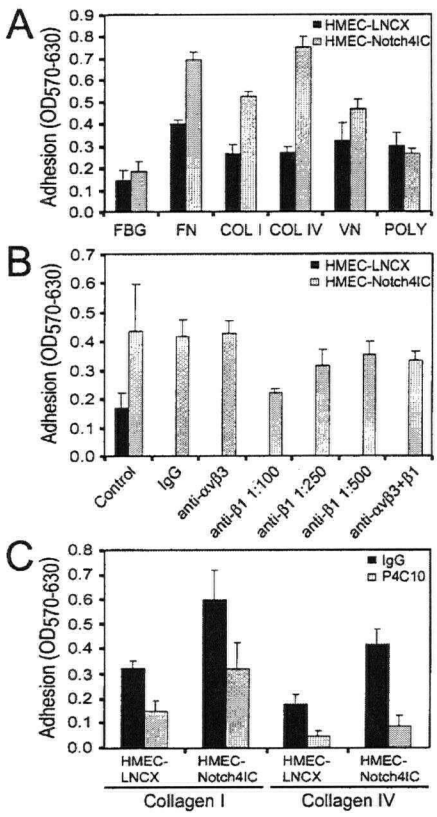

FIG. 6. Notch4 promotes endothelial cell adhesion to various extracellular matrix proteins through β1-integrins. (A) Adhesion of HMEC-LNCX and HMEC-Notch4IC to extracellular matrix proteins. Plates were coated with the following proteins: fibrinogen (FBG), fibronectin (FN), collagen type I (COL I), collagen type IV (COL IV), vitronectin (VN), and poly-L-lysine (POLY). Adherent cells were fixed, stained, and solubilized, and absorbance was read at 570 nm with background absorbance at 630 nm subtracted ($OD_{570-630}$). (B) Adhesion of HMEC-LNCX and HMEC-Notch4IC in the presence of function-blocking antibodies against αvβ3- and β1-integrins. Adhesion assays were performed on plates coated with collagen type I. HMEC-LNCX and HMEC-Notch4IC were preincubated with IgG2a (1:100 dilution), an anti-αvβ3 antibody (LM609; 10 μg/ml), and an anti-β1 antibody (P4C10; 1:100, 1:250, and 1:500 dilutions). For cells treated with both αvβ3 and β1 antibodies, 10 μg/ml and a 1:100 dilution, respectively, were used. (C) Adhesion of HMEC-LNCX and HMEC-Notch4IC in the presence of a function-blocking β1-integrin antibody. Adhesion assays were performed on plates coated with collagen type I or collagen type IV. Cells were preincubated with IgG2a (1:500 dilution) or an anti-β1 antibody (P4C10; 2.5 μg/ml). Adhesion data are the means ± standard deviations from a single experiment done in triplicate and are representative of at least three independent experiments.

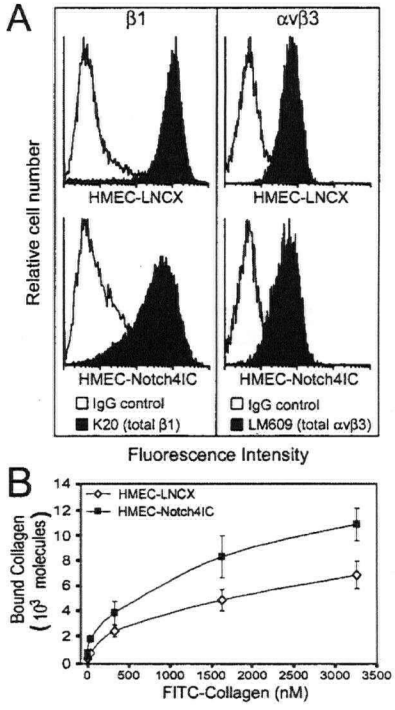

FIG. 7. Notch4 does not increase endothelial cell surface expression of β1-integrins but enhances binding of soluble collagen. (A) Surface expression of αvβ3- and β1-integrins on HMEC-LNCX and HMEC-Notch4IC. Cells were incubated with antibodies (IgG control, K20, and LM609) and analyzed by flow cytometry. Histograms are representative of at least three independent experiments. (B) Curves for binding of soluble collagen to HMEC-LNCX and HMEC-Notch4IC. FITC-conjugated collagen type I was incubated with cells at the indicated concentrations, and the samples were analyzed by flow cytometry. Binding data are the means ± standard deviations from two independent experiments.

(K20) (72) and mean fluorescence ratios (active β1/total β1) were determined by flow cytometry. Notch4IC-expressing cells, compared to control cells, displayed a greater proportion of β1-integrin receptors in a high-affinity state (Fig. 8A). Based on our findings, we reasoned that if β1-integrins expressed on HMEC-Notch4IC were already in a high-affinity state, we would not be able to further increase β1-integrin-mediated adhesion to collagen. Using a function-activating β1-integrin antibody (8A2) (42), we found that whereas HMEC-LNCX adhesion to collagen type I could be increased, 8A2 was unable to increase HMEC-Notch4IC adhesion to collagen type I (Fig. 8B). Taken together, our findings demonstrate that Notch4IC-expressing cells already display a fully active conformation of β1-integrins.

Increased β1-integrin-mediated adhesion plays a role in the Notch4 inhibition of endothelial sprouting. Our data suggest that the inhibited sprouting of Notch4IC-expressing cells in vitro may be explained in part by an increased affinity to gelatin-coated beads and that this high-affinity adhesive state (which presumably cannot be "turned off" due to the constitutive activation of Notch4) prevents the Notch4IC-expressing cells from migrating off the gelatin-coated beads and into the fibrin gel. This suggests that if Notch4IC-expressing cells were seeded onto beads by charge interaction rather than β1-integrin-mediated adhesion, the ability to form sprouts would be restored. To test this hypothesis, HMEC-Notch4IC were seeded onto dextran-coated microcarrier beads and the beads were embedded into fibrin gels. In this assay, we noted that HMEC-Notch4IC formed sprouts to a similar extent as HMEC-LNCX (Fig. 9). Hence in the absence of a β1-integrin substrate with which to interact, Notch4IC-expressing cells are capable of forming sprouts. As a control, dextran-coated beads were further coated with collagen type I and then seeded with HMEC-Notch4IC. Similar to results shown in Fig. 1B, sprout-

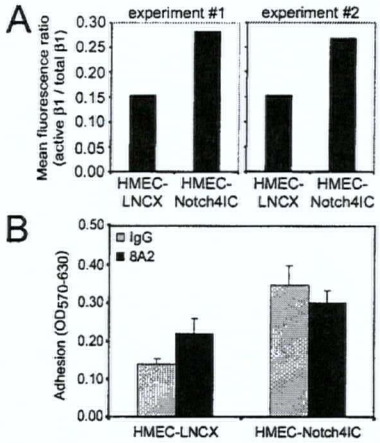

FIG. 8. Notch4-expressing cells display β1-integrins in a high-affinity conformation. (A) Mean fluorescence ratios of active β1 to total β1 on HMEC-LNCX and HMEC-Notch4IC. Cells were incubated with antibodies (B44, active β1; K20, total β1) and assessed by flow cytometry. Data are from two independent experiments. (B) HMEC-Notch4IC adhesion to collagen cannot be increased by function-activating β1-integrin antibodies. HMEC-LNCX and HMEC-Notch4IC preincubated with function-activating β1-integrin antibody 8A2 were added to collagen type I-coated wells. Adherent cells were fixed, stained, and solubilized, and absorbance was read at 570 nm with background absorbance at 630 nm subtracted ($OD_{570-630}$). Data are means ± standard deviations from a single experiment done in triplicate and are representative of at least three independent experiments. For the increased adhesion of HMEC-LNCX due to 8A2, the *P* value was 0.03 (analysis of variance).

ing of HMEC-Notch4IC from these collagen-recoated beads was inhibited (Fig. 9).

Activation of β1-integrins is sufficient to inhibit angiogenesis in vitro and in vivo. Our findings described thus far demonstrate that expression of activated Notch4 in endothelial cells inhibits angiogenesis both in vitro and in vivo, in part by promoting β1-integrin activation. To determine whether activation of β1-integrins alone (independent of constitutively active Notch4 expression) was sufficient to inhibit angiogenesis,

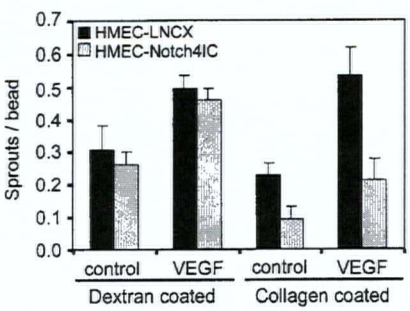

FIG. 9. Notch4 does not inhibit endothelial sprouting from dextran-coated microcarrier beads in vitro. Dextran-coated microcarrier beads were seeded with HMEC-LNCX or HMEC-Notch4IC. Equal numbers of beads were embedded in fibrin gels containing control medium or medium supplemented with VEGF (15 ng/ml). Endothelial sprout formation was quantitated after 3 days of incubation. As a control, dextran-coated beads were coated with collagen type I and were then seeded with HMEC lines. Data are the means ± standard deviations from a single experiment done in triplicate and are representative of at least three independent experiments.

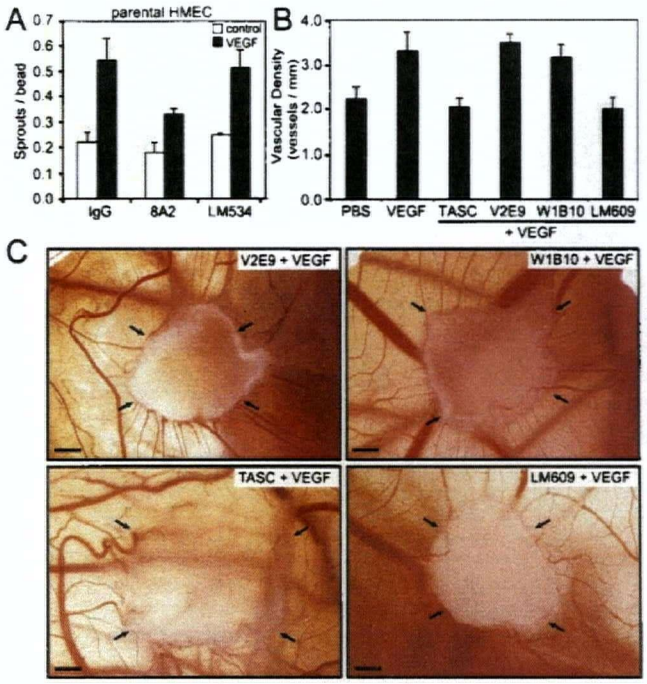

FIG. 10. Activation of β1-integrins alone, independent of Notch4 activation, is sufficient to inhibit endothelial sprouting in vitro and angiogenesis in vivo. (A) In vitro sprouting of parental HMEC from microcarrier beads coated with anti-β1-integrin antibodies. Dextran-coated microcarrier beads were preincubated with an IgG control antibody, a function-activating β1-integrin antibody (8A2), or a non-function-modifying β1-integrin antibody (LM534). Data are the means ± standard deviations from a single experiment done in triplicate and are representative of at least three independent experiments. (B) Angiogenesis in the chick CAM in the presence of anti-β1-integrin antibodies. The following antibodies were used: TASC (function-activating β1-integrin antibody), V2E9 (non-function-modifying β1-integrin antibody), W1B10 (function-blocking β1-integrin antibody), LM609 (function-blocking αvβ3-integrin antibody). Antibodies (10 μg/ml) plus VEGF (30 ng/ml) were loaded onto gelatin sponges, and the sponges were placed on the CAMs of day 8 embryos. As controls, sponges containing PBS or VEGF (30 ng/ml) were placed on CAMs. Angiogenesis was quantitated on day 10. Data are the means ± standard errors from two experiments each done in replicates of three to five eggs. (C) CAMs treated with V2E9, W1B10, TASC, and LM609 antibodies, all in the presence of VEGF. CAMs are representative of two independent experiments. Arrows, corners of the sponges. Bars, 1 mm.

we performed in vitro and in vivo experiments using antibodies that specifically activate β1-integrins.

Using the in vitro sprouting model with untransduced parental HMEC, we investigated the effect of function-activating β1-integrin antibody 8A2 on VEGF-induced sprouting. Dextran-coated beads were preincubated with either 8A2 or LM534, a non-function-modifying β1 antibody (72). These beads were subsequently seeded with parental HMEC and incubated for 3 days to allow parental HMEC to produce and secrete their own matrix proteins (many of which are β1-integrin substrates) onto the bead surface (44). Figure 10A shows that, whereas VEGF was able to induce sprouting of parental HMEC from beads coated with LM534, sprouting from 8A2-coated beads was reduced. Hence β1-integrin activation was sufficient to inhibit VEGF-induced endothelial

sprouting in vitro. The in vivo chick CAM assay was used to examine VEGF-induced angiogenesis in the presence of various anti-avian β1-integrin antibodies (Fig. 10B and C). CAMs were treated with TASC (a function-activating β1-integrin antibody) (16, 54), V2E9 (a non-function-modifying β1-integrin antibody) (31), or W1B10 (a function-blocking β1-integrin antibody) (16). Whereas VEGF was able to induce angiogenesis in CAMs treated with V2E9 and W1B10, CAMs treated with TASC exhibited decreased angiogenesis (Fig. 10B and C). In fact, angiogenesis in TASC-treated CAMs was reduced to a level similar to that for CAMs treated with LM609 (Fig. 10B and C), a function-blocking αvβ3-integrin antibody previously shown to attenuate VEGF-induced angiogenesis in the CAM (23). Taken together, our findings demonstrate that activation of β1-integrins, and hence increased adhesion through β1-integrins, is sufficient to inhibit VEGF-induced angiogenesis in vitro and in vivo.

DISCUSSION

There is good evidence to indicate that members of the Notch family of transmembrane receptors play an important role in regulating cell fate decisions and differentiation (2). More recently, several studies point to a role for Notch and its ligands in influencing vascular development. Mutations in Notch3 are responsible for the human vascular disorder cerebral autosomal dominant arteriopathy with subcortical infarcts and leukoencephalopathy, although in this case the defect appears to be mainly in vascular smooth muscle cells (37). Mutations in presenilin 1, a protein involved in Notch proteolytic processing, results in hemorrhaging (67, 79). Mice that are rendered null for Notch ligands Jagged1 and Delta1 exhibit vascular remodeling defects (80) and hemorrhaging (32), respectively. Antisense oligonucleotides directed against Jagged1 enhance FGF-2-induced endothelial tube formation in a collagen gel assay (81). Recently, a study examining the expression of four Notch receptors (Notch1 to -4) and five Notch ligands (Delta1, -3, and -4 and Jagged1 and -2) in the developing mouse vasculature was performed. Notch1, Notch3, Notch4, Delta4, Jagged1, and Jagged2 are all expressed in arteries but not veins (76). Notch2, Delta1, and Delta3, on the other hand, are not expressed in vessels (76). Nevertheless, a Notch2 hypomorphic allele disrupts vessel remodeling in multiple vascular beds (50). The combined loss of Notch4 and Notch1 functions due to gene targeting in the mouse results in defects in vascular remodeling (34, 45). Interestingly, expression of activated Notch4 in the mouse embryonic vasculature, under the control of the VEGF-R2 promoter, also results in vascular patterning defects (73). Although the last two studies demonstrate that both increases and decreases in Notch4 signaling result in a common vascular phenotype, disrupted blood vessel development, a mechanism(s) by which to explain this phenotype has not been elucidated.

The enforced expression of a constitutively active form of murine Notch4 in a mammary epithelial cell line has been shown to inhibit branching morphogenesis in a collagen gel assay (75). Because mammary epithelial tubulogenesis and blood vessel angiogenesis are similar morphogenic processes (52) and because Notch4 is primarily expressed in the endothelium (47, 74), we investigated whether enforced expression of activated Notch4 (Notch4IC) in endothelial cells could inhibit endothelial sprouting in vitro and angiogenesis in vivo. In an in vitro endothelial-tube formation assay, we show that Notch4IC inhibits spontaneous endothelial sprouting, as well as sprouting in response to FGF-2 and VEGF (Fig. 1). Furthermore, using an in vivo chick CAM assay, we demonstrate that Notch4IC expression is sufficient to inhibit VEGF-induced angiogenesis (Fig. 2 and 3).

Quiescent endothelial cells are normally anchored by their abluminal surface to a collagen-rich matrix (38). At the initiation of angiogenesis, the mature collagen-containing matrix is degraded and replaced by a provisional matrix of fibrin and fibronectin upon which endothelial cells migrate and proliferate (20, 59). The endothelial-sprouting assay used in our studies mimics angiogenesis in vivo. Specifically, microvascular endothelial cells are seeded as a monolayer onto gelatin-coated beads and are then induced by angiogenic factors to migrate into a fibrin matrix to form sprouts. We report that endothelial cells expressing Notch4IC exhibit inhibited sprouting in vitro (Fig. 1 and 9) and that this inhibition can be explained in part by an increase in HMEC-Notch4IC adhesion to collagen (Fig. 6 to 8). By enhancing cell adherence to collagen-coated beads, activated Notch4 prevents migration of the cells into the fibrin matrix. This is in accordance with our migration studies, where HMEC-Notch4IC migration through collagen, but not fibrinogen, was inhibited (Fig. 5). Proliferation rates, on the other hand, in HMEC-Notch4IC and control cells were found to be similar (Fig. 4). Our in vivo studies demonstrate that Notch4IC expression in the chick CAM inhibits VEGF-induced angiogenesis (Fig. 2 and 3). Based on our in vitro findings, the inhibition of angiogenesis in vivo may be due in part to enhanced endothelial cell adhesion to matrix proteins, thereby inhibiting vascular remodeling in the CAM.

Cell migration requires the coordinated activation and deactivation of integrins (46). As a cell migrates across a matrix, integrins at the leading edge of the cell adhere to the substrate (35). At the same time, receptors at the trailing edge of the cell detach from the substrate to allow the cell to progress forward (56). Thus, during the sprouting process of angiogenesis, integrin affinity states are constantly being modulated. The αvβ3-integrin has been shown to play a critical role in angiogenesis, but several studies also delineate the essential contribution of β1-integrins in endothelial morphogenesis (7, 21). Our data show that activated Notch4 increases endothelial cell adhesion (Fig. 6) and that enhanced β1-integrin affinity plays a role in this increased adhesion (Fig. 7 and 8).

Our work demonstrates that constitutive Notch4 activation inhibits vascular remodeling. Importantly, our studies provide a possible mechanism with which to explain the common vascular defects observed in mutant mice with either increased (73) or decreased (45) Notch signaling. Because Notch plays a role in cell fate decisions, Notch signaling must be precisely regulated and hence requires cessation of receptor signaling at certain times (2, 51, 77). Similarly, because cell adhesion influences cell functions such as migration and cell phenotype, modulation of cell adhesion must be strictly regulated (7, 26, 46, 57, 63). Therefore, it is possible that knocking out Notch4 and Notch1 results in a loss of cell-to-extracellular matrix adhesion and hence inhibited vascular remodeling, whereas constitutive Notch4 activation results in excessive cell-to-extracel-

lular matrix adhesion, thereby effectively fixing the cells in place. Taken together, our studies as well as the studies of Krebs et al. (45) and Uyttendaele et al. (73) reveal that altered Notch4 signaling results in disrupted blood vessel development.

Notch-like extracellular matrix protein Dell has been shown to induce integrin signaling and angiogenesis by binding endothelial αvβ3 and promoting migration (58). This is a case of signaling from the outside to the interior of the cell, as seen with many transmembrane receptors. In contrast, our studies suggest that activation of Notch4 propagates signals that induce an active, high-affinity conformation of the β1-integrin. To our knowledge, this is the first report demonstrating that any Notch member can regulate inside-out signaling of integrins. We are currently in the process of examining the potential pathways contributing to modulation of β1-integrin affinity by Notch4.

There is much evidence demonstrating that suppression of integrin activation is a physiological mechanism with which to control integrin-dependent cell adhesion and migration (33). In addition, regulation of integrin activation has been reported to precede differentiation in several cell types. Regulation of β1-integrin activity in neurogenic and myogenic differentiation, two processes that are also modulated by Notch, has been reported (8, 54). In a baboon model, it has previously been shown that in uninjured saphenous arteries endothelial cells and vascular smooth muscle cells express an epitope characteristic of β1-integrins in a high-affinity state (43). However, 6 weeks following balloon injury, regenerating endothelial cells did not express this ligand-induced epitope, although there was no decrease in the expression of total β1-integrin (43). In the same study, activation of β1-integrin with function-activating β1 antibody 8A2 inhibited the migration of endothelial cells in vitro (43). Together, these findings suggest that activated β1-integrin is required to maintain endothelial cells in a quiescent state, but, to repair arteries and possibly to allow neovascularization, dyshesion by downregulating β1-integrin affinity is required. In fact, activation of β1-integrins on human endothelial cells has been shown to inhibit capillary tube formation in collagen gels in vitro (25). We report that activation of β1-integrins on endothelial cells, independent of Notch4 activation, inhibits endothelial sprouting in vitro (Fig. 10A). Furthermore, we demonstrate that β1-integrin activation can inhibit angiogenesis in the chick CAM in vivo (Fig. 10B and C). In a previous study using function-blocking antibodies directed against specific α-integrin subunits, a combination of α1-blocking and α2-blocking antibodies was shown to inhibit VEGF-induced angiogenesis in a mouse Matrigel plug assay (66). These findings suggest that blocking α1β1- and α2β1-integrin function can inhibit VEGF-induced angiogenesis (66). Although these results may seem contradictory to our data demonstrating that blocking β1-integrin function does not inhibit VEGF-induced angiogenesis in the chick CAM (Fig. 10B and C), it is important to note that the effect of function-blocking and -activating antibodies directed against the β1-integrin subunit in the Matrigel plug assay was not reported. Because numerous αβ1-integrin heterodimers are implicated in angiogenesis (4, 17), blocking the function of only the α1 and α2 subunits may result in a different phenotype from that seen when the function of all β1-integrins is blocked. Alternatively, the different results may reflect intrinsic differences in the experimental models used. Indeed, function-blocking β1-integrin antibody CSAT has been reported to disrupt vascular development and lumen formation when microinjected into quail embryos (18), whereas the same CSAT antibody does not affect FGF-2- or tumor necrosis factor alpha-induced angiogenesis in the chick CAM (10).

Because Notch4 expression is restricted to the endothelium (74) and because Notch4 is the only Notch receptor expressed in the capillary endothelium (76), our findings implicate selective activation of Notch4 as a possible method by which to inhibit angiogenesis in pathological contexts. However, because our studies involve a constitutively active, overexpressed form of Notch4 in endothelial cells, the physiological relevance of the data must be interpreted with caution. Further studies using ligands specific for Notch4 will be important to determine whether modulated activation of Notch4 also inhibits angiogenesis. Recent studies suggest that Delta-like4 (Dll4) may be a potential ligand for Notch4, based on similar expression patterns for the two proteins (45, 69). However, it remains to be seen whether Dll4 can physically interact with and activate Notch4 and induce Notch4 signaling.

Hence the ability of Notch4 to inhibit endothelial sprouting in vitro and angiogenesis in vivo may be related in part to its ability to increase the ligand-binding affinity of β1-integrins, as we have demonstrated in this report. Other potential mechanisms, however, may act in concert with β1-integrin activation to mediate the observed Notch4 effect.

ACKNOWLEDGMENTS

We thank Mina Bissell and Nancy Boudreau for providing the avian retroviral vector CK and Nancy Boudreau for advice on the chick CAM assay. We also thank Kelly McNagny for the Q2bn cell line, John Harlan for the 8A2 antibody, John A. Wilkins for the B44 antibody, and Louis F. Reichardt for the TASC antibody. The V2E9 antibody, developed by Alan F. Horwitz, was obtained from the Developmental Studies Hybridoma Bank developed under the auspices of the NICHD and maintained by The University of Iowa, Department of Biological Sciences, Iowa City, Iowa. Thanks are also due to Penny Costello for assistance with the setup of the chick CAM assay and Linda Hughes for immunohistochemical staining of CAM sections.

This research was supported by grants to A.K. from the Heart and Stroke Foundation of British Columbia and the Yukon and the National Cancer Institute of Canada with funds from the Canadian Cancer Society and the Canadian Breast Cancer Foundation (BC Chapter) and to L.L. from the Stowers Institute for Medical Research. B.L. was supported by a Doctoral Research Award from the Heart and Stroke Foundation of Canada. K.G.L. was supported by a Doctoral Research Award from the Canadian Institutes of Health Research and a Predoctoral Fellowship Award from the Department of the Army (DAMD17-01-1-0164). The U.S. Army Medical Research Acquisition Activity, Fort Detrick, Md., is the awarding and administering acquisition office. A.K. is a Clinician-Scientist of the Canadian Institutes of Health Research and a Scholar of the Michael Smith Foundation for Health Research.

REFERENCES

1. **Ades, E. W., F. J. Candal, R. A. Swerlick, V. G. George, S. Summers, D. C. Bosse, and T. J. Lawley.** 1992. HMEC-1: establishment of an immortalized human microvascular endothelial cell line. J. Investig. Dermatol. **99**:683–690.
2. **Artavanis-Tsakonas, S., M. D. Rand, and R. J. Lake.** 1999. Notch signaling: cell fate control and signal integration in development. Science **284**:770–776.
3. **Auerbach, W., and R. Auerbach.** 1994. Angiogenesis inhibition. Pharmacol. Ther. **63**:265–311.
4. **Bauer, J., M. Margolis, C. Schreiner, C. J. Edgell, J. Azizkhan, E. Lazarowski, and R. L. Juliano.** 1992. In vitro model of angiogenesis using a human endothelium-derived permanent cell line: contributions of induced gene expression, G-proteins, and integrins. J. Cell Physiol. **153**:437–449.

5. **Bazoni, G., E. Dejana, and M. G. Lampugnani.** 1999. Endothelial adhesion molecules in the development of the vascular tree: the garden of forking paths. Curr. Opin. Cell Biol. **11**:573–581.
6. **Bigas, A., D. I. K. Martin, and L. A. Milner.** 1998. Notch1 and Notch2 inhibit myeloid differentiation in response to different cytokines. Mol. Cell. Biol. **18**:2324–2333.
7. **Bloch, W., E. Forsberg, S. Lentini, C. Brakebusch, K. Martin, H. W. Krell; U. H. Weidle, K. Addicks, and R. Fassler.** 1997. β1 integrin is essential for teratoma growth and angiogenesis. J. Cell Biol. **139**:265–278.
8. **Boettiger, D., M. Enomoto-Iwamoto, H. Y. Yoon, U. Hofer, A. S. Menko, and R. Chiquet-Ehrismann.** 1995. Regulation of integrin alpha 5 beta 1 affinity during myogenic differentiation. Dev. Biol. **169**:261–272.
9. **Boudreau, N., C. Andrews, A. Srebrow, A. Ravanpay, and D. A. Cheresh.** 1997. Induction of the angiogenic phenotype by Hox D3. J. Cell Biol. **139**: 257–264.
10. **Brooks, P. C., R. A. Clark, and D. A. Cheresh.** 1994. Requirement of vascular integrin alpha v beta 3 for angiogenesis. Science **264**:569–571.
11. **Brooks, P. C., A. M. Montgomery, and D. A. Cheresh.** 1999. Use of the 10-day-old chick embryo model for studying angiogenesis. Methods Mol. Biol. **129**:257–269.
12. **Carter, W. G., E. A. Wayner, T. S. Bouchard, and P. Kaur.** 1990. The role of integrins alpha 2 beta 1 and alpha 3 beta 1 in cell-cell and cell-substrate adhesion of human epidermal cells. J. Cell Biol. **110**:1387–1404.
13. **Celis, J. E. E.** 1998. Cell biology: a laboratory handbook, 2nd ed. Academic Press, San Diego, Calif.
14. **Cheresh, D. A.** 1987. Human endothelial cells synthesize and express an Arg-Gly-Asp-directed adhesion receptor involved in attachment to fibrinogen and von Willebrand factor. Proc. Natl. Acad. Sci. USA **84**:6471–6475.
15. **Cockerill, G. W., J. R. Gamble, and M. A. Vadas.** 1995. Angiogenesis: models and modulators. Int. Rev. Cytol. **159**:113–160.
16. **Cruz, M. T., C. L. Dalgard, and M. J. Ignatius.** 1997. Functional partitioning of beta1 integrins revealed by activating and inhibitory mAbs. J. Cell Sci. **110**:2647–2659.
17. **Davis, C. M., S. C. Danehower, A. Laurenza, and J. L. Molony.** 1993. Identification of a role of the vitronectin receptor and protein kinase C in the induction of endothelial cell vascular formation. J. Cell. Biochem. **51**:206–218.
18. **Drake, C. J., L. A. Davis, and C. D. Little.** 1992. Antibodies to beta 1-integrins cause alterations of aortic vasculogenesis, in vivo. Dev. Dyn. **193**:83–91.
19. **Duriez, P. J., F. Wong, K. Dorovini-Zis, R. Shahidi, and A. Karsan.** 2000. A1 functions at the mitochondria to delay endothelial apoptosis in response to tumor necrosis factor. J. Biol. Chem. **275**:18099–18107.
20. **Dvorak, H. F., L. F. Brown, M. Detmar, and A. M. Dvorak.** 1995. Vascular permeability factor/vascular endothelial growth factor, microvascular hyperpermeability, and angiogenesis. Am. J. Pathol. **146**:1029–1039.
21. **Eliceiri, B. P., and D. A. Cheresh.** 1999. The role of alphav integrins during angiogenesis: insights into potential mechanisms of action and clinical development. J. Clin. Investig. **103**:1227–1230.
22. **Ellison, L. W., J. Bird, D. C. West, A. L. Soreng, T. C. Reynolds, S. D. Smith, and J. Sklar.** 1991. TAN-1, the human homologue of the Drosophila *Notch* gene, is broken by chromosomal translocations in T lymphoblastic neoplasms. Cell **66**:649–661.
23. **Friedlander, M., P. C. Brooks, R. W. Shaffer, C. M. Kincaid, J. A. Varner, and D. A. Cheresh.** 1995. Definition of two angiogenic pathways by distinct alpha v integrins. Science **270**:1500–1502.
24. **Furriols, M., and S. Bray.** 2000. Dissecting the mechanisms of suppressor of hairless function. Dev. Biol. **227**:520–532.
25. **Gamble, J., G. Meyer, L. Noack, J. Furze, L. Matthias, N. Kovach, J. Harlan, and M. Vadas.** 1999. Beta(1) integrin activation inhibits in vitro tube formation: effects on cell migration, vacuole coalescence and lumen formation. Endothelium **7**:23–34.
26. **Gamble, J. R., L. J. Matthias, G. Meyer, P. Kaur, G. Russ, R. Faull, M. C. Berndt, and M. A. Vadas.** 1993. Regulation of in vitro capillary tube formation by anti-integrin antibodies. J. Cell Biol. **121**:931–943.
27. **Garces, C., M. J. Ruizhidalgo, J. F. Demora, C. Park, L. Miele, J. Goldstein, E. Bonvini, A. Porras, and J. Laborda.** 1997. Notch-1 controls the expression of fatty acid-activated transcription factors and is required for adipogenesis. J. Biol. Chem. **272**:29729–29734.
28. **Grant, D. S., K. I. Tashiro, B. Segui-Real, Y. Yamada, G. R. Martin, and H. K. Kleinman.** 1989. Two different laminin domains mediate the differentiation of human endothelial cells into capillary-like structures *in vitro*. Cell **58**:933–943.
29. **Greenwald, I.** 1994. Structure/function studies of lin-12/Notch proteins. Curr. Biol. **4**:556–562.
30. **Hanahan, D., and J. Folkman.** 1996. Patterns and emerging mechanisms of the angiogenic switch during tumorigenesis. Cell **86**:353–364.
31. **Hayashi, Y., B. Haimovich, A. Reszka, D. Boettiger, and A. Horwitz.** 1990. Expression and function of chicken integrin beta 1 subunit and its cytoplasmic domain mutants in mouse NIH 3T3 cells. J. Cell Biol. **110**:175–184.
32. **Hrabe de Angelis, M., J. McIntyre II, and A. Gossler.** 1997. Maintenance of somite borders in mice requires the Delta homologue Dll1. Nature **386**:717–721.
33. **Hughes, P. E., and M. Pfaff.** 1998. Integrin affinity modulation. Trends Cell Biol. **8**:359–364.
34. **Huppert, S. S., A. Le, E. H. Schroeter, J. S. Mumm, M. T. Saxena, L. A. Milner, and R. Kopan.** 2000. Embryonic lethality in mice homozygous for a processing-deficient allele of Notch1. Nature **405**:966–970.
35. **Huttenlocher, A., M. H. Ginsberg, and A. F. Horwitz.** 1996. Modulation of cell migration by integrin-mediated cytoskeletal linkages and ligand-binding affinity. J. Cell Biol. **134**:1551–1562.
36. **Jiang, B. H., J. Z. Zheng, M. Aoki, and P. K. Vogt.** 2000. Phosphatidylinositol 3-kinase signaling mediates angiogenesis and expression of vascular endothelial growth factor in endothelial cells. Proc. Natl. Acad. Sci. USA **97**: 1749–1753.
37. **Joutel, A., C. Corpechot, A. Ducros, K. Vahedi, H. Chabriat, P. Mouton, S. Alamowitch, V. Domenga, M. Cecillion, E. Marechal, J. Maciazek, C. Vayssiere, C. Cruaud, E. A. Cabanis, M. M. Ruchoux, J. Weissenbach, J. F. Bach, M. G. Bousser, and E. Tournier-Lasserve.** 1996. Notch3 mutations in CADASIL, a hereditary adult-onset condition causing stroke and dementia. Nature **383**:707–710.
38. **Karsan, A., and J. M. Harlan.** 1999. The blood vessel wall, p. 1770–1782. *In* R. Hoffman, E. J. J. Benz, S. J. Shattil, B. Furie, H. J. Cohen, L. E. Silberstein, and P. McGlave (ed.), Hematology: basic principles and practice. Churchill Livingstone, New York, N.Y.
39. **Karsan, A., E. Yee, and J. M. Harlan.** 1996. Endothelial cell death induced by tumor necrosis factor α is inhibited by the Bcl-2 family member, A1. J. Biol. Chem. **271**:27201–27204.
40. **Koblizek, T. I., C. Weiss, G. D. Yancopoulos, U. Deutsch, and W. Risau.** 1998. Angiopoietin-1 induces sprouting angiogenesis *in vitro*. Curr. Biol. **8**:529–532.
41. **Kopan, R., J. S. Nye, and H. Weintraub.** 1994. The intracellular domain of mouse Notch: a constitutively activated repressor of myogenesis directed at the basic helix-loop-helix region of *MyoD*. Development **120**:2385–2396.
42. **Kovach, N. L., T. M. Carlos, E. Yee, and J. M. Harlan.** 1992. A monoclonal antibody to beta 1 integrin (CD29) stimulates VLA-dependent adherence of leukocytes to human umbilical vein endothelial cells and matrix components. J. Cell Biol. **116**:499–509.
43. **Koyama, N., J. Seki, S. Vergel, E. J. Mattsson, T. Yednock, N. L. Kovach, J. M. Harlan, and A. W. Clowes.** 1996. Regulation and function of an activation-dependent epitope of the beta 1 integrins in vascular cells after balloon injury in baboon arteries and in vitro. Am. J. Pathol. **148**:749–761.
44. **Kramer, R. H., G. M. Fuh, and M. A. Karasek.** 1985. Type IV collagen synthesis by cultured human microvascular endothelial cells and its deposition into the subendothelial basement membrane. Biochemistry **24**:7423–7430.
45. **Krebs, L. T., Y. Xue, C. R. Norton, J. R. Shutter, M. Maguire, J. P. Sundberg, D. Gallahan, V. Closson, J. Kitajewski, R. Callahan, G. H. Smith, K. L. Stark, and T. Gridley.** 2000. Notch signaling is essential for vascular morphogenesis in mice. Genes Dev. **14**:1343–1352.
46. **Lauffenburger, D. A., and A. F. Horwitz.** 1996. Cell migration: a physically integrated molecular process. Cell **84**:359–369.
47. **Li, L., G. M. Huang, A. B. Banta, Y. Deng, T. Smith, P. Dong, C. Friedman, L. Chen, B. J. Trask, T. Spies, L. Rowen, and L. Hood.** 1998. Cloning, characterization, and the complete 56.8-kilobase DNA sequence of the human Notch4 gene. Genomics **51**:45–58.
48. **Li, L., I. D. Krantz, Y. Deng, A. Genin, A. B. Banta, C. C. Collins, M. Qi, B. J. Trask, L. Kuo, J. Cochran, T. Costa, M. E. M. Pierpont, E. B. Rand, D. A. Piccoli, L. Hood, and N. B. Spinner.** 1997. Alagille syndrome is caused by mutations in human *Jagged1*, which encodes a ligand for Notch1. Nat. Genet. **16**:243–251.
49. **Lowik, C. W., M. J. Alblas, M. van de Ruit, S. E. Papapoulos, and G. van der Pluijm.** 1993. Quantification of adherent and nonadherent cells cultured in 96-well plates using the supravital stain neutral red. Anal. Biochem. **213**: 426–433.
50. **McCright, B., X. Gao, L. Shen, J. Lozier, Y. Lan, M. Maguire, D. Herzlinger, G. Weinmaster, R. Jiang, and T. Gridley.** 2001. Defects in development of the kidney, heart and eye vasculature in mice homozygous for a hypomorphic Notch2 mutation. Development **128**:491–502.
51. **Milner, L. A., and A. Bigas.** 1999. Notch as a mediator of cell fate determination in hematopoiesis: evidence and speculation. Blood **93**:2431–2448.
52. **Montesano, R., J. V. Soriano, K. M. Malinda, M. L. Ponce, A. Bafico, H. K. Kleinman, D. P. Bottaro, and S. A. Aaronson.** 1998. Differential effects of hepatocyte growth factor isoforms on epithelial and endothelial tubulogenesis. Cell Growth Differ. **9**:355–365.
53. **Nehls, V., and D. Drenckhahn.** 1995. A novel, microcarrier-based *in vitro* assay for rapid and reliable quantification of three-dimensional cell migration and angiogenesis. Microvasc. Res. **50**:311–322.
54. **Neugebauer, K. M., and L. F. Reichardt.** 1991. Cell-surface regulation of beta 1-integrin activity on developing retinal neurons. Nature **350**:68–71.
55. **Ni, H., A. Li, N. Simonsen, and J. A. Wilkins.** 1998. Integrin activation by dithiothreitol or Mn2+ induces a ligand-occupied conformation and exposure of a novel NH2-terminal regulatory site on the beta1 integrin chain. J. Biol. Chem. **273**:7981–7987.
56. **Palecek, S. P., A. Huttenlocher, A. F. Horwitz, and D. A. Lauffenburger.**

1998. Physical and biochemical regulation of integrin release during rear detachment of migrating cells. J. Cell Sci. **111**:929–940.
57. **Palecek, S. P., J. C. Loftus, M. H. Ginsberg, D. A. Lauffenburger, and A. F. Horwitz.** 1997. Integrin-ligand binding properties govern cell migration speed through cell-substratum adhesiveness. Nature **385**:537–540.
58. **Penta, K., J. A. Varner, L. Liaw, C. Hidai, R. Schatzman, and T. Quertermous.** 1999. Del1 induces integrin signaling and angiogenesis by ligation of αvβ3. J. Biol. Chem. **274**:11101–11109.
59. **Pepper, M. S.** 1997. Manipulating angiogenesis: from basic science to the bedside. Arterioscler. Thromb. Vasc. Biol. **17**:605–619.
60. **Rak, J., and R. S. Kerbel.** 1997. bFGF and tumor angiogenesis--back in the limelight? Nat. Med. **3**:1083–1084.
61. **Rebay, I., R. G. Fehon, and S. Artavanis-Tsakonas.** 1993. Specific truncations of Drosophila Notch define dominant activated and dominant negative forms of the receptor. Cell **74**:319–329.
62. **Risau, W.** 1997. Mechanisms of angiogenesis. Nature **386**:671–674.
63. **Ruoslahti, E., and E. Engvall.** 1997. Integrins and vascular extracellular matrix assembly. J. Clin. Investig. **99**:1149–1152.
64. **Schroeter, E. H., J. A. Kisslinger, and R. Kopan.** 1998. Notch-1 signalling requires ligand-induced proteolytic release of intracellular domain. Nature **393**:382–386.
65. **Sehested, M., and K. Hou-Jensen.** 1981. Factor VIII related antigen as an endothelial cell marker in benign and malignant diseases. Virchows Arch. A Pathol. Anat. Histol. **391**:217–225.
66. **Senger, D. R., K. P. Claffey, J. E. Benes, C. A. Perruzzi, A. P. Sergiou, and M. Detmar.** 1997. Angiogenesis promoted by vascular endothelial growth factor: regulation through alpha1beta1 and alpha2beta1 integrins. Proc. Natl. Acad. Sci. USA **94**:13612–13617.
67. **Shen, J., R. T. Bronson, D. F. Chen, W. Xia, D. J. Selkoe, and S. Tonegawa.** 1997. Skeletal and CNS defects in Presenilin-1-deficient mice. Cell **89**:629–639.
68. **Shirayoshi, Y., Y. Yuasa, T. Suzuki, K. Sugaya, E. Kawase, T. Ikemura, and N. Nakatsuji.** 1997. Proto-oncogene of int-3, a mouse Notch homologue, is expressed in endothelial cells during early embryogenesis. Genes Cells **2**:213–224.
69. **Shutter, J. R., S. Scully, W. Fan, W. G. Richards, J. Kitajewski, G. A. Deblandre, C. R. Kintner, and K. L. Stark.** 2000. Dll4, a novel Notch ligand expressed in arterial endothelium. Genes Dev. **14**:1313–1318.
70. **Sriramarao, P., M. Mendler, and M. A. Bourdon.** 1993. Endothelial cell attachment and spreading on human tenascin is mediated by alpha 2 beta 1 and alpha v beta 3 integrins. J. Cell Sci. **105**:1001–1012.
71. **Struhl, G., and A. Adachi.** 1998. Nuclear access and action of *Notch* in vivo. Cell **93**:649–660.
72. **Takada, Y., and W. Puzon.** 1993. Identification of a regulatory region of integrin beta 1 subunit using activating and inhibiting antibodies. J. Biol. Chem. **268**:17597–17601.
73. **Uyttendaele, H., J. Ho, J. Rossant, and J. Kitajewski.** 2001. Vascular patterning defects associated with expression of activated Notch4 in embryonic endothelium. Proc. Natl. Acad. Sci. USA **98**:5643–5648.
74. **Uyttendaele, H., G. Marazzi, G. Wu, Q. Yan, D. Sassoon, and J. Kitajewski.** 1996. *Notch4/Int-3*, a mammary proto-oncogene, is an endothelial cell-specific mammalian *Notch* gene. Development **122**:2251–2259.
75. **Uyttendaele, H., V. J. Soriano, R. Montesano, and J. Kitajewski.** 1998. Notch4 and Wnt-1 proteins function to regulate branching morphogenesis of mammary epithelial cells in an opposing fashion. Dev. Biol. **196**:204–217.
76. **Villa, N., L. Walker, C. E. Lindsell, J. Gasson, M. L. Iruela-Arispe, and G. Weinmaster.** 2001. Vascular expression of Notch pathway receptors and ligands is restricted to arterial vessels. Mech. Dev. **108**:161–164.
77. **Weinmaster, G.** 2000. Notch signal transduction: a real rip and more. Curr. Opin. Genet. Dev. **10**:363–369.
78. **Wilkins, J. A., A. Li, H. Ni, D. G. Stupack, and C. Shen.** 1996. Control of beta1 integrin function. Localization of stimulatory epitopes. J. Biol. Chem. **271**:3046–3051.
79. **Wong, P. C., H. Zheng, H. Chen, M. W. Becher, D. J. Sirinathsinghji, M. E. Trumbauer, H. Y. Chen, D. L. Price, L. H. van der Ploeg, and S. S. Sisodia.** 1997. Presenilin 1 is required for Notch1 and Dll1 expression in the paraxial mesoderm. Nature **387**:288–292.
80. **Xue, Y., X. Gao, C. E. Lindsell, C. R. Norton, B. Chang, C. Hicks, M. Gendron-Maguire, E. B. Rand, G. Weinmaster, and T. Gridley.** 1999. Embryonic lethality and vascular defects in mice lacking the Notch ligand Jagged1. Hum. Mol. Genet. **8**:723–730.
81. **Zimrin, A. B., M. S. Pepper, G. A. McMahon, F. Nguyen, R. Montesano, and T. Maciag.** 1996. An antisense oligonucleotide to the notch ligand jagged enhances fibroblast growth factor-induced angiogenesis in vitro. J. Biol. Chem. **271**:32499–32502.

This page intentionally blank

American Journal of Hematology 70:22–30 (2002)

Role of the Microenvironment in Promoting Angiogenesis in Acute Myeloid Leukemia

Craig Litwin,[1] Kevin G. Leong,[2,4] Richard Zapf,[5] Heather Sutherland,[3,5] Sheldon C. Naiman,[1] and Aly Karsan[1,4,6*]

[1]Department of Pathology and Laboratory Medicine, University of British Columbia, Vancouver, Canada
[2]Department of Experimental Medicine, University of British Columbia, Vancouver, Canada
[3]Department of Medicine, University of British Columbia, Vancouver, Canada
[4]Department of Medical Biophysics, British Columbia Cancer Agency, Vancouver, Canada
[5]Terry Fox Laboratory, British Columbia Cancer Agency, Vancouver, Canada
[6]Department of Pathology and Laboratory Medicine, British Columbia Cancer Agency, Vancouver, Canada

Angiogenesis is a crucial event in the survival and progression of solid tumors. To determine whether angiogenesis in acute myeloid leukemia (AML) is an intrinsic property of leukemic cells, the vascularity of bone marrow biopsies was determined. Bone marrow vascularity in newly diagnosed or post-chemotherapy AML patients was increased 4-fold ($P < 0.01$) and 8.7-fold ($P < 0.01$), respectively, relative to controls. Vascular endothelial growth factor (VEGF) expression by AML blast cells was assessed by immunohistochemistry, and bone marrow cell supernatants were assayed for secretion of VEGF, fibroblast growth factor-2 (FGF-2), and endostatin by enzyme-linked immunosorbent assay. Diffuse cytoplasmic and strong extracellular VEGF immunoreactivity was seen in bone marrow aspirates from AML patients, but not controls. In contrast, there was no difference in the levels of VEGF, FGF-2, and endostatin secreted by mononuclear cells cultured from bone marrows of AML patients compared to normal controls following two days of culture in vitro. Total angiogenic potential of bone marrow cell supernatants was assessed by endothelial sprouting in vitro and by a chick chorioallantoic membrane assay. No differences were found between 2-day conditioned medium from normal and AML bone marrow mononuclear cells in either assay. Our data show a discrepancy between bone marrow vascularity and VEGF expression in vivo and VEGF expression and angiogenesis from 2-day conditioned medium ex vivo. This suggests that angiogenesis in AML likely represents a response to microenvironmental factors in vivo, rather than being an intrinsic property of leukemic cells. Am. J. Hematol. 70:22–30, 2002. © 2002 Wiley-Liss, Inc.

Key words: angiogenesis; leukemia; microenvironment; fibroblast growth factor; vascular endothelial growth factor

INTRODUCTION

Compelling experimental evidence attests to the fundamental role angiogenesis plays in both the growth and metastasis of solid tumors [1]. Neovascularization of solid tumors is required for a tumor to grow beyond 2–3 mm^3 and inhibition of angiogenesis reduces primary tumor volume and inhibits tumor metastasis [1]. Recent observations suggest that angiogenesis may also be important in the pathogenesis of hematologic malignancies. Increased microvessel density in bone marrow biopsies obtained from patients diagnosed with childhood acute lymphoblastic

Contract grant sponsor: Heart and Stroke Foundation of British Columbia the Yukon (to A.K.); Contract grant sponsor: National Cancer Institute of Canada (to A.K. and H.S.).

C. Litwin and K.G. Leong contributed equally to this work.

*Correspondence to: Aly Karsan, Department of Medical Biophysics, British Columbia Cancer Research Centre, 601 West 10th Ave., Vancouver, BC, Canada, V5Z 1L3.
E-mail: akarsan@bccancer.bc.ca

Received for publication 14 May 2001; Accepted 14 December 2001

Published online in Wiley InterScience (www.interscience.wiley.com). DOI: 10.1002/ajh.10092

leukemia (ALL) relative to control bone marrow biopsies has been reported [2]. The vessels in the leukemic bone marrow biopsies were architecturally abnormal and demonstrated a complex three-dimensional structure, uneven clustering (so-called "hot-spots"), and poorly formed lumina. Similarly, Vacca and colleagues reported increased density of architecturally abnormal blood vessels in bone marrow biopsies from patients diagnosed with multiple myeloma compared to patients with monoclonal gammopathy of unknown significance (MGUS) [3,4]. Others have demonstrated increased vascular density in bone marrow biopsies from patients with acute myeloid leukemia (AML) [5,6].

Malignant hematopoietic cells have been demonstrated to secrete a number of angiogenic growth factors. Elevated cellular vascular endothelial growth factor (VEGF) concentrations have been detected in patients with AML and portend a poorer prognosis [7]. Bellamy and colleagues identified expression of VEGF mRNA and the secretion of intact VEGF by each of twelve different cell lines representing lymphoma, leukemia, and multiple myeloma phenotypes, while expression of fibroblast growth factor-2 (FGF-2) mRNA was detected in half of the cell lines studied [8]. Fiedler and co-workers [9] detected expression of VEGF mRNA by blast cells in 20 of 28 patients newly diagnosed with AML. Intracellular VEGF immunoreactivity was present in two different leukemic cell lines and in freshly harvested blast cells obtained from 8 patients with AML. Secretion of VEGF into culture media has been demonstrated in a number of leukemic cell lines and cultured bone marrow cells derived from patients with chronic myelogenous leukemia [10]. Furthermore, VEGF mRNA synthesis and secretion of VEGF peptide by AML blasts has been reported [5]. Despite these observations, the role of angiogenesis in the pathophysiology of hematologic malignancies remains uncertain. An understanding of the regulation of the secretion of angiogenic factors by malignant hematologic cells and the response of malignant hematopoietic cells to environmental factors is almost completely lacking.

In the current report, we confirm increased vascular density in bone marrow biopsies obtained from patients diagnosed with AML. In newly diagnosed AML patients, bone marrow vascularity was increased 4-fold. Furthermore, an 8.7-fold increase in vascularity was noted in bone marrow biopsies obtained at 30 days post-induction chemotherapy. AML blast cells demonstrated strong cytoplasmic immunohistochemical reactivity to VEGF, providing evidence of increased VEGF content in the cellular compartment of AML bone marrows. In contrast, cultured bone marrow cells from patients with AML did not secrete increased amounts of either VEGF or FGF-2 relative to normal bone marrow cells. Despite the increased bone marrow vascularity and VEGF expression of AML marrows, results of two angiogenesis assays did not show an increased angiogenic potential of conditioned medium from cultured bone marrow of AML patients. Taken together, our findings suggest that bone marrow environmental factors likely play a crucial role in promoting angiogenesis in AML.

MATERIALS AND METHODS

Tissue Samples and Immunohistochemistry

Archival paraffin-embedded bone marrow core biopsy specimens were obtained from adult patients with AML at time of initial diagnosis or at 30 days post-induction chemotherapy. Diagnosis of AML conformed to criteria outlined by the standard French-American-British (FAB) system and the distribution of cases was as follows: M1 (7), M2 (3), M3 (3), M4 (5). Negative staging bone marrow biopsies from patients diagnosed with lymphoma were used as controls as described by others, as these patients had normal hematological parameters [2]. A total of 18 AML bone marrow core biopsies, 11 post-induction chemotherapy, and 10 lymphoma-negative biopsies were subsequently evaluated. Specimens were fixed in formalin or B5, surface decalcified in nitric acid, and embedded in paraffin.

Bone marrow sections were stained immunohistochemically for von Willebrand factor (vWF), a marker of vascular endothelial cells [11]. Immunohistochemical staining for vWF was performed using anti-human vWF rabbit polyclonal antibody (1:100 dilution, Dako, Glostrup, Denmark). Bone marrow aspirate VEGF immunohistochemistry was performed using anti-human VEGF (clone JH121, Neomarkers Laboratories, Union City, CA, 1:100 dilution with overnight incubation).

Bone Marrow Vascularity

Point counting of the bone marrow biopsies was performed according to published methods [12,13]. Briefly, a 13 × 13 point grid was projected upon five randomly selected medium power fields (ocular 10×, objective 10×) per biopsy. Individual cells falling upon the point grid were scored as either vascular or non-vascular. Points landing on bone were excluded. To normalize each specimen to the actual marrow space evaluated, the ratio of points landing on vascular endothelial cells to total points landing within the marrow space was calculated. All counts were performed by a blinded observer, with 5 random specimens counted by a second blinded observer to verify reproducibility of the counts.

Patient Cells

Bone marrow cells were obtained from 7 normal allogeneic bone marrow donors as an aliquot of their marrow harvest or as an aliquot of the diagnostic marrow from patients with AML, after informed and written consent according to a protocol approved by the Research Ethics Board of the University of British Columbia. Cells were treated with ammonium chloride to lyse red blood cells and were frozen in Dulbecco's Modified Eagle's medium (DMEM) (StemCell Technologies, Inc., Vancouver, Canada) with 30% fetal calf serum (FCS) and 10% DMSO. To obtain supernatants for assessment, cells were thawed and washed. Viability was determined by Trypan blue exclusion and was at least 80%. Cells were then cultured at 10^7 cells in 10 mL of MCDB medium with 5% FCS and maintained at 37°C in a 5% CO_2 humidified incubator.

Enzyme-Linked Immunosorbent Assay (ELISA)

Supernatants were assayed for the presence of VEGF, FGF-2, or endostatin by ELISA (Cytimmune Science Inc., College Park, MD) according to the manufacturer's instructions.

Endothelial Sprouting Assay

Endothelial sprouting was assessed by a modification of the method of Nehls and Drenckhahn [14]. Briefly, gelatin-coated microcarrier beads (Sigma, St. Louis, MO) were seeded with human microvascular endothelial cells (HMEC) [15]. When the cells reached confluence on the beads, equal numbers of HMEC-coated beads were embedded in fibrin gels in 96-well plates. FGF-2 (15 ng/mL) or VEGF (15 ng/mL) were used as positive controls. Negative controls contained FCS (5%) only. Fibrin gels for bone marrow supernatants were prepared by adding 50 μL of the appropriate supernatant to 50 μL of fibrinogen solution, yielding a final fibrinogen concentration of 2.5 mg/mL. Following transfer of the fibrinogen solution to 96-well plates, HMEC-coated beads were added at a density of 50 beads/well, and clotting was induced by the addition of thrombin (0.625 U/mL). After clotting was complete, gels were equilibrated with MCDB + 5% FCS at 37°C. Following 60 min of incubation, the overlying medium was changed for all wells. MCDB + 5% FCS containing FGF-2 (15 ng/mL), VEGF (15 ng/mL), or harvested culture supernatant (10^6 cells × 48 hr) was added. Each condition was tested in 3 replicate wells per experiment. After 3 days of incubation with daily medium changes, the number of capillary-like tubes formed was quantitated by counting the number of endothelial sprouts per microcarrier bead. Only sprouts greater than 150 μm in length and composed of at least 3 endothelial cells were counted.

Chick Embryo Chorioallantoic Membrane (CAM) Assay

Fertilized White Leghorn chicken eggs were incubated at 37°C under conditions of constant humidity. On day 6 of embryo incubation, the developing CAM was separated from the shell by opening a small circular window at the broad end of the egg above the air sac. The opening was sealed with Parafilm, and the eggs were incubated for 2 more days. On day 8, 20 μL of bone marrow supernatant was loaded onto 2 mm^3 gelatin sponges (Gelfoam; Pharmacia and Upjohn Co., Donmills, Canada) that were placed on the surface of the developing CAM. Sponges containing vehicle alone (MCDB medium + 5% FCS) were used as negative controls, whereas sponges containing either FGF-2 (30 ng/mL) or VEGF (30 ng/mL) were used as positive controls. Eggs were resealed and returned to the incubator. On day 10, images of the CAM were captured digitally using an Olympus SZX9 stereomicroscope (Olympus America Inc., Melville, NY) with the Spot RT digital imaging system (Diagnostic Instruments Inc., Sterling Heights, MI). The relative angiogenesis index was determined by grading according to a 5-point scale, with scores of 0 and 4 representing the angiogenic response to negative and positive controls, respectively, as has been previously described [16].

Statistical Analysis

Differences between groups were determined by ANOVA, and the Tukey test was used to determine significant differences between multiple groups [17]. A P value less than 0.05 was considered significant.

RESULTS

Increased Vascularity and Abnormal Vascular Architecture in AML Bone Marrow Biopsies

Identification of blood vessels was aided by positive immunohistochemical staining for vWF of the vascular endothelial cells. This procedure highlights small or poorly formed vessels which are less apparent on hematoxylin and eosin stained bone marrow biopsies and has been previously validated [2,5,11]. Figure 1 illustrates the typical immunohistology seen in bone marrow biopsies obtained from control patients (Fig. 1B), patients newly diagnosed with AML (Fig. 1C), and patients with AML at 30 days post-induction chemotherapy (Fig. 1D).

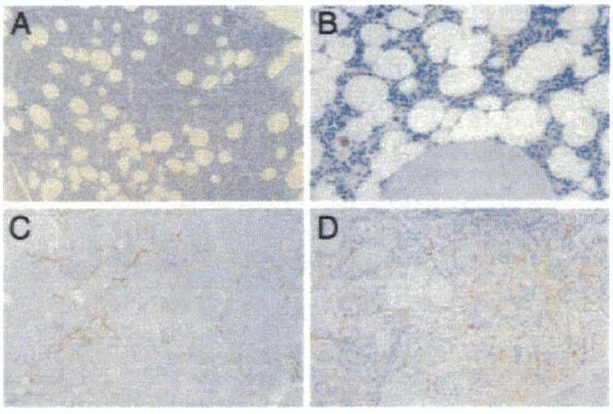

Fig. 1. Bone marrow biopsies immunostained for vWF to highlight marrow blood vessels. (A) Negative control. No vWF immunoreactivity is seen in an AML specimen in the absence of primary antibody (original magnification 50x). (B) Normal control biopsy showing occasional well-formed vessels. Immunoreactivity is restricted to megakaryocytes and the endothelial cells of blood vessels (original magnification 100×). Increased vascularity is evident in both newly diagnosed AML (C, original magnification 50×) or 30 day post-induction chemotherapy AML biopsies (D, original magnification 66×). [Color figure can be viewed in the online issue, which is available at www.interscience.wiley.com.]

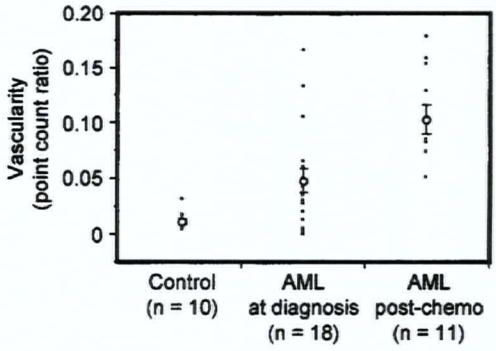

Fig. 2. Point count ratios of control and AML bone marrow biopsies. Blood vessel point counts were performed on control (n = 10), newly diagnosed AML (n = 18), and 30 day post-induction chemotherapy (n = 11) bone marrow biopsies and the point count ratios calculated as described. The mean of each group (O) and standard error are indicated.

Figure 1A shows an AML marrow biopsy where the primary antibody was omitted (negative control). Normal cellularity and characteristically low vascular density was typically observed in the control bone marrow biopsies (Fig. 1B). Megakaryocytes consistently stained for vWF as expected, and served as an internal control. Well-formed, non-clustered, small- to medium-sized vessels present at a density of less than one vessel per medium power (10×) microscopic field were typically observed.

Bone marrow biopsies obtained from patients newly diagnosed with AML were markedly hypercellular. An increased number of small- to medium-sized vWF-positive vessels was identifiable in the majority of microscopic fields examined (Fig. 1C). These vessels were architecturally abnormal with irregular outlines, and variable luminal caliber. Additionally, there was a noticeable tendency toward vessel clustering ("hot-spots") at points distant from bony trabeculae. Marrow biopsies obtained from AML patients 30 days post-induction chemotherapy were normocellular or hypocellular and demonstrated degenerative change (Fig. 1D). The overall histologic appearance of the blood vessels and tendency toward clustering reiterated that observed in the newly diagnosed AML biopsies. Somewhat unexpectedly, the vascularity of the post-chemotherapy biopsies qualitatively exceeded that seen in the pre-chemotherapy bone marrow biopsies.

Quantitative assessment of bone marrow vascularity was performed using point count methodology. Only those vWF-positive vascular endothelial cells falling on a defined computer-generated point were counted and subsequently utilized as markers of blood vessels. Point count data showed control marrow biopsies to have a relatively uniform low density of vascular endothelial cells. The number of vascular endothelial cells per microscopic field ranged from 0 to 8. Point counts from biopsies obtained from AML patients at diagnosis revealed an increased number of vWF-positive endothelial cells ranging from 0 to 28. The highest point counts were obtained in the 30 day post-induction chemotherapy bone marrow biopsies, in which counts ranged from 0 to 41 per 10× microscopic field.

To correct for differences in total marrow space evaluated between individual biopsies, the point count data were calculated as the ratio of vWF-positive points per total points counted ("point count ratio"). Calculation of the point count ratio for control biopsies yielded values of 0.003 to 0.031, with a mean of 0.012 ± 0.003 (n = 10) (Fig. 2). The values obtained fell within a relatively narrow range with minimal inter-biopsy variation. Confirming our qualitative assessment of newly diagnosed AML biopsy vascularity, the point count ratio was increased with values ranging from 0.002 to 0.166 with a mean value of 0.048 ± 0.011 (n = 18) (Fig. 2). This represents a 4-fold elevation in the point count ratio relative to control marrow biopsies ($P < 0.01$). Greater inter-field and inter-biopsy variability in the number of vWF-positive points was also noted relative to control biopsies. This variability can be accounted for by the tendency toward vessel clustering ("hot-spots") typically present in AML bone marrow

biopsies. Point count ratios from AML 30 day post-induction chemotherapy biopsies showed the greatest degree of variability and ranged from 0.05 to 0.178 with a mean value of 0.104 ± 0.013 (n = 11). This represents an 8.7-fold increase in the ratio relative to the control group ($P < 0.001$). As with the newly diagnosed AML bone marrow biopsies, significant inter-biopsy variability was observed.

VEGF Is Expressed by AML Blasts In Vivo

To account for the increased vascularity of bone marrow biopsies of patients with AML either at time of diagnosis or 30 days post-induction chemotherapy, we speculated that AML blast cells may synthesize and secrete angiogenic growth factors. VEGF is a potent angiogenic factor synthesized by hematopoietic cells [18]. To assess whether AML blast cells synthesize VEGF in vivo, bone marrow aspirate squash preparations obtained from control patients (lymphoma negative staging marrow biopsies, n = 6) or patients newly diagnosed with AML (n = 5) were examined by immunohistochemistry for VEGF. Bone marrow aspirates from control patients typically contained several granules of normal cellularity (Fig. 3B,C). Low-power magnification typically revealed weak-to-moderate and patchy VEGF immunohistochemical reactivity restricted to the marrow granule (Fig. 3B). At higher magnification, the VEGF immunoreactivity was confined primarily to the cytoplasm of megakaryocytes and mature granulocytes (Fig. 3C). This distribution of VEGF has been previously reported [19,20]. Little background VEGF immunoreactivity was present (Fig. 3C) and other hematopoietic cells did not stain for VEGF. Bone marrow aspirates obtained from patients with newly diagnosed AML contained large numbers of highly cellular granules. At low-power, the granules typically displayed diffuse moderate-to-strong VEGF immunohistochemical reactivity with a weaker halo of non-cellular VEGF immunostaining surrounding the granule. The range of staining intensity obtained is shown in Figure 3D (strong) and Figure 3E (moderate). Higher magnification confirmed that blast cells represented the dominant cell type and accounted for the majority of the VEGF immunoreactivity (Fig. 3F). The VEGF immunohistochemical staining pattern consisted of moderate-to-strong cytoplasmic immunoreactivity with a perinuclear prominence (Fig. 3F). Moderate background staining of areas immediately adjacent to blast cells within the granule and surrounding the granule was seen consistently and interpreted as immunohistochemical reactivity toward extracellular VEGF. Despite the overall increase in VEGF staining, occasional granules containing blast cells showed much lower immunoreactivity for VEGF. No staining was seen in the absence of primary antibody (Fig. 3A). The significantly stronger VEGF immunoreactivity present in the AML bone marrow aspirates suggests increased VEGF content within the cellular compartment of the bone marrow. AML blasts, therefore, may represent a significant source of VEGF and potentiate neovascularization of the bone marrow through secretion or release of VEGF.

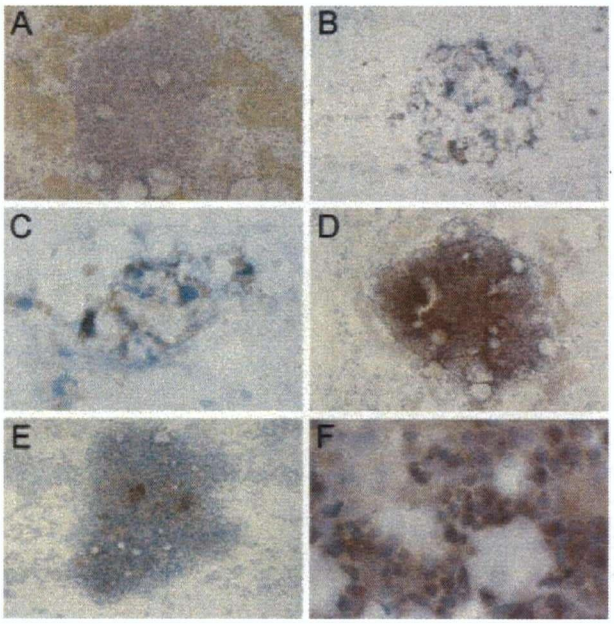

Fig. 3. Bone marrow aspirates immunostained for VEGF. (A) Granule from patient with AML. There is no VEGF immunoreactivity seen in the absence of primary antibody (original magnification 50×). (B, C) Control marrow aspirates (B, original magnification 50×; C, original magnification 400×) stained for VEGF. (D, E) Bone marrow aspirates from two different patients newly diagnosed with AML (original magnification 50×); (F) Higher power view (original magnification 500×) of AML patient granule immunostained for VEGF. [Color figure can be viewed in the online issue, which is available at www.interscience.wiley.com.]

Conditioned Media From AML Marrow Mononuclear Cells Do Not Show Increased Amounts of VEGF, FGF-2, or Endostatin

To further explore the ability of AML blasts to secrete angiogenic growth factors, mononuclear cells from AML and normal bone marrow were cultured for 48 hr, and the medium was assayed for VEGF, FGF-2, or endostatin by competitive ELISA. In addition to VEGF, FGF-2 is a potent angiogenic growth factor while endostatin is an inhibitor of angiogenesis [21]. As shown in Figure 4, VEGF, FGF-2, and endostatin were detected in the supernatants of

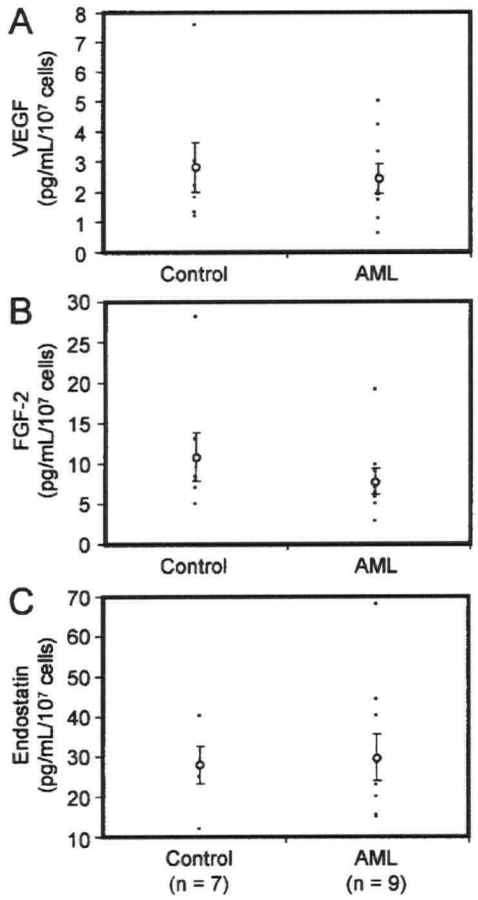

Fig. 4. Determination of VEGF, FGF-2, and endostatin levels. Concentrations of angiogenic or angiostatic factors by ELISA in supernatants of primary cultured AML blast cells or control bone marrow mononuclear cells following 48-hr incubation. (A) VEGF; (B) FGF-2; and (C) endostatin. The mean (O) and standard error for each group are given.

cultured normal bone marrow cells ($n = 7$) at average concentrations of 2.8 ± 0.8, 11 ± 3.0, and 28 ± 4.8 pg/mL, respectively. Expression of VEGF, FGF-2, and endostatin in AML marrow conditioned medium ($n = 9$) showed mean concentrations of 2.5 ± 0.5, 7.9 ± 1.6, and 30 ± 6.0 pg/mL, respectively.

Conditioned Media From AML Marrow Mononuclear Cells Do Not Show Increased Angiogenic Potential

Because immunological techniques will only detect factors that are specifically assayed, we used two different angiogenesis assays to screen for angiogenic factors potentially secreted by the cultured AML blasts. Under the influence of angiogenic growth factors, endothelial cells grown on microcarrier beads form tube-like structures with microscopic and ultrastructural features similar to that of rudimentary

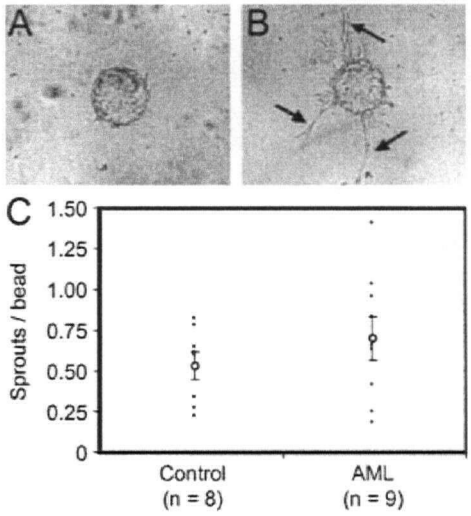

Fig. 5. Endothelial cell sprouting assay. Two-day conditioned medium from either normal marrow mononuclear cells or primary cultures of AML blast cells were tested. (A) Microcarrier bead coated with endothelial cells with a complete lack of sprout formation; (B) microcarrier bead showing three typical endothelial sprouts indicated by arrows; (C) average sprout formation per microcarrier bead shown for control and AML specimens. The mean (O) and standard error for each group are given.

capillaries. In the presence of medium and serum only, the endothelial cells form few tube-like structures (Fig. 5A). In the presence of angiogenic factors, however, the endothelial cells reorganize into branching tube-like structures extending beyond the surface of the microcarrier bead and into the supporting fibrin matrix (Fig. 5B). The results of the microcarrier bead assay are shown in Figure 5C. A range of angiogenic responses was obtained, with certain AML blast cell supernatants eliciting little endothelial tube formation while several control supernatants induced striking endothelial tube formation (Fig. 5C). Scoring of endothelial sprouting revealed that AML blast supernatants did not demonstrate greater angiogenic activity compared to control supernatants, with mean scores of 0.7 ± 0.1 sprout/bead and 0.5 ± 0.1 sprout/bead, respectively ($P = 0.313$). However, an occasional individual sample of AML conditioned medium showed significantly greater endothelial cell tube-forming activity.

The chick CAM assay is another well-established model to study angiogenesis. Grading of the degree of angiogenesis was performed on a 5-point scale as previously described [16]. Figure 6A shows a negative response elicited by medium only (Grade 0), and Figure 6B demonstrates a more prominent radial neovascularization pattern and blood vessel ingrowth involving greater than 80% of the sponge circumference (Grade 4). Conditioned media from control

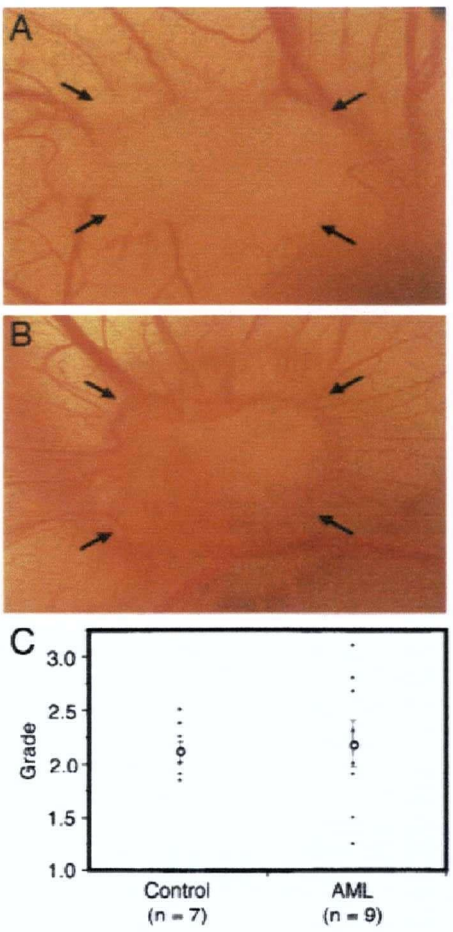

Fig. 6. Angiogenesis on the chick CAM using conditioned media from bone marrow aspirates. (A, B) Examples of Grade 0 (A, PBS control) and Grade 4 (B, VEGF 30 ng/mL) angiogenic responses. Controls or culture supernatants were applied to a gelatin sponge (arrows) implanted on top of the CAM. Note the presence of a radial growth pattern of small vessels, and penetration of vessels into the gelatin sponge in B. (C) Angiogenic activity of normal mononuclear bone marrow cell or AML blast cell supernatant in the chick CAM assay. The mean (O) and standard error for each group are given. [Color figure can be viewed in the online issue, which is available at www.interscience.wiley.com.]

marrow cells in general evoked a moderate response, with localized proliferation of small blood vessels in a radial pattern toward the sponge with focal penetration into the sponge. Typically, the vessels penetrated less than 50% of the sponge circumference. Overall, supernatants from AML blast cells elicited a similar angiogenic response (2.2 ± 0.2) as control (2.1 ± 0.1) specimens (Fig. 6C, $P = 0.796$). However, as with the endothelial sprouting assay, AML supernatants showed a greater range of response with specific individual samples demonstrating greatly increased angiogenesis.

DISCUSSION

Previous reports have identified increased vascularity within bone marrow biopsies from patients diagnosed with ALL, multiple myeloma, or AML [2,3,5–7]. The blood vessels in these biopsies differed in their pattern of growth and histologic appearance compared to blood vessels present in control bone marrow biopsies. We confirm these observations by demonstrating a significant increase in the number of blood vessels in bone marrow biopsies obtained from patients diagnosed with AML. An uneven distribution of vessels was also noted, as evidenced by increased variability in the point counts between individual fields and biopsies within the AML patient group. The observation that the highest point count ratios were seen in the biopsies obtained post-chemotherapy may be attributable to several causes. The most tenable explanation would be that leukemic cell lysis following chemotherapy results in the release of VEGF or other angiogenic factors directly from the blast cells. Alternatively, since VEGF is secreted in response to inflammatory stimuli, our findings may be due to a reactive process secondary to marrow damage from chemotherapy [1]. In a study of childhood ALL, day 31 post-induction chemotherapy marrow biopsies did not show a significant difference from diagnostic specimens in marrow vascularity [2]. In contrast to the current study, others have observed significantly decreased vascularity in post-chemotherapy AML bone marrows [6]. This discrepancy may be attributable to the time at which the post-chemotherapy biopsies were taken; in the present study, the post-chemotherapy biopsies studied were performed on day 30 while the biopsies analyzed by Padro and co-workers were undertaken on day 16. The difference between day 16 and day 30 post-induction chemotherapy marrows may suggest that antileukemic chemotherapy also has anti-vascular activity, but that leukemic cell lysis and reactive changes stimulate a rebound angiogenesis.

The results of the current study provide direct evidence that VEGF is actively synthesized by AML blasts in vivo. The strong cytoplasmic immunohistochemical reactivity of AML blasts to VEGF staining suggests that a prominent source of angiogenic factors resides within the AML blast cells. Lysis of AML blast cells, as may occur with increased cell turnover or chemotherapy, could result in the release of large quantities of VEGF, which may subsequently contribute to or elicit further neovascularization of the bone marrow.

Although the AML blasts were strongly immunoreactive for VEGF in vivo, elevated secretion of VEGF could not be demonstrated ex vivo, in cells

cultured from leukemic bone marrows. This suggests that microenvironmental factors promote the secretion of VEGF in vivo, and that we have not reproduced these conditions ex vivo. Two critical factors that promote VEGF expression are hypoxia and hypoglycemia, neither of which is present in vitro [22–25]. Further, the AML blast cells were cultured ex vivo without exogenous growth factors, and the presence of cytokines in vivo may act upon blast cells to promote VEGF secretion [22,26–28]. Another possibility is that other cell types in the bone marrow may also secrete angiogenic factors secondary to metabolic stress and thus contribute to bone marrow neovascularization in AML [29]. This is an important consideration given that Ratajczak and co-workers observed that cultured normal bone marrow stromal cells secreted VEGF at concentrations significantly higher than all malignant hematopoietic cell lines examined in their study [10]. In addition, infiltration of the bone marrow by blast cells may induce VEGF secretion by stromal cells, and an increased expression of VEGF has been demonstrated in bone marrow stromal cells of mice with metastatic disease to the bone marrow [29]. Given that we were clearly able to detect VEGF in blast cells, the secretion of VEGF by stromal cells is unlikely to be the sole reason for the discrepancy between our in vivo and in vitro findings. However, the variable VEGF expression in different granules of the same bone marrow aspirate again suggests that the microenvironment of the marrow and/or direct leukemic-stromal cell interactions play a significant role in promoting VEGF expression in AML blast cells.

It is also possible that certain populations of blast cells actively synthesize VEGF but are less efficient at secretion or lack a stimulus for secretion of VEGF. As a result, supernatant concentrations of VEGF may be lower relative to other cell populations. While the regulation of VEGF transcriptional activation is better understood, the regulation of VEGF secretion is less clear [25,30]. Hence, additional stimuli may be necessary to elicit secretion of VEGF in vitro.

We also considered that AML blast cells secreted additional angiogenic growth factors. To address this possibility, two angiogenesis assays were utilized to screen for angiogenic growth factors. To date, the use of angiogenesis assays in the evaluation of primary cultured AML blasts has not been reported. The endothelial cell tube formation assay offers the advantage of utilizing a human endothelial cell line under controlled experimental conditions. The CAM assay represents a true in vivo system allowing for potential interaction of multiple signaling factors and cell types. This is an important feature as synergism between VEGF and FGF-2 in angiogenesis has been documented [31]. Although in both assays there were individual AML specimens that elicited a greater angiogenic response, the difference between the mean scores of control and AML marrow specimens was not statistically significant. In contrast, others have reported significant stimulation of angiogenesis in the CAM assay induced by cultured multiple myeloma cells [4].

Alternatively, or in addition to the above possibilities, it may be that under the conditions in vitro there is increased secretion or stability of angiogenic inhibitors with respect to angiogenic promoters. Indeed, it has been postulated that one reason that a primary tumor is able to suppress the growth of metastases in some cases is the longer circulating half-life of certain angiogenic inhibitors such as endostatin and angiostatin [21,32]. Our results do not demonstrate a difference in the levels of endostatin between control and AML specimens, but this does not preclude the presence of other long-lived inhibitors.

Notwithstanding the above comments, the fact that an occasional specimen shows increased angiogenesis and VEGF expression ex vivo suggests that, in some cases, myeloid blasts may have an intrinsic propensity to stimulate angiogenesis. It has also been reported that there is individual variability in VEGF expression in response to hypoxia [33]. It might be anticipated that if AML blast cells constitutively secrete VEGF or other angiogenic factors, a more uniform pattern of neovascularization should result, reflecting the distribution of the blast cells. Rather, the pattern of vascularity observed in our study suggests that local factors are critical in the angiogenic response of the bone marrow. This hypothesis does not discount the possibility that blast cells may be more acutely sensitive to environmental stresses, and that a lowered threshold for angiogenic growth factor secretion may impart a survival advantage to the malignant cells. Clearly, further studies are required to elucidate the mechanisms of increased angiogenesis in AML, and to determine whether this finding has prognostic or therapeutic significance.

ACKNOWLEDGMENTS

We thank Harvey Coxson for assistance with point counting. A.K. is a Clinician-Scientist of the Canadian Institutes of Health Research.

REFERENCES

1. Folkman J. Angiogenesis in cancer, vascular, rheumatoid and other disease. Nat Med 1995;1:27–31.
2. Perez-Atayde AR, Sallan SE, Tedrow U, Connors S, Allred E, Folkman J. Spectrum of tumor angiogenesis in the bone marrow of children with acute lymphoblastic leukemia. Am J Pathol 1997;150:815–821.

3. Vacca A, Ribatti D, Roncali L, Ranieri G, Serio G, Silvestris F, Dammacco F. Bone marrow angiogenesis and progression in multiple myeloma. Br J Haematol 1994;87:503–508.
4. Vacca A, Ribatti D, Presta M, Minischetti M, Iurlaro M, Ria R, Albini A, Bussolino F, Dammacco F. Bone marrow neovascularization, plasma cell angiogenic potential, and matrix metalloproteinase-2 secretion parallel progression of human multiple myeloma. Blood 1999;93:3064–3073.
5. Hussong JW, Rodgers GM, Shami PJ. Evidence of increased angiogenesis in patients with acute myeloid leukemia. Blood 2000;95:309–313.
6. Padro T, Ruiz S, Bieker R, Burger H, Steins M, Kienast J, Buchner T, Berdel WE, Mesters RM. Increased angiogenesis in the bone marrow of patients with acute myeloid leukemia. Blood 2000;95:2637–2644.
7. Aguayo A, Estey E, Kantarjian H, Mansouri T, Gidel C, Keating M, Giles F, Estrov Z, Barlogie B, Albitar M. Cellular vascular endothelial growth factor is a predictor of outcome in patients with acute myeloid leukemia. Blood 1999;94:3717–3721.
8. Bellamy WT, Richter L, Frutiger Y, Grogan TM. Expression of vascular endothelial growth factor and its receptors in hematopoietic malignancies. Cancer Res 1999;59:728–733.
9. Fiedler W, Graeven U, Ergun S, Verago S, Kilic N, Stockschlader M, Hossfeld DK. Vascular endothelial growth factor, a possible paracrine growth factor in human acute myeloid leukemia. Blood 1997;89:1870–1875.
10. Ratajczak MZ, Ratajczak J, Machalinski B, Majka M, Marlicz W, Carter A, Pietrzkowski Z, Gewirtz AM. Role of vascular endothelial growth factor (VEGF) and placenta-derived growth factor (PlGF) in regulating human haemopoietic cell growth. Br J Haematol 1998;103:969–979.
11. Burgdorf WH, Mukai K, Rosai J. Immunohistochemical identification of factor VIII-related antigen in endothelial cells of cutaneous lesions of alleged vascular nature. Am J Clin Pathol 1981;75:167–171.
12. Doerschuk CM, Markos J, Coxson HO, English D, Hogg JC. Quantitation of neutrophil migration in acute bacterial pneumonia in rabbits. J Appl Physiol 1994;77:2593–2599.
13. Hogg JC, Coxson HO, Brumwell ML, Beyers N, Doerschuk CM, MacNee W, Wiggs BR. Erythrocyte and polymorphonuclear cell transit time and concentration in human pulmonary capillaries. J Appl Physiol 1994;77:1795–1800.
14. Nehls V, Drenckhahn D. A novel, microcarrier-based in vitro assay for rapid and reliable quantification of three-dimensional cell migration and angiogenesis. Microvasc Res 1995;50:311–322.
15. Ades EW, Candal FJ, Swerlick RA, George VG, Summers S, Bosse DC, Lawley TJ. HMEC-1: establishment of an immortalized human microvascular endothelial cell line. J Invest Dermatol 1992;99:683–690.
16. Vu MT, Smith CF, Burger PC, Klintworth GK. An evaluation of methods to quantitate the chick chorioallantoic membrane assay in angiogenesis. Lab Invest 1985;53:499–508.
17. Zar JH, editor. Biostatistical analysis. 4th edition. Englewood Cliffs, NJ: Prentice Hall, Inc.; 1999. p 210–214.
18. Mohle R, Green D, Moore MA, Nachman RL, Rafii S. Constitutive production and thrombin-induced release of vascular endothelial growth factor by human megakaryocytes and platelets. Proc Natl Acad Sci U S A 1997;94:663–668.
19. Pruneri G, Bertolini F, Soligo D, Carboni N, Cortelezzi A, Ferrucci PF, Buffa R, Lambertenghi-Deliliers G, Pezzella F. Angiogenesis in myelodysplastic syndromes. Br J Cancer 1999;81: 1398–1401.
20. Gaudry M, Bregerie O, Andrieu V, El Benna J, Pocidalo MA, Hakim J. Intracellular pool of vascular endothelial growth factor in human neutrophils. Blood 1997;90:4153–4161.
21. O'Reilly MS, Boehm T, Shing Y, Fukai N, Vasios G, Lane WS, Flynn E, Birkhead JR, Olsen BR, Folkman J. Endostatin: an endogenous inhibitor of angiogenesis and tumor growth. Cell 1997;88:277–285.
22. Larrivee B, Karsan A. Signaling pathways induced by vascular endothelial growth factor (review). Int J Mol Med 2000;5:447–456.
23. Stein I, Neeman M, Shweiki D, Itin A, Keshet E. Stabilization of vascular endothelial growth factor mRNA by hypoxia and hypoglycemia and co-regulation with other ischemia-induced genes. Mol Cell Biol 1995;15:5363–5368.
24. Damert A, Machein M, Breier G, Fujita MQ, Hanahan D, Risau W, Plate KH. Up-regulation of vascular endothelial growth factor expression in a rat glioma is conferred by two distinct hypoxia-driven mechanisms. Cancer Res 1997;57:3860–3864.
25. Shweiki D, Neeman M, Itin A, Keshet E. Induction of vascular endothelial growth factor expression by hypoxia and by glucose deficiency in multicell spheroids: implications for tumor angiogenesis. Proc Natl Acad Sci U S A 1995;92:768–772.
26. Abramovitch R, Neeman M, Reich R, Stein I, Keshet E, Abraham J, Solomon A, Marikovsky M. Intercellular communication between vascular smooth muscle and endothelial cells mediated by heparin-binding epidermal growth factor-like growth factor and vascular endothelial growth factor. FEBS Lett 1998;425: 441–447.
27. Valter MM, Wiestler OD, Pietsch T. Differential control of VEGF synthesis and secretion in human glioma cells by IL-1 and EGF. Int J Dev Neurosci 1999;17:565–577.
28. Hellwig-Burgel T, Rutkowski K, Metzen E, Fandrey J, Jelkmann W. Interleukin-1beta and tumor necrosis factor-alpha stimulate DNA binding of hypoxia-inducible factor-1. Blood 1999;94: 1561–1567.
29. Fukumura D, Xavier R, Sugiura T, Chen Y, Park EC, Lu N, Selig M, Nielsen G, Taksir T, Jain RK, Seed B. Tumor induction of VEGF promoter activity in stromal cells. Cell 1998;94:715–725.
30. Shweiki D, Itin A, Soffer D, Keshet E. Vascular endothelial growth factor induced by hypoxia may mediate hypoxia-initiated angiogenesis. Nature 1992;359:843–845.
31. Pepper MS, Ferrara N, Orci L, Montesano R. Potent synergism between vascular endothelial growth factor and basic fibroblast growth factor in the induction of angiogenesis in vitro. Biochem Biophys Res Commun 1992;189:824–831.
32. O'Reilly MS, Holmgren L, Shing Y, Chen C, Rosenthal RA, Moses M, Lane WS, Cao Y, Sage EH, Folkman J. Angiostatin: a novel angiogenesis inhibitor that mediates the suppression of metastases by a Lewis lung carcinoma. Cell 1994;79:315–328.
33. Schultz A, Lavie L, Hochberg I, Beyar R, Stone T, Skorecki K, Lavie P, Roguin A, Levy AP. Inter-individual heterogeneity in the hypoxic regulation of VEGF: significance for the development of the coronary artery collateral circulation. Circulation 1999;100: 547–552.

This page intentionally blank

Brief report

Bacterial lipopolysaccharide directly induces angiogenesis through TRAF6-mediated activation of NF-κB and c-Jun N-terminal kinase

Ingrid Pollet, Christy J. Opina, Carla Zimmerman, Kevin G. Leong, Fred Wong, and Aly Karsan

The intracellular pathways by which inflammatory mediators transmit their angiogenic signals is not well studied. The effects of a potent inflammatory mediator, bacterial lipopolysaccharide (LPS), are transmitted through Toll-like receptors (TLRs). A major, although not exclusive, LPS/TLR intracellular signaling pathway is routed through TNF (tumor necrosis factor) receptor associated factor 6 (TRAF6). In this report we demonstrate that LPS directly stimulates endothelial sprouting in vitro. By blocking TRAF6 activity using retroviral expression of a dominant-negative TRAF6 in endothelial cells, we show that TRAF6 is absolutely required for the LPS-initiated angiogenic response in vitro and in vivo. Inhibition of either c-Jun N-terminal kinase (JNK) activity or nuclear factor κB (NF-κB) activity, downstream of TRAF6, is sufficient to inhibit LPS-induced endothelial sprouting. In contrast, only inhibition of NF-κB, but not JNK, activity blocks basic fibroblast growth factor (bFGF)–induced angiogenesis. Our findings thus demonstrate a direct endothelial-stimulatory role of LPS in initiating angiogenesis through activation of TRAF6-dependent signaling pathways. (Blood. 2003;102: 1740-1742)

Introduction

Although several angiogenic cytokines have been described, the understanding of signaling pathways through which these factors transduce their message remains in its infancy. In particular, little has been reported on the intracellular angiogenic signaling mediated by inflammatory mediators. There is controversy as to whether inflammatory mediators such as tumor necrosis factor (TNF) and bacterial lipopolysaccharide (LPS) directly stimulate endothelial sprouting and angiogenesis, or whether these mediators act by stimulating the release of intermediary growth factors/cytokines.[1-4] Several studies have demonstrated the angiogenic potential of LPS.[2,5-7] However, in some cases it has been suggested that the angiogenic effect of LPS may be secondary to the release of angiogenic factors from adjacent nonendothelial cells, rather than a direct effect on the endothelium.[2,8] In this report we demonstrate that, in contrast to TNF, LPS directly stimulates endothelial sprouting in vitro. Because TNF receptor associated factor 6 (TRAF6) is a major route of the LPS/Toll-like receptor (TLR) signaling pathway, we have used dominant-negative constructs of TRAF6 and downstream signaling molecules to dissect the intracellular signal transduction pathway required for LPS-mediated induction of angiogenesis in vitro and in vivo.[9-11]

Study design

Reagents and cell lines

Generation and characterization of retrovirally transduced human dermal microvascular endothelial cell lines (HMEC-vector, HMEC-TRAF6-C, HMEC-IκBmt, HMEC-JNK-APF) has been reported previously.[11] The avian retroviral packaging cell line Q2bn was a gift from K. McNagny (University of British Columbia, Vancouver, Canada).

Endothelial sprouting assay

Endothelial sprouting was assessed as previously described.[12] Briefly, microcarrier beads coated with gelatin were seeded with HMEC lines and embedded in fibrin gels in 96-well plates. Fibrin gels were supplemented with basic fibroblast growth factor (bFGF; 1 ng/mL), LPS (100 ng/mL), or TNF (10 ng/mL) according to the experiment. The overlying medium contained either MCDB medium + 2% fetal bovine serum (FBS) alone or was supplemented with bFGF (1 ng/mL), LPS (100 ng/mL), or TNF (10 ng/mL). After 3 days of incubation with daily medium changes, the number of capillary-like tubes formed was quantitated by counting the number of tubelike structures more than 150 μm in length per microcarrier bead (sprouts per bead).

Chick chorioallantoic membrane (CAM) assay

The chick CAM assay was performed as previously described.[12] Briefly, on embryonic day 8, the developing CAM was separated from the shell by

From the Department of Medical Biophysics, British Columbia Cancer Agency; Department of Pathology and Laboratory Medicine, University of British Columbia; Experimental Medicine Program, University of British Columbia; and Department of Pathology and Laboratory Medicine, British Columbia Cancer Agency, Vancouver, BC, Canada.

Submitted January 29, 2003; accepted April 11, 2003. Prepublished online as *Blood* First Edition Paper, April 24, 2003; DOI 10.1182/blood-2003-01-0288.

Supported by the Canadian Institutes of Health Research, the Heart and Stroke Foundation of British Columbia and the Yukon, and the National Cancer Institute of Canada with funds from the Canadian Cancer Society. K.G.L. is supported by a Doctoral Research Award from the Canadian Institutes of Health Research, and a Predoctoral Fellowship Award from the U.S. Department of the Army (DAMD17-01-1-0164).

Reprints: Aly Karsan, Department of Medical Biophyics, British Columbia Cancer Research Centre, 601 West 10th Ave, Vancouver, BC, Canada, V5Z 1L3; e-mail: akarsan@bccancer.bc.ca.

The publication costs of this article were defrayed in part by page charge payment. Therefore, and solely to indicate this fact, this article is hereby marked "advertisement" in accordance with 18 U.S.C. section 1734.

opening a small circular window at the broad end of the egg. On day 10, Q2bn avian retroviral producer cell lines were transfected with either empty vector (CK) or dominant-negative TRAF6 (CK-TRAF6-C), resuspended in phosphate-buffered saline (PBS) alone or supplemented with bFGF (30 ng/mL) or LPS (10 ng/mL), and placed onto nylon meshes on the CAM. Expression of the TRAF6-C construct was confirmed by immunoblotting. The retroviral producer cells distribute throughout the mesh and secrete virus (control or TRAF6-C) which mainly infects the proliferating endothelial cells.[12,13] On day 14, images of the CAMs were captured digitally, and neovascularization was quantitated for each CAM by counting the number of vessels that entered the mesh area and dividing by the perimeter of the mesh (vessels per millimeter).

Statistics

Results were analyzed by analysis of variance (ANOVA) to ascertain differences between groups, followed by a Tukey test for multiple comparisons.

Results and discussion

Tissues exhibiting inflammation show increased vascularity.[14,15] We first attempted to determine whether the inflammatory mediators TNF and LPS could directly stimulate endothelial sprouting using an in vitro tube-forming morphogenesis assay. Microcarrier beads seeded with human microvascular endothelial cells (HMECs) were embedded in fibrin gels and stimulated with LPS, TNF, or bFGF (positive control). Interestingly, LPS but not TNF was able to directly stimulate endothelial sprouting in this assay. Figure 1A demonstrates endothelial sprout formation in response to LPS. Figure 1B shows the number of sprouts per bead in response to LPS or TNF, with bFGF used as a positive control. These findings suggest that TLRs activate specific downstream signals promoting angiogenesis, which are distinct from TNF receptors.

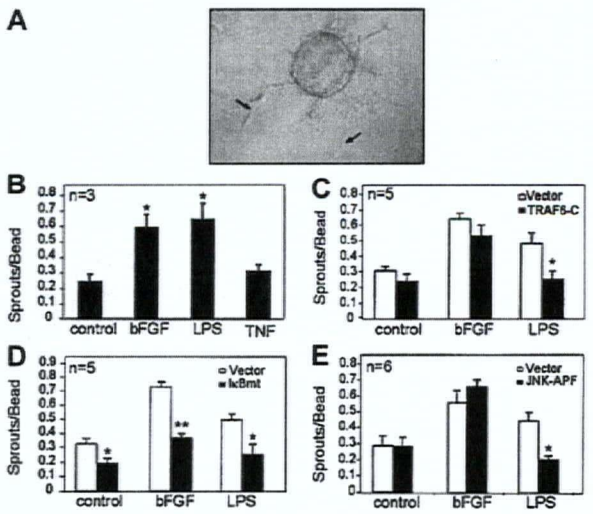

Figure 1. LPS signals endothelial sprouting through a TRAF6-mediated pathway that activates NF-κB and JNK. Microcarrier beads seeded with endothelial cells were embedded in fibrin gels and exposed to various stimuli. (A) An example of endothelial sprouts (arrows) formed in this assay following LPS (100 ng/mL) stimulation. (B) Quantitation of the number of sprouts formed following stimulation by serum-only (control), bFGF (1 ng/mL), LPS (100 ng/mL), or TNF (10 ng/mL). Effect of inhibiting (C) TRAF6 activation, (D) NF-κB activation, or (E) JNK activation on endothelial sprouting in response to bFGF (1 ng/mL) or LPS (100 ng/mL). Each experiment was done in triplicate, and the total number of experiments done in each case is indicated on the graph. Results shown are the mean + SEM of the total number of experiments. $^*P \leq .05$, $^{**}P \leq .01$.

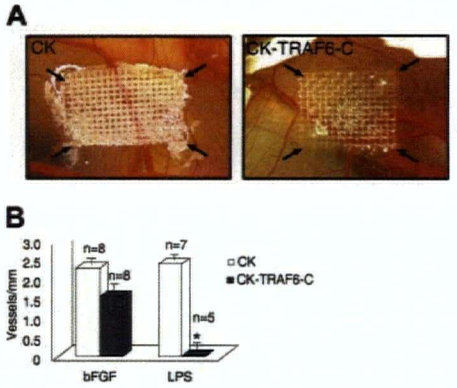

Figure 2. Inhibition of TRAF6 signaling on the chick CAM inhibits LPS- but not bFGF-induced angiogenesis. Avian retroviral producer lines were used to infect the proliferating cells (mainly endothelial) on the chick CAM with either empty vector (CK) or a dominant-negative TRAF6 (CK-TRAF6-C). (A) A representative CAM showing LPS-induced angiogenesis following infection of the CAM by empty vector (left panel) or TRAF6-C (right panel). The arrows point to the corners of the mesh on which the retroviral producer lines are seeded. (B) Quantitation of vessel number entering the mesh following retroviral infection and stimulation with bFGF (30 ng/mL) or LPS (10 ng/mL). Results shown are the number of vessels entering the mesh perimeter over baseline control (medium only). The number of experiments for each condition is shown over the bars. Results shown are the mean + SEM. $^*P \leq .05$.

A critical intermediary signaling molecule used by the TLRs is TRAF6.[9,11,16,17] To determine whether TRAF6 is involved in signaling the endothelial sprouting response, we used endothelial cells that overexpress a dominant-negative TRAF6 construct that lacks amino acids 1-289 (TRAF6-C).[11] HMEC-TRAF6-C or vector-transduced cells were seeded onto microcarrier beads, and sprouting in response to LPS or bFGF was assessed. Figure 1D demonstrates that TRAF6-C inhibited LPS-induced endothelial sprouting, indicating the importance of TRAF6 activation in LPS-induced sprouting. The lack of effect of TRAF6-C on bFGF-induced endothelial sprouting (Figure 1D) confirms the specificity of the inhibitory effect of this dominant-negative construct as previously shown.[11]

We have shown that LPS-induced NF-κB activation and c-Jun N-terminal kinase (JNK) activation lie downstream of TRAF6 in endothelial cells.[11] To determine whether NF-κB activation was required for LPS-induced sprouting, we used endothelial cells that express a super-repressor IκBα protein that is resistant to degradation and, thus, retains NF-κB in the cytoplasm despite activating signals.[18] Figure 1E demonstrates that abrogation of NF-κB activation inhibited endothelial sprouting in response to either LPS or bFGF. Interestingly, blockade of NF-κB also inhibited baseline sprouting in response to serum stimulation only (control, Figure 1E), highlighting the general importance of this pathway in endothelial sprouting. However, we did not find that IκBmt inhibited endothelial cell proliferation (data not shown), suggesting that NF-κB activation is required for morphogenesis rather than endothelial proliferation in this context.

To test whether JNK activation was similarly necessary for LPS-induced sprouting, we used endothelial cells transduced with a dominant-negative JNK (JNK-APF) construct.[11] We have previously shown that this mutant JNK specifically blocks JNK activation without affecting other mitogen-activated protein (MAP) kinase pathways.[11] Figure 1F demonstrates that, although JNK activation is required for LPS-induced endothelial sprouting, bFGF-induced sprouting can proceed independently of JNK. Thus, in contrast to the critical role of NF-κB in signaling endothelial morphogenesis in response to diverse stimuli, the role of JNK appears to be limited to specific angiogenic activators.

To confirm that our findings can be translated to angiogenesis in vivo, we used the chick CAM assay to test whether LPS can induce angiogenesis. We found that LPS (10 ng/mL) was able to induce angiogenesis on the chick CAM to a degree similar to bFGF (30 ng/mL) (data not shown). Next, we used an avian retroviral producer line to infect the chick CAM with the TRAF6-C construct. We and others have previously shown that most of the cells transduced using this technique are vascular endothelial cells.[12,13] As seen in Figure 2A-B, angiogenesis on the chick CAM is blocked by the dominant-negative TRAF6 when LPS is the stimulus, but not when bFGF is the angiogenic agent, thereby corroborating our in vitro findings.

Our findings demonstrate that LPS-induced activation of TRAF6 in endothelial cells signals angiogenesis through activation of both NF-κB and JNK. LPS has been demonstrated to promote tumor angiogenesis and metastasis in mouse models.[2,6] Thus, our results may be of relevance in cancer therapeutics, given that clinical trials with a lipid A analog, the bioactive domain of LPS, are in progress.[19]

Acknowledgment

A.K. is a Clinician-Scientist of the Canadian Institutes of Health Research and a Scholar of the Michael Smith Foundation for Health Research.

References

1. Koolwijk P, van Erck MG, de Vree WJ, et al. Cooperative effect of TNFalpha, bFGF, and VEGF on the formation of tubular structures of human microvascular endothelial cells in a fibrin matrix: role of urokinase activity. J Cell Biol. 1996;132:1177-1188.
2. Pidgeon GP, Harmey JH, Kay E, Da Costa M, Redmond HP, Bouchier-Hayes DJ. The role of endotoxin/lipopolysaccharide in surgically induced tumour growth in a murine model of metastatic disease. Br J Cancer. 1999;81:1311-1317.
3. Norrby K. Interleukin-1-alpha and de novo mammalian angiogenesis. Microvasc Res. 1997;54:58-64.
4. Yoshida S, Ono M, Shono T, et al. Involvement of interleukin-8, vascular endothelial growth factor, and basic fibroblast growth factor in tumor necrosis factor alpha-dependent angiogenesis. Mol Cell Biol. 1997;17:4015-4023.
5. Mattsby-Baltzer I, Jakobsson A, Sorbo J, Norrby K. Endotoxin is angiogenic. Int J Exp Pathol. 1994;75:191-196.
6. Harmey JH, Bucana CD, Lu W, et al. Lipopolysaccharide-induced metastatic growth is associated with increased angiogenesis, vascular permeability and tumor cell invasion. Int J Cancer. 2002;101:415-422.
7. Li WW, Grayson G, Folkman J, D'Amore PA. Sustained-release endotoxin: a model for inducing corneal neovascularization. Invest Ophthalmol Vis Sci. 1991;32:2906-2911.
8. Leibovich SJ, Chen JF, Pinhal-Enfield G, et al. Synergistic up-regulation of vascular endothelial growth factor expression in murine macrophages by adenosine A(2A) receptor agonists and endotoxin. Am J Pathol. 2002;160:2231-2244.
9. Ishida T, Mizushima S, Azuma S, et al. Identification of TRAF6, a novel tumor necrosis factor receptor-associated factor protein that mediates signaling from an amino-terminal domain of the CD40 cytoplasmic region. J Biol Chem. 1996;271:28745-28748.
10. O'Neill LA. Signal transduction pathways activated by the IL-1 receptor/toll-like receptor superfamily. Curr Top Microbiol Immunol. 2002;270:47-61.
11. Hull C, McLean G, Wong F, Duriez PJ, Karsan A. Lipopolysaccharide signals an endothelial apoptosis pathway through TNF receptor-associated factor 6-mediated activation of c-Jun NH2-terminal kinase. J Immunol. 2002;169:2611-2618.
12. Leong KG, Hu X, Li L, et al. Activated Notch4 inhibits angiogenesis: role of beta 1-integrin activation. Mol Cell Biol. 2002;22:2830-2841.
13. Boudreau N, Andrews C, Srebrow A, Ravanpay A, Cheresh DA. Induction of the angiogenic phenotype by Hox D3. J Cell Biol. 1997;139:257-264.
14. Margetts PJ, Kolb M, Yu L, et al. Inflammatory cytokines, angiogenesis, and fibrosis in the rat peritoneum. Am J Pathol. 2002;160:2285-2294.
15. Griffioen AW, Molema G. Angiogenesis: potentials for pharmacologic intervention in the treatment of cancer, cardiovascular diseases, and chronic inflammation. Pharmacol Rev. 2000;52:237-268.
16. Cao Z, Xiong J, Takeuchi M, Kurama T, Goeddel DV. TRAF6 is a signal transducer for interleukin-1. Nature. 1996;383:443-446.
17. Zhang FX, Kirschning CJ, Mancinelli R, et al. Bacterial lipopolysaccharide activates nuclear factor-kappaB through interleukin-1 signaling mediators in cultured human dermal endothelial cells and mononuclear phagocytes. J Biol Chem. 1999;274:7611-7614.
18. Hu X, Yee E, Harlan JM, Wong F, Karsan A. Lipopolysaccharide induces the antiapoptotic molecules, A1 and A20, in microvascular endothelial cells. Blood. 1998;92:2759-2765.
19. de Bono JS, Dalgleish AG, Carmichael J, et al. Phase I study of ONO-4007, a synthetic analogue of the lipid A moiety of bacterial lipopolysaccharide. Clin Cancer Res. 2000;6:397-405.

This page intentionally blank